Bergen, 25th March 2023

To
The Evaluation Committee
Falchs Fund for Medical Research

Ref: Nomination of Siddharth Shanbhag for the Falchs Junior Prize for Young Researchers 2023

We hereby nominate Siddharth Shanbhag for the Falchs Junior Prize 2023. Shanbhag is currently a Postdoctoral Fellow at the Laboratory Clinic, Haukeland University Hospital (HUH) and a Researcher at the Department of Clinical Dentistry (IKO), Faculty of Medicine UiB.

Shanbhag (27.01.1985) graduated as a dentist in India and completed his postgraduate training in UK and Sweden, and his doctoral training at IKO, UiB (2016-2020). Shanbhag also completed the 'Qualification Program' for dentists to obtain a Norwegian dental license (2022).

Since 2015, Shanbhag's research has focused on novel strategies for regeneration of oro-facial tissues, particularly bone. Replacement of missing/lost teeth to restore patients' oral function and quality of life is an important aspect of modern dentistry. Very often, regeneration of the jaw bones is first needed to allow the safe and predictable replacement of teeth with dental implants. Current strategies for **bone regeneration** are largely based on synthetic biomaterials, which present several limitations. Shanbhag's research focuses on strategies to overcome the limitations of traditional biomaterials using adult stem cells and 'tissue engineering' based approaches. Patients requiring these treatments are mostly those with advanced stages of disease and/or in whom conventional treatments have failed; therefore, the **clinical and social impact** of this research is large. Shanbhag has performed multiple original, in-depth, and methodologically complex research works, documented by several high-impact peer-reviewed publications in top journals in the field. Shanbhag's research on bone regeneration can be divided into two categories as follows:

1. *Cell-based* approaches (doctoral research)

The PhD thesis titled *"Xeno-free 3D cultures of mesenchymal stromal cells for bone tissue engineering"* involved novel, multi-disciplinary, and translational studies to optimize constructs of mesenchymal stem cells (MSC) for bone regeneration. A variety of in-vitro and in-vivo methods were used to achieve the objectives, with the central focus being clinical relevance and translatability of findings. The choice of in-vitro methods was evidence-based, and multiple methods were used to confirm findings in a single experiment. For in-vivo studies, both 'ectopic' (skin implantation) and 'orthotopic' models (bone implantation) in immune-compromised animals were used to test *human* derived cells, to ensure **clinical relevance**.

A key aspect of the PhD thesis was the optimization of a 'xeno-free' supplement for ex-vivo stem cell expansion. Cell production for clinical applications requires the exclusion of animal-derived products and their replacement with 'humanized' or 'xeno-free' alternatives. Human platelet lysate (HPL) represents the optimal xeno-free source of growth factors for cost-effective cell production (*Shanbhag S, et al. Tissue Eng Part B Rev. 2017; 23:552*). Several aspects of HPL production were optimized during the PhD, resulting in a new product – **BergenLys™** (*Shanbhag et al. Stem Cell Res Ther. 2020;11:351*). In collaboration with HUH and Vestlandets Innovasjonsselskap (VIS), current activity is focused on transferring HPL production to the new *Ex Vivo Facility (EVF)* for cell production at HUH, to enable safe and effective production of stem cells for clinical trials in Bergen. This project has received funding from the Research Council of Norway (Milestone Project), reflecting the **innovation potential** of Shanbhag's work.

The thesis comprised of **six** original articles (all as first author), with **nine** additional contributions (six as first author). Importantly, several new collaborations (local, national, and international) were established during this time, which have been highly productive and are still ongoing. For his doctoral work, Shanbhag received the **Best PhD Thesis Award 2020** from the Faculty of Medicine UiB.

2. *Cell-free* approaches (postdoctoral research)

Despite the tremendous promise of cell therapy, several limitations exist with current strategies, for example, extremely high costs and stringent regulation by health authorities. Moreover, recent studies, including those from Shanbhag's thesis, have shown that MSC mainly act via paracrine secretions rather than direct engraftment in tissues. Therefore, in addition to his work on MSC, Shanbhag is leading an **international consortium** to develop new 'cell-free' strategies for bone regeneration based on MSC 'secretomes'.

Overall, this multi-disciplinary project aims to produce a safer, simpler, and more cost-effective alternative to cell transplantation. The strategy has been extensively tested in both in-vitro and in-vivo experimental models. Preliminary results have indicated superior outcomes of the cell-free approach in comparison with current cell-based (*Shanbhag S, et al. Cells. 2023;12:767*) and growth factor-based approaches (*Shanbhag S, et al. submitted manuscript*). A key aspect of this work has been the proteomic analysis of MSC secretomes based on state-of-the-art mass spectrometry and bioinformatic methods, in collaboration with the Proteomics Unit at UiB (PROBE). The project has received **major funding** from reputed agencies such as the International Association for Dental Research (IADR, USA), Osteology Foundation (Switzerland), and ITI Foundation (Switzerland), reflecting its **clinical and translational potential**.

Shanbhag has also been active in the international scientific community. In 2018, he was invited to lead a systematic review and meta-analysis for the prestigious *XV European Workshop on Periodontology*, a meeting of global experts organized by the European Federation of Periodontology. This paper (*Shanbhag S, et al. J Clin Periodontol. 2019;46 Suppl 21:162*) was used to draft **clinical guidelines** on the use of cell therapy for bone regeneration. Moreover, Shanbhag has presented at several national and international **scientific meetings**, including the EuroPerio Congress (Copenhagen), Global Bone Regeneration Symposium (Santiago) and the *Norsk Tannlegeforenings Landsmøte* (Lillestrøm). He has received several **awards** from leading organizations, such as the IADR's Aubrey Sheiham Award (2014), Nordic Hatton Award (2017), Karring-Nyman Award in Periodontal Research (2018), and the prestigious New Investigator Award in Oral Tissue Regeneration (2022).

Shanbhag is also involved in **teaching and supervision** at IKO at Masters, PhD, and Specialist levels. Currently, Shanbhag is supervising a Master's project to compare the proteomes of oral cells from healthy individuals vs. patients with periodontitis, a chronic inflammatory oral disease with systemic implications. The findings could provide new insights into disease mechanisms, biomarkers of severity, and cues for targeted therapy, thus having a significant clinical impact.

Since 2016, Shanbhag has established **new collaborations** with internationally renowned experts at HUH (Bloodbank, Prof. Einar K. Kristoffersen), NTNU (Dept. of Physics, Prof. Catharina Davies), University of Malmö (Dept. of Periodontology, Prof. Andreas Stavropoulos), University Complutense of Madrid (ETEP Research Group, Prof. Mariano Sanz) and University of Vienna (Dept. of Oral Biology, Prof. Reinhard Gruber), highlighting a strong **network building** capacity. Shanbhag was recently awarded a Helse Vest Overseas Fellowship (2023) to the Faculty of Odontology, University Complutense of Madrid, Spain.

Shanbhag is a motivated dentist and researcher and has become an active member both in local and well-established international research groups, contributing remarkably to the scientific environment. His scientific output together with multiple awards and honors in a relatively short period indicates his outstanding performance as a researcher and makes him a strong asset for IKO and UiB in the future. We therefore nominate Shanbhag for the Falchs Junior Prize 2023.

Sincerely,

Anne Isine Bolstad, professor
Section for Periodontology
IKO, UiB

Kamal Mustafa, professor
Leader, Centre for Translational Oral Research
IKO, UiB

Asgeir Bårdsen, professor
Leader, IKO
UiB

Einar K. Kristoffersen, professor
Leader, Dept. of Immunology and Transfusion Medicine, HUH and Dept. of Clinical Medicine, UiB

Curriculum vitae

PERSONAL INFORMATION

Family name, First name:	Shanbhag, Siddharth Vivek		
Date of birth:	27.01.1985	Sex:	Male
Nationality:	Norwegian		

HIGHER EDUCATION/OTHER TRAINING

	Subjects/degree	Name of institution, country
2023	Authorization, Dentistry	Norwegian Directorate of Health
2022	Qualification program, Dentistry	Department of Clinical Dentistry (IKO), Faculty of Medicine, University of Bergen (UiB)
2020	PhD, Tissue Engineering	IKO, Faculty of Medicine, UiB
2010	MSc (Master), Dentistry	Institute of Dentistry, Queen Mary University of London, UK
2008	BDS (Bachelor), Dentistry	SDM Dental College, Rajiv Gandhi University of Health Sciences, Dharwad, India

POSITIONS, CURRENT AND PREVIOUS

	Job title/name of employer
2021 -	Postdoctoral Fellow, Laboratory Clinic, Haukeland University Hospital
2021 -	Researcher, Centre for Translational Oral Research (TOR), IKO, UiB
2016-2020	PhD Research Fellow, IKO, UiB
2014-2016	Researcher (assoc.), Dept. of Periodontology, Faculty of Odontology, Malmö University, Malmö, Sweden
2012-2016	Dentist, Private Practice, Mumbai, India
2010-2012	Researcher, Centre for Oral Sciences, Institute of Dentistry, Queen Mary University of London, UK

PROJECT MANAGEMENT EXPERIENCE

	Role /project /topic /funding from /status
2023 -	PI, Stem Cell Secretomes for Peri-Implant Bone Regeneration, ITI Foundation (Switzerland), ongoing
2022 -	PI, Cell-free Therapies for Bone Regeneration, International Association for Dental Research (IADR, USA) and Osteology Foundation (Switzerland), ongoing
2021 -	Co-PI, Stem Cell Therapies for Clinical Trials in Bergen, Helse Vest (Norway)
2019-2021	PI, Stem Cell Secretomes for Bone Regeneration, Osteology Foundation (Switzerland), completed
2015-2018	Co-PI, Cell Cocultures for Vascularized Bone Tissue Engineering, ITI Foundation (Switzerland), completed

EXPERIENCE FROM RELEVANT RESEARCH & INNOVATION ACTIVITIES

	Project /type of R&I activity and R&I content /role and tasks /funding from /status
2019 -	**Functionalized biomaterials to enhance bone regeneration,** novel biomaterials functionalized with stem cell-conditioned media; preclinical testing in rodent and swine models, PI in an international consortium (Norway, Spain, Austria), funding: IADR (USA) and Osteology Foundation (Switzerland), ongoing
2017-2022	**BergenLys - a human platelet lysate supplement to enhance stem cell cultures,** new product to improve ex vivo stem cell expansion for regenerative applications, co-PI, in collaboration with Vestlandets Innovasjonsselskap (VIS) and Helse Bergen, funding: Helse Vest (Innovation) and Research Council of Norway (Milestone Project), completed

EXPERIENCE FROM NATIONAL/INTERNATIONAL COLLABORATION/NETWORKING

	Activity or project /tasks /framework and names of key partners (companies, institutions)
2021 -	**Functionalized biomaterials to enhance bone regeneration,** PI, international consortium: UiB (Prof. Kamal Mustafa), University Complutense of Madrid (Prof. Mariano Sanz) and Medical University of Vienna (Prof. Reinhard Gruber)
2020 -	**L-PRF for bone regeneration,** PI, preclinical and clinical efficacy-testing of leukocyte- and platelet-rich fibrin (L-PRF), BioHorizons Camlog GmBH
2018-2019	**XV European Workshop in Periodontology – Workshop on Bone Regeneration,** invited first author of a systematic review, European Federation of Periodontology (EFP) workshop to formulate consensus guidelines in the field of bone regeneration
2015-2020	**Cell-biomaterial interactions in inflammatory conditions,** co-PI, collaboration with Malmö University, Sweden (Prof. Andreas Stavropoulos)

AWARDS/HONORS

	Award
2023	Helse Vest Overseas Research Fellowship at University Complutense of Madrid, Spain
2022	IADR Osteology Foundation New Investigator Award in Oral Tissue Regeneration, USA
2022	International Team for Implantology (ITI) Research Grant
2022	Osteology Foundation Advanced Researcher Grant
2021	Best PhD Thesis Award 2020, Faculty of Medicine, UiB
2019	UiB Overseas Research Grant at Medical University of Vienna, Austria
2019	Osteology Foundation Young Researcher Grant
2019	Finalist, IADR Unilever Hatton Competition, London, UK
2018	IADR Karring-Nyman Sunstar Guidor Award in Periodontal Research
2017	Nordisk Odontologisk Förening (NOF) Hatton Award
2017	Meltzer Research Fund Award
2016	Nordic Young Scientist in Odontology Best Oral Presentation Award, Tuusula, Finland
2015	IADR Aubrey Sheiham Award for Distinguished Research

MEETINGS/CONFERENCE PRESENTATIONS

	Event / Invited speaker / Oral presentation / Poster presentation
2023	Oral Reconstruction Foundation Global Symposium, Rome, Italy - Invited Speaker
2023	Osteology Foundation International Symposium, Barcelona, Spain - Invited Speaker
2023	Norsk Peridontistforening Course on Peri-implant Diseases, Stavanger - Invited Speaker
2022	Norsk Tannlegeforening (NTF) Annual Meeting, Lillestrøm - Invited Speaker
2022	Workshop on Translational Oral Research, IKO, Bergen - Invited Speaker
2022	European Federation of Periodontology EuroPerio Congress, Copenhagen, Denmark - Oral
2021	Bone Regeneration Global Symposium, Santiago de Compostela, Spain - Invited Speaker
2019	Nordic Young Scientist Conference in Odontology, 5th meeting, Oslo - Oral
2019	Tissue Engineering Regenerative Medicine Society EU Congress, Rhodos, Greece - Poster
2018	IADR General Session, London, UK - Oral
2018	Bergen Stem Cell Consortium 3rd Annual Meeting, Bergen - Oral
2017	Tissue Engineering Regenerative Medicine Society World Congress, Kyoto, Japan - Poster
2017	IADR Continental European & Scandinavian divisions Meeting, Vienna, Austria - Oral
2016	Nordic Young Scientist Conference in Odontology, 4th meeting, Tuusula, Finland - Oral
2015	European Federation of Periodontology EuroPerio Congress, London, UK - Oral

TEACHING/SUPERVISION

2022 -	Master project (MAOD-ODONT, 2 students) at IKO, UiB
2022 -	Research Methods Course (ODO-FORSK) at IKO, UiB
2019 -	Future Medicine Course (ELMED303) at K2, UiB

PUBLICATIONS

1. **Shanbhag S,** Al-Sharabi N, Kampleitner C, Mohamed-Ahmed S, Tangl S, Kristoffersen EK, Mustafa K, Gruber R, Sanz M. The use of mesenchymal stromal cell secretome to enhance guided bone regeneration in comparison with leukocyte and platelet-rich fibrin. *(submitted)*
2. Al-Sharabi N, Mohamed-Ahmed S, **Shanbhag S,** Kampleitner C, Tangl S, Rana N, Gruber R, Mustafa K. Extracellular vesicles secreted by osteogenic-differentiated mesenchymal stem cells promote bone regeneration. *(submitted)*
3. Al-Sharabi N, Mohamed-Ahmed S, Kristoffersen EK, Gruber R, Mustafa K, Sanz M, **Shanbhag S.** Proteomic analysis of conditioned media from mesenchymal stromal cells and leukocyte and platelet-rich fibrin. *(submitted)*
4. **Shanbhag S,** Kampleitner C, Al-Sharabi N, Mohamed-Ahmed S, Apaza K, Tangl S, Rana N, Sanz M, Kristoffersen EK, Mustafa K, Gruber R. Functionalizing collagen membranes with MSC conditioned media promotes guided bone regeneration. *Cells.* **2023**; 12:767.
5. **Shanbhag S,** Rana N, Suliman S, Idris S, Mustafa K, Stavropoulos A. Influence of bone substitutes on mesenchymal stromal cell responses in an inflammatory microenvironment. *Int J Mol Sci.* **2023**; 24:438.
6. **Shanbhag S,** Al-Sharabi N, Mohamed-Ahmed S, Gruber R, Kristoffersen EK, Mustafa K. Brief communication: Effects of conditioned media from human platelet lysate cultured MSC on osteogenic cell differentiation in vitro. *Front Bioeng Biotechnol.* **2022**; 10:969275.
7. **Shanbhag S,** Kampleitner C, Al-Sharabi N, Mohamed-Ahmed S, Apaza K, Tangl S, Rana N, Sanz M, Kristoffersen EK, Mustafa K, Gruber R. O073: Cell conditioned media functionalized collagen membranes promote in vivo guided bone regeneration. *J Clin Periodontol.* **2022**; 49 Suppl 23:35.
8. Yamada S, **Shanbhag S,** Mustafa K. Scaffolds in periodontal regenerative treatment. *Dent Clin North Am.* **2022**; 66:111.
9. **Shanbhag S,** Kampleitner C, Mohamed-Ahmed S, Yassin MA, Dongre H, Costea DE, Tangl S, Stavropoulos A, Bolstad AI, Suliman S, Mustafa K. Ectopic bone tissue engineering in mice using human gingiva or bone marrow derived stromal cells in scaffold-hydrogel constructs. *Front Bioeng Biotechnol.* **2021**; 9:783468.
10. **Shanbhag S,** Suliman S, Mohamed-Ahmed S, Kampleitner C, Hassan MN, Heimel P, Dobsak T, Tangl S, Bolstad AI, Mustafa K. Bone regeneration in rat calvarial defects using dissociated or spheroid mesenchymal stromal cells in scaffold-hydrogel constructs. *Stem Cell Res Ther.* **2021**; 12:575.
11. Helgeland E, Mohamed-Ahmed S, **Shanbhag S,** Pedersen TO, Rosén A, Mustafa K, Rashad A. 3D printed gelatin-genipin scaffolds for temporomandibular joint cartilage regeneration. *Biomed Phys Eng Express.* **2021**; 7:5.
12. **Shanbhag S,** Rashad A, Nymark EH, Suliman S, de Lange Davies C, Stavropoulos A, Bolstad AI, Mustafa K. Spheroid coculture of human gingiva-derived progenitor cells with endothelial cells in modified platelet lysate hydrogels. *Front Bioeng Biotechnol.* **2021**; 9:739225.
13. **Shanbhag S,** Xeno-free three-dimensional culture of human mesenchymal stromal cells for bone tissue engineering (PhD thesis). Faculty of Medicine, *University of Bergen,* **2020**.
14. **Shanbhag S,** Mohamed-Ahmed S, Lunde THF, Suliman S, Bolstad AI, Hervig T, Mustafa K. Influence of platelet storage time on human platelet lysates and platelet lysate-expanded mesenchymal stromal cells for bone tissue engineering. *Stem Cell Res Ther.* **2020**; 11:351.
15. **Shanbhag S,** Suliman S, Bolstad AI, Stavropoulos A, Mustafa K. Xeno-free spheroids of human gingiva derived progenitor cells for bone tissue engineering. *Front Bioeng Biotechnol.* **2020**; 8:968.
16. Gjerde CG, **Shanbhag S,** Neppelberg E, Mustafa K, Gjengedal H. Patient experience following iliac crest-derived alveolar bone grafting and implant placement. *Int J Implant Dent.* **2020**; 6:4.
17. **Shanbhag S,** Suliman S, Pandis N, Stavropoulos A, Sanz M, Mustafa K. Cell therapy for orofacial bone regeneration: A systematic review and meta-analysis. *J Clin Periodontol.* **2019**; 46 Suppl 21:162.
18. **Shanbhag S,** Suliman S, Mustafa K. Secretome of 3-D and 2-D cultured MSCs in xeno-free conditions. *Eur Cell Mater. Meeting Abstracts* **2019**, Collection 3:1122.
19. Helgeland E, **Shanbhag S,** Pedersen TO, Mustafa K, Rosén A. Scaffold-based temporomandibular joint tissue regeneration in experimental animal models: a systematic review. *Tissue Eng Part B Rev.* **2018**; 24:300.

20. **Shanbhag S,** Mohamed-Ahmed S, Suliman S, Stavropoulos A, Bolstad AI, Mustafa K. Characterization of human gingiva- and pdl-derived progenitor cells in xeno-free conditions. *J Dent Res.* **2018**; 97(Spec Iss B):1840.
21. **Shanbhag S,** Pandis N, Mustafa K, Nyengaard JR, Stavropoulos A. Bone tissue engineering in oral peri-implant defects in preclinical in vivo research: A systematic review and meta-analysis. *J Tissue Eng Regen Med.* **2018**; 12:e336.
22. **Shanbhag S,** Stavropoulos A, Suliman S, Hervig T, Mustafa K. Efficacy of humanized mesenchymal stem cell cultures for bone tissue engineering: a systematic review with a focus on platelet derivatives. *Tissue Eng Part B Rev.* **2017**; 23:552.
23. **Shanbhag S,** Mohamed-Ahmed S, Lunde THF, Hervig T, Mustafa K. Human platelet-derivatives for clinical-grade expansion of mesenchymal stem cells from different tissue sources. *Eur Cell Mater. Meeting Abstracts* **2017**; Collection 2:P693.
24. **Shanbhag S,** Pandis N, Mustafa K, Nyengaard JR, Stavropoulos A. Cell cotransplantation strategies for vascularized craniofacial bone tissue engineering: a systematic review and meta-analysis of preclinical in vivo studies. *Tissue Eng Part B Rev.* **2017**; 23:101.
25. **Shanbhag S,** Pandis N, Mustafa K, Nyengaard JR, Stavropoulos A. Alveolar bone tissue engineering in critical-size defects of experimental animal models: a systematic review and meta-analysis. *J Tissue Eng Regen Med.* **2016**; 11:2935.
26. **Shanbhag S,** Shanbhag V, Stavropoulos A. Genomic analyses of early peri-implant bone healing in humans: a systematic review. *Int J Implant Dent.* **2015**; 1:5.
27. **Shanbhag S,** Shanbhag V. Clinical applications of cell-based approaches in alveolar bone augmentation: a systematic review. *Clin Implant Dent Relat Res.* **2015**; 17 Suppl 1:e17-34.
28. **Shanbhag S,** Shanbhag V, Stavropoulos A. Volume changes of maxillary sinus augmentations over time: a systematic review. *Int J Oral Maxillofac Implants* **2014**; 29:881-92.
29. **Shanbhag S,** Karnik P, Shirke P, Shanbhag V. Cone-beam computed tomographic analysis of sinus membrane thickness, ostium patency, and residual ridge heights in the posterior maxilla: implications for sinus floor elevation. *Clin Oral Implants Res*. **2014**; 25:755-60.
30. **Shanbhag S,** Karnik P, Shirke P, Shanbhag V. Association between periapical lesions and maxillary sinus mucosal thickening: a retrospective cone-beam computed tomographic study. *J Endod.* **2013**;39:853-7.
31. **Shanbhag S,** Dahiya M, Croucher R. The impact of periodontal therapy on oral health-related quality of life in adults: a systematic review. *J Clin Periodontol.* **2012**; 39:725-35.
32. Croucher R, **Shanbhag S,** Dahiya M, Kassim S, Csikar J. Smokeless tobacco cessation in South Asian communities: a multicentre prospective study. *Addiction* **2012**; 107 Suppl 2:45-52.
33. Croucher R, **Shanbhag S,** Dahiya M, Kassim S, McNeill A. Predictors of successful short-term tobacco cessation in UK resident female Bangladeshi tobacco chewers. *Addiction* **2012**; 107:1354-8.

Complete list of publications: https://www.ncbi.nlm.nih.gov/myncbi/1HeIarjn_jdk8/bibliography/public/

Falchs Junior Prize for Young Researchers 2023

Siddharth Shanbhag

Documented results of research (2016 - present)

Stem Cell Research & Therapy

The use of mesenchymal stromal cell secretome to enhance guided bone regeneration in comparison with leukocyte and platelet-rich fibrin

--Manuscript Draft--

Manuscript Number:	
Full Title:	The use of mesenchymal stromal cell secretome to enhance guided bone regeneration in comparison with leukocyte and platelet-rich fibrin
Article Type:	Research
Funding Information:	Osteology Foundation (YRG 18-152) — Dr. Siddharth Shanbhag Helse Vest (F-12124) — Dr. Siddharth Shanbhag Trond Mohn stiftelse (BFS2018TMT10) — Prof Kamal Mustafa Norges Forskningsråd (273551, 302043) — Prof Kamal Mustafa
Abstract:	Background: Secretomes of mesenchymal stromal cells (MSC) are emerging as a novel strategy for growth factor delivery and a promising alternative to cell therapies for tissue regeneration. The objective of this study was to compare the efficacy of adjunctive use of conditioned media of human MSC (MSC-CM) with collagen barrier membranes (MEM) for guided bone regeneration (GBR) vs. adjunctive use of conditioned media of leukocyte- and platelet-rich fibrin (PRF-CM). Methods: MSC-CM and PRF-CM were prepared from three human donors each and subjected to quantitative proteomic analysis using mass spectrometry and multiplex immunoassay. Early responses (48 h) of MSC to MSC-CM and PRF-CM were studied via gene expression analysis. Next, MEM functionalized with pooled MSC-CM or PRF-CM were applied on critical-size rat calvaria defects and new bone formation was analyzed via micro-computed tomography (µCT, 2 and 4 weeks) and histology (4 weeks). Results: Proteomic analysis revealed several proteins representing biological processes related to bone formation in both MSC-CM and PRF-CM, although more differentially expressed proteins ($p < 0.05$) were observed in MSC-CM. Similar trends for differential expression of a subset of proteins related to bone remodeling were observed in the multiplex assay. More bone-related genes were upregulated ($p < 0.05$) in MSC exposed to MSC-CM vs. PRF-CM. In calvaria defects, µCT revealed greater bone coverage in the MSC-CM group after 2 and 4 weeks ($p < 0.05$). Histologically, both groups showed a combination of regular new bone and ‘hybrid’ new bone, which was formed within the membrane compartment and characterized by incorporation of mineralized collagen fibers. Greater hybrid bone formation occurred in the MSC-CM group ($p < 0.05$), while total new bone area was similar between groups. Conclusion: Based on the proteomic analysis and in vivo investigation, MSC-CM was superior to PRF-CM when functionalizing MEM to enhance bone regeneration and represents a promising new strategy for GBR.
Corresponding Author:	Siddharth Shanbhag Universitetet i Bergen NORWAY
Corresponding Author E-Mail:	siddharth.shanbhag@uib.no
Corresponding Author Secondary Information:	
Corresponding Author's Institution:	Universitetet i Bergen
Corresponding Author's Secondary Institution:	
First Author:	Siddharth Shanbhag
First Author Secondary Information:	

Powered by Editorial Manager® and ProduXion Manager® from Aries Systems Corporation

Order of Authors:	Siddharth Shanbhag
	Niyaz Al-Sharabi
	Carina Kampleitner
	Samih Mohamed-Ahmed
	Einar K Kristoffersen
	Stefan Tangl
	Kamal Mustafa
	Reinhard Gruber
	Mariano Sanz
Order of Authors Secondary Information:	
Additional Information:	
Question	**Response**
Is this study a clinical trial?<hr>A clinical trial is defined by the World Health Organisation as 'any research study that prospectively assigns human participants or groups of humans to one or more health-related interventions to evaluate the effects on health outcomes'.	No

Manuscript
Click here to access/download;Manuscript;PRF CM draft_SCRT2.docx
Click here to view linked References

The use of mesenchymal stromal cell secretome to enhance guided bone regeneration in comparison with leukocyte and platelet-rich fibrin

Siddharth Shanbhag[1,2]*, Niyaz Al-Sharabi[2], Carina Kampleitner[3,4,5], Samih Mohamed-Ahmed[2], Einar K Kristoffersen[1], Stefan Tangl[3,5], Kamal Mustafa[2], Reinhard Gruber[5,6,7 T] and Mariano Sanz[8 T]

[1] Department of Immunology and Transfusion Medicine, Haukeland University Hospital, Bergen, Norway

[2] Center for Translational Oral Research (TOR), Department of Clinical Dentistry, Faculty of Medicine, University of Bergen, Bergen, Norway

[3] Karl Donath Laboratory for Hard Tissue and Biomaterial Research, Division of Oral Surgery, University Clinic of Dentistry, Medical University of Vienna, Vienna, Austria

[4] Ludwig Boltzmann Institute for Experimental and Clinical Traumatology, The Research Center in Cooperation with AUVA, Vienna, Austria

[5] Austrian Cluster for Tissue Regeneration, Vienna, Austria

[6] Department of Oral Biology, University Clinic of Dentistry, Medical University of Vienna, Vienna, Austria

[7] Department of Periodontology, School of Dental Medicine, University of Bern, Bern, Switzerland

[8] ETEP Research Group, Faculty of Odontology, University Complutense of Madrid, Madrid, Spain

[T] *Equal contribution and shared senior authors*

* Corresponding author:
Siddharth Shanbhag
Center for Translational Oral Research (TOR)
Department of Clinical Dentistry, University of Bergen
Årstadveien 19, 5009 Bergen, Norway
+47 55 58 60 59
siddharth.shanbhag@uib.no

Abstract

Background: Secretomes of mesenchymal stromal cells (MSC) are emerging as a novel strategy for growth factor delivery and a promising alternative to cell therapies for tissue regeneration. The objective of this study was to compare the efficacy of adjunctive use of conditioned media of human MSC (MSC-CM) with collagen barrier membranes (MEM) for guided bone regeneration (GBR) vs. adjunctive use of conditioned media of leukocyte- and platelet-rich fibrin (PRF-CM).

Methods: MSC-CM and PRF-CM were prepared from three human donors each and subjected to quantitative proteomic analysis using mass spectrometry and multiplex immunoassay. Early responses (48 h) of MSC to MSC-CM and PRF-CM were studied via gene expression analysis. Next, MEM functionalized with pooled MSC-CM or PRF-CM were applied on critical-size rat calvaria defects and new bone formation was analyzed via micro-computed tomography (μCT, 2 and 4 weeks) and histology (4 weeks).

Results: Proteomic analysis revealed several proteins representing biological processes related to bone formation in both MSC-CM and PRF-CM, although more differentially expressed proteins ($p < 0.05$) were observed in MSC-CM. Similar trends for differential expression of a subset of proteins related to bone remodeling were observed in the multiplex assay. More bone-related genes were upregulated ($p < 0.05$) in MSC exposed to MSC-CM vs. PRF-CM. In calvaria defects, μCT revealed greater bone coverage in the MSC-CM group after 2 and 4 weeks ($p < 0.05$). Histologically, both groups showed a combination of regular new bone and 'hybrid' new bone, which was formed within the membrane compartment and characterized by incorporation of mineralized collagen fibers. Greater hybrid bone formation occurred in the MSC-CM group ($p < 0.05$), while total new bone area was similar between groups.

Conclusion: Based on the proteomic analysis and *in vivo* investigation, MSC-CM was superior to PRF-CM when functionalizing MEM to enhance bone regeneration and represents a promising new strategy for GBR.

Key words: mesenchymal stromal cells; conditioned media; guided bone regeneration; bone tissue engineering; regenerative medicine

1. Background

Presence of bone defects in the edentulous alveolar ridge usually jeopardizes the ability of placing dental implants in the adequate position to rehabilitate the lost dentition. To overcome this limitation different bone regenerative interventions have been tested both staged and simultaneously with dental implant placement (1). Among these regenerative therapies the most widely used is guided bone regeneration (GBR) based on filling the bone defect with a bone replacement graft and covering it with a barrier membrane (2-4).

Autologous bone has been the gold standard bone replacement graft material since it behaves as a true bioactive scaffold not only filling the defect and maintaining the reconstructed space during healing, but its osteogenic (cells), osteoinductive (signaling molecules) and osteoconductive (scaffold) properties, promote bone regeneration and defect resolution. However, bone harvesting, especially for large defects, is associated with patient morbidity and risks for clinical complications (5). Moreover, due to the rapid resorption rate of autologous bone, other natural bone biomaterials as xenogeneic and allogenic bone substitutes have been gradually replacing its clinical use, mainly when used with barrier membranes and other bioactive substances.

Bioabsorbable collagen membranes (MEM) are frequently used in GBR, either applied alone or combined with bone substitute materials (6). These membranes primarily act as *passive* occlusive barriers limiting epithelial cell invasion and promoting osseous cell population (homing). In addition to their barrier effect, MEM can adsorb and release signaling molecules with the potential of becoming bioactive mediators of GBR (7-11). Recent attempts to functionalize MEM with growth factors (GF) have demonstrated enhanced GBR *in vivo* (9, 10).

The use of GF to enhance bone regeneration has been extensively investigated as an alternative to autologous bone grafting, both using recombinant human GF [e.g., bone morphogenetic protein-2 (BMP2), platelet-derived growth factor-B (PDGFB), etc.] or tissue fractions containing autologous GF, mainly through the use of autologous platelet concentrates of the first- [platelet-rich plasma (PRP)] and second-generation [platelet-rich fibrin (PRF) and its variants] (12, 13). Recently, leukocyte- and platelet-rich fibrin (L-PRF) has received widespread interest due to its relative ease of preparation, high concentration and sustained release of GF, and promising clinical outcomes (14-16). L-PRF matrices can be prepared via ‘chair-side’ centrifugation of whole blood without any additives or anticoagulants (17), resulting in a fibrin mesh with entrapped platelets, leucocytes, monocytes

and progenitor cells (18, 19). Moreover, the secretome of L-PRF matrices also contains a complex mixture of GF and other bioactive molecules (20-22), which drive wound healing (23-25). The biological activity of L-PRF and its conditioned media (PRF-CM), demonstrated *in vitro* in terms of GF-release and cellular activity [see review (25)], forms the basis for its clinical efficacy [see review (26)].

In recent years, tissue engineering approaches using GF in combination with cells and biomaterial scaffolds have been proposed as another alternative to autologous bone grafting, to further enhance regenerative efficacy (27). Bone tissue engineering strategies combine adult mesenchymal stromal cells (MSC) – usually from the bone marrow (BMSC), with biomaterial scaffolds and/or GF, to replicate the properties of autogenous bone grafts (28, 29). However, the need for expensive *ex vivo* laboratories and stringent regulation of MSC as Advanced Therapeutic Medicinal Products (ATMP) by health authorities limits the widespread application of cell therapies (27). Recent preclinical data, however, suggest alternative mechanisms of MSC bioactivity based on paracrine secretions and immune modulation, instead of engraftment and direct replacement of injured tissues (30, 31), which has led to emergence of so-called 'cell-free' strategies (32). These strategies are based on the secretion of a wide range of bioactive factors by MSC, including soluble proteins (GF, cytokines, chemokines), lipids, nucleic acids, and extracellular vesicles (31, 33, 34) involved in the wound healing process (35). These data provide the biological basis for utilizing the secretome or conditioned media (CM) of MSC for tissue regeneration (36, 37).

We have recently reported a method to functionalize MEM with MSC-CM and demonstrated its superior efficacy for bone regeneration compared to MEM alone and MEM with MSC (38). There is, however, lack of evidence on whether MSC-CM may have superior biological activity than currently used GF-based strategies, e.g., L-PRF, for bone regeneration. It was therefore the objective of the present study to compare MSC-CM vs. CM from L-PRF matrices (PRF-CM), firstly, based on their proteomic profiles, and, secondly, based on their respective *in vivo* efficacy to enhance GBR in critical-size rat calvaria defects using a MEM functionalization model.

2. Materials and methods

2.1. Cell culture

BMSC isolation and culture was performed following ethical approval (Regional Committees for Medical Research Ethics in Norway, 2013-1248/REK-sør-øst and 2016-1266/REK-nord)

and informed consent, as previously described (39). Briefly, bone marrow specimens were obtained following parental consent from healthy donors (2 females and 3 males; 8–10 years) undergoing reconstructive surgery at the Department of Plastic Surgery, Haukeland University Hospital, Norway. BMSC were cultured using sterile filtered growth media (GM) comprising of Dulbecco's Modified Eagle's medium (DMEM, Invitrogen, Carlsbad, CA, USA) supplemented with 5% (v/v) pooled human platelet lysate (Bergenlys, Bergen, Norway), 1% (v/v) penicillin/streptomycin (GE Healthcare, South Logan, UT, USA) and 1 IU/mL heparin (Leo Pharma AS, Lysaker, Norway) under standard incubation conditions of 37 °C and 5% CO_2 (39). Passage 1 (p1) and 2 (p2) BMSC were characterized based on immunophenotype and multi-lineage differentiation potential as previously reported (39). Three BMSC donors were used for MSC-CM preparation and the two other BMSC donors were used for cell culture experiments. Cell growth and morphology were regularly monitored under an inverted light microscope (Nikon Eclipse TS100, Tokyo, Japan).

2.2. Preparation of MSC-CM

MSC-CM was prepared from BMSC of three donors as previously described (40). Briefly, p1 and p2 BMSC were expanded in GM until 70-80% confluency under standard incubation. At this point, cells were washed three times with phosphate-buffered saline (PBS; Invitrogen) and then cultured in plain DMEM (without HPL or antibiotics) for another 48 h. After 48 h, the supernatant media (MSC-CM) from p1 and p2 BMSC were collected and pooled for each of the three donors. For the *in vivo* study, MSC-CM from the three donors were pooled (pooled MSC-CM), to minimize inter-donor variation. The individual donor and pooled MSC-CM were centrifuged (4000× *g*, 10 min) to remove any debris, aliquoted and stored at –80° C until further use.

2.3. Preparation of L-PRF and PRF-CM

L-PRF was prepared according to published protocols (21). Following local approval (Haukeland University Hospital Bloodbank, Bergen, Norway; AIT-69993) and informed consent, whole blood samples were obtained from healthy volunteer donors (3 women and 2 men; 23-46 years). Three 10 mL glass tubes (A-PRF tubes, Process for PRF, Nice, France) of whole blood were collected per donor via venipuncture and immediately centrifuged (Intra-Spin, BioHorizons, Birmingham, AL, USA) using the recommended settings, i.e., 408× *g* (RCF_{clot}) and 653× *g* (RCF_{max}) for 12 min at RT (21). The resulting fibrin clots were gently

compressed using the Xpression kit (BioHorizons) for 5 min under gravity pressure to produce the L-PRF membranes.

L-PRF membranes from three donors (three membranes per donor) were each placed in 5 mL supplement-free DMEM under standard incubation with intermittent shaking for 4 h, to remove most of the dead cells and plasma proteins. Next, the membranes were washed three times with PBS (Invitrogen), placed in 6-well plates and cultured in supplement-free DMEM for 72 h (21, 22). After 72 h, the supernatant media (PRF-CM) were collected and pooled for each of the three donors. Additionally, PRF-CM from the three donors were also pooled to produce pooled PRF-CM for use in the *in vivo* study. The individual donor and pooled PRF-CM were centrifuged (4000× *g*, 10 min) to remove any debris, aliquoted and stored at –80° C until further use.

2.4.CM ultrafiltration

Individual donor and pooled MSC-CM and PRF-CM were concentrated using Amicon Ultra-15 3 kDa centrifugal filter devices (Merck Millipore, Billerica, MA, USA) following the manufacturer's protocol. Briefly, after PBS equilibration, MSC-CM and PRF-CM were centrifuged in the Ultra-15 tubes at 4000× *g* for 30 min at 4° C, followed by buffer exchange with PBS and re-centrifugation at 4000× *g* for 30 min at 4° C. The corresponding concentrated media (~30-fold) were collected, aliquoted and stored at –80° C or used for MEM functionalization/lyophilization. Prior to freezing, the media were supplemented with mannitol (Sigma Aldrich) at a final concentration of 0.5% (v/v) to enhance cryo-preservation (32, 41). Individual donor MSC-CM and PRF-CM were used for proteomic analysis, while pooled MSC-CM and PRF-CM were used for MEM functionalization.

2.5. Liquid chromatography with tandem mass spectrometry (LC-MS/MS)

The proteomic profiles of individual donor MSC-CM (n=3 donors) and PRF-CM (n=3 donors) were analyzed using LC-MS/MS (42). Briefly, total protein concentrations of MSC-CM and PRF-CM were measured using bicinchoninic acid assay (Pierce BCA Kit, Thermo Fisher) and 10 µg protein was processed to obtain tryptic peptides. About 0.5 µg protein as tryptic peptides dissolved in 2% acetonitrile and 0.5% formic acid, was injected into an Ultimate 3000 RSLC system connected online to a Exploris 480 mass spectrometer equipped with EASY-spray nano-electrospray ion source (all from Thermo Scientific, Sunnyvale, CA, USA). Additional details of LC-MS/MS are reported in the **Supplementary methods**.

2.6. Bioinformatic analysis

For purposes of the present study, the bioinformatic analysis was limited to proteins relevant for bone formation. First, the LC-MS/MS raw files were searched using Proteome Discoverer software (version 2.5.0.400; Thermo Scientific). Perseus software (version 2.3.0.1; Max Planck Institute for Biochemistry, Martinsread, Germany) was used to process the dataset. The distributions of proteins in each CM group were determined using an online Venn diagram software (https://bioinformatics.psb.ugent.be/webtools/Venn/). Precise quantification of proteins was based detection in at least two donors in each group (43). Next, differentially expressed proteins (DEPs) in each group were identified using the Student's t-test and a Benjamini-Hochberg false discovery rate (FDR) < 0.05 in Perseus. Based on the human genome (Homo sapiens) as reference, relevant gene ontology (GO) terms for biological process related to bone formation were retrieved from the QuickGO database (https://www.ebi.ac.uk/QuickGO/, EMBL-EMI, Cambridge, UK, accessed on 14th November 2022), and compared to the DEPs in each group (42). A list of bone related DEPs is presented in **Supplementary Table S1.**

2.7. Multiplex immunoassay

The Quantibody Human Bone Metabolism Array Q1 (RayBiotech Inc., Norcross, GA, USA) was used for analysis of bone related cytokines (**Supplementary Table S2**) according to the manufacturer's protocol. This array is based on the sandwich enzyme-linked immunosorbent assay (ELISA) technology, and each antibody is spotted in quadruplicate. Array hybridization was performed using individual donor MSC-CM (n=3 donors) and PRF-CM (n=3 donors) (0.15-0.5 mg/mL of total protein) and standard cytokines. Array scanning was performed using a laser scanner (GenePix 4000B, Axon Instruments, San Jose, CA, USA) at different photomultiplier tube gains. Data extraction was performed using the GenePix Pro software ver. 5.0 (Axon Instruments). Concentrations of candidate proteins were calculated based on linear standard curves and normalized to the corresponding total protein concentrations.

2.8. MEM functionalization and bioassay

MEM were functionalized using pooled MSC-CM or pooled PRF-CM for the *in vivo* study. A bi-layered, non-cross-linked MEM (25 mm × 25 mm; Bio- Gide®, Geistlich Pharma, Wolhusen, Switzerland) was used in this study. MEM were cut using sterile scissors into smaller pieces (7 mm × 6 mm) and incubated with pooled MSC-CM or PRF-CM at 37° C for 1 h (8). After 1 h, the supernatants were aspirated, and all MEM were stored overnight in a –

80° C freezer for subsequent lyophilization. Lyophilization has been shown to preserve the biological activity of GF and, when used to functionalize biomaterials, has been shown to enhance *in vivo* release and bone regeneration (44). Lyophilization was performed overnight in a FreeZone™ freeze dryer (Labconco, Kansas, MO, USA) at 0.014 mBar pressure and at –51° C. The lyophilized MEM/MSC-CM and MEM/PRF-CM were stored at 4° C until use in experiments (up to 24 h).

As a bioassay, the effects of pooled MSC-CM and PRF-CM (alone and after MEM functionalization) were tested on human BMSC via quantitative real-time polymerase chain reaction (qPCR) using TaqMan® real-time PCR assays (Thermo Scientific), as previously described (45). Primary BMSC (different from those used for CM preparation) were exposed to GM, MSC-CM and PRF-CM in monolayer culture, and on MEM functionalized with MSC-CM and PRF-CM for 48 h. Expressions of osteogenesis-related genes runt-related transcription factor 2 (RUNX2), bone morphogenetic protein 2 (BMP2), collagen type 1A (COLIA), osteopontin (OPN/SPP1) and osteocalcin (BGLAP/OCN) (**Supplementary Table S3**) were assessed via quantitative real-time polymerase chain reaction (qPCR) using TaqMan® real-time PCR assays (Thermo Fisher, Carlsbad, CA, USA), as previously described (45). Data were normalized to the reference gene glyceraldehyde 3-phosphate dehydrogenase (GAPDH) and analyzed by the ΔΔCt method. Results are presented as fold changes in the MSC-CM and PRF-CM groups relative to the control group.

2.9. Calvarial defect model

Animal experiments were approved by the Norwegian Animal Research Authority (Mattilsynet; FOTS-17443) and performed in accordance with Directive 2010/63/EU and the ARRIVE guidelines (46). Nine male Lewis rats (LEW/OrlRj, Janvier Labs, Le Genest-Saint-Isle, France), 7-weeks-old and weighing 200-350 g were housed in stable conditions (22 ± 2 °C) with a 12 h dark/light cycle and *ad libitum* access to food and water. Surgeries were performed as previously described (47). Briefly, two full thickness calvarial defects (5 mm Φ; one in each parietal bone) were created per animal under general anesthesia. The experimental treatments, i.e., MEM/MSC-CM and MEM/PRF-CM, were then randomly applied to the defects (n=9 per group). In additional animals, native MEM (non-functionalized) were applied on similar defects; these data are part of another study and will be reported separately. MEM were fixed to the calvaria using 3-5 µL of tissue adhesive (Histoacryl®; B. Braun, Tuttingen, Germany) (48, 49). Treatment allocation was adapted such

that each animal received both treatments. After 2 weeks, an *in vivo* micro-computed tomography (μCT) scan was performed, and after 4 weeks, the animals were euthanized with an overdose of CO_2. The primary outcome was new bone formation after 2 (*in vivo* μCT) and 4 weeks (*ex vivo* μCT, histology). For all handling/analyses, the animals/specimens were identified by numbers to facilitate blinding of operators to treatment groups.

2.10. μCT analysis

To track early bone formation, *in vivo* μCT scans of the animals were obtained at 2 weeks using a small-animal CT scanner and Mediso workstation (both from nanoScan, Mediso, Budapest, Hungary) with voxel size of 40 μm, energy 70 kV, exposure time 300 ms, projections 720, and 1:1 binning. After euthanasia at 4 weeks, the calvaria were harvested, fixed in 4% paraformaldehyde, and scanned again using a SCANCO 50 μCT scanner (SCANCO Medical AG, Bruttisellen, Switzerland) at 90 kV and 200 μA with an isotropic resolution of 20 μm. Scans were reconstructed using Amira software (Thermo Scientific) and analyzed using ImageJ software (NIH, USA) using custom defined rulesets (47). The percentages of bone coverage and new bone volume relative to total defect volume (BV/TV%) were calculated.

2.11. Histology and histomorphometry

Based on μCT scanning, selected calvaria specimens were processed for undecalcified histology. Specimens were dehydrated in ascending grades of alcohol and embedded in light-curing resin (Technovit 7200 + 1% benzoyl peroxide, Kulzer & Co., Wehrheim, Germany). The embedded specimens were re-scanned (μCT) and central defect regions were visualized by applying a slice simulating the planned histological section, i.e., in the geometric centre of the defect, parallel to the sagittal suture and perpendicular to the parietal bone (47). Blocks were further processed using EXAKT cutting and grinding equipment (EXAKT Apparatebau, Norderstedt, Germany). Standardized thin-ground sections (~100 μm) were prepared in the centre of each defect and stained with Levai-Laczko dye (Morphisto GmbH, Frankfurt, Germany). In this staining, mature bone appears light pink, woven bone dark pink and soft tissues (including collagen) dark blue. The sections were scanned using an Olympus BX61VS digital virtual microscopy system (DotSlide 2.4, Olympus, Tokyo, Japan) with a 20× objective resulting in a resolution of 0.32 μm per pixel. For the histomorphometric analysis (50), using Photoshop software (version 2022; Adobe, San Jose, CA, USA), two regions of interest (ROI) were defined for each sample based on the position of the

membrane in relation to the defect: a *central defect* region and a *defect edge* or 'side' region, i.e., the area adjacent to the central defect on both sides (**Supplementary figure S1**). In both ROIs, the respective areas of new bone without embedded MEM fibers (hereafter termed 'new bone'), new bone with embedded MEM fibers (hereafter termed 'hybrid bone'), total new bone (sum of new bone and hybrid bone), mineralized MEM fibers, residual MEM (non-mineralized MEM fibers) and soft tissues were measured, and corresponding percentages were calculated as a ratio of the ROI area.

2.12. Statistical analysis

Statistical analysis was performed using the Prism 9 software (GraphPad Software, San Diego, CA, USA). Data are presented as means (± SD and/or range), unless specified. Analyses of gene expression data are based on delta-CT values and results are presented as relative (log/non-linear) fold changes using scatter plots. Normality testing was performed via the Shapiro-Wilk test. An independent samples t-test with a 0.05 significance level was applied for the μCT and histomorphometric analyses.

3. Results

3.1. Biological processes related to bone formation were enriched in MSC-CM

Proteomic analysis revealed a total of 2925 and 2500 proteins in MSC-CM (n=3 donors) and PRF-CM (n=3 donors), respectively. Both groups showed considerable inter-donor variation in the total number of proteins; this variation was relatively greater in PRF-CM (**Figure 1A**). After a filtration step based on detection of proteins in at least two donors in each group (43), 1983 common proteins were detected in MSC-CM and PRF-CM (**Figure 1B**); a majority (65%) of these proteins were detected in all three donors in each CM-group. From the common proteins, statistical analysis revealed 727 DEPs in MSC-CM ($p < 0.05$) and 190 DEPs in PRF-CM ($p < 0.05$).

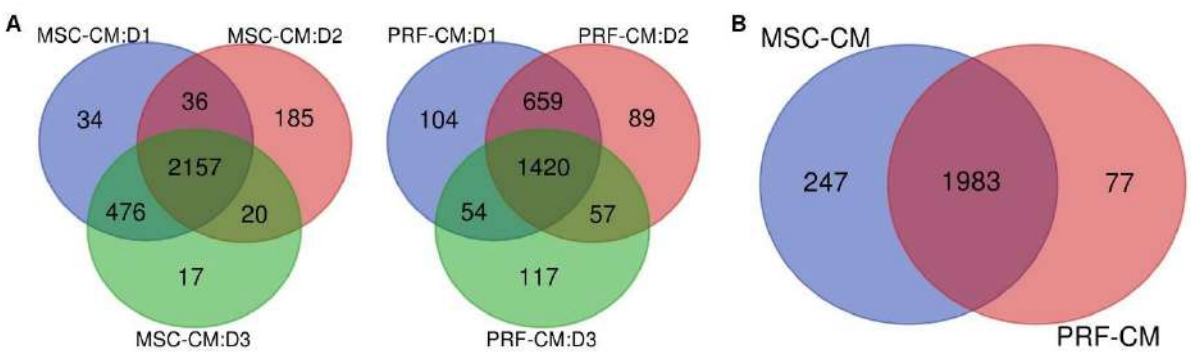

Figure 1: Proteomic analysis. (A) Venn diagrams showing total numbers of common and exclusively identified proteins in MSC-CM and PRF-CM each from three individual donors (D1-3; Note: MSC and L-PRF were obtained from different donor-groups). (B) Venn diagram showing numbers of common and exclusively identified proteins in MSC-CM and PRF-CM after filtration.

Among the classical GF, transforming growth factor beta-1 (TGFβ1), TGFβ2, BMP1, PDGFB, vascular endothelial growth factor-C (VEGFC), insulin-like growth factor (IGF), epidermal growth factor receptor (EGFR), stem cell factor (SCF/KITLG), stem cell growth factor (SCGF/CLECL11A), and colony stimulating factor-1 (CSF1) were identified. Additionally, several key proteins related to angiogenesis [von Willebrand factor (VWF), vascular cell adhesion molecule-1 (VCAM1), platelet endothelial cell adhesion molecule-1 (PECAM1), chemokine ligand-2 (CCL2/MCP1), etc.], extracellular matrix (ECM) [periostin (POSTN), osteonectin (ON/SPARC), connective tissue growth factor (CTGF), collagen-I (COL1A1/2) and -V (COL5A1/2), etc.] and bone remodeling [osteoprotegerin (OPG/TNFRSF11B), osteoclast stimulating factor-1 (OSTF1), matrix metalloproteinases (MMPs), tissue inhibitors of metalloproteinases (TIMPs), etc.] were differentially expressed in MSC-CM and PRF-CM. A greater subset of bone related proteins was upregulated in MSC-CM vs. PRF-CM (77 vs. 15 proteins), i.e., proteins within each GO subset of selected biological processes relevant for bone formation (**Table 1**). Among these were ECM organization (27 vs. 3 proteins), BMP signaling pathway (4 vs. 0 proteins), regulation of osteoblast differentiation (5 vs. 2 proteins), bone mineralization (6 vs. 0 proteins), ossification (15 vs. 2 proteins), Wnt signaling pathway (5 vs. 1 proteins), and angiogenesis (29 vs. 7 proteins).

Table 1: Summary of differentially expressed proteins (DEPs) in MSC-CM and PRF-CM representing selected biological processes related to bone formation

Upregulated in MSC-CM (77)	Upregulated in PRF-CM (15)
GO:0030198 Extracellular matrix organization	
27 proteins: MMP2, MMP13, COL1A1, TNFRSF11B, PXDN, B4GALT1, NDNF, COL5A2, ABI3BP, MMP1, ADAMTS12, COL4A2, ECM2, MMP3, POSTN, CCDC80, COL14A1, RECK, SMOC1(SPARC)*, OLFML2B, COL4A1, COL5A1, COL11A1, COL8A2, TGFBI, ADAMTSL1, COL1A2	3 proteins: MMP8, MMP9, ADAMTSL4
GO:0030509 BMP signaling pathway	
4 proteins: TGFB2, EXT1, COMP, TWSG1	
GO:0030513 Regulation of BMP signaling pathway (positive regulation)	

	2 proteins: NUMA1, TWSG1	
GO:0045667/9 Regulation of osteoblast differentiation (positive regulation)		
	5 proteins: FERMT2, FBN2, SMOC1(SPARC)*, CTNNB1, CTHRC1	2 proteins: IL6ST, LTF
GO:0060349 Bone morphogenesis		
	4 proteins: MMP13, EXT1, COMP, GLG1	LTF
GO:0030282 Bone mineralization		
	6 proteins: MMP13, MINPP1, COMP, SBDS, ENPP1, COL1A2	
GO:0030500/1 Regulation of bone mineralization (positive regulation)		
	4 proteins: FBN2, COMP, ENPP1, ISG15	
GO:0001503 Ossification		
	15 proteins: EXT1, EXT2, COL1A1, EGFR, OSTF1, CSF1, MINPP1, LRRC17, COMP, BMP1, COL5A2, COL11A1, CDH11, TWSG1, ADAMTS12	2 proteins: LTF, MMP9
GO:0030278/ 0045778 Regulation of ossification (positive regulation)		
	3 proteins: TGFB2, CSF1, MAPK14	
GO:0045670 Regulation of osteoclast differentiation (positive and negative regulation)		
	6 proteins: CSF1, TNFRSF11B, LRRC17, TNFAIP6, CTNNB1, FBN1	LTF
GO:0016055 Wnt signaling pathway		
	5 proteins: PTK7, CTNNB1, DAB2, TAX1BP3, RECK	TGFB1I1
GO:0030111 Regulation of Wnt signaling pathway		
	PPP2CA	
GO:0007219 Notch signaling pathway		
	2 proteins: GOT1, ADAM17	KMT2A
GO:0008593 Regulation of Notch signaling pathway		
	3 proteins: TGFB2, POSTN, ROBO1	3 proteins: IL6ST, TSPAN14, PDCD10
GO:0001525 Angiogenesis		
	29 proteins: MMP2, CSPG4, NRP1, PXDN, NRP2, ERAP1, NDNF, MAPK14, VEGFC, ITGAV, THY1, CCL2, COL4A2, FAP, CLIC4, SRPX2, GLUL, AIMP1, MYDGF, NCL, COL4A1, SERPINE1, VCAM1, CCBE1, CALD1, COL8A2, ADAM15, TGFBI, HSPG2	7 proteins: HRG, CXCL8, VWF, PDCD10, PDCD6, PECAM1, ITGA2B

GO, gene ontology subset. *SMOC1 is a protein related to SPARC (osteonectin), which was also detected in MSC-CM. A complete list of gene names is provided in Supplementary Table S1.

The concentrations of selected cytokines involved in bone remodeling, were further determined using a multiplex immunoassay. On average, MMP2, MMP13 and CCL2/MCP1 were significantly greater in MSC-CM, while MMP9 and interleukin-8 (IL8/CXCL8) were greater in PRF-CM (**Figure 2**), which was consistent with the proteomic analysis.

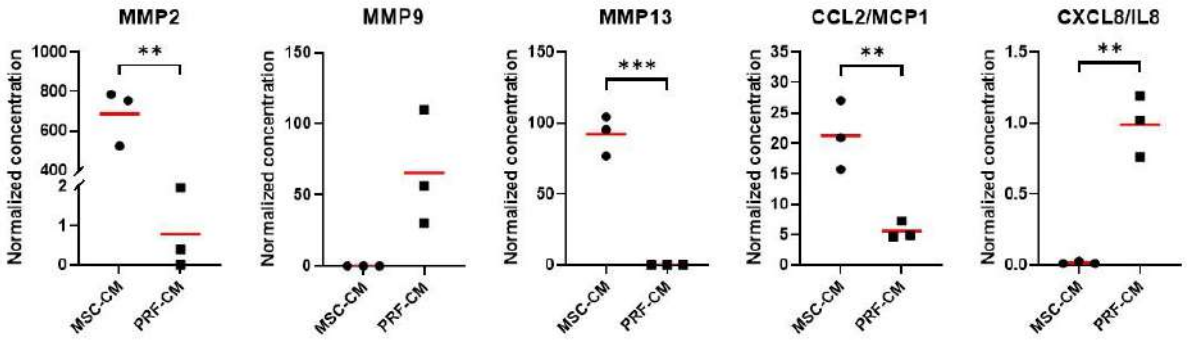

Figure 2: Multiplex immunoassay. Normalized concentrations (pg cytokine/µg total protein) of cytokines detected in MSC-CM and PRF-CM using a human bone metabolism array (Supplementary Table S2). Data represent means of 3 donors (each data point represents the average of 4 technical replicates). ** $p < 0.01$, *** $p < 0.001$.

We have previously reported the pro-osteogenic effects of MSC-CM on human BMSC (40). Consistently, in the present study, more osteogenesis related genes, namely RUNX2, COL1A2, SPP1/OPN and BGLAP/OCN, were upregulated in BMSC exposed to MSC-CM vs. PRF-CM after 48 h in monolayer culture (**Figure 3**). As a bioassay for MEM functionalization, gene expression was also evaluated in BMSC seeded on MEM/MSC-CM and MEM/PRF-CM, although cell culture on native MEM itself (regardless of functionalization) resulted in significant upregulation of all tested genes (**Figure 3**).

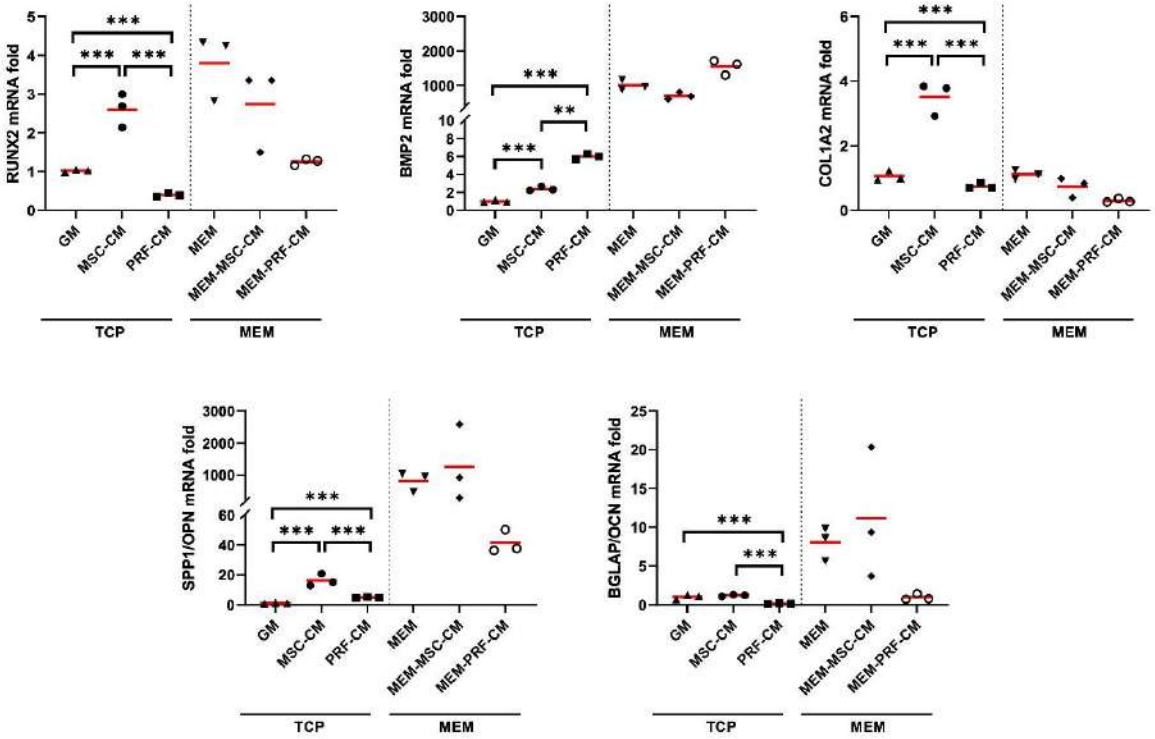

Figure 3: Gene expression analysis. Relative mRNA fold changes of osteogenic gene markers in human BMSC exposed to MSC-CM or PRF-CM for 48 hours in monolayer culture or on functionalized membranes. Data represent means (n = 3 experimental replicates); ** $p < 0.01$, *** $p < 0.001$. GM, growth media; TCP, tissue culture plastic; MEM, functionalized membranes; RUNX2, runt-related transcription factor 2; BMP2, bone morphogenetic protein 2; COL1A2 Collagen type 1 alpha 2; SPP1/OPN, osteopontin; BGLAP/OCN, osteocalcin.

3.2. MSC-CM functionalized MEM enhanced bone coverage in calvarial defects

All experimental animals recovered from the surgeries without adverse events. After 2 weeks, *in vivo* μCT revealed significantly greater defect coverage in MEM/MSC-CM (54.56 ± 15.03%) vs. MEM/PRF-CM (28.21 ± 16.94%; $p = 0.003$); a similar trend was observed with regards to BV/TV, i.e., MEM/MSC-CM (1.94 ± 0.91%) vs. MEM/PRF-CM (0.93 ± 0.90%; $p = 0.03$) (**Figure 4A-C**). After 4 weeks, *ex vivo* μCT revealed substantial increases in bone coverage in both MEM/MSC-CM (70.76 ± 22.63%) and MEM/PRF-CM (48.07 ± 19.74%), with significant differences between the groups ($p = 0.03$). Similarly, BV/TV after 4 weeks was greater in MEM/MSC-CM (5.83 ± 2.71%) vs. MEM/PRF-CM (2.83 ± 1.78%; $p = 0.013$) (**Figure 4C**). Both groups showed considerable intra-group variations, especially with regards to BV/TV. Some degree of mineralization within the membrane compartment was also observed, particularly in the MSC-CM group. Although the membrane per se was not visible in the μCT, mineralization of MEM fibres and/or formation of 'hybrid' bone (see section 3.3) allowed detection of the membrane in the μCT images (**Figure 4B**).

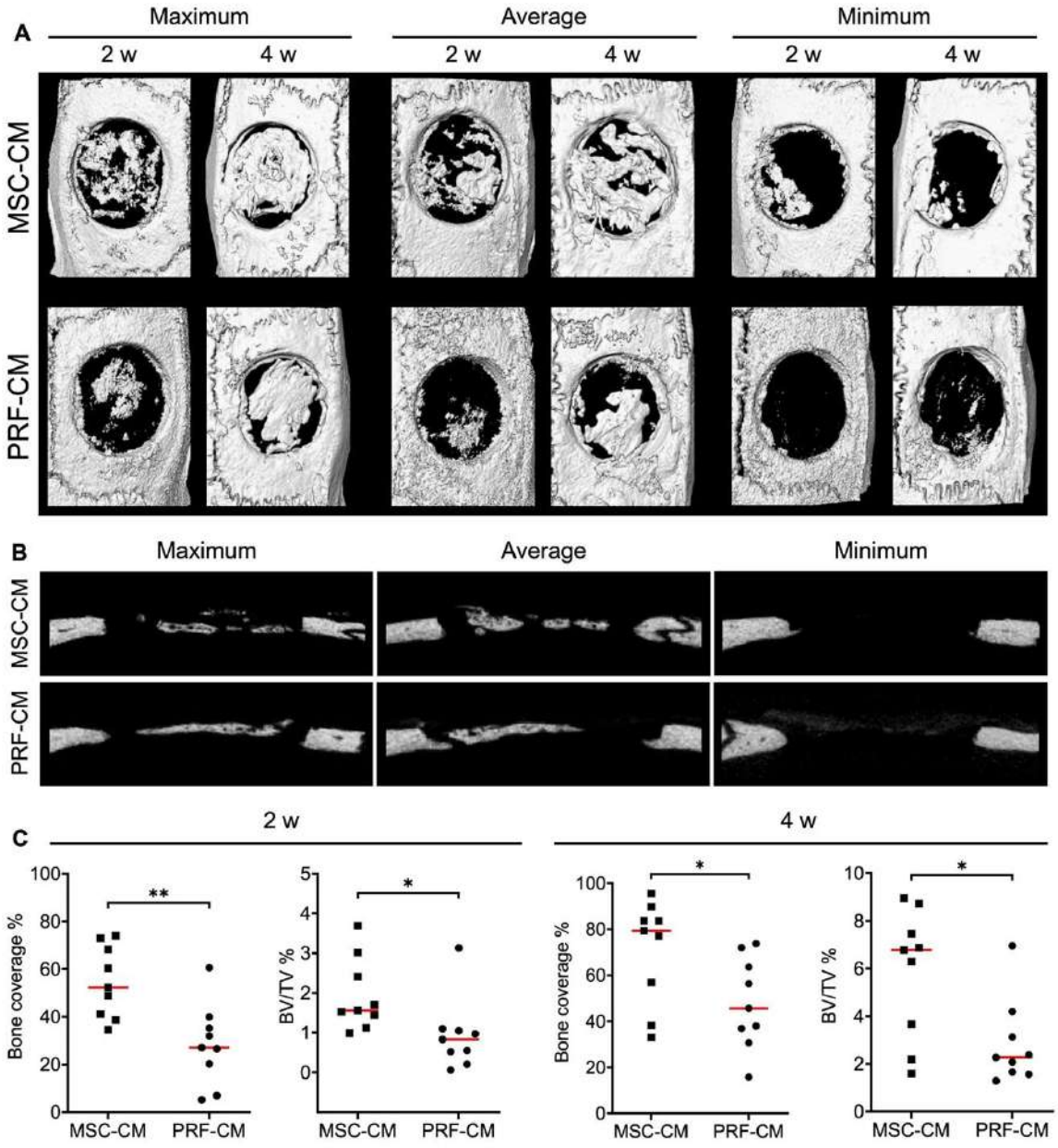

Figure 4: µCT analysis. (A) Representative reconstructed µCT images after 2 (*in vivo*) and 4 weeks (*ex vivo*) showing maximum, average and minimum bone coverage in MEM with MSC-CM PRF-CM. (B) Corresponding central slices of maximum, average and minimum bone coverage after 4 weeks in MEM with MSC-CM and PRF-CM. (C) Quantification of percentage bone coverage and bone volume per tissue volume (BV/TV%) after 2 and 4 weeks in MEM with MSC-CM and PRF-CM. w, weeks. Data represent means (n = 9); * $p < 0.05$, ** $p < 0.01$.

3.3. MSC-CM functionalized MEM enhanced hybrid bone formation in calvarial defects

After 4 weeks, both groups revealed a heterogeneous histological pattern inside the defect with the following tissue components: regular new bone, i.e., newly formed bone in the defect area without incorporated MEM fibers, new bone with incorporated MEM fibers hereafter called hybrid bone, mineralized MEM fibers not embedded in surrounding bone

tissue, unmineralized residual MEM, and soft tissues (**Figures 5-7**). The term 'new bone' in this case refers to characteristic woven or lamellar bone in the defect ROI at 4 weeks. In the MEM/MSC-CM group, new bone was typically seen at the base of the defect towards the dura, characterized by well-structured woven bone (dark pink) enclosed by layers of parallel-fibered bone (light pink). Adjacent to this new bone, areas of hybrid bone [characterized by immature woven bone incorporating collagen MEM fibers (pink)] were evident, indicating bone formation *within* the membrane compartment (**Figure 6**). Often, the hybrid bone was partially enclosed by new bone without incorporated MEM fibers, but in direct contact with the membrane. By following the outline of the membrane, it could be estimated that hybrid bone is initially formed within the membrane and subsequently remodeled to regular new bone. The MEM/PRF-CM group revealed a similar pattern with regards to new bone (without MEM fibers) directly above the dura but with a comparatively smaller area of hybrid bone in the membrane compartment (**Figure 7**). All samples revealed some degree of free-standing mineralized MEM fibers (without surrounding woven bone), remnant collagen MEM fibers (unmineralized) and non-specific mineralization, which could not be attributed to hybrid bone or mineralized MEM fibers. Finally, all samples revealed clear peripheral zones of osteoid tissue with characteristic osteoblast seams, suggesting still ongoing bone formation after 4 weeks (**Supplementary Figure S2**).

Quantification of tissues revealed significantly greater hybrid bone in MEM/MSC-CM (12.40 $\pm$ 3.68%) vs. MEM/PRF-CM (3.59 $\pm$ 3.68%; $p = 0.002$) (**Figure 5**). The area fraction of new bone was similar in MEM/MSC-CM (22.23 $\pm$ 6.76%) and MEM/PRF-CM (21.18 $\pm$ 12.85; $p = 0.87$). A trend for greater total new bone (new bone + hybrid bone) was observed in MEM/MSC-CM (34.63 $\pm$ 4.94%) vs. MEM/PRF-CM (24.77 $\pm$ 15.05%), although this was not statistically significant ($p = 0.20$). No significant differences were observed in terms of mineralized MEM fibers or residual MEM between the groups ($p > 0.05$). Notably, one sample from the MEM/PRF-CM group showed only MEM mineralization (11.76%) without relevant new (0.61%) or hybrid bone formation (0%). Quantification of tissue fractions in the defect edge areas revealed no significant differences between the groups for any of the histomorphometric parameters (**Supplementary figure S3**).

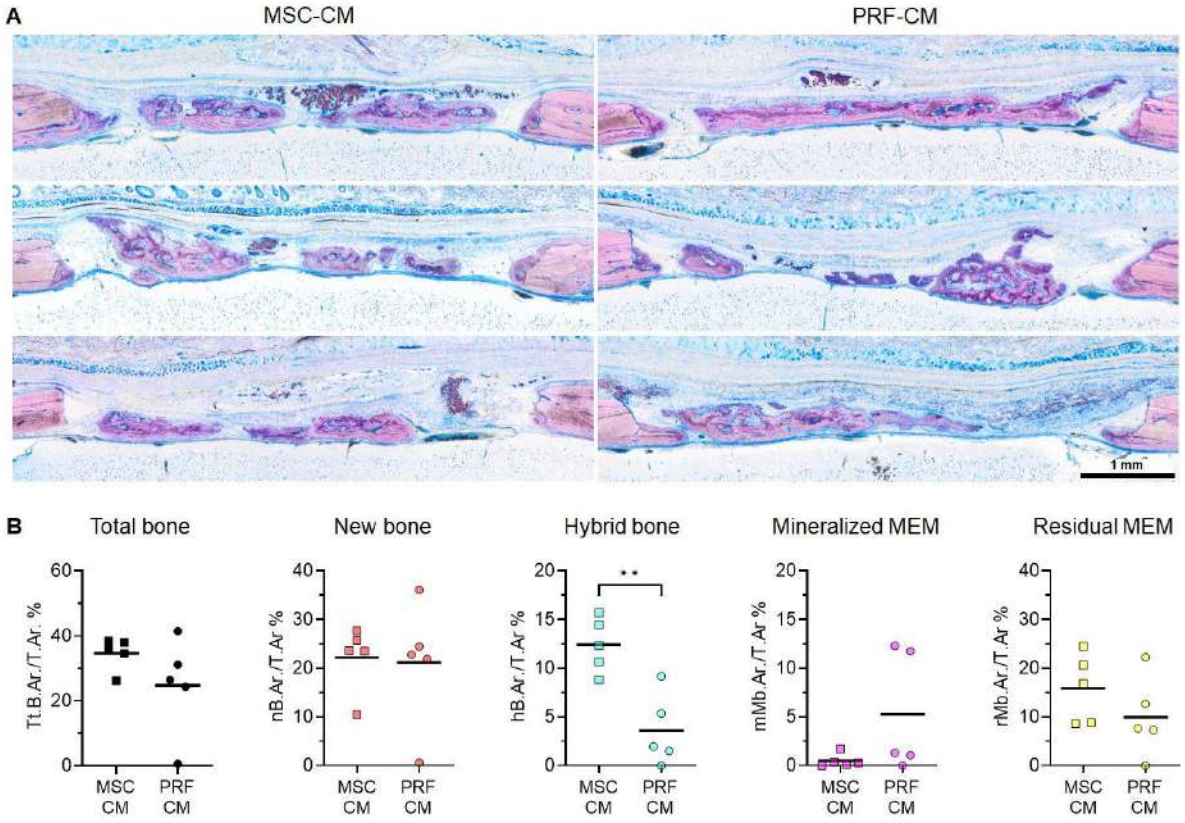

Figure 5: Histological analysis. (A) Representative undecalcified central histological sections (~100 μm) showing bone regeneration in MEM with MSC-CM or PRF-CM; scale bar 1 mm. (B) Quantification of histomorphometric parameters. Data represent means (n = 5); ** $p < 0.01$. MEM, membrane; T.Ar., Tissue Area; nB.Ar., New Bone Area; hB.Ar., Hybrid Bone Area; Tt.B.Ar., Total New Bone Area (New Bone + Hybrid Bone Area); mMb.Ar., Mineralized Membrane Area; rMb.Ar., Residual Membrane Area.

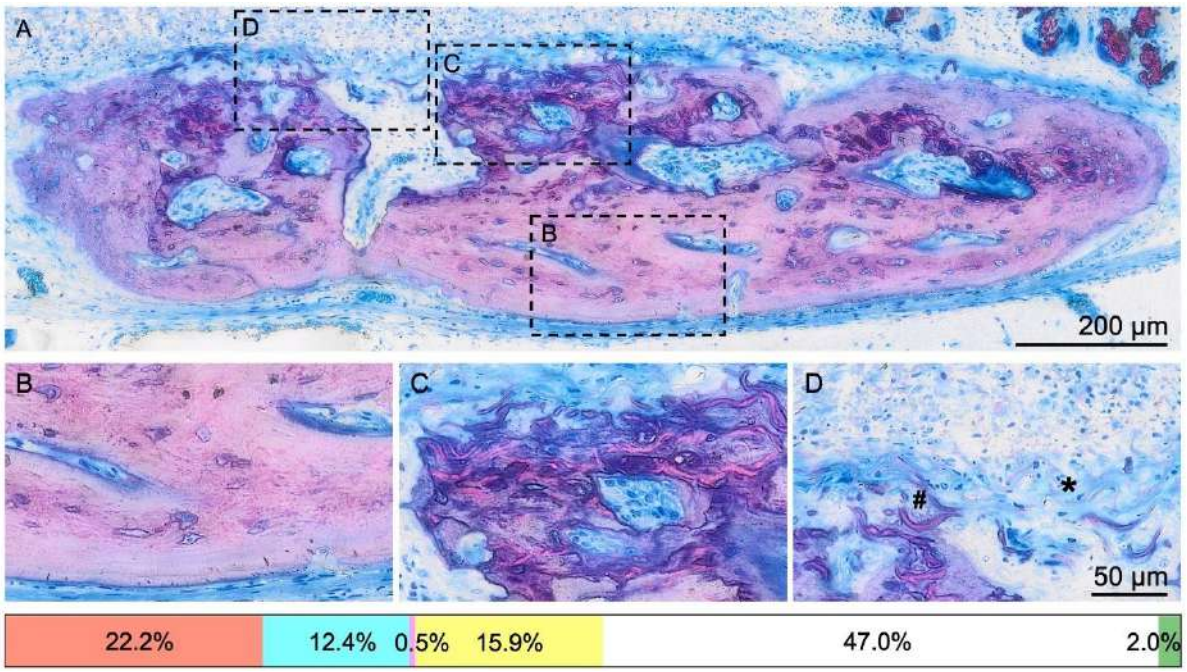

Figure 6: Histological analysis of MEM with MSC-CM. Representative images showing overview (A) and higher magnification areas of new bone (B), hybrid bone (C) and membrane (D) consisting of mineralized fibers (#) and residual membrane (*); scale bars: panel above 200 µm, panel below 50 µm. Numbers on the bottom panel indicate relative percentages for the treatment group of new bone (red), hybrid bone (cyan), mineralized membrane fibers (pink), non-specific mineralization (green), residual unmineralized membrane (yellow) and soft tissues area (white).

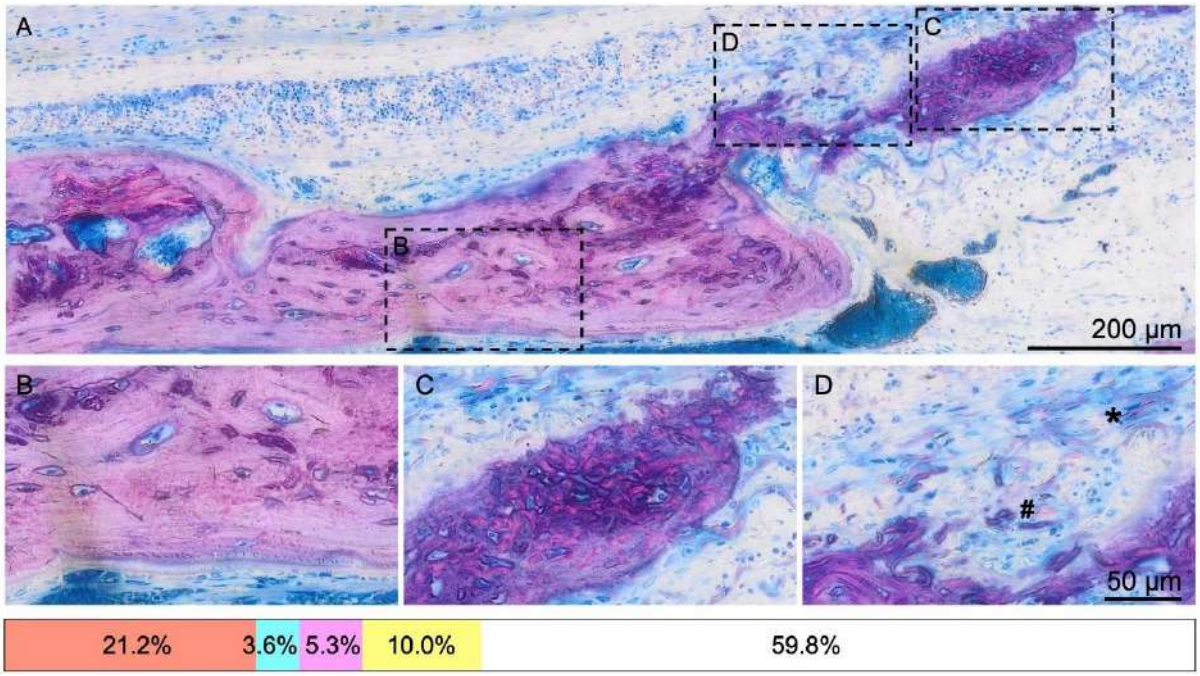

Figure 7: Histological analysis of MEM with PRF-CM. Representative images showing overview (A) and higher magnification areas of new bone (B), hybrid bone (C) and membrane (D) consisting of mineralized fibers (#) and residual membrane (*); scale bars: panel above 200 µm, panel below 50 µm. Numbers on the bottom panel indicate relative percentages for the treatment group of new bone (red), hybrid bone (cyan), mineralized membrane fibers (pink), residual unmineralized membrane (yellow) and soft tissues area (white).

4. Discussion

The objectives of the present study were to investigate the biological activity of MSC-CM for enhancing bone regeneration compared to a currently used GF strategy, i.e., L-PRF (PRF-CM). The principal findings herein were, firstly, that the proteome of MSC-CM was more enriched for biological processes related to bone formation compared to that of PRF-CM, and that superior bone regeneration was observed in rat calvaria defects treated with MEM functionalized with MSC-CM vs. PRF-CM.

The secretome of MSC (MSC-CM) has gained significant attention in the tissue engineering literature based on emerging evidence for paracrine mechanisms of MSC bioactivity. Moreover, practical benefits of MSC-CM over cell therapy include relative ease of preparation, 'off-the-shelf' application, and cost-efficacy (51). In the context of bone regeneration, previous data suggest that MSC-CM may be at least equally, if not more, effective than MSC transplantation (52-54). MSC-CM likely exerts its *in vivo* effects by stimulating tissue-resident progenitor cells and modulating immune cells (33). The former mechanism was demonstrated herein via upregulation of several osteogenesis related genes in human BMSC exposed to MSC-CM. It is of interest to note that pure MSC-CM (without additional supplements) caused greater upregulation of osteogenic genes than GM (supplemented with HPL), which itself is known to cause osteogenic gene upregulation and lineage commitment (39).

Proteomic characterizations of MSC secretomes have revealed several growth factors as well as various chemokines and cytokines (55, 56). Previous proteomic analyses of PRF lysates identified 652 (20), 1791 (57), and 705 total proteins (22), but only a few growth factors, e.g., TGFβ1, insulin-like growth factor-2, myeloid-derived growth factor, epidermal growth factor, and hepatocyte growth factor-like protein (57). These observations were partially confirmed by our proteomic analysis of PRF-CM. However, 727 proteins were significantly upregulated in MSC-CM compared to only 190 upregulated proteins in PRF-CM. The effects of donor-related variations in the properties and efficacy of both MSC(-CM) and L-PRF have been well-documented (58-63). Indeed, considerable variation in the total numbers of identified proteins was observed between the three donors within each group; this variation was relatively greater in PRF-CM. However, in terms of expression levels of the common proteins, i.e., DEPs, inter-donor variations were small in both MSC-CM and PRF-CM groups, based on mass spectrometry and multiplex analysis. Nevertheless, MSC-CM and PRF-CM from the different donors were each pooled prior to use in the *in vivo* experiments.

Pooling of CM has been proposed as a strategy to minimize donor-related variation while maintaining functional properties and increasing volumes for clinical translation (61, 64).

Overall, MSC-CM presented a more favourable proteomic profile than PRF-CM for bone regeneration; 77 proteins involved in selected bone related processes were upregulated in MSC-CM compared to only 15 proteins in PRF-CM. Expression of a subset of these proteins related to bone remodeling was also confirmed via multiplex assay. Interestingly, several key proteins involved in bone remodeling (MMPs, TIMPs, CCL2, OPG, OSTF1, etc.) were upregulated in MSC-CM. These proteins, which mainly regulate osteoclast activity, are critical for bone regeneration and their impaired function is reported to compromise healing (65). Moreover, key growth factors (TGFβ2, VEGFC, etc.), signaling pathways (BMP, Wnt, Notch) and ECM proteins (COL1A1/2, COL5A1/2, POSTN, ON, etc.) relevant for bone regeneration (66) were enriched in MSC-CM. In the context of MEM functionalization, our group has previously demonstrated that growth factor activity, specifically TGFβ, from L-PRF is adsorbed onto MEM (20). Indeed, TGFβ-proteins were detected in MSC-CM and PRF-CM herein. Therefore, it is reasonable to assume that growth factor activity from MSC-CM and PRF-CM was also adsorbed onto the MEM and subsequently released *in vivo*. Nevertheless, further studies are indicated to investigate which specific proteins, particularly from MSC-CM, are adsorbed (and released) from the MEM to mediate the *in vivo* effects.

The *in vivo* efficacy of MSC-CM and PRF-CM was investigated using a rat calvarial defect model. Despite considerable biological variation within each treatment group, significantly greater radiographic bone formation was observed in MSC-CM vs. PRF-CM after 2 and 4 weeks. Histologically, all samples revealed some degree of regular new bone as well as hybrid bone formation; the area of hybrid bone was significantly greater in the MSC-CM group. This pattern of new bone formation based on the incorporation of MEM fibers, i.e., new bone and hybrid bone, has previously been reported when using MEM in this animal model (50). Although yet unconfirmed by detailed time-course studies, our data suggest that hybrid bone formation may be an 'intermediate' stage, characterized by an early and swift mineralization of MEM fibers, their incorporation into new woven bone, which is spared the task of producing those collagen fibers itself, and subsequent remodeling to mature parallel-fibered bone. This pattern was evident in areas where 'islands' of hybrid bone were seen to be surrounded by (and in direct contact) new bone without fibers. Thus, the increased area fraction of hybrid bone in the MSC-CM group indicates superior MEM incorporation and, potentially, a greater likelihood of new bone formation (secondary to hybrid bone remodeling) at a later time-point.

Some limitations of the present study must be acknowledged. Firstly, MSC-CM and PRF-CM were prepared from relatively few (n=3) donors. Although similar sample sizes are commonly reported in the literature (43, 67-69), inclusion of additional donors may have provided a clearer picture of donor-related variations and a more 'standardized' CM-product after pooling. Next, the exclusion of a MEM-only control group in the *in vivo* analyses may have confounded the results. Nevertheless, in a previous study (38), we observed a clear benefit of MEM/MSC-CM, prepared in the same manner as in the present study, over native MEM based on μCT and histological analysis. It must also be acknowledged that PRF-CM may not accurately represent the clinical product, i.e., L-PRF. However, despite its wide clinical use (14), the overall evidence does not demonstrate a clear significant benefit of L-PRF over conventional therapies for bone regeneration (14, 16, 70, 71). Nevertheless, L-PRF has some practical advantages over MSC-CM, given its relative ease of 'chair-side' preparation and low cost. Moreover, the efficacy of MSC-CM for bone regeneration remains to be demonstrated in well-designed clinical studies in comparison to conventional GBR procedures.

5. Conclusions

In summary, MEM functionalized with MSC-CM resulted in faster and greater NBF in rat calvaria defects compared to MEM functionalized with PRF-CM. Significantly greater radiographic bone coverage was observed after 2 and 4 weeks in MSC-CM treated defects. Histologically, both groups showed comparable total new bone formation, although significantly greater hybrid bone (with embedded MEM fibres) was formed in the MSC-CM group. The results herein may be explained by differences in the proteomic profiles of MSC-CM and PRF-CM, with the former demonstrating greater enrichment for several biological processes related to bone formation. Thus, while both MSC-CM and L-PRF(-CM) are feasible approaches for GF delivery, functionalizing MEM with MSC-CM may represent a more effective and clinically relevant strategy to enhance GBR.

List of abbreviations

GBR	guided bone regeneration
MEM	collagen membranes
GF	growth factors
BMP2	bone morphogenetic protein-2
PDGFB	platelet-derived growth factor-B
PRF	platelet-rich fibrin
L-PRF	leukocyte- and platelet-rich fibrin
MSC	mesenchymal stromal cells
BMSC	bone marrow mesenchymal stromal cells
CM	conditioned media
MSC-CM	conditioned media from mesenchymal stromal cells
PRF-CM	conditioned media from leukocyte- and platelet-rich fibrin
ATMP	Advanced Therapeutic Medicinal Products
GM	growth media
DMEM	Dulbecco's Modified Eagle's medium
PBS	phosphate-buffered saline
DEPs	differentially expressed proteins
FDR	false discovery rate
ELISA	enzyme-linked immunosorbent assay
μCT	micro-computed tomography
BV/TV	new bone volume relative to total defect volume
ROI	regions of interest
TGFβ1	transforming growth factor beta-1
VEGFC	vascular endothelial growth factor-C
EGFR	epidermal growth factor receptor
ECM	extracellular matrix

List of abbreviations of all analyzed proteins is provided in Supplementary Tables S1 and S2.

Declarations

Ethical approvals

The use of human cells and tissues was approved by the Regional Committees for Medical Research Ethics (REK) in Norway (2013-1248/REK sør-øst C). Animal experiments were approved by the Norwegian Animal Research Authority (Mattilsynet; FOTS-17443) and performed in accordance with the ARRIVE guidelines.

Consent for publication

Not applicable

Competing interests

The authors confirm that there are no known conflicts of interest associated with this publication and there has been no significant financial support for this work that could have influenced its outcome.

Funding

This work was supported by the Osteology Foundation, Switzerland (18-152), Helse Vest Research Funding, Norway (F-12124), and Trond Mohn Foundation, Norway (BFS2018TMT10).

Authors' contributions

S.S., M.S., and R.G. conceived and designed the study. S.S. performed the experiments, data collection, data analysis and drafted the manuscript. N.A.S., C.K., S.M.A., E.K.K., and S.T. assisted with experiments, sample preparation, data collection, data analysis/interpretation and/or drafting the manuscript. M.S., E.K.K, K.M. and R.G. assisted with data analysis/interpretation, drafting the manuscript and funding acquisition. All authors read and approved the final version of the manuscript.

Acknowledgements

We thank the Bloodbank at Haukeland University Hospital for assistance with the L-PRF preparation, and Heidi Espedal from the Dept. of Clinical Medicine, University of Bergen, for assistance with the in vivo CT scanning. The Intra-Spin L-PRF kit was a kind donation from CAMLOG Biotechnologies GmbH. Mass spectrometry-based proteomic analyses were performed by the Proteomics Unit at the University of Bergen (PROBE). This facility is a member of the National Network of Advanced Proteomics Infrastructure (NAPI), which is funded by the Research Council of Norway (INFRASTRUKTUR-program project number: 295910).

Availability of data and materials

Additional data are included in the Supplementary data file and can be made available by the authors upon request.

Legends

Figure 1: Proteomic analysis. (A) Venn diagrams showing total numbers of common and exclusively identified proteins in MSC-CM and PRF-CM from three individual donors (D1-3; MSC and L-PRF were obtained from different donor-groups). (B) Venn diagram showing total numbers of common and exclusively identified proteins in MSC-CM and PRF-CM based on detection in at least 2 donors in each group.

Figure 2: Multiplex immunoassay. Normalized concentrations (pg cytokine/µg total protein) of cytokines detected in MSC-CM and PRF-CM using a human bone metabolism array (Supplementary Table S2). Data represent means of CM from MSC/PRF of 3 independent donors (each data point represent the average of 4 technical replicates). ** $p < 0.01$, *** $p < 0.001$.

Figure 3: Gene expression analysis. Relative mRNA fold changes of osteogenic gene markers in human BMSC exposed to MSC-CM or PRF-CM for 48 hours in monolayer culture or on functionalized membranes. Data represent means (n = 3 experimental replicates); ** $p < 0.01$, *** $p < 0.001$. GM, growth media; TCP, tissue culture plastic; MEM, functionalized membranes; RUNX2, runt-related transcription factor 2; BMP2, bone morphogenetic protein 2; COL1A2 Collagen type 1 alpha 2; SPP1/OPN, osteopontin; BGLAP/OCN, osteocalcin.

Figure 4: µCT analysis. (A) Representative reconstructed µCT images after 2 (*in vivo*) and 4 weeks (*ex vivo*) showing maximum, average and minimum bone formation in MEM with MSC-CM or PRF-CM. (B) Corresponding central slices of maximum, average and minimum bone formation after 4 weeks in MEM with MSC-CM and PRF-CM. (C) Quantification of percentage bone coverage and bone volume per tissue volume (BV/TV) after 2 and 4 weeks in MEM with MSC-CM and PRF-CM. w, weeks. Data represent means (n = 9); * $p < 0.05$, ** $p < 0.01$.

Figure 5: Histological analysis. (A) Representative undecalcified central histological sections (~100 µm) showing bone regeneration in MEM with MSC-CM or PRF-CM after 4 weeks; scale bar 1 mm. (B) Quantification of histomorphometric parameters. Data represent means (n = 5); ** $p < 0.01$. MEM, membrane; T.Ar., Tissue Area; nB.Ar., New Bone Area; hB.Ar., Hybrid Bone Area; Tt.B.Ar., Total New Bone Area (New Bone + Hybrid Bone Area); mMb.Ar., Mineralized Membrane Area; rMb.Ar., Residual Membrane Area.

Figure 6: Histological analysis of MEM with MSC-CM. Representative images showing overview (A) and higher magnification areas of new bone (B), hybrid bone (C) and membrane (D) consisting of mineralized fibers (#) and residual membrane (*); scale bars: panel above 200 µm, panel below 50 µm. Numbers on the bottom panel indicate relative percentages for the treatment group of new bone (red), hybrid bone (cyan), mineralized membrane fibers (pink), non-specific mineralization (green), residual unmineralized membrane (yellow) and soft tissues area (white).

Figure 7: Histological analysis of MEM with PRF-CM. Representative images showing overview (A) and higher magnification areas of new bone (B), hybrid bone (C) and membrane (D) consisting of mineralized fibers (#) and residual membrane (*); scale bars: panel above 200 µm, panel below 50 µm. Numbers on the bottom panel indicate relative percentages for the treatment group of new bone (red), hybrid bone (cyan), mineralized membrane fibers (pink), residual unmineralized membrane (yellow) and soft tissues area (white).

References

1. Sanz-Sánchez I, Ortiz-Vigón A, Sanz-Martín I, Figuero E, Sanz M. Effectiveness of lateral bone augmentation on the alveolar crest dimension: A systematic review and meta--analysis. Journal of Dental Research. 2015;94(9).
2. Thoma DS, Bienz SP, Figuero E, Jung RE, Sanz-Martin I. Efficacy of lateral bone augmentation performed simultaneously with dental implant placement: A systematic review and meta-analysis. J Clin Periodontol. 2019;46 Suppl 21:257-76.
3. Urban IA, Montero E, Monje A, Sanz-Sanchez I. Effectiveness of vertical ridge augmentation interventions: A systematic review and meta-analysis. J Clin Periodontol. 2019;46 Suppl 21:319-39.
4. Benic GI, Hammerle CH. Horizontal bone augmentation by means of guided bone regeneration. Periodontol 2000. 2014;66(1):13-40.
5. Gimbel M, Ashley RK, Sisodia M, Gabbay JS, Wasson KL, Heller J, et al. Repair of alveolar cleft defects: Reduced morbidity with bone marrow stem cells in a resorbable matrix. The Journal of Craniofacial Surgery. 2007;18:895-901.
6. Caballe-Serrano J, Munar-Frau A, Ortiz-Puigpelat O, Soto-Penaloza D, Penarrocha M, Hernandez-Alfaro F. On the search of the ideal barrier membrane for guided bone regeneration. J Clin Exp Dent. 2018;10(5):e477-e83.
7. Turri A, Elgali I, Vazirisani F, Johansson A, Emanuelsson L, Dahlin C, et al. Guided bone regeneration is promoted by the molecular events in the membrane compartment. Biomaterials. 2016;84:167-83.
8. Caballe-Serrano J, Sawada K, Miron RJ, Bosshardt DD, Buser D, Gruber R. Collagen barrier membranes adsorb growth factors liberated from autogenous bone chips. Clin Oral Implants Res. 2017;28(2):236-41.
9. Kuchler U, Rybaczek T, Dobask T, Heimel P, Tangl S, Klehm J, et al. Bone-conditioned medium modulates the osteoconductive properties of collagen membranes in a rat calvaria defect model. Clin Oral Implants Res. 2018;29(4):381-8.
10. Strauss FJ, Kuchler U, Kobatake R, Heimel P, Tangl S, Gruber R. Acid bone lysates reduce bone regeneration in rat calvaria defects. J Biomed Mater Res A. 2021;109(5):659-65.
11. Omar O, Elgali I, Dahlin C, Thomsen P. Barrier membranes: More than the barrier effect? J Clin Periodontol. 2019;46 Suppl 21:103-23.
12. Farmani AR, Nekoofar MH, Ebrahimi Barough S, Azami M, Rezaei N, Najafipour S, et al. Application of Platelet Rich Fibrin in Tissue Engineering: Focus on Bone Regeneration. Platelets. 2021;32(2):183-8.
13. Donos N, Dereka X, Calciolari E. The use of bioactive factors to enhance bone regeneration: A narrative review. J Clin Periodontol. 2019;46 Suppl 21:124-61.
14. Strauss FJ, Stahli A, Gruber R. The use of platelet-rich fibrin to enhance the outcomes of implant therapy: A systematic review. Clin Oral Implants Res. 2018;29 Suppl 18:6-19.
15. Castro AB, Meschi N, Temmerman A, Pinto N, Lambrechts P, Teughels W, et al. Regenerative potential of leucocyte- and platelet-rich fibrin. Part A: intra-bony defects, furcation defects and periodontal plastic surgery. A systematic review and meta-analysis. J Clin Periodontol. 2017;44(1):67-82.
16. Castro AB, Meschi N, Temmerman A, Pinto N, Lambrechts P, Teughels W, et al. Regenerative potential of leucocyte- and platelet-rich fibrin. Part B: sinus floor elevation, alveolar ridge preservation and implant therapy. A systematic review. J Clin Periodontol. 2017;44(2):225-34.
17. Dohan DM, Choukroun J, Diss A, Dohan SL, Dohan AJ, Mouhyi J, et al. Platelet-rich fibrin (PRF): a second-generation platelet concentrate. Part I: technological concepts and evolution. Oral Surg Oral Med Oral Pathol Oral Radiol Endod. 2006;101(3):e37-44.

18. Dohan Ehrenfest DM, Del Corso M, Diss A, Mouhyi J, Charrier JB. Three-dimensional architecture and cell composition of a Choukroun's platelet-rich fibrin clot and membrane. J Periodontol. 2010;81(4):546-55.
19. Di Liddo R, Bertalot T, Borean A, Pirola I, Argentoni A, Schrenk S, et al. Leucocyte and Platelet-rich Fibrin: a carrier of autologous multipotent cells for regenerative medicine. J Cell Mol Med. 2018;22(3):1840-54.
20. Di Summa F, Kargarpour Z, Nasirzade J, Stahli A, Mitulovic G, Panic-Jankovic T, et al. TGFbeta activity released from platelet-rich fibrin adsorbs to titanium surface and collagen membranes. Sci Rep. 2020;10(1):10203.
21. Castro AB, Andrade C, Li X, Pinto N, Teughels W, Quirynen M. Impact of g force and timing on the characteristics of platelet-rich fibrin matrices. Sci Rep. 2021;11(1):6038.
22. Hermida-Nogueira L, Barrachina MN, Moran LA, Bravo S, Diz P, Garcia A, et al. Deciphering the secretome of leukocyte-platelet rich fibrin: towards a better understanding of its wound healing properties. Sci Rep. 2020;10(1):14571.
23. Dohan DM, Choukroun J, Diss A, Dohan SL, Dohan AJ, Mouhyi J, et al. Platelet-rich fibrin (PRF): a second-generation platelet concentrate. Part II: platelet-related biologic features. Oral Surg Oral Med Oral Pathol Oral Radiol Endod. 2006;101(3):e45-50.
24. Dohan DM, Choukroun J, Diss A, Dohan SL, Dohan AJ, Mouhyi J, et al. Platelet-rich fibrin (PRF): a second-generation platelet concentrate. Part III: leucocyte activation: a new feature for platelet concentrates? Oral Surg Oral Med Oral Pathol Oral Radiol Endod. 2006;101(3):e51-5.
25. Strauss FJ, Nasirzade J, Kargarpoor Z, Stahli A, Gruber R. Effect of platelet-rich fibrin on cell proliferation, migration, differentiation, inflammation, and osteoclastogenesis: a systematic review of in vitro studies. Clin Oral Investig. 2020;24(2):569-84.
26. Dragonas P, Katsaros T, Avila-Ortiz G, Chambrone L, Schiavo JH, Palaiologou A. Effects of leukocyte-platelet-rich fibrin (L-PRF) in different intraoral bone grafting procedures: a systematic review. Int J Oral Maxillofac Surg. 2019;48(2):250-62.
27. Shanbhag S, Suliman S, Pandis N, Stavropoulos A, Sanz M, Mustafa K. Cell therapy for orofacial bone regeneration: A systematic review and meta-analysis. J Clin Periodontol. 2019;46 Suppl 21:162-82.
28. Sandor GK, Numminen J, Wolff J, Thesleff T, Miettinen A, Tuovinen VJ, et al. Adipose stem cells used to reconstruct 13 cases with cranio--maxillofacial hard--tissue defects. Stem Cells Translational Medicine. 2014;3:530-40.
29. Gjerde C, Mustafa K, Hellem S, Rojewski M, Gjengedal H, Yassin MA, et al. Cell therapy induced regeneration of severely atrophied mandibular bone in a clinical trial. Stem Cell Res Ther. 2018;9(1):213.
30. Haumer A, Bourgine PE, Occhetta P, Born G, Tasso R, Martin I. Delivery of cellular factors to regulate bone healing. Advanced Drug Delivery Reviews. 2018;129:285-94.
31. Caplan AI, Dennis JE. Mesenchymal stem cells as trophic mediators. J Cell Biochem. 2006;98(5):1076-84.
32. Bari E, Perteghella S, Di Silvestre D, Sorlini M, Catenacci L, Sorrenti M, et al. Pilot Production of Mesenchymal Stem/Stromal Freeze-Dried Secretome for Cell-Free Regenerative Nanomedicine: A Validated GMP-Compliant Process. Cells. 2018;7(11).
33. Gnecchi M, Danieli P, Malpasso G, Ciuffreda MC. Paracrine Mechanisms of Mesenchymal Stem Cells in Tissue Repair. Methods Mol Biol. 2016;1416:123-46.
34. Pittenger MF, Discher DE, Péault BM, Phinney DG, Hare JM, Caplan AI. Mesenchymal stem cell perspective: cell biology to clinical progress. NPJ Regen Med. 2019;4:22.
35. Weiss ARR, Dahlke MH. Immunomodulation by Mesenchymal Stem Cells (MSCs): Mechanisms of Action of Living, Apoptotic, and Dead MSCs. Front Immunol. 2019;10:1191.

36. Veronesi F, Borsari V, Sartori M, Orciani M, Mattioli-Belmonte M, Fini M. The use of cell conditioned medium for musculoskeletal tissue regeneration. J Cell Physiol. 2018;233(6):4423-42.
37. Benavides-Castellanos MP, Garzon-Orjuela N, Linero I. Effectiveness of mesenchymal stem cell-conditioned medium in bone regeneration in animal and human models: a systematic review and meta-analysis. Cell Regen. 2020;9(1):5.
38. Shanbhag S, Kampleitner C, Al-Sharabi N, Mohamed-Ahmed S, Apaza Alccayhuaman KA, Heimel P, et al. Functionalizing Collagen Membranes with MSC-Conditioned Media Promotes Guided Bone Regeneration in Rat Calvarial Defects. Cells. 2023;12(5).
39. Shanbhag S, Mohamed-Ahmed S, Lunde THF, Suliman S, Bolstad AI, Hervig T, et al. Influence of platelet storage time on human platelet lysates and platelet lysate-expanded mesenchymal stromal cells for bone tissue engineering. Stem Cell Res Ther. 2020;11(1):351.
40. Shanbhag S, Al-Sharabi N, Mohamed-Ahmed S, Gruber R, Kristoffersen EK, Mustafa K. Brief communication: Effects of conditioned media from human platelet lysate cultured MSC on osteogenic cell differentiation in vitro. Front Bioeng Biotechnol. 2022;10:969275.
41. Peng Y, Xuan M, Zou J, Liu H, Zhuo Z, Wan Y, et al. Freeze-dried rat bone marrow mesenchymal stem cell paracrine factors: a simplified novel material for skin wound therapy. Tissue Eng Part A. 2015;21(5-6):1036-46.
42. Aasebo E, Brenner AK, Hernandez-Valladares M, Birkeland E, Berven FS, Selheim F, et al. Proteomic Comparison of Bone Marrow Derived Osteoblasts and Mesenchymal Stem Cells. Int J Mol Sci. 2021;22(11).
43. Shin S, Lee J, Kwon Y, Park KS, Jeong JH, Choi SJ, et al. Comparative Proteomic Analysis of the Mesenchymal Stem Cells Secretome from Adipose, Bone Marrow, Placenta and Wharton's Jelly. Int J Mol Sci. 2021;22(2).
44. Zhao J, Wang S, Bao J, Sun X, Zhang X, Zhang X, et al. Trehalose maintains bioactivity and promotes sustained release of BMP-2 from lyophilized CDHA scaffolds for enhanced osteogenesis in vitro and in vivo. PLoS One. 2013;8(1):e54645.
45. Mohamed-Ahmed S, Fristad I, Lie SA, Suliman S, Mustafa K, Vindenes H, et al. Adipose-derived and bone marrow mesenchymal stem cells: a donor-matched comparison. Stem Cell Res Ther. 2018;9(1):168.
46. Kilkenny C, Browne WJ, Cuthill IC, Emerson M, Altman DG. Improving bioscience research reporting: the ARRIVE guidelines for reporting animal research. PLoS Biol. 2010;8:1000412.
47. Shanbhag S, Suliman S, Mohamed-Ahmed S, Kampleitner C, Hassan MN, Heimel P, et al. Bone regeneration in rat calvarial defects using dissociated or spheroid mesenchymal stromal cells in scaffold-hydrogel constructs. Stem Cell Res Ther. 2021;12(1):575.
48. Toriumi DM, Raslan WF, Friedman M, Tardy ME. Histotoxicity of cyanoacrylate tissue adhesives. A comparative study. Arch Otolaryngol Head Neck Surg. 1990;116(5):546-50.
49. Rezende ML, Cunha Pde O, Damante CA, Santana AC, Greghi SL, Zangrando MS. Cyanoacrylate Adhesive as an Alternative Tool for Membrane Fixation in Guided Tissue Regeneration. J Contemp Dent Pract. 2015;16(6):512-8.
50. Feher B, Apaza Alccayhuaman KA, Strauss FJ, Lee JS, Tangl S, Kuchler U, et al. Osteoconductive properties of upside-down bilayer collagen membranes in rat calvarial defects. Int J Implant Dent. 2021;7(1):50.
51. Marolt Presen D, Traweger A, Gimona M, Redl H. Mesenchymal Stromal Cell-Based Bone Regeneration Therapies: From Cell Transplantation and Tissue Engineering to Therapeutic Secretomes and Extracellular Vesicles. Front Bioeng Biotechnol. 2019;7:352.
52. Osugi M, Katagiri W, Yoshimi R, Inukai T, Hibi H, Ueda M. Conditioned media from mesenchymal stem cells enhanced bone regeneration in rat calvarial bone defects. Tissue Eng Part A. 2012;18(13-14):1479-89.

53. Hiraki T, Kunimatsu R, Nakajima K, Abe T, Yamada S, Rikitake K, et al. Stem cell-derived conditioned media from human exfoliated deciduous teeth promote bone regeneration. Oral Dis. 2020;26(2):381-90.
54. Sanchooli T, Norouzian M, Ardeshirylajimi A, Ghoreishi S, Abdollahifar M, Nazarian H, et al. Adipose Derived Stem Cells Conditioned Media in Combination with Bioceramic-Collagen Scaffolds Improved Calvarial Bone Healing in Hypothyroid Rats. Iranian Red Crescent Medical Journal. 2017;In Press.
55. Kupcova Skalnikova H. Proteomic techniques for characterisation of mesenchymal stem cell secretome. Biochimie. 2013;95(12):2196-211.
56. Kehl D, Generali M, Mallone A, Heller M, Uldry AC, Cheng P, et al. Proteomic analysis of human mesenchymal stromal cell secretomes: a systematic comparison of the angiogenic potential. NPJ Regen Med. 2019;4:8.
57. Kargarpour Z, Nasirzade J, Panahipour L, Mitulovic G, Miron RJ, Gruber R. Platelet-Rich Fibrin Increases BMP2 Expression in Oral Fibroblasts via Activation of TGF-beta Signaling. Int J Mol Sci. 2021;22(15).
58. Trivedi A, Miyazawa B, Gibb S, Valanoski K, Vivona L, Lin M, et al. Bone marrow donor selection and characterization of MSCs is critical for pre-clinical and clinical cell dose production. J Transl Med. 2019;17(1):128.
59. Sagaradze G, Grigorieva O, Nimiritsky P, Basalova N, Kalinina N, Akopyan Z, et al. Conditioned Medium from Human Mesenchymal Stromal Cells: Towards the Clinical Translation. Int J Mol Sci. 2019;20(7).
60. Miron RJ, Dham A, Dham U, Zhang Y, Pikos MA, Sculean A. The effect of age, gender, and time between blood draw and start of centrifugation on the size outcomes of platelet-rich fibrin (PRF) membranes. Clin Oral Investig. 2019;23(5):2179-85.
61. Assoni A, Coatti G, Valadares MC, Beccari M, Gomes J, Pelatti M, et al. Different Donors Mesenchymal Stromal Cells Secretomes Reveal Heterogeneous Profile of Relevance for Therapeutic Use. Stem Cells Dev. 2017;26(3):206-14.
62. Mindaye ST, Ra M, Lo Surdo JL, Bauer SR, Alterman MA. Global proteomic signature of undifferentiated human bone marrow stromal cells: evidence for donor-to-donor proteome heterogeneity. Stem Cell Res. 2013;11(2):793-805.
63. Weibrich G, Kleis WK, Hafner G, Hitzler WE. Growth factor levels in platelet-rich plasma and correlations with donor age, sex, and platelet count. J Craniomaxillofac Surg. 2002;30:97.
64. Silini AR, Papait A, Cargnoni A, Vertua E, Romele P, Bonassi Signoroni P, et al. CM from intact hAM: an easily obtained product with relevant implications for translation in regenerative medicine. Stem Cell Res Ther. 2021;12(1):540.
65. Xing Z, Lu C, Hu D, Yu YY, Wang X, Colnot C, et al. Multiple roles for CCR2 during fracture healing. Dis Model Mech. 2010;3(7-8):451-8.
66. Majidinia M, Sadeghpour A, Yousefi B. The roles of signaling pathways in bone repair and regeneration. J Cell Physiol. 2018;233(4):2937-48.
67. Chen J, Li Y, Hao H, Li C, Du Y, Hu Y, et al. Mesenchymal Stem Cell Conditioned Medium Promotes Proliferation and Migration of Alveolar Epithelial Cells under Septic Conditions In Vitro via the JNK-P38 Signaling Pathway. Cell Physiol Biochem. 2015;37(5):1830-46.
68. Winkel A, Jaimes Y, Melzer C, Dillschneider P, Hartwig H, Stiesch M, et al. Cell culture media notably influence properties of human mesenchymal stroma/stem-like cells from different tissues. Cytotherapy. 2020;22(11):653-68.
69. Mead B, Chamling X, Zack DJ, Ahmed Z, Tomarev S. TNFalpha-Mediated Priming of Mesenchymal Stem Cells Enhances Their Neuroprotective Effect on Retinal Ganglion Cells. Invest Ophthalmol Vis Sci. 2020;61(2):6.

70. Alrayyes Y, Al-Jasser R. Regenerative Potential of Platelet Rich Fibrin (PRF) in Socket Preservation in Comparison with Conventional Treatment Modalities: A Systematic Review and Meta-Analysis. Tissue Eng Regen Med. 2022;19(3):463-75.
71. Wang X, Fok MR, Pelekos G, Jin L, Tonetti MS. Increased local concentrations of growth factors from leucocyte- and platelet-rich fibrin do not translate into improved alveolar ridge preservation: An intra-individual mechanistic randomized controlled trial. J Clin Periodontol. 2022;49(9):889-98.

cells

MDPI

Article

Functionalizing Collagen Membranes with MSC-Conditioned Media Promotes Guided Bone Regeneration in Rat Calvarial Defects

Siddharth Shanbhag [1,2,*], Carina Kampleitner [3,4,5,†], Niyaz Al-Sharabi [2,†], Samih Mohamed-Ahmed [2], Karol Ali Apaza Alccayhuaman [6], Patrick Heimel [3,4,5], Stefan Tangl [3,5], Andreas Beinlich [7], Neha Rana [2], Mariano Sanz [8], Einar K. Kristoffersen [1], Kamal Mustafa [2,‡] and Reinhard Gruber [5,6,9,*,‡]

1 Department of Immunology and Transfusion Medicine, Haukeland University Hospital, 5021 Bergen, Norway
2 Center for Translational Oral Research (TOR), Department of Clinical Dentistry, Faculty of Medicine, University of Bergen, 5009 Bergen, Norway
3 Karl Donath Laboratory for Hard Tissue and Biomaterial Research, University Clinic of Dentistry, Medical University of Vienna, 1090 Vienna, Austria
4 Ludwig Boltzmann Institute for Traumatology, The Research Center in Cooperation with AUVA, 1200 Vienna, Austria
5 Austrian Cluster for Tissue Regeneration, 1200 Vienna, Austria
6 Department of Oral Biology, University Clinic of Dentistry, Medical University of Vienna, 1090 Vienna, Austria
7 Department of Earth Science, Faculty of Mathematics and Natural Sciences, University of Bergen, 5009 Bergen, Norway
8 ETEP Research Group, Faculty of Odontology, University Complutense of Madrid, 28040 Madrid, Spain
9 Department of Periodontology, School of Dental Medicine, University of Bern, 3010 Bern, Switzerland
* Correspondence: siddharth.shanbhag@uib.no (S.S.); reinhard.gruber@meduniwien.ac.at (R.G.); Tel.: +47-55586059 (S.S.); +43-(0)69910718472 (R.G.)
† These authors contributed equally to this work.
‡ Equal contribution and shared senior authors.

check for updates

Citation: Shanbhag, S.; Kampleitner, C.; Al-Sharabi, N.; Mohamed-Ahmed, S.; Apaza Alccayhuaman, K.A.; Heimel, P.; Tangl, S.; Beinlich, A.; Rana, N.; Sanz, M.; et al. Functionalizing Collagen Membranes with MSC-Conditioned Media Promotes Guided Bone Regeneration in Rat Calvarial Defects. *Cells* **2023**, *12*, 767. https://doi.org/10.3390/cells12050767

Academic Editors: Roberta Di Pietro and Florelle Gindraux

Received: 8 February 2023
Revised: 21 February 2023
Accepted: 24 February 2023
Published: 28 February 2023

Copyright: © 2023 by the authors. Licensee MDPI, Basel, Switzerland. This article is an open access article distributed under the terms and conditions of the Creative Commons Attribution (CC BY) license (https://creativecommons.org/licenses/by/4.0/).

Abstract: Functionalizing biomaterials with conditioned media (CM) from mesenchymal stromal cells (MSC) is a promising strategy for enhancing the outcomes of guided bone regeneration (GBR). This study aimed to evaluate the bone regenerative potential of collagen membranes (MEM) functionalized with CM from human bone marrow MSC (MEM-CM) in critical size rat calvarial defects. MEM-CM prepared via soaking (CM-SOAK) or soaking followed by lyophilization (CM-LYO) were applied to critical size rat calvarial defects. Control treatments included native MEM, MEM with rat MSC (CEL) and no treatment. New bone formation was analyzed via micro-CT (2 and 4 weeks) and histology (4 weeks). Greater radiographic new bone formation occurred at 2 weeks in the CM-LYO group vs. all other groups. After 4 weeks, only the CM-LYO group was superior to the untreated control group, whereas the CM-SOAK, CEL and native MEM groups were similar. Histologically, the regenerated tissues showed a combination of regular new bone and hybrid new bone, which formed within the membrane compartment and was characterized by the incorporation of mineralized MEM fibers. Areas of new bone formation and MEM mineralization were greatest in the CM-LYO group. Proteomic analysis of lyophilized CM revealed the enrichment of several proteins and biological processes related to bone formation. In summary, lyophilized MEM-CM enhanced new bone formation in rat calvarial defects, thus representing a novel 'off-the-shelf' strategy for GBR.

Keywords: mesenchymal stromal cells; conditioned media; guided bone regeneration; bone tissue engineering; regenerative medicine

1. Introduction

The reconstruction of complex bone defects, where tissue deficiency occurs tri-dimensionally, is a clinical challenge [1]. In the alveolar bone, the recommended treat-

ment approaches for such defects have been either guided bone regeneration (GBR) using autologous bone grafts in combination with a bone substitute material and a barrier membrane or autogenous or allogeneic bone blocks [2,3]. Although GBR has demonstrated a high degree of clinical success and predictability [4,5], in the presence of large defects, the need for extensive autologous bone harvesting may result in additional patient morbidity and risks of clinical complications [6].

Bone tissue engineering is increasingly being used to overcome these limitations [7] by combining autologous transplantation of ex vivo expanded adult mesenchymal stromal cells (MSC), usually from the bone marrow (BMSC), with biomaterial scaffolds [8,9]. However, this approach has important logistic and regulatory complications that limit its efficiency and predictability. In fact, in a recent meta-analysis, our group reported that the clinical evidence for effectiveness of cell therapy was limited, i.e., there were relatively small effect sizes vs. traditional GBR/grafting procedures, and these were mainly limited to studies of maxillary sinus augmentation [7]. Moreover, the large-scale translation of this strategy is limited by the need for expensive Good Manufacturing Practice (GMP)-grade laboratories for ex vivo cell expansion and stringent regulation of MSC as Advanced Therapeutic Medicinal Products (ATMP) by health authorities. Furthermore, the traditional hypothesis that MSC act via engraftment, differentiation and replacement at the injury site has, in recent years, been challenged by evidence of a predominantly paracrine mechanism of action [10,11].

It is widely accepted that MSC may exert their beneficial effects by secreting a wide range of bioactive factors, including soluble proteins (growth factors, cytokines and chemokines), lipids, nucleic acids and extracellular vesicles at or near the site of injury [11–13]. These factors, in turn, stimulate tissue-resident progenitor (osteogenesis), endothelial (angiogenesis) and immune cells (immune modulation) to drive the subsequent regeneration processes [14]. These findings have provided the biological basis for developing 'cell-free' strategies, which use the secretome contained in MSC-conditioned media (CM) to stimulate tissue regeneration. An additional advantage of this strategy is the possibility of storing and using MSC-CM as 'off-the-shelf' products [15]. Although the preclinical efficacy of MSC-CM for bone regeneration has previously been reported [16,17], data for the optimal dose(s) and mode(s) of CM delivery are lacking.

GBR techniques are based on the use of barrier membranes that act as occlusive barriers to the rapidly proliferating cells of epithelial and connective tissues, while promoting repopulation with slower-growing osteoprogenitor cells [18,19]. Bioabsorbable collagen membranes (MEM) are the most frequently used membranes in GBR, and are either applied alone or combined with bone substitute materials [20]. In addition to functioning as occlusive barriers, MEM have also shown an inherent biological activity via their ability to adsorb and release signaling molecules, e.g., growth factors [21,22]. This property has been exploited in several preclinical studies where MEM have been functionalized with bioactive molecules, e.g., bone-derived proteins [23,24] and recombinant growth factors (see review [4]). We have previously demonstrated that MEM can adsorb the growth factor-activity from human biological products ex vivo [25]. Thus, it is reasonable to hypothesize that MEM can also adsorb bioactive factors from CM and serve as carriers or 'scaffolds' in GBR settings [14,25]. To test this hypothesis, we propose using the calvarial critical size defect model in rodents, since this model is extensively used for testing other GBR strategies [26]. Thus, the objective of the present study was to investigate the efficacy of CM-functionalized MEM (MEM-CM) for promoting GBR in vivo in rat calvarial defects. A secondary objective was to compare two different methods, i.e., soaking vs. lyophilization of CM, for MEM functionalization.

2. Methods

2.1. Cell Culture

The use of human cells and tissues was approved by the Regional Committees for Medical Research Ethics in Norway (2013-1248/REK-sør-øst and 2016-1266/REK-nord). Bone marrow specimens were obtained following parental consent from five independent donors (2 females and 3 males; 8–10 years) undergoing reconstructive surgery at the Department of Plastic Surgery, Haukeland University Hospital. BMSC were isolated and expanded following previous protocols [27]. Briefly, the cells were cultured in T75 or T175 flasks (Thermo Fisher Scientific, Carlsbad, CA, USA) using sterile filtered growth media (GM) comprising of Dulbecco's Modified Eagle's medium (DMEM, Invitrogen, Carlsbad, CA, USA) supplemented with 5% (*v/v*) pooled human platelet lysate (HPL; Bergenlys, Bergen, Norway), 1% (*v/v*) penicillin/streptomycin (GE Healthcare, South Logan, UT, USA) and 1 IU/mL heparin (Leo Pharma AS, Lysaker, Norway) [27]. The cells were sub-cultured and expanded under standard incubation conditions, i.e., 37 °C and 5% CO_2, following a validated protocol with a seeding density of 4000 cells/cm^2 [28]. Passage 1 (p1) and 2 (p2) BMSC were characterized based on immunophenotype and multi-lineage differentiation potential, as previously reported [27]. For all the cell cultures, growth and morphology were monitored regularly under an inverted light microscope (Nikon Eclipse TS100, Tokyo, Japan).

2.2. CM Preparation

Pooled CM were prepared from BMSC (n = 3 donors) as previously described [29]. Briefly, p1 and p2 BMSC were expanded in T175 flasks in GM until 70–80% confluency under standard incubation. At this point, the cells were washed three times with phosphate-buffered saline (PBS; Invitrogen), and then cultured in plain DMEM (without HPL or antibiotics) for another 48 h to produce CM. After 48 h, the CM from p1 and p2 BMSC from each of the three donors were collected, pooled, centrifuged at 4000× *g* for 10 min to remove any debris, aliquoted and stored at −80 °C. The CM were further concentrated using 3 kDa Amicon Ultra-15 centrifugal filter devices (Merck Millipore, Billerica, MA, USA) using the manufacturers protocol. Briefly, following the equilibration of filter devices with PBS, the CM were centrifuged at 4000× *g* for 30 min at 4 °C, followed by PBS buffer exchange and another centrifugation cycle (4000× *g* for 30 min), resulting in concentrated CM (~30-fold). Based on previous reports [15,30], mannitol (Sigma Aldrich, St. Louis, MO, USA) was added as a cryo-preservative (0.5% *v/v*), and the concentrated CM were then used for MEM functionalization.

2.3. MEM Functionalization and Bioassay

Bi-layered, non-cross-linked MEM (25 mm × 25 mm; Bio-Gide®, Geistlich Pharma, Wolhusen, Switzerland) were used in this study. The MEM were cut using sterile scissors into smaller pieces (7 mm × 6 mm) and incubated with 100 µL of serum-free DMEM (control) or concentrated CM at 37 °C for 1 h based on previous experiments where the incubation conditions for optimal adsorption of proteins were determined [22]. For equal comparison, mannitol was also added to serum-free DMEM at a final concentration of 0.5% (*v/v*). After 1 h, the supernatants were aspirated, and MEM soaked with serum-free DMEM (native MEM, control group) and half of the MEM soaked with CM (CM-SOAK) were stored at 4 °C. The remaining MEM soaked with CM were stored in a −80 °C freezer for subsequent lyophilization. Lyophilization of the MEM-CM was performed in a FreeZone™ freeze dryer (Labconco, Kansas, MO, USA) at 0.014 mBar of pressure and at −51 °C. The lyophilized MEM-CM (CM-LYO) were stored at 4 °C until their use in the experiments (up to 24 h). As a bioassay, the effects of CM alone and MEM-CM (CM-SOAK and CM-LYO) on BMSC were tested via a quantitative real-time polymerase chain reaction (qPCR) using TaqMan® real-time PCR assays (Thermo Scientific) as previously described [31]. Primary BMSC (different from those used for CM preparation) were exposed to GM and CM in a monolayer culture, and to CM-SOAK, CM-LYO and native MEM in a three-dimensional

(3D) culture for 48 h. Expressions of osteogenesis-related genes (Supplementary Table S1) were assessed as previously described [31].

2.4. Cell Viability on MEM

To test the cytocompatibility of the functionalized MEM-CM (CM-SOAK and CM-LYO), i.e., whether the resident cells could populate the MEM following in vivo implantation, the in vitro viability of rat MSC (rMSC) seeded on native and functionalized MEM was determined after 1 and 3 days using the LIVE/DEAD cell viability assay (Invitrogen) as previously described [32]. Briefly, previously isolated rMSC [33] were cultured in DMEM supplemented with 10% (*v/v*) fetal bovine serum (FBS) and 1% (*v/v*) penicillin/streptomycin; p3-5 cells were used in experiments. Pooled rMSC (~10^5 cells) were seeded on MEM and allowed to attach for 1 h before supplementing them with the corresponding growth media for 1–3 days. At each time point, MEM were stained and observed under a confocal microscope (Andor Dragonfly 5050, Oxford Instruments, Abingdon, UK) coupled with Imaris software ver. 9.5.1 (Oxford Instruments), and green (live) and red (dead) cells were visualized qualitatively in each condition. For the animal experiment, pooled rMSC (1.5×10^6 cells) were seeded on the MEM as described above and cultured in growth media for 24 h before implantation. Cell viability was confirmed just prior to implantation using the aforementioned viability assay.

2.5. Rat Calvaria Defect Model

The calvarial defect model in rats was performed following ethical approval (Norwegian Animal Research Authority, FOTS-17443) and in accordance with the ARRIVE guidelines, as previously described [32]. Briefly, 20 male Lewis rats (LEW/OrlRj, Janvier Labs, Le Genest-Saint-Isle, France) that were 8 weeks old and weighing 200–350 g were used. Following acclimatization, the animals were anesthetized (Sevoflurane, Abbott Laboratories, Berkshire, UK), and two full-thickness defects were surgically created, one in each parietal bone, using a trephine bur with an outer diameter of 5 mm (Meisinger GmbH, Neuss, Germany) under saline irrigation. Three animals died during the surgery due to anesthesia-related complications; therefore 17 animals were available for the experiment. The following treatments were then randomly applied to the defects: CM-LYO (n = 8), CM-SOAK (n = 8), MEM seeded with allogeneic pooled rMSC (CEL, 1.5×10^6 cells; n = 7), native MEM soaked with serum-free DMEM (MEM; n = 6) and no treatment ('empty' defects; n = 5). Membranes were fixed to the calvaria using 3–5 µL of tissue adhesive (Histoacryl®, B. Braun, Tuttingen, Germany) at the defect edges [34,35]; the fixation of MEM is advised to prevent micromovements and promote healing [36]. Randomization of defects/groups was performed using the Research Randomizer online software [37], and the animals were coded via ear clips. For all subsequent handling/analyses, the animals/specimens were identified by numbers to facilitate blinding of the observers to the treatment groups. After 2 weeks, the animals were subjected to in vivo micro-computed tomography (µCT), and after 4 weeks, they were euthanized with an overdose of CO_2. The primary outcome was new bone formation after 2 weeks via in vivo µCT and after 4 weeks via ex vivo µCT, histology and histomorphometry. The secondary outcomes included the characterization of new bone tissues via scanning electron microscopy (SEM), microhardness testing, relative bone density and Raman spectroscopy.

2.6. µ CT

To track early in vivo bone regeneration, the live animals were scanned at 2 weeks post-surgery under anesthesia using a small-animal CT scanner and Mediso workstation (both from nanoScan Mediso, Budapest, Hungary) with a voxel size of 40 µm (resolution), 70 kV energy, an exposure time of 300 ms, 720 projections and 1:1 binning. After a period of observation, the animals were returned to their original cages and housing locations until euthanasia. After 4 weeks, the calvaria were harvested and fixed in 10% buffered formalin. The specimens were scanned using a SCANCO 50 µCT scanner (SCANCO Medical AG,

Bruttisellen, Switzerland) at 90 kV and 200 µA with an isotropic resolution of 20 µm. Reconstruction and analysis were performed as previously described [32]. Briefly, scans were reconstructed using Amira software (Thermo Scientific) by orienting the drill direction along the *Z*-axis, with the defect in the approximate center of the image. Using ImageJ software (NIH, Bethesda, MD, USA), a standardized volume of interest (VOI) including the entire thickness of the calvaria and excluding 0.5 mm of marginal bone was defined for each defect. Specific density thresholds were defined for in vivo and ex vivo µCT scans (based on scanning resolutions) and percentages of new bone volume relative to total defect volume (BV/TV%) and bone coverage (%) were calculated in ImageJ (NIH) using custom defined rulesets.

2.7. Histology and Histomorphometry

After µCT scanning, the calvaria specimens were processed for undecalcified histology as previously described [32]. Briefly, the specimens were dehydrated in ascending grades of alcohol and embedded in light-curing resin (Technovit 7200 + 1% benzoyl peroxide, Kulzer & Co., Wehrheim, Germany). The blocks were further processed using EXAKT cutting and grinding equipment (EXAKT Apparatebau, Norderstedt, Germany). Standardized thin-ground sections (~100 µm) were prepared in the centre of each defect, parallel to the sagittal suture and perpendicular to the parietal bone, and stained with Levai-Laczko dye (Morphisto GmbH, Frankfurt, Germany). In this staining process, mature bone appears light pink, woven bone is dark pink and soft tissues (including collagen) are dark blue. The sections were scanned using an Olympus BX61VS digital virtual microscopy system (DotSlide 2.4, Olympus, Tokyo, Japan) with a 20× objective, resulting in a resolution of 0.32 µm per pixel.

Histomorphometric analysis was performed to analyze the tissue components filling the defects as previously described [38]. Briefly, the scanned images were manually segmented using Photoshop CS 6 (Adobe Systems Inc., San Jose, CA, USA) and quantified using a custom script in ImageJ (NIH). Two regions of interest (ROI) were defined for each sample based on the position of the membrane in relation to the defect: the central defect region, delimited superiorly by the MEM, inferiorly by the dura and laterally by the defect edges, and the defect edge or 'side' region, which was the area adjacent to the central defect on both sides (Supplementary Figure S1). In both ROIs, the respective areas of new bone without embedded MEM fibers (hereafter termed 'new bone'), new bone with embedded MEM fibers (hereafter termed 'hybrid bone'), total new bone (sum of new and hybrid bone), mineralized MEM fibers, residual MEM (non-mineralized MEM fibers) and soft tissue were measured, and corresponding percentages were calculated as a ratio of the ROI area.

2.8. Characterization of New Bone Tissues

The structural, mechanical and compositional properties of new bone tissues were analyzed based on SEM, microhardness, relative bone density and Raman spectroscopy. The objective herein was to compare the different tissue types, i.e., regular new bone and hybrid new bone, and not the different treatment conditions. Representative sections from each experimental group (MEM, CM-LYO, CM-SOAK and CEL) were used, and native calvarial bone was analyzed as a control.

SEM: The ultrastructure of the new bone tissues, i.e., regular new bone and hybrid bone, was further analyzed using SEM. Briefly, back-scattered electron imaging of carbon coated resin-embedded calvaria sections was performed using a Zeiss Supra 55VP microscope (Carl Zeiss, Oberkochen, Germany), with an acceleration voltage of 15 kV and an 8 mm working distance.

Microhardness: Vickers microhardness testing was performed as previously described [39]. Briefly, micro-indentations were created on the tissue surfaces using an MHT-10 microhardness tester equipped with a Vickers diamond indenter tip and a video measuring system (Anton Paar, Graz, Austria) attached to a light microscope with a 50× objective (Leica DMR, Wetzlar, Germany). A load of 50 g was applied for 10 s to produce each indentation; at least 10 separated indentations were made per tissue type, per section. The length of the diagonals of each indentation was measured using the inbuilt software (Anton Paar), and a Vickers hardness value (H_V) was automatically calculated.

Relative bone density: The selected sections were scanned using a SkyScan 1172 µCT scanner (Bruker, Kontich, Belgium) with an X-ray source of 60 kV/200 µA and 0.5 mm aluminum filter for a resolution of 13.3 µm; beam hardening was adjusted to compensate for the difference in density between the plastic microscope slides. A maximum intensity projection of each slide was created, and using a custom ImageJ script, the average intensity in each tissue type was measured. Details of the measurement protocol are presented in the Supplementary Materials.

Raman spectroscopy: This technique was used to study bone composition via an estimation of the crystallinity and mineral-to-matrix ratio. Raman spectra of each tissue type were collected using a confocal Raman microscope (LabRam, Horiba Jobin Yvon, Edison, NJ, USA) equipped with a 488 nm excitation laser and 50× objective coupled with the LabSpec ver. 5 software (Horiba Jobin Yvon) with the following settings: a spatial resolution of 0.5 cm^{-1}, a spectral range of 400–1800 cm^{-1} and 10 accumulations with 1 s exposure time per measurement. The spectral measurements were calibrated using a silicon standard, and at least five measurements were taken per tissue type per section. The spectra were processed using a custom script in Matlab (Mathworks, Natick, MA, USA) for the selected peaks of interest, i.e., v_1 phosphate (v_1 PO_4^3) at ~960 cm^{-1}, representing the mineral/inorganic phase of bone, and CH_2 wag at ~1448 cm^{-1}, representing the organic/matrix phase, i.e., collagens, lipids and non-collagenous proteins [40]. Background fluorescence correction and smoothing using the Savitzky–Golay polynomial function in the 2nd order were applied to the spectra in the appropriate wave number range (±80 cm^{-1}) using a custom MatLab script. The following parameters were determined for the selected peaks of interest: peak height, peak area and the full peak width at half maximum intensity (FWHM). To ensure the correct identification of the different tissue types, stained histological sections were used, which resulted in an additional background peak from the dye (pararosaniline); the dye-peak at 913 cm^{-1} [41] could be clearly differentiated from the bone peaks and did not interfere with the analysis. The following compositional parameters were then calculated: *crystallinity*, represented by the inverse of the full peak width at half maximum intensity ($FWHM^{-1}$) for v_1 PO_4^3, and mineral/matrix ratio, represented by the peak height ratio of v_1 PO_4^3 to CH_2 wag.

2.9. Liquid Chromatography with Tandem Mass Spectrometry (LC-MS/MS) of Lyophilized CM

The proteomic composition of the pooled CM were analyzed using LC-MS/MS as previously described [42]. Briefly, the total protein concentration was measured using a bicinchoninic acid assay (Pierce BCA Kit, Thermo Fisher), and 10 µg of lyophilized protein was processed to obtain tryptic peptides. About 0.5 µg protein as tryptic peptides dissolved in 2% acetonitrile and 0.5% formic acid was injected into an Ultimate 3000 RSLC system connected online to a Exploris 480 mass spectrometer equipped with EASY-spray nano-electrospray ion source (all from Thermo Scientific, Sunnyvale, CA, USA). Additional details of LC-MS/MS are reported in the Supplementary Materials.

2.10. Bioinformatic Analysis

The LC-MS/MS raw files were searched using Proteome Discoverer software (version 2.5.0.400; Thermo Scientific). Perseus software (version 2.3.0.1; Max Planck Institute for Biochemistry, Martinsread, Germany) was used to process and filter the results. An over-representation analysis of the exclusive proteins in each CM group was performed using the WebGestalt tool (wGSEA) [43,44]. Gene ontology (GO) slim subsets were retrieved based on the human genome (Homo sapiens) as a reference. Relevant GO terms (Homo sapiens) for bone-related biological processes were retrieved from the QuickGO database (https://www.ebi.ac.uk/QuickGO/, accessed on 14 November 2022), and the corresponding gene names were compared to the proteins identified in CM [42]. A list of identified bone-related proteins is presented in Supplementary Table S2.

2.11. Multiplex Immunoassay

The Quantibody Human Bone Metabolism Array Q1 (RayBiotech Inc., Norcross, GA, USA) was used to analyze 31 bone related cytokines (Supplementary Table S3) according to the manufacturer's protocol. This array is based on the sandwich enzyme-linked immunosorbent assay (ELISA) technology, and each antibody is spotted in quadruplicate. Array hybridization was performed using concentrated CM (0.1–0.2 mg/mL of total protein) and standard cytokines. Array scanning was performed using a laser scanner (GenePix 4000B, Axon Instruments, San Jose, CA, USA) at different photomultiplier tube gains. Data extraction was performed using the GenePix Pro software ver. 5.0 (Axon Instruments). Concentrations of candidate proteins were calculated based on linear standard curves and normalized to the corresponding total protein concentration.

2.12. Statistical Analysis

Statistical analysis was performed using the Prism 9 software (GraphPad, San Diego, CA, USA). Data are presented as means (± SD and/or range), unless they are specified. Analyses of the gene expression data are based on delta-CT values, and the results are presented as relative (log/non-linear) fold changes using scatter plots. All other linear data are presented as scatter or bar graphs. Normality testing was performed via the Shapiro–Wilk test. The one-way analysis of variance (ANOVA), followed by a post hoc Tukey's test, was applied, and statistical significance was set at $p < 0.05$.

3. Results

3.1. Functionalized MEM Supported Cell Growth and Function

The live/dead assay revealed the high viability of rMSC on the MEM-CM, i.e., CM-LYO and CM-SOAK (Figure 1A), both of which were similar to that on the native MEM. The stacking of z-sections revealed the 3D migration of cells between the fibrillar network (pores) of the MEM (Figure 1B). The viability of rMSC on native MEM was also confirmed just prior to in vivo implantation (Supplementary Figure S2). With regard to cell function, the qPCR bioassay showed a significant upregulation of osteogenic gene markers in the BMSC exposed to CM vs. those in GM in monolayer cultures (Supplementary Figure S3). In the 3D cultures, i.e., BMSC seeded on native or functionalized MEM, a remarkable upregulation of all osteogenic genes was observed compared to cells in monolayer cultures, regardless of MEM functionalization. Thus, in 3D cultures, the effect of the MEM itself on the BMSC confounded the effects of MEM-CM. Although it was not statistically significant, a trend for enhanced gene expression was observed in the CM-LYO vs. CM-SOAK MEM-CM (Supplementary Figure S3).

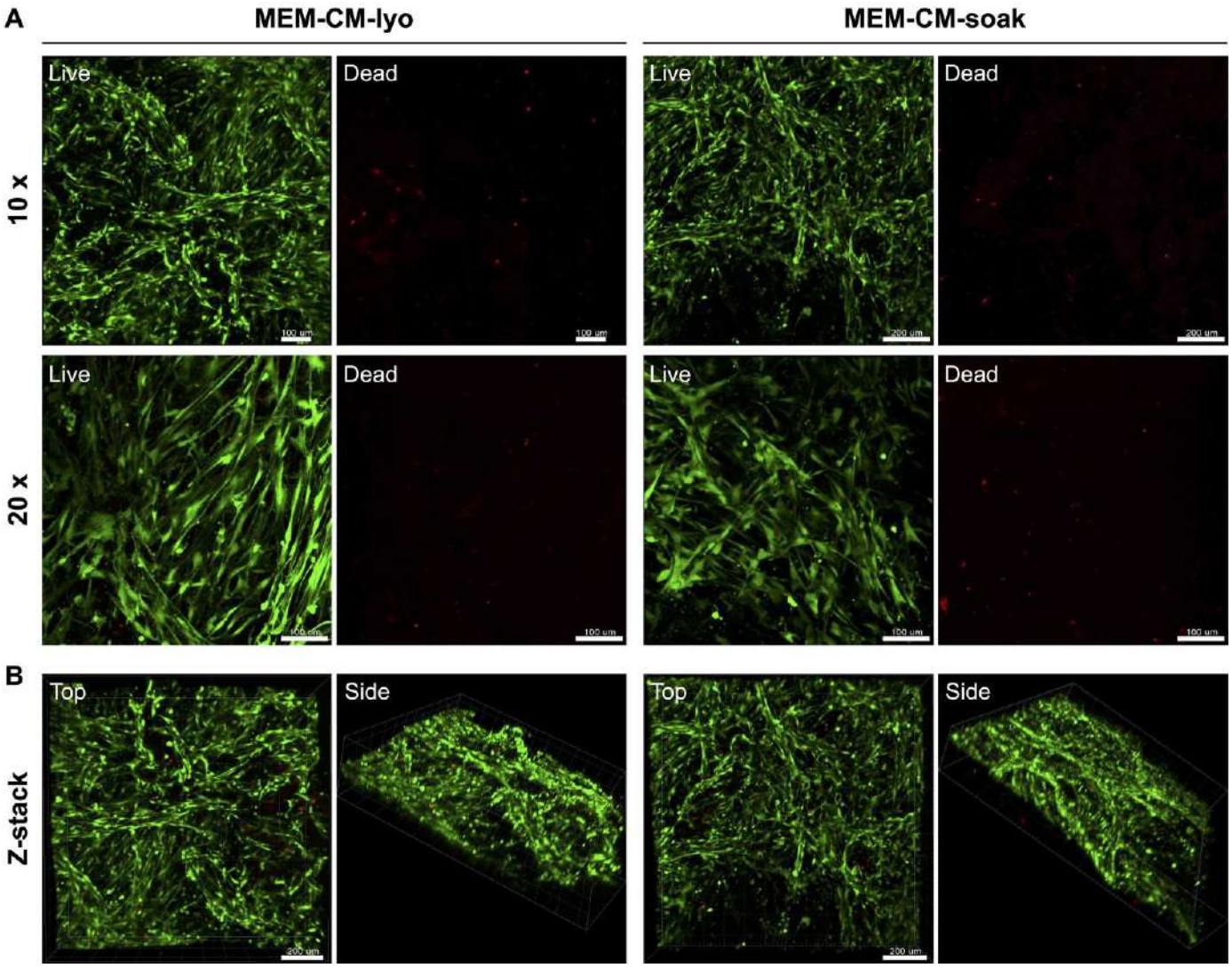

Figure 1. Evaluation of cell viability on MEM-CM. Representative 2D (**A**) and 3D (**B**) confocal images of rMSC viability (live/dead assay) on CM functionalized MEM either soaked (CM-SOAK) or lyophilized (CM-LYO) after 3 days. Scale bars: 100 μm (A) and 200 μm (B).

3.2. CM-LYO Enhanced In Vivo New Bone Formation More than Other Treatments Did

All animals included in the experiment recovered from the surgery, and no adverse events were observed. After 2 weeks, μCT revealed a significantly greater coverage of bone defects in the CM-LYO (85.5 ± 15.49%) vs. that in the CM-SOAK group (21.67 ± 21.13%; $p < 0.001$), suggesting a clear benefit of lyophilization (Figure 2A,B). Moreover, the bone coverage was also greater in CM-LYO vs. that in the CEL (18.81 ± 20.03%; $p < 0.001$), native MEM (18.57 ± 20.83%; $p < 0.001$) and empty groups (11.67 ± 12.02%; $p < 0.001$). A similar trend was observed with regard to BV/TV in CM-LYO (4.48 ± 1.4%) vs. CM-SOAK (0.72 ± 0.74; $p < 0.001$), CEL (0.98 ± 1.17; $p < 0.001$), native MEM (0.69 ± 0.77; $p < 0.001$) and empty groups (0.56 ± 0.83; $p < 0.001$) (Figure 2B). Early mineralization within the membrane compartment occurred more frequently in CM-LYO (8/8) vs. in the CM-SOAK (0/8), CEL (1/7) and MEM (2/6) groups (Figure 3).

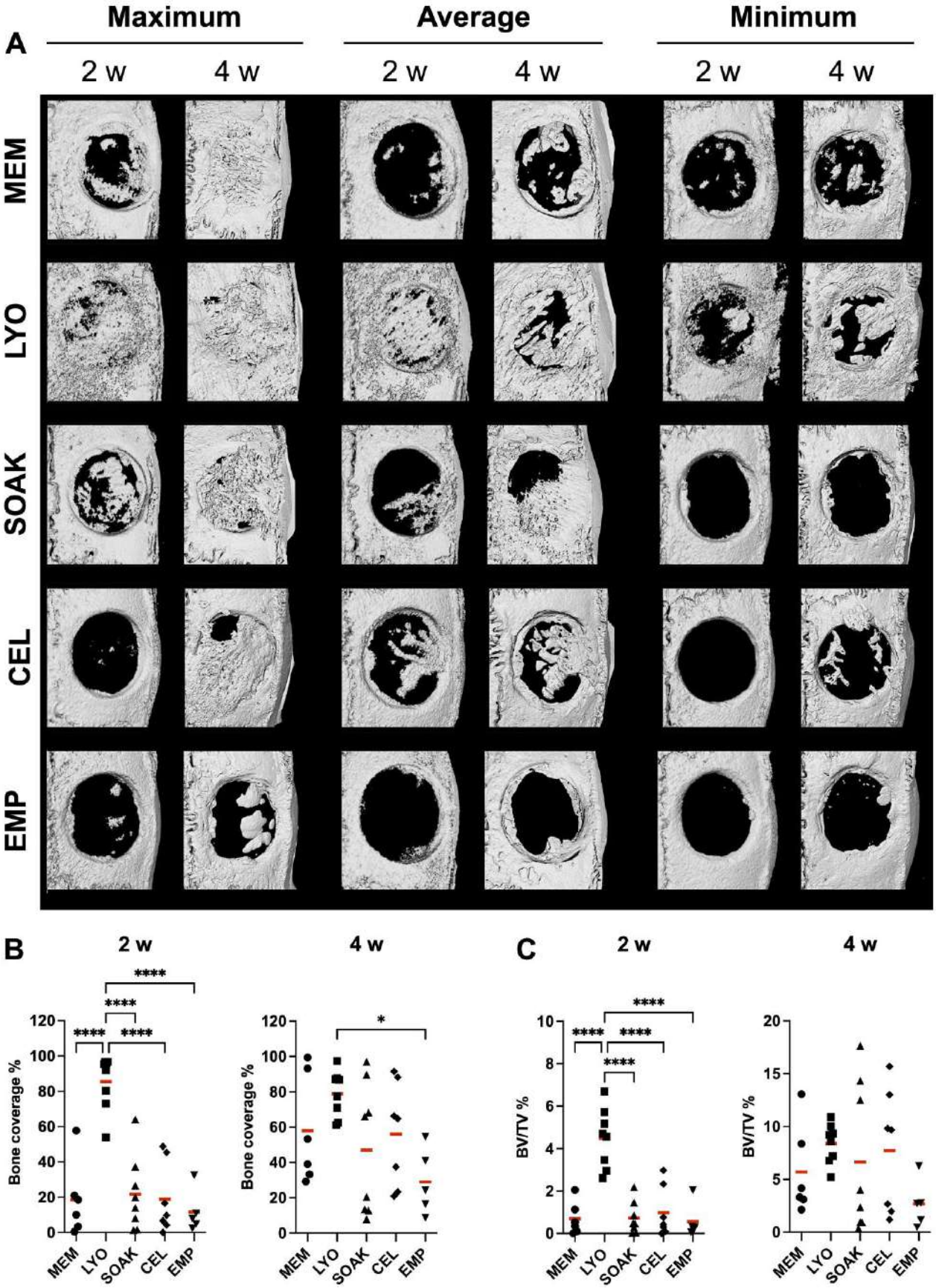

Figure 2. μCT analysis. (**A**) Representative reconstructed μCT images after 2 (in vivo) and 4 weeks

(ex vivo) showing maximum, average and minimum bone formation in the different groups. Quantification of bone coverage (**B**) and bone volume per tissue volume (BV/TV) (**C**) in the different groups. MEM, native membrane; LYO, lyophilized membrane with conditioned media; SOAK, soaked membrane with conditioned media; CEL, membrane with rMSC; EMP, empty defects. Data represent means (n ≥ 5). * $p < 0.05$, **** $p < 0.001$.

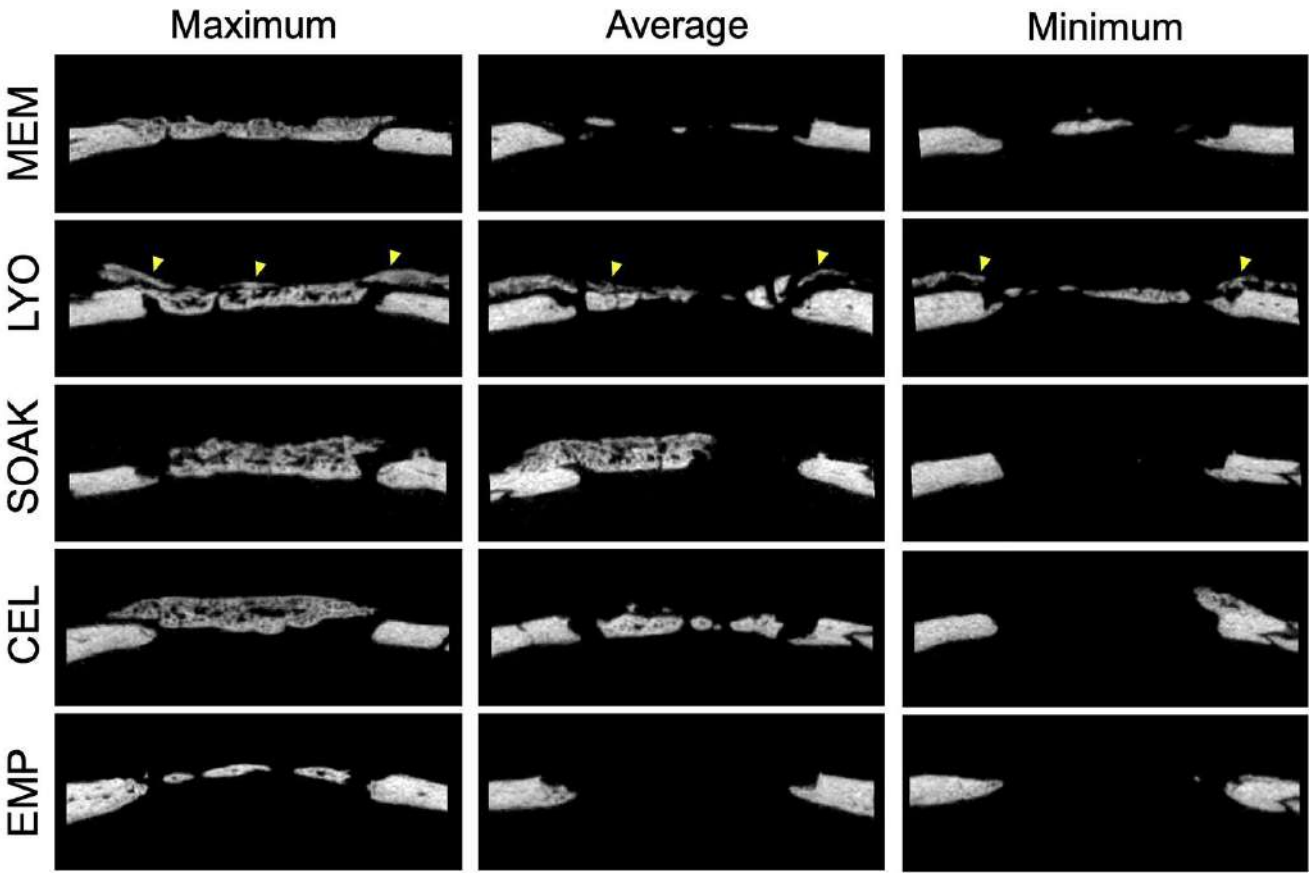

Figure 3. µCT analysis (continued). Representative µCT images of central slices at 4 weeks showing maximum, average and minimum bone formation in the different groups. Mineralization within the membrane component is indicated by yellow arrows in the LYO group representing hybrid bone and/or mineralized MEM fibers. MEM, native membrane; LYO, lyophilized membrane with conditioned media; SOAK, soaked membrane with conditioned media; CEL, membrane with rMSC; EMP, empty defects.

After 4 weeks, only CM-LYO (78.9 ± 13.08%) showed significantly greater bone coverage than the untreated control group did (28.99 ± 18.64%; $p = 0.027$); those of the CM-SOAK (46.97 ± 37.12%), CEL (56.07 ± 29.22%) and native MEM groups (57.89 ± 30.9%) were similar. No differences in BV/TV were observed in CM-LYO (8.41 ± 1.87%) vs. that in the CM-SOAK (6.64 ± 7.01%; $p = 0.947$), CEL (7.72 ± 5.78%; $p = 0.99$), native MEM (5.7 ± 4.21%; $p = 0.83$) and empty groups (2.68 ± 2.24%; $p = 0.25$). Notably, the smallest intra-group variation was observed in the CM-LYO group (Figures 2A,B and 3).

3.3. CM-LYO Promoted Histological New Bone Formation Better than Other Treatments Did

After 4 weeks, all the groups revealed a heterogeneous histological pattern combining the following tissue components: regular new bone (without incorporated MEM fibers), hybrid new bone (with incorporated MEM fibers), mineralized MEM fibers, residual MEM and soft tissues (Figures 4 and 5). New bone was typically seen at the base of the defect towards the dura, i.e., outside the MEM compartment, characterized by well-structured woven bone (dark pink) and enclosed by layers of parallel-fibered bone (light pink) and

osteoid matrix (grey). Adjacent to this newly formed bone, areas with a hybrid pattern characterized by the presence of immature woven bone and incorporated collagen fibers from the MEM (pink) were evident, indicating that some new bone formation occurred *within* the MEM compartment. In some cases, the MEM fibers appeared to be mineralized and formed bridges to the woven bone, while in other instances we observed mineralized 'free-standing' fibers (without surrounding woven bone) or remnant collagen fibers (unmineralized). Hybrid bone also appeared to vary based on the degree of mineralization of the embedded MEM fibers; the orientation of fibers followed the structure of the MEM. These different tissue types were observed in all the experimental groups, albeit in different proportions, as revealed in the histomorphometric analysis (Figures 5 and 6).

The quantification of tissues in the central defect area revealed significantly greater amount of new bone in CM-LYO (34.35 ± 17.27%) vs. that in the CM-SOAK (9.66 ± 11.36%; $p = 0.005$), native MEM (8.63 ± 9.09%; $p = 0.007$) and CEL groups (13.46 ± 12.76%; $p = 0.025$) (Figure 6). Conversely, CM-LYO revealed the least amount of hybrid bone (5.42 ± 3.77%) vs. that in the CM-SOAK (11.67 ± 11.89%), MEM (18.5 ± 20.74%) and CEL groups (13.7 ± 19.23%), although this was not statistically significant ($p = 0.43$). The quantification of total new bone (new bone + hybrid bone) revealed a non-significant trend ($p = 0.45$) in CM-LYO (39.77 ± 19.85%) vs. that in the CM-SOAK (21.33 ± 22.25%), MEM (27.14 ± 28.02%) and CEL groups (27.16 ± 23.24%). CM-LYO also revealed the greatest area of mineralized MEM fibers (12.88 ± 16.01%) and the least area of residual MEM (5.5 ± 10.79%) vs. that of the other groups; the latter comparison was statistically significant ($p < 0.001$) (Figure 6). The intra-group variations, particularly for new bone, total new bone and residual MEM areas were relatively large. The quantification of tissue fractions in the defect edge areas revealed similar trends for the total new bone, mineralized MEM fibers and residual MEM between the groups (Supplementary Figure S4).

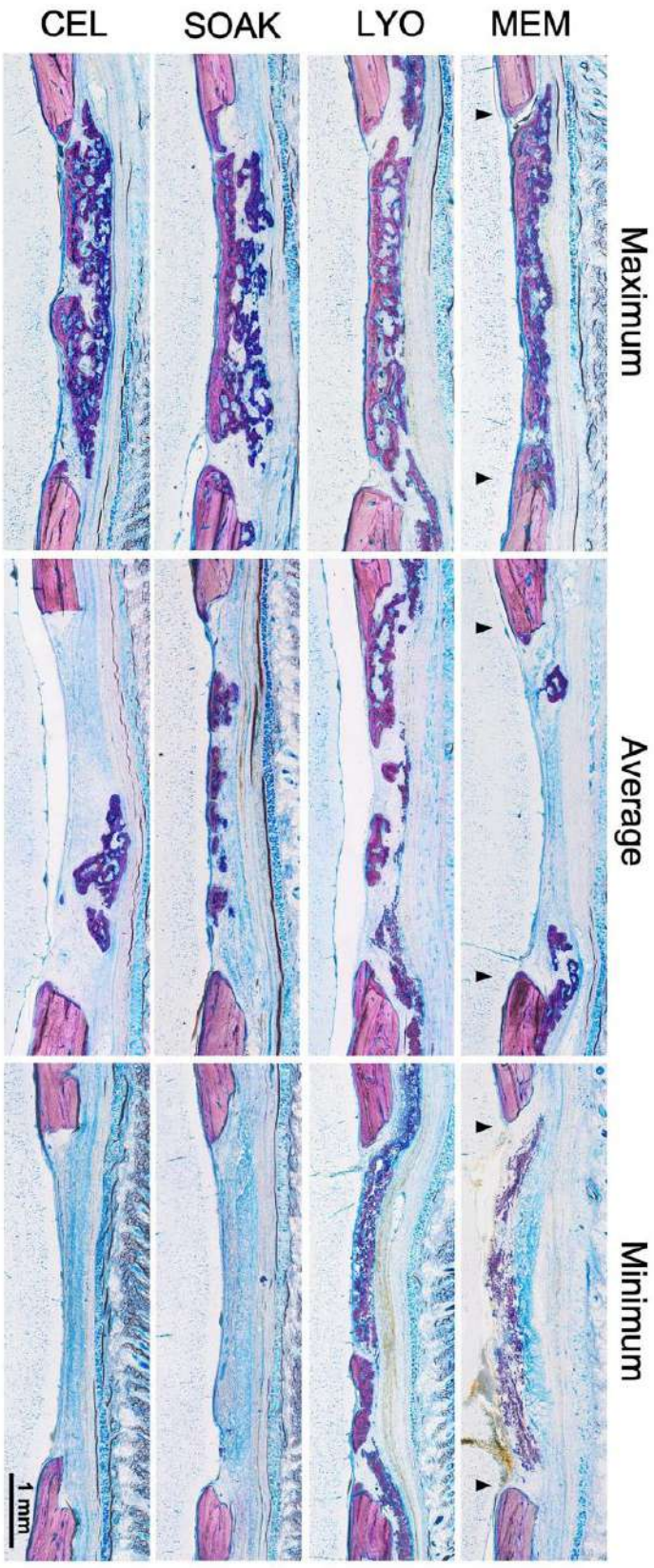

Figure 4. Histological analysis. Representative histological images after 4 weeks showing maximum, average and minimum bone regeneration in the different groups. Arrows indicate the defect edges. MEM, native membrane; LYO, lyophilized membrane with conditioned media; SOAK, soaked membrane with conditioned media; CEL, membrane with rMSC. Scale bar: 1 mm.

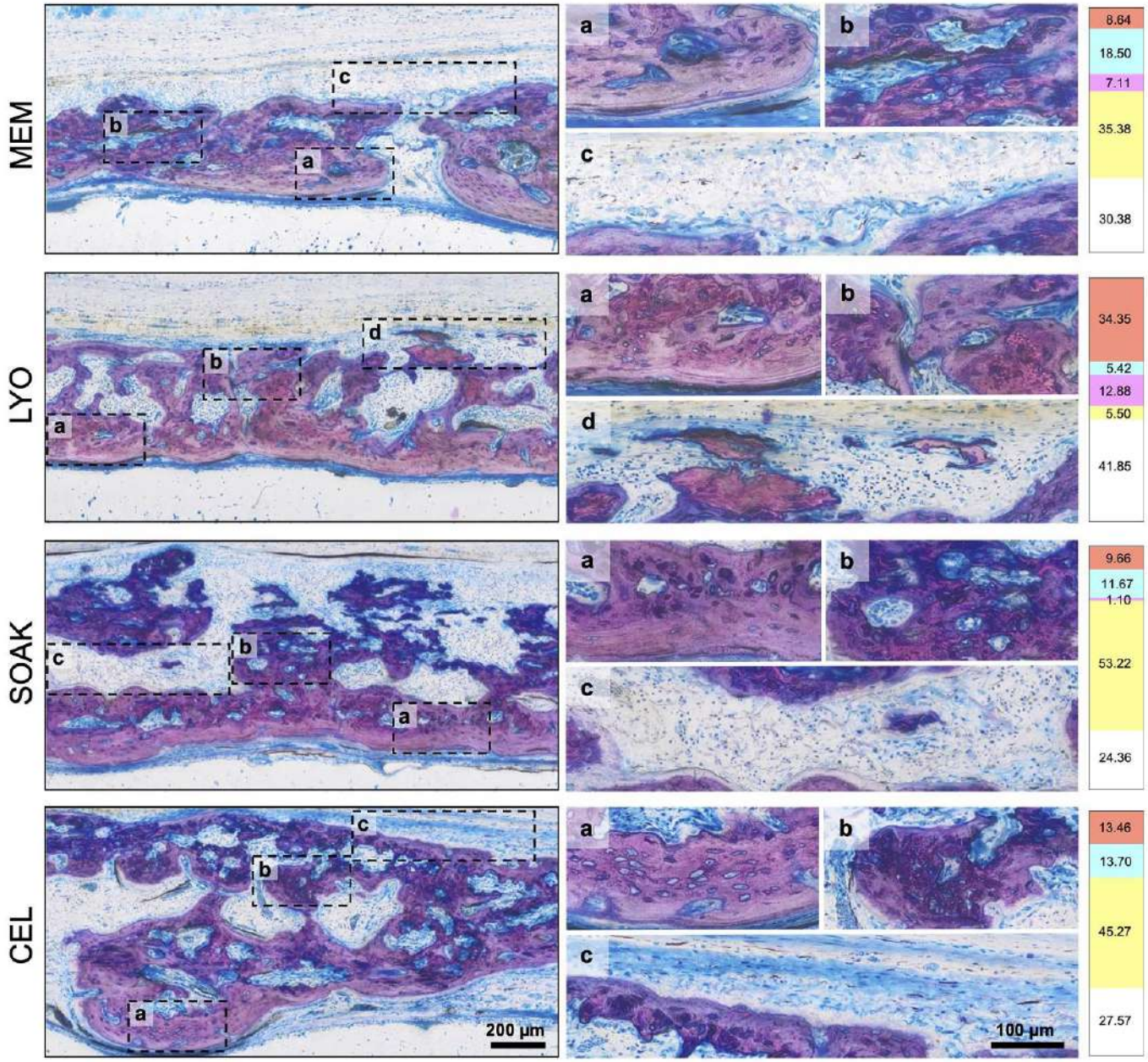

Figure 5. Histological analysis (continued). Representative histological images at higher magnification showing the different analyzed tissues in the experimental groups. The left panel shows a region of interest in each group with outlined sub-regions, which are enlarged in the right panel (scale bars: left panel 200 µm; right panel 100 µm). Each sub-region shows a specific tissue type indicated by letters (a–d). Numbers in the far right panel indicate relative percentages of tissue area in each group (for the whole group) based on color coding. Letters and colors indicate each tissue type: new bone (a, red), hybrid bone (b, cyan), residual membrane (c, yellow) and mineralized fibers (d, pink). White color in the far right panel indicates soft tissue areas.

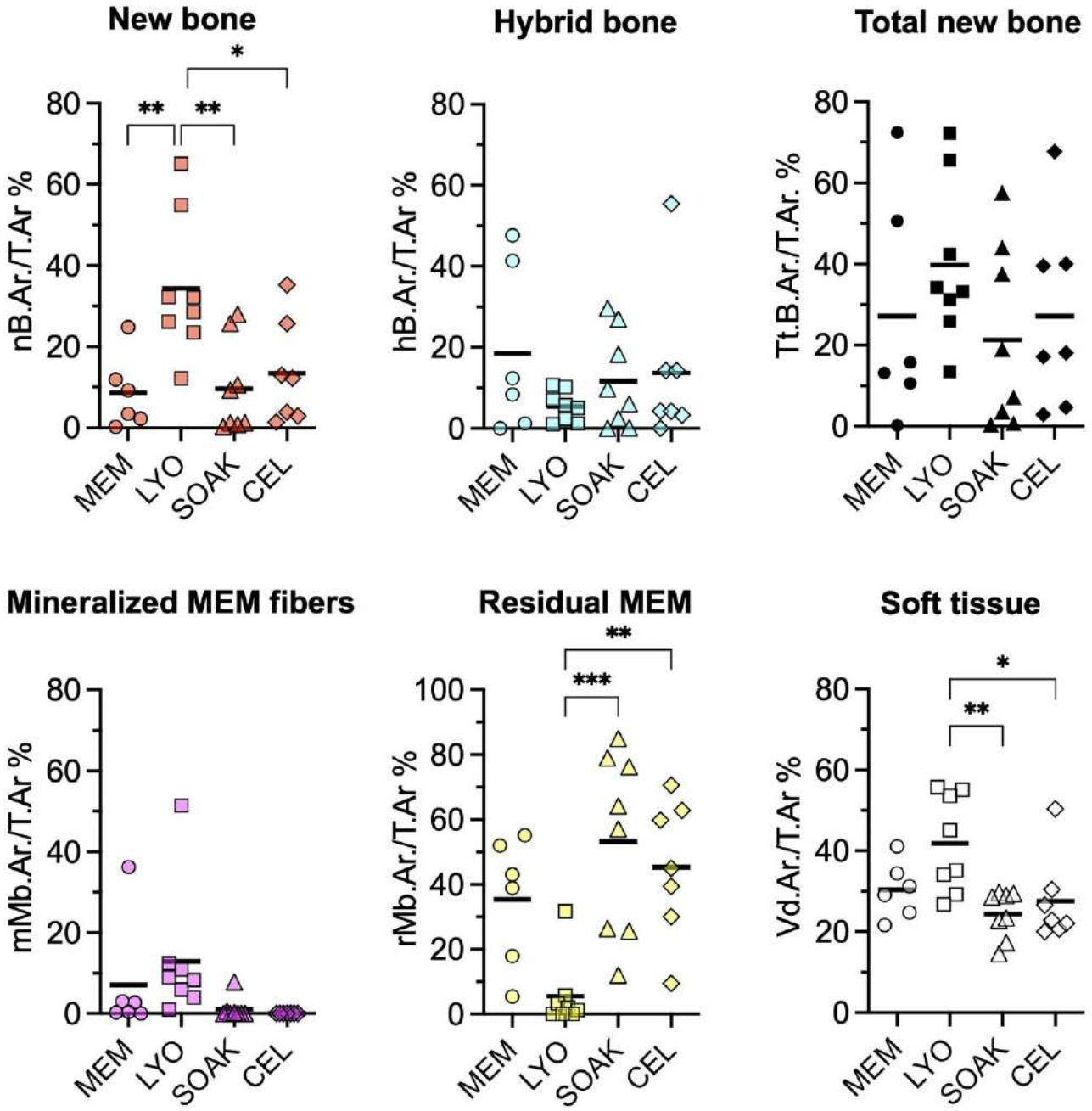

Figure 6. Histomorphometry of central defect regions. Quantification of histomorphometric parameters: T.Ar., Total Area; nB.Ar., New Bone Area; hB.Ar., Hybrid Bone Area; Tt.B.Ar., Total New Bone Area (New Bone + Hybrid Bone Area); mMb.Ar., Mineralized Membrane Area; rMb.Ar., Residual Membrane Area; Vd.Ar., Void Area; MEM, native membrane; LYO, lyophilized membrane with conditioned media; SOAK, soaked membrane with conditioned media; CEL, membrane with rMSC. Data represent means ($n \geq 5$). * $p < 0.05$, ** $p < 0.01$, *** $p < 0.001$.

3.4. Structural, Mechanical and Compositional Differences Were Observed between Regular New Bone and Hybrid New Bone

The SEM analysis of the ultrastructure of new bone tissues confirmed that new bone (without incorporated MEM fibers) was most similar to the native calvaria bone, while hybrid bone (with incorporated MEM fibers) was more heterogenous. Detailed SEM analysis of hybrid bone revealed clear differences based on the degree of mineralization of the incorporated MEM fibers. Accordingly, the hybrid bone was further categorized as stage 1 (early stage, less mature and moderately mineralized) or stage 2 hybrid bone (later stage,

more mature and highly mineralized) (Figure 7A). In the corresponding histology and SEM, stage 2 hybrid bone revealed evidence of resorption (cement lines) and remodeling, with the associated new bone deposition enveloping the hybrid bone (Figure 7A).

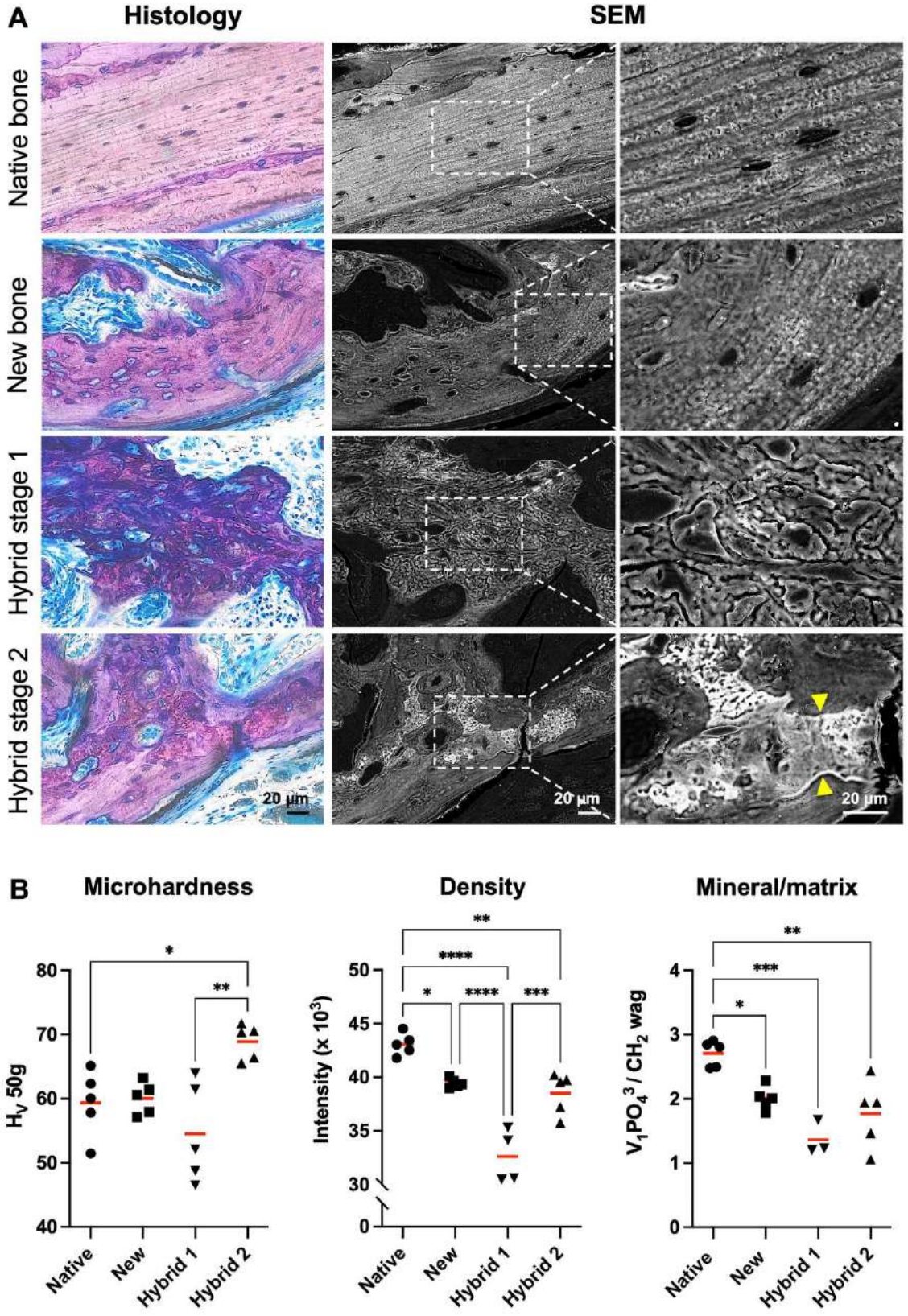

Figure 7. Characterization of new and hybrid bone. (**A**) Representative histological and corresponding

scanning electron microscopy (SEM) images of native calvarial bone, new bone, hybrid stage 1 and hybrid stage 2 bones. Hybrid stage 1 and stage 2 bones are differentiated by degree of mineralization reflected by brightness in SEM images (a brighter area = more mineralized bone). Yellow arrows indicate cement lines characteristic of bone remodeling. Scale bars: 20 µm. (**B**) Quantification of microhardness (Vickers test), relative bone density (µCT), and mineral/matrix ratio (Raman spectroscopy) in native calvarial bone (Native), new bone (New), hybrid bone at stage 1 (Hybrid 1) and hybrid bone at stage 2 (Hybrid 2) in representative histological sections from each group ($n \geq 3$ per group). Hv, Vickers hardness value; v_1 PO_4^3, v_1 phosphate peak; $FWHM^{-1}$, full peak width at half maximum intensity for v_1 PO_4^3 peak. Data represent means. * $p < 0.05$, ** $p < 0.01$, *** $p = 0.001$, **** $p < 0.001$.

The quantitative analysis of the regular and hybrid new bone tissues was also performed based on their microhardness (Vickers test) and composition (µCT and Raman spectroscopy), in comparison to the native calvaria bone. Mechanical loading by Vickers indentation revealed significantly greater hardness in stage 2 vs. that in stage 1 hybrid bone and new bone ($p = 0.002$; Figure 7B). The bone density analysis demonstrated similar densities in the stage 2 hybrid bone and new bone, but a significantly lower density in stage 1 hybrid bone ($p < 0.001$; Figure 7B). No significant differences were observed in the mineral/matrix ratio (v_1 PO_4^3/CH_2 wag) (Figure 7B) or crystallinity (v_1 PO_4^3 $FWHM^{-1}$) between the new bone and stage 1 and 2 hybrid bones. A trend for lower mineral/matrix ratio was observed in stage 1 vs. stage 2 hybrid bone and new bone ($p = 0.07$). However, mineral/matrix ratios of all three tissues were significantly lower than that of native bone (Figure 7B). Representative Raman spectra are presented in Supplementary Figure S5**.**

3.5. Qualitative Proteomic Analysis of Lyophilized CM Revealed Enrichment of Biological Processes Related to Bone Formation

The proteomic analysis revealed 2684 proteins in the lyophilized pooled CM, of which 255 proteins were involved in selected biological processes related to bone formation (Table 1, Supplementary Table S2). Among the classical growth factors, transforming growth factor beta-1 (TGFβ1), TGFβ2, BMP1, platelet derived growth factor subunit-A (PDGFA), vascular endothelial growth factor-C (VEGFC), insulin-like growth factor-2 (IGF2), c-type lectin domain containing 11A or stem cell growth factor (CLEC11A/SCGF) and colony stimulating factor-1 (CSF1) were identified. Several proteins related to angiogenesis (VEGF-C, von Willebrand factor (VWF), vascular cell adhesion molecule-1 (VCAM1) and platelet endothelial cell adhesion molecule-1 (PECAM1), etc.) and ECM (collagens, laminins, fibronectin, etc.) were also identified in the CM.

Table 1. Summary of proteins in lyophilized pooled CM representing selected biological processes related to bone formation.

Bone-Related Process (GO Term) and Associated Proteins Identified in CM (Gene Name)
GO:0030198 Extracellular matrix organization
63 proteins: MMP2, COL1A1, EMILIN1, COL18A1, PXDN, TNXB, PRDX4, COL5A2, ADAMTSL4, MMP1, COL4A2, MMP3, MMP8, POSTN, COL4A1, COL11A1, COL8A2, ADAMTSL1, CYR61, COL1A2, NID1, MMP13, COL15A1, TNFRSF11B, B4GALT1, FBLN1, VTN, ABI3BP, ADAMTSL2, PTX3, COL3A1, ECM2, CCDC80, COL14A1, RECK, OLFML2B, MATN2, COL5A1, TGFBI, APP, MMP9, COL4A5, ADAMTS2, NDNF, MMP20, OLFML2A, COL8A1, ADAMTS12, COL5A3, MMP14, COL16A1, PDGFRA, COL24A1, ADAMTS7, COL4A3, ELN, ADAMTS4, MATN3, ADAMTS1, COL2A1, SMOC1, COL10A1, ADAMTS5
GO:0030509 BMP signaling pathway
15 proteins: PDCD4, TGFB1, TWSG1, EXT1, USP15, COMP, TGFB2, MEGF8, SMAD4, ENG, FST, WNT5A, NOTCH2, RGMB, TGFB3
GO:0030513 Positive Regulation of BMP signaling pathway
10 proteins: TWSG1, UBE2O, ILK, SMAD4, ENG, NUMA1, CDH5, SCUBE3, NOTCH2, SULF1

Table 1. *Cont.*

Bone-Related Process (GO Term) and Associated Proteins Identified in CM (Gene Name)
GO:0045667/9 Regulation of osteoblast differentiation (positive regulation) 19 proteins: PPP3CA, PTK2, CTNNB1, CLIC1, PRKACA, PDLIM7, FBN2, JAG1, ILK, FERMT2, LTF, IL6ST, YAP1, SCUBE3, FAM20C, IL6, SMOC1, TMEM119, CTHRC1
GO:0060349 Bone morphogenesis 8 proteins: GLG1, EXT1, COMP, MMP13, PAPPA2, LTF, LTBP3, SFRP4
GO:0046849 Bone remodeling 4 proteins: RAB7A, NOTCH2, LTBP3, GJA1
GO:0046850/GO:0045780 Regulation of bone remodeling (positive and negative regulation) 9 proteins: TF, SPP1, SRC, TFRC, SYK, ITGB3, LTBP3, GREM1, MDK
GO:0030282 Bone mineralization 12 proteins: CLEC3B, MINPP1, COMP, SBDS, COL1A2, MMP13, ENPP1, LOX, LTBP3, ALPL, PTN, ALOX15
GO:0030500/1 Regulation of bone mineralization (positive regulation) 13 proteins: OMD, TGFB1, COMP, AHSG, FBN2, ECM1, ISG15, ENPP1, FAM20C, PTN, TGFB3, TMEM119, ATP2B1
GO:0001503 Ossification 34 proteins: COL1A1, CLEC3B, COL5A2, SPP1, CDH11, TWSG1, EXT1, EGFR, MINPP1, COMP, BMP1, AHSG, CLEC11A, COL11A1, EXT2, PDLIM7, OSTF1, CSF1, ECM1, CBFB, IGF2, LTF, FSTL3, GPLD1, MMP9, ADAMTS12, MMP14, ADAMTS7, PTN, LRRC17, ALOX15, STC1, COL2A1, TMEM119
GO:0030278/GO:0045778 Regulation of ossification (positive regulation) 7 proteins: MAPK1, TGFB2, PTPN11, CSF1, MAPK14, WNT5A, PTN
GO:0016055 Wnt signaling pathway 20 proteins: DDB1, SLC9A3R1, CTNNB1, CUL3, TAX1BP3, CPE, TGFB1I1, PTK7, DAB2, PLCG2, RECK, TMEM198, STRN, WNT5A, NXN, CTNND1, ROR1, SFRP4, WNT5B, DDX3X
GO:0030111 Regulation of Wnt signaling pathway 4 proteins: PPP2CA, PPP2R1A, APP, SNX3
GO:0007219 Notch signaling pathway 16 proteins: FAT4, GOT1, TGFB1, ADAM17, CFD, JAG1, ADAM10, POFUT1, ANXA4, APP, WDR12, SORBS2, NOTCH2, EPN1, IFT74, TGFBR2
GO:0008593 Regulation of Notch signaling pathway 6 proteins: POSTN, ADAM10, CD46, IL6ST, POFUT1, LFNG
GO:0001525 Angiogenesis 86 proteins: MMP2, ITGA5, PDCL3, CSPG4, HRG, SHC1, PTK2, COL18A1, PXDN, FN1, YWHAZ, THY1, EPHB3, BSG, ANXA2, PDCD6, COL4A2, HMOX1, ANGPTL4, MFGE8, CLIC4, PDGFA, APOD, MYDGF, NCL, COL4A1, CALD1, COL8A2, ACTG1, TYMP, UNC5B, NRP1, COL15A1, MYH9, NRP2, ERAP1, JAG1, CXCL8, ECM1, MAPK14, VEGFC, ITGAV, VWF, MCAM, ANG, VAV2, CCL2, PDCD10, ANGPT1, ENG, PECAM1, FAP, ITGA2B, PIK3CA, SYK, GLUL, AIMP1, ANPEP, SERPINE1, VCAM1, POFUT1, ADAM15, TGFBI, HSPG2, FLNA, WASF2, EPGN, NDNF, PDGFRB, VEGFA, COL8A1, PLXND1, MMP14, SRPX2, CCBE1, EPHB2, FLT4, ESM1, PARVA, EGFL7, NPR3, GREM1, TNFRSF12A, AAMP, EFNB2, CAV1

GO, gene ontology. A complete list of gene names is provided in Supplementary Table S2.

The concentrations of selected bone-related cytokines in the lyophilized CM were further determined using a multiplex immunoassay; of the 31 array cytokines, 7 were present at detectable concentrations (Figure 8). Consistent with the proteomic analysis, matrix metalloproteinases-2 (MMP2) and -13 (MMP13), interleukins-6 (IL6) and -11 (IL11) and VCAM1 were detected in the pooled CM.

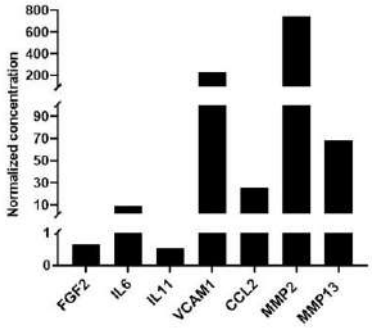

Figure 8. Multiplex immunoassay. Normalized concentrations of cytokines (pg cytokine/μg total protein) detected in CM using a human bone metabolism array (Supplementary Table S3). Data represent means of 4 technical replicates of a single sample of pooled CM (3 MSC donors).

4. Discussion

Cell-free strategies using MSC-CM are emerging as cost-effective, 'off-the-shelf' alternatives to MSC transplantation for the regeneration of bone defects [17]. In the present study, we tested the efficacy of CM-functionalized MEM (CM-LYO, CM-SOAK) vs. that of native MEM or MEM seeded with allogeneic rMSC (CEL) for GBR in critical size rat calvaria defects. The main finding was that a trend for enhanced bone regeneration was observed in the CM-LYO group compared to the CM-SOAK, native MEM and CEL groups based on μCT and histological analysis.

The secretome/CM of MSC contains a plethora of different proteins, including growth factors, cytokines, chemokines and cell adhesion molecules, as well as lipids, nucleic acids and extracellular vesicles, which promote tissue healing and regeneration [45–48]. Consistent with previous reports [16], the data from the present study show that the exposure of BMSC to CM resulted in a significant upregulation of osteogenic gene markers. Additionally, we have recently reported that CM contain several antiapoptotic and antioxidative factors, which may inhibit apoptosis and/or promote cell survival [49]. From a clinical perspective, CM delivery presents clear advantages compared to implementing autologous cell therapies, since it is easier, cheaper and enables large-scale production [50,51]. Moreover, its application may be under less stringent regulation compared to that of cell therapies, which may facilitate faster clinical translation.

In the present study, MSC cultured in 'xeno-free' HPL-supplemented media were used for CM preparation. Most studies thus far have investigated CM from MSC cultured in 'xenogeneic', i.e., FBS-supplemented media, both in vitro [16] and in vivo (Supplementary Table S4). However, the exclusion of animal-derived supplements in MSC cultures is important for clinical translation and is in fact recommended by regulatory authorities [52]. Pooled HPL has been identified as the optimal xeno-free supplement for clinical grade MSC cultures [53], with particular benefits for osteogenic differentiation [27,54]. Indeed, the type of supplement can influence the composition and efficacy of the CM [55,56]. A few studies have investigated the composition of CM from HPL- vs. FBS-cultured MSC [47,57,58]. Recent evidence suggests that CM from HPL-cultured MSC are more 'enriched' in certain growth factors related to wound healing, angiogenesis and extra-cellular matrix (ECM) production [58], which may further promote their in vivo regenerative potential.

The in vivo applications of MSC-CM for bone regeneration have recently been reviewed [17] and are summarized in Supplementary Table S4. All the studies reported superior outcomes in bone defects treated with CM vs. those of control treatments in experimental in vivo investigations (mainly in rodent or rabbit models), although one study in a canine model also reported superior periodontal regeneration when comparing CM vs. PBS [59]. While a majority of the studies applied CM to bone defects using biomaterials, interestingly, CM also promoted regeneration when injected locally [60,61] and systemically [62] in challenging rodent models. Overall, while the current literature supports the use of CM for bone regeneration, certain aspects of this strategy remain unclear, such as,

the optimal method/biomaterial for CM delivery and the optimal method of biomaterial functionalization for the best in vivo efficacy.

CM have been delivered using different biomaterials including collagen sponges, hydrogels, bone substitutes, barrier membranes and other scaffolds (Supplementary Table S4). Specifically, barrier membranes such as poly(lactic-co-glycolic acid) [63] and collagen [64,65] have been used, given their ability to absorb and release biomolecules at regeneration sites [19,21]. These biomolecules have included bone-derived proteins [23,24], BMP2 [66–68], fibroblast growth factor-2 [69] and dexamethasone [70], as recently summarized [4]. With regard to the collagen membranes used in the present study (MEM), we have previously demonstrated their ability to adsorb growth factor, specifically TGFβ, activity from human biological material [25]. Furthermore, Qiu et al. [19] recently reported the application of MEM soaked with CM from human periodontal- or gingiva-derived MSC in rat periodontal defects; significantly greater bone formation was observed in the defects treated with MEM-CM vs. those treated with native MEM [65]. Together, these data suggest that MEM are efficient carriers of bioactive factors, including CM, for GBR applications.

To identify the optimal method of functionalization herein, MEM were treated with concentrated CM (~30-fold) by either soaking only (CM-SOAK) or soaking followed by lyophilization (CM-LYO). The application of concentrated CM is reported to enhance tissue regeneration as compared that of unconcentrated CM [71]. Moreover, lyophilization or 'freeze drying' is reported to preserve the biological activity of proteins, e.g., growth factors, and other biological components for long-term storage [72]. Following MEM functionalization, both CM-LYO and CM-SOAK showed high cell viability, suggesting that they could be rapidly populated by resident cells following in vivo implantation. In the context of growth factors, the lyophilization of BMP2 on scaffolds, as compared to soaking, has been shown to enhance in vivo release and bone regeneration [73]. Indeed, CM-LYO showed superior bone regeneration compared to CM-SOAK in the present study. The lyophilization process may have resulted in superior concentration/immobilization and the subsequent in vivo release of proteins on/from the MEM, thus enhancing bone formation [74,75]. To exclude any effect of lyophilization on the MEM properties, we later studied the effects of lyophilized MEM (with serum-free DMEM) in the same calvaria defect model; a similar histological pattern was seen for the lyophilized MEM group as in the present study, suggesting no significant effect of the lyophilization process (unpublished data). Since lyophilization is a well-established and GMP-compliant process, this strategy could offer new possibilities for 'off-the-shelf' CM-based therapies for GBR.

Allogeneic MSC transplantation has been proposed as an easier, more cost-effective, and equally safe and efficacious alternative to autologous cell therapy [76]. This is based on the unique ability of MSC to modulate immune responses and avoid detection/rejection in dissimilar hosts [77]. Comparable or superior outcomes have been reported in in vivo models of bone regeneration when the researchers were using allogeneic vs. autologous cells [78–82]. In the present study, MEM seeded with pooled non-autologous rMSC (CEL) from syngeneic donor rats were also transplanted into calvarial defects. Trends of greater bone regeneration were observed in CM-LYO vs. that of the CEL-treated defects, which is consistent with previous reports of using CM and the corresponding cells, i.e., human BMSC [83], stem cells from human exfoliated deciduous teeth (SHED) [84] or rat adipose MSC [85]. Indeed, the present study used an inbred/syngeneic strain of rats, where the genetic diversity between the individuals, i.e., donor and recipient rats, was limited, and therefore, the cell source may not be strictly allogeneic. Moreover, immunological reactions to allogeneic/xenogeneic cells may not be accurately reflected in simple rodent models [86]. Thus, the true efficacy of CM vs. that of allogeneic MSC should be verified in large animal models of bone regeneration.

Inherent clinical limitations of resorbable MEM are their poor dimensional stability and sub-optimal mechanical strength and stiffness, which may result in their collapse into the bony defect unless they are supported by a biomaterial scaffold [20]. To enhance their

long-term rigidity and stability, the concept of in vivo "self-mineralizing" membranes has been reported [87,88]. In the present study, in vivo MEM mineralization was observed, especially in the CM-LYO-treated MEM. This phenomenon of in vivo mineralization of collagen MEM was previously described by Feher et al. and is attributed to a potentially cell-independent mechanism [38]. It is reported that the hydrophobic nature of collagen MEM can facilitate calcium binding and mineralization by enhanced protein adsorption [89]. In the present study, the CM-LYO group exhibited the greatest histological area fraction of mineralized MEM fibers and new bone (without MEM fibers). The presence of stage 2 hybrid bone around the mineralized MEM fibers clearly indicates that MEM mineralization proceeded to new bone formation within the MEM compartment. Therefore, it is reasonable to hypothesize that MEM mineralization may have contributed to the overall bone regeneration, especially in the CM-LYO group.

An interesting finding in the present study was the heterogeneous pattern of new bone formation based on whether MEM collagen fibers were incorporated or not into the newly formed bone, i.e., new bone formation *within* and *outside* the membrane compartment. Indeed, the new bone outside the membrane compartment was histologically most similar to the native calvarial bone. In contrast, the hybrid bone (within the membrane compartment) was notably different from the native bone. A further analysis revealed distinct stages of hybrid bone formation based on the degree of mineralization of the MEM fibers, i.e., stage 1 (less mineralized) and stage 2 (more mineralized). This most likely reflects the stage of maturation, since an increasing degree of mineralization is a known age-related change in mineralized tissue [90]. Consequently, stage 2 hybrid bone demonstrated significantly greater hardness—an important indicator of bone strength mainly determined by the degree of mineralization [91]—than the new bone and even the native calvarial bone did. However, both the hybrid bone (stage 1 and 2) and new bone revealed significantly lower mineral/matrix ratios vs. that of the native calvaria bone. These data are similar to previous comparisons between new and native bone in rat calvaria [92,93] and to recent studies of bone regeneration following cell [94] and/or scaffold implantation [95]. With regard to its 'fate', the hybrid bone, particularly stage 2, showed signs of remodeling and replacement by new bone. This could potentially explain the relatively lower area of hybrid bone and the greater area of new bone (without MEM fibers) in the CM-LYO group. Taken together, the current data suggest that the use of MEM in rat calvaria results in a combination of regular new bone and hybrid new bone characterized by the incorporation of MEM in the newly formed bone. While further time course studies are needed to determine the exact sequence of events (with regard to MEM mineralization and hybrid bone formation), it appears that the hybrid bone is ultimately remodeled and replaced by regular new bone, and this process may be accelerated in CM-LYO-treated MEM.

The proteomic composition of lyophilized pooled CM was analyzed as the potential basis for its in vivo effects. Indeed, previous studies have comprehensively described the general proteomic profile of MSC [47,96], therefore, in the present study, we focused only on bone-related processes. Several key growth factors (TGFβ1, TGFβ2, PDGFA, VEGFC, etc.) involved in biological processes relevant to bone regeneration (Table 1) were identified in MSC-CM. Correspondingly, the expressions of several osteogenesis-related genes were enhanced in human BMSC upon exposure to CM for 48 h (Supplementary Figure S3), suggesting a pro-osteogenic effect. Moreover, several proteins related to Wnt/β-catenin signaling, a key signaling pathway during osteoblastogenesis [97], and angiogenesis were enriched in CM. In the context of MEM, Wnt-related [98] and angiogenesis-related proteins [4], in addition to TGFβ [25], have been shown to adsorb to collagen, revealing the potential mechanisms of MEM-CM activity. Correspondingly, areas of active in vivo bone formation (Supplementary Figure S6) and angiogenesis were observed in the present study. However, no remarkable differences in these events could be detected between the groups, which could be due to the relatively late time point of the histological analysis (4 weeks). Therefore, no reliable correlations between the in vitro and in vivo data could be drawn. The inclusion of earlier time points (1–2 weeks) and immunohistochemical methods in

future studies to detect specific cells/processes may reveal such associations and their effects on in vivo bone regeneration. Nevertheless, the present study supports the current evidence for the efficacy of MSC-CM for in vivo bone regeneration [59–65,99–108].

Some limitations of the present study must be acknowledged. Firstly, the proteomic analysis was performed using only pooled CM (3 MSC donors) and not CM from independent donor-MSC, thus precluding the assessment of donor related variations. Secondly, human-derived MSC-CM were compared to rat-derived MSC (from syngeneic rats) in vivo, which may have cofounded the findings. However, the use of human-derived MSC would necessitate the use of immunocompromised animals, while the use of rat-derived MSC-CM would limit the clinical relevance of the therapy. The intra-group variations in the in vivo data were relatively large, reflecting biological differences in the healing response between the animals. Nevertheless, the measures of central tendency were reliable enough to allow the detection of statistically significant differences between the groups. Finally, in vitro assessments of protein adsorption and 'release' from the different functionalized membranes (CM-LYO and CM-SOAK) in future studies could shed light on potential differences in their mechanisms of action and their in vivo effects on bone regeneration.

5. Conclusions

Application of CM-LYO-functionalized MEM revealed a trend for enhanced GBR in rat calvaria defects compared to that of conventional GBR (MEM alone) and cell therapy (MEM with rMSC). The regenerated tissues presented a combination of regular new bone and hybrid new bone characterized by bone formation within the membrane compartment and incorporation of MEM in the newly formed bone. Further research is needed to determine the functional properties of these new bone tissues in terms of supporting implant osseointegration and prosthetic loading in more clinically relevant animal models. Moreover, future refinements of the study design and methodology may reveal correlations between the proteome of CM and in vivo processes. In summary, functionalizing MEM with MSC-CM represents a clinically relevant, 'off-the-shelf' strategy to promote GBR.

Supplementary Materials: The following supporting information can be downloaded at: https://www.mdpi.com/article/10.3390/cells12050767/s1, Figure S1: Histomorphometry segmentation; Figure S2: Cell viability on MEM; Figure S3: Gene expression assay; Figure S4: Histomorphometry of side regions; Figure S5: Raman spectroscopy; Figure S6: Histology; Table S1: Real time PCR primers; Table S2: List of proteins in CM representing selected bone-related processes; Table S3: List of cytokines included in the human bone metabolism multiplex array (n = 31); Table S4: In vivo studies of CM for bone regeneration..

Author Contributions: S.S., R.G. and K.M. conceived and designed the study. S.S. performed the experiments, data collection, data analysis and drafted the manuscript. C.K., N.A.-S., S.M.-A., K.A.A.A., P.H., S.T., A.B. and N.R. assisted with experiments, sample preparation, data collection, data analysis/interpretation and/or drafting the manuscript. M.S., E.K.K., K.M. and R.G. assisted with data analysis/interpretation, drafting the manuscript and funding acquisition. All authors have read and agreed to the published version of the manuscript.

Funding: This work was supported by the Osteology Foundation, Switzerland (18-152), Helse Vest Research Funding, Norway (F-12124), Research Council of Norway (273551 and 302043), Olav Thon Foundation, Norway, and Trond Mohn Foundation, Norway (BFS2018TMT10).

Institutional Review Board Statement: The use of human cells and tissues was approved by the Regional Committees for Medical Research Ethics (REK) in Norway (2013-1248/REK sør-øst C). Animal experiments were approved by the Norwegian Animal Research Authority (Mattilsynet; FOTS-17443) and performed in accordance with the ARRIVE guidelines.

Informed Consent Statement: Informed consent was obtained from all subjects involved in the study.

Data Availability Statement: Additional data are included in the Supplementary File and can further be made available by the authors upon request.

Acknowledgments: We thank the Bloodbank at Haukeland University Hospital for assistance with HPL production, the Molecular Imaging Center (MIC), University of Bergen, for assistance with microscopy, Heidi Espedal from the Dept. of Clinical Medicine, University of Bergen, for assistance with the in vivo CT scanning, Irene Heggstad from the Electron Microscopy lab, University of Bergen, for assistance with SEM, and Nils Roar Gjerdet and Odd Johan Lundberg from the Dept. of Clinical Dentistry, University of Bergen, for assistance with the Vickers testing. Mass spectrometry-based proteomic analyses were performed by the Proteomics Unit at the University of Bergen (PROBE). This facility is a member of the National Network of Advanced Proteomics Infrastructure (NAPI), which is funded by the Research Council of Norway (INFRASTRUKTUR-program project number: 295910).

Conflicts of Interest: The authors confirm that there are no known conflict of interest associated with this publication and there has been no significant financial support for this work that could have influenced its outcome.

References

1. Benic, G.I.; Hammerle, C.H. Horizontal bone augmentation by means of guided bone regeneration. *Periodontol. 2000* **2014**, *66*, 13–40. [CrossRef] [PubMed]
2. Thoma, D.S.; Bienz, S.P.; Figuero, E.; Jung, R.E.; Sanz-Martin, I. Efficacy of lateral bone augmentation performed simultaneously with dental implant placement: A systematic review and meta-analysis. *J. Clin. Periodontol.* **2019**, *46* (Suppl. S21), 257–276. [CrossRef] [PubMed]
3. Urban, I.A.; Montero, E.; Monje, A.; Sanz-Sanchez, I. Effectiveness of vertical ridge augmentation interventions: A systematic review and meta-analysis. *J. Clin. Periodontol.* **2019**, *46* (Suppl. S21), 319–339. [CrossRef] [PubMed]
4. Omar, O.; Elgali, I.; Dahlin, C.; Thomsen, P. Barrier membranes: More than the barrier effect? *J. Clin. Periodontol.* **2019**, *46* (Suppl. S21), 103–123. [CrossRef] [PubMed]
5. Chappuis, V.; Rahman, L.; Buser, R.; Janner, S.F.M.; Belser, U.C.; Buser, D. Effectiveness of Contour Augmentation with Guided Bone Regeneration: 10-Year Results. *J. Dent. Res.* **2018**, *97*, 266–274. [CrossRef] [PubMed]
6. Gimbel, M.; Ashley, R.K.; Sisodia, M.; Gabbay, J.S.; Wasson, K.L.; Heller, J.; Wilson, L.; Kawamoto, H.; Bradley, J. Repair of alveolar cleft defects: Reduced morbidity with bone marrow stem cells in a resorbable matrix. *J. Craniofacial Surg.* **2007**, *18*, 895–901. [CrossRef] [PubMed]
7. Shanbhag, S.; Suliman, S.; Pandis, N.; Stavropoulos, A.; Sanz, M.; Mustafa, K. Cell therapy for orofacial bone regeneration: A systematic review and meta-analysis. *J. Clin. Periodontol.* **2019**, *46* (Suppl. S21), 162–182. [CrossRef]
8. Sandor, G.K.; Numminen, J.; Wolff, J.; Thesleff, T.; Miettinen, A.; Tuovinen, V.J.; Mannerström, B.; Patrikoski, M.; Seppänen, R.; Miettinen, S.; et al. Adipose stem cells used to reconstruct 13 cases with cranio- maxillofacial hard- tissue defects. *Stem Cells Transl. Med.* **2014**, *3*, 530–540. [CrossRef]
9. Gjerde, C.; Mustafa, K.; Hellem, S.; Rojewski, M.; Gjengedal, H.; Yassin, M.A.; Feng, X.; Skaale, S.; Berge, T.; Rosen, A.; et al. Cell therapy induced regeneration of severely atrophied mandibular bone in a clinical trial. *Stem Cell Res. Ther.* **2018**, *9*, 213. [CrossRef]
10. Haumer, A.; Bourgine, P.E.; Occhetta, P.; Born, G.; Tasso, R.; Martin, I. Delivery of cellular factors to regulate bone healing. *Adv. Drug Deliv. Rev.* **2018**, *129*, 285–294. [CrossRef]
11. Caplan, A.I.; Dennis, J.E. Mesenchymal stem cells as trophic mediators. *J. Cell Biochem.* **2006**, *98*, 1076–1084. [CrossRef] [PubMed]
12. Gnecchi, M.; Danieli, P.; Malpasso, G.; Ciuffreda, M.C. Paracrine Mechanisms of Mesenchymal Stem Cells in Tissue Repair. *Methods Mol. Biol.* **2016**, *1416*, 123–146. [PubMed]
13. Pittenger, M.F.; Discher, D.E.; Péault, B.M.; Phinney, D.G.; Hare, J.M.; Caplan, A.I. Mesenchymal stem cell perspective: Cell biology to clinical progress. *NPJ Regen. Med.* **2019**, *4*, 22. [CrossRef]
14. Weiss, A.R.R.; Dahlke, M.H. Immunomodulation by Mesenchymal Stem Cells (MSCs): Mechanisms of Action of Living, Apoptotic, and Dead MSCs. *Front. Immunol.* **2019**, *10*, 1191. [CrossRef] [PubMed]
15. Bari, E.; Perteghella, S.; Di Silvestre, D.; Sorlini, M.; Catenacci, L.; Sorrenti, M.; Marrubini, G.; Rossi, R.; Tripodo, G.; Mauri, P.; et al. Pilot Production of Mesenchymal Stem/Stromal Freeze-Dried Secretome for Cell-Free Regenerative Nanomedicine: A Validated GMP-Compliant Process. *Cells* **2018**, *7*, 190. [CrossRef]
16. Veronesi, F.; Borsari, V.; Sartori, M.; Orciani, M.; Mattioli-Belmonte, M.; Fini, M. The use of cell conditioned medium for musculoskeletal tissue regeneration. *J. Cell Physiol.* **2018**, *233*, 4423–4442. [CrossRef] [PubMed]
17. Benavides-Castellanos, M.P.; Garzon-Orjuela, N.; Linero, I. Effectiveness of mesenchymal stem cell-conditioned medium in bone regeneration in animal and human models: A systematic review and meta-analysis. *Cell Regen.* **2020**, *9*, 5. [CrossRef]
18. Dahlin, C.; Linde, A.; Gottlow, J.; Nyman, S. Healing of bone defects by guided tissue regeneration. *Plast Reconstr. Surg.* **1988**, *81*, 672–676. [CrossRef]
19. Elgali, I.; Omar, O.; Dahlin, C.; Thomsen, P. Guided bone regeneration: Materials and biological mechanisms revisited. *Eur. J. Oral Sci.* **2017**, *125*, 315–337. [CrossRef]
20. Caballe-Serrano, J.; Munar-Frau, A.; Ortiz-Puigpelat, O.; Soto-Penaloza, D.; Penarrocha, M.; Hernandez-Alfaro, F. On the search of the ideal barrier membrane for guided bone regeneration. *J. Clin. Exp. Dent.* **2018**, *10*, e477–e483. [CrossRef]

21. Turri, A.; Elgali, I.; Vazirisani, F.; Johansson, A.; Emanuelsson, L.; Dahlin, C.; Thomsen, P.; Omar, O. Guided bone regeneration is promoted by the molecular events in the membrane compartment. *Biomaterials* **2016**, *84*, 167–183. [CrossRef]
22. Caballe-Serrano, J.; Sawada, K.; Miron, R.J.; Bosshardt, D.D.; Buser, D.; Gruber, R. Collagen barrier membranes adsorb growth factors liberated from autogenous bone chips. *Clin. Oral Implant. Res.* **2017**, *28*, 236–241. [CrossRef] [PubMed]
23. Kuchler, U.; Rybaczek, T.; Dobask, T.; Heimel, P.; Tangl, S.; Klehm, J.; Menzel, M.; Gruber, R. Bone-conditioned medium modulates the osteoconductive properties of collagen membranes in a rat calvaria defect model. *Clin. Oral Implant. Res.* **2018**, *29*, 381–388. [CrossRef] [PubMed]
24. Strauss, F.J.; Kuchler, U.; Kobatake, R.; Heimel, P.; Tangl, S.; Gruber, R. Acid bone lysates reduce bone regeneration in rat calvaria defects. *J. Biomed Mater. Res. A* **2021**, *109*, 659–665. [CrossRef] [PubMed]
25. Di Summa, F.; Kargarpour, Z.; Nasirzade, J.; Stahli, A.; Mitulovic, G.; Panic-Jankovic, T.; Koller, V.; Kaltenbach, C.; Müller, H.; Panahipour, L.; et al. TGFbeta activity released from platelet-rich fibrin adsorbs to titanium surface and collagen membranes. *Sci. Rep.* **2020**, *10*, 10203. [CrossRef]
26. Donos, N.; Dereka, X.; Mardas, N. Experimental models for guided bone regeneration in healthy and medically compromised conditions. *Periodontol 2000* **2015**, *68*, 99–121. [CrossRef]
27. Shanbhag, S.; Mohamed-Ahmed, S.; Lunde, T.H.F.; Suliman, S.; Bolstad, A.I.; Hervig, T.; Mustafa, K. Influence of platelet storage time on human platelet lysates and platelet lysate-expanded mesenchymal stromal cells for bone tissue engineering. *Stem Cell Res. Ther.* **2020**, *11*, 351. [CrossRef]
28. Rojewski, M.T.; Lotfi, R.; Gjerde, C.; Mustafa, K.; Veronesi, E.; Ahmed, A.B.; Wiesneth, M.; Körper, S.; Sensebé, L.; Layrolle, P.; et al. Translation of a standardized manufacturing protocol for mesenchymal stromal cells: A systematic comparison of validation and manufacturing data. *Cytotherapy* **2019**, *21*, 468–482. [CrossRef]
29. Al-Sharabi, N.; Mustafa, M.; Ueda, M.; Xue, Y.; Mustafa, K.; Fristad, I. Conditioned medium from human bone marrow stromal cells attenuates initial inflammatory reactions in dental pulp tissue. *Dent. Traumatol.* **2017**, *33*, 19–26. [CrossRef]
30. Peng, Y.; Xuan, M.; Zou, J.; Liu, H.; Zhuo, Z.; Wan, Y.; Cheng, B. Freeze-dried rat bone marrow mesenchymal stem cell paracrine factors: A simplified novel material for skin wound therapy. *Tissue Eng. Part A* **2015**, *21*, 1036–1046. [CrossRef]
31. Mohamed-Ahmed, S.; Fristad, I.; Lie, S.A.; Suliman, S.; Mustafa, K.; Vindenes, H.; Idris, S.B. Adipose-derived and bone marrow mesenchymal stem cells: A donor-matched comparison. *Stem Cell Res. Ther.* **2018**, *9*, 168. [CrossRef] [PubMed]
32. Shanbhag, S.; Suliman, S.; Mohamed-Ahmed, S.; Kampleitner, C.; Hassan, M.N.; Heimel, P.; Dobsak, T.; Tangl, S.; Bolstad, A.I.; Mustafa, K. Bone regeneration in rat calvarial defects using dissociated or spheroid mesenchymal stromal cells in scaffold-hydrogel constructs. *Stem Cell Res. Ther.* **2021**, *12*, 575. [CrossRef] [PubMed]
33. Yassin, M.A.; Leknes, K.N.; Pedersen, T.O.; Xing, Z.; Sun, Y.; Lie, S.A.; Finne-Wistrand, A.; Mustafa, K. Cell seeding density is a critical determinant for copolymer scaffolds-induced bone regeneration. *J. Biomed Mater. Res. A* **2015**, *103*, 3649–3658. [CrossRef]
34. Toriumi, D.M.; Raslan, W.F.; Friedman, M.; Tardy, M.E. Histotoxicity of cyanoacrylate tissue adhesives. A comparative study. *Arch. Otolaryngol. Head Neck. Surg.* **1990**, *116*, 546–550. [CrossRef]
35. Rezende, M.L.; Cunha Pde, O.; Damante, C.A.; Santana, A.C.; Greghi, S.L.; Zangrando, M.S. Cyanoacrylate Adhesive as an Alternative Tool for Membrane Fixation in Guided Tissue Regeneration. *J. Contemp Dent. Pract.* **2015**, *16*, 512–518. [CrossRef] [PubMed]
36. An, Y.Z.; Strauss, F.J.; Park, J.Y.; Shen, Y.Q.; Thoma, D.S.; Lee, J.S. Membrane fixation enhances guided bone regeneration in standardized calvarial defects: A pre-clinical study. *J. Clin. Periodontol.* 2021. [CrossRef] [PubMed]
37. Urbaniak, G.; Plous, S. *Research Randomizer, version 4.0*. Computer Software. 2013. Available online: http://www.randomizer.org/ (accessed on 22 June 2013).
38. Feher, B.; Apaza Alccayhuaman, K.A.; Strauss, F.J.; Lee, J.S.; Tangl, S.; Kuchler, U.; Gruber, R. Osteoconductive properties of upside-down bilayer collagen membranes in rat calvarial defects. *Int. J. Implant Dent.* **2021**, *7*, 50. [CrossRef] [PubMed]
39. Boivin, G.; Bala, Y.; Doublier, A.; Farlay, D.; Ste-Marie, L.G.; Meunier, P.J.; Delmas, P. The role of mineralization and organic matrix in the microhardness of bone tissue from controls and osteoporotic patients. *Bone* **2008**, *43*, 532–538. [CrossRef]
40. Unal, M.; Ahmed, R.; Mahadevan-Jansen, A.; Nyman, J.S. Compositional assessment of bone by Raman spectroscopy. *Analyst* **2021**, *146*, 7464–7490. [CrossRef]
41. Cesaratto, A.; Lombardi, J.; Leona, M. Tracking photo-degradation of triarylmethane dyes with surface-enhanced Raman spectroscopy. *J. Raman Spectrosc.* **2016**, *48*, 418–424. [CrossRef]
42. Aasebo, E.; Brenner, A.K.; Hernandez-Valladares, M.; Birkeland, E.; Berven, F.S.; Selheim, F.; Bruserud, Ø. Proteomic Comparison of Bone Marrow Derived Osteoblasts and Mesenchymal Stem Cells. *Int. J. Mol. Sci.* **2021**, *22*, 5665. [CrossRef] [PubMed]
43. Bahlas, S.; Damiati, L.A.; Al-Hazmi, A.S.; Pushparaj, P.N. Decoding the Role of Sphingosine-1-Phosphate in Asthma and Other Respiratory System Diseases Using Next Generation Knowledge Discovery Platforms Coupled With Luminex Multiple Analyte Profiling Technology. *Front. Cell Dev. Biol.* **2020**, *8*, 444. [CrossRef] [PubMed]
44. Liao, Y.; Wang, J.; Jaehnig, E.J.; Shi, Z.; Zhang, B. WebGestalt 2019: Gene set analysis toolkit with revamped UIs and APIs. *Nucleic Acids Res.* **2019**, *47*, W199–W205. [CrossRef] [PubMed]
45. Maffioli, E.; Nonnis, S.; Angioni, R.; Santagata, F.; Cali, B.; Zanotti, L.; Negri, A.; Viola, A.; Tedeschi, G. Proteomic analysis of the secretome of human bone marrow-derived mesenchymal stem cells primed by pro-inflammatory cytokines. *J. Proteomics.* **2017**, *166*, 115–126. [CrossRef]

46. Baberg, F.; Geyh, S.; Waldera-Lupa, D.; Stefanski, A.; Zilkens, C.; Haas, R.; Schroeder, T.; Stühler, K. Secretome analysis of human bone marrow derived mesenchymal stromal cells. *Biochim. Biophys. Acta Proteins Proteom.* **2019**, *1867*, 434–441. [CrossRef]
47. Kehl, D.; Generali, M.; Mallone, A.; Heller, M.; Uldry, A.C.; Cheng, P.; Gantenbein, B.; Hoerstrup, S.P.; Weber, B. Proteomic analysis of human mesenchymal stromal cell secretomes: A systematic comparison of the angiogenic potential. *NPJ Regen. Med.* **2019**, *4*, 8. [CrossRef]
48. Shin, S.; Lee, J.; Kwon, Y.; Park, K.S.; Jeong, J.H.; Choi, S.J.; Bang, S.I.; Chang, J.W.; Lee, C. Comparative Proteomic Analysis of the Mesenchymal Stem Cells Secretome from Adipose, Bone Marrow, Placenta and Wharton's Jelly. *Int. J. Mol. Sci.* **2021**, *22*, 845. [CrossRef]
49. Saleem, R.; Mohamed-Ahmed, S.; Elnour, R.; Berggreen, E.; Mustafa, K.; Al-Sharabi, N. Conditioned Medium from Bone Marrow Mesenchymal Stem Cells Restored Oxidative Stress-Related Impaired Osteogenic Differentiation. *Int. J. Mol. Sci.* **2021**, *22*, 13458. [CrossRef]
50. Sagaradze, G.; Grigorieva, O.; Nimiritsky, P.; Basalova, N.; Kalinina, N.; Akopyan, Z.; Efimenko, A. Conditioned Medium from Human Mesenchymal Stromal Cells: Towards the Clinical Translation. *Int. J. Mol. Sci.* **2019**, *20*, 1656. [CrossRef]
51. Marolt Presen, D.; Traweger, A.; Gimona, M.; Redl, H. Mesenchymal Stromal Cell-Based Bone Regeneration Therapies: From Cell Transplantation and Tissue Engineering to Therapeutic Secretomes and Extracellular Vesicles. *Front. Bioeng. Biotechnol.* **2019**, *7*, 352. [CrossRef]
52. Bieback, K.; Fernandez-Munoz, B.; Pati, S.; Schafer, R. Gaps in the knowledge of human platelet lysate as a cell culture supplement for cell therapy: A joint publication from the AABB and the. *Int. Soc. Cell Gene Ther. Transfus.* **2019**, *59*, 3448–3460.
53. Fekete, N.; Rojewski, M.T.; Lotfi, R.; Schrezenmeier, H. Essential components for ex vivo proliferation of mesenchymal stromal cells. *Tissue Eng. Part C Methods* **2014**, *20*, 129. [CrossRef] [PubMed]
54. Shanbhag, S.; Suliman, S.; Bolstad, A.I.; Stavropoulos, A.; Mustafa, K. Xeno-Free Spheroids of Human Gingiva-Derived Progenitor Cells for Bone Tissue Engineering. *Front. Bioeng. Biotechnol.* **2020**, *8*, 968. [CrossRef] [PubMed]
55. Madrigal, M.; Rao, K.S.; Riordan, N.H. A review of therapeutic effects of mesenchymal stem cell secretions and induction of secretory modification by different culture methods. *J. Transl. Med.* **2014**, *11*, 260. [CrossRef] [PubMed]
56. Nikolits, I.; Nebel, S.; Egger, D.; Kress, S.; Kasper, C. Towards Physiologic Culture Approaches to Improve Standard Cultivation of Mesenchymal Stem Cells. *Cells* **2021**, *10*, 886. [CrossRef]
57. Palombella, S.; Guiotto, M.; Higgins, G.C.; Applegate, L.L.; Raffoul, W.; Cherubino, M.; Hart, A.; Riehle, M.O.; di Summa, P.G. Human platelet lysate as a potential clinical-translatable supplement to support the neurotrophic properties of human adipose-derived stem cells. *Stem Cell Res. Ther.* **2020**, *11*, 432. [CrossRef]
58. Kim, S.N.; Lee, C.J.; Nam, J.; Choi, B.; Chung, E.; Song, S.U. The Effects of Human Bone Marrow-Derived Mesenchymal Stem Cell Conditioned Media Produced with Fetal Bovine Serum or Human Platelet Lysate on Skin Rejuvenation Characteristics. *Int. J. Stem Cells* **2021**, *14*, 94–102. [CrossRef]
59. Inukai, T.; Katagiri, W.; Yoshimi, R.; Osugi, M.; Kawai, T.; Hibi, H.; Ueda, M. Novel application of stem cell-derived factors for periodontal regeneration. *Biochem Biophys Res. Commun.* **2013**, *430*, 763–768. [CrossRef]
60. Xu, J.; Wang, B.; Sun, Y.; Wu, T.; Liu, Y.; Zhang, J.; Lee, W.Y.; Pan, X.; Chai, Y.; Li, G. Human fetal mesenchymal stem cell secretome enhances bone consolidation in distraction osteogenesis. *Stem Cell Res. Ther.* **2016**, *7*, 134. [CrossRef]
61. Fujio, M.; Xing, Z.; Sharabi, N.; Xue, Y.; Yamamoto, A.; Hibi, H.; Ueda, M.; Fristad, I.; Mustafa, K. Conditioned media from hypoxic-cultured human dental pulp cells promotes bone healing during distraction osteogenesis. *J. Tissue Eng. Regen. Med.* **2017**, *11*, 2116–2126. [CrossRef]
62. Ogata, K.; Katagiri, W.; Osugi, M.; Kawai, T.; Sugimura, Y.; Hibi, H.; Nakamura, S.; Ueda, M. Evaluation of the therapeutic effects of conditioned media from mesenchymal stem cells in a rat bisphosphonate-related osteonecrosis of the jaw-like model. *Bone* **2015**, *74*, 95–105. [CrossRef] [PubMed]
63. Tsuchiya, S.; Ohmori, M.; Hara, K.; Fujio, M.; Ikeno, M.; Hibi, H.; Ueda, M. An Experimental Study on Guided Bone Regeneration Using a Polylactide-co-glycolide Membrane-Immobilized Conditioned Medium. *Int. J. Oral Maxillofac. Implant.* **2015**, *30*, 1175–1186. [CrossRef] [PubMed]
64. Diomede, F.; D'Aurora, M.; Gugliandolo, A.; Merciaro, I.; Orsini, T.; Gatta, V.; Piattelli, A.; Trubiani, O.; Mazzon, E. Biofunctionalized Scaffold in Bone Tissue Repair. *Int. J. Mol. Sci.* **2018**, *19*, 1022. [CrossRef] [PubMed]
65. Qiu, J.; Wang, X.; Zhou, H.; Zhang, C.; Wang, Y.; Huang, J. Enhancement of periodontal tissue regeneration by conditioned media from gingiva-derived or periodontal ligament-derived mesenchymal stem cells: A comparative study in rats. *Stem Cell Res. Ther.* **2020**, *11*, 42. [CrossRef] [PubMed]
66. Lai, C.H.; Zhou, L.; Wang, Z.L.; Lu, H.B.; Gao, Y. Use of a collagen membrane loaded with recombinant human bone morphogenetic protein-2 with collagen-binding domain for vertical guided bone regeneration. *J. Periodontol.* **2013**, *84*, 950–957. [CrossRef] [PubMed]
67. Chang, Y.Y.; Lee, J.S.; Kim, M.S.; Choi, S.H.; Chai, J.K.; Jung, U.W. Comparison of collagen membrane and bone substitute as a carrier for rhBMP-2 in lateral onlay graft. *Clin. Oral Implants Res.* **2015**, *26*, e13–e19. [CrossRef]
68. Jo, J.Y.; Jeong, S.I.; Shin, Y.M.; Kang, S.S.; Kim, S.E.; Jeong, C.M.; Huh, J.-B. Sequential delivery of BMP-2 and BMP-7 for bone regeneration using a heparinized collagen membrane. *Int. J. Oral Maxillofac. Surg.* **2015**, *44*, 921–928. [CrossRef]

69. Furuhata, M.; Takayama, T.; Yamamoto, T.; Ozawa, Y.; Senoo, M.; Ozaki, M.; Yamano, S.; Sato, S. Real-time assessment of guided bone regeneration in critical size mandibular bone defects in rats using collagen membranes with adjunct fibroblast growth factor-2. *J. Dent. Sci.* **2021**, *16*, 1170–1181. [CrossRef]
70. Piao, Z.G.; Kim, J.S.; Son, J.S.; Lee, S.Y.; Fang, X.H.; Oh, J.S.; You, J.-S.; Kim, S.-G. Osteogenic evaluation of collagen membrane containing drug-loaded polymeric microparticles in a rat calvarial defect model. *Tissue Eng. Part A* **2014**, *20*, 3322–3331. [CrossRef]
71. Nagata, M.; Iwasaki, K.; Akazawa, K.; Komaki, M.; Yokoyama, N.; Izumi, Y.; Morita, I. Conditioned Medium from Periodontal Ligament Stem Cells Enhances Periodontal Regeneration. *Tissue Eng. Part A* **2017**, *23*, 367–377. [CrossRef]
72. Steil, L.; Thiele, T.; Hammer, E.; Bux, J.; Kalus, M.; Völker, U.; Greinacher, A. Proteomic characterization of freeze-dried human plasma: Providing treatment of bleeding disorders without the need for a cold chain. *Transfusion* **2008**, *48*, 2356–2363. [CrossRef] [PubMed]
73. Zhao, J.; Wang, S.; Bao, J.; Sun, X.; Zhang, X.; Zhang, X.; Ye, D.; Wei, J.; Liu, C.; Jiang, X.; et al. Trehalose maintains bioactivity and promotes sustained release of BMP-2 from lyophilized CDHA scaffolds for enhanced osteogenesis in vitro and in vivo. *PLoS ONE* **2013**, *8*, e54645. [CrossRef] [PubMed]
74. Bari, E.; Di Silvestre, D.; Mastracci, L.; Grillo, F.; Grisoli, P.; Marrubini, G.; Nardini, M.; Mastrogiacomo, M.; Sorlini, M.; Rossi, R.; et al. GMP-compliant sponge-like dressing containing MSC lyo-secretome: Proteomic network of healing in a murine wound model. *Eur. J. Pharm. Biopharm.* **2020**, *155*, 37–48. [CrossRef] [PubMed]
75. Zhang, C.; Wang, T.; Zhang, L.; Chen, P.; Tang, S.; Chen, A.; Li, M.; Peng, G.; Gao, H.; Weng, H.; et al. Combination of lyophilized adipose-derived stem cell concentrated conditioned medium and polysaccharide hydrogel in the inhibition of hypertrophic scarring. *Stem Cell Res. Ther.* **2021**, *12*, 23. [CrossRef]
76. Kot, M.; Baj-Krzyworzeka, M.; Szatanek, R.; Musial-Wysocka, A.; Suda-Szczurek, M.; Majka, M. The Importance of HLA Assessment in "Off-the-Shelf" Allogeneic Mesenchymal Stem Cells Based-Therapies. *Int. J. Mol. Sci.* **2019**, *20*, 5680. [CrossRef]
77. Ankrum, J.A.; Ong, J.F.; Karp, J.M. Mesenchymal stem cells: Immune evasive, not immune privileged. *Nat. Biotechnol.* **2014**, *32*, 252–260. [CrossRef]
78. Kang, S.H.; Chung, Y.G.; Oh, I.H.; Kim, Y.S.; Min, K.O.; Chung, J.Y. Bone regeneration potential of allogeneic or autogeneic mesenchymal stem cells loaded onto cancellous bone granules in a rabbit radial defect model. *Cell Tissue Res.* **2014**, *355*, 81–88. [CrossRef]
79. Mahalingam, V.D.; Behbahani-Nejad, N.; Horine, S.V.; Olsen, T.J.; Smietana, M.J.; Wojtys, E.M.; Wellik, D.M.; Arruda, E.M.; Larkin, L.M. Allogeneic versus autologous derived cell sources for use in engineered bone-ligament-bone grafts in sheep anterior cruciate ligament repair. *Tissue Eng. Part A* **2015**, *21*, 1047–1054. [CrossRef]
80. Rapp, A.E.; Bindl, R.; Erbacher, A.; Kruchen, A.; Rojewski, M.; Schrezenmeier, H.; Müller, I.; Ignatius, A. Autologous Mesenchymal Stroma Cells Are Superior to Allogeneic Ones in Bone Defect Regeneration. *Int. J. Mol. Sci.* **2018**, *19*, 2526. [CrossRef]
81. Maiti, S.K.; Shivakumar, M.U.; Mohan, D.; Kumar, N.; Singh, K.P. Mesenchymal Stem Cells of Different Origin-Seeded Bioceramic Construct in Regeneration of Bone Defect in Rabbit. *Tissue Eng. Regen. Med.* **2018**, *15*, 477–492. [CrossRef]
82. Lopez-Fernandez, A.; Barro, V.; Ortiz-Hernandez, M.; Manzanares, M.C.; Vivas, D.; Vives, J.; Vélez, R.; Ginebra, M.P.; Aguirre, M. Effect of Allogeneic Cell-Based Tissue-Engineered Treatments in a Sheep Osteonecrosis Model. *Tissue Eng. Part A* **2020**, *26*, 993–1004. [CrossRef] [PubMed]
83. Osugi, M.; Katagiri, W.; Yoshimi, R.; Inukai, T.; Hibi, H.; Ueda, M. Conditioned media from mesenchymal stem cells enhanced bone regeneration in rat calvarial bone defects. *Tissue Eng. Part A* **2012**, *18*, 1479–1489. [CrossRef] [PubMed]
84. Hiraki, T.; Kunimatsu, R.; Nakajima, K.; Abe, T.; Yamada, S.; Rikitake, K.; Tanimoto, K. Stem cell-derived conditioned media from human exfoliated deciduous teeth promote bone regeneration. *Oral Dis.* **2020**, *26*, 381–390. [CrossRef] [PubMed]
85. Sanchooli, T.; Norouzian, M.; Ardeshirylajimi, A.; Ghoreishi, S.; Abdollahifar, M.; Nazarian, H.; Piryaei, A. Adipose Derived Stem Cells Conditioned Media in Combination with Bioceramic-Collagen Scaffolds Improved Calvarial Bone Healing in Hypothyroid Rats. *Iran. Red Crescent Med. J.* **2017**, in press. [CrossRef]
86. Mehler, V.J.; Burns, C.; Moore, M.L. Concise Review: Exploring Immunomodulatory Features of Mesenchymal Stromal Cells in Humanized Mouse Models. *Stem Cells* **2019**, *37*, 298–305. [CrossRef]
87. Wang, J.; Qu, Y.; Chen, C.; Sun, J.; Pan, H.; Shao, C.; Tang, R.; Gu, X. Fabrication of collagen membranes with different intrafibrillar mineralization degree as a potential use for GBR. *Mater. Sci. Eng. C Mater. Biol. Appl.* **2019**, *104*, 109959. [CrossRef]
88. Li, J.; Yan, J.F.; Wan, Q.Q.; Shen, M.J.; Ma, Y.X.; Gu, J.T.; Gao, P.; Tang, X.-Y.; Yu, F.; Chen, J.-H.; et al. Matrix stiffening by self-mineralizable guided bone regeneration. *Acta Biomater.* **2021**, *125*, 112–125. [CrossRef]
89. Vo, T.N.; Ekenseair, A.K.; Spicer, P.P.; Watson, B.M.; Tzouanas, S.N.; Roh, T.T.; Mikos, A.G. In vitro and in vivo evaluation of self-mineralization and biocompatibility of injectable, dual-gelling hydrogels for bone tissue engineering. *J. Control. Release* **2015**, *205*, 25–34. [CrossRef]
90. Bailey, A.J.; Sims, T.J.; Ebbesen, E.N.; Mansell, J.P.; Thomsen, J.S.; Mosekilde, L. Age-related changes in the biochemical properties of human cancellous bone collagen: Relationship to bone strength. *Calcif Tissue Int.* **1999**, *65*, 203–210. [CrossRef]
91. Ibrahim, A.; Magliulo, N.; Groben, J.; Padilla, A.; Akbik, F.; Abdel Hamid, Z. Hardness, an Important Indicator of Bone Quality, and the Role of Collagen in Bone Hardness. *J. Funct. Biomater.* **2020**, *11*, 85. [CrossRef]
92. Ahmed, R.; Law, A.W.L.; Cheung, T.W.; Lau, C. Raman spectroscopy of bone composition during healing of subcritical calvarial defects. *Biomed. Opt. Express* **2018**, *9*, 1704–1716. [CrossRef] [PubMed]

93. Ahmed, R.; Wang, W.; Zia, A.W.; Lau, C. Collagen formation observed from healing calvarial defects with principal component analysis of Raman scattering. *Analyst* **2018**, *143*, 4614–4622. [CrossRef]
94. Du, F.; Wang, Q.; Ouyang, L.; Wu, H.; Yang, Z.; Fu, X.; Liu, X.; Yan, L.; Cao, Y.; Xiao, R. Comparison of concentrated fresh mononuclear cells and cultured mesenchymal stem cells from bone marrow for bone regeneration. *Stem Cells Transl. Med.* **2021**, *10*, 598–609. [CrossRef] [PubMed]
95. Omar, O.; Engstrand, T.; Kihlstrom Burenstam Linder, L.; Aberg, J.; Shah, F.A.; Palmquist, A.; Birgersson, U.; Elgali, I.; Pujari-Palmer, M.; Engqvist, H.; et al. In situ bone regeneration of large cranial defects using synthetic ceramic implants with a tailored composition and design. *Proc. Natl. Acad. Sci. USA* **2020**, *117*, 26660–26671. [CrossRef]
96. Kupcova Skalnikova, H. Proteomic techniques for characterisation of mesenchymal stem cell secretome. *Biochimie* **2013**, *95*, 2196–2211. [CrossRef] [PubMed]
97. Okamoto, M.; Udagawa, N.; Uehara, S.; Maeda, K.; Yamashita, T.; Nakamichi, Y.; Kato, H.; Saito, N.; Minami, Y.; Takahashi, N.; et al. Noncanonical Wnt5a enhances Wnt/beta-catenin signaling during osteoblastogenesis. *Sci. Rep.* **2014**, *4*, 4493. [CrossRef] [PubMed]
98. Hiraiwa, T.; Nakai, Y.; Yamada, T.G.; Tanimoto, R.; Kimura, H.; Matsumoto, Y.; Miki, N.; Hiroi, N.; Funahashi, A. Quantitative analysis of sensitivity to a Wnt3a gradient in determination of the pole-to-pole axis of mitotic cells by using a microfluidic device. *FEBS Open Bio.* **2018**, *8*, 1920–1935. [CrossRef]
99. Linero, I.; Chaparro, O. Paracrine effect of mesenchymal stem cells derived from human adipose tissue in bone regeneration. *PLoS ONE* **2014**, *9*, e107001. [CrossRef]
100. Wang, K.X.; Xu, L.L.; Rui, Y.F.; Huang, S.; Lin, S.E.; Xiong, J.H.; Li, Y.-H.; Lee, W.Y.-W.; Li, G. The effects of secretion factors from umbilical cord derived mesenchymal stem cells on osteogenic differentiation of mesenchymal stem cells. *PLoS ONE* **2015**, *10*, e0120593. [CrossRef]
101. Katagiri, W.; Sakaguchi, K.; Kawai, T.; Wakayama, Y.; Osugi, M.; Hibi, H. A defined mix of cytokines mimics conditioned medium from cultures of bone marrow-derived mesenchymal stem cells and elicits bone regeneration. *Cell Prolif.* **2017**, *50*, e012059. [CrossRef]
102. Katagiri, W.; Osugi, M.; Kawai, T.; Ueda, M. Novel cell-free regeneration of bone using stem cell-derived growth factors. *Int. J. Oral Maxillofac. Implant.* **2013**, *28*, 1009–1016. [CrossRef] [PubMed]
103. Katagiri, W.; Kawai, T.; Osugi, M.; Sugimura-Wakayama, Y.; Sakaguchi, K.; Kojima, T.; Kobayashi, T. Angiogenesis in newly regenerated bone by secretomes of human mesenchymal stem cells. *Maxillofac. Plast Reconstr. Surg.* **2017**, *39*, 8. [CrossRef] [PubMed]
104. Kawai, T.; Katagiri, W.; Osugi, M.; Sugimura, Y.; Hibi, H.; Ueda, M. Secretomes from bone marrow-derived mesenchymal stromal cells enhance periodontal tissue regeneration. *Cytotherapy* **2015**, *17*, 369–381. [CrossRef] [PubMed]
105. Wang, C.Y.; Yang, H.B.; Hsu, H.S.; Chen, L.L.; Tsai, C.C.; Tsai, K.S.; Yew, T.-L.; Kao, Y.-H.; Hung, S.-C. Mesenchymal stem cell-conditioned medium facilitates angiogenesis and fracture healing in diabetic rats. *J. Tissue Eng. Regen. Med.* **2012**, *6*, 559–569. [CrossRef]
106. Ogisu, K.; Fujio, M.; Tsuchiya, S.; Tsuboi, M.; Qi, C.; Toyama, N.; Kamio, H.; Hibi, H. Conditioned media from mesenchymal stromal cells and periodontal ligament fibroblasts under cyclic stretch stimulation promote bone healing in mouse calvarial defects. *Cytotherapy* **2020**, *22*, 543–551. [CrossRef]
107. Diomede, F.; Gugliandolo, A.; Scionti, D.; Merciaro, I.; Cavalcanti, M.F.; Mazzon, E. Biotherapeutic effect of gingival stem cells conditioned medium in bone tissue restoration. *Int. J. Mol. Sci.* **2018**, *19*, 329. [CrossRef]
108. Pranskunas, M.; Simoliunas, E.; Alksne, M.; Martin, V.; Gomes, P.S.; Puisys, A.; Kaupinis, A.; Juodzbalys, G. Assessment of the Bone Healing Process Mediated by Periosteum-Derived Mesenchymal Stem Cells' Secretome and a Xenogenic Bioceramic-An In Vivo Study in the Rabbit Critical Size Calvarial Defect Model. *Materials* **2021**, *14*, 3512. [CrossRef]

Disclaimer/Publisher's Note: The statements, opinions and data contained in all publications are solely those of the individual author(s) and contributor(s) and not of MDPI and/or the editor(s). MDPI and/or the editor(s) disclaim responsibility for any injury to people or property resulting from any ideas, methods, instructions or products referred to in the content.

International Journal of
Molecular Sciences

MDPI

Article

Influence of Bone Substitutes on Mesenchymal Stromal Cells in an Inflammatory Microenvironment

Siddharth Shanbhag [1,2,†], Neha Rana [1,†], Salwa Suliman [1], Shaza Bushra Idris [3], Kamal Mustafa [1] and Andreas Stavropoulos [4,5,*]

[1] Center for Translational Oral Research (TOR), Department of Clinical Dentistry, Faculty of Medicine, University of Bergen, 5009 Bergen, Norway
[2] Department of Immunology and Transfusion Medicine, Haukeland University Hospital, 5021 Bergen, Norway
[3] Private Practice, Voss Tannspesialist Team, 5700 Voss, Norway
[4] Division of Conservative Dentistry and Periodontology, University Clinic of Dentistry, Medical University of Vienna, 1090 Vienna, Austria
[5] Department of Periodontology, Faculty of Odontology, Malmö University, 205 06 Malmö, Sweden
* Correspondence: andreas.stavropoulos@mau.se; Tel.: +46-040-6658066
† These authors contributed equally to this work.

Abstract: Bone regeneration is driven by mesenchymal stromal cells (MSCs) via their interactions with immune cells, such as macrophages (MPs). Bone substitutes, e.g., bi-calcium phosphates (BCPs), are commonly used to treat bone defects. However, little research has focused on MSC responses to BCPs in the context of inflammation. The objective of this study was to investigate whether BCPs influence MSC responses and MSC–MP interactions, at the gene and protein levels, in an inflammatory microenvironment. In setup A, human bone marrow MSCs combined with two different BCP granules (BCP 60/40 or BCP 20/80) were cultured with or without cytokine stimulation (IL1β + TNFα) to mimic acute inflammation. In setup B, U937 cell-line-derived MPs were introduced via transwell cocultures to setup A. Monolayer MSCs with and without cytokine stimulation served as controls. After 72 h, the expressions of genes related to osteogenesis, healing, inflammation and remodeling were assessed in the MSCs via quantitative polymerase chain reactions. Additionally, MSC-secreted cytokines related to healing, inflammation and chemotaxis were assessed via multiplex immunoassays. Overall, the results indicate that, under both inflammatory and non-inflammatory conditions, the BCP granules significantly regulated the MSC gene expressions towards a pro-healing genotype but had relatively little effect on the MSC secretory profiles. In the presence of the MPs (coculture), the BCPs positively regulated both the gene expression and cytokine secretion of the MSCs. Overall, similar trends in MSC responses were observed with BCP 60/40 and BCP 20/80. In summary, within the limits of in vitro models, these findings suggest that the presence of BCP granules at a surgical site may not necessarily have a detrimental effect on MSC-mediated wound healing, even in the event of inflammation.

Keywords: mesenchymal stromal cells; bone substitutes; immune modulation; bone regeneration

check for updates

Citation: Shanbhag, S.; Rana, N.; Suliman, S.; Idris, S.B.; Mustafa, K.; Stavropoulos, A. Influence of Bone Substitutes on Mesenchymal Stromal Cells in an Inflammatory Microenvironment. *Int. J. Mol. Sci.* **2023**, *24*, 438. https://doi.org/10.3390/ijms24010438

Academic Editor: Nicola Alessio

Received: 19 November 2022
Revised: 19 December 2022
Accepted: 23 December 2022
Published: 27 December 2022

Copyright: © 2022 by the authors. Licensee MDPI, Basel, Switzerland. This article is an open access article distributed under the terms and conditions of the Creative Commons Attribution (CC BY) license (https://creativecommons.org/licenses/by/4.0/).

1. Introduction

Bone regeneration is the result of the interplay between osteogenic progenitor cells and immune cells [1]. Of these, mesenchymal stromal cells (MSCs), which give rise to osteoblasts, and peripheral blood monocytes, which give rise to macrophages/osteoclasts, are arguably the most relevant [2]. The carefully coordinated cellular and molecular events that drive wound-healing processes form the biological basis for the treatment of bone defects using guided bone regeneration or tissue engineering approaches [3].

MSCs are key players in the wound-healing process and have been shown to be the most active during the early stages of healing [4–6]. MSCs are hypothesized to promote bone regeneration via various mechanisms, including direct differentiation into osteoblasts,

the paracrine stimulation of resident progenitor cells, the modulation of inflammatory and immune responses or a combination thereof [7], providing the basis for tissue engineering strategies for bone regeneration [8,9]. These processes, i.e., osteogenic differentiation, wound healing, immune modulation, remodeling, etc., are regulated by the interplay between several genes and proteins expressed by MSCs. For example, runt-related transcription factor 2 (*RUNX2*), a master transcription factor of osteoblast differentiation, and bone morphogenetic protein 2 (BMP2) together regulate MSC osteogenic differentiation [10,11]. Wound healing is mediated by growth factors, such as vascular endothelial growth factor (VEGF), basic fibroblast growth factor (FGF2), granulocyte colony-stimulating factor (GCSF) and platelet-derived growth factors (PDGF-AA/BB/AB). Interleukins (ILs) such as IL10 facilitate a "switch" from an inflammatory to a healing microenvironment, while others, such as IL5, IL6, IL7, IL8 and IL9, regulate inflammation and interactions with immune cells, e.g., macrophages (MPs), during the early stages of healing [12,13]. For example, MSCs have been shown to direct MP "polarization", i.e., induce a phenotype shift from a pro-inflammatory (M1) phenotype towards an anti-inflammatory or pro-healing (M2) phenotype conducive to resolving inflammation and accelerating wound healing [14–16]. Moreover, in the later stages of healing, cytokines, such as the receptor activator of nuclear factor-κ β ligand (RANKL) and osteoprotegerin (OPG), regulate bone remodeling, especially in the presence of biomaterials [17].

Another factor usually present at an early bone healing site is the biomaterial; regardless of the clinical approach, most current strategies involve the use of bone substitutes for the treatment of alveolar and peri-implant bone defects [18,19]. Since human bone is composed of ~70% calcium phosphate (CaP), commonly used bone substitute materials are also CaP-based, e.g., hydroxyapatite (HA); β-tricalcium phosphate (β-TCP); or their mixtures, i.e., biphasic CaP (BCP). BCPs are commercially available as different products based on the ratio of HA/β-TCP, e.g., an HA/β-TCP ratio of 60/40 (BoneCeramic®, Institut Straumann AG, Basel, Switzerland) or an HA/β-TCP ratio of 20/80 (MBCP+®, Biomatlante, Vigneux de Bretagne, France). BCPs function as three-dimensional (3D) scaffolds for cellular attachment and growth (osteoconduction) during bone healing. Moreover, BCP-based bone substitutes are also used in tissue engineering strategies as scaffolds for MSC delivery [12,13]. In addition to functioning as scaffolds, bone substitutes may also provide instructive microenvironments to direct cellular (MSC) functions, such as differentiation, paracrine secretion and immune modulation [20,21]. Thus, the biomaterial may also modulate cellular responses and influence healing outcomes.

While several studies have investigated the cellular responses to bone substitutes in standard in vitro conditions [22], relatively little research has focused on the cellular responses to bone substitutes in the context of inflammation. From a clinical perspective, this is relevant since bone substitutes are often present at the sites of existing inflammation, e.g., peri-implant defects [23–25]. Moreover, in its early stages (48–72 h), the healing microenvironment is characterized by the presence of pro-inflammatory cytokines, primarily interleukin-1-beta (IL1β), tumor necrosis factor-alpha (TNFα) and interferon-gamma (IFNγ), which may further modulate cellular responses and regulate the healing process [26]. It is therefore of interest to study the effects of bone substitutes on cellular responses and interactions in an inflammatory microenvironment. Thus, the objective of the present study was to address the following research question: how do bone substitutes (BCP) influence MSC responses and MSC–MP interactions, at the gene and protein levels, in an inflammatory microenvironment? That is, does the presence of a bone substitute pose a risk for modulating early cellular responses and possibly delay healing at sites of inflammation?

2. Results

2.1. BCP Strongly Modulated MSC Gene Expression under Inflammatory Conditions

In setup A, the responses of primary human MSCs (Figure 1) to two different BCP granules (BCP 60/40 and BCP 20/80), with or without cytokine stimulation (IL1β + TNFα), were assessed via analyses of genes related to osteogenesis (*RUNX2* and *BMP2*), healing

(*VEGF* and *IL10*), inflammation (IL6 and IL8) and remodeling (*RANKL* and *OPG*). The control cultures included monolayer MSCs with or without cytokine stimulation.

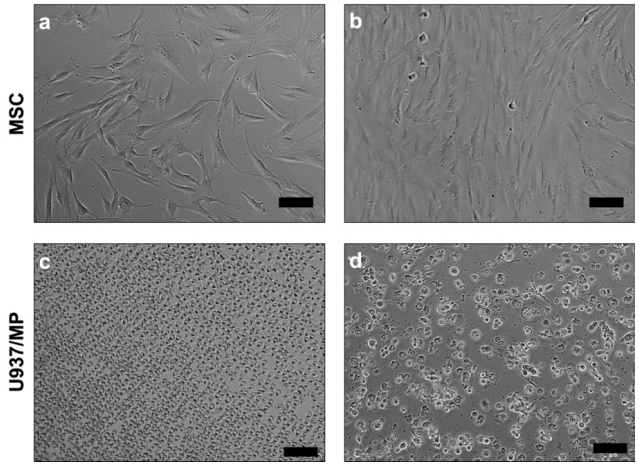

Figure 1. Representative phase contrast images of human bone-marrow-derived MSCs (**a**,**b**), U937 monocytes (**c**) and U937-derived macrophages (**d**); scale bars 100 µm.

Overall, after 72 h, the presence of the BCP granules enhanced the expressions of the osteogenesis-, healing- and remodeling-related genes in the MSCs to varying degrees. In the presence of BCP 60/40, the expressions of the *BMP2, VEGF, IL10* and *RANKL* genes were enhanced compared to those of the control, while the inflammation-related genes (*IL6* and *IL8*) remained unchanged. Under inflammatory conditions, the BCP 60/40 granules further enhanced the expressions of these genes in the MSCs, in addition to *RUNX2, IL6* and *IL8* (Figure 2). The gene expression data were validated by performing an enzyme-linked immunosorbent assay (ELISA) for the BMP2 protein, which revealed a similar trend in levels under inflammatory and non-inflammatory conditions (Supplementary Figure S1).

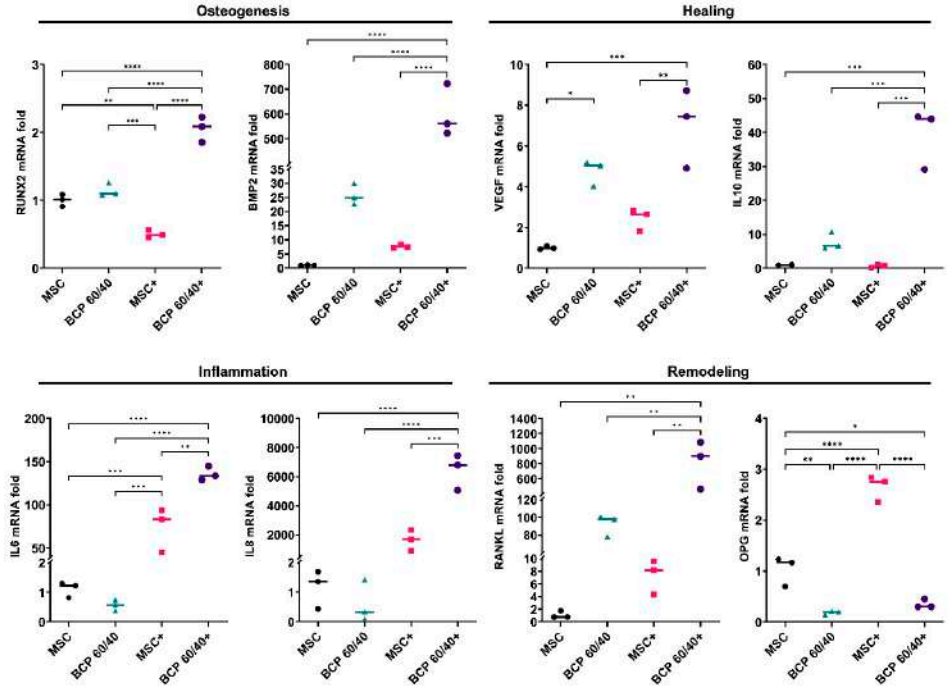

Figure 2. Relative mRNA expressions (fold changes) of osteogenesis-, healing-, inflammation- and remodeling-related genes in MSCs cultured as monolayers (control) or with BCP 60/40; + represents cytokine stimulation (n = 3). Statistical analyses are based on one-way ANOVA with Tukey's multiple comparison tests on delta-Ct values; * $p < 0.05$; ** $p < 0.001$; *** $p = 0.0001$; **** $p < 0.0001$.

A similar trend in MSC gene expression was observed in the presence of the BCP 20/80 granules: *BMP2*, *VEGF*, *IL10* and *RANKL* were enhanced, in addition to OPG, compared to the control. In contrast to the BCP 60/40 culture, *IL6* expression was enhanced in the presence of BCP 20/80. Under inflammatory conditions, the BCP 20/80 granules further enhanced the expressions of *BMP2*, *IL10* and *RANKL* in the MSCs, along with those of the inflammation-related genes, i.e., *IL6* and *IL8* (Figure 3).

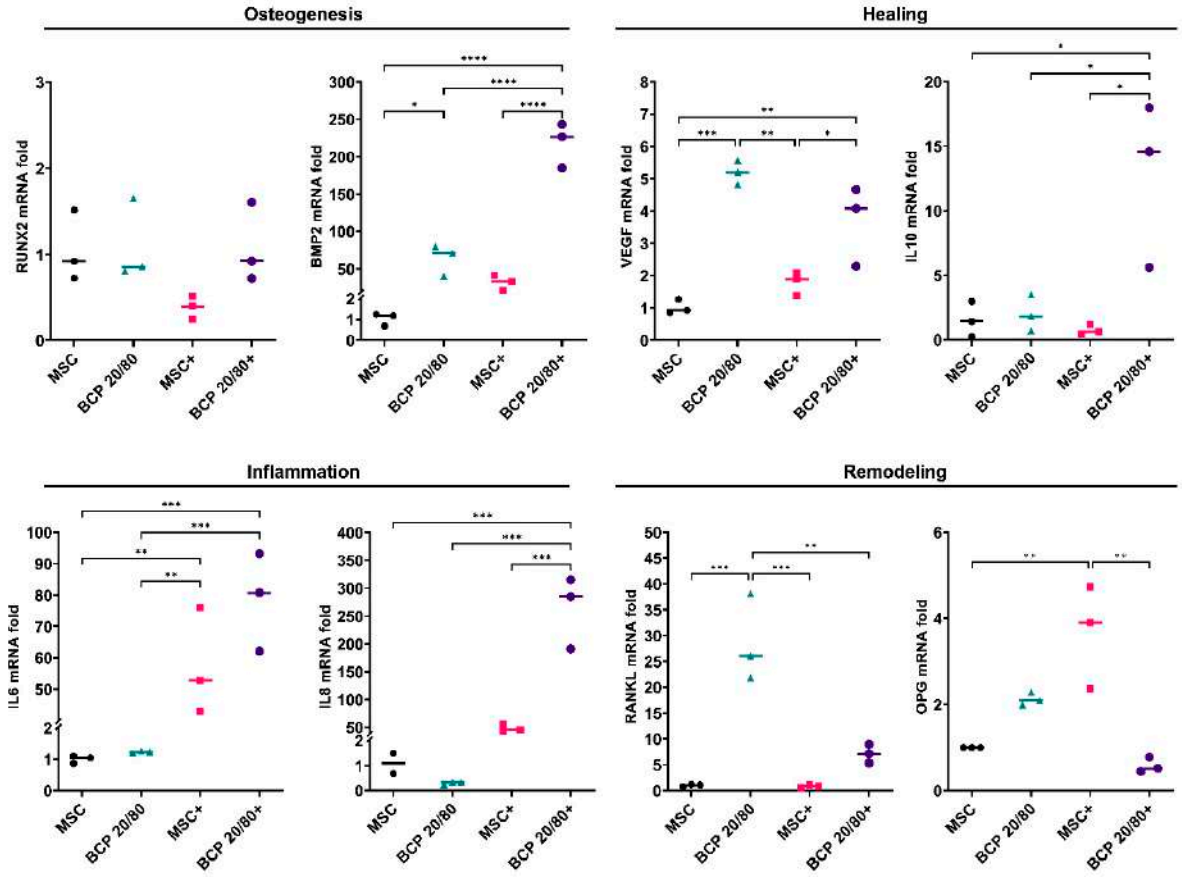

Figure 3. Relative mRNA expressions (fold changes) of osteogenesis-, healing-, inflammation- and remodeling-related genes in MSCs cultured as monolayers (control) or with BCP 20/80; + represents cytokine stimulation (n = 3). Statistical analyses are based on one-way ANOVA with Tukey's multiple comparison tests on delta-Ct values; * $p < 0.05$; ** $p < 0.001$; *** $p = 0.0001$; **** $p < 0.0001$.

2.2. BCP Did Not Additionally Alter MSC Cytokine Profiles under Inflammatory Conditions

The secreted protein concentrations in the supernatant media of the BCP-cultured MSCs, with or without cytokine stimulation, were measured via a multiplex assay (setup A). Of the 27 tested cytokines, consistent and reliable readings were obtained for 11 cytokines related to healing (FGF2, VEGF, PDGF-BB, GCSF and IL10) and inflammation (IL5, IL7 and IL9). Additionally, chemokines such as C-C motif ligands 11 (CCL11), 4 (CCL4) and 5 (CCL5) were identified. The presence of the BCP granules, either 60/40 or 20/80, did not significantly alter the cytokine profiles of the MSCs compared to those of the control. Under inflammatory conditions, BCP 20/80 enhanced the secretion of FGF2, IL5 and CCL11, while BCP 60/40 enhanced CCL5 compared to that of the cytokine-stimulated controls (Figure 4).

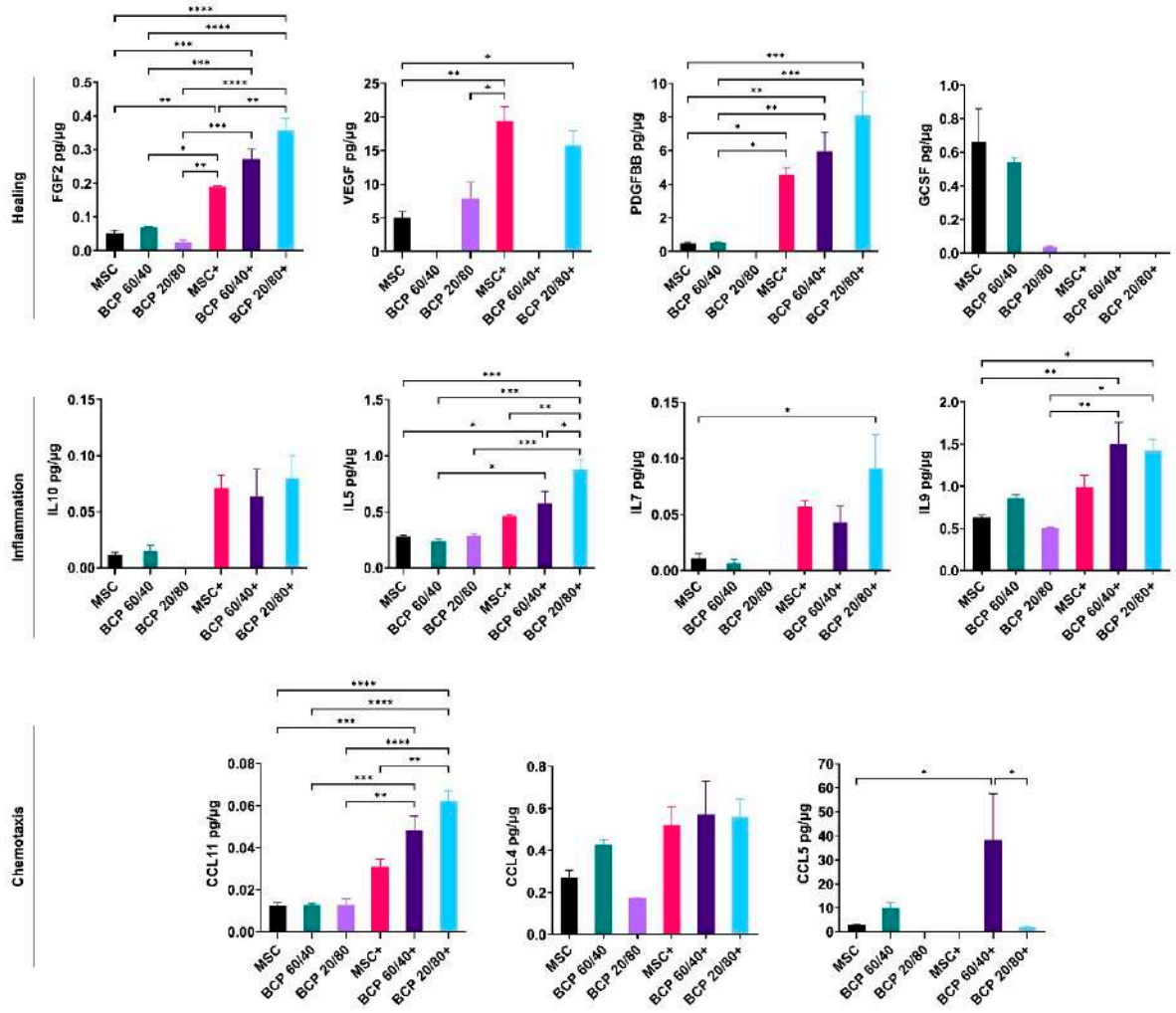

Figure 4. Multiplex cytokine assay of MSCs cultured with BCP granules (BCP 60/40 or BCP 20/80). Cytokines related to healing, inflammation and chemotaxis were measured after 72 h. + indicates cytokine stimulation. Concentration of each analyte (pg/mL) was normalized to total protein concentration of the conditioned media (µg/mL). Statistical analyses are based on one-way ANOVA with Tukey's multiple comparison tests; * $p < 0.05$; ** $p < 0.001$; *** $p = 0.0001$; **** $p < 0.0001$.

2.3. BCP Altered MSC Gene Expression in Cocultures

In setup B, the paracrine interactions between the MPs and the MSCs in the presence of the BCP granules and/or cytokine stimulation were assessed by using a transwell coculture assay via the expressions of the same panel of genes analyzed in setup A. After 72 h, the coculture of the MPs with the monolayer MSCs enhanced the expressions of all the analyzed genes related to osteogenesis (*RUNX2* and *BMP2*), healing (*VEGF* and *IL10*), inflammation (*IL6* and *IL8*) and remodeling (*RANKL* and *OPG*) compared to those of the monolayer controls. In comparison, the coculture of the MPs with MSC + BCP 60/40 revealed the further upregulation of *BMP2, VEGF* and *OPG*, while the *IL10, IL6, IL8* and *RANKL* expressions remained unchanged. Under inflammatory conditions, BCP 60/40 remarkably enhanced the expressions of *BMP2, IL10, IL6* and *IL8* in the MSCs, while the remodeling genes (*RANKL* and *OPG*) were downregulated (Figure 5).

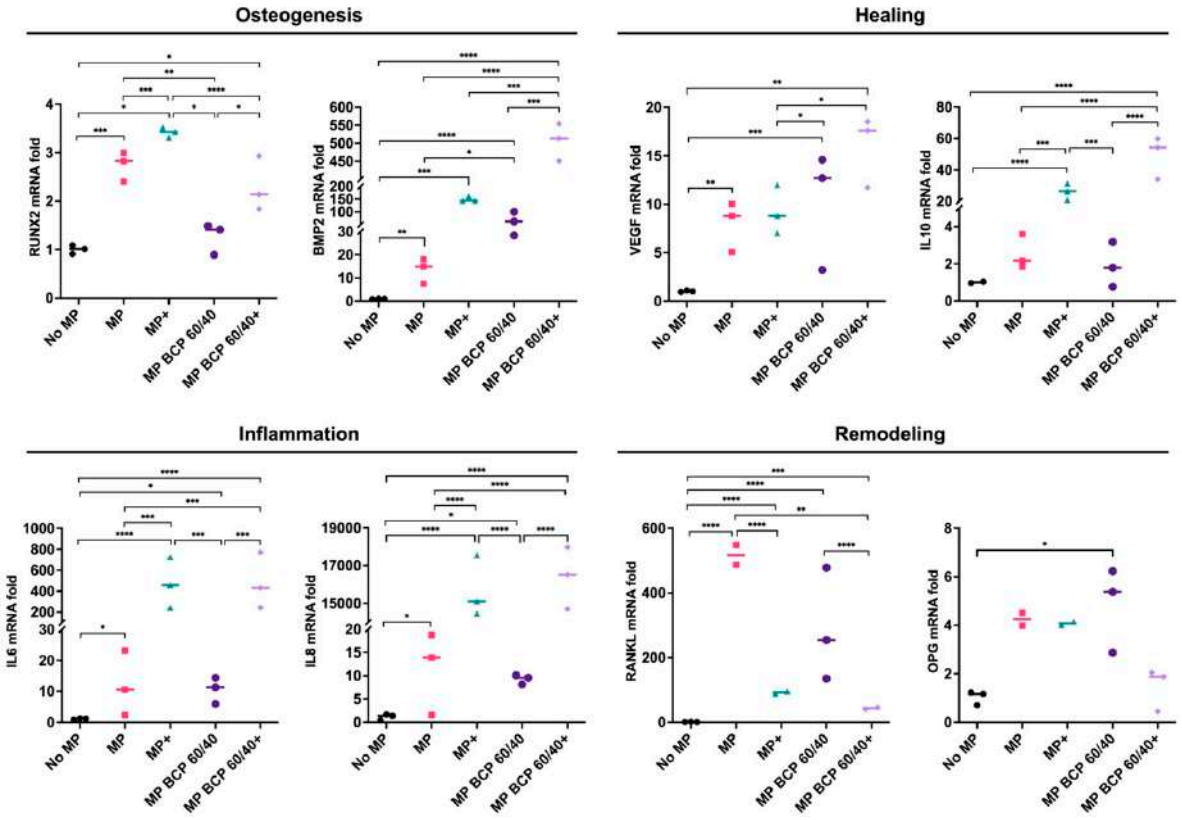

Figure 5. Relative mRNA expressions (fold changes) of osteogenesis-, healing-, inflammation- and remodeling-related genes in MSCs cultured with BCP 60/40 and/or MPs (n = 3). No MP, monolayer MSC control; MP, monolayer MSCs cocultured with MPs; + represents cytokine stimulation. Statistical analyses are based on one-way ANOVA with Tukey's multiple comparison tests on delta-Ct values; * $p < 0.05$; ** $p < 0.001$; *** $p = 0.0001$; **** $p < 0.0001$.

The coculture of the MPs with MSC + BCP 20/80 revealed the upregulation of *BMP2*, *VEGF* and *IL10* vs. the coculture of the MPs with the monolayer MSCs, while the inflammation (*IL6* and *IL8*) and remodeling genes (*RANKL* and *OPG*) remained unchanged. In contrast to BCP 60/40, the coculture of the MPs with MSC + BCP 20/80 under inflammatory conditions revealed the upregulation of the *IL10* gene only, whereas *IL6* and *IL8* were not upregulated in comparison to those in the control cocultures with cytokine stimulation (Figure 6).

The influences of the BCP-cultured MSCs on the gene expressions of the MPs were also assessed after 72 h of coculture. The genes commonly associated with the M1 (*IL1β*, *IL6* and *IL8*) and M2 MP phenotypes (*IL10* and *VEGF*) were evaluated. No significant differences in MP differentiation were observed when cocultured with either monolayer MSCs or BCP 20/80-cultured MSCs, regardless of cytokine stimulation. However, in the BCP 60/40-cultured MSCs, cytokine stimulation led to the upregulation of M1 macrophage markers (*IL1β*, *IL6* and *IL8*) (Supplementary Figure S2). This suggests a predisposition towards the M1 MP subtype, providing further evidence of an acute inflammatory microenvironment, although no clear evidence of an MP phenotype "switch" was observed.

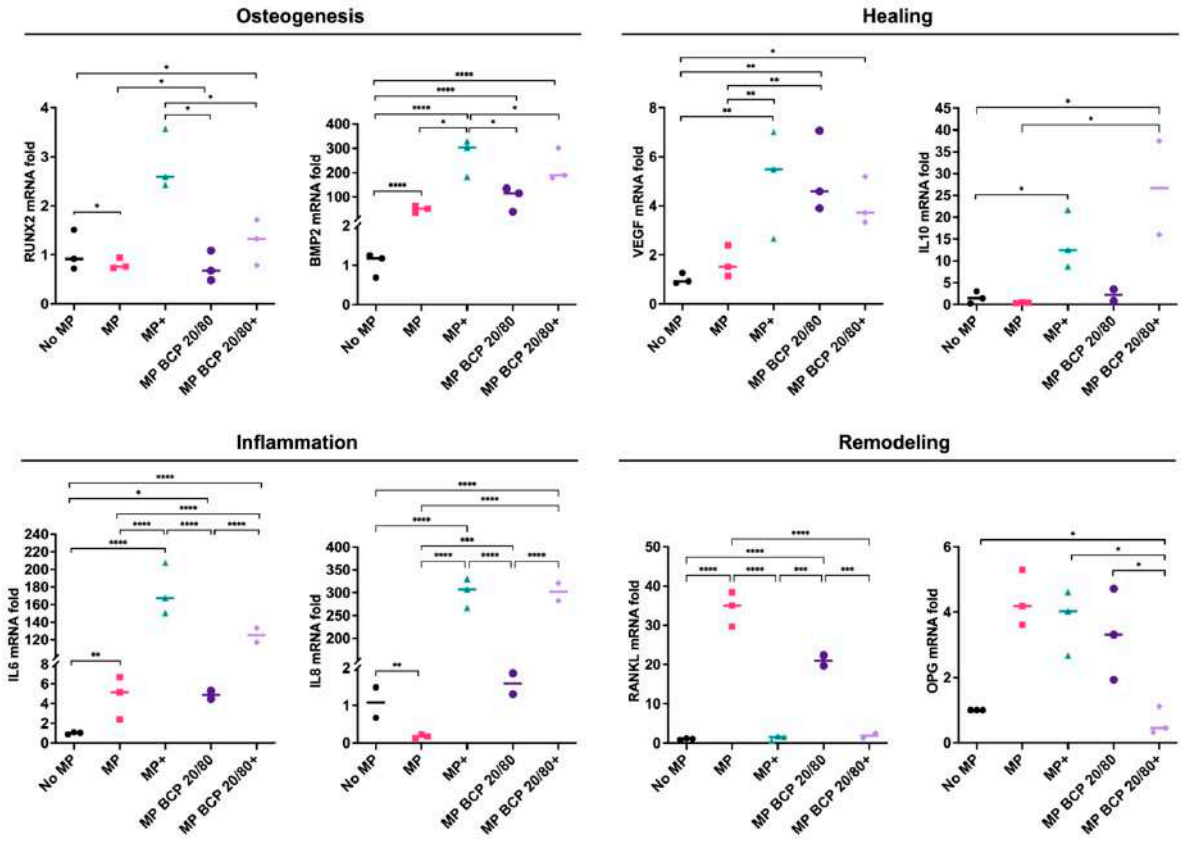

Figure 6. Relative mRNA expressions (fold changes) of osteogenesis-, healing-, inflammation- and remodeling-related genes in MSCs cultured with BCP 20/80 and/or MPs (n = 3). No MP, monolayer MSC control; MP, monolayer MSCs cocultured with MPs; + represents cytokine stimulation. Statistical analyses are based on one-way ANOVA with Tukey's multiple comparison tests on delta-Ct values; * $p < 0.05$; ** $p < 0.001$; *** $p = 0.0001$; **** $p < 0.0001$.

2.4. BCP Altered MSC Cytokine Profile in Cocultures

In setup B, the coculture with the MPs did not significantly alter the cytokine profiles of the MSCs based on the evaluated panel of cytokines. With regards to the BCP granules, the secretion of VEGF and CCL4 was enhanced in MSC + BCP 60/40, while IL5, IL7 and IL9 were enhanced in MSC + BCP 20/80 compared to those in the control cocultures. In the presence of cytokine stimulation, the secretion of GCSF, IL10 and IL9 was enhanced in MSC + BCP 60/40, while no increased secretion was observed in MSC + BCP 20/80 compared to that in the cytokine-stimulated control cocultures. In fact, the secretion of PDGFBB, IL7 and CCL5 was significantly reduced in stimulated MSC + BCP 20/80 (Figure 7).

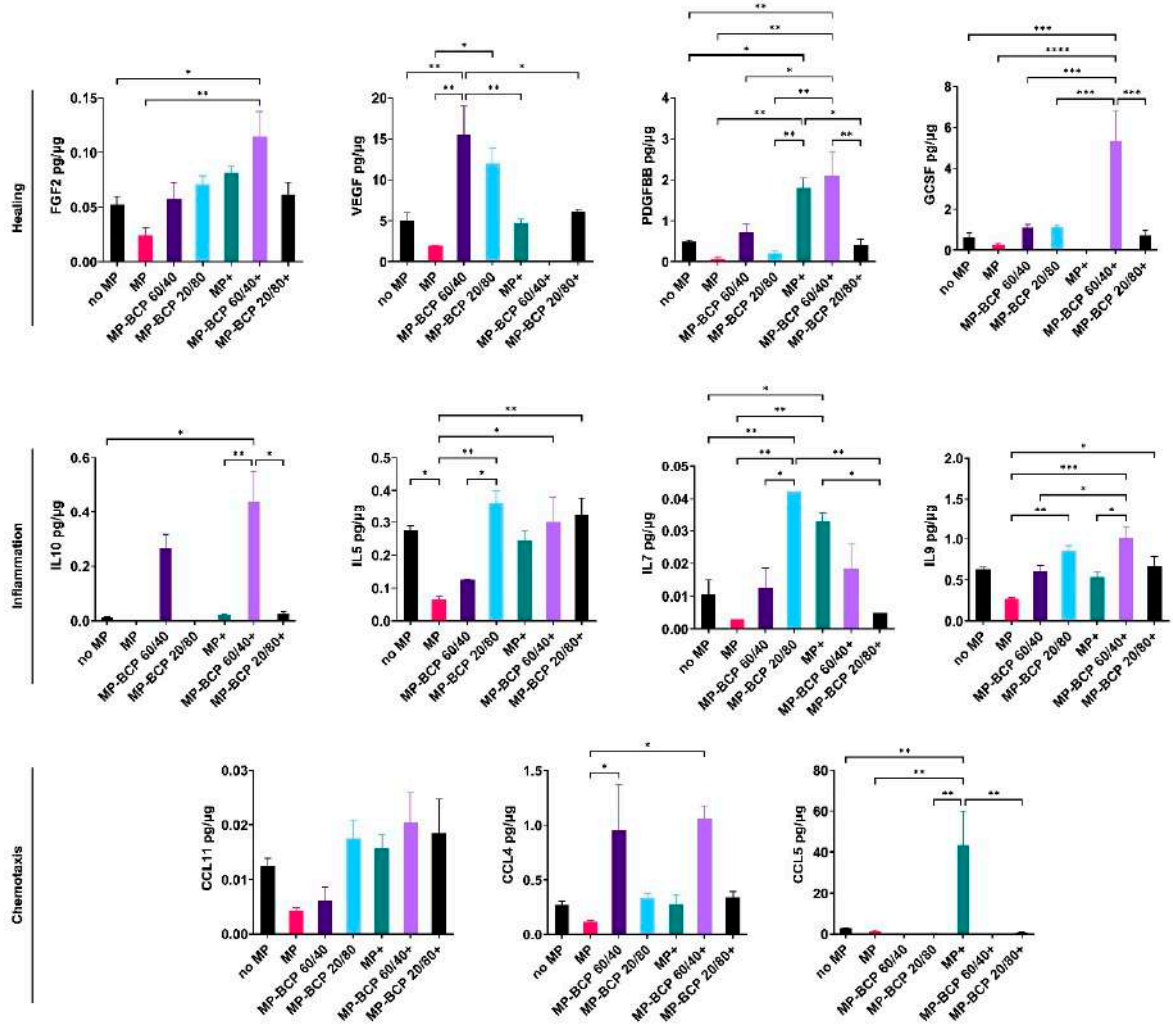

Figure 7. Multiplex cytokine assay of MPs co-cultured with MSCs and BCP granules (BCP 60/40 or BCP 20/80). Cytokines related to healing, inflammation and chemotaxis were measured after 72 h. + indicates cytokine stimulation. Concentration of each analyte (pg/mL) was normalized to total protein concentration of the conditioned media (µg/mL). Statistical analyses are based on one-way ANOVA with Tukey's multiple comparison tests; * $p < 0.05$; ** $p < 0.001$; *** $p = 0.0001$; **** $p < 0.0001$.

3. Discussion

Tissue engineering strategies for bone regeneration frequently involve the use of MSCs seeded on biomaterials, e.g., alloplastic bone substitutes, used as carrier scaffolds. The objective of the present study was to assess whether BCP bone substitutes influence vitro MSC responses and MSC–MP interactions in an inflammatory microenvironment. The research question in a clinical context was whether, within the limitations of in vitro models, the presence of a bone substitute poses a risk for aggravating early cellular responses and, possibly, delaying healing at sites of active inflammation. MSCs were cultured in the presence of BCP granules (BCP 60/40 or 20/80) and cytokine stimulation (IL1β + TNFα) to mimic acute inflammation, either alone or in a coculture with MPs. Overall, our findings indicate that the BCP granules (a) significantly modulated MSC gene expressions, both in the presence and absence of inflammation; (b) did not significantly alter MSC cytokine secretion, regardless of inflammation; and (c) in the indirect coculture with the MPs, did not significantly alter MSC gene expressions or cytokine secretion, regardless of inflammation.

Emerging concepts suggest that the mechanisms of MSC bioactivity primarily involve the paracrine modulation of host responses rather than direct differentiation and tissue-specific cell replacement [6,27]. It has been proposed that MSCs exert their effects via

interactions with resident immune cells in the early stages of wound healing. Moreover, the resulting paracrine secretions may continue to stimulate other immune cells over time and guide the healing process [28,29]. MSCs respond to inflammation by adjusting their immunoregulatory repertoire and by differentially modulating their gene expressions and cytokine profiles [30]. With regards to the inflammatory cytokines used herein, IL1β has been reported to prime MSCs towards anti-inflammatory and pro-trophic phenotypes in vitro, while TNFα triggers a more potent pro-inflammatory profile to instrument effective tissue repair [31]. The stimulation of MSCs with a combination of pro-inflammatory cytokines may lead to additional or synergistic effects, such as increased cytokine secretion [32]. While several studies have investigated the effects of inflammatory cytokines on MSCs [33], few studies have reported on the responses of MSCs in the presence of BCP bone substitutes [13].

In setup A, regardless of cytokine stimulation, the BCP granules enhanced the expressions of osteogenesis- (BMP2) and healing-related genes (*VEGF* and *IL10*) but suppressed those of inflammation-related genes (*IL6* and *IL8*) in the MSCs, suggesting positive effects of BCP in terms of pro-healing MSC activity. Similar trends in MSC responses were observed with BCP 60/40 and BCP 20/80. Surprisingly, the expression of *RUNX2* was not significantly altered by the BCP granules after 72 h, despite the strong upregulation of *BMP2*, which is reported to be an upstream regulator of *RUNX2* [10,11]. Similar results have been reported in previous studies regarding *RUNX2* expression by MSCs on BCP granules. One possible reason could be the relatively early time point (72 h) used in the present study, as previous studies analyzed *RUNX2* expression after 7 and 14 days [34,35]. Despite the changes in the gene expressions of the MSCs, the secretion of healing- and inflammation-related cytokines was not significantly altered by the presence of the BCPs, either BCP 60/40 or BCP 20/80. Moreover, while cytokine stimulation significantly altered the secretory profiles of the MSCs, the additional effect of the BCP granules under inflammatory conditions was minimal. Nevertheless, the presence of the BCP granules seemed to elicit a "pro-healing" response in the MSCs, at least at the gene level, in an inflammatory microenvironment. In context, a previous study has shown that the expressions of several pro-inflammatory genes were attenuated in MSCs cultured on BCP [36]. Together, these findings highlight the relevance of BCP and the microenvironment in MSC activity.

To better simulate the in vivo scenario, it is important to study MSC behaviors in the context of other cells. MSCs interact extensively with immune cells to drive the healing process, and recent evidence has shown the key role played by immune cells, particularly MPs, in the regulation of MSCs during bone regeneration [21,37,38]. In setup B in the present study, the coculture of the MPs with the MSCs in the presence of the BCP granules strongly promoted MSC gene expressions. Specifically, the presence of either BCP 60/40 or BCP 80/20 revealed enhanced MSC expressions of osteogenesis- (*BMP2*) and healing-related genes (*VEGF* and *IL10*), especially in the presence of inflammation. Interestingly, the expressions of inflammation- (*IL6* and *IL8*) and remodeling-related genes (*RANKL* and *OPG*) remained unchanged. In fact, in the presence of BCP 60/40, *RANKL* and *OPG* were downregulated in the MSCs under inflammatory conditions, suggesting that the BCP granules did not aggravate pro-inflammatory MSC responses when cocultured with the MPs.

Inflammation and/or other pathological stimuli lead naive macrophages (M0) to activate into either a classical, pro-inflammatory type (M1) or an alternative anti-inflammatory type (M2) [29]. Signaling molecules from non-activated MPs, particularly BMP2, have been implicated in MSC–MP crosstalk [39]. Our results reveal a sharp upregulation of *BMP2* gene expression in the MSCs when cocultured with the MPs. This expression was further upregulated in the presence of the BCP granules, together with a downregulation of *RANKL* expression. These observations suggest the commitment of MSCs towards an osteogenic phenotype in the presence of non-activated MPs, and they may reflect the physiological role of tissue-resident MPs in bone homeostasis. Further, the role of BCP in the coculture system is also of interest. While the coculture of the MPs with the control MSCs under inflammatory conditions promoted gene expression but not cytokine secretion, both gene

expression and cytokine secretion were strongly promoted in the MSC–MP cocultures in the presence of BCP. Therefore, we hypothesize that the presence of BCP granules endorsed the cytokine stimulation of the MSCs, allowing for an accelerated protein translation.

Although two different commercial BCP bone substitutes were used in the present study (BCP 60/40 and 20/80), the objective herein was not to perform a biological comparison of the two biomaterials but rather to investigate whether a similar trend in MSC responses could be observed with BCP granules with different HA/β-TCP ratios. While the trends in MSC gene expressions and cytokine secretion were generally similar between the two BCPs, some differences were observed. For example, the MSCs showed remarkable differences in the secretion of GCSF in the presence of BCP 60/40 and BCP 20/80. GCSF has been shown to play distinct roles in normal state conditions, as well as in inflammatory conditions [40], and it has been shown to be produced in higher amounts by cytokine-stimulated MSCs [31,41], which could elucidate the differences observed herein. This was further demonstrated in the coculture setup, where the MSCs secreted higher levels of GCSF in the presence of BCP 60/40. Together, these findings highlight the impact of subtle biomaterial properties on the immunomodulatory responses of MSCs.

Some limitations of the present study must be acknowledged. Firstly, the results herein are based on MSCs derived from a single donor, and, therefore, the findings should be verified using multiple donors' MSCs to exclude the effects of donor variation. Moreover, we differentiated MPs from a promonocytic cell line (U937) and not from primary peripheral blood monocytes. Although widely used as an economical and reliable in vitro model, U937-derived MPs may not accurately replicate the "plasticity" and/or responses of the M1/M2 phenotype in the context of other cells, i.e., in cocultures. For example, the increased secretion of anti-inflammatory cytokines observed in the BCP-cultured MSCs did not translate to altered gene expressions of the U937-derived MPs in the corresponding cocultures. A similar trend in LPS-treated BV2 cells has been observed when exposed to conditioned medium from cytokine-stimulated MSCs [41]. Cell-line-derived MPs are reported to differ from primary MPs in their cytokine profiles, which could also explain the differences in gene expression patterns [42]. Another limitation herein was the lack of functional assays to demonstrate MP activity, e.g., via direct culture on BCP, and to demonstrate MSC function, e.g., the suppression of T-cell proliferation, in order to support the gene and protein analyses. Finally, the role of other innate immune cells (particularly neutrophils) in MSC- and biomaterial-mediated healing should be investigated in future studies [43,44].

4. Materials and Methods

4.1. Cell Culture

The use of human cells and tissues was approved by the Regional Committees for Medical Research Ethics (REK) in Norway (2013-1248, REK sør-øst C). Primary human bone marrow MSCs from a healthy 10-year-old male donor were cultured in growth medium (GM) composed of Dulbecco's modified Eagle's medium (DMEM, Invitrogen, Carlsbad, CA, USA) supplemented with 1% penicillin/streptomycin (GE Healthcare, South Logan, UT, USA) and 10% fetal bovine serum (FBS; GE Healthcare). The details of MSC isolation and characterization via immunophenotyping and tri-lineage differentiation assays have been reported elsewhere [45]. Cells were sub-cultured (4000 cells/cm^2) and expanded in humidified 5% CO_2 at 37 °C; passage 2–4 cells were used in experiments.

MPs were derived from the human pro-monocytic U937 cell line (CRL-1593.2, ATCC, Rockville, MD, USA); cells were cultured in GM as described above. To induce differentiation into the MPs, U937 cells were stimulated with 50 ng/mL phorbol 12-myristate 13-acetate (PMA; Sigma-Aldrich, St. Louis, MO, USA) for 48 h [46]. Subsequently, the PMA-treated cells were washed in phosphate-buffered saline (PBS; Invitrogen), to remove the PMA along with nonadherent cells, and further maintained in GM. Cell growth and the morphology of the MSCs and MPs were regularly monitored under a phase-contrast microscope (Nikon Eclipse TS100, Tokyo, Japan).

4.2. BCP Bone Substitutes

Two different commercial BCP bone substitutes were used in this study: BoneCeramic® (BC; Institut Straumann AG, Basel, Switzerland) porous granules (0.5–1 mm) with HA/β-TCP in a 60/40 ratio and Biomatlante MBCP+® (BM; Biomatlante, Vigneux de Bretagne, France) micro-porous granules (0.5–1 mm) with HA/β-TCP in a 20/80 ratio. Both BCPs were supplied in sterile packaging and used under sterile conditions in the experiments. Both BCPs have previously been used to deliver MSCs in clinical studies of bone tissue engineering [47,48].

4.3. Experimental Setup

Two experimental setups were used in this study: setup A, where MSCs were seeded on BCP with and without cytokine stimulation, and setup B, where MSCs were seeded on BCP and cocultured with MPs with and without cytokine stimulation to simulate an inflammatory microenvironment. The experimental setups are summarized in Table 1.

Table 1. Summary of experimental setups and groups.

Setup, Group	
A: MSC monoculture	
MSC	MSC+
MSC/BCP 60/40	MSC/BCP 60/40+
MSC/BCP 20/80	MSC/BCP 20/80+
B: MP-MSC coculture	
MP-MSC	MP-MSC+
MP-MSC/BCP 60/40+	MP-MSC/BCP 60/40+
MP-MSC/BCP 20/80+	MP-MSC/BCP 20/80+

MSC, bone marrow mesenchymal stromal cell; BCP 60/40, BoneCeramic®; BCP 20/80, Biomatlante MBCP+®; +, cytokine stimulation; MP, U937-derived macrophage.

4.4. Cell Seeding

The BCP 60/40 and BCP 20/80 granules (~100 mg per well) were separately loaded in 24-well tissue culture plates and pre-conditioned with GM overnight at 37 °C to promote cell attachment. Next, MSCs suspended in GM (150×10^3 cells in 100 µL per well) were uniformly seeded on the granules and allowed to attach for 2 h. Subsequently, an additional 900 µL of GM (total 1 mL) was added and cultured for 72 h. Monolayer MSCs on the tissue culture plastic served as controls.

4.5. MSC–MP Coculture

In setup B, the cocultures of the MPs with the MSCs (1:4 MP:MSC) and BCP 60/40 or BCP 20/80 granules were set up via transwell assays using polyester membrane inserts with a 0.4 µm pore size (Corning, Lowell, MA, USA); transwell membranes allow cellular interactions without direct cell-to-cell contact. The MPs cocultured with the monolayer MSCs served as controls. The MSCs were seeded on the BCP granules in notched 24-well plates as described above. Separately, the U937 cells were seeded in transwell inserts and stimulated with PMA for 48 h to induce MP differentiation, and they were allowed to mature in GM for an additional 24 h. Thereafter, the inserts with adherent MPs were transferred to the notched wells with the MSCs, and the coculture was initiated in GM for an additional 72 h. In relevant groups, the culture media were supplemented with cytokines to simulate an inflammatory microenvironment.

4.6. Cytokine Stimulation

To simulate inflammation, the MSCs in setups A and B were stimulated with a combination of recombinant human IL1β (10 ng/mL) and TNFα (10 ng/mL) (both from R&D Systems, Minneapolis, MN, USA). Cytokines were added to GM in order to stimulate the MSCs for an additional 72 h, corresponding to the duration of the "acute inflammatory phase" in the in vivo wound-healing cascade. The expressions of genes and secretions of

cytokines (proteins) were assessed in standard (unstimulated) and stimulated monolayer MSCs (control) and BCP-cultured MSCs.

4.7. Gene Expression Analysis

In setups A and B, the expressions of the genes associated with osteogenesis, healing, inflammation and remodeling (Supplementary Table S1) were assessed in the MSCs after 72 h. Gene expression was assessed via quantitative real-time polymerase chain reaction (qPCR) using TaqMan® real-time PCR assays (Thermo Scientific). RNA extraction and cDNA synthesis were performed as previously described [45]. Briefly, total RNA was extracted using an RNA extraction kit (Maxwell, Promega, Madison, WI, USA), and cDNA was synthesized using a high-capacity cDNA reverse transcription kit (Applied Biosystems, Foster City, CA, USA), following the manufacturers' protocols. qPCR was performed using a TaqMan Fast Universal PCR Master Mix with amplification in a StepOne Real-Time PCR System (both from Applied Biosystems), following the manufacturers' protocols. The expressions of the genes of interest were normalized to that of the housekeeping gene glyceraldehyde 3-phosphate dehydrogenase (GAPDH). Data were analyzed by using the $\Delta\Delta Ct$ method, and the results are presented as fold changes relative to the results of the control group (unstimulated monolayer MSCs).

4.8. Multiplex Cytokine Assay

In setups A and B, the concentrations of various cytokines (Supplementary Table S2) in the supernatant media of the MSCs were measured using a human cytokine 27-plex assay and the Bio-Plex® 200 System (both from Bio-Rad Laboratories, CA, USA), according to the manufacturer's instructions. Supernatant media from the MSCs in the different culture conditions were collected after 72 h for cytokine analyses. The total protein concentrations (µg/mL) in all samples were measured using a Pierce® Bicinchoninic Acid Protein Assay (Thermo Scientific) according to the manufacturer's instructions. As the total protein concentrations were significantly different between the groups, individual cytokine concentrations in the multiplex assay were normalized to the corresponding total protein (pg/µg) for each group.

4.9. Statistical Analysis

Statistical analyses were performed using Prism 9.0 software (GraphPad Software, San Diego, CA, USA). Data are presented as means (±SD) unless otherwise specified. Gene expression analyses are based on delta-CT values, and the results are presented as relative (log/non-linear) fold changes using scatter plots. All other linear data are presented as bar graphs. Normality testing was performed via the Shapiro–Wilk test. A one-way analysis of variance (ANOVA, followed by post hoc Tukey's test for multiple comparisons) was applied, and $p < 0.05$ was considered statistically significant.

5. Conclusions

Overall, the findings herein indicate that, under both inflammatory and non-inflammatory conditions, the BCP granules significantly regulated the expressions of osteogenesis-, healing- and inflammation-related genes in the MSCs towards a pro-healing phenotype but had relatively little effect on the MSC secretory profiles. In the presence of the MPs (indirect coculture), BCP positively regulated both the gene expressions and cytokine secretion of the MSCs. Overall, similar trends in MSC responses were observed with BCP 60/40 and BCP 20/80. Thus, within the limitations of in vitro models, we postulate that the presence of a BCP bone substitute at the surgical site does not have a detrimental effect on MSC-mediated healing, even in the event of inflammation. Future studies using primary human immune cells may more accurately reveal the mechanisms of crosstalk with MSCs in the context of bone regeneration.

Supplementary Materials: The supporting information can be downloaded at: https://www.mdpi.com/article/10.3390/ijms24010438/s1.

Author Contributions: S.S. (Siddharth Shanbhag), N.R., S.S. (Salwa Suliman), K.M. and A.S. conceived and designed the study. S.S. (Siddharth Shanbhag), N.R., and S.B.I. performed the experiments, data collection and data analysis and drafted the manuscript. S.S. (Salwa Suliman), K.M. and A.S. assisted in data analysis and drafting the manuscript. K.M. and A.S. were responsible for funding acquisition. All authors have read and agreed to the published version of the manuscript.

Funding: This work was supported by Helse Vest, Norway (project no. F-12124); MAXIBONE EU H2020 (project no. 779322); and the International Team for Implantology (ITI), Switzerland (project no. 1117_2015).

Institutional Review Board Statement: The use of human cells and tissues was approved by the Regional Committees for Medical Research Ethics (REK) in Norway (2013-1248, REK sør-øst C).

Informed Consent Statement: Informed consent was obtained from all subjects involved in the study.

Data Availability Statement: All data are provided in either the figures or Supplementary Material; otherwise, they are available upon request.

Acknowledgments: We thank Ying Xue from the Department of Clinical Dentistry, University of Bergen, for assistance with the multiplex experiments.

Conflicts of Interest: The authors confirm that there are no known conflict of interest associated with this publication and there has been no significant financial support for this work that could have influenced its outcome.

References

1. Gruber, R.; Stadlinger, B.; Terheyden, H. Cell-to-cell communication in guided bone regeneration: Molecular and cellular mechanisms. *Clin. Oral Implants. Res.* **2017**, *28*, 1139–1146. [CrossRef] [PubMed]
2. Yang, N.; Liu, Y. The Role of the Immune Microenvironment in Bone Regeneration. *Int. J. Med. Sci.* **2021**, *18*, 3697–3707. [CrossRef] [PubMed]
3. Papachristou, D.J.; Georgopoulos, S.; Giannoudis, P.V.; Panagiotopoulos, E. Insights into the Cellular and Molecular Mechanisms That Govern the Fracture-Healing Process: A Narrative Review. *J. Clin. Med.* **2021**, *10*, 3554. [CrossRef]
4. Parekkadan, B.; Milwid, J.M. Mesenchymal Stem Cells as Therapeutics. *Annu. Rev. Biomed. Eng.* **2010**, *12*, 87–117. [CrossRef] [PubMed]
5. Sohni, A.; Verfaillie, C.M. Mesenchymal Stem Cells Migration Homing and Tracking. *Stem Cells Int.* **2013**, *2013*, 130763. [CrossRef]
6. Gamblin, A.-L.; Brennan, M.A.; Renaud, A.; Yagita, H.; Lézot, F.; Heymann, D.; Trichet, V.; Layrolle, P. Bone tissue formation with human mesenchymal stem cells and biphasic calcium phosphate ceramics: The local implication of osteoclasts and macrophages. *Biomaterials* **2014**, *35*, 9660–9667. [CrossRef]
7. Oryan, A.; Kamali, A.; Moshiri, A.; Baghaban Eslaminejad, M. Role of Mesenchymal Stem Cells in Bone Regenerative Medicine: What Is the Evidence? *Cells Tissues Organs* **2017**, *204*, 59–83. [CrossRef]
8. Henkel, J.; Woodruff, M.A.; Epari, D.R.; Steck, R.; Glatt, V.; Dickinson, I.C.; Choong, P.F.M.; Schuetz, M.A.; Hutmacher, D.W. Bone Regeneration Based on Tissue Engineering Conceptions—A 21st Century Perspective. *Bone Res.* **2013**, *1*, 216–248. [CrossRef]
9. Shanbhag, S.; Suliman, S.; Pandis, N.; Stavropoulos, A.; Sanz, M.; Mustafa, K. Cell therapy for orofacial bone regeneration: A systematic review and meta-analysis. *J. Clin. Periodontol.* **2019**, *46* (Suppl. 21), 162–182. [CrossRef]
10. Jang, W.G.; Kim, E.J.; Kim, D.K.; Ryoo, H.M.; Lee, K.B.; Kim, S.H.; Choi, H.S.; Koh, J.T. BMP2 protein regulates osteocalcin expression via Runx2-mediated Atf6 gene transcription. *J. Biol. Chem.* **2012**, *287*, 905–915. [CrossRef]
11. Phimphilai, M.; Zhao, Z.; Boules, H.; Roca, H.; Franceschi, R.T. BMP signaling is required for RUNX2-dependent induction of the osteoblast phenotype. *J. Bone Miner. Res.* **2006**, *21*, 637–646. [CrossRef] [PubMed]
12. Ponzetti, M.; Rucci, N. Updates on Osteoimmunology: What's New on the Cross-Talk Between Bone and Immune System. *Front. Endocrinol.* **2019**, *10*, 236. [CrossRef]
13. Chen, Z.; Wu, C.; Gu, W.; Klein, T.; Crawford, R.; Xiao, Y. Osteogenic differentiation of bone marrow MSCs by β-tricalcium phosphate stimulating macrophages via BMP2 signalling pathway. *Biomaterials* **2014**, *35*, 1507–1518. [CrossRef] [PubMed]
14. Maggini, J.; Mirkin, G.; Bognanni, I.; Holmberg, J.; Piazzón, I.M.; Nepomnaschy, I.; Costa, H.; Cañones, C.; Raiden, S.; Vermeulen, M.; et al. Mouse Bone Marrow-Derived Mesenchymal Stromal Cells Turn Activated Macrophages into a Regulatory-Like Profile. *PLoS One* **2010**, *5*, e9252. [CrossRef] [PubMed]
15. Wise, A.F.; Williams, T.M.; Kiewiet, M.B.; Payne, N.L.; Siatskas, C.; Samuel, C.S.; Ricardo, S.D. Human mesenchymal stem cells alter macrophage phenotype and promote regeneration via homing to the kidney following ischemia-reperfusion injury. *Am. J. Physiol. Renal Physiol.* **2014**, *306*, F1222–F1235. [CrossRef]

16. Tylek, T.; Schilling, T.; Schlegelmilch, K.; Ries, M.; Rudert, M.; Jakob, F.; Groll, J. Platelet lysate outperforms FCS and human serum for co-culture of primary human macrophages and hMSCs. *Sci. Rep.* **2019**, *9*, 3533. [CrossRef]
17. Boyce, B.F.; Xing, L. Functions of RANKL/RANK/OPG in bone modeling and remodeling. *Arch Biochem. Biophys.* **2008**, *473*, 139–146. [CrossRef]
18. Sanz, M.; Dahlin, C.; Apatzidou, D.; Artzi, Z.; Bozic, D.; Calciolari, E.; De Bruyn, H.; Dommisch, H.; Donos, N.; Eickholz, P.; et al. Biomaterials and regenerative technologies used in bone regeneration in the craniomaxillofacial region: Consensus report of group 2 of the 15th European Workshop on Periodontology on Bone Regeneration. *J. Clin. Periodontol.* **2019**, *46* (Suppl. 21), 82–91. [CrossRef]
19. Jepsen, S.; Schwarz, F.; Cordaro, L.; Derks, J.; Hammerle, C.H.F.; Heitz-Mayfield, L.J.; Hernandez-Alfaro, F.; Meijer, H.J.A.; Naenni, N.; Ortiz-Vigon, A.; et al. Regeneration of alveolar ridge defects. Consensus report of group 4 of the 15th European Workshop on Periodontology on Bone Regeneration. *J. Clin. Periodontol.* **2019**, *46* (Suppl. 21), 277–286. [CrossRef]
20. Humbert, P.; Brennan, M.Á.; Davison, N.; Rosset, P.; Trichet, V.; Blanchard, F.; Layrolle, P. Immune Modulation by Transplanted Calcium Phosphate Biomaterials and Human Mesenchymal Stromal Cells in Bone Regeneration. *Front. Immunol.* **2019**, *10*, 663. [CrossRef]
21. Rana, N.; Suliman, S.; Al-Sharabi, N.; Mustafa, K. Extracellular Vesicles Derived from Primed Mesenchymal Stromal Cells Loaded on Biphasic Calcium Phosphate Biomaterial Exhibit Enhanced Macrophage Polarization. *Cells* **2022**, *11*, 470. [CrossRef] [PubMed]
22. Leach, J.K.; Whitehead, J. Materials-Directed Differentiation of Mesenchymal Stem Cells for Tissue Engineering and Regeneration. *ACS Biomater. Sci. Eng.* **2018**, *4*, 1115–1127. [CrossRef] [PubMed]
23. Vasandan, A.B.; Jahnavi, S.; Shashank, C.; Prasad, P.; Kumar, A.; Prasanna, S.J. Human Mesenchymal stem cells program macrophage plasticity by altering their metabolic status via a PGE(2)-dependent mechanism. *Sci. Rep.* **2016**, *6*, 38308. [CrossRef] [PubMed]
24. Jin, L.; Deng, Z.; Zhang, J.; Yang, C.; Liu, J.; Han, W.; Ye, P.; Si, Y.; Chen, G. Mesenchymal stem cells promote type 2 macrophage polarization to ameliorate the myocardial injury caused by diabetic cardiomyopathy. *J. Transl. Med.* **2019**, *17*, 251. [CrossRef] [PubMed]
25. Wang, J.; Liu, Y.; Ding, H.; Shi, X.; Ren, H. Mesenchymal stem cell-secreted prostaglandin E(2) ameliorates acute liver failure via attenuation of cell death and regulation of macrophage polarization. *Stem Cell Res. Ther.* **2021**, *12*, 15. [CrossRef]
26. Noronha, N.d.C.; Mizukami, A.; Caliári-Oliveira, C.; Cominal, J.G.; Rocha, J.L.M.; Covas, D.T.; Swiech, K.; Malmegrim, K.C.R. Priming approaches to improve the efficacy of mesenchymal stromal cell-based therapies. *Stem Cell Res. Ther.* **2019**, *10*, 131. [CrossRef]
27. Brennan, M.Á.; Renaud, A.; Amiaud, J.; Rojewski, M.T.; Schrezenmeier, H.; Heymann, D.; Trichet, V.; Layrolle, P. Pre-clinical studies of bone regeneration with human bone marrow stromal cells and biphasic calcium phosphate. *Stem Cell Res. Ther.* **2014**, *5*, 114. [CrossRef]
28. Medhat, D.; Rodríguez, C.I.; Infante, A. Immunomodulatory Effects of MSCs in Bone Healing. *Int. J. Mol. Sci.* **2019**, *20*, 5467. [CrossRef]
29. Luque-Campos, N.; Bustamante-Barrientos, F.A.; Pradenas, C.; García, C.; Araya, M.J.; Bohaud, C.; Contreras-López, R.; Elizondo-Vega, R.; Djouad, F.; Luz-Crawford, P.; et al. The Macrophage Response Is Driven by Mesenchymal Stem Cell-Mediated Metabolic Reprogramming. *Front. Immunol.* **2021**, *12*, 624746. [CrossRef]
30. Najar, M.; Ouhaddi, Y.; Bouhtit, F.; Melki, R.; Afif, H.; Boukhatem, N.; Merimi, M.; Fahmi, H. Empowering the immune fate of bone marrow mesenchymal stromal cells: Gene and protein changes. *Inflamm. Res.* **2019**, *68*, 167–176. [CrossRef]
31. Redondo-Castro, E.; Cunningham, C.; Miller, J.; Martuscelli, L.; Aoulad-Ali, S.; Rothwell, N.J.; Kielty, C.M.; Allan, S.M.; Pinteaux, E. Interleukin-1 primes human mesenchymal stem cells towards an anti-inflammatory and pro-trophic phenotype in vitro. *Stem Cell Res. Ther.* **2017**, *8*, 79. [CrossRef] [PubMed]
32. Crisostomo, P.R.; Wang, Y.; Markel, T.A.; Wang, M.; Lahm, T.; Meldrum, D.R. Human mesenchymal stem cells stimulated by TNF-alpha, LPS, or hypoxia produce growth factors by an NF kappa B- but not JNK-dependent mechanism. *Am. J. Physiol. Cell Physiol.* **2008**, *294*, C675–C682. [CrossRef] [PubMed]
33. Lin, T.; Pajarinen, J.; Nabeshima, A.; Lu, L.; Nathan, K.; Jämsen, E.; Yao, Z.; Goodman, S.B. Preconditioning of murine mesenchymal stem cells synergistically enhanced immunomodulation and osteogenesis. *Stem Cell Res. Ther.* **2017**, *8*, 277. [CrossRef] [PubMed]
34. Chamary, S.; Grenho, L.; Fernandes, M.H.; Bouchart, F.; Monteiro, F.J.; Hornez, J.C. Influence of a Macroporous β-TCP Structure on human mesenchymal stem cell proliferation and differentiation in vitro. *Open Ceram.* **2021**, *7*, 100141. [CrossRef]
35. Lobo, S.E.; Glickman, R.; Da Silva, W.N.; Arinzeh, T.L.; Kerkis, I. Response of stem cells from different origins to biphasic calcium phosphate bioceramics. *Cell Tissue Res.* **2015**, *361*, 477–495. [CrossRef]
36. Zhu, Y.; Zhang, K.; Zhao, R.; Ye, X.; Chen, X.; Xiao, Z.; Yang, X.; Zhu, X.; Zhang, K.; Fan, Y.; et al. Bone regeneration with micro/nano hybrid-structured biphasic calcium phosphate bioceramics at segmental bone defect and the induced immunoregulation of MSCs. *Biomaterials* **2017**, *147*, 133–144. [CrossRef]
37. Wang, Y.H.; Zhao, C.Z.; Wang, R.Y.; Du, Q.X.; Liu, J.Y.; Pan, J. The crosstalk between macrophages and bone marrow mesenchymal stem cells in bone healing. *Stem Cell Res. Ther.* **2022**, *13*, 511. [CrossRef]
38. Chen, R.; Hao, Z.; Wang, Y.; Zhu, H.; Hu, Y.; Chen, T.; Zhang, P.; Li, J. Mesenchymal Stem Cell-Immune Cell Interaction and Related Modulations for Bone Tissue Engineering. *Stem Cells Int.* **2022**, *2022*, 7153584. [CrossRef]

39. Champagne, C.M.; Takebe, J.; Offenbacher, S.; Cooper, L.F. Macrophage cell lines produce osteoinductive signals that include bone morphogenetic protein-2. *Bone* **2002**, *30*, 26–31. [CrossRef]
40. Granulocyte colony-stimulating factor (G-CSF). *Meyler's Side Effects of Drugs*, 16th ed.; Aronson, J.K., Ed.; Elsevier: Oxford, UK, 2016; pp. 605–619. [CrossRef]
41. Redondo-Castro, E.; Cunningham, C.J.; Miller, J.; Brown, H.; Allan, S.M.; Pinteaux, E. Changes in the secretome of tri-dimensional spheroid-cultured human mesenchymal stem cells in vitro by interleukin-1 priming. *Stem Cell Res. Ther.* **2018**, *9*, 11. [CrossRef]
42. Riddy, D.M.; Goy, E.; Delerive, P.; Summers, R.J.; Sexton, P.M.; Langmead, C.J. Comparative genotypic and phenotypic analysis of human peripheral blood monocytes and surrogate monocyte-like cell lines commonly used in metabolic disease research. *PLoS ONE* **2018**, *13*, e0197177. [CrossRef] [PubMed]
43. Summers, C.; Rankin, S.M.; Condliffe, A.M.; Singh, N.; Peters, A.M.; Chilvers, E.R. Neutrophil kinetics in health and disease. *Trends Immunol.* **2010**, *31*, 318–324. [CrossRef] [PubMed]
44. Jhunjhunwala, S.; Aresta-DaSilva, S.; Tang, K.; Alvarez, D.; Webber, M.J.; Tang, B.C.; Lavin, D.M.; Veiseh, O.; Doloff, J.C.; Bose, S.; et al. Neutrophil Responses to Sterile Implant Materials. *PLoS ONE* **2015**, *10*, e0137550. [CrossRef]
45. Mohamed-Ahmed, S.; Fristad, I.; Lie, S.A.; Suliman, S.; Mustafa, K.; Vindenes, H.; Idris, S.B. Adipose-derived and bone marrow mesenchymal stem cells: A donor-matched comparison. *Stem Cell Res. Ther.* **2018**, *9*, 168. [CrossRef] [PubMed]
46. Jin, L.; Wu, J.; Yuan, G.; Chen, T. In vitro study of the inflammatory cells response to biodegradable Mg-based alloy extract. *PLoS ONE* **2018**, *13*, e0193276. [CrossRef] [PubMed]
47. Prins, H.J.; Schulten, E.A.; Ten Bruggenkate, C.M.; Klein-Nulend, J.; Helder, M.N. Bone Regeneration Using the Freshly Isolated Autologous Stromal Vascular Fraction of Adipose Tissue in Combination With Calcium Phosphate Ceramics. *Stem Cells Transl. Med.* **2016**, *5*, 1362–1374. [CrossRef]
48. Gjerde, C.; Mustafa, K.; Hellem, S.; Rojewski, M.; Gjengedal, H.; Yassin, M.A.; Feng, X.; Skaale, S.; Berge, T.; Rosen, A.; et al. Cell therapy induced regeneration of severely atrophied mandibular bone in a clinical trial. *Stem Cell Res. Ther.* **2018**, *9*, 213. [CrossRef]

Disclaimer/Publisher's Note: The statements, opinions and data contained in all publications are solely those of the individual author(s) and contributor(s) and not of MDPI and/or the editor(s). MDPI and/or the editor(s) disclaim responsibility for any injury to people or property resulting from any ideas, methods, instructions or products referred to in the content.

frontiers | Frontiers in Bioengineering and Biotechnology

TYPE Brief Research Report
PUBLISHED 29 September 2022
DOI 10.3389/fbioe.2022.969275

Check for updates

OPEN ACCESS

EDITED BY
Anna Lange-Consiglio,
University of Milan, Italy

REVIEWED BY
Jia Xian Law,
Universiti Kebangsaan Malaysia, Malaysia
Masahiro Nishimura,
Kagoshima University, Japan
Pavel Karalkin,
I.M. Sechenov First Moscow State Medical University, Russia
Morten Juhl,
Department of Cardiology, Rigshospitalet, Denmark

*CORRESPONDENCE
Siddharth Shanbhag,
siddharth.shanbhag@uib.no

SPECIALTY SECTION
This article was submitted to Tissue Engineering and Regenerative Medicine, a section of the journal Frontiers in Bioengineering and Biotechnology

RECEIVED 14 June 2022
ACCEPTED 14 September 2022
PUBLISHED 29 September 2022

CITATION
Shanbhag S, Al-Sharabi N, Mohamed-Ahmed S, Gruber R, Kristoffersen EK and Mustafa K (2022), Brief communication: Effects of conditioned media from human platelet lysate cultured MSC on osteogenic cell differentiation in vitro. *Front. Bioeng. Biotechnol.* 10:969275. doi: 10.3389/fbioe.2022.969275

COPYRIGHT
© 2022 Shanbhag, Al-Sharabi, Mohamed-Ahmed, Gruber, Kristoffersen and Mustafa. This is an open-access article distributed under the terms of the Creative Commons Attribution License (CC BY). The use, distribution or reproduction in other forums is permitted, provided the original author(s) and the copyright owner(s) are credited and that the original publication in this journal is cited, in accordance with accepted academic practice. No use, distribution or reproduction is permitted which does not comply with these terms.

Brief communication: Effects of conditioned media from human platelet lysate cultured MSC on osteogenic cell differentiation *in vitro*

Siddharth Shanbhag[1,2]*, Niyaz Al-Sharabi[2], Samih Mohamed-Ahmed[2], Reinhard Gruber[3,4,5], Einar K. Kristoffersen[1,6] and Kamal Mustafa[2]

[1]Department of Immunology and Transfusion Medicine, Haukeland University Hospital, Bergen, Norway, [2]Center for Translational Oral Research, Department of Clinical Dentistry, Faculty of Medicine, University of Bergen, Bergen, Norway, [3]Department of Oral Biology, University Clinic of Dentistry, Medical University of Vienna, Vienna, Austria, [4]Department of Periodontology, School of Dental Medicine, University of Bern, Bern, Switzerland, [5]Austrian Cluster for Tissue Regeneration, Vienna, Austria, [6]Department of Clinical Sciences, Faculty of Medicine, University of Bergen, Bergen, Norway

Culturing mesenchymal stromal cells (MSC) in human platelet lysate (HPL) supplemented media can enhance their osteogenic differentiation potential. The objective of this study was to test the hypothesis that conditioned media (CM) derived from HPL-cultured MSC also have pro-osteogenic effects. Pooled CM was prepared from HPL-cultured human bone marrow MSC (BMSC) of multiple donors and applied on BMSC of different donors (than those used for CM preparation), with or without additional supplementation [HPL, fetal bovine serum (FBS)] and osteogenic stimulation. At various time-points, cell proliferation, alkaline phosphatase (ALP) activity, osteogenic gene expression and *in vitro* mineralization were assessed. BMSC in standard unstimulated growth media served as controls. After 3–7 days, CM alone did not promote BMSC proliferation or ALP activity; supplementation of CM with HPL slightly improved these effects. After 2 and 7 days, CM alone, but not CM supplemented with HPL, promoted osteogenic gene expression. After 14 days, only CM supplemented with FBS and osteogenic stimulants supported *in vitro* BMSC mineralization; CM alone and CM supplemented with HPL did not support mineralization, regardless of osteogenic stimulation. In summary, CM from HPL-cultured BMSC promoted osteogenic gene expression but not *in vitro* mineralization in allogeneic BMSC even when supplemented with HPL and/or osteogenic stimulants. Future studies should investigate the role and relevance of supplementation and osteogenic induction in *in vitro* assays using CM from MSC.

KEYWORDS

mesenchymal stromal cells, conditioned media, platelet lysate, bone tissue engineering, osteogenic differentation

Introduction

Bone tissue engineering strategies are increasingly being used to overcome the limitations of autogenous bone grafts and existing biomaterials to reconstruct complex bone defects (Shanbhag et al., 2019). Conventional tissue engineering strategies involve the transplantation of autologous adult mesenchymal stromal cells (MSC)—usually from the bone marrow (BMSC), in combination with biomaterial scaffolds and/or signaling molecules at bone defect sites. However, certain limitations of this approach have been discussed. Firstly, in a recent meta-analysis, we found the clinical evidence for the effectiveness of this strategy to be limited; the effect sizes of cell therapy over traditional GBR or grafting procedures were relatively small and mainly limited to studies of maxillary sinus augmentation (Shanbhag et al., 2019). Secondly, large scale translation of autologous cell therapy is limited by the need for expensive Good Manufacturing Practice (GMP) grade laboratories for *ex vivo* cell expansion for each patient/production. Thirdly, the traditional hypothesis that MSC exert their bioactivity *via* engraftment, differentiation, and replacement at injury sites, has in recent years been challenged by evidence of a predominantly paracrine mechanism of action (Haumer et al., 2018).

It is now widely believed that MSC exert their effects *via* the secretion of a wide range of bioactive factors, including soluble proteins (growth factors, cytokines, chemokines), nucleic acids and microparticles [extracellular vesicles (EV)] at or near sites of injury (Gnecchi et al., 2016). These factors in turn stimulate tissue-resident progenitor (osteogenesis), endothelial (angiogenesis) and immune cells (immune modulation), to drive subsequent regeneration processes. Moreover, pre-conditioning or "priming" of MSC with various stimulants (growth factors, inflammatory cytokines, etc.) may further enhance their paracrine activity and immunomodulatory potential (Ferreira et al., 2018). These findings provide the biological basis for the development of "cell-free" strategies, which exploit the secretome contained in MSC conditioned media (CM) for tissue regeneration. A major advantage of this strategy is the possibility to produce secretomes on a large scale from a single (or limited) cell expansion cycle(s), and to use these factors as "off-the-shelf" products. The preclinical efficacy of MSC secretomes/CM for bone regeneration has recently been summarized (Veronesi et al., 2018; Benavides-Castellanos et al., 2020).

A critical aspect in the clinical translation of cell therapies is the use of safe and standardized culture conditions resulting in safe-to-use cell constructs. Exclusion of animal-derived supplements, e.g., fetal bovine serum (FBS), in *ex vivo* culture systems is considered important to facilitate clinical translation of cell therapies and is also a recommendation by regulatory health authorities (Bieback et al., 2019). This consideration may also be extended to cell-derivatives such as CM. Pooled human platelet lysate (HPL) has been identified as the optimal "xeno-free" supplement for MSC culture, with particular benefits for MSC osteogenic differentiation (Fekete et al., 2012; Shanbhag et al., 2017). We have recently reported that HPL-cultured MSC demonstrate superior proliferation, osteogenic gene expression and *in vitro* mineralization vs. corresponding FBS-cultured cells (Shanbhag et al., 2020a; Shanbhag et al., 2020b). Indeed, the type of supplement used to culture MSC can influence the composition and efficacy of their CM (Madrigal et al., 2014; Nikolits et al., 2021). In context, few studies have assessed the composition of CM from HPL-cultured MSC or compared the composition of CM from HPL- vs. FBS-cultured MSC (Kehl et al., 2019; Palombella et al., 2020; Kim et al., 2021). Several growth factors related to wound healing, angiogenesis and extracellular matrix production were found to be more abundant in the CM of HPL- vs. FBS-cultured BMSC (Kim et al., 2021). Thus, based on these data, it is reasonable to hypothesize that CM from HPL-cultured MSC may be more enriched and potentially pro-osteogenic.

In the context of bone tissue engineering, the efficacy of CM is often studied *in vitro via* its effects on MSC proliferation and osteogenic differentiation. In this regard, previous studies reported that CM promotes MSC osteogenic differentiation; CM in most cases, was derived from FBS-cultured MSC and applied on cells of rodent origin (see review Veronesi et al., 2018). However, for *in vitro* assays, CM is usually supplemented with serum since CM alone does not support longer term cell culture. For differentiation assays, usually lasting 14–21 days, CM is supplemented with both serum and osteogenesis-inducing supplements, i.e., L-ascorbic acid 2-phosphate, dexamethasone and/or β glycerophosphate, in various concentrations (Brauer et al., 2016). To our knowledge, no studies have tested the effects of CM from HPL-cultured human MSC on the osteogenic differentiation of human MSC, which would more closely simulate a clinical scenario. As previously discussed, it is reasonable to hypothesize that CM from HPL-cultured MSC may have pro-osteogenic effects. Thus, the main objective of this preliminary study was to investigate the effects of pooled CM derived from HPL-cultured human BMSC of multiple donors on the *in vitro* proliferation and osteogenic differentiation of allogeneic (different donor) BMSC. A secondary objective was to assess the need for additional supplementation and/or osteogenic stimulation in the *in vitro* assays.

Methods

Cell culture

The use of human cells and tissues was approved by the Regional Committees for Medical Research Ethics (REK) in Norway (2013-1248/REK-sør-øst and 2016-1266/REK-nord). Bone marrow specimens were obtained following parental

consent from five independent donors (2 females and 3 males; 8–10 years) undergoing reconstructive surgery at the Department of Plastic Surgery, Haukeland University Hospital, Bergen, Norway; BMSC were isolated and expanded following previous protocols (Shanbhag et al., 2020b). Briefly, cells were cultured in T75 or T175 flasks (Thermo Fisher Scientific, Carlsbad, CA, United States) using sterile filtered growth media (GM) comprising of Dulbecco's Modified Eagle's medium (DMEM, Invitrogen, Carlsbad, CA, United States) supplemented with 5% (v/v) pooled human platelet lysate (HPL; Bergenlys, Bergen, Norway), 1% (v/v) penicillin/streptomycin (GE Healthcare, South Logan, UT, United States) and 1 IU/ml heparin (Leo Pharma AS, Lysaker, Norway). HPL was produced 'in-house' as described elsewhere (Shanbhag et al., 2020b). Cells were sub-cultured and expanded under standard incubation, i.e., 37°C and 5% CO_2, according to a clinically validated protocol with a seeding density of 4000 cells/cm^2 (Rojewski et al., 2019). Passage 1 (p1) and 2 (p2) BMSC were characterized based on immunophenotype and multi-lineage differentiation potential as previously reported (Shanbhag et al., 2020b), and used for CM preparation. In indicated experiments, BMSC from two separate donors (different from those used for CM preparation) were used to study the paracrine effects of CM. BMSC (p2) were seeded in 12-well plates (4000 cells/cm^2) and exposed to CM for various durations in proliferation and differentiation assays. Cell attachment and morphology were regularly monitored under a light microscope (Nikon Eclipse TS100, Tokyo, Japan).

Conditioned media preparation

CM was prepared from BMSC of three independent donors, as previously described (Al-Sharabi et al., 2017). Briefly, p1 and p2 BMSC were expanded in T175 flasks in GM until 70%–80% confluency under standard incubation. At this point, cells were washed three times with phosphate-buffered saline (PBS; Invitrogen) and then cultured in plain DMEM (without HPL or antibiotics) for another 48 h. After 48 h, CM from p1 and p2 BMSC from each of the three donors was collected, pooled, and centrifuged at 4000× *g* for 10 min to remove any debris. The supernatant was aliquoted and stored at −80°C. For all experiments, CM from −80°C storage was thawed overnight at 4°C and sterile filtered (0.2 µm) before use.

DNA quantification and alkaline phosphatase activity assays

BMSC were seeded in 24-well plates at a density of 4000 cells/cm^2 and cultured in GM. After 24 h, corresponding wells were washed with PBS and exposed to CM or CM-HPL (1% HPL); the concentration of HPL was adjusted in comparison to GM (5% HPL) to avoid overconfluency after 24 h. After 3 and 7 days, cells were lysed in 0.1% Triton X-100 (Sigma Aldrich) and DNA quantification and ALP activity assay were performed using the Quant-IT® PicoGreen dsDNA Assay Kit (Thermo Fisher Scientific) and SIGMAFAST BCIP/NBT assay (Sigma-Aldrich), respectively, according to manufacturers' instructions. DNA concentrations (ng/ml), calculated based on known standards, were used to normalize ALP activity of the corresponding cell-lysates.

TABLE 1 Real time qPCR primers.

Gene (human)	TaqMan® assay ID	Amplicon length
References		
GAPDH	Hs 02758991_g1	93
Osteogenesis-related		
RUNX2	Hs01047973_m1	86
COL1A2	Hs00164099_m1	68
OPN (SPP1)	Hs00959010_m1	84
OCN (BGLAP)	Hs01587814_g1	138

GAPDH glyceraldehyde 3-phosphate dehydrogenase, RUNX2 runt-related transcription factor 2, COL1A2 Collagen type 1 alpha 2, OPN/SPP1 osteopontin, OCN/BGLAP osteocalcin.

Gene expression analysis

Expressions of osteogenesis-related genes (Table 1) were assessed after 2 and 7 days *via* quantitative real-time polymerase chain reaction (qPCR) using TaqMan® real-time PCR assays (Thermo Scientific). BMSC in GM were seeded in 12-well plates; after 24 h, corresponding wells were washed with PBS and exposed to different media formulations: GM, CM alone (CM) and CM supplemented with 5% HPL (CM-PL). RNA extraction and cDNA synthesis were performed as previously described (Mohamed-Ahmed et al., 2018) and expressions of genes of interest were normalized to that of a reference gene—glyceraldehyde 3-phosphate dehydrogenase (GAPDH). Data were analyzed by the ΔΔCt method and results are presented as fold changes relative to the reference group (GM) on a log(2)-transformed scale.

In vitro mineralization assay

In vitro mineralization was assessed using the Alizarin red-S assay. BMSC in GM were seeded in 12-well plates; after 24 h, corresponding wells were washed with PBS and exposed to different media formulations with osteogenic induction supplements: growth media (GM+), CM (CM+) and CM with 5% HPL (CM-PL+). To induce osteogenic differentiation, media were supplemented with final

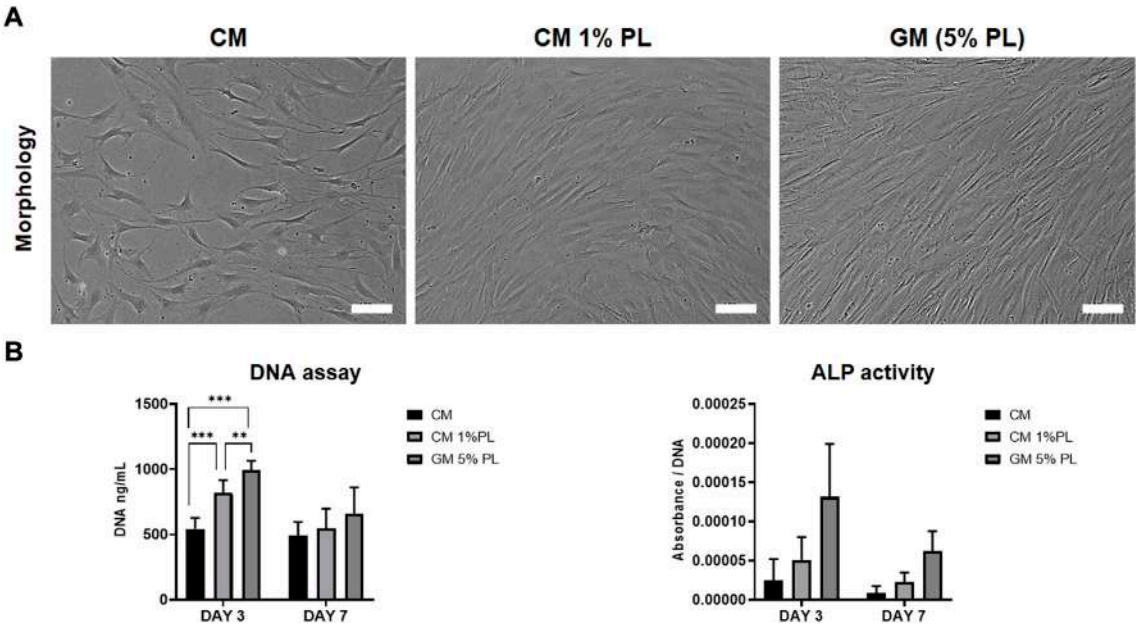

FIGURE 1
Proliferation and ALP activity. **(A)** Representative images of BMSC cultured in CM, CM supplemented with HPL (1% PL) or growth media (5% PL; control) after 3 days, scale bars 100 μm. **(B)** Quantification of total DNA (fluorescence) and ALP activity (absorbance) in BMSC cultured in CM, CM+1% PL and GM after 3 and 7 days (n = 2 donors; 3 experimental replicates per donor); $^{**}p < 0.005$, $^{***}p < 0.001$.

concentrations of 0.05 mM L-ascorbic acid 2-phosphate, 10 nM dexamethasone and 10 mM β glycerophosphate (all from Sigma-Aldrich, St. Louis, MO, United States). Additionally, the following groups were included: CM supplemented with 2.5% HPL and osteogenic supplements and CM supplemented with 10% FBS and osteogenic supplements (CM-FBS+). After 14 days, formation of extracellular calcium deposits was assessed *via* Alizarin red S staining, as previously described (Mohamed-Ahmed et al., 2018). Briefly, after fixation with 4% paraformaldehyde, cells were stained with 2% Alizarin red S solution (Sigma Aldrich) for 30 min at RT, then washed and dried, before images were acquired.

Statistical analysis

Statistical analysis was performed using the Prism 9 software (GraphPad Software, San Diego, CA, United States). Data are presented as means (± SD and/or range), unless specified. All linear data are presented as bar graphs. Normality testing was performed *via* the Shapiro-Wilk test. The student t test, Mann-Whitney U test, one-way analysis of variance (ANOVA; followed by a *post hoc* Tukey's test) or Kruskal-Wallis test (followed by a *post hoc* Dunn's test) were applied as appropriate, and $p < 0.05$ was considered as statistically significant.

Results

Conditioned media supplemented with platelet lysate did not enhance cell proliferation

The *in vitro* paracrine effects of CM were evaluated *via* proliferation and ALP activity assays using BMSC from two independent donors. DNA content of BMSC was lower in CM vs. GM (5% HPL) after 3 ($p < 0.001$) and 7 days ($p > 0.05$); supplementation of CM with 1% HPL did not attenuate this difference at 3 days (Figures 1A,B). A similar trend was observed for ALP activity between the groups, although without statistical significance (Figure 1B).

Conditioned media supplemented with platelet lysate did not enhance osteogenic gene expression

After 2 d, compared to the reference group (GM), expressions of selected osteogenesis related genes, i.e., runt-related transcription factor 2 (RUNX2), collagen type 1A (COLIA), and osteopontin (SPP1/OPN), were significantly upregulated in BMSC exposed to CM alone after 2 and 7 days ($p < 0.05$ for all genes; Figures 2A,B). In particular, expression of SPP1/OPN was remarkably upregulated in CM. Expression of

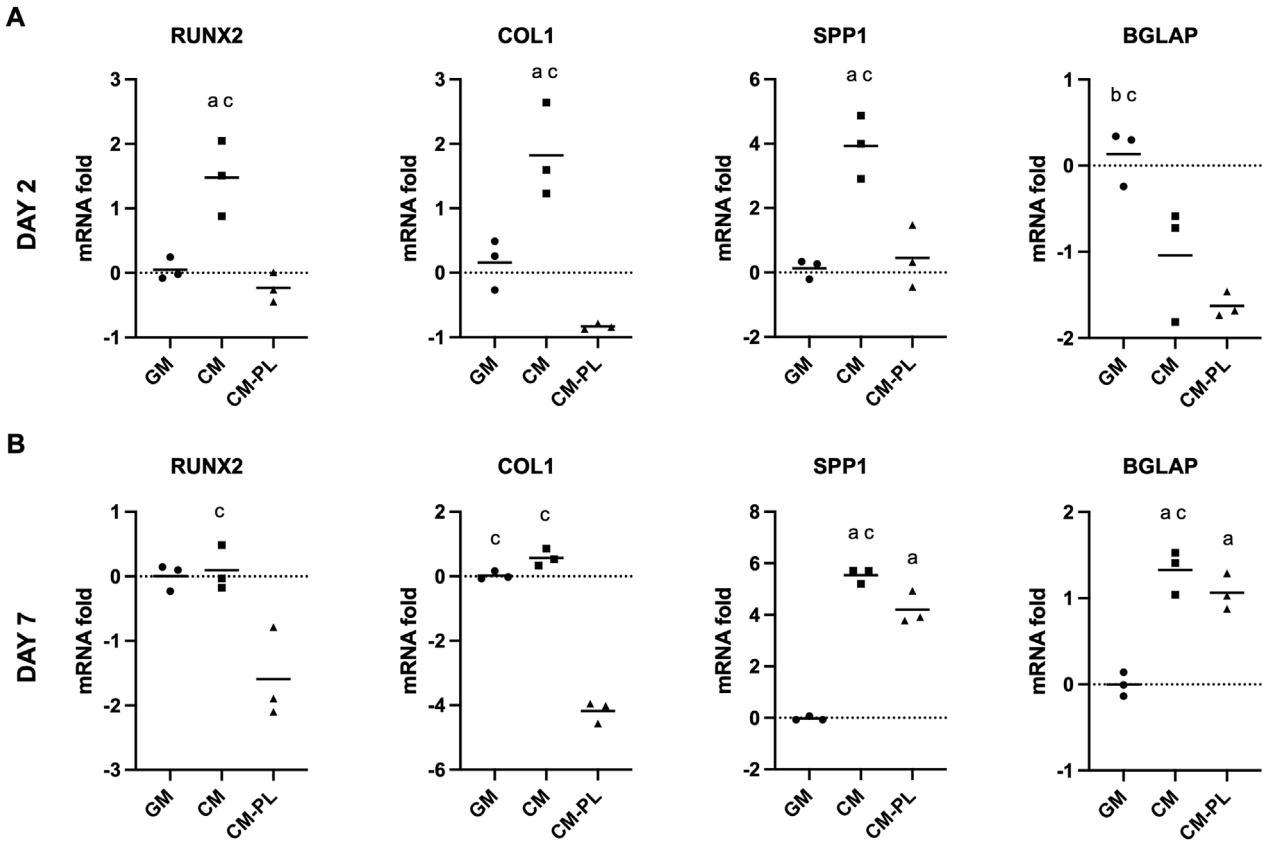

FIGURE 2
Osteogenic gene expression. Relative mRNA fold changes in BMSC after 2 **(A)** and 7 days **(B)**. Data indicate means of 3 experimental replicates for BMSC from one representative donor [Log(2)-transformed y-axis; negative values indicate gene downregulation]. Significance ($p < 0.05$) is denoted by alphabetical letterings: a, compared to GM; b, compared to CM; c, compared to CM-PL; GM, growth media; CM, conditioned media; conditioned media with platelet lysate.

osteocalcin (BGLAP/OCN) was upregulated only after 7 days. When CM was supplemented with HPL (CM-PL), gene expression was either unchanged or downregulated compared to standard GM after 2 days. After 7 days, expressions of SPP1 and BGLAP were upregulated also in CM-PL (Figure 2B).

Conditioned media supplemented with platelet lysate did not promote *in vitro* mineralization

Initially, for the *in vitro* mineralization assay, BMSC were exposed to CM alone or CM supplemented 5% HPL, both with osteogenic stimulants. After 14 days, no mineralization was observed in any of the test groups (Figure 3). Reduction of HPL concentration (from 5% to 2.5%) did not affect the results (data not shown). However, supplementation of CM with 10% FBS (CM-FBS+) revealed *in vitro* mineralization of BMSC comparable to the positive GM control (Figure 3).

Discussion

Since HPL-cultured MSC demonstrate enhanced osteogenic differentiation and the CM of HPL-cultured MSC is more enriched than their FBS-cultured counterparts, the present study hypothesized that the CM of HPL-cultured BMSC has pro-osteogenic effects, i.e., the use of such CM could possibly reduce the need for additional serum/supplementation and/or osteogenic stimulation. Although previous studies have reported that CM promotes MSC osteogenic differentiation (Veronesi et al., 2018; Zhong et al., 2019), these have mainly assessed the effects of CM derived from FBS-cultured cells on MSC of non-human origin. Thus, little is known about the effects of CM from HPL-cultured MSC on allogeneic MSC of human origin. Such an *in vitro* setup would more closely simulate a clinical scenario of CM application, since: 1) current regulations recommend substitution of animal derivatives such as FBS in clinical-grade MSC cultures; and 2) CM would most likely be used as an allogeneic (pooled from multiple donors) "off-the-

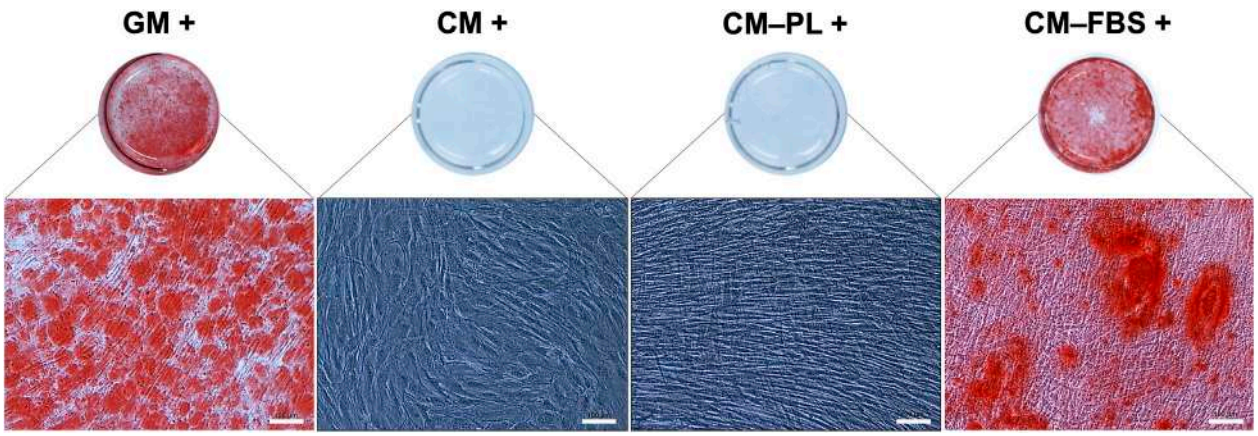

FIGURE 3
In vitro mineralization assay. Representative images of Alizarin red S stained BMSC after 14 days (n = 2 donors; 3 experimental replicates per donor), scale bars 100 μm. +, osteogenic induction added; GM, growth media; CM, conditioned media, PL, platelet lysate; FBS, fetal bovine serum.

shelf" product. Therefore, the objective of this preliminary study was to investigate the effects of CM derived from HPL-cultured MSC (pooled CM from multiple donors) on the *in vitro* osteogenic differentiation of allogeneic (different donors) human MSC. The main findings were that: 1) CM alone promoted osteogenic gene expression, but not *in vitro* mineralization of BMSC, and 2) CM supplemented with HPL promoted neither osteogenic gene expression nor *in vitro* mineralization of BMSC.

In the present study, we investigated the influence of CM supplemented with different concentrations of HPL on the *in vitro* proliferation and osteogenic differentiation of BMSC. We observed that pure CM (without HPL) did not have positive effects on BMSC proliferation and *in vitro* mineralization, despite promoting significant upregulation of several osteogenesis-related genes. In previous studies, we showed that HPL-cultured MSC have an enhanced capacity for osteogenic differentiation (Shanbhag et al., 2020a; Shanbhag et al., 2020b). Therefore, we hypothesized that the secretomes of HPL-cultured BMSC (contained in CM) might have a stimulatory effect on cellular metabolic activity and osteogenic differentiation. However, based on the results herein, it seems that CM alone without added supplements (HPL/FBS) might impair the cultured BMSC *via* nutrient deprivation, thus reducing their metabolic activity and functions (Nuschke et al., 2016). It has also been reported that the "serum starvation" method used to collect CM might be associated with the lower content of the specific growth factors with metabolic activity in CM, e.g., hepatocyte growth factor (HGF), brain-derived neurotrophic factor (BDNF), and fibroblast growth factor 2 (FGF-2) (Petrenko et al., 2020). Further investigations to determine the effects of collection methods on the composition and concentrations of secreted molecules in CM are needed.

Cell metabolism and survival are controlled by the action of growth factors and cytokines through inhibition of apoptosis or promotion of cell survival. In previous studies, we have shown that CM from FBS-cultured BMSC contains several growth factors and cytokines with antiapoptotic and antioxidant properties, including platelet-derived growth factor (PDGF) and vascular endothelial growth factor A (VEGFA), and enhances *in vitro* osteogenic differentiation of MSC (Al-Sharabi et al., 2014; Al-Sharabi et al., 2016; Saleem et al., 2021). In context, HPL also contains several growth factors and cytokines, including PDGF, epidermal growth factor (EGF), insulin-like growth factor (IGF), transforming growth factor (TGF), FGF2, stem cell-growth factor-beta (SCGF), interleukin (IL)-1β, IL-2, -6, -10, -12p70, and IL-17A, tumor necrosis factor (TNF)-α and interferon (IFN) (Cañas-Arboleda et al., 2020; Shanbhag et al., 2020a). Therefore, it is reasonable to postulate that CM of HPL-cultured MSC would be correspondingly more enriched. Indeed, in a recent study, the concentrations of important growth factors such as VEGF, TGF-β1, and HGF were found to be significantly greater in the CM of HPL- vs. FBS-cultured MSC (Kim et al., 2021). However, we found that proliferation and osteogenic differentiation rates were insufficient in BMSC treated with 5% vs. 1% HPL-supplemented CM; a 5% concentration was selected based on current recommendations for HPL supplementation for *ex vivo* MSC expansion (Becherucci et al., 2018).

Regarding osteogenic differentiation, previous studies have reported that CM increased osteogenic differentiation and mineralization of MSC in a paracrine manner (Ogata et al., 2015; Zhong et al., 2019). However, most studies have not

adequately addressed whether CM alone exerts this effect or whether the addition of FBS or HPL, with or without osteogenic supplements, is necessary. Such information would be important to standardize experimental setups and compare the results across different *in vitro* studies. In the present study, we found that pure CM stimulates neither ALP activity nor *in vitro* mineralization, as detected by Alizarin red staining. This was in line with a study conducted to evaluate proliferation and differentiation of osteoblasts under the induction of different concentrations of CM (Sun et al., 2012). When 1% HPL was added to CM, a slight improvement in ALP activity was detected although this was not equivalent to the control, i.e., GM containing 5% HPL. CM also promoted the expression of osteogenesis-related genes in BMSC, although this effect appears to be insufficient to stimulate *in vitro* mineralization, as no mineralization nodules were detected after 14 days. Thus, despite CM-induced gene upregulation in BMSC (without osteogenic supplementation), the impairment in promoting mineralization (with or without osteogenic supplementation) potentially reflects the safety of using BMSC as sources for CM production for different applications rather than specifically for bone regeneration.

In the context of osteogenic differentiation, we have previously reported that HPL supplementation alone (vs. FBS) enhances the expression of osteogenesis-related genes in MSC, suggesting particular benefits of HPL-supplemented MSC expansion for bone tissue engineering (Shanbhag et al., 2020a). Indeed, in the present study, exposure to CM resulted in an upregulation of osteogenic genes which was greater than that of HPL supplementation. However, the combination of HPL and CM did not exert a synergistic effect in terms of BMSC gene expression. This might indicate that a certain concentration of HPL together with CM might only allow the maintenance of the original microenvironment in BMSC, possibly *via* reduction of overexposure to cytokines and other stimulatory factors (Kandoi et al., 2018). On the contrary, the combination of CM and HPL may have antagonistic effects, which may distort the positive biological activity of CM. Therefore, future molecular research is warranted to study the effects of different combinational ratios of CM and HPL *in vitro* osteogenic differentiation of MSC (Aghamohamadi et al., 2020). Moreover, while the present study focused on osteogenic stimulatory capacity, other pathways of CM bioactivity, particularly angiogenesis (Quade et al., 2020) and immune-modulation (Jin et al., 2022), are also highly relevant for bone regeneration.

Some limitations of the present preliminary study must be acknowledged. The objective herein was to test the hypothesis that CM from HPL-cultured MSC may have pro-osteogenic effects, and not to compare per se CM from HPL- vs. FBS-cultured MSC or the osteogenic effects of CM supplemented with HPL vs. FBS. Therefore, we did not include FBS supplemented CM as a control group in all experiments, but only in the *in vitro* mineralization assay. Secondly, although the CM used herein was produced and pooled from multiple BMSC donors (n = 3), which is clinically relevant in terms of scaling up production and minimizing individual donor variations, the number of allogeneic BMSC donors for the *in vitro* assays was limited (n = 2). It is well known that BMSC may demonstrate significant donor-related variations in their growth and differentiation potential (Al-Sharabi et al., 2017) and therefore, the experiments should be repeated with BMSC from additional donors to validate the findings. Lastly, in this preliminary study, we did not perform any mechanistic assays, e.g., identification of specific signaling pathways, to determine the molecular basis for reduced mineralization in CM, with or without additional supplements. This would be relevant mainly for future *in vitro* assessments of MSC responses to CM to potentially predict (within the limitations of *in vitro* models) the *in vivo* effects of CM for bone regeneration. Clear descriptions of *in vitro* experimental setups, i.e., addition of serum/supplements and osteogenic stimulants, in future studies of CM efficacy are warranted to allow standardization and comparison of data.

Conclusion

In summary, pooled CM from HPL-cultured human BMSC promoted osteogenic gene expression but not *in vitro* mineralization in allogeneic BMSC, even when supplemented with HPL and/or osteogenic stimulants. The role and relevance of CM supplementation and osteogenic stimulation in *in vitro* assays should be investigated in future studies to better understand the underlying molecular mechanisms and allow standardized comparisons of results.

Data availability statement

The original contributions presented in the study are included in the article/Supplementary Material, further inquiries can be directed to the corresponding author.

Ethical statement

The use of human cells and tissues was approved by the Regional Committees for Medical Research Ethics (REK) in Norway (2013-1248/REK-sør-øst and 2016-1266/REK-nord).

Author contributions

SS and NA-S conceived and designed the study. SS performed the experiments, data collection, data analysis and drafted the manuscript. NA-S and SM-A assisted with experiments, sample preparation, data collection, data analysis/interpretation and/or drafting the manuscript. RG,

EK, and KM assisted with data analysis/interpretation, drafting the manuscript and funding acquisition. All authors read and approved the final version of the manuscript.

Funding

This work was supported by the Osteology Foundation, Switzerland (18-152), Helse Vest Research Funding, Norway (F-12124), and Trond Mohn Foundation, Norway (BFS2018TMT10).

Acknowledgments

We thank the Bloodbank at Haukeland University Hospital for assistance with HPL production.

Conflict of interest

The authors declare that the research was conducted in the absence of any commercial or financial relationships that could be construed as a potential conflict of interest.

Publisher's note

All claims expressed in this article are solely those of the authors and do not necessarily represent those of their affiliated organizations, or those of the publisher, the editors and the reviewers. Any product that may be evaluated in this article, or claim that may be made by its manufacturer, is not guaranteed or endorsed by the publisher.

References

Aghamohamadi, Z., Kadkhodazadeh, M., Torshabi, M., and Tabatabaei, F. (2020). A compound of concentrated growth factor and periodontal ligament stem cell-derived conditioned medium. *Tissue Cell* 65, 101373. doi:10.1016/j.tice.2020.101373

Al-Sharabi, N., Mustafa, M., Ueda, M., Xue, Y., Mustafa, K., and Fristad, I. (2017). Conditioned medium from human bone marrow stromal cells attenuates initial inflammatory reactions in dental pulp tissue. *Dent. Traumatol.* 33 (1), 19–26. doi:10.1111/edt.12277

Al-Sharabi, N., Xue, Y., Fujio, M., Ueda, M., Gjerde, C., Mustafa, K., et al. (2014). Bone marrow stromal cell paracrine factors direct osteo/odontogenic differentiation of dental pulp cells. *Tissue engineering.Part A* 20 (21-22), 3063–3072. doi:10.1089/ten.TEA.2013.0718

Al-Sharabi, N., Xue, Y., Udea, M., Mustafa, K., and Fristad, I. (2016). Influence of bone marrow stromal cell secreted molecules on pulpal and periodontal healing in replanted immature rat molars. *Dent. Traumatol.* 32 (3), 231–239. doi:10.1111/edt.12246

Becherucci, V., Piccini, L., Casamassima, S., Bisin, S., Gori, V., Gentile, F., et al. (2018). Human platelet lysate in mesenchymal stromal cell expansion according to a GMP grade protocol: A cell factory experience. *Stem Cell Res. Ther.* 9 (1), 124. doi:10.1186/s13287-018-0863-8

Benavides-Castellanos, M. P., Garzon-Orjuela, N., and Linero, I. (2020). Effectiveness of mesenchymal stem cell-conditioned medium in bone regeneration in animal and human models: A systematic review and meta-analysis. *Cell Regen.* 9 (1), 5. doi:10.1186/s13619-020-00047-3

Bieback, K., Fernandez-Munoz, B., Pati, S., and Schafer, R. (2019). Gaps in the knowledge of human platelet lysate as a cell culture supplement for cell therapy: A joint publication from the AABB and the, international society for cell & gene therapy. *Transfusion* 59, 3448–3460. doi:10.1111/trf.15483

Brauer, A., Pohlemann, T., and Metzger, W. (2016). Osteogenic differentiation of immature osteoblasts: Interplay of cell culture media and supplements. *Biotech. Histochem.* 91 (3), 161–169. doi:10.3109/10520295.2015.1110254

Cañas-Arboleda, M., Beltrán, K., Medina, C., Camacho, B., and Salguero, G. (2020). Human platelet lysate supports efficient expansion and stability of wharton's jelly mesenchymal stromal cells via active uptake and release of soluble regenerative factors. *Int. J. Mol. Sci.* 21, 6284. doi:10.3390/ijms21176284

Fekete, N., Gadelorge, M., Furst, D., Maurer, C., Dausend, J., Fleury-Cappellesso, S., et al. (2012). Platelet lysate from whole blood-derived pooled platelet concentrates and apheresis-derived platelet concentrates for the isolation and expansion of human bone marrow mesenchymal stromal cells: Production process, content and identification of active components. *Cytotherapy* 14 (5), 540–554. doi:10.3109/14653249.2012.655420

Ferreira, J. R., Teixeira, G. Q., Santos, S. G., Barbosa, M. A., Almeida-Porada, G., and Goncalves, R. M. (2018). Mesenchymal stromal cell secretome: Influencing therapeutic potential by cellular pre-conditioning. *Front. Immunol.* 9, 2837. doi:10.3389/fimmu.2018.02837

Gnecchi, M., Danieli, P., Malpasso, G., and Ciuffreda, M. C. (2016). Paracrine mechanisms of mesenchymal stem cells in tissue repair. *Methods Mol. Biol.* 1416, 123–146. doi:10.1007/978-1-4939-3584-0_7

Haumer, A., Bourgine, P. E., Occhetta, P., Born, G., Tasso, R., and Martin, I. (2018). Delivery of cellular factors to regulate bone healing. *Adv. Drug Deliv. Rev.* 129, 285–294. doi:10.1016/j.addr.2018.01.010

Jin, Q. H., Kim, H. K., Na, J. Y., Jin, C., Seon, J. K., Kim, H. K., et al. (2022). Anti-inflammatory effects of mesenchymal stem cell-conditioned media inhibited macrophages activation *in vitro*. *Sci. Rep.* 12, 4754. doi:10.1038/s41598-022-08398-4

Kandoi, S., Praveen.kumar, L., Patra, B., Vidyasekar, P., Sivanesan, D., Vijayalakshmi, S., et al. (2018). Evaluation of platelet lysate as a substitute for FBS in explant and enzymatic isolation methods of human umbilical cord MSCs. *Sci. Rep.* 8 (1), 12439. doi:10.1038/s41598-018-30772-4

Kehl, D., Generali, M., Mallone, A., Heller, M., Uldry, A. C., Cheng, P., et al. (2019). Proteomic analysis of human mesenchymal stromal cell secretomes: A systematic comparison of the angiogenic potential. *npj Regen. Med.* 4, 8. doi:10.1038/s41536-019-0070-y

Kim, S. N., Lee, C. J., Nam, J., Choi, B., Chung, E., and Song, S. U. (2021). The effects of human bone marrow-derived mesenchymal stem cell conditioned media produced with fetal bovine serum or human platelet lysate on skin rejuvenation characteristics. *Int. J. Stem Cells* 14 (1), 94–102. doi:10.15283/ijsc20070

Madrigal, M., Rao, K. S., and Riordan, N. H. (2014). A review of therapeutic effects of mesenchymal stem cell secretions and induction of secretory modification by different culture methods. *J. Transl. Med.* 11, 260. doi:10.1186/s12967-014-0260-8

Mohamed-Ahmed, S., Fristad, I., Lie, S. A., Suliman, S., Mustafa, K., Vindenes, H., et al. (2018). Adipose-derived and bone marrow mesenchymal stem cells: A donor-matched comparison. *Stem Cell Res. Ther.* 9 (1), 168. doi:10.1186/s13287-018-0914-1

Nikolits, I., Nebel, S., Egger, D., Kress, S., and Kasper, C. (2021). Towards physiologic culture approaches to improve standard cultivation of mesenchymal stem cells. *Cells* 10 (4), 886. doi:10.3390/cells10040886

Nuschke, A., Rodrigues, M., Wells, A. W., Sylakowski, K., and Wells, A. (2016). Mesenchymal stem cells/multipotent stromal cells (MSCs) are glycolytic and thus glucose is a limiting factor of *in vitro* models of MSC starvation. *Stem Cell Res. Ther.* 7 (1), 179. doi:10.1186/s13287-016-0436-7

Ogata, K., Katagiri, W., Osugi, M., Kawai, T., Sugimura, Y., Hibi, H., et al. (2015). Evaluation of the therapeutic effects of conditioned media from mesenchymal stem cells in a rat bisphosphonate-related osteonecrosis of the jaw-like model. *Bone.* 74, 95–105. doi:10.1016/j.bone.2015.01.011

Palombella, S., Guiotto, M., Higgins, G. C., Applegate, L. L., Raffoul, W., Cherubino, M., et al. (2020). Human platelet lysate as a potential clinical-translatable supplement to support the neurotrophic properties of human adipose-derived stem cells. *Stem Cell Res. Ther.* 11 (1), 432. doi:10.1186/s13287-020-01949-4

Petrenko, Y., Vackova, I., Kekulova, K., Chudickova, M., Koci, Z., Turnovcova, K., et al. (2020). A comparative analysis of multipotent mesenchymal stromal cells derived from different sources, with a focus on neuroregenerative potential. *Sci. Rep.* 10 (1), 4290. doi:10.1038/s41598-020-61167-z

Quade, M., Munch, P., Lode, A., Duin, S., Vater, C., Gabrielyan, A., et al. (2020). The secretome of hypoxia conditioned hMSC loaded in a central depot induces chemotaxis and angiogenesis in a biomimetic mineralized collagen bone replacement material. *Adv. Healthc. Mat.* 9 (2), e1901426. doi:10.1002/adhm.201901426

Rojewski, M. T., Lotfi, R., Gjerde, C., Mustafa, K., Veronesi, E., Ahmed, A. B., et al. (2019). Translation of a standardized manufacturing protocol for mesenchymal stromal cells: A systematic comparison of validation and manufacturing data. *Cytotherapy* 21 (4), 468–482. doi:10.1016/j.jcyt.2019.03.001

Saleem, R., Mohamed-Ahmed, S., Elnour, R., Berggreen, E., Mustafa, K., and Al-Sharabi, N. (2021). Conditioned medium from bone marrow mesenchymal stem cells restored oxidative stress-related impaired osteogenic differentiation. *Int. J. Mol. Sci.* 22 (24), 13458. doi:10.3390/ijms222413458

Shanbhag, S., Mohamed-Ahmed, S., Lunde, T. H. F., Suliman, S., Bolstad, A. I., Hervig, T., et al. (2020a). Influence of platelet storage time on human platelet lysates and platelet lysate-expanded mesenchymal stromal cells for bone tissue engineering. *Stem Cell Res. Ther.* 11 (1), 351. doi:10.1186/s13287-020-01863-9

Shanbhag, S., Stavropoulos, A., Suliman, S., Hervig, T., and Mustafa, K. (2017). Efficacy of humanized mesenchymal stem cell cultures for bone tissue engineering: A systematic review with a focus on platelet derivatives. *Tissue Eng. Part B Rev.* 23, 552–569. doi:10.1089/ten.teb.2017.0093

Shanbhag, S., Suliman, S., Bolstad, A. I., Stavropoulos, A., and Mustafa, K. (2020b). Xeno-free spheroids of human gingiva-derived progenitor cells for bone tissue engineering. *Front. Bioeng. Biotechnol.* 8, 968. doi:10.3389/fbioe.2020.00968

Shanbhag, S., Suliman, S., Pandis, N., Stavropoulos, A., Sanz, M., and Mustafa, K. (2019). Cell therapy for orofacial bone regeneration: A systematic review and meta-analysis. *J. Clin. Periodontol.* 46 (21), 162–182. doi:10.1111/jcpe.13049

Sun, J., Zhou, H., Deng, Y., Zhang, Y., Gu, P., Ge, S., et al. (2012). Conditioned medium from bone marrow mesenchymal stem cells transiently retards osteoblast differentiation by downregulating runx2. *Cells Tissues Organs* 196 (6), 510–522. doi:10.1159/000339245

Veronesi, F., Borsari, V., Sartori, M., Orciani, M., Mattioli-Belmonte, M., and Fini, M. (2018). The use of cell conditioned medium for musculoskeletal tissue regeneration. *J. Cell. Physiol.* 233 (6), 4423–4442. doi:10.1002/jcp.26291

Zhong, S., He, X., Li, Y., and Lou, X. (2019). Conditioned medium enhances osteogenic differentiation of induced pluripotent stem cell-derived mesenchymal stem cells. *Tissue Eng. Regen. Med.* 16 (2), 141–150. doi:10.1007/s13770-018-0173-3

Scaffolds in Periodontal Regenerative Treatment

Shuntaro Yamada, DDS, MSc[a], Siddharth Shanbhag, DDS, PhD[a,b], Kamal Mustafa, DDS, PhD[a,*]

KEYWORDS

• Periodontal regeneration • Biomimetic • scaffolds • 3D printing • Tissue engineering

KEY POINTS

- Periodontal regeneration requires the hierarchical reorganization of soft and hard tissues, namely, periodontal ligament, cementum, alveolar bone, and gingiva.
- Three-dimensional microporous scaffolds offer structural support and spatiotemporal guidance for cell growth and differentiation.
- Biomimetic periodontal extracellular matrix scaffold may be produced by combining periodontal ligament cells and microporous scaffolds with the prospect of off-the-shelf products.
- Selection of scaffold architecture, functionalization techniques, and cell types determines the functionality of scaffolds.
- Three-dimensional printing technology allows for designing personalized scaffolds for periodontal regeneration.

INTRODUCTION

Advanced periodontitis results in the damage and loss of hard and soft tissues, which impairs oral function, aesthetics, and the patient's overall quality of life.[1] Although conventional therapies such as scaling and root planing and flap surgery effectively interrupt disease progression, it often necessitates regenerative interventions to regain the original architecture and function of periodontal tissues because of limitation in spontaneous regeneration.[2,3] This requires newly formed cementum and alveolar bone bridged by functional periodontal ligament. Conventional regenerative approaches aim at promoting the growth and differentiation of tissue-resident progenitor cells into fibroblasts, cementoblasts, and osteoblasts, while preventing the downgrowth of epithelial tissues into the periodontal defect. This approach, termed guided tissue

[a] Department of Clinical Dentistry, Faculty of Medicine - Tissue Engineering Group, University of Bergen, Årstadveien 19, 5009 Bergen, Norway; [b] Department of Immunology and Transfusion Medicine, Haukeland University Hospital, Jonas Lies vei 65, 5021 Bergen, Norway
* Corresponding author.
E-mail address: kamal.mustafa@uib.no

Dent Clin N Am 66 (2022) 111–130
https://doi.org/10.1016/j.cden.2021.06.004 **dental.theclinics.com**
0011-8532/22/© 2021 The Authors. Published by Elsevier Inc. This is an open access article under the CC BY-NC-ND license (http://creativecommons.org/licenses/by-nc-nd/4.0/).

regeneration, is represented by the application of barrier membranes with or without bioactive molecules such as enamel matrix derivative and recombinant growth factors.[4] Additionally, autogenous bone or bone substitutes of allogeneic, xenogeneic, or alloplastic origin, may be applied as scaffolds for cell growth and migration. These interventions have been shown to be effective clinically. However, a large heterogeneity among studies affirms the unpredictability of the treatments, and none of the existing treatment options have achieved complete periodontal regeneration.[5,6]

A conventional regenerative strategy, namely, bone grafting, mainly uses autogenous bone and various bone substitutes. Autogenous bone is considered as the golden standard because it has osteoconductive, osteoinductive, and osteogenic properties attributed to the components: autologous cells (eg, osteoblasts and their progenitor cells), extracellular matrix (ECM) components (eg, collagen, hydroxyapatite), and bioactive molecules (eg, bone morphogenetic protein-2 [BMP-2]).[7] However, owing to limitations in the amount of harvestable bone and the necessity of surgical intervention to donor sites, the use of allografts and xenografts, which are obtained from a donor of the same or different species, respectively, have been preferred as alternatives. Nevertheless, they carry the risk of unforeseen infection, disease transmission, and/or immune rejection.[8] In contrast, alloplastic or synthetic bone substitutes, which are mostly made from hydroxyapatite, for example, tricalcium phosphate, calcium sulfate, biphasic calcium phosphate, possess osteoconductivity, but are not of biological origin and, therefore, do not carry the risk of disease transmission. Bone substitute materials are delivered to osseous defects, including periodontal defects as scaffolds, and their osteoconductivity is hypothesized to stimulate endogenous progenitors to grow and differentiate into mature osteoblasts.[9] However, a systematic review has revealed that the outcome of periodontal therapy solely with bone grafting, that is, without accompanying barrier membranes, is predominantly ascribed to bone regeneration with an attachment of long junctional epithelium, but with a lack of newly formed cementum and periodontal ligament.[10] Moreover, the effect of such combinational therapies seems to be limited in horizontal and 2-walled intrabony defects, and inadequate in 3-walled intrabony and advanced furcation defects.[3]

Although conventional approaches to periodontal regeneration predominantly rely on the regenerative capacity of endogenous cells, the comparatively newer tissue engineering approach aims to combine exogeneous progenitor cells, biomaterial scaffolds, and bioactive molecules (signals) to address the complex architecture and function of the periodontal tissues.[11,12] In nature, ECM possesses optimal structural patterns and bioactivity, which regulate the growth and fate of the residing cells spatiotemporally. Meanwhile, the concept of biomimetics was brought into the fabrication of tissue engineered constructs for periodontal regeneration. Despite a large variance among studies, most of the designing concepts converge in mimicking the hierarchical organization of the native periodontal tissues, particularly the ECM, structurally and functionally in an ex vivo setting.[13] Scaffolds, therefore, serve as the core of tissue engineered construct because they offer 3-dimensional (3D) structural support and spatial guidance for cells. Moreover, their functionality may be further enhanced by incorporating bioactive molecules, for example, growth factors.[14] A wide variety of conventional and state-of-art scaffold fabrication methodologies such as decellularization, salt leaching, electrospinning, and 3D printing have been tested to fabricate biomimetic scaffolds to challenge the complex nature of periodontal tissues.[15] The aim of this article is to review the concepts of scaffold designing and fabrication, and to summarize the recent advancements in tissue engineering-based applications of biomimetic scaffolds for periodontal regeneration.

SCAFFOLD DESIGNING AND FABRICATION CONCEPT FOR PERIODONTAL REGENERATION

Scaffolds act as the core of tissue-engineered constructs because they offer spatiotemporal guidance for cells by providing architectural and biochemical clues.[14] Scaffold designing requires the selection of material, fabrication techniques, and functionalization methods (**Fig. 1**). This section summarizes scaffold designing and fabrication concept for periodontal applications.

Scaffold Architectures and Fabrication Techniques

Scaffolds provide the structural support and the guidance for exogenous and/or endogenous cells.[14] Generally, 3D scaffolds with high porosity and interconnectivity are preferable to achieve structural and functional restoration, because the architecture offers a suitable microenvironment for cell-to-cell interaction and scaffold-to-tissue integration at the implanted site.[15,16] In the early phase of implantation, the porous structures facilitate blood infiltration to the scaffolds and stabilize the blood clots, which is considered as a key initiator of tissue repair and regeneration through enriched vascularization.[17,18] Particularly, macropores ranging from 100 to 700 μm enhance vascularization at the implanted sites, whereas micropores of less than 100 μm may suppress cell growth owing to local ischemia.[16,19–22] High porosity also supports the diffusion of nutrients and gases as well as waste removal, which improves cellular metabolism and growth.[23–26] Various fabrication techniques have been used to design highly porous scaffolds.[15,27]

In nature, the ECM has an amorphous porous structure, acting as a scaffold. It regulates the recruitment, growth, and differentiation of resident cells via bioactive molecules, spatial patterning, and mechanical stimuli.[28] As an exogeneous complete form

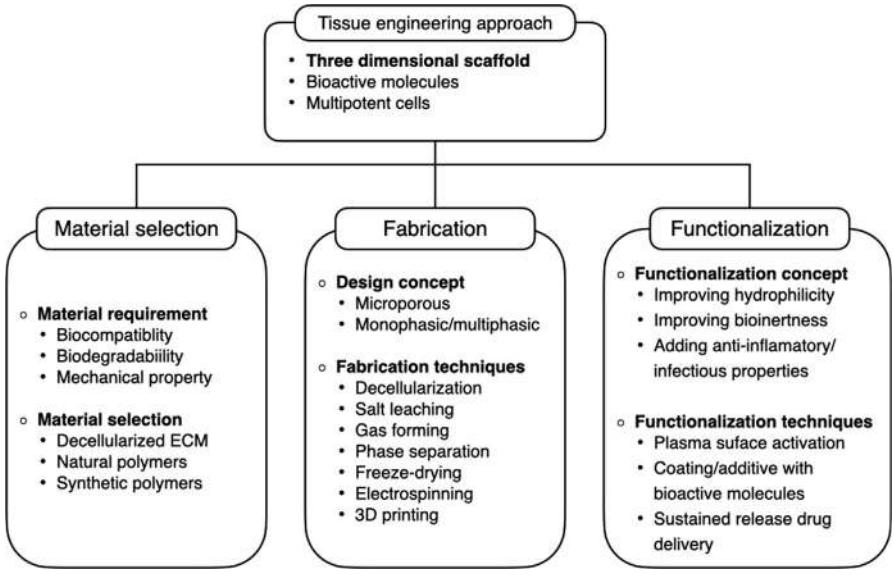

Fig. 1. Summary of scaffold designing and fabrication concept. Tissue engineering approach involves the combination of scaffolds, bioactive molecules, and multipotent cells. Scaffold functionality is determined by the selection of materials, fabrication methods, and functionalization techniques.

of ECM, decellularized ECM are widely applied to reproduce a 3D microenvironment at the implanted sites for tissue repair and regeneration. Decellularized ECM products from various origins, including human, porcine, or bovine dermis, and human amniotic membrane (hAM) are commercially available and used in clinical practice.[29] Recently, donor sites have been extended to the periodontal ligament itself, and attempts have been made to produce biomimetic periodontal scaffolds using decellularized ECM in combination with periodontal progenitor cells.[30–32] To reproduce the structural pattern of ECM artificially, various techniques have been translated into regenerative medicine. Salt leaching, gas forming, phase separation, and freeze drying are representative conventional methods to produce highly porous amorphous scaffolds (see the previous review on fabrication methods).[15] Salt leaching and gas forming techniques use salt and gas as porogen additives, whereas phase separation and freeze drying techniques use volatilization and sublimation of solvent and/or water in the polymer solution. Electrospinning is one of the representative engineering techniques used to produce fine fibrous scaffolds. It generates nonwoven nanoscaled-to-microscaled fibers, which reportedly mimic the native collagen fibrous network.[33–36] The electrospinning process requires a solvent–polymer mixture in a syringe pump, a collector, and a high voltage supply. When the high gradient of electric potential difference is applied between the metal syringe tip and the collector, electric charge accumulates on the polymer solution at the needle tip, and the polymer solution is ejected as a liquid jet toward the collector. When the jet reaches the collector, the polymer gets solidified because of evaporation of the solvent. These techniques allow for the fabrication of highly porous scaffolds, and resulting structures incorporate pores with various shapes and sizes, as if to recapitulate the structural pattern of the native ECM.[27] However, the controllability of internal architecture, that is, pore size, pore distribution, and pore orientation, is relatively low in comparison with rapid prototyping methods represented by 3D printing.[15] Furthermore, the resulting structures are considered as monophasic; it is characterized by the consistency in overall physical and chemical properties within the structures (**Fig. 2A**).

Provided that periodontal regeneration requires the hierarchical orientation of multiple tissues, a multiphasic design (ie, biphasic or triphasic) is considered to direct

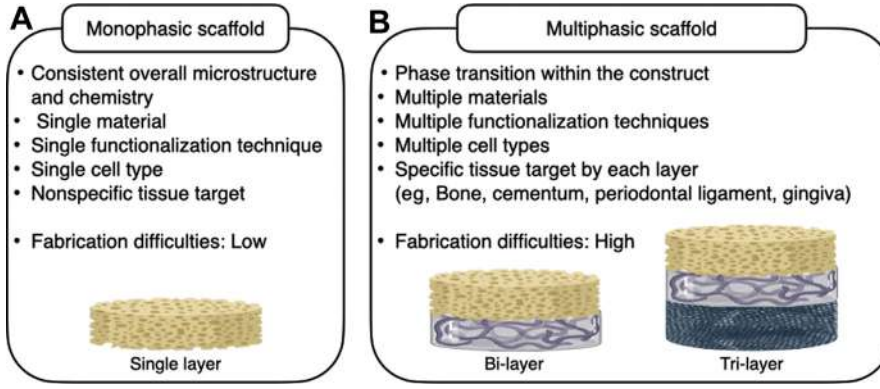

Fig. 2. Summary of the characteristics of monophasic and multiphasic scaffolds. (*A*) Monophasic scaffolds consist of single layer with consistency in microstructural pattern and chemical property within the construct. (*B*) Multiphasic scaffolds are characterized by phasal transition within the construct. This includes the combination of different materials, functionalization techniques, and/or cell types.

progenitors to specific cell types more rigorously (Fig. 2B). This structure can be designed by layering components with different characteristics such as material composition, architectures, and functionalization.[27,37] Depending on designing concepts, countless combinations are possible. Although there is no perfect combination, a number of proof-of-concept studies have developed prototype designs that potentially favor the regeneration of the hierarchical structures.[37–44] In particular, 3D printing technology has recently emerged as a promising strategy to produce multilayered constructs for tissue engineering, because it overcomes the limitation of conventional fabrication techniques. Namely, difficulties in precise structural control and reproducibility are avoided. Moreover, recent advances in bioprinting have empowered the possibility of producing functional artificial organs in vitro.[45] With the help of 3D computer-aided design (CAD) modeling software, constructs can be built up in a layer-by-layer fashion in accordance with the blueprints. Currently, 3D printers for biomedical applications can achieve a minimum of 10 μm resolution with high accuracy.[46–48] The major advantage of 3D printing for scaffold fabrication is attributable to its designing flexibility. Controlling porosity, pore size, interconnectivity, and strand alignment pattern creates structural gradient within the construct, which may guide tissue orientation. The 3D printed scaffolds could be produced in a monophasic or multiphasic form depending on its design. Further advantage of 3D printing derives from its compatibility with diagnostic imaging equipment such as a cone beam computed tomography (CT) scan and intraoral 3D scanner. The geometry of periodontal defects is scanned and transferred into CAD modeling software to produce custom-designed 3D scaffolds adapting to the defect.[49] This personalized medicine approach is expected to increase the predictability of periodontal therapy for advanced tissue defects.

Polymeric Scaffold Materials and Functionalization

Material development and scaffold designing have been the major interest in biomaterial research for regenerative medicine.[11] Although natural ECM serves as the ideal scaffold in nature, particular attention has been paid to the generation of biomimetic scaffolds using polymeric biomaterials. Polymeric biomaterials possess biodegradability and biocompatibility, which allow the materials to be used for a wide range of medical application as implants for soft and hard tissue regeneration.[50] Polymeric biomaterials are categorized based on their origin: natural and synthetic polymers.

Natural polymers represented by proteins (eg, collagen, silk) and polysaccharides (eg, cellulose, alginate, chitosan) are often referred as the first biodegradable biomaterials applied in clinical settings.[51–53] They possess inherent bioactive properties that actively interact with cellular components. For example, integrin-binding ligands are presented on protein-based polymers, which regulate cell adhesion, migration, proliferation, and differentiation.[54] However, natural polymers generally lack mechanical stability, and their mechanical/biological properties may significantly vary depending on extraction procedures.[50] Furthermore, their high susceptibility to enzymatic degradation may result in disharmonized scaffold resorption and tissue remodeling.[55] Therefore, reinforcement with resilient materials such as fibers or hydroxyapatites is often considered.[56]

In contrast, synthetic polymers such as polylactic acid, polycaprolactone (PCL), and poly(DL-lactide-*co*-glycolide) present superior mechanical properties and formability for clinical use in a variety of applications in addition to decent biocompatibility and biodegradability. By altering molecular weight and chemical composition, favorable biodegradability and mechanical properties are delivered to the scaffold.[57] However,

unlike natural polymers synthetic polymers are biologically inert, and their hydrophobic nature may hinder blood infiltration, which potentially prevents the scaffold from integrating to the implanted site.[58] To supplement the bioinertness of the synthetic polymers, functionalization using techniques such as plasma surface activation and the coating/additive of bioactive molecules are preferably performed.[33,59] These include ECM proteins (eg, collagen, fibronectin, gelatin),[59–61] growth factors (eg, BMP-2, BMP-7, fibroblast growth factor-2, and platelet-derived growth factor BB),[43,62–65] specialized proresolving mediators (eg, resolving D1),[66] and various types of antibiotics and anti-inflammatory drugs.[67–69] Generally, functionalization to the synthetic polymer does not alter the bulk property of the materials but increases interaction between material and tissues.[50] With this background in scaffold design and fabrication, the subsequent sections discuss the applications of various scaffold-based tissue engineering strategies in experimental settings for periodontal regeneration.

MONOPHASIC SCAFFOLD APPROACHES FOR PERIODONTAL REGENERATION

Decellularized Extracellular Matrix as an Exogeneous Natural Matrix

ECM is a natural form of complete scaffold, providing a suitable biochemical and biomechanical microenvironment for the residing cells. In a current clinical practice, an autologous connective tissue graft (CTG) is a frequent procedure to augment soft tissue. In addition to soft tissue regain, a histologic evaluation has revealed that CTG leads to the regeneration of cementum on the dentin surface, which may be bound to newly formed periodontal ligament, indicating connective tissue exhibits cementoconductivity.[70] However, the procedure is accompanied by a number of complications not only at the recipient site, but at the donor site such as pain, infection, bleeding, and necrosis.[71]

To overcome the limitation of the autologous soft tissue graft, decellularized ECM from allogenic or xenogeneic origin have been an alternative (**Fig. 3**). Acellular dermal matrix (ADM) from human skin is the most common decellularized ECM scaffold in periodontal treatment.[29] Although most of the clinical application in dentistry is limited to periodontal plastic surgery, its cementoconductivity and osteoconductivity supported by periodontal ligament regeneration has been suggested by in vivo models. A study using mini pigs with surgically created fenestration defects showed that clinical attachment gain by ADM was comparable with by CTG after 3 months of healing period, but ADM implantation led to greater new cementum regeneration with the narrower length of epithelial and connective tissue attachment.[72] The regenerative capacity of ADM may be further enhanced by combining bone substitute, as shown previously in beagle dogs that ADM in combination with beta-tricalcium phosphate induced the greater periodontal regeneration with thick cementum layers and alveolar bone formation that were bridged by periodontal ligament than ADM alone and coronally repositioned flap surgery.[73] Similarly, xenogeneic decellularized matrix possess comparable effects on the regeneration of periodontal tissue, although soft tissue response may differ.[72,74,75] There is a lack of evidence in the use of ADM to intrabony or furcation defects, but it supports the adhesion, robust proliferation of human periodontal ligament cells (PDLC) and possesses optimal biocompatibility and biodegradability for periodontal regeneration, suggesting its potency as a scaffold material.[76]

The hAM obtained from maternal donors undergoing caesarian section is another source of allogenic ECM, mainly for soft tissue repair and regeneration.[77] There is an absence of blood vessels and lymphatic tissue in hAM, and it has high durability and superior mechanical property attributed to the tight network of collagen and

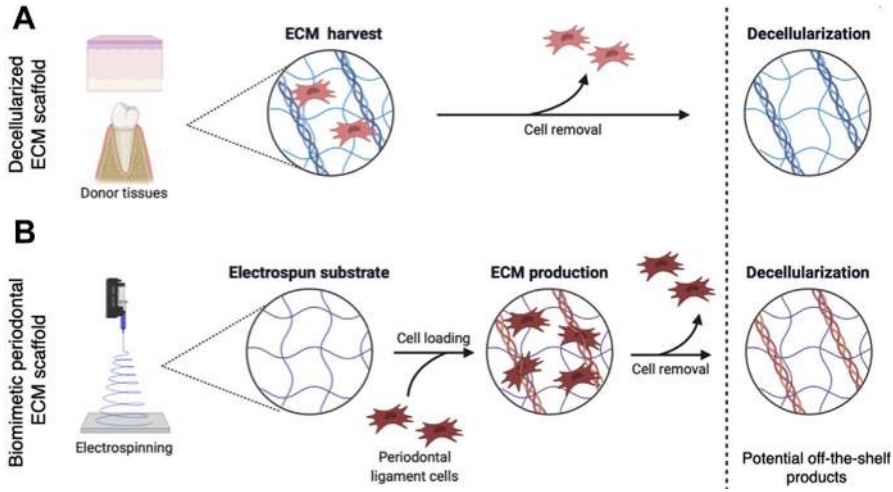

Fig. 3. Schematic illustration of the fabrication workflow of decellularized ECM scaffolds and biomimetic periodontal ECM scaffolds. (*A*) Decellularized ECM scaffolds are produced by harvesting ECM from donor sites such as dermis, amniotic membrane, and periodontal tissues followed by decellularization process. (*B*) Biomimetic periodontal ECM scaffolds are produced by the combination of nano-scaled electrospun substrate and allogenic PDLCs. The cells loaded on the substrate produce periodontal-specific ECM, which remains deposited after decellularization.

elastin fibers.[78] Human AM has been proven to contains rich growth factors such as epithelial growth factor, basic fibroblast growth factor, transforming growth factor-α and -β, vascular endothelial growth factor, and hepatocyte growth factor, all of which are positively corelated to periodontal regeneration through anti-inflammatory effects, immunomodulatory effects, antibacterial effects, and promotion of endogenous progenitor growth.[79–82] On hAM, PDLC are able to maintain their phenotype as in vivo with robust expression of ki-67, vimentin, desmoplakin, and ZO-1, but not keratins 4 and 13, suggesting its compatibility for periodontal regeneration.[70] It was shown that the use of hAM as a barrier membrane in combination with hydroxyapatite granules had advantageous effects on the suppression of the local inflammation at the recipient site, resulting in greater clinical attachment gain with increased bone generation than the bone substitutes only.[83,84] Although the efficacy of hAM alone to induce periodontal regeneration remains elusive, it was proven to be a promising scaffold for cell-based periodontal therapy.[85,86] An in vivo study in immunodeficient mice showed that hAM loaded with periodontal ligament stem cells (PDLSC) induced bone regeneration in surgically created class II furcation defects.[85] The histologic analysis confirmed new cementum formation, with single-layered cementblast-like cells on the surface, in which Sharpey's fibers were inserted. Similarly, the transplantation of adipose-derived mesenchymal stem cells on hAM regenerated 2-wall osseous defects in a rat model.[86] These results confirmed that hAM supported cementogenesis, osteogenesis, and fibrogenesis in experimental periodontal defects.

The ECM could also be obtained from dental tissues. Indeed, a detailed protocol to harvest and decellularize ECM from dental tissues without deteriorating intermingled collagen fiber networks have been recently reported, and it was successfully applied to periodontal tissues.[32,87] Naturally, the ECM of periodontal origin could be considered to possess the ideal microenvironment (eg, topography, protein composition)

for periodontal regeneration. An in vitro study investigating the fatal determination of PDLSC on decellularized periodontal ECM from tooth slice has indicated its unique usability as a scaffold.[32] In the study, decellularized periodontal ECM was repopulated by PDLCS. Strikingly, PDLSC that were found near the decellularized cementum layer selectively expressed cementoblast markers, cementum protein-23 and osteocalcin, while keeping fibrous network within the decellularized area of periodontal ligament. This finding has confirmed that decellularized periodontal tissues maintains spatial information, which may guide the fate of PDLSC. Although no study has tested the regenerative capacity of decellularized periodontal EMC in periodontal defects, a tooth replantation model in beagle dogs has suggested that it potentially regenerates periodontal tissues structurally and functionally.[44] In the study, mandibular premolars were extracted and processed to decellularize the residual periodontal tissues on the root surface. The teeth were then replanted in the surgically expanded extraction socket. Interestingly, there was no significant difference between the freshly extracted teeth and the decellularized teeth in root resorption, recovered periodontal ligament area and new cementum formation. The study also showed rich revascularization in the decellularized matrix, suggesting that decellularized periodontal ECM was sufficient to retrieve its hierarchical structure and function by recruiting endogenous progenitors.

Nevertheless, the clinical translation of decellularized ECM originated from periodontal tissues seems challenging although periodontal ligament can be obtained from deciduous teeth, wisdom teeth, and extracted teeth for orthodontics treatment and then cryopreserved. The technique requires the provision of infrastructure, namely, “tooth banks,” and improved cost efficiency before being manufactured as off-the-shelf products for example, ADM and hAM.[88]

Bioengineered Periodontal Extracellular Matrix as a Biomimetic Approach

Contrary to natural ECM-based approaches, bioengineering techniques may be used to produce biomimetic periodontal scaffolds in combination with progenitor cells and/or bioactive molecules. A nanotopographical pattern of scaffolds, such as pores, grooves, and ridges, regulates cell growth, mobility, and fate.[89–91] Various techniques have been used to produce biomimetic ECM which has close resemblance to natural fibrous ECM. In particular, electrospinning has caught appreciable attention because of the unique features of the end products. Electrospun scaffolds consist of nonwoven nano-to-micro filaments with favorable porosity and interconnectivity for cell growth, which resemble to the structural pattern of natural ECM.[92] It is compatible with various natural and synthetic polymers, and further functionalization may be combined by adding bioactive molecules in the melts.[33]

Electrospun constructs have been used as a substrate to produce biomimetic periodontal ECM in combination with progenitor cells (**Fig. 2**B). Simply, PDLC seeded on an electrospun substrate were able to produce ECM by secreting collagen I, fibronectin, and rich growth factors, which are found in native periodontal tissues, such as basic fibroblast growth factor, vascular endothelial growth factor, and hepatocyte growth factor.[30,93] Importantly, the secreted proteins were preserved on the substrate after the decellularization process, indicating that the engineered construct mimicked the architecture and function of the native periodontal ECM.[30,31] Furthermore, the electrospun substrate provided a structural reinforcement during production process, which prevented the construct from being deformed and damaged during production process.[31] This allowed for further preclinical assessment of the biomimetic periodontal ECM in surgically created periodontal fenestration defects in rat, showing that it significantly promoted the regeneration of periodontal ligament, cementum,

and alveolar bone in comparison to electrospun PCL scaffolds alone.[35] It has been shown that decellularized bioengineered ECM did not show immunogenicity, and it could be repopulated by allogenic and xenogeneic cells[30,35,93,94] Therefore, the concept of biomimetic periodontal ECM has a potential to be clinically transferred as off-the-shelf products.

The idea of biomimetic periodontal ECM may be further enhanced by controlling nanofiber orientation. On parallelly aligned PCL electrospun nanofibers, PDLC upregulated the expression of periostin, which regulates homeostasis of periodontal tissues in response to occlusal load.[95,96] Further in vivo observation in a periodontal fenestration defect model in rat showed that aligned PCL electrospun nanofibers loaded by PDLC noticeably regenerated periodontal ligament, which was perpendicularly oriented to the root surface, whereas randomly aligned nanofibers resulted in irregular ligament orientation.[96] This finding suggests that fiber orientation governs the architecture and function at the regenerated sites.

The functionalization of electrospun constructs may also expand the feasibility of hierarchical periodontal regeneration. For example, adding collagen type 1 and nanohydroxyapatites in PCL solution before extrusion allowed the end product to be osteoinductive, promoting the expression of alkaline phosphatase and osteocalcin expression by PDLCs.[97] Provided that periodontitis is an inflammatory disease caused by bacterial infection, functionalization with nonsteroidal anti-inflammatory drugs or antibiotics in anticipation of sustained drug release seems valid. The immobilization of nonsteroidal anti-inflammatory drugs such as meloxicam and ibuprofen in electrospun fibers allowed the construct to possess a long-term anti-inflammatory effect.[67–69] Interestingly, PCL electrospun scaffolds functionalized with ibuprofen selectively suppressed the proliferation of gingival cells subjected to *Porphyromonas gingivalis* lipopolysaccharide.[67] In an experimentally induced periodontitis model, PCL electrospun scaffolds functionalized with ibuprofen significantly decreased local inflammation and further progression but improved the clinical attachment level in comparison with the nonfunctionalized counterpart. Functionalization with antibiotics such as doxycycline hydrochloride, metronidazole, and tetracycline hydrochloride has been also suggested to be efficacious against the progression of periodontitis and to provide better sustainability after implantation.[98–100] These functionalization techniques do not alter the bulk properties of the polymeric scaffolds, but may offer additional benefits to periodontal regenerative therapy.[100]

MULTIPHASIC SCAFFOLD APPROACH FOR TARGETING TISSUE-SPECIFIC REGENERATION

Periodontal regeneration requires the spatiotemporal reorganization of newly formed periodontal ligament, cementum, and alveolar bone. These components are suggestive of porous medium with approximately 70% to 90% porosity, but each component has unique cellular components, matrix pattern, and functionality.[101–103] Therefore, multiphasic scaffolds are designed to consist of multiple components layer by layer, each of which specifically targets their corresponding tissue. There are countless designing concepts to achieve compartmentalized periodontal regeneration; it can be the combination of differential materials, architectural patterns, functionalization, and cell types.[37]

Biphasic scaffolds are often designed to combine bone compartment and periodontal compartment. Vaquette and colleagues (2012) developed double-layered PCL scaffolds which consisted of a bone compartment produced by 3D printing and an electrospun periodontal compartment.[38] In this study, osteoblasts in

suspension and PDLC in sheet were loaded on their corresponding components, and then the construct was placed on a dentin block as the periodontal compartment was in contact with the dentin surface before subcutaneous transplantation in an immunodeficiency rat model. The histologic evaluation noted that a cementum-like tissue was formed on the dentin surface in which fibrous attachment supported, whereas the expression of alkaline phosphatase was promoted on the bone compartment side. The following study further optimized the scaffold design by functionalizing the bone compartment with calcium phosphates, showing improved bone formation.[39] The other common biphasic approach is to combine a barrier membrane and porous scaffold as one unit. Despite differences in designing concept among studies, it would be concluded the concept may improve the tissue regeneration in comparison with barrier membrane or scaffold alone.[40–42] However, further comparative studies between the biphasic scaffold approach and the conventional combination of barrier membrane and graft material separately are needed to verify its additional therapeutic benefit.

Triphasic scaffolds are mostly designed to individually target each of 3 components in periodontal tissues to provide more specific spaciotemporal guidance. Despite complexity in fabrication methods, several studies have successfully produced triphasic scaffolds for periodontal application. For example, 3D printing technology facilitates producing triphasic scaffolds by changing strand alignment patterns. Lee and colleagues[43] (2014) verified the triphasic concept by the orthodox tissue engineering approach, namely, by combining scaffolds, bioactive molecules, and progenitor cells. In this study, triphasic 3D printed scaffolds of nanohydroxyapatite-containing PCL were designed by changing porous patterns. Three phases were designed with 100 μm, 600 μm, and 300 μm microchannels to approach cementum/dentin interface, periodontal ligament, and alveolar bone, respectively. Subsequently, layers for the cementum–dentin interface, periodontal ligament, and alveolar bone were functionalized with human amelogenin, connective tissue growth factor, and BMP-2, respectively, before the scaffold was loaded by dental pulp stem cells and transplanted subcutaneously in immunodeficient mice. Notably, phase-specific tissue formation was observed: dense and polarized mineral formation with the upregulation of dentin sialophosphoprotein and cement matrix protein 1 in the cementum/dentin phase, aligned fibrous matrix formation with the upregulation of collagen type 1 in the periodontal ligament phase, and scattered mineral formation with the upregulation of bone sialoprotein in the bone phase. This finding suggests that multiphasic structures effectively guide tissue-specific regeneration by providing optimal microstructure and spatiotemporal delivery of bioactive molecules. Another example is the combination of differential cell types and mechanical properties. Varoni and colleagues[44] (2017) produced chitosan-based porous scaffolds that consisted of bone and periodontal layers produced by the freeze-drying method and a dense mesh gingival layers by electrochemical deposition. Differential stiffness was given to each of the layers by controlling molecular weight of cross-linking reagent: a stiff layer aiming for bone regeneration and a soft layer for the interaction with the gingiva and the periodontal ligament. Osteoblast, PDLC, and gingival fibroblast were then seeded to their corresponding layers. In an in vivo ectopic periodontal model, as expected, robust expression of tissue specific markers was found: periostin and collagen type 1 in the periodontal ligament layer, osteopontin and bone sialoprotein in the bone layer, and cement matrix protein-1 adjacent to the dentin surface. Also, putative cementum and bone were newly formed in the bone and periodontal layers.

It is also relevant to mention other studies that have introduced novel fabrication techniques for triphasic scaffolds that may potentially guide hierarchical regeneration,

albeit without testing their in vivo efficacy.[37,104,105] Nevertheless, scaffold fabrication is complicated with each additional phase, particularly with regard to small scaffolds for periodontal applications, and a lack of in vivo evidence for the efficacy of such complex scaffolds precludes a conclusion on their current clinical relevance.

CUSTOM-DESIGNED 3-DIMENSIONAL SCAFFOLD FOR A PERSONALIZED PERIODONTAL APPROACH

A personalized medicine approach underlies the concept of pathologic variation among patients.[106] Optimal periodontal regeneration requires spatial guidance to progenitor cells with rich vascularization while preventing epithelial downgrowth.[107] Therefore, 3D scaffolds with defect-specific geometry may enhance periodontal regeneration. This goal could be achieved by applying a medical imaging system such as a high-resolution cone beam CT scan in scaffold designing. The prototype workflow of custom-designed 3D scaffolds for periodontal regeneration was introduced by Park and colleagues[49,63] (2010, 2012). Surgically created periodontal fenestration defects were scanned by a micro-CT scan, and the scanned files were then transferred into CAD software as 3D image data in *.stl* format, where the scaffold geometry was designed to adapt to the defect. In the scaffold, microchannel architectures were included in the scaffold to provide an orientational guide to periodontal ligament fibers. Subsequently, a wax mold was created by a wax printer, and PCL was casted in the mold.[49,63] After the sterilization process, PDLC were loaded on the custom-designed scaffold and transplanted to the defect site.[63] After 4 weeks of healing, the custom-designed scaffold resulted in a significant increase in bone mass and mineral density, and the alignment of regenerated periodontal ligament was oriented more regularly in comparison with amorphous scaffolds with random pores produced by the freeze-drying method. Strikingly, the expression of periostin, which is the regulator of collagen fibrogenesis found in functional periodontal ligament,[108] was evident in the treated site by the custom-designed scaffold, but not by the amorphous scaffold.[63] The development of high-resolution 3D printing technology has facilitated the fabrication of on-demand scaffolds (**Fig. 4**). The clinical implication of the approach was reported by Rasperini and colleagues[62] (2015) in which a fenestration defect in the mandibular canine was treated by 3D printed custom-designed scaffold. The scaffold was designed based on CT data and printed by selective laser sintering. During periodontal surgery, the scaffold was immersed in recombinant human platelet-derived growth factor BB and then transplanted in the defect site. After 12 months of the treatment, clinical attachment gain and radiological bone regeneration was observed without complication. In this case, however, the scaffold was exposed at 13 months, and then the entire scaffold was removed owing to infection. After histologic assessment and gel permeation chromatography showed that a great amount of the scaffold was still found with approximately 76% of PCL molecular weight remained. Also, the new bone formation was limited. This suggests that custom-designed scaffold may guide the tissue regeneration, but the prognosis largely depends on concordant material degradation and biological interaction between materials and tissues. Further optimization of internal microstructure, polymer selection, and polymer functionalization may contribute to an improved outcome.

Bioprinting technology has been emerging as a state-of-art tool to fabricate 3D biofunctional hierarchical architecture with one or multiple type(s) of living cell incorporated. It adds biological functionality to a conventional 3D printed scaffold because it mimics an in vivo cell-to-cell and cell-to matrix interaction within the construct. Currently, the technique has been used with trial-and-error steps to fabricate

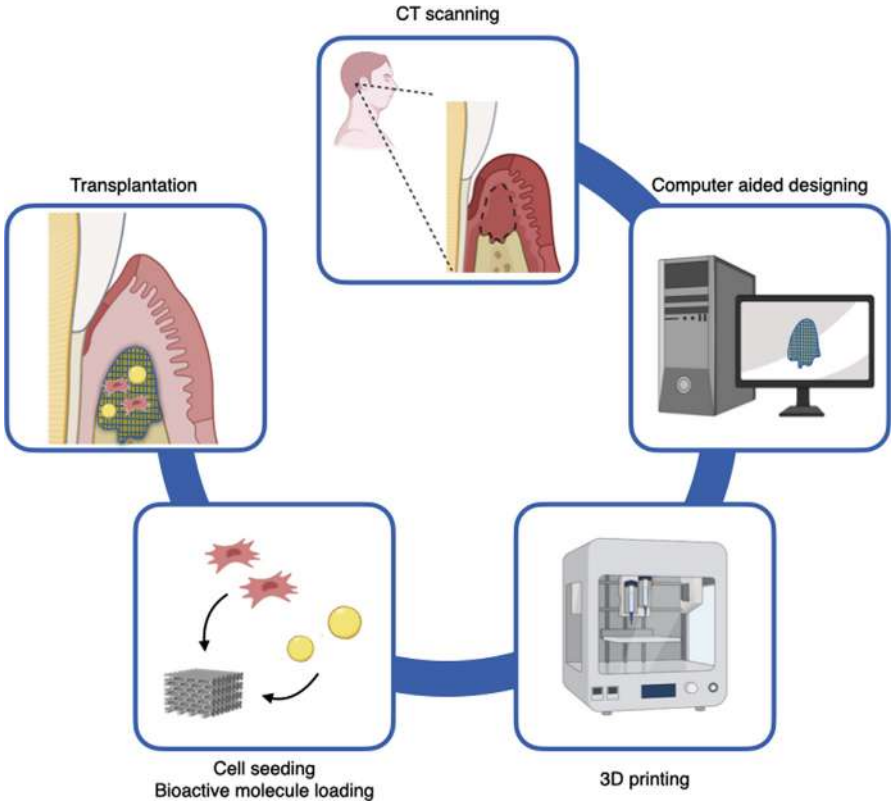

Fig. 4. Schematic illustration of the fabrication workflow of personalized 3D-printed scaffolds for periodontal regeneration. The geometry of periodontal defect obtained by CT scanning is processed in computer aided designing (CAD) software to design a scaffold which may adapt to the defect. Using CAD file, the scaffold is produced by 3D printing with a desired biomaterial. Multipotent cells and bioactive molecules may be incorporated to improve the functionality of the scaffold before transplantation.

bioartificial organs such as skin, bone, cartilage, liver, heart, kidney, lung, and nerve.[109] Owing to its immaturity, there are considerable challenges to overcome. These include the optimization of bioink, referring to a mixture of biomaterial and cells, and cytocompatible extrusion parameters.[109] For future application to periodontal regeneration, the optimization of bioink using PDLC has been just launched. By now, photocrosslinkable hydrogels, gelatin-methacryloyl and poly(ethylene glycol) dimethacrylate hydrogel were proposed as base materials, and the optimization of printability, mechanical stability, and cytocompatibility has been performed by testing different extrusion parameters and crosslinking methods.[110,111] The progress is in an early phase, but given the necessity of hierarchical regeneration, bioprinting in the field of periodontal regeneration is likely to gain more and more research attention.

CONCLUSION AND FUTURE IMPLICATIONS

Periodontal regeneration involves a high degree of complexity owing to the specialized nature and hierarchical structure of the periodontium. It requires a spatiotemporal coordination of both soft and hard tissues, namely gingival epithelium, periodontal

ligament, cementum, and alveolar bone. Additionally, it is highly susceptible to oral microflora, and therefore controlling local inflection and inflammation determines the prognosis and therapeutic efficacy. Based on our current knowledge, the conventional grafting approach to periodontal defects with bone substitutes results in mainly bone regeneration with a long junctional epithelium regardless of material properties, and the regenerative potency of current therapies such as guided tissue regeneration and enamel matrix derivative is limited despite their clinical popularity. This warrants the necessity of further advancement in periodontal regenerative therapy based on the tissue engineering approach.

Indeed, tissue engineering in periodontics is a growing field: since the mid-1990s when its therapeutic potential was suggested, the number of studies has been exponentially increasing.[112] Advancement of material development, fabrication techniques, and digital solutions are remarkably propelling this novel approach to periodontal regeneration. Several studies have introduced prototypical scaffold designs that can potentially guide site-specific regeneration. This concept is based on the production of biomimetic periodontal scaffolds ex vivo by combining different materials and functionalization methods. The architectural patterns of scaffolds provide a spatial guidance to endogenous and exogeneous progenitor cells, whose functionality may be further enhanced by the inclusion of bioactive molecules on the scaffolds. Currently, high-resolution 3D printing technology allows for a rapid production of polymeric scaffolds in prescribed forms. The technique seems highly compatible with dental clinical settings where a CT scan and 3D intraoral scanner systems are now widely in use. This will allow to produce patient-specific scaffolds in a chair-side setting or in, for example, laboratories. Although clinical evidence for the efficacy of 3D-printed scaffolds is currently limited, further optimization of microstructure, material selection, and functionalization to add bioactive features may improve future clinical outcomes. Furthermore, advances in bioprinting technology may allow the production of patient-specific biomimetic periodontal implants.

Nevertheless, there is admittedly limited evidence on the advantage of the tissue engineering approach in comparison with the currently available treatment owing to the lack of in vivo and clinical evaluation in periodontal defect models. Challenges of preclinical testing notwithstanding, future studies should consider including more clinically relevant animal models of periodontitis, ideally in large animal models, to facilitate clinical translation. Furthermore, additional challenges, including compliance with good manufacturing practices and regulatory authorities must be overcome to facilitate the translation of novel tissue engineering therapies.[113] This involves the need for infrastructure improvements and quality control, with considerably higher costs of therapy as a consequence. Therefore, further investigations on clinical efficiency as well as cost effectiveness are required to validate the clinical applicability of tissue engineered constructs for periodontal regeneration.

CLINICS CARE POINTS

- Extracellular matrix obtained from periodontal ligament may be developed as off-the-shelf products.
- Biomimetic periodontal extracellular matrix can be produced by combining polymeric substrate and periodontal ligament-derived cells.
- Development of tooth-bank and stable provision of cell source are necessary for extracellular matrix approach.

- Multiphasic scaffolds may guide periodontal progenitor cells to specifically targeted cell types (i.e., fibroblasts, cementblasts, osteoblasts) despite difficulty in fabrication
- Defect-specific scaffolds produced by 3D printer may support periodontal regeneration for short-term, but there is currently no evidence on long-term prognosis
- Further in-vivo and clinical studies are needed to optimize scaffold design and material selection.

DISCLOSURE

The authors declare no potential conflict of interest.

ACKNOWLEDGMENTS

The authors gratefully acknowledge the Trond Mohn Foundation (Grant No. BFS2018TMT10) for financial support of this article.

REFERENCES

1. Gerritsen AE, Allen PF, Witter DJ, et al. Tooth loss and oral health-related quality of life: a systematic review and meta-analysis. Health Qual Life Outcomes 2010; 8:126.
2. Hughes FJ, Ghuman M, Talal A. Periodontal regeneration: a challenge for the tissue engineer? Proc Inst Mech Eng H 2010;224:1345–58.
3. Sculean A, Nikolidakis D, Schwarz F. Regeneration of periodontal tissues: combinations of barrier membranes and grafting materials - biological foundation and preclinical evidence: a systematic review. J Clin Periodontol 2008;35: 106–16.
4. Murphy KG, Gunsolley JC. Guided tissue regeneration for the treatment of periodontal intrabony and furcation defects. A systematic review. Ann Periodontol 2003;8:266–302.
5. Esposito M, Grusovin MG, Coulthard P, et al. Enamel matrix derivative (Emdogain) for periodontal tissue regeneration in intrabony defects. A Cochrane systematic review. Cochrane Database Syst Rev 2005;CD003875.
6. Needleman IG, V Worthington H, Giedrys-Leeper E, et al. Guided tissue regeneration for periodontal infra-bony defects. Cochrane Database Syst Rev 2006;CD001724.
7. Misch CM. Autogenous bone: is it still the gold standard? Implant Dent 2010; 19:361.
8. Eppley BL, Pietrzak WS, Blanton MW. Allograft and alloplastic bone substitutes: a review of science and technology for the craniomaxillofacial surgeon. J Craniofac Surg 2005;16:981–9.
9. Jimi E, Hirata S, Osawa K, et al. The current and future therapies of bone regeneration to repair bone defects. Int J Dent 2012;2012:1–7.
10. Sculean A, Nikolidakis D, Nikou G, et al. Biomaterials for promoting periodontal regeneration in human intrabony defects: a systematic review. Periodontol. 2000 2015;68:182–216.
11. Langer R, Vacanti JP. Tissue engineering. Science 1993;260:920–6.
12. Tollemar V, Collier ZJ, Mohammed MK, et al. Stem cells, growth factors and scaffolds in craniofacial regenerative medicine. Genes Dis 2016;3:56–71.
13. Green DW, Lee J-S, Jung H-S. Small-scale fabrication of biomimetic structures for periodontal regeneration. Front Physiol 2016;7:1–8.

14. O'Brien FJ. Biomaterials & scaffolds for tissue engineering. Mater Today 2011; 14:88–95.
15. Loh QL, Choong C. Three-dimensional scaffolds for tissue engineering applications: role of porosity and pore size. Tissue Eng B Rev 2013;19:485–502.
16. Karageorgiou V, Kaplan D. Porosity of 3D biomaterial scaffolds and osteogenesis. Biomaterials 2005;26:5474–91.
17. Tran PA. Blood clots and tissue regeneration of 3D printed dual scale porous polymeric scaffolds. Mater Lett 2021;285:129184.
18. Li Z, Lv X, Chen S, et al. Improved cell infiltration and vascularization of three-dimensional bacterial cellulose nanofibrous scaffolds by template biosynthesis. RSC Adv 2016;6:42229–39.
19. Hong WX, Hu MS, Esquivel M, et al. The role of hypoxia-inducible factor in wound healing. Adv Wound Care 2014;3:390–9.
20. Darby IA, Hewitson TD. Hypoxia in tissue repair and fibrosis. Cell Tissue Res 2016;553–62.
21. Klenke FM, Liu Y, Yuan H, et al. Impact of pore size on the vascularization and osseointegration of ceramic bone substitutes in vivo. J Biomed Mater Res A 2008;85A:777–86.
22. Murphy CM, O'Brien FJ. Understanding the effect of mean pore size on cell activity in collagen-glycosaminoglycan scaffolds. Cell Adhes Migr 2010;4:377–81.
23. Jin H, Zhuo Y, Sun Y, et al. Microstructure design and degradation performance in vitro of three-dimensional printed bioscaffold for bone tissue engineering. Adv Mech Eng 2019;11. 168781401988378.
24. Botchwey EA, Dupree MA, Pollack SR, et al. Tissue engineered bone: measurement of nutrient transport in three-dimensional matrices. J Biomed Mater Res 2003;67A:357–67.
25. Mastrullo V, Cathery W, Velliou E, et al. Angiogenesis in tissue engineering: As nature intended? Front Bioeng Biotechnol 2020;8:188.
26. Dutta RC, Dey M, Dutta AK, et al. Competent processing techniques for scaffolds in tissue engineering. Biotechnol Adv 2017;35:240–50.
27. Jeon JE, Vaquette C, Klein TJ, et al. Perspectives in multiphasic osteochondral tissue engineering. Anat Rec (Hoboken) 2014;297:26–35.
28. Nakayama KH, Hou L, Huang NF. Role of extracellular matrix signaling cues in modulating cell fate commitment for cardiovascular tissue engineering. Adv Healthc Mater 2014;3:628–41.
29. Tavelli L, McGuire MK, Zucchelli G, et al. Extracellular matrix-based scaffolding technologies for periodontal and peri-implant soft tissue regeneration. J Periodontol 2020;91:17–25.
30. Farag A, Vaquette C, Theodoropoulos C, et al. Decellularized periodontal ligament cell sheets with recellularization potential. J Dent Res 2014;93:1313–9.
31. Farag A, Vaquette C, Hutmacher DW, et al. Fabrication and characterization of decellularized periodontal ligament cell sheet constructs. Methods Mol Biol 2017;37:403–12.
32. Son H, Jeon M, Choi H-J, et al. Decellularized human periodontal ligament for periodontium regeneration. PLoS One 2019;14:e0221236.
33. Kurokawa N, Endo F, Maeda T, et al. Electrospinning and surface modification methods for functionalized cell scaffolds. In: Ficai D, Grumezescu AM, editors. Micro and Nano Technologies, Nanostructures for Novel Therapy. Elsevier; 2017. p. 201–25.
34. Lannutti J, Reneker D, Ma T, et al. Electrospinning for tissue engineering scaffolds. Mater Sci Eng C 2007;27:504–9.

35. Farag A, Hashimi SM, Vaquette C, et al. The effect of decellularized tissue engineered constructs on periodontal regeneration. J Clin Periodontol 2018;45:586–96.
36. Cortez Tornello PR, Caracciolo PC, Igartúa Roselló JI, et al. Electrospun scaffolds with enlarged pore size: porosimetry analysis. Mater Lett 2018;227:191–3.
37. Ivanovski S, Vaquette C, Gronthos S, et al. Multiphasic scaffolds for periodontal tissue engineering. J Dent Res 2014;93:1212–21.
38. Vaquette C, Fan W, Xiao Y, et al. A biphasic scaffold design combined with cell sheet technology for simultaneous regeneration of alveolar bone/periodontal ligament complex. Biomaterials 2012;33:5560–73.
39. Costa PF, Vaquette C, Zhang Q, et al. Advanced tissue engineering scaffold design for regeneration of the complex hierarchical periodontal structure. J Clin Periodontol 2014;41:283–94.
40. Requicha JF, Viegas CA, Muñoz F, et al. A tissue engineering approach for periodontal regeneration based on a biodegradable double-layer scaffold and adipose-derived stem cells. Tissue Eng A 2014;20:2483–92.
41. Requicha JF, Viegas CA, Hede S, et al. Design and characterization of a biodegradable double-layer scaffold aimed at periodontal tissue-engineering applications. J Tissue Eng Regen Med 2016;10:392–403.
42. Carlo Reis EC, Borges APB, Araújo MVF, et al. Periodontal regeneration using a bilayered PLGA/calcium phosphate construct. Biomaterials 2011;32:9244–53.
43. Lee CH, Hajibandeh J, Suzuki T, et al. Three-dimensional printed multiphase scaffolds for regeneration of periodontium complex. Tissue Eng Part A 2014;20:1342–51.
44. Varoni EM, Vijayakumar S, Canciani E, et al. Chitosan-based trilayer scaffold for multitissue periodontal regeneration. J Dent Res 2018;97:303–11.
45. Murphy SV, Atala A. 3D bioprinting of tissues and organs. Nat Biotechnol 2014;32:773–85.
46. Liu F, Wang X. Synthetic polymers for organ 3D printing. Polymers (Basel) 2020;12:1765.
47. Han T, Kundu S, Nag A, et al. 3D printed sensors for biomedical applications: a review. Sensors 2019;19:1706.
48. Derakhshanfar S, Mbeleck R, Xu K, et al. 3D bioprinting for biomedical devices and tissue engineering: a review of recent trends and advances. Bioact Mater 2018;3:144–56.
49. Park CH, Rios HF, Jin Q, et al. Biomimetic hybrid scaffolds for engineering human tooth-ligament interfaces. Biomaterials 2010;31:5945–52.
50. Tallawi M, Rosellini E, Barbani N, et al. Strategies for the chemical and biological functionalization of scaffolds for cardiac tissue engineering: a review. J R Soc Interf 2015;12:20150254.
51. Nair LS, Laurencin CT. Biodegradable polymers as biomaterials. Prog Polym Sci 2007;32:762–98.
52. Dhandayuthapani B, Yoshida Y, Maekawa T, et al. Polymeric scaffolds in tissue engineering application: a review. Int J Polym Sci 2011;2011:1–19.
53. Filippi M, Born G, Chaaban M, et al. Natural polymeric scaffolds in bone regeneration. Front Bioeng Biotechnol 2020;8:474.
54. Zhao J, Santino F, Giacomini D, et al. Integrin-targeting peptides for the design of functional cell-responsive biomaterials. Biomedicines 2020;8:307.
55. Banerjee A, Chatterjee K, Madras G. Enzymatic degradation of polymers: a brief review. Mater Sci Technol 2014;30:567–73.

56. Mano J, Silva G, Azevedo H, et al. Natural origin biodegradable systems in tissue engineering and regenerative medicine: present status and some moving trends. J R Soc Interf 2007;4:999–1030.
57. Heljak MK, Swieszkowski W, Kurzydlowski KJ. Modeling of the degradation kinetics of biodegradable scaffolds: the effects of the environmental conditions. J Appl Polym Sci 2014;131:40280.
58. Baican M, Stoleru E, Vasile C. Cellular response to synthetic polymers. In: Mozafari M, editor. Woodhead Publishing Series in Biomaterials, Handbook of Biomaterials Biocompatibility. Woodhead Publishing; 2020. p. 269–319.
59. Campos DM, Gritsch K, Salles V, et al. Surface entrapment of fibronectin on electrospun PLGA scaffolds for periodontal tissue engineering. Biores Open Access 2014;3:117–26.
60. Liu Z, Yin X, Ye Q, et al. Periodontal regeneration with stem cells-seeded collagen-hydroxyapatite scaffold. J Biomater Appl 2016;31:121–31.
61. Carmagnola D, Tarce M, Dellavia C, et al. Engineered scaffolds and cell-based therapy for periodontal regeneration. J Appl Biomater Funct Mater 2017;15:e303–12.
62. Rasperini G, Pilipchuk SP, Flanagan CL, et al. 3D-printed bioresorbable scaffold for periodontal repair. J Dent Res 2015;94:153S–7S.
63. Park CH, Rios HF, Jin Q, et al. Tissue engineering bone-ligament complexes using fiber-guiding scaffolds. Biomaterials 2012;33:137–45.
64. Vasconcelos DP, Costa M, Neves N, et al. Chitosan porous 3D scaffolds embedded with resolvin D1 to improve in vivo bone healing. J Biomed Mater Res Part A 2018;106:1626–33.
65. Nakamura S, Ito T, Okamoto K, et al. Acceleration of bone regeneration of horizontal bone defect in rats using collagen-binding basic fibroblast growth factor combined with collagen scaffolds. J Periodontol 2019;90:1043–52.
66. Van Dyke TE. Pro-resolving mediators in the regulation of periodontal disease. Mol Aspects Med 2017;58:21–36.
67. Batool F, Morand D-N, Thomas L, et al. Synthesis of a novel electrospun polycaprolactone scaffold functionalized with ibuprofen for periodontal regeneration: an in vitro and in vivo study. Materials (Basel) 2018;11:580.
68. Yar M, Farooq A, Shahzadi L, et al. Novel meloxicam releasing electrospun polymer/ceramic reinforced biodegradable membranes for periodontal regeneration applications. Mater Sci Eng C 2016;64:148–56.
69. Farooq A, Yar M, Khan AS, et al. Synthesis of piroxicam loaded novel electrospun biodegradable nanocomposite scaffolds for periodontal regeneration. Mater Sci Eng C 2015;56:104–13.
70. Goldstein M, Boyan BD, Cochran DL, et al. Human histology of new attachment after root coverage using subepithelial connective tissue graft. J Clin Periodontol 2001;28:657–62.
71. Aguirre-Zorzano L-A, García-De La Fuente AM, Estefanía-Fresco R, et al. Complications of harvesting a connective tissue graft from the palate. A retrospective study and description of a new technique. J Clin Exp Dent 2017;9:e1439–45.
72. Núñez J, Caffesse R, Vignoletti F, et al. Clinical and histological evaluation of an acellular dermal matrix allograft in combination with the coronally advanced flap in the treatment of miller class I recession defects: an experimental study in the mini-pig. J Clin Periodontol 2009;36:523–31.
73. Okubo N, Fujita T, Ishii Y, et al. Coverage of gingival recession defects using acellular dermal matrix allograft with or without beta-tricalcium phosphate. J Biomater Appl 2013;27:627–37.

74. de Carvalho Formiga M, Nagasawa MA, Moraschini V, et al. Clinical efficacy of xenogeneic and allogeneic 3D matrix in the management of gingival recession: a systematic review and meta-analysis. Clin Oral Investig 2020;24:2229–45.
75. Aragoneses J, Suárez A, Rodríguez C, et al. Histomorphometric comparison between two types of acellular dermal matrix grafts: a mini pig animal model study. Int J Environ Res Public Health 2021;18:3881.
76. Guo J, Chen H, Wang Y, et al. A novel porcine acellular dermal matrix scaffold used in periodontal regeneration. Int J Oral Sci 2013;5:37–43.
77. Leal-Marin S, Kern T, Hofmann N, et al. Human amniotic membrane: a review on tissue engineering, application, and storage. J Biomed Mater Res B Appl Biomater 2020;109(8):1198–215.
78. Mamede AC, Botelhoeditors MF. Amniotic membrane. Dordrecht: Springer Netherlands; 2015.
79. Koizumi N, Inatomi T, Sotozono C, et al. Growth factor mRNA and protein in preserved human amniotic membrane. Curr Eye Res 2000;20:173–7.
80. Bosshardt DD, Schroeder HE. Cementogenesis reviewed: a comparison between human premolars and rodent molars. Anat Rec 1996;245:267–92.
81. Howell TH, Martuscelli G, Oringer J. Polypeptide growth factors for periodontal regeneration. Curr Opin Periodontol 1996;3:149–56.
82. Ferenczy PAH, de Souza LB. Comparison of the preparation and preservation techniques of amniotic membrane used in the treatment of ocular surface diseases. Rev Bras Oftalmol 2020;79:71–80.
83. Adachi K, Amemiya T, Nakamura T, et al. Human periodontal ligament cell sheets cultured on amniotic membrane substrate. Oral Dis 2014;20:582–90.
84. Kumar A, Chandra RV, Reddy AA, et al. Evaluation of clinical, antiinflammatory and antiinfective properties of amniotic membrane used for guided tissue regeneration: a randomized controlled trial. Dent Res J (Isfahan) 2015;12:127–35.
85. Iwasaki K, Komaki M, Yokoyama N, et al. Periodontal regeneration using periodontal ligament stem cell-transferred amnion. Tissue Eng Part A 2013;20.131209065021003.
86. Wu P-H, Chung H-Y, Wang J-H, et al. Amniotic membrane and adipose-derived stem cell co-culture system enhances bone regeneration in a rat periodontal defect model. J Formos Med Assoc 2016;115:186–94.
87. Song JS, Takimoto K, Jeon M, et al. Decellularized human dental pulp as a scaffold for regenerative endodontics. J Dent Res 2017;96:640–6.
88. Zeitlin BD. Banking on teeth – stem cells and the dental office. Biomed J 2020;43:124–33.
89. Wang WY, Pearson AT, Kutys ML, et al. Extracellular matrix alignment dictates the organization of focal adhesions and directs uniaxial cell migration. APL Bioeng 2018;2:046107.
90. Janson IA, Putnam AJ. Extracellular matrix elasticity and topography: material-based cues that affect cell function via conserved mechanisms. J Biomed Mater Res Part A 2015;103:1246–58.
91. Ermis M, Antmen E, Hasirci V. Micro and nanofabrication methods to control cell-substrate interactions and cell behavior: a review from the tissue engineering perspective. Bioact Mater 2018;3:355–69.
92. Wang X, Ding B, Li B. Biomimetic electrospun nanofibrous structures for tissue engineering. Mater Today 2013;16:229–41.

93. Jiang Y, Liu J-M, Huang J-P, et al. Regeneration potential of decellularized periodontal ligament cell sheets combined with 15-deoxy-Δ 12,14 -prostaglandin J 2 nanoparticles in a rat periodontal defect. Biomed Mater 2021;16:045008.
94. Heng BC, Zhu S, Xu J, et al. Effects of decellularized matrices derived from periodontal ligament stem cells and SHED on the adhesion, proliferation and osteogenic differentiation of human dental pulp stem cells in vitro. Tissue Cell 2016; 48:133–43.
95. Rios HF, Ma D, Xie Y, et al. Periostin is essential for the integrity and function of the periodontal ligament during occlusal loading in mice. J Periodontol 2008;79: 1480–90.
96. Yang M, Gao X, Shen Z, et al. Gelatin-assisted conglutination of aligned polycaprolactone nanofilms into a multilayered fibre-guiding scaffold for periodontal ligament regeneration. RSC Adv 2019;9:507–18.
97. Wu X, Miao L, Yao Y, et al. Electrospun fibrous scaffolds combined with nanoscale hydroxyapatite induce osteogenic differentiation of human periodontal ligament cells. Int J Nanomedicine 2014;9:4135.
98. Jia L, Zhang X, Xu H, et al. Development of a doxycycline hydrochloride-loaded electrospun nanofibrous membrane for GTR/GBR applications. J Nanomater 2016;2016:1–10.
99. Verma P, Chaturvedi T, Gupta V, et al. Evaluation of metronidazole nanofibers in patients with chronic periodontitis: a clinical study. Int J Pharm Investig 2012; 2:213.
100. Ranjbar-Mohammadi M, Zamani M, Prabhakaran MP, et al. Electrospinning of PLGA/gum tragacanth nanofibers containing tetracycline hydrochloride for periodontal regeneration. Mater Sci Eng C 2016;58:521–31.
101. Bergomi M, Cugnoni J, Galli M, et al. Hydro-mechanical coupling in the periodontal ligament: a porohyperelastic finite element model. J Biomech 2011; 44:34–8.
102. Ortún-Terrazas J, Cegoñino J, Santana-Penín U, et al. Approach towards the porous fibrous structure of the periodontal ligament using micro-computerized tomography and finite element analysis. J Mech Behav Biomed Mater 2018;79:135–49.
103. Ho SP, Yu B, Yun W, et al. Structure, chemical composition and mechanical properties of human and rat cementum and its interface with root dentin. Acta Biomater 2009;5:707–18.
104. Shah AT, Zahid S, Ikram F, et al. Tri-layered functionally graded membrane for potential application in periodontal regeneration. Mater Sci Eng C 2019;103:109812.
105. Sprio S, Campodoni E, Sandri M, et al. A graded multifunctional hybrid scaffold with superparamagnetic ability for periodontal regeneration. Int J Mol Sci 2018; 19:3604.
106. Hamburg MA, Collins FS. The path to personalized medicine. N Engl J Med 2010;301–4.
107. Ramseier CA, Rasperini G, Batia S, et al. Advanced reconstructive technologies for periodontal tissue repair. Periodontol. 2000 2012;59:185–202.
108. Wen W, Chau E, Jackson-Boeters L, et al. TGF-β1 and FAK regulate periostin expression in PDL fibroblasts. J Dent Res 2010;89:1439–43.
109. Matai I, Kaur G, Seyedsalehi A, et al. Progress in 3D bioprinting technology for tissue/organ regenerative engineering. Biomaterials 2020;226:119536.
110. Thattaruparambil Raveendran N, Vaquette C, Meinert C, et al. Optimization of 3D bioprinting of periodontal ligament cells. Dent Mater 2019;35:1683–94.

111. Ma Y, Ji Y, Huang G, et al. Bioprinting 3D cell-laden hydrogel microarray for screening human periodontal ligament stem cell response to extracellular matrix. Biofabrication 2015;7:044105.
112. Bell E. Strategy for the selection of scaffolds for tissue engineering. Tissue Eng 1995;1:163–79.
113. Giancola R, Bonfini T, Iacone A. Cell therapy: cGMP facilities and manufacturing. Muscles Ligaments Tendons J 2012;2:243–7.

Stem Cell Research & Therapy

RESEARCH Open Access

Bone regeneration in rat calvarial defects using dissociated or spheroid mesenchymal stromal cells in scaffold-hydrogel constructs

Siddharth Shanbhag[1,2*], Salwa Suliman[1], Samih Mohamed-Ahmed[1], Carina Kampleitner[3,4,5], Mohamed Nageeb Hassan[1], Patrick Heimel[3,4,5], Toni Dobsak[3,5], Stefan Tangl[3,5], Anne Isine Bolstad[1] and Kamal Mustafa[1*]

Abstract

Background: Three-dimensional (3D) spheroid culture can promote the osteogenic differentiation of bone marrow mesenchymal stromal cells (BMSC). 3D printing offers the possibility to produce customized scaffolds for complex bone defects. The aim of this study was to compare the potential of human BMSC cultured as 2D monolayers or 3D spheroids encapsulated in constructs of 3D-printed poly-L-lactide-co-trimethylene carbonate scaffolds and modified human platelet lysate hydrogels (PLATMC-HPLG) for bone regeneration.

Methods: PLATMC-HPLG constructs with 2D or 3D BMSC were assessed for osteogenic differentiation based on gene expression and in vitro mineralization. Subsequently, PLATMC-HPLG constructs with 2D or 3D BMSC were implanted in rat calvarial defects for 12 weeks; cell-free constructs served as controls. Bone regeneration was assessed via in vivo computed tomography (CT), ex vivo micro-CT and histology.

Results: Osteogenic gene expression was significantly enhanced in 3D versus 2D BMSC prior to, but not after, encapsulation in PLATMC-HPLG constructs. A trend for greater in vitro mineralization was observed in constructs with 3D versus 2D BMSC ($p > 0.05$). In vivo CT revealed comparable bone formation after 4, 8 and 12 weeks in all groups. After 12 weeks, micro-CT revealed substantial regeneration in 2D BMSC (62.47 ± 19.46%), 3D BMSC (51.01 ± 24.43%) and cell-free PLATMC-HPLG constructs (43.20 ± 30.09%) ($p > 0.05$). A similar trend was observed in the histological analysis.

Conclusion: Despite a trend for superior in vitro mineralization, constructs with 3D and 2D BMSC performed similarly in vivo. Regardless of monolayer or spheroid cell culture, PLATMC-HPLG constructs represent promising scaffolds for bone tissue engineering applications.

Keywords: Xeno-free, Platelet lysate, MSC, Spheroid culture, Bone tissue engineering

Background

Reconstruction of advanced maxillofacial bone deficiencies is a clinical challenge. Bone tissue engineering (BTE) strategies are increasingly being used to overcome the limitations of autogenous bone grafts and existing bone-substitute materials to reconstruct such defects [1]. BTE aims to combine the cellular (*osteogenic* cells), extracellular (*osteoconductive* scaffolds) and/or molecular elements (*osteoinductive* growth factors) required for bone healing [2]. The potential of BTE for orofacial bone regeneration as demonstrated in several preclinical and clinical studies has recently been summarized [1, 3–5].

*Correspondence: siddharth.shanbhag@uib.no; kamal.mustafa@uib.no
[1] Center for Translational Oral Research (TOR), Department of Clinical Dentistry, Faculty of Medicine, University of Bergen, Årstadveien 19, 5009 Bergen, Norway
Full list of author information is available at the end of the article

© The Author(s) 2021. **Open Access** This article is licensed under a Creative Commons Attribution 4.0 International License, which permits use, sharing, adaptation, distribution and reproduction in any medium or format, as long as you give appropriate credit to the original author(s) and the source, provide a link to the Creative Commons licence, and indicate if changes were made. The images or other third party material in this article are included in the article's Creative Commons licence, unless indicated otherwise in a credit line to the material. If material is not included in the article's Creative Commons licence and your intended use is not permitted by statutory regulation or exceeds the permitted use, you will need to obtain permission directly from the copyright holder. To view a copy of this licence, visit http://creativecommons.org/licenses/by/4.0/. The Creative Commons Public Domain Dedication waiver (http://creativecommons.org/publicdomain/zero/1.0/) applies to the data made available in this article, unless otherwise stated in a credit line to the data.

BTE strategies usually involve the use of adult mesenchymal stromal cells (MSC), most frequently derived from the bone marrow (BMSC) and expanded as plastic-adherent monolayers [6, 7]. This expansion process can be further enhanced by replacing animal-derived supplements, e.g., fetal bovine serum (FBS), in MSC cultures with humanized or "xeno-free" alternatives such as human platelet lysate (HPL) [8–10]. This step is important not only to enhance the efficacy of MSC expansion but also to facilitate clinical translation of cell therapies according to current regulations [11]. Despite these advances, the two-dimensional (2D) monolayer expansion system is not representative of the in vivo MSC microenvironment and may alter the phenotype and properties of MSC [12, 13]. In contrast, self-assembly or aggregation of MSC into three-dimensional (3D) spheroids simulates more closely their in vivo microenvironment or niche [12, 14]. In the context of bone regeneration, the cytoskeletal changes induced by 3D culture may be particularly beneficial [15, 16]. We have recently reported that 3D spheroid culture of BMSC promotes the expression of several genes and proteins associated with self-renewal and osteogenic differentiation; the latter is independent of osteogenic stimulation [17]. Moreover, several studies have demonstrated benefits of spheroid culture for promoting the differentiation [18–20], paracrine function [21] and regeneration potential of MSC [22–25].

Traditional cell delivery methods involve direct seeding and attachment of MSC on biomaterial scaffolds before in vivo transplantation [26]. However, this method may not be optimal for the delivery of cell spheroids where the 3D structure, essential to maximize their in vivo effects, is lost by direct seeding. To preserve the 3D structure, encapsulation of spheroids in hydrogels represents an effective delivery system for BTE applications [27–29]. Recent reports also suggest that hydrogel properties may modulate the efficacy of MSC spheroids [30]. Since HPL is increasingly being used, and even recommended, for clinical-grade MSC culture [31], extending its application as a hydrogel carrier represents a clinically relevant and cost-effective strategy for BTE. In addition to functioning as cell carriers, HPL hydrogels (HPLG) may offer an additional benefit of sustained cytokine release at regeneration sites [32].

While hydrogel scaffolds may be used in self-contained bone defects, larger, non-contained defects often necessitate the use of rigid biomaterials. These "bone substitute" biomaterials represent the cornerstone of bone regenerative therapies, and various materials have been investigated to date [33]. Among these are synthetic polymers, e.g., poly(L-lactic acid) (PLA), poly(glycolic acid) (PGA), and their *co*polymers, e.g., polylactic-co-glycolic acid (PLGA). A major advantage of synthetic (co)polymers is the possibility to adjust their structure, biomechanical properties and biodegradability to suit the required application(s), in addition to a reduced risk of undesirable immunological reactions (34, 35). Moreover, current advances in 3D printing allow the fabrication of customized (co)polymer scaffolds with highly controlled macro- and micro-architecture for bone regeneration [36]. Although PLA, PGA and PLGA represent some of the most frequently used materials for 3D-printed bone scaffolds, a major disadvantage is the local pH alterations caused by the acidic by-products from their hydrolytic degradation, which may be unfavorable for cell growth and differentiation [35]. Trimethylene carbonate (TMC) is a polymer which degrades via surface erosion; when combined with PLA (PLATMC), it stabilizes the PLA resulting in less hydrolysis and thereby less by-products and local pH alterations [35]. The suitability of PLATMC for producing 3D-printed scaffolds, which support MSC attachment, growth and differentiation, has recently been demonstrated [37].

A combination of MSC with growth factor-rich hydrogels (HPLG) and biomaterial scaffolds (PLATMC), reflecting the classical tissue engineering "triad," may represent a novel and effective strategy for bone regeneration in challenging defects [38, 39]. Therefore, the objectives of the present study were to develop constructs of BMSC encapsulated in HPLG and PLATMC constructs as dissociated (2D) cells or 3D spheroids and to compare their in vivo bone regeneration potential in an orthotopic defect model.

Methods

Cell culture

The use of human cells and tissues was approved by the Regional Committees for Medical Research Ethics (REK) in Norway (2013-1248/REK sør-øst C). Bone marrow aspirates were obtained from three donors (1 female and 2 males; 8–10 years) undergoing corrective surgery at the Department of Plastic Surgery, Haukeland University Hospital, Bergen, Norway. BMSC were isolated and expanded in growth media (GM) comprising of Dulbecco's modified Eagle's medium (DMEM, Invitrogen, Carlsbad, CA, USA) supplemented with 5% (v/v) pooled HPL (Bergenlys, Bergen, Norway), 1% (v/v) penicillin/streptomycin (GE Healthcare, South Logan, UT, USA) and 1 IU/mL heparin (Leo Pharma AS, Lysaker, Norway). The preparation of HPL is described elsewhere [10]. Cells were sub-cultured (4000 cells/cm^2) and expanded in humidified 5% CO_2 at 37 °C; passage 2–4 cells were used in experiments. Monolayer (2D) BMSC were characterized based on immunophenotype, proliferation

and multi-lineage differentiation potential as previously described [10].

To generate 3D spheroids, monolayer BMSC (passage 2) were seeded in microwell-patterned 24-well plates (Kugelmeiers Ltd, Erlenbach, Switzerland) in GM; after 24 h, aggregates of ~1000 cells were formed via guided self-assembly [17]. To induce differentiation of 2D and 3D BMSC, osteogenic induction media (OIM) were prepared by supplementing GM with final concentrations of 0.05 mM L-ascorbic acid 2-phosphate, 10 nM dexamethasone and 10 mM β glycerophosphate (all from Sigma-Aldrich, St. Louis, MO, USA).

Characterization of 2D and 3D BMSC

Monolayer (2D) and spheroid (3D) BMSC were characterized at gene and protein levels. Expressions of genes associated with multipotency and osteogenesis (Additional file 1: Table 1), normalized to that of glyceraldehyde 3-phosphate dehydrogenase (GAPDH), were assessed after 7 days via quantitative real-time polymerase chain reaction (qPCR) using TaqMan PCR assays (Thermo Scientific, Carlsbad, CA, USA). Osteogenic gene expression was assessed in both GM and OIM cultures. RNA extraction and cDNA synthesis were performed as previously described [40]. Mineralization in 2D and 3D BMSC was confirmed via Alizarin red S staining (Sigma-Aldrich) after 21 days of OIM culture.

For protein-level characterization, conditioned media (CM) from 2D (2D-CM) and 3D BMSC (3D-CM) were collected after culturing the cells for 48 h in HPL-free media and characterized via a multiplex cytokine assay as previously described [17]. Briefly, the concentrations of 15 cytokines (Additional file 1: Table 2) were measured using a custom multiplex assay and Bio-Plex R 200 System (both from Bio-Rad Laboratories, CA, USA), according to the manufacturer's instructions. To account for differences in cell proliferation rates between 2 and 3D cultures, cytokine concentrations (pg/mL) were normalized to the corresponding total cellular DNA (ng/mL). DNA quantification was performed using the Quant-IT PicoGreen dsDNA Assay (Invitrogen) according to the manufacturer's instructions. The efficacy of 2D- and 3D-CM was tested in an in vitro wound healing assay of rat BMSC (Additional file 1).

3D printing of PLATMC scaffolds

3D-printed PLATMC scaffolds were produced as described elsewhere [37]. Briefly, a 3D CAD model was designed using the Magics software integrated with a 3D-Bioplotter (both from EnvisionTEC, Gladbeck, Germany). Granules of medical-grade PLATMC (RESOMER® LT-706-S 70:30, Evonik GmBh, Essen, Germany) were loaded into the printer cartridge (pre-heated to 220 °C), and rectangular sheets of three layers with an orientation of 0°–90°–0° were printed at 190 °C with an inner nozzle diameter of 400 μm and strand spacing of 0.7 mm [37]. Disc-shaped scaffolds measuring 5 mm × 1.2 mm were punched out and placed in 48-well plates. Prior to use in experiments, the scaffolds were sterilized by soaking in 70% ethanol for 30 min, followed by washing with phosphate-buffered saline (PBS; Invitrogen) and 2-h exposure to UV light in sterile conditions.

Production of hydrogels and constructs

HPLG were produced by combining previously reported methods for platelet-rich plasma (PRP) and fibrin gel preparation, both of which are commonly used as scaffolds in BTE applications. To prepare the hydrogels, sterile-filtered HPL (same as for cell culture) was supplemented with 20 mg/mL fibrinogen (Sigma-Aldrich) to increase the stiffness and mechanical properties of the hydrogel. Gelation was achieved by adding a "thrombin solution" containing 1 IU/mL human thrombin and 1 TIU/mL aprotinin in 20 mM $CaCl_2$ solution (all from Sigma-Aldrich), followed by incubation at 37 °C for 15 min.

To prepare the PLATMC-HPLG constructs, HPL/fibrinogen and thrombin solutions were mixed and 50 μL were quickly seeded on the PLATMC scaffolds (pre-wetted with HPL), followed by incubation at 37 °C for 15 min. Imaging of constructs was performed using a stereomicroscope (Leica M205C, Heerbrugg, Switzerland) and, after gold/palladium sputter-coating, using a scanning electron microscope (SEM; Phenom XL, Thermo Scientific).

Cell encapsulation in constructs

For cell encapsulation, equal numbers of dissociated (2D) or spheroid (3D) BMSC were uniformly suspended in fibrin-supplemented HPL, mixed with thrombin solution and seeded on scaffolds (1×10^6 cells in 50 μL) as described above. The distribution of 2D and 3D BMSC within PLATMC-HPLG constructs was observed under a light microscope (Nikon Eclipse TS100, Tokyo, Japan). Cell morphology and viability were assessed after 1, 7 and 21 days using the LIVE/DEAD cell viability assay (Invitrogen) and observed under a high-speed Andor Dragonfly 5050 confocal microscope equipped with an iXon 888 Life EMCCD camera (1024 × 1024 resolution, 100–200 × magnification; Oxford Instruments, Abingdon, UK). Z-stacks were acquired from the top of each construct, with steps of 4 μm to a depth of up to 200 μm. Images were processed using the Imaris software (Oxford Instruments).

To assess osteogenic differentiation, PLATMC-HPLG constructs with 2D or 3D BMSC were cultured in GM

and OIM for up to 21 days. Expressions of early, intermediate and late osteogenesis-related genes (Additional file 1: Table 1) were assessed after 7 days via qPCR. In vitro mineralization was assessed via Alizarin red S staining (Sigma-Aldrich) after 14 and 21 days, as previously described [40]. For quantification, the stain was dissolved in 10% cetylpyridinium chloride (Sigma-Aldrich) and absorbance was measured at 540 nm using a microplate reader.

Implantation in rat calvarial defects

Animal experiments were approved by the Norwegian Animal Research Authority (Mattilsynet; FOTS-17443) and performed in accordance with the ARRIVE guidelines [41]. Twelve male athymic nude rats (Rj:ATHYM-Foxn1rnu, Janvier Labs, Le Genest-Saint-Isle, France), 7 weeks old and weighing 300 ± 15.58 g were used. Animals were housed in stable conditions (22 ± 2 °C) with a 12-h dark/light cycle and ad libitum access to food and water. Animals were allowed to acclimatize for one week prior to experiments and were regularly monitored for signs of pain/infection, food intake and activity during the entire experimental period. Pre-operatively, animals were anesthetized with a mixture of sevoflurane (Abbott Laboratories, Berkshire, UK) and O_2 using a custom-made mask. Following anesthesia, a 2-cm sagittal incision was made in the midline of the cranium to reflect the periosteum and expose the parietal bones. In each animal, two full-thickness defects of 5 mm diameter [42] were created on either side using a trephine bur (Meisinger GmbH, Neuss, Germany) attached to a slow-speed handpiece under saline irrigation. Special care was taken to preserve the sagittal suture and underlying dura mater. The following constructs were then randomly implanted in the defects: PLATMC-HPLG containing 2×10^6 2D BMSC ($n = 8$), PLATMC-HPLG containing 2×10^6 3D BMSC ($n = 8$) or cell-free PLATMC-HPLG constructs ($n = 6$); PLATMC scaffolds without HPLG were implanted in two defects ($n = 2$). The critical-size nature of 5 mm defects was previously tested showing no healing within the observation time (data not shown). All constructs were cultured in GM for 36 h prior to implantation. Randomization was performed so that no animal received two constructs from the same group and animals were coded via ear clips. Post-operatively, the skin was sutured (Vicryl, Ethicon, Somerville, NJ, USA) and animals were injected subcutaneously with buprenorphine (Temgesic 0.03 mg/kg, Schering-Plough, UK) for up to 2 days thereafter. After 12 weeks, the animals were euthanized with an overdose of CO_2. The primary outcome was assessment of bone regeneration in the defects via radiography and histology. For all subsequent handling/analyses, the animals were identified by numbers to facilitate blinding of observers to the treatment groups.

In vivo *computed tomography (CT)*

To track in vivo bone regeneration, the calvaria were scanned 4, 6, 8 and 12 weeks after surgery using a small-animal CT scanner (nanoScan, Mediso, Budapest, Hungary) as previously described [43]. At each time point, 0.04 mm resolution scans were obtained and analyzed using PMOD software (PMOD Technologies LLC, Zurich, Switzerland). A standardized volume of interest (VOI)—including the entire thickness of the defect and excluding 0.5 mm of marginal bone, was defined for each defect. A density threshold was applied to exclude the scaffold (determined by scanning blank scaffolds using the same parameters) and classify only mineralized tissues. Percentage defect fills in the VOI, i.e., new bone volume per total defect volume (nBV/TV), were calculated using the PMOD software.

Ex vivo *micro-CT and histology*

Immediately after euthanasia, the calvaria were harvested and fixed in 10% buffered formalin. For micro-CT (μCT) analysis, specimens were scanned using a SCANCO 50 μCT scanner (SCANCO Medical AG, Bruttisellen, Switzerland) at 90 kV and 200 μA with an isotropic resolution of 17.2 μm. Scans were reconstructed by orienting the drill direction along the Z-axis, with the defect in the approximate center of the image, using Amira software (Thermo Scientific). A standardized VOI (as described for in vivo CT) and threshold were applied to all samples. In addition to nBV/TV (as described for the CT), the formation of bone "islands" or isolated areas of new bone not connected to the host bone [isolated bone volume per total defect volume (iBV/TV)], was calculated using ImageJ software [44].

After μCT scanning, the calvaria specimens were processed for undecalcified histology. Specimens were dehydrated in ascending grades of alcohol and embedded in light-curing resin (Technovit 7200 + 1% benzoyl peroxide, Kulzer & Co., Wehrheim, Germany). Blocks were further processed using EXAKT cutting and grinding equipment (EXAKT Apparatebau, Norderstedt, Germany). Standardized thin-ground sections (~ 100 μm) parallel to the sagittal suture and perpendicular to the parietal bone (Additional file 1: Figure 1), were prepared from all specimens and stained with Levi-Laczko dye (Morphisto GmbH, Frankfurt, Germany). In this staining, mature bone appears light pink, woven bone appears dark pink, and soft tissue (including collagen) appears dark blue [45]. Further, the sections were scanned using an Olympus BX61VS digital virtual microscopy system (DotSlide 2.4, Olympus, Tokyo, Japan) with a

20 × objective resulting in a resolution of 0.32 μm per pixel.

For histomorphometric analysis, a standardized region of interest (ROI) was defined within each defect excluding 1 mm of marginal bone. Using Definiens Developer XD2 software (Definiens, Munich, Germany), the different tissue types (bone/soft tissue/scaffold) were semi-automatically classified from digital images and further corrected using Adobe Photoshop software (Adobe, San Jose, CA, USA). The percentage of new bone formation in the ROI was calculated as a ratio of the area of newly formed bone to the total available area (nB.Ar/T.Ar). Blood vessels, identified by endothelial lining and entrapped erythrocytes, were manually counted in the ROI.

Statistical analysis

Statistical analysis was performed using the Prism 9 software (GraphPad Software, San Diego, CA, USA). Data are presented as means (± SD and/or range), unless specified. Analyses of gene expression data are based on delta-CT values, and results are presented as relative (log/nonlinear) fold changes in 3D versus 2D BMSC using scatter plots. Multiplex proteomic data are presented on a logarithmic (log_{10}) scale. All other linear data are presented as bar graphs. Normality testing was performed via the Shapiro–Wilk test. The Student's *t* test, Mann–Whitney U test, one-way analysis of variance (ANOVA; followed by a post hoc Tukey's test) or Kruskal–Wallis test, were applied as appropriate, and $p < 0.05$ was considered statistically significant.

Results

Gene expression and cytokine secretion are altered in spheroid BMSC

Monolayer BMSC showing characteristic morphology, immunophenotype and multi-lineage differentiation potential were expanded in HPL supplemented GM (Additional file 1: Figure 2); passage 2 cells were used to form 3D spheroids as previously described [17] (Fig. 1a). After 7 days, significant upregulations of genes associated with early osteogenic [bone morphogenetic protein 2 (BMP2), 13.20-fold, $p = 0.0001$] and adipogenic differentiation [peroxisome proliferator-activated receptor gamma (PPARG), 2.63-fold, $p = 0.0028$] were observed in 3D versus 2D BMSC; upregulation of chondrogenic differentiation gene SRY-box transcription factor 9 (SOX9) was not statistically significant (1.45-fold, $p > 0.05$) (Fig. 1b). Genes for extracellular matrix (ECM) components associated with late-stage osteogenic differentiation, i.e., bone sialoprotein (BSP; 20.45-fold, $p < 0.0001$), osteocalcin (OCN/BGLAP; 150.83-fold, $p < 0.0001$) and osteopontin (OPN/SPP1; 143.73-fold, $p < 0.0001$), were also upregulated in 3D versus 2D BMSC, regardless of osteogenic induction (Fig. 1c). In vitro mineralization was confirmed after 21 days of induction in both 2D and 3D BMSC (Fig. 1e).

The concentrations of various growth factors and chemokines were measured in 2D- and 3D-CM. Several growth factors were elevated in 3D- versus 2D-CM: fibroblast growth factor (FGF2; $p < 0.05$), hepatocyte growth factor (HGF; $p > 0.05$), granulocyte colony-stimulating factor (GCSF; $p < 0.05$), platelet-derived growth factor (PDGF-BB; $p > 0.05$) and transforming growth factor beta (TGF-β2; $p < 0.05$). Chemokine ligands 1 (CXCL1/GROα; $p < 0.05$), 10 (CXCL10; $p < 0.05$) and 5 (CCL5; $p < 0.05$) were also elevated in 3D-CM. Stem cell factor (SCF; $p > 0.05$), vascular endothelial growth factor (VEGF; $p < 0.05$) and stem cell growth factor beta (SCGF-β; $p < 0.05$) were greater in 2D-CM (Fig. 1d). Comparable in vitro wound closure was observed in rat BMSC exposed to 2D- or 3D-CM for 24–48 h ($p < 0.05$; Additional file 1: Figure 3).

PLATMC-HPLG constructs maintain the activity of 2D and 3D BMSC in vitro

PLATMC scaffolds were 3D-printed with a pore size of 350–400 μm and total porosity of 53.96% ± 2.91% as determined by μCT. Modified HPLG were prepared by addition of fibrinogen and thrombin. When combined with HPLG, the scaffold filaments and pores were completely covered, indicating the potential for high "cell-seeding efficacy" (Fig. 2a, b).

Constructs containing equal numbers of 2D or 3D BMSC were produced; uniform distribution of cells/spheroids was confirmed soon after encapsulation (Fig. 3a). After 24 h, both single and spheroid BMSC appeared rounded and suspended mainly within the gels and not directly attaching to the scaffold surface (Fig. 3b). After 7 days, proliferation and spreading of cells within the hydrogels was observed, with a tendency for more dead cells in 2D versus 3D BMSC constructs. In the case of 3D BMSC, the spheroid structure appeared to still be maintained, although several cells appeared to migrate from the spheroids into the gel. After 21 days, the hydrogel was substantially degraded and 2D BMSC appeared to attach and spread on the surface of the PLATMC filaments. In 3D BMSC, the spheroid structure was still preserved after 21 days, and, in contrast to 2D BMSC, the cells appeared to spread both on the PLATMC filaments and in the spaces in between (Fig. 3b).

Gene expression analysis of encapsulated 2D and 3D BMSC revealed no significant changes in early [runt-related transcription factor 2 (RUNX2)], intermediate [alkaline phosphatase (ALP), collagen type 1 (COL1)] or late (OCN) osteogenic differentiation markers after

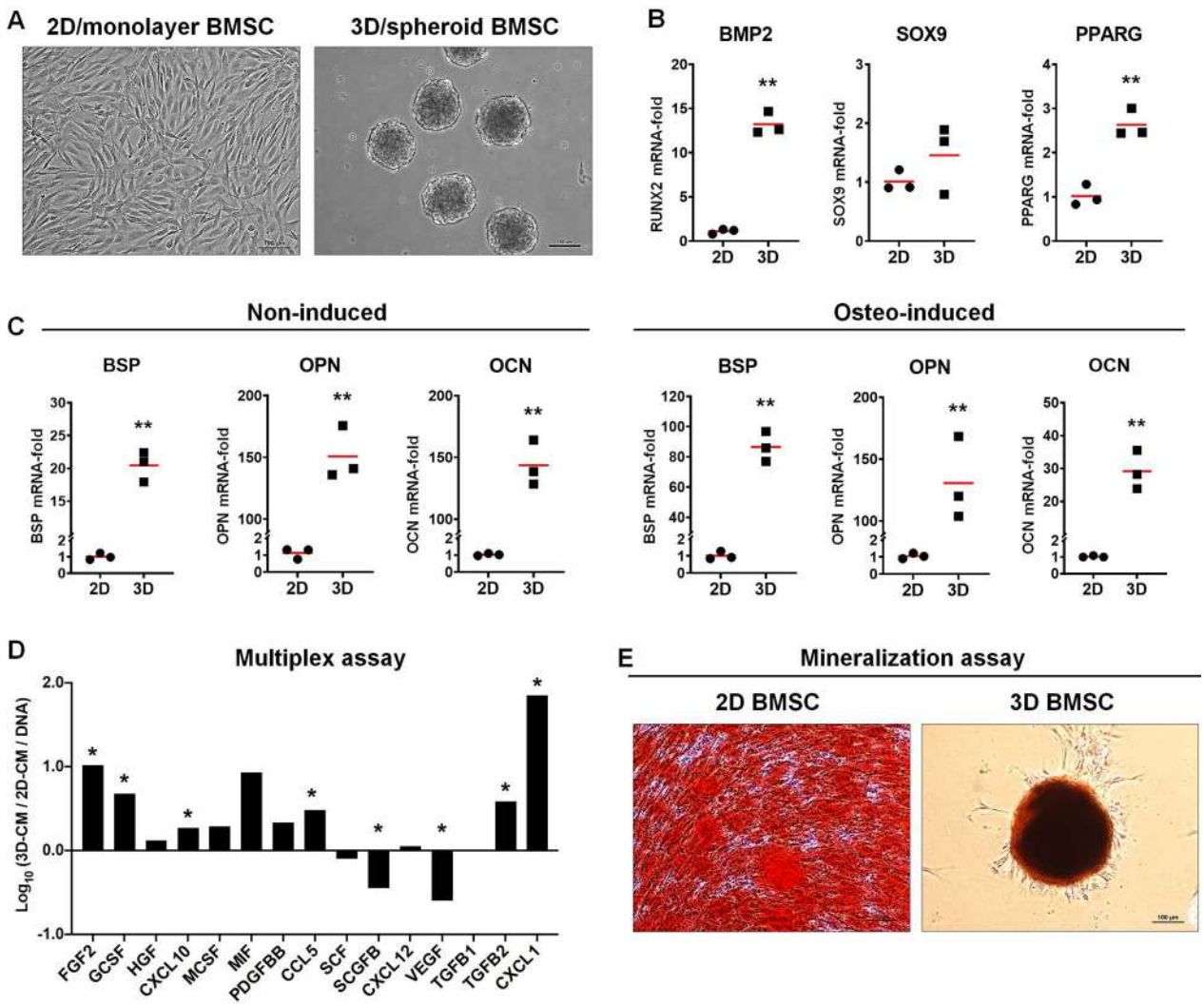

Fig. 1 Characterization of 2D and 3D BMSC. **a** Representative images of 2D and 3D BMSC, scale bars 100 µm. Expression (fold changes) of multipotency-related genes (**b**) and osteogenesis-related genes (**c**) in 3D BMSC relative to 2D BMSC after 7 days; the latter were assessed in growth (non-induced) or induction media (osteo-induced). Data represent means of 3 experimental replicates; statistical analyses are based on delta-Ct values; *$p < 0.05$; **$p < 0.001$. **d** Protein (cytokine) concentrations (pg/mL) in the conditioned media (CM) of 2D and 3D BMSC normalized to corresponding DNA contents (ng/mL); data are presented as the logarithm (log10) of the ratio of means of each cytokine in 3D-CM/2D-CM; *$p < 0.05$. **e** Mineralization in 2D and 3D BMSC detected via Alizarin red staining, scale bars 100 µm. BMP2, bone morphogenetic protein 2; SOX9, sex determining region Y-box 9; PPARG, peroxisome proliferator-activated receptor gamma; BSP, bone sialoprotein; OPN/SPP1, osteopontin; OCN/BGLAP osteocalcin. Multiplex assay (see Additional file 1: Table 2)

7 days, regardless of induction (Fig. 4a); a trend for upregulation of RUNX2 (1.43-fold) and OCN (1.47-fold) was observed in induced 3D versus 2D BMSC ($p > 0.05$). Alizarin red staining revealed comparable in vitro mineralization in 2D versus 3D BMSC constructs after 14 days in OIM. After 21 days, a trend for greater mineralization was observed in 3D versus 2D BMSC constructs in OIM ($p > 0.05$; Fig. 4b, c). Evidence of mineralization was also observed in non-induced constructs of 2D and 3D BMSC, although significantly lower than in the corresponding induced constructs ($p < 0.05$).

Comparable bone regeneration in PLATMC-HPLG constructs with 2D or 3D BMSC in vivo

All experimental animals recovered from surgery and no adverse events were observed. In vivo CT scanning revealed bone regeneration of varying degrees in all defects after 4 weeks, increasing progressively up to 12 weeks, in all groups, i.e., PLATMC-HPLG constructs

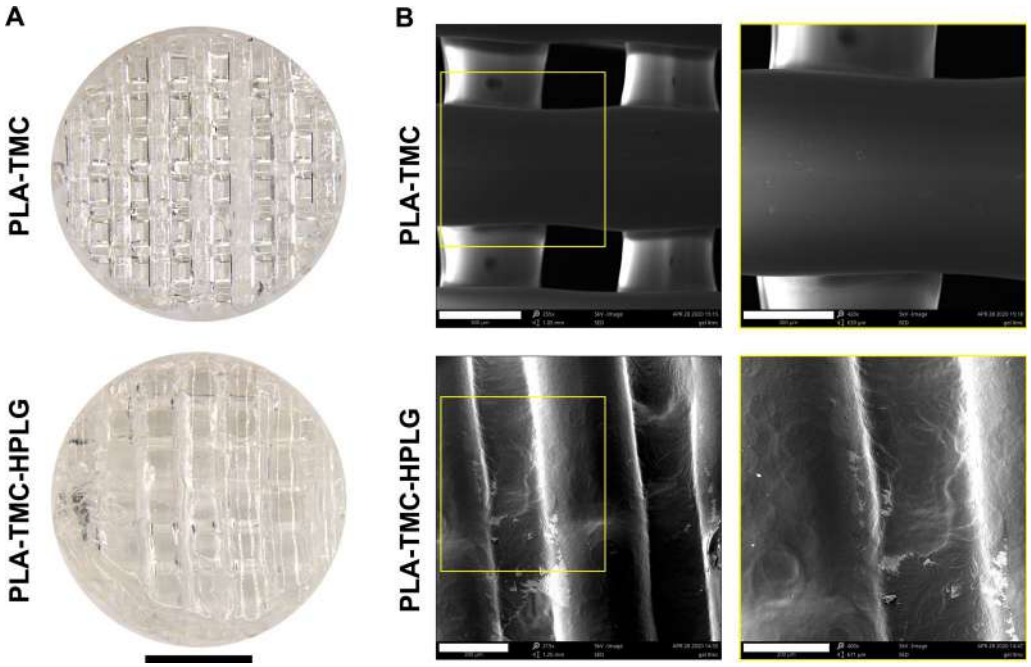

Fig. 2 Scaffold-hydrogel constructs. **a** Stereomicroscopic images of PLATMC scaffolds before (top) and after encapsulation in HPLG (bottom), scale bar 2 mm. **b** Corresponding SEM images of PLATMC and PLATMC-HPLG constructs in low (left; scale bars 300 µm) and high magnification (right; scale bars 200 µm)

with 2D BMSC, 3D BMSC or no cells (Fig. 5a). In constructs with 2D BMSC and 3D BMSC, the increase in bone formation from 4 to 12 weeks was statistically significant ($p < 0.05$; Fig. 5b). Bone formation typically started from the defect margins and progressed towards the center, closely following the structure of the scaffolds, i.e., in the pores and along the printed filaments. Islands of new bone, not connected to the host bone, were also observed. Although a trend for greater bone formation was observed in constructs with 2D BMSC, no significant differences were observed between the groups at 4 ($p = 0.437$), 8 ($p = 0.355$) or 12 weeks ($p = 0.383$).

The in vivo CT findings were confirmed by ex vivo µCT after 12 weeks (Fig. 6a). Central slices revealed bone formation throughout the entire thickness of the defects with complete bridging, i.e., transverse defect closure, in 75%, 62.5% and 33.3% of constructs with 2D BMSC, 3D BMSC and no cells, respectively. Mean nBV/TV was 62.47% (SD 19.46%), 51.01% (SD 24.43%) and 43.20% (SD 30.09%) in constructs with 2D BMSC, 3D BMSC and no cells, respectively ($p > 0.05$). Mean iBV/TV was generally low but greater in constructs with 3D BMSC (0.29%, range 0.03–0.96) versus 2D BMSC (0.08%, range 0–0.44; $p > 0.05$) and no cells (0.03%, range 0–0.07; $p < 0.05$) (Fig. 6b).

Morphology of the regenerated bone was evaluated via undecalcified histology of standardized sagittal sections in the centre of each defect. New bone mainly originated from the endocranial margins of the host calvarial bone and consisted predominantly of plexiform bone which is a combination of woven bone in the center and parallel-fibered bone on the superficial layers of bone trabeculae. This type of bone is formed during the initial stages of the healing of bone defects, and the process of primary bone formation was already completed at 12 weeks. No active osteoblasts or osteoblast seams were detectable on the trabecular surfaces (Fig. 7a). Blood vessels were strongly associated with areas of bone regeneration. The process of resorption of plexiform bone and replacement with lamellar bone, i.e., remodeling, could be observed via bone surfaces displaying resorption lacunae (Fig. 5b). No remarkable cellular inflammatory response was observed. A thin layer of fibrous tissue was always seen surrounding the scaffold and bone formation never seemed to occur directly on the scaffold surface (Fig. 7b). No visible signs of scaffold degradation were observed in any of the groups; scaffolds occupied ~ 50% of the defect area. Histomorphometry revealed a similar trend as the µCT analysis, with mean nB.Ar./T.Ar. of 28.09% (SD: 18.9%), 24.37% (SD: 18.49%) and 15.34% (SD: 19.51%) in constructs with 2D BMSC, 3D BMSC and no cells, respectively ($p > 0.05$, Fig. 7c). A similar degree of new vessel formation was observed in all groups ($p > 0.05$, Fig. 7c).

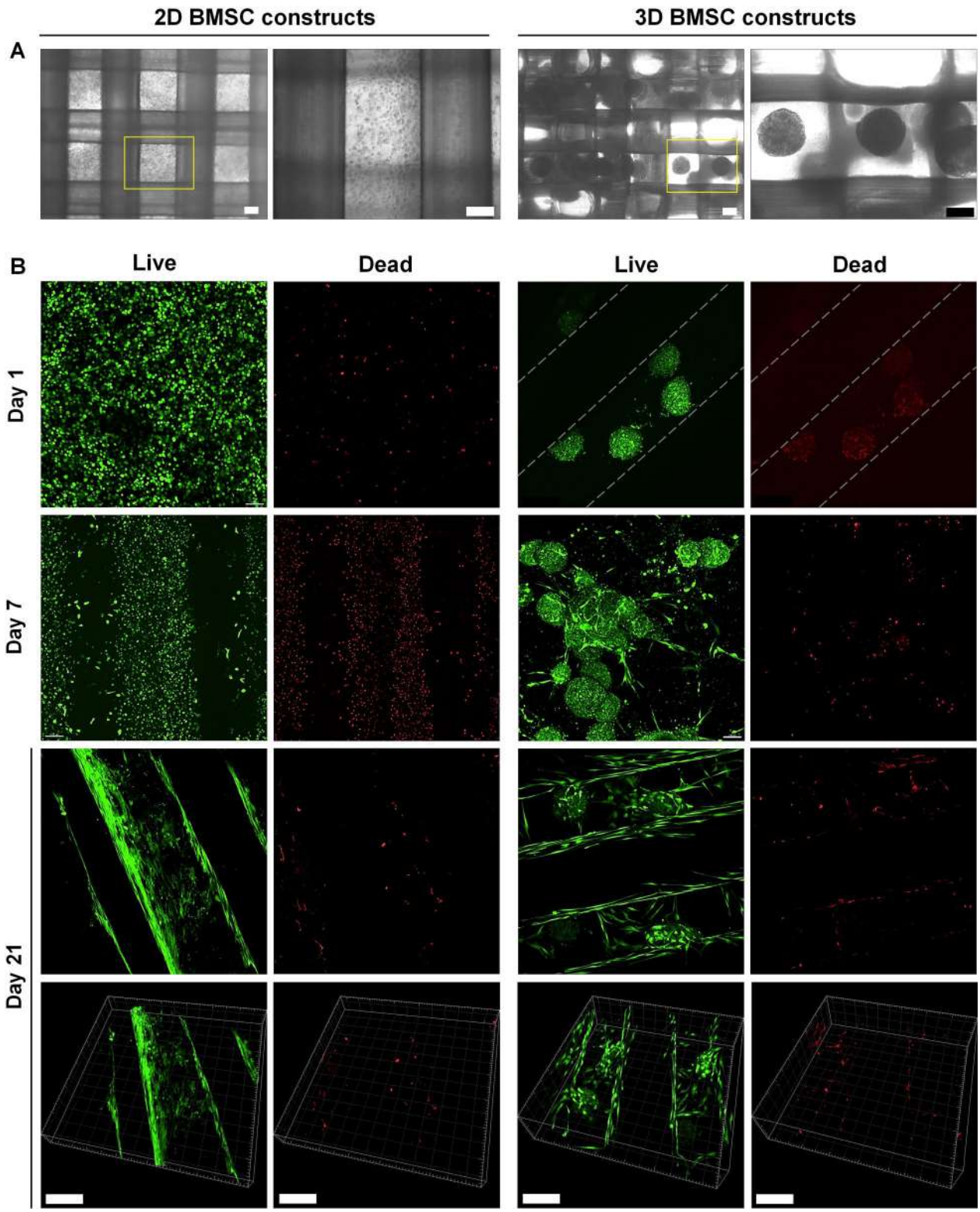

Fig. 3 Cell seeding in scaffold-hydrogel constructs. **a** Distribution of 2D and 3D BMSC in constructs after seeding, scale bars 100 μm. **c** Representative confocal images showing cell viability based on the live (green) and dead (red) assay after 1, 7 and 21 days; corresponding 3D z-stack views of constructs at 21 days showing cell spreading on and/or in between the scaffold filaments; dotted lines indicate outlines of the printed filaments; scale bars 200 μm

Discussion

BTE is a promising strategy to treat advanced critical-size bone defects. In the present study, we compared the efficacy of PLATMC-HPLG constructs loaded with either dissociated (2D) BMSC, spheroid (3D) BMSC or no cells (cell-free controls) for bone regeneration in rat-calvarial defects. The main findings herein were (a) robust and comparable bone formation in constructs containing 2D or 3D BMSC and (b) favorable but non-significantly lower bone formation in cell-free PLATMC-HPLG constructs.

The efficacy of BMSC in BTE applications may be enhanced via xeno-free and spheroid culture. We recently reported the characterization of xeno-free spheroid cultures of BMSC in HPL [17]. Advantages of spheroid culture for multipotency, via upregulation of key regulator genes (BMP2, PPARG and SOX9), were confirmed herein. Consistent with previous results [17], upregulation of osteogenesis-related genes (BSP, OPN, OCN) was observed in 3D versus 2D BMSC herein, even in the absence of osteogenic supplements. Moreover, the secretion of several growth factors (FGF2, PDGF-BB, HGF, TGF-β2) and chemokines involved in tissue regeneration was also enhanced in 3D versus 2D BMSC. Thus, the two major mechanisms of MSC action, i.e., differentiation and paracrine function, appeared to be enhanced in 3D spheroids. Additionally, others have reported benefits of spheroid culture for MSC immunomodulatory functions in the context of tissue regeneration [21, 46, 47].

Although accumulating evidence suggests clear benefits of spheroid culture to enhance MSC efficacy, the optimal mode of spheroid delivery to regeneration sites has not been adequately investigated. Conventional strategies for in vivo delivery involve seeding of cells directly on scaffolds to allow attachment and spreading in vitro for a defined period prior to implantation. However, this method may not be optimal for delivering spheroids as it facilitates dissociation and migration of cells from the spheres during in vitro culture, thus compromising the benefits of cell aggregation. Interestingly, in one study, superior bone formation in rat-calvaria defects was observed when BMSC spheroids were transplanted as "suspensions" rather than when seeded on beta-tricalcium phosphate (β-TCP) granules [22]. In contrast to direct seeding, encapsulation of spheroids in hydrogel scaffolds maintains their 3D assembly at the time of in vivo implantation. Recent studies have reported superior in vitro function and in vivo bone formation when using BMSC spheroids versus dissociated cells encapsulated in alginate hydrogels [29, 48, 49]. Since HPL was used as a xeno-free supplement for BMSC culture, its application was extended as a hydrogel carrier, via modification of previous methods [32]. Further, HPLG were supplemented with fibrin to improve their mechanical properties and prolong degradation, without compromising MSC function [28, 50–52].

In addition to HPLG, copolymer scaffolds were used to deliver the cells in vivo. Complex bone defects often necessitate the use of rigid biomaterial scaffolds, and in such cases hydrogels alone may be insufficient. 3D printing technology offers promising solutions for producing customized scaffolds to treat such defects. Although several designs and materials for 3D-printed scaffolds have been studied, their in vivo applications as carriers for human MSC have been limited [36]. PLATMC is reported to be a promising copolymer for various tissue engineering applications, particularly due to its mechanical properties and biocompatibility [37]; to our knowledge, no studies have yet tested its feasibility for BTE. Therefore, in the present study, human BMSC encapsulated in HPLG were combined with 3D-printed PLATMC scaffolds to represent the classical tissue engineering "triad" [53].

In a previous study we reported spontaneous upregulation of several osteogenesis-related genes in 3D versus 2D BMSC, regardless of osteogenic induction [13]. However, in the present study, no significant upregulation of RUNX2, ALP, COL1 or OCN was observed in 3D versus 2D BMSC following encapsulation in HPLG, regardless of osteogenic induction. This suggested that encapsulation in HPLG attenuated differences in gene expression between 2 and 3D BMSC. Nevertheless, a trend for superior in vitro mineralization was observed in encapsulated 3D versus 2D BMSC after 21 days of osteogenic induction. Considerable mineralization was also observed in non-induced constructs of 3D and 2D BMSC, suggesting a promotive effect of the HPLG on the osteogenic differentiation. Taken together, these findings suggest that the HPLG may have itself initiated the osteogenic differentiation of 2D and 3D BMSC (regardless of media

(See figure on next page.)

Fig. 4 In vitro osteogenic differentiation. **a** mRNA fold changes of osteogenesis-related genes in 3D-relative to 2D-BMSC constructs after non-induced or osteogenic (osteo-induced) culture for 7 days. Data represent means ($n = 3$); no significant differences in 3D versus 2D BMSC for any of the genes. **b** Representative macroscopic and corresponding microscopic images of in vitro mineralization (Alizarin red S) in 2D and 3D BMSC constructs after non-induced or osteo-induced culture for 21 days, scale bars 100 µm. **c** Quantification of Alizarin red staining via absorbance measurements in non-induced and induced 2D and 3D BMSC constructs; data represent means and SD ($n = 3$ or 4) of absorbance values relative to the non-induced 2D BMSC group. RUNX2 runt-related transcription factor 2; ALPL alkaline phosphatase, COL1A2, collagen type 1-alpha 2; OCN/BGLAP, osteocalcin

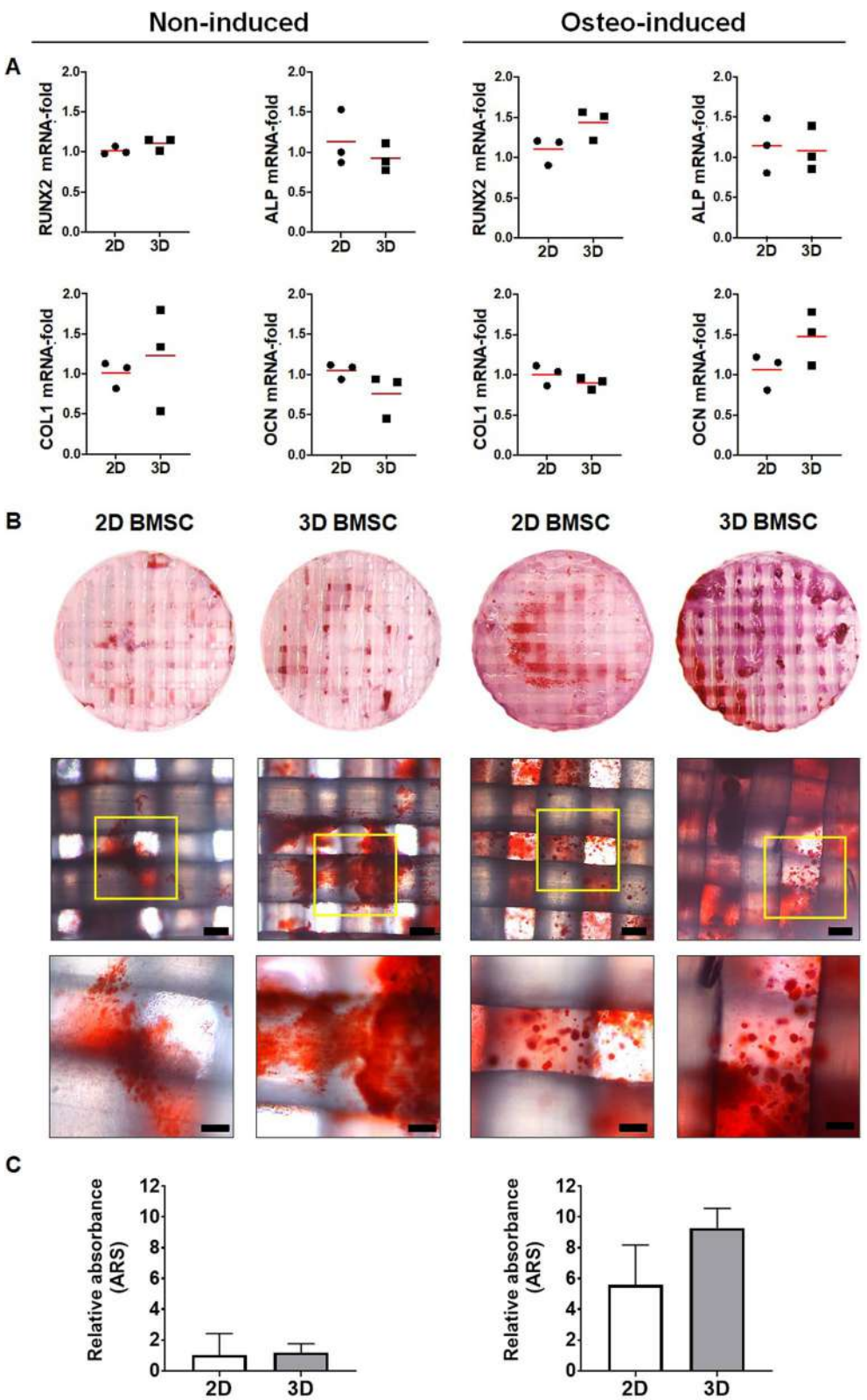

Fig. 4 (See legend on previous page.)

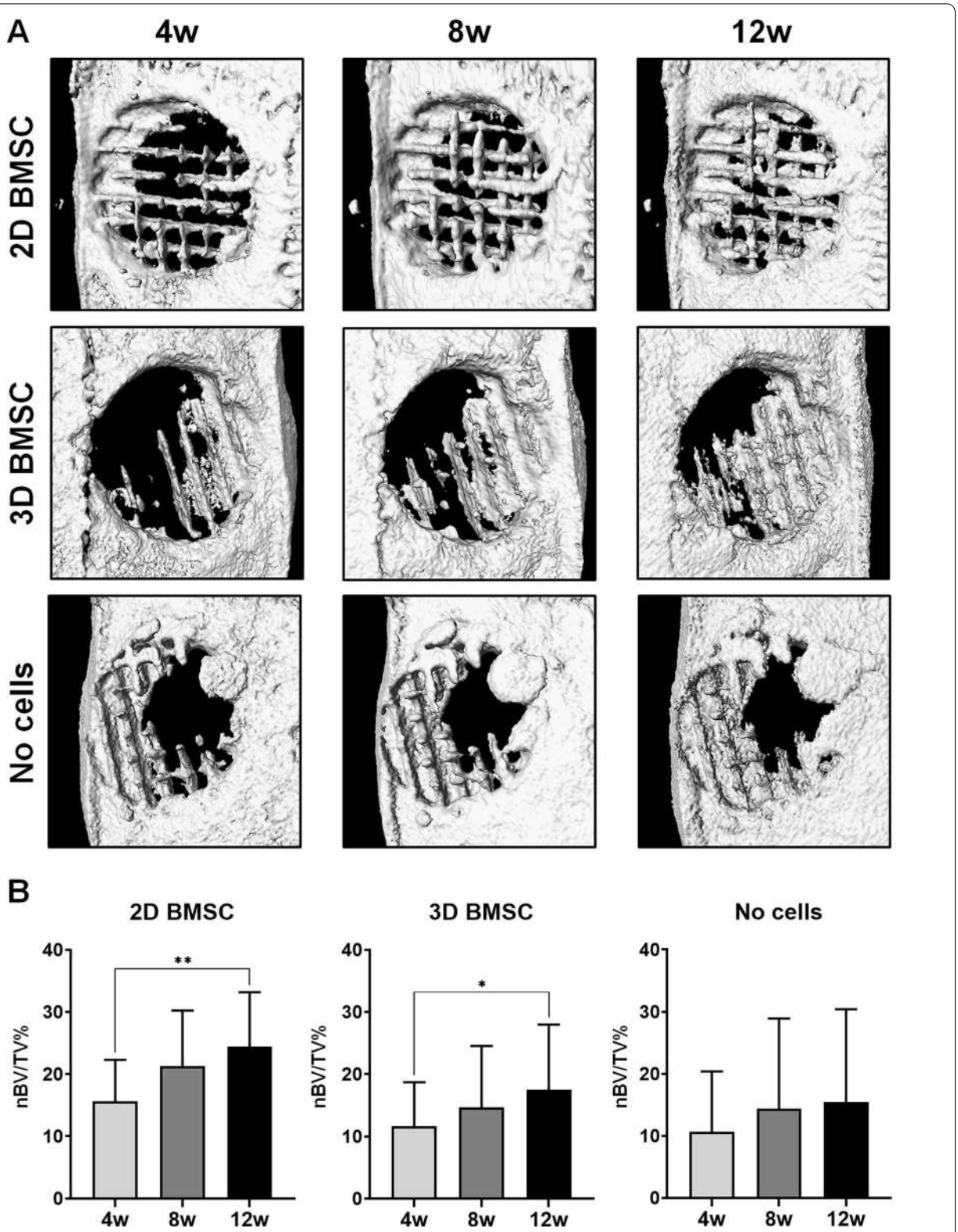

Fig. 5 In vivo CT scanning. Representative reconstructed CT scans showing progression and distribution of bone regeneration (**a**) and corresponding quantification (**b**) in constructs with 2D BMSC, 3D BMSC and no cells from 4 to 12 weeks (w); data represent means ± SD; $^{**}p < 0.01$; $^{*}p < 0.05$

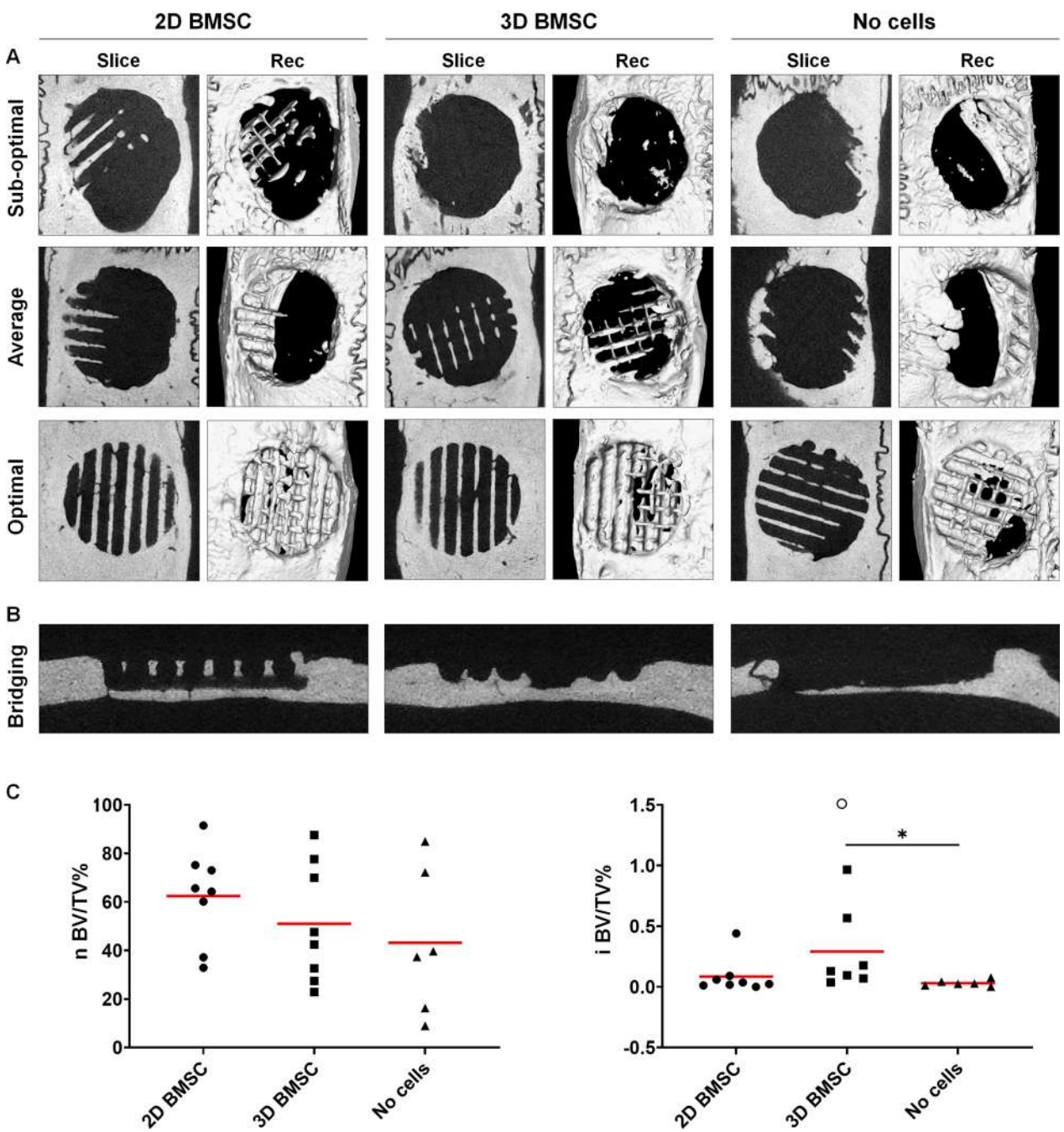

Fig. 6 Micro-CT analysis. **a** Representative slice and 3D reconstructed (Rec) images of sub-optimal, average and optimal bone regeneration (based on quantitative analysis) in constructs with 2D BMSC, 3D BMSC and no cells after 12 weeks. **b** Representative images of defect bridging. **c** Quantification of total bone (nBV/TV%) and island bone regeneration (iBV/TV%); o indicates an outlier value (iBV/TV 1.70%); data represent means, *$\mathbf{p} < 0.05$

supplements), thereby attenuating differences in gene expression, but promoting mineralization. Indeed, when used as a culture supplement, HPL promotes the osteogenic differentiation of MSC in vitro [54–56]. Moreover, several studies have reported positive effects of platelet-derived growth factors, e.g., PRP, on MSC osteogenic differentiation both in vitro and in vivo [23, 57–60]. Since HPL is being increasingly used for clinical-grade MSC expansion and may be easily and inexpensively produced using outdated platelet concentrates from blood

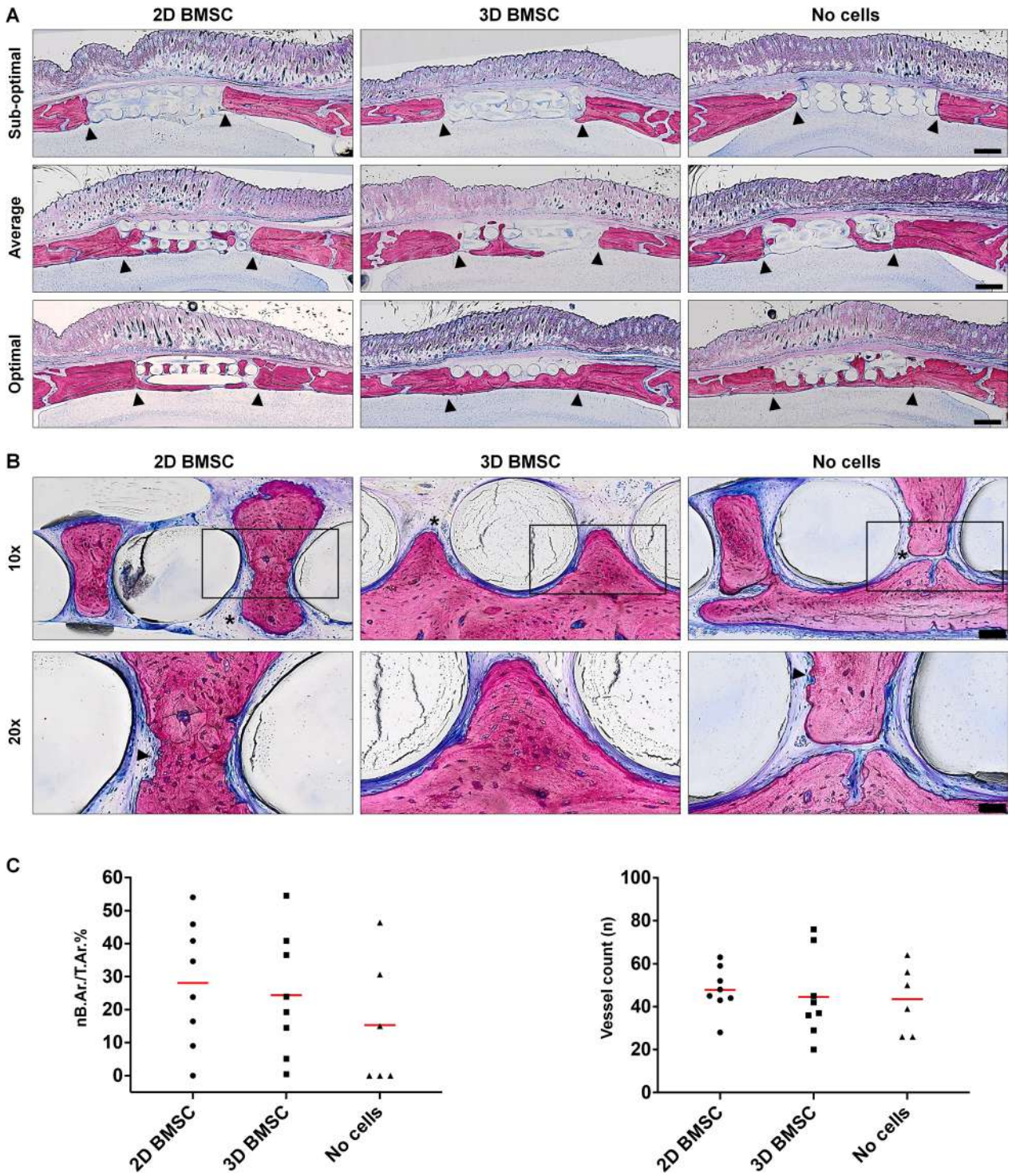

Fig. 7 Histological analysis. **a** Representative low-magnification images from central sections of defects receiving constructs of 2D BMSC, 3D BMSC or no cells after 12 weeks, scale bars 1 mm; black arrows indicate original defect margins. Scalp and brain tissues are intact; mature bone appears light pink, woven bone dark pink and collagen dark blue. **b** Corresponding high-magnification images of newly formed bone, scale bars 100 µm (top panel) and 50 µm (bottom panel); black arrows indicate resorption lacunae suggestive of active remodeling. **c** Quantification of new bone formation (nB.Ar./T.Ar.%) and vessel counts (n = number/defect); data represent means

establishments [10], HPLG represents a promising and cost-effective tool for BTE.

To test their potential for bone regeneration, PLATMC-HPLG constructs with 2D BMSC or 3D BMSC were implanted into rat-calvarial defects. In both groups, substantial bone regeneration could already be detected in the earliest in vivo CT scans after 4 weeks. After 12 weeks, robust bone regeneration was observed in both groups with maximum nBV/TV values of 91.5% and 87.56% and complete bridging in 6/8 and 5/8 defects in 2D and 3D BMSC constructs, respectively. Indeed, μCT analysis revealed a higher incidence of de novo bone island formation (iBV/TV) in 3D BMSC constructs, which could be attributed to in situ mineralization of the implanted spheroids with subsequent remodeling by host cells. However, since the formation of similar bone islands has also been reported in calvarial defects treated with only growth factors [44], i.e., without exogenous cells or scaffolds, the cellular origin of the bone islands remains elusive. In context, previous studies have reported enhanced regeneration in experimental bone defects treated with 3D versus 2D BMSC from allogeneic (rat) [25] or human sources [22, 29]. Similar outcomes were reported also in the context of periodontal ligament-derived cells (PDLC) in mouse calvarial defects [24]. Conversely, a recent study reported no differences in the healing of mouse femoral defects treated with either 2D or 3D human BMSC encapsulated in fibrin gels [61]. Consistent with this finding, no significant differences in the overall quantity or quality of regenerated bone were observed between 2 and 3D BMSC constructs in the present study. Notably, in the previous studies [22, 25, 29, 61], BMSC were cultured in OIM prior to implantation. Indeed, our in vitro data indicated superior mineralization in induced versus non-induced 2D and 3D BMSC constructs, despite some mineralization also being observed in non-induced constructs ("induction" in this context refers to the use of chemical stimulants such as dexamethasone, L-ascorbic acid and β-glycerophosphate, and not recombinant growth factors, such as BMP2). Nevertheless, for the in vivo experiments herein, non-induced constructs were used based on trends in recent clinical studies of BTE, and a preference for "minimal manipulation" of cells by regulatory authorities [1].

Although immunocompromised rodents are commonly reported animal models for testing human MSC [62], the precise mechanism(s) of bone formation in these animals, and the interactions between transplanted (human) and native (recipient) cells, have not been fully elucidated. In the present study, the histological technique (undecalcified) and lack of human-specific antibodies with low host-tissue cross-reactivity, precluded determination of the origin of newly formed bone tissues, i.e., whether these were formed by engraftment and differentiation of the transplanted human BMSC or via recruitment of host (rat) cells. Nevertheless, previous studies have reported that, depending on the immune status of experimental animals, transplanted BMSC may not differentiate into osteoblasts, but rather promote bone formation via paracrine stimulation of host cells [63–66]. In context, although significant differences were observed herein between the CM, i.e., paracrine effectors, of 2D and 3D BMSC, there were no differences in their ability to promote in vitro wound healing in rat BMSC (Additional file 1: Figure 3). Moreover, differences in cytokine secretions of 2D and 3D BMSC were not assessed following encapsulation in the constructs, which, like the differences in gene expression, may have been attenuated following encapsulation. Therefore, it may be speculated whether differences in paracrine functions between 2 and 3D BMSC (or a lack thereof), in addition to cross-species-related factors, contributed to the observed in vivo outcomes.

Comparatively lower, but favorable, regeneration was observed in cell-free (versus cell-loaded) PLATMC-HPLG constructs herein, with up to 84.9% nBV/TV (maximum) and bridging in 2/6 defects. This suggested (a) a possible stimulatory effect from HPLG on in vivo bone formation and (b) further supported the reports that osteogenesis mainly occurs via tissue-resident progenitor cells, and not via differentiation of the transplanted BMSC [63]. Indeed, HPL is known to contain a wide array of physiological growth factors which promote MSC differentiation in vitro [10]. In context, one study reported superior bone regeneration in calvarial defects when using 3D-printed PCL scaffolds coated with "freeze-dried PRP" versus uncoated scaffolds; optimal bone regeneration was observed when using PRP activated via freezing/thawing (similar to HPL) versus thrombin/calcium activation [67]. Indeed, the PLATMC scaffolds alone showed substantially lower bone regeneration herein, i.e., 9% and 15% defect fill, in two animals. Notably, no differences in bone regeneration were observed between PLATMC scaffolds with and without HPLG in these two animals (Additional file 1: Figure 4). Nevertheless, we cannot rule out a possible stimulatory effect of the hydrogel on bone regeneration in our experiments. Such a potentially confounding effect, together with a lack of osteogenic pre-induction of cells, and the presence of local physiological stimuli in the defect sites, may have masked differences between 2 and 3D BMSC in this orthotopic model.

In context of the in vivo outcomes herein, it must be acknowledged that the scaffold itself, although excluded from the μCT analysis, occupied a considerable volume of the defects and did not show any signs of degradation

or replacement during the experimental period. PLATMC is reported to be a promising copolymer for various tissue engineering applications mainly due to its biocompatibility [35], although little is known regarding its in vivo degradation profile. Optimal properties of scaffolds for bone regeneration have been defined, such as an average pore size of 300–400 μm (with ≥ 50% total porosity) [68], and a degradation profile corresponding to the physiological rate of bone formation [69]. Although the recommendations for physical properties, i.e., pore size of ~ 400 μm and total porosity > 50%, were incorporated into the design of the scaffolds herein, no prior assessment of their degradation profile was performed. Our in vivo observations revealed that bone formation occurred around—but not in direct contact with, the printed filaments, i.e., the scaffolds were incorporated within but not replaced by the regenerated bone. However, no specific in vitro or in vivo assessment of scaffold degradation was performed herein. Moreover, no mechanical testing of the regenerated tissues was performed. Thus, longer-term outcomes such as in vivo degradation of PLATMC and the mechanical and biological function of these scaffold-bone "composite tissues," require further investigation.

Conclusions

Encapsulation of spheroid (3D) and dissociated (2D) BMSC in PLATMC-HPLG constructs attenuated the differences in osteogenic gene expression observed in standard 3D spheroid versus 2D monolayer cultures. Despite a non-significant trend for superior in vitro mineralization in constructs of 3D BMSC versus 2D BMSC, in vivo implantation revealed comparable bone regeneration between the groups in rat-calvarial defects. Interestingly, favorable but non-significantly lower bone regeneration was also observed in cell-free PLATMC-HPLG constructs. In summary, regardless of spheroid or monolayer cell culture, PLATMC-HPLG constructs represent promising scaffolds for BTE applications.

Abbreviations

BTE: Bone tissue engineering; MSC: Mesenchymal stromal cells; BMSC: Bone marrow MSC; 2D: Two-dimensional; 3D: Three-dimensional; MCC: Mesenchymal cell condensations; HPL: Human platelet lysate; PLA: Poly-L-lactic acid; PGA: Polyglycolic acid; PCL: Polycaprolactone; PLGA: Poly-lactic-co-glycolic acid; TMC: Trimethylene carbonate; PLATMC: Poly-L-lactide-co-trimethylene carbonate; HPLG: HPL hydrogels; GM: Growth media; OIM: Osteogenic induction media; qPCR: Polymerase chain reaction; CM: Conditioned media; PBS: Phosphate-buffered saline; PRP: Platelet-rich plasma; CT: Computed tomography; VOI: Volume of interest; nBV/TV: New bone volume per total defect volume; μCT: Micro-CT; iBV/TV: Isolated bone volume per total defect volume; nB.Ar/T.Ar: Area of newly formed bone to the total available area; ANOVA: One-way analysis of variance; BMP2: Bone morphogenetic protein 2; PPARG: Peroxisome proliferator-activated receptor gamma; SOX9: SRY-box transcription factor 9; OCN/BGLAP: Osteocalcin; OPN/SPP1: Osteopontin; FGF2: Fibroblast growth factor; HGF: Hepatocyte growth factor; GCSF: Granulocyte colony-stimulating factor; TGF-β2: Transforming growth factor beta; CXCL1/GROα: Chemokine ligand 1; CXCL10: Chemokine ligand 10; CCL5: Chemokine ligand 5; SCF: Stem cell factor; VEGF: Vascular endothelial growth factor; SCGF-β: Stem cell growth factor beta; RUNX2: Runt-related transcription factor 2; ALP: Alkaline phosphatase; COL1: Collagen type 1; β-TCP: Beta-tri-calcium phosphate; PDLC: Periodontal ligament-derived cells.

Supplementary Information

The online version contains supplementary material available at https://doi.org/10.1186/s13287-021-02642-w.

Additional file 1. Supplementary methods.

Acknowledgements

We thank the Bloodbank at Haukeland University Hospital for assistance with HPL production, the Molecular Imaging Center (MIC), University of Bergen, for assistance with microscopy, and Heidi Espedal from the Dept. of Clinical Medicine, University of Bergen, for assistance with the in vivo CT scanning.

Authors' contributions

SSh and KM conceived and designed the study. SSh performed the experiments, data collection, data analysis and drafted the manuscript. SSu, SMA, CK, MNH, PH, TD and ST assisted with samples preparation, data collection, data analysis/interpretation and/or drafting the manuscript. AIB and KM assisted with data analysis/interpretation and drafting the manuscript. All authors read and approved the final manuscript.

Funding

This work was supported by Helse Vest Strategic Research Funding, Norway (502027), Research Council of Norway (BEHANDLING/273551), Trond Mohn Foundation, Norway (BFS2018TMT10), and the Osteology Foundation, Switzerland (18-152).

Availability of data and materials

Additional data are included in Additional file 1 and can be made available by the authors upon request.

Declarations

Ethical approval and consent to participate

The use of human cells and tissues was approved by the Regional Committees for Medical Research Ethics (REK) in Norway (2013-1248/REK sør-øst C). Animal experiments were approved by the Norwegian Animal Research Authority (Mattilsynet; FOTS-17443) and performed in accordance with the ARRIVE guidelines.

Consent for publication

Not applicable.

Competing interests

The authors confirm that there are no known conflicts of interest associated with this publication and there has been no significant financial support for this work that could have influenced its outcome.

Author details

[1]Center for Translational Oral Research (TOR), Department of Clinical Dentistry, Faculty of Medicine, University of Bergen, Årstadveien 19, 5009 Bergen, Norway. [2]Department of Immunology and Transfusion Medicine, Haukeland University Hospital, Bergen, Norway. [3]Core Facility Hard Tissue and Biomaterial Research/Karl Donath Laboratory, University Clinic of Dentistry, Medical University of Vienna, Vienna, Austria. [4]Ludwig Boltzmann Institute for Traumatology, The research center in cooperation with AUVA, Vienna, Austria. [5]Austrian Cluster for Tissue Regeneration, Vienna, Austria.

Received: 16 August 2021 Accepted: 22 October 2021
Published online: 14 November 2021

References

1. Shanbhag S, Suliman S, Pandis N, Stavropoulos A, Sanz M, Mustafa K. Cell therapy for orofacial bone regeneration: a systematic review and meta-analysis. J Clin Periodontol. 2019;46(Suppl 21):162–82.
2. Oppenheimer AJ, Mesa J, Buchman SR. Current and emerging basic science concepts in bone biology: implications in craniofacial surgery. J Craniofac Surg. 2012;23:30.
3. Shanbhag S, Pandis N, Mustafa K, Nyengaard JR, Stavropoulos A. Alveolar bone tissue engineering in critical-size defects of experimental animal models: a systematic review and meta-analysis. J Tissue Eng Regen Med. 2016;11:2935–49.
4. Shanbhag S, Pandis N, Mustafa K, Nyengaard JR, Stavropoulos A. Bone tissue engineering in oral peri-implant defects in preclinical in vivo research: a systematic review and meta-analysis. J Tissue Eng Regen Med. 2018;12:336–49.
5. Janssen NG, Weijs WL, Koole R, Rosenberg AJ, Meijer GJ. Tissue engineering strategies for alveolar cleft reconstruction: a systematic review of the literature. Clin Oral Investig. 2014;18:219–26.
6. Pittenger MF, Mackay AM, Beck SC, Jaiswal RK, Douglas R, Mosca J. Multilineage potential of adult human mesenchymal stem cells. Science. 1999;284:143–7.
7. Pittenger MF, Discher DE, Péault BM, Phinney DG, Hare JM, Caplan AI. Mesenchymal stem cell perspective: cell biology to clinical progress. NPJ Regen Med. 2019;4:22.
8. Fekete N, Gadelorge M, Furst D, Maurer C, Dausend J, Fleury-Cappellesso S, et al. Platelet lysate from whole blood-derived pooled platelet concentrates and apheresis-derived platelet concentrates for the isolation and expansion of human bone marrow mesenchymal stromal cells: production process, content and identification of active components. Cytotherapy. 2012;14(5):540–54.
9. Shanbhag S, Stavropoulos A, Suliman S, Hervig T, Mustafa K. Efficacy of humanized mesenchymal stem cell cultures for bone tissue engineering: a systematic review with a focus on platelet derivatives. Tissue Eng B Rev. 2017;23:552–69.
10. Shanbhag S, Mohamed-Ahmed S, Lunde THF, Suliman S, Bolstad AI, Hervig T, et al. Influence of platelet storage time on human platelet lysates and platelet lysate-expanded mesenchymal stromal cells for bone tissue engineering. Stem Cell Res Ther. 2020;11(1):351.
11. Bieback K, Fernandez-Munoz B, Pati S, Schafer R. Gaps in the knowledge of human platelet lysate as a cell culture supplement for cell therapy: a joint publication from the AABB and the. Int Soc Cell Gene Therapy Transfus. 2019;59:3448–60.
12. Sart S, Tsai AC, Li Y, Ma T. Three-dimensional aggregates of mesenchymal stem cells: cellular mechanisms, biological properties, and applications. Tissue Eng B Rev. 2014;20:365–80.
13. Ghazanfari R, Zacharaki D, Li H, Ching Lim H, Soneji S, Scheding S. Human primary bone marrow mesenchymal stromal cells and their in vitro progenies display distinct transcriptional profile signatures. Sci Rep. 2017;7:10338.
14. Ahmadbeigi N, Soleimani M, Babaeijandaghi F, Mortazavi Y, Gheisari Y, Vasei M. The aggregate nature of human mesenchymal stromal cells in native bone marrow. Cytotherapy. 2012;14:917–24.
15. Hall BK, Miyake T. All for one and one for all: condensations and the initiation of skeletal development. BioEssays. 2000;22:138–47.
16. Kale S, Biermann S, Edwards C, Tarnowski C, Morris M, Long MW. Three-dimensional cellular development is essential for ex vivo formation of human bone. Nat Biotechnol. 2000;18:954–8.
17. Shanbhag S, Suliman S, Bolstad AI, Stavropoulos A, Mustafa K. Xeno-free spheroids of human gingiva-derived progenitor cells for bone tissue engineering. Front Bioeng Biotechnol. 2020;8:968.
18. Frith JE, Thomson B, Genever PG. Dynamic three-dimensional culture methods enhance mesenchymal stem cell properties and increase therapeutic potential. Tissue Eng C Methods. 2010;16(4):735–49.
19. Cheng NC, Wang S, Young TH. The influence of spheroid formation of human adipose-derived stem cells on chitosan films on stemness and differentiation capabilities. Biomaterials. 2012;33(6):1748–58.
20. Wang W, Itaka K, Ohba S, Nishiyama N, Chung UI, Yamasaki Y, et al. 3D spheroid culture system on micropatterned substrates for improved differentiation efficiency of multipotent mesenchymal stem cells. Biomaterials. 2009;30(14):2705–15.
21. Follin B, Juhl M, Cohen S, Pedersen AE, Kastrup J, Ekblond A. Increased paracrine immunomodulatory potential of mesenchymal stromal cells in three-dimensional culture. Tissue Eng B Rev. 2016;22(4):322–9.
22. Suenaga H, Furukawa KS, Suzuki Y, Takato T, Ushida T. Bone regeneration in calvarial defects in a rat model by implantation of human bone marrow-derived mesenchymal stromal cell spheroids. J Mater Sci Mater Med. 2015;26:254.
23. Chatterjea A, LaPointe VL, Barradas A, Garritsen H, Yuan H, Renard A, et al. Cell aggregation enhances bone formation by human mesenchymal stromal cells. Eur Cell Mater. 2017;33:121–9.
24. Moritani Y, Usui M, Sano K, Nakazawa K, Hanatani T, Nakatomi M. Spheroid culture enhances osteogenic potential of periodontal ligament mesenchymal stem cells. J Periodontal Res. 2018;53:870–82.
25. Yamaguchi Y, Ohno J, Sato A, Kido H, Fukushima T. Mesenchymal stem cell spheroids exhibit enhanced in-vitro and in-vivo osteoregenerative potential. BMC Biotechnol. 2014;14:105.
26. Shanbhag S, Shanbhag V. Clinical applications of cell-based approaches in alveolar bone augmentation: a systematic review. Clin Implant Dent Relat Res. 2015;17(Suppl 1):e17-34.
27. Murphy KC, Fang SY, Leach JK. Human mesenchymal stem cell spheroids in fibrin hydrogels exhibit improved cell survival and potential for bone healing. Cell Tissue Res. 2014;357:91–9.
28. Murphy KC, Hughbanks ML, Binder BY, Vissers CB, Leach JK. Engineered fibrin gels for parallel stimulation of mesenchymal stem cell proangiogenic and osteogenic potential. Ann Biomed Eng. 2015;43(8):2010–21.
29. Ho SS, Hung BP, Heyrani N, Lee MA, Leach JK. Hypoxic preconditioning of mesenchymal stem cells with subsequent spheroid formation accelerates repair of segmental bone defects. Stem Cells. 2018;36(9):1393–403.
30. Whitehead J, Griffin KH, Gionet-Gonzales M, Vorwald CE, Cinque SE, Leach JK. Hydrogel mechanics are a key driver of bone formation by mesenchymal stromal cell spheroids. Biomaterials. 2021;269:120607.
31. Bieback K, Fernandez-Munoz B, Pati S, Schafer R. Gaps in the knowledge of human platelet lysate as a cell culture supplement for cell therapy: a joint publication from the AABB and the International Society for Cell & Gene Therapy. Transfusion. 2019;59(11):3448–60.
32. Robinson ST, Douglas AM, Chadid T, Kuo K, Rajabalan A, Li H, et al. A novel platelet lysate hydrogel for endothelial cell and mesenchymal stem cell-directed neovascularization. Acta Biomater. 2016;36:86–98.
33. Haugen HJ, Lyngstadaas SP, Rossi F, Perale G. Bone grafts: which is the ideal biomaterial? J Clin Periodontol. 2019;46(Suppl 21):92–102.
34. Yassin MA, Mustafa K, Xing Z, Sun Y, Fasmer KE, Waag T. A copolymer scaffold functionalized with nanodiamond particles enhances osteogenic metabolic activity and bone regeneration. Macromol Biosci. 2017;17:1600427.
35. Yassin MA, Fuoco T, Mohamed-Ahmed S, Mustafa K, Finne-Wistrand A. 3D and porous RGDC-functionalized polyester-based scaffolds as a niche to induce osteogenic differentiation of human bone marrow stem cells. Macromol Biosci. 2019;19(6):e1900049.
36. Hassan MN, Yassin MA, Suliman S, Lie SA, Gjengedal H, Mustafa K. The bone regeneration capacity of 3D-printed templates in calvarial defect models: a systematic review and meta-analysis. Acta Biomater. 2019;91:1–23.
37. Jain S, Yassin MA, Fuoco T, Liu H, Mohamed-Ahmed S, Mustafa K, et al. Engineering 3D degradable, pliable scaffolds toward adipose tissue regeneration; optimized printability, simulations and surface modification. J Tissue Eng. 2020;11:2041731420954316.
38. Schantz JT, Hutmacher DW, Lam CX, Brinkmann M, Wong KM, Lim TC, et al. Repair of calvarial defects with customised tissue-engineered bone grafts II. Evaluation of cellular efficiency and efficacy in vivo. Tissue Eng. 2003;9:S127–39.
39. Cameron JA, Milner DJ, Lee JS, Cheng J, Fang NX, Jasiuk IM. Employing the biology of successful fracture repair to heal critical size bone defects. Curr Top Microbiol Immunol. 2013;367:113–32.
40. Mohamed-Ahmed S, Fristad I, Lie SA, Suliman S, Mustafa K, Vindenes H, et al. Adipose-derived and bone marrow mesenchymal stem cells: a donor-matched comparison. Stem Cell Res Ther. 2018;9(1):168.
41. Kilkenny C, Browne WJ, Cuthill IC, Emerson M, Altman DG. Improving bioscience research reporting: the ARRIVE guidelines for reporting animal research. PLoS Biol. 2010;8:1000412.

42. Vajgel A, Mardas N, Farias BC, Petrie A, Cimoes R, Donos N. A systematic review on the critical size defect model. Clin Oral Implants Res. 2014;25:879.
43. Mohamed-Ahmed S, Yassin MA, Rashad A, Espedal H, Idris SB, Finne-Wistrand A, et al. Comparison of bone regenerative capacity of donor-matched human adipose-derived and bone marrow mesenchymal stem cells. Cell Tissue Res. 2020;383:1061–75.
44. Kuchler U, Rybaczek T, Dobask T, Heimel P, Tangl S, Klehm J, et al. Bone-conditioned medium modulates the osteoconductive properties of collagen membranes in a rat calvaria defect model. Clin Oral Implants Res. 2018;29(4):381–8.
45. Jeno L, Geza L. A simple differential staining method for semi-thin sections of ossifying cartilage and bone tissues embedded in epoxy resin. Mikroskopie. 1975;31(1–2):1–4.
46. Zhang Q, Nguyen AL, Shi S, Hill C, Wilder-Smith P, Krasieva TB. Three-dimensional spheroid culture of human gingivaderived mesenchymal stem cells enhances mitigation of chemotherapyinduced oral mucositis. Stem Cells Dev. 2012;21:937–47.
47. Miranda JP, Camoes SP, Gaspar MM, Rodrigues JS, Carvalheiro M, Barcia RN. The secretome derived from 3D-cultured umbilical cord tissue MSCs counteracts manifestations typifying rheumatoid arthritis. Front Immunol. 2019;10:18.
48. Ho SS, Keown AT, Addison B, Leach JK. Cell migration and bone formation from mesenchymal stem cell spheroids in alginate hydrogels are regulated by adhesive ligand density. Biomacromol. 2017;18(12):4331–40.
49. Ho SS, Murphy KC, Binder BY, Vissers CB, Leach JK. Increased survival and function of mesenchymal stem cell spheroids entrapped in instructive alginate hydrogels. Stem Cells Transl Med. 2016;5(6):773–81.
50. Jaquiery C, Schaeren S, Farhadi J, Mainil-Varlet P, Kunz C, Zeilhofer HF, et al. In vitro osteogenic differentiation and in vivo bone-forming capacity of human isogenic jaw periosteal cells and bone marrow stromal cells. Ann Surg. 2005;242(6):859–67 (**discussion 67-8**).
51. Kim BS, Kim HJ, Choi JG, You HK, Lee J. The effects of fibrinogen concentration on fibrin/atelocollagen composite gel: an in vitro and in vivo study in rabbit calvarial bone defect. Clin Oral Implants Res. 2015;26(11):1302–8.
52. Linsley CS, Wu BM, Tawil B. Mesenchymal stem cell growth on and mechanical properties of fibrin-based biomimetic bone scaffolds. J Biomed Mater Res A. 2016;104(12):2945–53.
53. Langer R, Vacanti JP. Tissue engineering. Science. 1993;260(5110):920–6.
54. Xia W, Li H, Wang Z, Xu R, Fu Y, Zhang X, et al. Human platelet lysate supports ex vivo expansion and enhances osteogenic differentiation of human bone marrow-derived mesenchymal stem cells. Cell Biol Int. 2011;35(6):639–43.
55. Chevallier N, Anagnostou F, Zilber S, Bodivit G, Maurin S, Barrault A, et al. Osteoblastic differentiation of human mesenchymal stem cells with platelet lysate. Biomaterials. 2010;31(2):270–8.
56. Kuterbekov M, Machillot P, Baillet F, Jonas AM, Glinel K, Picart C. Design of experiments to assess the effect of culture parameters on the osteogenic differentiation of human adipose stromal cells. Stem Cell Res Ther. 2019;10(1):256.
57. Kasten P, Vogel J, Luginbuhl R, Niemeyer P, Weiss S, Schneider S, et al. Influence of platelet-rich plasma on osteogenic differentiation of mesenchymal stem cells and ectopic bone formation in calcium phosphate ceramics. Cells Tissues Organs. 2006;183(2):68–79.
58. Huang S, Jia S, Liu G, Fang D, Zhang D. Osteogenic differentiation of muscle satellite cells induced by platelet-rich plasma encapsulated in three-dimensional alginate scaffold. Oral Surg Oral Med Oral Pathol Oral Radiol. 2012;114(5 Suppl):S32-40.
59. Zhang S, Mao T, Chen F. Influence of platelet-rich plasma on ectopic bone formation of bone marrow stromal cells in porous coral. Int J Oral Maxillofac Surg. 2011;40(9):961–5.
60. Trouillas M, Prat M, Doucet C, Ernou I, Laplace-Builhe C, Blancard PS, et al. A new platelet cryoprecipitate glue promoting bone formation after ectopic mesenchymal stromal cell-loaded biomaterial implantation in nude mice. Stem Cell Res Ther. 2013;4(1):1.
61. Findeisen L, Bolte J, Vater C, Petzold C, Quade M, Muller L, et al. Cell spheroids are as effective as single cells suspensions in the treatment of critical-sized bone defects. Bmc Musculoskel Dis. 2021;22:1.
62. Scott MA, Levi B, Askarinam A, Nguyen A, Rackohn T, Ting K, et al. Brief review of models of ectopic bone formation. Stem Cells Dev. 2012;21:655.
63. Tsujigiwa H, Hirata Y, Katase N, Buery RR, Tamamura R, Ito S, et al. The role of bone marrow-derived cells during the bone healing process in the GFP mouse bone marrow transplantation model. Calcif Tissue Int. 2013;92(3):296–306.
64. Takabatake K, Tsujigiwa H, Song Y, Matsuda H, Kawai H, Fujii M, et al. The role of bone marrow-derived cells during ectopic bone formation of mouse femoral muscle in GFP mouse bone marrow transplantation model. Int J Med Sci. 2018;15(8):748–57.
65. Gamblin AL, Brennan MA, Renaud A, Yagita H, Lezot F, Heymann D, et al. Bone tissue formation with human mesenchymal stem cells and biphasic calcium phosphate ceramics: the local implication of osteoclasts and macrophages. Biomaterials. 2014;35(36):9660–7.
66. Haumer A, Bourgine PE, Occhetta P, Born G, Tasso R, Martin I. Delivery of cellular factors to regulate bone healing. Adv Drug Deliv Rev. 2018;129:285–94.
67. Li JD, Chen ML, Wei XY, Hao YS, Wang JM. Evaluation of 3D-printed polycaprolactone scaffolds coated with freeze-dried platelet-rich plasma for bone regeneration. Materials. 2017;10(7):831.
68. Wu SL, Liu XM, Yeung KWK, Liu CS, Yang XJ. Biomimetic porous scaffolds for bone tissue engineering. Mater Sci Eng R. 2014;80:1–36.
69. Lim J, Lee J, Yun HS, Shin HI, Park EK. Comparison of bone regeneration rate in flat and long bone defects: calvarial and tibial bone. Tissue Eng Regener Med. 2013;10(6):336–40.

Publisher's Note

Springer Nature remains neutral with regard to jurisdictional claims in published maps and institutional affiliations.

Ready to submit your research? Choose BMC and benefit from:

- fast, convenient online submission
- thorough peer review by experienced researchers in your field
- rapid publication on acceptance
- support for research data, including large and complex data types
- gold Open Access which fosters wider collaboration and increased citations
- maximum visibility for your research: over 100M website views per year

At BMC, research is always in progress.

Learn more biomedcentral.com/submissions

frontiers in Bioengineering and Biotechnology

ORIGINAL RESEARCH
published: 30 November 2021
doi: 10.3389/fbioe.2021.783468

Ectopic Bone Tissue Engineering in Mice Using Human Gingiva or Bone Marrow-Derived Stromal/Progenitor Cells in Scaffold-Hydrogel Constructs

Siddharth Shanbhag[1,2], Carina Kampleitner[3,4,5], Samih Mohamed-Ahmed[1], Mohammed Ahmad Yassin[1], Harsh Dongre[6,7], Daniela Elena Costea[6,7], Stefan Tangl[4,5], Andreas Stavropoulos[8,9], Anne Isine Bolstad[1], Salwa Suliman[1] and Kamal Mustafa[1]**

[1]Center for Translational Oral Research (TOR), Department of Clinical Dentistry, Faculty of Medicine, University of Bergen, Bergen, Norway, [2]Department of Immunology and Transfusion Medicine, Haukeland University Hospital, Bergen, Norway, [3]Ludwig Boltzmann Institute for Traumatology, The Research Center in Cooperation With AUVA, Vienna, Austria, [4]Karl Donath Laboratory for Hard Tissue and Biomaterial Research, University Clinic of Dentistry, Medical University of Vienna, Vienna, Austria, [5]Austrian Cluster for Tissue Regeneration, Vienna, Austria, [6]Gade Laboratory for Pathology, Department of Clinical Medicine, Faculty of Medicine, University of Bergen, Bergen, Norway, [7]Centre for Cancer Biomarkers (CCBIO), Faculty of Medicine, University of Bergen, Bergen, Norway, [8]Department of Periodontology, Faculty of Odontology, Malmö University, Malmö, Sweden, [9]Division of Conservative Dentistry and Periodontology, University Clinic of Dentistry, Medical University of Vienna, Vienna, Austria

OPEN ACCESS

Edited by:
Nikos Donos,
Queen Mary University of London,
United Kingdom

Reviewed by:
Joaquim Vives,
Banc de Sang i Teixits, Spain
Deborah Stanco,
University of Zurich, Switzerland

***Correspondence:**
Siddharth Shanbhag
siddharth.shanbhag@uib.no
Kamal Mustafa
Kamal.Mustafa@uib.no

Specialty section:
This article was submitted to Tissue Engineering and Regenerative Medicine, a section of the journal Frontiers in Bioengineering and Biotechnology

Received: 26 September 2021
Accepted: 16 November 2021
Published: 30 November 2021

Citation:
Shanbhag S, Kampleitner C, Mohamed-Ahmed S, Yassin MA, Dongre H, Costea DE, Tangl S, Stavropoulos A, Bolstad AI, Suliman S and Mustafa K (2021) Ectopic Bone Tissue Engineering in Mice Using Human Gingiva or Bone Marrow-Derived Stromal/Progenitor Cells in Scaffold-Hydrogel Constructs. Front. Bioeng. Biotechnol. 9:783468. doi: 10.3389/fbioe.2021.783468

Three-dimensional (3D) spheroid culture can promote the osteogenic differentiation and bone regeneration capacity of mesenchymal stromal cells (MSC). Gingiva-derived progenitor cells (GPC) represent a less invasive alternative to bone marrow MSC (BMSC) for clinical applications. The aim of this study was to test the *in vivo* bone forming potential of human GPC and BMSC cultured as 3D spheroids or dissociated cells (2D). 2D and 3D cells encapsulated in constructs of human platelet lysate hydrogels (HPLG) and 3D-printed poly (L-lactide-co-trimethylene carbonate) scaffolds (HPLG-PLATMC) were implanted subcutaneously in nude mice; cell-free HPLG-PLATMC constructs served as a control. Mineralization was assessed using micro-computed tomography (μCT), histology, scanning electron microscopy (SEM) and *in situ* hybridization (ISH). After 4–8 weeks, μCT revealed greater mineralization in 3D-BMSC vs. 2D-BMSC and 3D-GPC ($p < 0.05$), and a similar trend in 2D-GPC vs. 2D-BMSC ($p > 0.05$). After 8 weeks, greater mineralization was observed in cell-free constructs vs. all 2D- and 3D-cell groups ($p < 0.05$). Histology and SEM revealed an irregular but similar mineralization pattern in all groups. ISH revealed similar numbers of 2D and 3D BMSC/GPC within and/or surrounding the mineralized areas. In summary, spheroid culture promoted ectopic mineralization in constructs of BMSC, while constructs of dissociated GPC and BMSC performed similarly. The combination of HPLG and PLATMC represents a promising scaffold for bone tissue engineering applications.

Keywords: xeno-free, platelet lysate, MSc, spheroid culture, bone tissue engineering

INTRODUCTION

Adult mesenchymal stromal cells (MSC) are increasingly being used in bone tissue engineering (BTE) for the reconstruction of clinically challenging bone defects, and to overcome the limitations of existing bone-substitute materials (Shanbhag et al., 2019). Although MSC derived from bone marrow (BMSC) are the most widely tested, progenitor cells from other tissues requiring less-invasive harvesting, e.g., oral tissues, are being explored (Sharpe, 2016; Pittenger et al., 2019). Gingiva, in particular, can be harvested with minimal morbidity and contains a subpopulation of multipotent progenitor cells (GPCs), which demonstrate an MSC-like phenotype, immunomodulatory properties, and osteogenic potential both *in vitro* and *in vivo* (Fournier et al., 2010; Mitrano et al., 2010; Tomar et al., 2010).

A critical aspect in the clinical translation of cell therapies is the use of safe and standardized culture conditions resulting in safe-to-use cell constructs. Exclusion of animal-derived supplements, e.g., fetal bovine serum (FBS), in *ex vivo* culture systems is considered important to facilitate clinical translation of cell therapies and is also a recommendation by regulatory health authorities (Bieback et al., 2019). Pooled human platelet lysate (HPL) has been identified as the optimal "xeno-free" supplement for MSC culture, with particular benefits for BTE by promoting MSC osteogenic differentiation (Fekete et al., 2012; Shanbhag et al., 2017). We have recently reported that HPL cultured GPC and BMSC demonstrate superior proliferation, osteogenic gene expression and *in vitro* mineralization vs. corresponding FBS-based cultures (Shanbhag et al., 2020a; Shanbhag et al., 2020b).

Compared to two-dimensional (2D) monolayer cultures, the self-assembly or aggregation of MSC into 3D spheroids is mediated by unique cell-cell and cell-extracellular matrix (ECM) interactions, biomechanical cues and activated signaling pathways, simulating more closely the *in vivo* microenvironment (Sart et al., 2014; Cesarz and Tamama, 2016). Several studies have reported that, compared to conventional 2D monolayers, spheroid MSC show enhanced "stemness", differentiation capacity, paracrine activity and immunomodulatory potential (Kale et al., 2000; Follin et al., 2016; Petrenko et al., 2017). We have recently reported that the expressions of several genes associated with self-renewal and osteogenic differentiation were significantly enhanced in xeno-free 3D spheroid vs. 2D monolayer cultures of GPC and BMSC, independent of osteogenic induction via media supplements (Shanbhag et al., 2020b). GPC and BMSC spheroids also demonstrated *in situ* mineralization and ECM formation following *in vitro* osteogenic induction, altogether, suggesting a promising potential for use in BTE (Shanbhag et al., 2020b).

Traditional cell delivery methods involve direct seeding of cells on the surface of biomaterial scaffolds before *in vivo* transplantation (Shanbhag and Shanbhag, 2015). However, this may not be optimal for MSC spheroids where the 3D structure is lost by direct seeding, thus potentially compromising their efficacy. To preserve the 3D structure, encapsulation of spheroids in hydrogel scaffolds maintains their 3D assembly and represents an effective delivery system (Murphy et al., 2014; Murphy et al., 2015; Ho et al., 2018). Since HPL is increasingly being used for clinical-grade MSC culture, extending its application as a hydrogel scaffold represents a clinically relevant and cost-effective strategy (Robinson et al., 2016). Additionally, using 3D-printing technology, pliable scaffolds of novel copolymers, e.g., poly (L-lactide-co-trimethylene carbonate) (PLATMC) (Jain et al., 2020), can be custom designed to support the cell-hydrogel constructs in non-contained critical-size bone and/or periodontal defects (Hassan et al., 2019; Yamada et al., 2021). As a preliminary step, the regenerative potential of tissue engineered constructs is frequently tested in ectopic, e.g., subcutaneous or intramuscular, sites (Scott et al., 2012). The absence of local osteogenic cells and stimuli surmises that any observed mineralization is from exogenous origins and/or stimuli. Therefore, the objective of the present study was to compare the potential of xeno-free GPC and BMSC, as dissociated cells (2D) or spheroids (3D), encapsulated in constructs of HPL hydrogels (HPLG) and PLATMC (HPLG-PLATMC), for ectopic BTE in a subcutaneous immunocompromised mouse model.

MATERIALS AND METHODS

Cell Culture

The use of human cells and tissues was approved by the Regional Committees for Medical Research Ethics (REK) in Norway (2013-1248/REK-sør-øst C and 2016-1266/REK-nord) and obtained following appropriate informed consent. Bone marrow aspirates were obtained from three donors (one female and two males; 8–10 years) undergoing corrective surgery at the Department of Plastic Surgery, Haukeland University Hospital, Bergen, Norway. Gingival biopsies were collected from three systemically healthy, non-smoking patients (two females and one male; 18–31 years) undergoing dental surgery at the Department of Clinical Dentistry, University of Bergen, Bergen, Norway. BMSC and GPC were isolated as previously described (Mohamed-Ahmed et al., 2018; Shanbhag et al., 2020b). Briefly, primary monolayer cultures of GPC and BMSC were separately established in growth media comprising Dulbecco's Modified Eagle's medium (DMEM; Invitrogen, Carlsbad, CA, United States) supplemented with 5% (v/v) HPL (Bergenlys®, Bergen, Norway), 1% (v/v) penicillin/streptomycin (GE Healthcare, South Logan, UT, United States) and 1 IU/ml heparin (Leo Pharma AS, Lysaker, Norway). Cells were sub-cultured (4,000 cells/cm^2) and expanded in humidified 5% CO_2 at 37°C. Characterization of monolayer GPC and BMSC according to the "minimal MSC criteria" (Dominici et al., 2006), i.e., plastic adherence, stromal-like immunophenotype and multi-lineage differentiation potential, has been reported elsewhere (Shanbhag et al., 2020a; Shanbhag et al., 2020b).

To generate 3D spheroids, passage-2 dissociated monolayer GPC and BMSC (n = 3 donors, pooled) were separately seeded in microwell-patterned 24-well plates (Kugelmeiers Ltd., Erlenbach, CH); after 24 h, aggregate spheroids of ~1000 cells were formed via guided self-assembly (Shanbhag et al., 2020b).

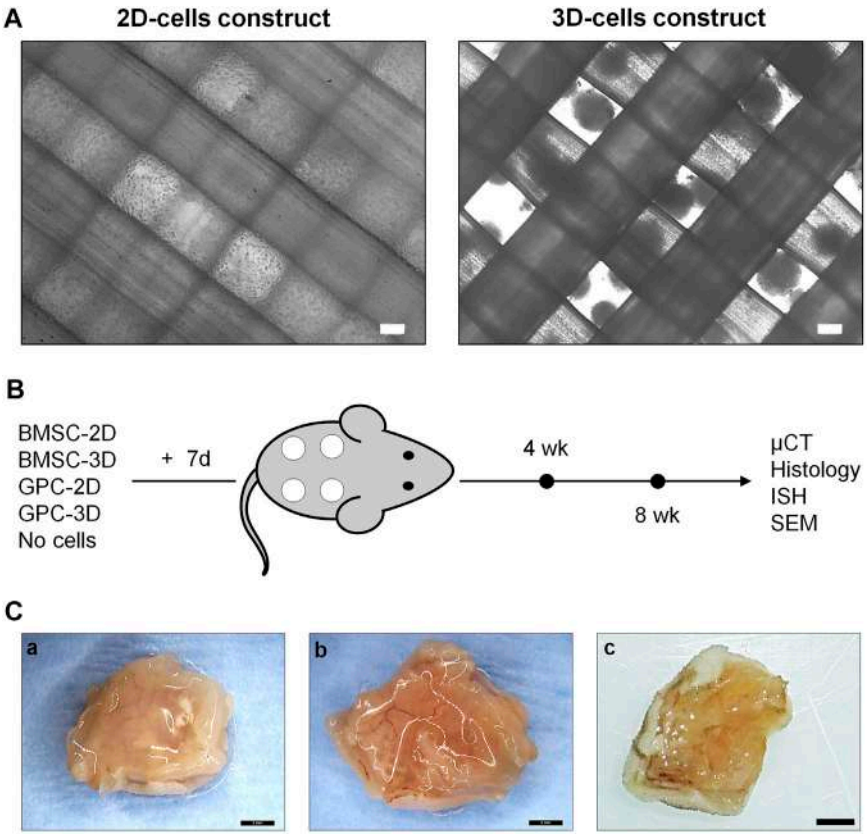

FIGURE 1 | Study design. **(A)** Representative phase microscopic images of 2D (single cells) and 3D (spheroids) cell constructs; scale bars 100 µm. **(B)** Schema of study design, experimental groups and outcomes; constructs were cultured *in vitro* in osteogenic induction medium for 7 days prior to implantation (+7 days). **(C)** Representative macroscopic images of 8-weeks tissue specimens containing BMSC (a), GPC (b) or cell-free constructs (c); scale bars 2 mm.

Characterization of GPC and BMSC spheroids based on gene expression, cytokine secretion and *in vitro* mineralization, has been reported elsewhere (Shanbhag et al., 2020b).

Fabrication of HPLG-PLATMC Constructs

PLATMC scaffolds were produced as described elsewhere (Jain et al., 2020). Briefly, a 3D CAD model was designed using the Magics® software integrated with a 3D-Bioplotter® (both from EnvisionTEC, Gladbeck, Germany). Granules of medical-grade PLATMC (RESOMER® LT-706-S 70:30, Evonik GmBh, Essen, Germany) were loaded into the printer cartridge (pre-heated to 220°C) and rectangular sheets of three layers with an orientation of 0°–90°–0° were printed at 190°C with an inner nozzle diameter of 400 µm and strand spacing of 0.7 mm. Disc-shaped scaffolds measuring 6 mm × ~1.2 mm were punched out and placed in 48-well plates. Prior to use in experiments, the scaffolds were sterilized by soaking in 70% ethanol for 30 min, followed by washing with phosphate-buffered saline (PBS, Invitrogen) and 2 h exposure to UV light.

To avoid direct seeding on scaffolds and aiming to preserve the morphology of 3D spheroids, HPLG was added to the construct. To prepare HPLG, sterile-filtered HPL (same as in growth media) was supplemented with 20 mg/ml fibrinogen (Sigma-Aldrich, St. Louis, MO, United States) to increase the stiffness and mechanical properties of the hydrogel (Murphy et al., 2015). Gelation was achieved by adding a "thrombin solution" containing 1 IU/ml human thrombin and 1 TIU/ml aprotinin in 20 mM $CaCl_2$ solution (all from Sigma-Aldrich), followed by incubation at 37°C for 15 min. To prepare the (cell-free) constructs, the HPL and thrombin solutions were mixed and 50 µl were quickly seeded on pre-wetted scaffolds. To prepare cell-loaded constructs, equal numbers of passage-2 2D or 3D GPC or BMSC were uniformly suspended in fibrin supplemented HPL, mixed with thrombin solution and seeded on scaffolds (2×10^6 cells in 50 µl) as described above. Cell distribution within the constructs was observed under a light microscope (Nikon Eclipse TS100, Tokyo, Japan) (**Figure 1A**). Constructs were cultured in osteogenic induction media, i.e., growth media supplemented with final concentrations of 0.05 mM L-ascorbic acid 2-phosphate, 10 nM dexamethasone and 10 mM β glycerophosphate (all from Sigma-Aldrich), for 1 week prior to *in vivo* implantation.

Ectopic Implantation in Nude Mice

Animal experiments were approved by the Norwegian Animal Research Authority (Mattilsynet; FOTS-18738) and reported in accordance with the ARRIVE guidelines for all relevant items (Kilkenny et al., 2010; Berglundh and Stavropoulos, 2012).

Twenty female athymic nude mice (Rj:Athym-Foxn1nu/nu, Janvier Labs, France), 7-weeks-old and weighing 19.4 ± 1.12 g, were used. Animals were housed in stable conditions (22 ± 2°C) with a 12 h dark/light cycle and *ad libitum* access to food and water. Animals were allowed to acclimatize for 1 week prior to experiments and were regularly monitored for signs of pain/infection, food intake and activity during the entire experimental period.

Pre-operatively, animals were anesthetized with a mixture of sevoflurane (Abbott Laboratories, Berkshire, United Kingdom) and O_2 using a custom-made mask. Following anaesthesia, two 1-cm incisions were made in the midline of the dorsum, and four subcutaneous pouches were created using blunt dissection. Next, four constructs per animal containing either suspension [2×10^6 2D-BMSC or 2D-GPC], spheroid [2×10^6 3D-BMSC or 3D-GPC] or no cells were randomly implanted in the pouches (5 groups; $n = 8$ constructs per group per time point). GPC and BMSC were never implanted in the same animals. Post-operatively, the skin was sutured (Vicryl, Ethicon, Somerville, NJ, United States) and animals were injected subcutaneously with buprenorphine (Temgesic 0.03 mg/kg, Schering-Plough, United Kingdom) for up to 2 days thereafter. After 4 or 8 weeks, the animals were euthanized with an overdose of CO_2 and constructs were harvested. The primary outcome, i.e., ectopic mineralized tissue formation, was assessed via micro-computed tomography (μCT) and histology. Secondary outcomes included identification of transplanted human cells by *in situ* hybridization (ISH) and assessment of mineralized ultrastructure by scanning electron microscopy and energy dispersive x-ray spectroscopy (SEM/EDX) analysis. Animals were coded via ear clips and identified by numbers for all subsequent handling/analyses to facilitate blinding of personnel.

μCT

Immediately after euthanasia, the specimens were harvested along with the overlying skin and underlying muscle tissues and fixed in 10% buffered formalin (Sigma-Aldrich). Specimens were scanned using a SkyScan 1172 μCT scanner (Bruker, Kontich, Belgium) with an X-ray source of 60 kV/200 μA and 0.5 mm aluminum filter for a 10 μm resolution. Scans were reconstructed by applying a standardized volume of interest (5 mm × 1 mm to exclude the tissue margins) and a global grey threshold of 110–255 using the CTAn v.1.18 software (Bruker). Quantification of mineralization as a ratio of the total construct volume (MdV/TV) was performed in a blinded fashion using the CTAn software (Bruker).

Histology

Specimens were processed for histology by both decalcified (paraffin-embedded) and undecalcified (resin-embedded) methods. Selected specimens were decalcified in 20% ethylenediaminetetraacetic acid solution (EDTA; Sigma-Aldrich) for 7 days. Next, formalin-fixed tissues were dehydrated in ascending grades of alcohol and embedded in paraffin (FFPE) or light-curing resin (RE; Technovit 7200 + 1% benzoyl peroxide, Kulzer & Co., Wehrheim, Germany). FFPE tissue sections were cut (~5 μm) and stained with hematoxylin and eosin, Alizarin red S (Sigma-Aldrich) or Trichrome dyes (Roche Diagnostics, Oslo, Norway); Alizarin red staining was performed on undecalcified FFPE sections. RE specimens were further processed using EXAKT cutting and grinding equipment (EXAKT Apparatebau, Norderstedt, Germany) and thin ground sections (~100 μm) were stained with Levi-Lazko dye (Morphisto GmbH, Frankfurt, Germany). FFPE and RE sections were scanned and digitized using a Nanozoomer XR (Hamamatsu, Photonics Ltd., Hertfordshire, United Kingdom; ×40 magnification) and Olympus BX61VS system (DotSlide 2.4; Olympus, Japan, Tokyo, ×20 magnification), respectively. Quantification of total collagen (area in μm^2) in Trichrome stained FFPE sections was performed using QuPath open-source image analysis software (Bankhead et al., 2017).

ISH

Detection of transplanted human cells was performed using ISH for the human specific repetitive *Alu* sequence, which comprises approximately 5% of the total human genome (Mankani et al., 2007). ISH was performed using the RNAscope 2.5 High-Definition Brown Assay according to the manufacturer's instructions (all reagents and probes from Advanced Cell Diagnostics, Newark, CA, United States). Briefly, tissue slides were baked at 60°C for 1 h followed by deparaffinization in 100% xylene twice for 5 min each and two changes of 100% ethanol. The slides were treated with an endogenous peroxidase-blocking reagent, incubated for 15 min in boiling 1× target retrieval solution and treated with protease digestion buffer for 30 min at 40°C. The slides were then incubated with the target *Alu* probe for 2 h at 40°C, followed by signal amplification as detailed in the manufacturer's guide. For colorimetric detection, 3,3′-Diaminobenzidine (DAB) was applied for 5 min at RT followed by counterstaining with hematoxylin. A peptidylprolyl isomerase B (*PPIB*) Positive Control Probe was used to validate the assay. Quantification of brown stained *Alu* + cells in ISH sections was performed using the QuPath software (Bankhead et al., 2017).

SEM

Ultrastructure of mineralization in the undecalcified ground sections was analyzed using SEM and EDX. Briefly, the slides were sputter coated with carbon and imaged at a voltage of 15 kV with an electron microscope (Supra 55VP, Carl Zeiss, Oberkochen, Germany). EDX analysis was performed using the Pathfinder software (Thermo Scientific) and atomic weight percentages of various elements such as calcium (Ca) and phosphorous (P) were automatically calculated. EDX analysis was performed at least three different regions of the mineralized tissues in each section. Sections of histologically validated ectopic bone from a previous study in mouse intramuscular sites were analyzed as positive controls.

Statistical Analysis

Statistical analysis was performed using the Prism 9.0 software (GraphPad Software, San Diego, CA, United States). Data are presented as means ± SD, unless specified. Normality testing was performed using the Shapiro-Wilk test. The student *t* test,

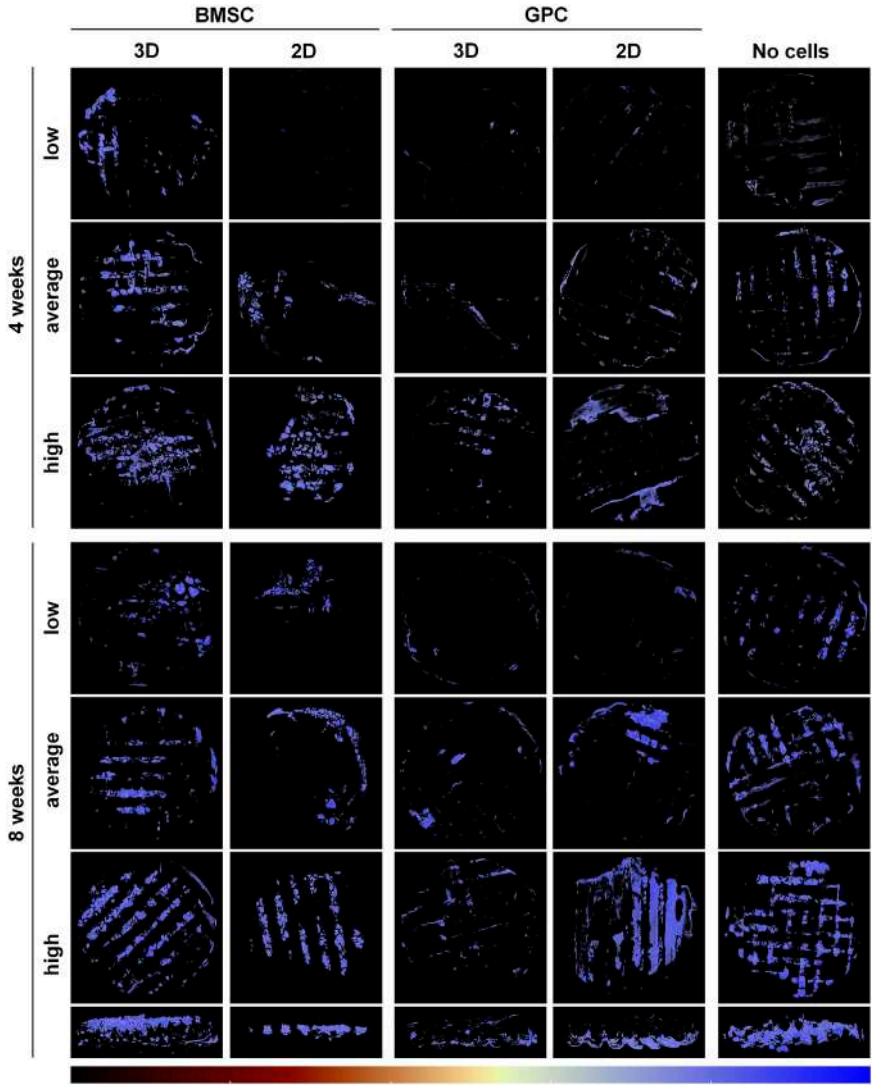

FIGURE 2 | μCT analysis of ectopic mineralization. Representative reconstructed images showing "low, average and high" degrees of mineralization in BMSC, GPC and control constructs (no cells) after 4 and 8 weeks; the bottom row shows cross-sectional views of the corresponding "high" constructs at 8 weeks. The color bar indicates relative mineral density from minimum (black) to maximum (blue).

Mann-Whitney U test and one-way analysis of variance (ANOVA), followed by a post-hoc Tukey's (parametric) or Dunn's test (non-parametric) for multiple comparisons, were applied as appropriate, and $p < 0.05$ was considered statistically significant.

RESULTS

General Outcomes

HPLG-PLATMC constructs containing equal numbers of 2D or 3D GPC or BMSC were implanted subcutaneously in nude mice (**Figures 1A,B**). One animal died 2 days postoperatively due to an eye infection unrelated to the implants and was excluded from the analysis. All other animals recovered from surgery and no adverse events were recorded. Constructs were analyzed after 4 weeks [2D-BMSC ($n = 8$), 3D-BMSC ($n = 8$), 2D-GPC ($n = 6$), 3D-GPC ($n = 6$), cell-free ($n = 8$)] or 8 weeks [2D-BMSC ($n = 8$), 3D-BMSC ($n = 8$), 2D-GPC ($n = 8$), 3D-GPC ($n = 8$), cell-free ($n = 8$)]. No signs of inflammation were observed on either the skin or muscle surface. Abundant blood vessels were observed in the muscle layer directly underlying the constructs in all groups.

Spheroid Culture of BMSC Promoted Ectopic Mineralization

μCT analysis revealed mineralization of varying degrees in all groups. The pattern of mineralization typically followed the scaffold architecture, i.e., along the surface of the printed filaments in between the pores (**Figure 2**). Cross-sectional images demonstrated mineralization throughout the entire

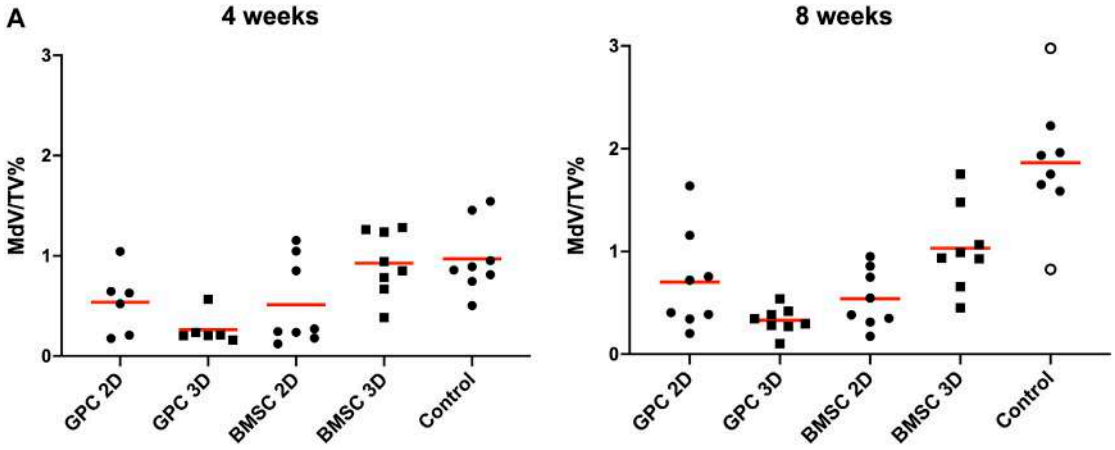

B

4 weeks	Mean MdV/TV	*p*	8 weeks	Mean MdV/TV	*p*
BMSC-3D*	0.92		BMSC-3D*	1.03	
vs BMSC-2D	0.51	0.0467	*vs* BMSC-2D	0.54	0.0154
vs GPC-3D	0.26	0.0006	*vs* GPC-3D	0.33	0.0004
Control*	0.97		Control*	1.86	
vs GPC-2D	0.53	0.0387	*vs* GPC-2D	0.70	0.0001
vs GPC-3D	0.26	0.0011	*vs* GPC-3D	0.33	<0.0001
			vs BMSC-2D	0.54	<0.0001
			vs BMSC-3D	1.03	0.0041
			vs Control 4 w	0.97	0.0030

FIGURE 3 | Quantification of mineralization by μCT. **(A)** Percentage mineralization in BMSC, GPC and control constructs (no cells) after 4 and 8 weeks; MdV/TV, mineral volume/total construct volume; data represent means; o represents outliers. **(B)** Inter-group comparisons showing statistically significant differences ($p < 0.05$); * reference group in the analysis (Kruskal-Wallis one-way ANOVA).

thickness of the construct. Significantly greater mineralization (MdV/TV) was observed in 3D-BMSC vs. 2D-BMSC constructs after 4 (0.92 ± 0.32 vs. 0.51 ± 0.42; $p = 0.046$) and 8 weeks (1.03 ± 0.41 vs. 0.54 ± 0.28; $p = 0.015$) (**Figures 3A,B**). In the case of GPC, a non-significant trend for greater MdV/TV was observed in 2D-GPC vs. 3D-GPC constructs at 4 (0.53 ± 0.32 vs. 0.26 ± 0.15; $p > 0.05$) and 8 weeks (0.70 ± 0.48 vs. 0.33 ± 0.12; $p > 0.05$). Comparable mineralization was observed in 2D-GPC vs. 2D-BMSC constructs at 4 and 8 weeks ($p > 0.05$). Significantly greater mineralization was observed in 3D-BMSC vs. 3D-GPC constructs at 4 and 8 weeks ($p < 0.05$).

Cell-Free Constructs Produced Robust Ectopic Mineralization

Substantial mineralization was also observed in the control, i.e., cell-free HPLG-PLATMC, constructs after 4 weeks; μCT analysis revealed comparable MdV/TV to that of 3D-BMSC constructs at 4 weeks (0.97 ± 0.35 vs. 0.92 ± 0.32; $p > 0.05$). Only the cell-free group showed a significant increase in mineralization from 4 to 8 weeks (0.97 ± 0.35 to 1.86 ± 0.60; $p = 0.003$). After 8 weeks, mineralization in the cell-free group was significantly greater than all other groups ($p < 0.05$) (**Figures 3A,B**).

Irregular Histological Appearance of Ectopic Mineralization

Generally, histological analysis of all explants (cell-loaded and cell-free) revealed fibrous encapsulation of the constructs, with little or no inflammatory cell-infiltrate around the capsules. The scaffold material within the construct was well-defined, could be clearly distinguished from the host tissues and did not indicate any signs of resorption or degradation, even after 8 weeks. The hydrogel between the scaffold pores was degraded and replaced by well-vascularized host tissues (**Figures 4–6**).

In paraffin-embedded (FFPE) sections, areas of diffuse mineralization were seen along the scaffold margins and between the filaments, often in direct contact with the scaffold. Alizarin red staining of undecalcified FFPE sections confirmed the presence of calcium in the tissues; *Alu* + cells were detected within/surrounding these tissues (**Supplementary Figure S1**). Presence of collagen was confirmed via Trichrome (blue) staining. After 8 weeks, a trend for higher collagen content

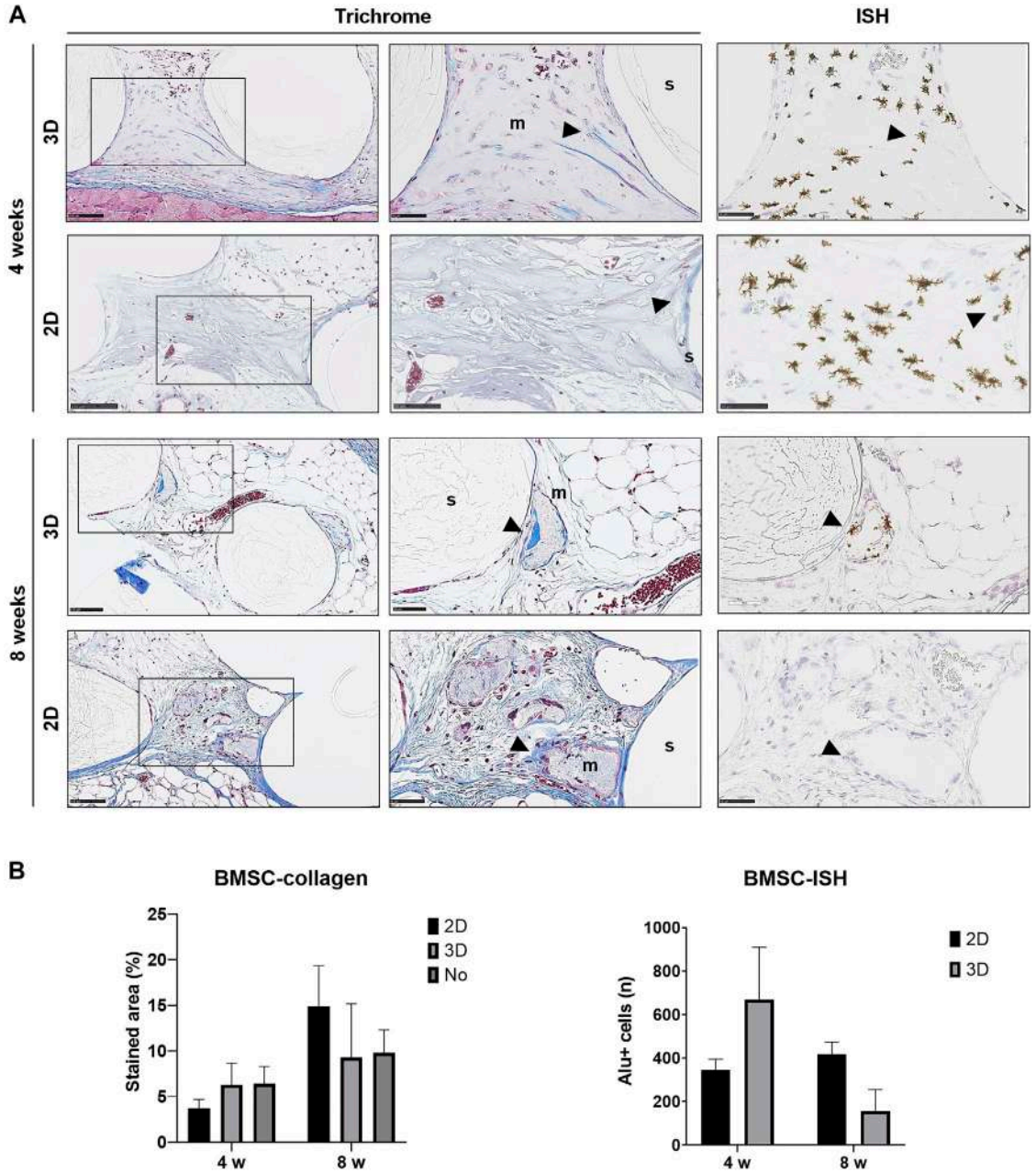

FIGURE 4 | Histology of BMSC constructs. **(A)** Representative images of Trichrome and corresponding ISH stained sections of 2D and 3D BMSC constructs after 4 and 8 weeks; m, mineralization; s, scaffold; wb, woven bone; arrows indicate dense collagen (Trichrome) and Alu + cells (ISH)—except in the ISH section of 2D-GPC at 8 weeks where dense collagen does not correlate with Alu + cells in ISH; scale bars 100 μm. **(B)** Quantification of collagen staining (Trichrome) and Alu + cells (ISH); *n*, total number; data represent means ± SD ($n = 3$).

was observed in 2D vs. 3D groups of both GPC and BMSC constructs ($p > 0.05$). Overall, no differences in morphology of the mineralized areas or collagen content were observed between cell-loaded and cell-free constructs. A trend for greater collagen and *Alu* + cells was observed in GPC vs. BMSC constructs ($p > 0.05$). In the 3D-BMSC and 3D-GPC groups, the spheroidal form of cell aggregates was retained after 4 weeks and often showed signs of mineralization *en masse* (**Supplementary Figure S1**).

In FFPE sections, the mineralized areas lacked the organized structure of normal bone tissue, with no evidence of embedded (osteocytes) or lining cells. Similar observations were made in undecalcified RE sections, where the mineralized areas mostly showed an irregular and acellular pattern (**Figure 7**). Only one instance of organized bone-like tissue with embedded osteocytes was observed in a single specimen from the 2D-BMSC group at 8 weeks. In this case, the new bone was seen to be formed on the

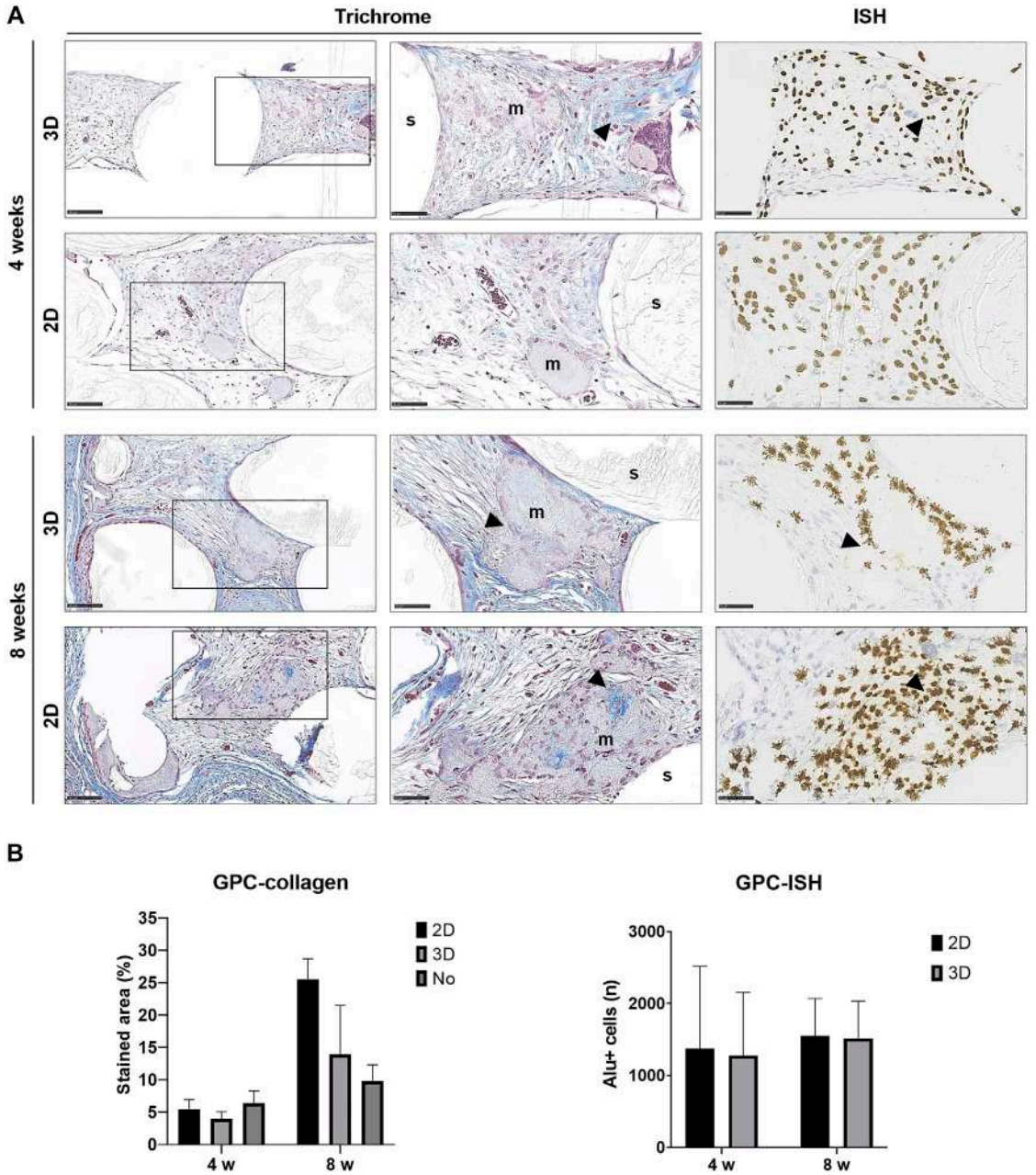

FIGURE 5 | Histology of GPC constructs. **(A)** Representative images of Trichrome and corresponding ISH stained sections of 2D and 3D GPC constructs after 4 and 8 weeks; m, mineralization; s, scaffold; arrows indicate dense collagen (Trichrome) and Alu + cells (ISH); scale bars 100 μm. **(B)** Quantification of collagen staining (Trichrome) and Alu + cells (ISH); n, total number; data represent means ± SD (n = 3).

surface of an irregular mineralization, which showed roughened borders indicative of resorption (**Figure 7**).

Comparable Ultrastructure of Different Mineralization Patterns

Composition of the different ectopic mineralization patterns in RE sections was further determined via SEM/EDX analysis; SEM and histological images were correlated to analyze specific regions within the mineralized areas. Based on appearance, the different mineralization patterns were categorized as follows (in order of decreasing frequency): globular, plate-like and filament-like (**Figure 8**). EDX analysis revealed similar compositions in terms of Ca, P and Ca:P ratios between the different mineralization types; average values of Ca, P and Ca:P were 37.31% (range 33.46–41.12%), 17.77% (range 15.73–19.02%) and 2.10 (range 2.02–2.17), respectively. These values were comparable to historical controls of "true" ectopic bone (**Supplementary Figure S2**).

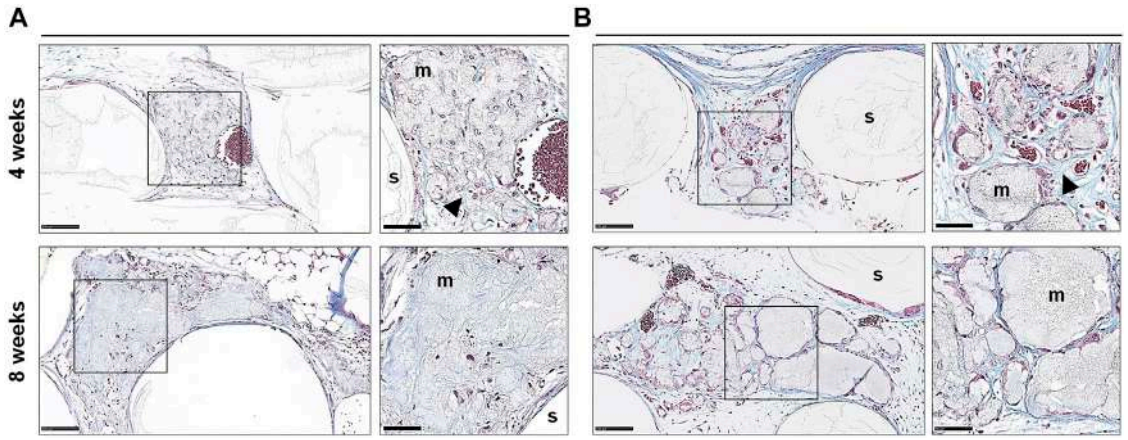

FIGURE 6 | Histology of cell-free constructs. Representative images of Trichrome stained sections of cell-free constructs showing different patterns of mineralization **(A,B)** after 4 and 8 weeks; m, mineralization; s, scaffold; arrows indicate dense collagen; scale bars 100 μm (20x) and 50 μm (40x).

Transplanted Cells Detected *in situ* After 8 weeks

Detection of transplanted human cells was performed using ISH for the human specific *Alu* sequence; no *Alu* + cells were detected in cell-free constructs (data not shown). High numbers of *Alu* + cells were detected after 4 and 8 weeks in constructs of both 2D and 3D GPC and BMSC. In 3D GPC/BMSC, cell aggregation was evident even after 8 weeks. *Alu* + cells were uniformly distributed throughout the constructs and associated with markedly denser connective tissue. In several instances, *Alu* + cells were detected within and around the areas of mineralization, although not showing the characteristic lacunae of embedded osteocytes. In BMSC constructs, a trend for greater numbers of *Alu* + cells was observed in the 3D vs. 2D group at 4 but not at 8 weeks (**Figure 4B**). In GPC constructs, similar numbers of *Alu* + cells were observed in the 3D vs. 2D group at both 4 and 8 weeks (**Figure 5B**). No significant differences in the numbers of *Alu* + cells were detected between the groups at 4 or 8 weeks ($p > 0.05$).

DISCUSSION

The present study investigated the ectopic BTE potential of HPLG-PLATMC constructs containing spheroid (3D) or dissociated (2D) BMSC or GPC in a subcutaneous mouse model. The main findings were 1) significantly greater mineralization in constructs of 3D vs. 2D BMSC, 2) comparable mineralization in 2D GPC vs. 2D BMSC, and 3) robust mineralization in cell-free constructs.

In the context of BTE, aggregation of MSC into 3D spheroids has been reported to recapitulate embryonic events during skeletal development and thereby promote their osteogenic differentiation (Hall and Miyake, 2000; Kale et al., 2000). We have recently reported significant upregulations of genes associated with self-renewal and osteogenic differentiation in xeno-free cultures of 3D vs. 2D GPC and BMSC, suggesting a greater potential for *in vivo* osteogenesis (Shanbhag et al., 2020b). Consistently, recent studies have reported superior bone regeneration in rodent orthotopic models when using 3D vs. 2D BMSC encapsulated in Matrigel® (Corning) (Yamaguchi et al., 2014) or alginate-based hydrogels (Ho et al., 2018); similar results were reported for periodontal ligament-derived cells (PDLCs) encapsulated in Matrigel® (Moritani et al., 2018). Conversely, a recent study reported no differences in the healing of mouse femoral defects treated with either 2D or 3D BMSC encapsulated in a commercial fibrin gel (Findeisen et al., 2021). In the present study, significantly greater ectopic mineralization was observed via μCT in 3D vs. 2D BMSC constructs. To our knowledge, only one previous study has reported μCT analysis of ectopic bone formation (Ruminski et al., 2018); another study reported conventional X-ray but not μCT-based assessment of spheroid-hydrogel constructs (Ho et al., 2016). Nevertheless, our findings are supported by previous studies, which reported superior ectopic bone formation by 3D vs. 2D BMSC in calcium phosphate + platelet-rich plasma (PRP) complexes (Chatterjea et al., 2017) or RGD-modified alginate hydrogels (Ho et al., 2016). In the former study (Chatterjea et al., 2017), ectopic bone formation by spheroid BMSC was further enhanced in the presence of PRP, suggesting a synergistic effect of BMSC and platelet-derived growth factors (Shanbhag et al., 2017).

Fibrin- and platelet-based hydrogels, e.g., PRP, have been extensively used as scaffolds for bone regeneration (Soffer et al., 2003). In the present study, a fibrin supplemented HPLG was used to encapsulate the GPC and BMSC spheroids—to preserve their 3D architecture during *in vivo* delivery (Robinson et al., 2016). Indeed, platelet growth factors are known to promote MSC osteogenic differentiation *in vitro* (Kasten et al., 2006; Zhang et al., 2011; Huang et al., 2012; Trouillas et al., 2013; Chatterjea et al., 2017) and bone formation *in vivo* (Kasten et al., 2006; Trouillas et al., 2013; Chatterjea et al., 2017). However, an interesting (and potentially confounding) observation herein was the robust mineralization in cell-free HPLG-PLATMC constructs; after

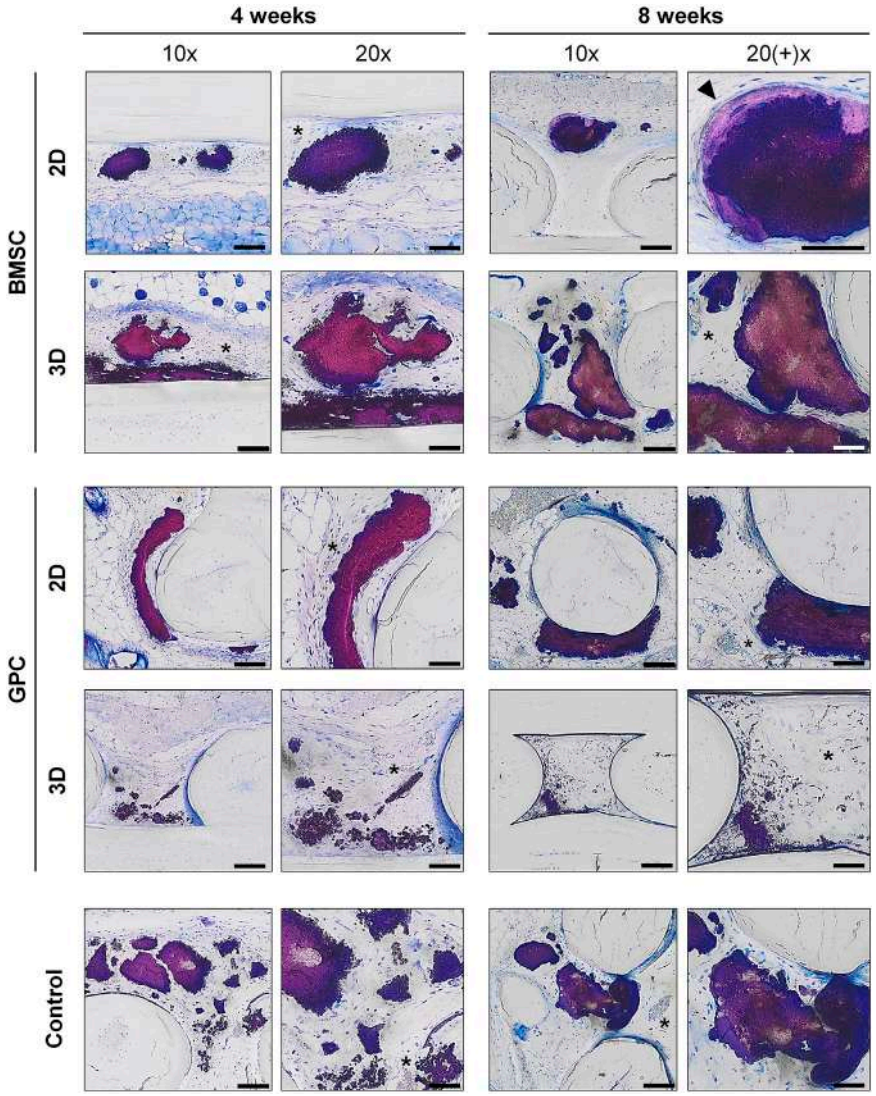

FIGURE 7 | Undecalcified histology. Representative images of BMSC, GPC and control constructs (no cells) after 4 and 8 weeks (thin ground sections, Levi Lazko staining); * indicate blood vessels; arrow indicates the only instance of "bone-like" tissue observed in the study; scale bars 100 µm (10x) and 50 µm (20x).

8 weeks, the greatest µCT-based mineralization was observed in the cell-free group. Since PLATMC is biologically inert, the observed mineralization could be attributed to the HPLG. As already mentioned, although platelet growth factors (PRP) have been shown to enhance MSC-mediated ectopic bone formation, to our knowledge, no studies have detected ectopic bone formation in cell-free fibrin- or PRP-constructs alone (Yamada et al., 2003; Osathanon et al., 2008; Murphy et al., 2015). In context, previous studies have tested "HPL coated" ceramic scaffolds for ectopic and orthotopic bone formation; scaffolds were immersed in HPL for 24 h prior to experiments (Leotot et al., 2013; Bolte et al., 2019). While the HPL coating itself did not promote bone formation, it enhanced the osteogenic potential of BMSC seeded on the scaffolds (Leotot et al., 2013; Bolte et al., 2019). Therefore, whether (and if so, how) human HPL (G) alone can lead to ectopic bone formation requires further investigation.

When comparing cell types herein, comparable ectopic mineralization was observed in constructs of 2D-GPC (MdV/TV 0.70%) vs. 2D-BMSC (0.54%) after 8 weeks. Even constructs of 3D-BMSC (1.03%) did not significantly outperform those of 2D-GPC (0.70%), suggesting that GPC may have the potential to substitute BMSC in future BTE applications. Several studies have investigated *in vivo* bone formation by GPC; some studies have compared the ectopic bone forming potential of GPC and BMSC, of which, three (Fournier et al., 2010; Tomar et al., 2010; Zorin et al., 2014) reported comparable histological "bone formation" between GPC and BMSC (**Supplementary Table S1**). However, the morphology of mineralized tissues formed by GPC is highly variable in the reported literature—to our knowledge, only few studies have reported regular organized bone tissue with

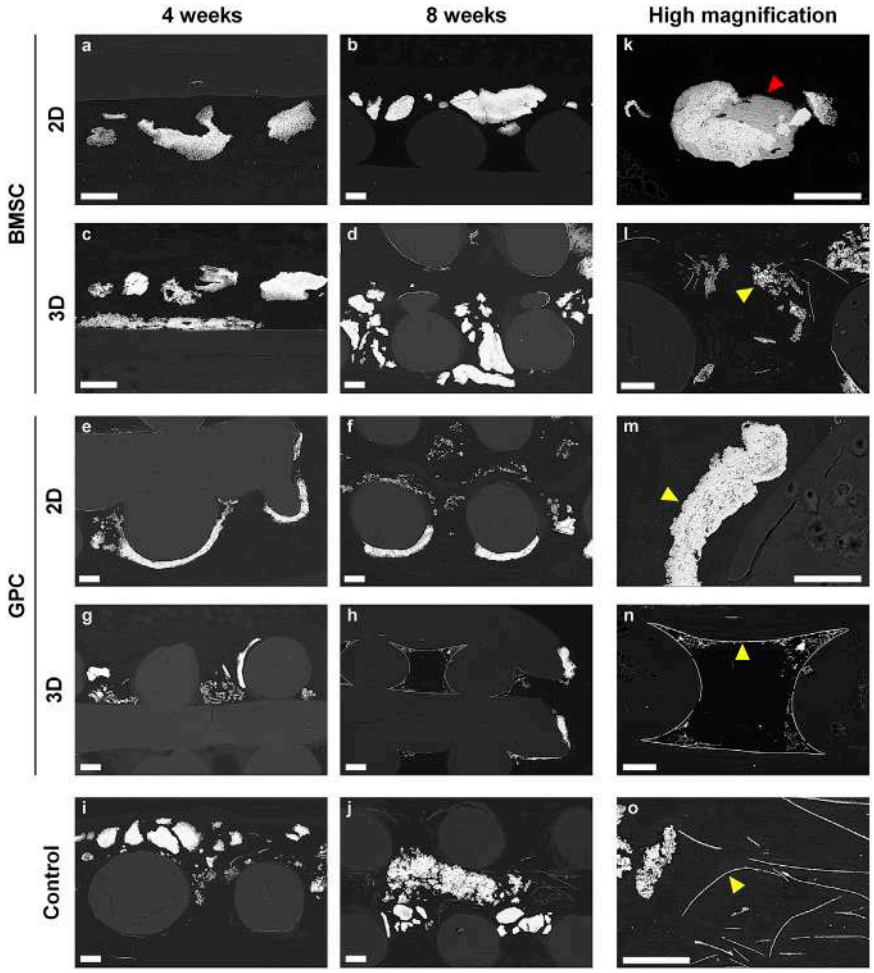

FIGURE 8 | SEM analysis. **(A–J)** Representative images of BMSC, GPC and control constructs (no cells) after 4 and 8 weeks. **(K–O)** Corresponding high magnification images from each group; yellow arrows indicate the different patterns of mineralization: **(K,M)** sheet/plate, **(L)** globular, **(N,O)** filament-like; red arrow indicates the only instance of "bone-like" tissue observed in the study; scale bars 100 μm.

embedded (osteocytes) and/or bone forming cells (osteoblasts) (**Supplementary Table S1**). These differences in mineralization produced by GPC and BMSC may be explained by the so-called "tissue source variability" (Xu et al., 2017). BMSC are naturally resident in the bone marrow—a specialized tissue niche, and have an inherent propensity for osteogenic differentiation (Hoch and Leach, 2015). Conversely, gingiva is a connective tissue with a mainly supportive function and a large fibroblast-population. Indeed, fibroblasts from various tissues including gingiva are reported to be indistinguishable from BMSC *in vitro* based on the "minimal MSC criteria" (Denu et al., 2016), and the presence of a "true" MSC-like population in gingiva remains to be identified *in vivo* (da Silva Meirelles et al., 2008). Nevertheless, gingiva represents a promising alternative source of progenitor cells for BTE applications.

In contrast to the traditional histological picture of lamellar bone with embedded (osteocytes) and lining cells, an atypical pattern of mineral deposition/precipitation was observed in the constructs herein, regardless of the type or presence of cells. The mineralized areas often appeared as solid masses or aggregates, with no internal lamellar structure or canals containing blood vessels. However, in several instances the mineralized areas revealed the presence of embedded cells, including transplanted BMSC and GPC; in one instance of 2D-BMSC, organized bone-like tissue with embedded osteocytes was observed. A similar pattern of atypical mineralization has previously been reported in rat calvarial defects treated with collagen membranes (Kuchler et al., 2018; Feher et al., 2021). It has been hypothesized that the collagen fibres underwent mineralization via cell-independent mechanisms and thereby served as "scaffolds" for subsequent bone formation (Nudelman et al., 2013) and may explain the observations herein. We observed organized and cellular (osteocyte containing) bone-like tissue around the mineral deposits in one specimen of the 2D-BMSC group at 8 weeks—the mineral deposits showed roughened borders characteristic of surface resorption. This finding supports the hypothesis that the mineral deposits may first undergo resorption and

subsequently serve as scaffolds for new bone formation. Other studies have reported dystrophic mineralization of biomaterials in ectopic sites, related to nucleation of calcium-phosphate complexes (Schoen and Levy, 2013; Lotsari et al., 2018). However, extending these hypotheses to the mineralization patterns observed herein is rather speculative, and the exact mechanism(s) of mineralization remains unclear.

Alu + GPC and BMSC were detected in the ectopic transplants herein. Detection of transplanted cells via ISH is well established and may assist in understanding the mechanism(s) of *in vivo* bone formation (Mankani et al., 2007; Janicki et al., 2011). It is relevant to note herein that cells (both GPC and BMSC) from pooled donors were used in the present study—to minimize donor-related variation and as a potential future strategy for allogeneic "off-the-shelf" cell therapy. The current literature is inconclusive regarding the mechanism(s) of bone formation by transplanted human MSC—either from independent or pooled donors, i.e., whether this occurs primarily via direct osteogenic differentiation of transplanted cells, paracrine stimulation of host cells, immune modulation, or a combination of factors (Moll et al., 2020). Indeed, *Alu* + cells were identified in the areas of mineralization herein; in several instances, these cells were embedded within the mineralization(s) and/or associated with areas of dense collagen deposition. However, the embedded cells did not demonstrate the well-defined surrounding lacunae characteristic of osteocytes. Previous studies have characterized the role of exogenous cells in ectopic and orthotopic bone formation. For example, transplantation of allogeneic BMSC in immunocompetent mice revealed immune modulation rather than osteoblastic differentiation in one study (Tsujigiwa et al., 2013; Takabatake et al., 2018). In another study, no transplanted human BMSC could be detected in ectopic mouse transplants beyond 2 weeks, despite robust bone formation at 8 weeks (Gamblin et al., 2014). These reports further suggest that transplanted BMSC contribute to bone formation via stimulation of tissue-resident progenitor cells rather than direct differentiation into osteoblasts (Tsujigiwa et al., 2013; Takabatake et al., 2018). Indeed, the type and immune status of the animal-model may also influence *in vivo* osteogenesis (Garske et al., 2020). Based on previous literature, we selected the athymic "nude" mouse model (Scott et al., 2012), where the absence of functional T lymphocytes (and partial defect of B cells) allows for xenogeneic transplantation of human cells without immune rejection. Others have reported favourable ectopic bone formation by human BMSC in NMRI-nude (Brennan et al., 2014; Gamblin et al., 2014) and NOD-SCID mice (Suliman et al., 2019), which present certain differences in immune status compared to our mouse model. Nevertheless, the exact mechanism(s) of osteogenesis and/or mineralization by xeno-transplanted BMSC in immunocompromised rodent models remains to be elucidated.

CONCLUSION

In summary, ectopic implantation of the various HPLG-PLATMC constructs revealed significantly greater mineralization in those with 3D-BMSC vs. 2D-BMSC and comparable mineralization in those with 2D-GPC vs. 2D-BMSC. However, the effect of cell transplantation was confounded by that of HPLG, based on the robust mineralization observed in cell-free constructs. Although transplanted GPC and BMSC were detected *in situ* after 8 weeks, their direct contribution to mineralization could neither be confirmed nor excluded. GPC represents a promising alternative to BMSC for BTE. The HPLG-PLATMC constructs herein represent promising and clinically relevant scaffolds for BTE applications.

DATA AVAILABILITY STATEMENT

The raw data supporting the conclusion of this article will be made available by the authors, without undue reservation.

ETHICS STATEMENT

The animal study was reviewed and approved by Norwegian Animal Research Authority (Mattilsynet; FOTS-18738).

AUTHOR CONTRIBUTIONS

SSh and KM conceived and designed the study. SSh performed the experiments, data collection, data analysis and drafted the manuscript. CK, SM-A, MY, HD, DE, and ST assisted with data collection, data analysis/interpretation and drafting the manuscript. AS, AB, SSu, and KM assisted with data analysis/interpretation and drafting the manuscript. All authors read and approved the final version of the manuscript.

FUNDING

This work was supported by Helse Vest Strategic Research Funding, Norway (502027 and 912260/2019), Research Council of Norway (BEHANDLING-273551 and Centers of Excellence-22325), Trond Mohn Foundation, Norway (BFS2018TMT10) and the ITI Foundation, Switzerland (117/2015).

ACKNOWLEDGMENTS

We thank the Bloodbank at Haukeland University Hospital for supplying the platelets and the Molecular Imaging Center (MIC), University of Bergen, for assistance with microscopy and imaging. We also thank Bendik Nordanger, Siren Fromreide and Randi Lavik from the Department of Clinical Medicine, University of Bergen, for assistance with the histology.

SUPPLEMENTARY MATERIAL

The Supplementary Material for this article can be found online at: https://www.frontiersin.org/articles/10.3389/fbioe.2021.783468/full#supplementary-material

REFERENCES

Bankhead, P., Loughrey, M. B., Fernández, J. A., Dombrowski, Y., McArt, D. G., Dunne, P. D., et al. (2017). QuPath: Open Source Software for Digital Pathology Image Analysis. *Sci. Rep.* 7 (1), 16878. doi:10.1038/s41598-017-17204-5

Berglundh, T., and Stavropoulos, A. (2012). Preclinical *In Vivo* Research in Implant Dentistry. Consensus of the Eighth European Workshop on Periodontology. *J. Clin. Periodontol.* 39 (Suppl. 12), 1–5. doi:10.1111/j.1600-051X.2011.01827.x

Bieback, K., Fernandez-Muñoz, B., Pati, S., and Schäfer, R. (2019). Gaps in the Knowledge of Human Platelet Lysate as a Cell Culture Supplement for Cell Therapy: a Joint Publication from the AABB and the International Society for Cell & Gene Therapy. *Int. Soc. Cel Gene TherapyTransfusion* 59, 3448–3460. doi:10.1111/trf.15483

Bolte, J., Vater, C., Culla, A. C., Ahlfeld, T., Nowotny, J., Kasten, P., et al. (2019). Two-step Stem Cell Therapy Improves Bone Regeneration Compared to Concentrated Bone Marrow Therapy. *J. Orthop. Res.* 37 (6), 1318–1328. doi:10.1002/jor.24215

Brennan, M. Á., Renaud, A., Amiaud, J., Rojewski, M. T., Schrezenmeier, H., Heymann, D., et al. (2014). Pre-clinical Studies of Bone Regeneration with Human Bone Marrow Stromal Cells and Biphasic Calcium Phosphate. *Stem Cel Res Ther* 5, 114. doi:10.1186/scrt504

Cesarz, Z., and Tamama, K. (2016). Spheroid Culture of Mesenchymal Stem Cells. *Stem Cell Int.* 2016, 1–11. doi:10.1155/2016/9176357

Chatterjea, A., LaPointe, V. L., LaPointe, V., Barradas, A., Garritsen, H., Yuan, H., et al. (2017). Cell Aggregation Enhances Bone Formation by Human Mesenchymal Stromal Cells. *eCM* 33, 121–129. doi:10.22203/eCM.v033a09

da Silva Meirelles, L., Caplan, A. I., and Nardi, N. B. (2008). In Search of the *In Vivo* Identity of Mesenchymal Stem Cells. *Stem Cells* 26 (9), 2287–2299. doi:10.1634/stemcells.2007-1122

Denu, R. A., Nemcek, S., Bloom, D. D., Goodrich, A. D., Kim, J., Mosher, D. F., et al. (2016). Fibroblasts and Mesenchymal Stromal/stem Cells Are Phenotypically Indistinguishable. *Acta Haematol.* 136, 85–97. doi:10.1159/000445096

Dominici, M., Le Blanc, K., Mueller, I., Slaper-Cortenbach, I., Marini, F. C., Krause, D. S., et al. (2006). Minimal Criteria for Defining Multipotent Mesenchymal Stromal Cells. The International Society for Cellular Therapy Position Statement. *Cytotherapy* 8 (4), 315–317. doi:10.1080/14653240600855905

Feher, B., Apaza Alccayhuaman, K. A., Strauss, F. J., Lee, J.-S., Tangl, S., Kuchler, U., et al. (2021). Osteoconductive Properties of Upside-Down Bilayer Collagen Membranes in Rat Calvarial Defects. *Int. J. Implant Dent* 7 (1), 50. doi:10.1186/s40729-021-00333-y

Fekete, N., Gadelorge, M., Fürst, D., Maurer, C., Dausend, J., Fleury-Cappellesso, S., et al. (2012). Platelet Lysate from Whole Blood-Derived Pooled Platelet Concentrates and Apheresis-Derived Platelet Concentrates for the Isolation and Expansion of Human Bone Marrow Mesenchymal Stromal Cells: Production Process, Content and Identification of Active Components. *Cytotherapy* 14 (5), 540–554. doi:10.3109/14653249.2012.655420

Findeisen, L., Bolte, J., Vater, C., Petzold, C., Quade, M., Müller, L., et al. (2021). Cell Spheroids Are as Effective as Single Cells Suspensions in the Treatment of Critical-Sized Bone Defects. *BMC Musculoskelet. Disord.* 22 (1), 401, 2021 . ARTN 401. doi:10.1186/s12891-021-04264-y

Follin, B., Juhl, M., Cohen, S., Pedersen, A. E., Kastrup, J., and Ekblond, A. (2016). Increased Paracrine Immunomodulatory Potential of Mesenchymal Stromal Cells in Three-Dimensional Culture. *Tissue Eng. B: Rev.* 22 (4), 322–329. doi:10.1089/ten.TEB.2015.0532

Fournier, B. P. J., Ferre, F. C., Couty, L., Lataillade, J.-J., Gourven, M., Naveau, A., et al. (2010). Multipotent Progenitor Cells in Gingival Connective Tissue. *Tissue Eng. A* 16, 2891–2899. doi:10.1089/ten.tea.2009.0796

Gamblin, A.-L., Brennan, M. A., Renaud, A., Yagita, H., Lézot, F., Heymann, D., et al. (2014). Bone Tissue Formation with Human Mesenchymal Stem Cells and Biphasic Calcium Phosphate Ceramics: the Local Implication of Osteoclasts and Macrophages. *Biomaterials* 35 (36), 9660–9667. doi:10.1016/j.biomaterials.2014.08.018

Garske, D. S., Schmidt-Bleek, K., Ellinghaus, A., Dienelt, A., Gu, L., Mooney, D. J., et al. (2020). Alginate Hydrogels for *In Vivo* Bone Regeneration: The Immune Competence of the Animal Model Matters. *Tissue Eng. Part A* 26 (15-16), 852–862. doi:10.1089/ten.TEA.2019.0310

Hall, B. K., and Miyake, T. (2000). All for One and One for All: Condensations and the Initiation of Skeletal Development. *Bioessays* 22, 138–147. doi:10.1002/(sici)1521-1878(200002)22:2<138:aid-bies5>3.0.co;2-4

Hassan, M. N., Yassin, M. A., Suliman, S., Lie, S. A., Gjengedal, H., and Mustafa, K. (2019). The Bone Regeneration Capacity of 3D-Printed Templates in Calvarial Defect Models: A Systematic Review and Meta-Analysis. *Acta Biomater.* 91, 1–23. doi:10.1016/j.actbio.2019.04.017

Ho, S. S., Hung, B. P., Heyrani, N., Lee, M. A., and Leach, J. K. (2018). Hypoxic Preconditioning of Mesenchymal Stem Cells with Subsequent Spheroid Formation Accelerates Repair of Segmental Bone Defects. *Stem Cells* 36 (9), 1393–1403. doi:10.1002/stem.2853

Ho, S. S., Murphy, K. C., Binder, B. Y. K., Vissers, C. B., and Leach, J. K. (2016). Increased Survival and Function of Mesenchymal Stem Cell Spheroids Entrapped in Instructive Alginate Hydrogels. *STEM CELLS Translational Med.* 5 (6), 773–781. doi:10.5966/sctm.2015-0211

Hoch, A. I., and Leach, J. K. (2015). Concise Review: Optimizing Expansion of Bone Marrow Mesenchymal Stem/stromal Cells for Clinical Applications. *Stem Cell Transl Med* 4 (4), 412. doi:10.5966/sctm.2013-0196erratum

Huang, S., Jia, S., Liu, G., Fang, D., and Zhang, D. (2012). Osteogenic Differentiation of Muscle Satellite Cells Induced by Platelet-Rich Plasma Encapsulated in Three-Dimensional Alginate Scaffold. *Oral Surg. Oral Med. Oral Pathol. Oral Radiol.* 114 (5 Suppl. l), S32–S40. doi:10.1016/j.tripleo.2011.07.048

Jain, S., Yassin, M. A., Fuoco, T., Liu, H., Mohamed-Ahmed, S., Mustafa, K., et al. (2020). Engineering 3D Degradable, Pliable Scaffolds toward Adipose Tissue Regeneration; Optimized Printability, Simulations and Surface Modification. *J. Tissue Eng.* 11, 204173142095431. doi:10.1177/2041731420954316

Janicki, P., Boeuf, S., Boeuf, S., Steck, E., Egermann, M., Kasten, P., et al. (2011). Prediction of *In Vivo* Bone Forming Potency of Bone Marrow-Derived Human Mesenchymal Stem Cells. *eCM* 21, 488–577. doi:10.22203/ecm.v021a37

Kale, S., Biermann, S., Edwards, C., Tarnowski, C., Morris, M., and Long, M. W. (2000). Three-dimensional Cellular Development Is Essential for *Ex Vivo* Formation of Human Bone. *Nat. Biotechnol.* 18, 954–958. doi:10.1038/79439

Kasten, P., Vogel, J., Luginbühl, R., Niemeyer, P., Weiss, S., Schneider, S., et al. (2006). Influence of Platelet-Rich Plasma on Osteogenic Differentiation of Mesenchymal Stem Cells and Ectopic Bone Formation in Calcium Phosphate Ceramics. *Cells Tissues Organs* 183 (2), 68–79. doi:10.1159/000095511

Kilkenny, C., Browne, W. J., Cuthill, I. C., Emerson, M., and Altman, D. G. (2010). Improving Bioscience Research Reporting: the ARRIVE Guidelines for Reporting Animal Research. *Plos Biol.* 8, e1000412. doi:10.1371/journal.pbio.1000412

Kuchler, U., Rybaczek, T., Dobask, T., Heimel, P., Tangl, S., Klehm, J., et al. (2018). Bone-conditioned Medium Modulates the Osteoconductive Properties of Collagen Membranes in a Rat Calvaria Defect Model. *Clin. Oral Impl Res.* 29 (4), 381–388. doi:10.1111/clr.13133

Leotot, J., Coquelin, L., Bodivit, G., Bierling, P., Hernigou, P., Rouard, H., et al. (2013). Platelet Lysate Coating on Scaffolds Directly and Indirectly Enhances Cell Migration, Improving Bone and Blood Vessel Formation. *Acta Biomater.* 9, 6630–6640. doi:10.1016/j.actbio.2013.02.003

Lotsari, A., Rajasekharan, A. K., Halvarsson, M., and Andersson, M. (2018). Transformation of Amorphous Calcium Phosphate to Bone-like Apatite. *Nat. Commun.* 9 (1), 4170. doi:10.1038/s41467-018-06570-x

Mankani, M. H., Kuznetsov, S. A., and Robey, P. G. (2007). Formation of Hematopoietic Territories and Bone by Transplanted Human Bone Marrow Stromal Cells Requires a Critical Cell Density. *Exp. Hematol.* 35 (6), 995–1004. doi:10.1016/j.exphem.2007.01.051

Mitrano, T. I., Grob, M. S., Carrión, F., Nova-Lamperti, E., Luz, P. A., Fierro, F. S., et al. (2010). Culture and Characterization of Mesenchymal Stem Cells from Human Gingival Tissue. *J. Periodontol.* 81, 917–925. doi:10.1902/jop.2010.090566

Mohamed-Ahmed, S., Fristad, I., Lie, S. A., Suliman, S., Mustafa, K., Vindenes, H., et al. (2018). Adipose-derived and Bone Marrow Mesenchymal Stem Cells: a Donor-Matched Comparison. *Stem Cel Res Ther* 9 (1), 168. doi:10.1186/s13287-018-0914-1

Moll, G., Hoogduijn, M. J., and Ankrum, J. A. (2020). Editorial: Safety, Efficacy and Mechanisms of Action of Mesenchymal Stem Cell Therapies. *Front. Immunol.* 11, 243. doi:10.3389/fimmu.2020.00243

Moritani, Y., Usui, M., Sano, K., Nakazawa, K., Hanatani, T., Nakatomi, M., et al. (2018). Spheroid Culture Enhances Osteogenic Potential of Periodontal

Ligament Mesenchymal Stem Cells. *J. Periodont Res.* 53, 870–882. doi:10.1111/jre.12577

Murphy, K. C., Fang, S. Y., and Leach, J. K. (2014). Human Mesenchymal Stem Cell Spheroids in Fibrin Hydrogels Exhibit Improved Cell Survival and Potential for Bone Healing. *Cell Tissue Res* 357, 91–99. doi:10.1007/s00441-014-1830-z

Murphy, K. C., Hughbanks, M. L., Binder, B. Y. K., Vissers, C. B., and Leach, J. K. (2015). Engineered Fibrin Gels for Parallel Stimulation of Mesenchymal Stem Cell Proangiogenic and Osteogenic Potential. *Ann. Biomed. Eng.* 43 (8), 2010–2021. doi:10.1007/s10439-014-1227-x

Nudelman, F., Lausch, A. J., Sommerdijk, N. A. J. M., and Sone, E. D. (2013). *In Vitro* models of Collagen Biomineralization. *J. Struct. Biol.* 183 (2), 258–269. doi:10.1016/j.jsb.2013.04.003

Osathanon, T., Linnes, M. L., Rajachar, R. M., Ratner, B. D., Somerman, M. J., and Giachelli, C. M. (2008). Microporous Nanofibrous Fibrin-Based Scaffolds for Bone Tissue Engineering. *Biomaterials* 29 (30), 4091–4099. doi:10.1016/j.biomaterials.2008.06.030

Petrenko, Y., Syková, E., and Kubinová, Š. (2017). The Therapeutic Potential of Three-Dimensional Multipotent Mesenchymal Stromal Cell Spheroids. *Stem Cel Res Ther* 8, 94. doi:10.1186/s13287-017-0558-6

Pittenger, M. F., Discher, D. E., Péault, B. M., Phinney, D. G., Hare, J. M., and Caplan, A. I. (2019). Mesenchymal Stem Cell Perspective: Cell Biology to Clinical Progress. *NPJ Regen. Med.* 4, 22. doi:10.1038/s41536-019-0083-6

Robinson, S. T., Douglas, A. M., Chadid, T., Kuo, K., Rajabalan, A., Li, H., et al. (2016). A Novel Platelet Lysate Hydrogel for Endothelial Cell and Mesenchymal Stem Cell-Directed Neovascularization. *Acta Biomater.* 36, 86–98. doi:10.1016/j.actbio.2016.03.002

Rumiński, S., Ostrowska, B., Jaroszewicz, J., Skirecki, T., Włodarski, K., Święszkowski, W., et al. (2018). Three-dimensional Printed Polycaprolactone-Based Scaffolds Provide an Advantageous Environment for Osteogenic Differentiation of Human Adipose-Derived Stem Cells. *J. Tissue Eng. Regen. Med.* 12 (1), e473–e485. doi:10.1002/term.2310

Sart, S., Tsai, A.-C., Li, Y., and Ma, T. (2014). Three-dimensional Aggregates of Mesenchymal Stem Cells: Cellular Mechanisms, Biological Properties, and Applications. *Tissue Eng. Part B: Rev.* 20, 365–380. doi:10.1089/ten.teb.2013.0537

Schoen, F. J., and Levy, R. J. (2013). "Pathological Calcification of Biomaterials," in *Biomaterials Science*. Editors B.D. Ratner, A.S. Hoffman, F.J. Schoen, and J.E. Lemons. Third Edition (Academic Press), 739–754. doi:10.1016/b978-0-08-087780-8.00063-2

Scott, M. A., Levi, B., Askarinam, A., Nguyen, A., Rackohn, T., Ting, K., et al. (2012). Brief Review of Models of Ectopic Bone Formation. *Stem Cell Dev* 21 (655), 655–667. doi:10.1089/scd.2011.0517

Shanbhag, S., Mohamed-Ahmed, S., Lunde, T. H. F., Suliman, S., Bolstad, A. I., Hervig, T., et al. (2020a). Influence of Platelet Storage Time on Human Platelet Lysates and Platelet Lysate-Expanded Mesenchymal Stromal Cells for Bone Tissue Engineering. *Stem Cel Res Ther* 11 (1), 351. doi:10.1186/s13287-020-01863-9

Shanbhag, S., and Shanbhag, V. (2015). Clinical Applications of Cell-Based Approaches in Alveolar Bone Augmentation: a Systematic Review. *Clin. Implant Dentistry Relat. Res.* 17 (Suppl. 1), e17–e34. doi:10.1111/cid.12103

Shanbhag, S., Stavropoulos, A., Suliman, S., Hervig, T., and Mustafa, K. (2017). Efficacy of Humanized Mesenchymal Stem Cell Cultures for Bone Tissue Engineering: a Systematic Review with a Focus on Platelet Derivatives. *Tissue Eng. Part B: Rev.* 23, 552–569. doi:10.1089/ten.teb.2017.0093

Shanbhag, S., Suliman, S., Bolstad, A. I., Stavropoulos, A., and Mustafa, K. (2020b). Xeno-Free Spheroids of Human Gingiva-Derived Progenitor Cells for Bone Tissue Engineering. *Front. Bioeng. Biotechnol.* 8, 968. doi:10.3389/fbioe.2020.00968

Shanbhag, S., Suliman, S., Pandis, N., Stavropoulos, A., Sanz, M., and Mustafa, K. (2019). Cell Therapy for Orofacial Bone Regeneration: A Systematic Review and Meta-Analysis. *J. Clin. Periodontol.* 46 (Suppl. 21), 162–182. doi:10.1111/jcpe.13049

Sharpe, P. T. (2016). Dental Mesenchymal Stem Cells. *Development* 143, 2273–2280. doi:10.1242/dev.134189

Soffer, E., Ouhayoun, J. P., and Anagnostou, F. (2003). Fibrin Sealants and Platelet Preparations in Bone and Periodontal Healing. *Oral Surg. Oral Med. Oral Pathol. Oral Radiol. Endodontology* 95 (5), 521–528. doi:10.1067/moe.2003.152

Suliman, S., Ali, H. R. W., Karlsen, T. A., Amiaud, J., Mohamed-Ahmed, S., Layrolle, P., et al. (2019). Impact of Humanised Isolation and Culture Conditions on Stemness and Osteogenic Potential of Bone Marrow Derived Mesenchymal Stromal Cells. *Sci. Rep.* 9 (1), 16031. doi:10.1038/s41598-019-52442-9

Takabatake, K., Tsujigiwa, H., Song, Y., Matsuda, H., Kawai, H., Fujii, M., et al. (2018). The Role of Bone Marrow-Derived Cells during Ectopic Bone Formation of Mouse Femoral Muscle in GFP Mouse Bone Marrow Transplantation Model. *Int. J. Med. Sci.* 15 (8), 748–757. doi:10.7150/ijms.24605

Tomar, G. B., Srivastava, R. K., Gupta, N., Barhanpurkar, A. P., Pote, S. T., Jhaveri, H. M., et al. (2010). Human Gingiva-Derived Mesenchymal Stem Cells Are superior to Bone Marrow-Derived Mesenchymal Stem Cells for Cell Therapy in Regenerative Medicine. *Biochem. Biophysical Res. Commun.* 393, 377–383. doi:10.1016/j.bbrc.2010.01.126

Trouillas, M., Prat, M., Doucet, C., Ernou, I., Laplace-Builhé, C., Blancard, P. S., et al. (2013). A New Platelet Cryoprecipitate Glue Promoting Bone Formation after Ectopic Mesenchymal Stromal Cell-Loaded Biomaterial Implantation in Nude Mice. *Stem Cel Res Ther* 4 (1), 1. doi:10.1186/scrt149

Tsujigiwa, H., Hirata, Y., Katase, N., Buery, R. R., Tamamura, R., Ito, S., et al. (2013). The Role of Bone Marrow-Derived Cells during the Bone Healing Process in the GFP Mouse Bone Marrow Transplantation Model. *Calcif Tissue Int.* 92 (3), 296–306. doi:10.1007/s00223-012-9685-3

Xu, L., Liu, Y., Sun, Y., Wang, B., Xiong, Y., Lin, W., et al. (2017). Tissue Source Determines the Differentiation Potentials of Mesenchymal Stem Cells: a Comparative Study of Human Mesenchymal Stem Cells from Bone Marrow and Adipose Tissue. *Stem Cel Res Ther* 8 (1), 275. doi:10.1186/s13287-017-0716-x

Yamada, S., Shanbhag, S., and Mustafa, K. (2022). Scaffolds in Periodontal Regenerative Treatment. *Dental Clin. North America* 66, 111–130. doi:10.1016/j.cden.2021.06.004

Yamada, Y., Seong Boo, J., Ozawa, R., Nagasaka, T., Okazaki, Y., Hata, K.-i., et al. (2003). Bone Regeneration Following Injection of Mesenchymal Stem Cells and Fibrin Glue with a Biodegradable Scaffold. *J. Craniomaxillofac. Surg.* 31 (1), 27–33. doi:10.1016/s1010-5182(02)00143-9

Yamaguchi, Y., Ohno, J., Sato, A., Kido, H., and Fukushima, T. (2014). Mesenchymal Stem Cell Spheroids Exhibit Enhanced *In-Vitro* and *In-Vivo* Osteoregenerative Potential. *BMC Biotechnol.* 14, 105. doi:10.1186/s12896-014-0105-9

Zhang, S., Mao, T., and Chen, F. (2011). Influence of Platelet-Rich Plasma on Ectopic Bone Formation of Bone Marrow Stromal Cells in Porous Coral. *Int. J. Oral Maxillofac. Surg.* 40 (9), 961–965. doi:10.1016/j.ijom.2011.02.037

Zorin, V. L., Komlev, V. S., Zorina, A. I., Khromova, N. V., Solovieva, E. V., Fedotov, A. Y., et al. (2014). Octacalcium Phosphate Ceramics Combined with Gingiva-Derived Stromal Cells for Engineered Functional Bone Grafts. *Biomed. Mater.* 9 (5), 055005. doi:10.1088/1748-6041/9/5/055005

Conflict of Interest: The authors declare that the research was conducted in the absence of any commercial or financial relationships that could be construed as a potential conflict of interest.

Publisher's Note: All claims expressed in this article are solely those of the authors and do not necessarily represent those of their affiliated organizations, or those of the publisher, the editors and the reviewers. Any product that may be evaluated in this article, or claim that may be made by its manufacturer, is not guaranteed or endorsed by the publisher.

Copyright © 2021 Shanbhag, Kampleitner, Mohamed-Ahmed, Yassin, Dongre, Costea, Tangl, Stavropoulos, Bolstad, Suliman and Mustafa. This is an open-access article distributed under the terms of the Creative Commons Attribution License (CC BY). The use, distribution or reproduction in other forums is permitted, provided the original author(s) and the copyright owner(s) are credited and that the original publication in this journal is cited, in accordance with accepted academic practice. No use, distribution or reproduction is permitted which does not comply with these terms.

frontiers in Bioengineering and Biotechnology

ORIGINAL RESEARCH
published: 26 August 2021
doi: 10.3389/fbioe.2021.739225

Spheroid Coculture of Human Gingiva-Derived Progenitor Cells With Endothelial Cells in Modified Platelet Lysate Hydrogels

Siddharth Shanbhag[1,2], Ahmad Rashad[1], Ellen Helgeland Nymark[3], Salwa Suliman[1], Catharina de Lange Davies[3], Andreas Stavropoulos[4,5], Anne Isine Bolstad[1] and Kamal Mustafa[1]**

[1]Center for Translational Oral Research (TOR), Department of Clinical Dentistry, Faculty of Medicine, University of Bergen, Bergen, Norway, [2]Department of Immunology and Transfusion Medicine, Haukeland University Hospital, Bergen, Norway, [3]Department of Physics, Norwegian University of Science and Technology, Trondheim, Norway, [4]Department of Periodontology, Faculty of Odontology, Malmö University, Malmö, Sweden, [5]Division of Regenerative Medicine and Periodontology, University Clinics of Dental Medicine, University of Geneva, Geneva, Switzerland

OPEN ACCESS

Edited by:
Guangdong Zhou, Shanghai Jiao Tong University, China

Reviewed by:
Menekse Ermis Sen, Middle East Technical University, Turkey
Fengxuan Han, Soochow University, China

***Correspondence:**
Siddharth Shanbhag
siddharth.shanbhag@uib.no
Kamal Mustafa
kamal.mustafa@uib.no

Specialty section:
This article was submitted to Tissue Engineering and Regenerative Medicine, a section of the journal Frontiers in Bioengineering and Biotechnology

Received: *10 July 2021*
Accepted: *12 August 2021*
Published: *26 August 2021*

Citation:
Shanbhag S, Rashad A, Nymark EH, Suliman S, de Lange Davies C, Stavropoulos A, Bolstad AI and Mustafa K (2021) Spheroid Coculture of Human Gingiva-Derived Progenitor Cells With Endothelial Cells in Modified Platelet Lysate Hydrogels. Front. Bioeng. Biotechnol. 9:739225. doi: 10.3389/fbioe.2021.739225

Cell coculture strategies can promote angiogenesis within tissue engineering constructs. This study aimed to test the angiogenic potential of human umbilical vein endothelial cells (HUVEC) cocultured with gingiva-derived progenitor cells (GPC) as spheroids in a xeno-free environment. Human platelet lysate (HPL) was used as a cell culture supplement and as a hydrogel matrix (HPLG) for spheroid encapsulation. HUVEC and HUVEC + GPC (1:1 or 5:1) spheroids were encapsulated in various HPLG formulations. Angiogenesis was assessed via *in vitro* sprouting and *in vivo* chick chorioallantoic membrane (CAM) assays. HUVEC revealed characteristic *in vitro* sprouting in HPL/HPLG and this was significantly enhanced in cocultures with GPC ($p < 0.05$). A trend for greater sprouting was observed in 5:1 vs 1:1 HUVEC + GPC spheroids and in certain HPLG formulations ($p > 0.05$). Both HUVEC and HUVEC + GPC spheroids in HPLG revealed abundant and comparable neoangiogenesis in the CAM assay ($p > 0.05$). Spheroid coculture of HUVEC + GPC in HPLG represents a promising strategy to promote angiogenesis.

Keywords: spheroid culture, coculture (co-culture), angiogenesis, bone tissue engineering, platelet lysate

INTRODUCTION

In the context of bone tissue engineering (BTE), timely vascularization of *in vivo* implanted constructs is critical for cell survival, especially in regions distant from the host vasculature, since diffusion of oxygen and nutrients is only limited to a distance of 150–200 µm (Jain et al., 2005; Nguyen et al., 2012). Angiogenesis is an essential component of the bone regeneration cascade and its insufficiency is a major limiting factor for the clinical translation of BTE strategies (Kanczler and Oreffo, 2008). Mesenchymal stromal cells (MSC) are increasingly being used for BTE (Pittenger et al., 2019; Shanbhag et al., 2019), and one strategy has been to coculture MSC with endothelial cells (EC), to create *in vitro* "pre-vascularized" constructs with a network of primitive vessels that functionally anastomose with the host vasculature when implanted *in vivo* (Levenberg et al., 2005; Rouwkema et al., 2006). MSC are reported to stabilize these networks by adopting a pericyte-like phenotype, thereby enhancing EC-mediated angiogenesis and in turn, bone regeneration (Keramaris et al., 2012; Loibl et al., 2014; Shanbhag et al., 2017a).

MSC derived from bone marrow (BMSC) are the most widely tested. However, progenitor cells from less-invasive sources, e.g., adipose and oral tissues, are being explored (Friedenstein et al., 1968; Pittenger et al., 2019). Oral tissues, such as dental pulp, periodontal ligament and gingiva, represent alternative sources of "MSC-like" progenitor cells (Sharpe, 2016). Gingiva, in particular, can be harvested with minimal morbidity and contains a subpopulation of multipotent progenitor cells (GPC), which demonstrate an MSC-like phenotype, immunomodulatory properties, and osteogenic potential both *in vitro* and *in vivo* (Fournier et al., 2010; Mitrano et al., 2010), thus representing promising alternatives to BMSC for BTE applications (Stefanska et al., 2020).

A critical aspect in the clinical translation of cell therapies is the use of safe and standardized culture conditions. Although commonly used for MSC expansion, several limitations of xenogeneic fetal bovine serum (FBS) supplementation have been highlighted, and current recommendations from health authorities advocate the use of "xeno-free" protocols whenever possible (Bieback et al., 2019a). Accordingly, xeno-free alternatives such as pooled human platelet lysate (HPL), have emerged and have been shown to be comparable, and often superior, to FBS for the proliferation and differentiation of various types of MSC (Fekete et al., 2012; Shanbhag et al., 2017b; Shanbhag et al., 2020a). We have recently reported that xeno-free culture of human GPC in HPL vs FBS media results in enhanced growth, gene expression and differentiation (Shanbhag et al., 2020b). Moreover, the proliferation and tube formation of EC is reported to be enhanced in HPL (Tasev et al., 2015) and other xeno-free media (Bauman et al., 2018).

Current BTE strategies rely mainly on monolayer expansion of MSC in plastic-adherent cultures (Rojewski et al., 2019). However, this two-dimensional (2D) culture system is not representative of the 3D *in vivo* microenvironment of MSC and may therefore alter their phenotype and diminish their regenerative and immunomodulatory potential (Banfi et al., 2000; Hoch and Leach, 2015; Ghazanfari et al., 2017). Similar observations have been reported in EC; single dissociated EC are reported to be more likely to undergo apoptosis (Korff and Augustin, 1998). In contrast, the self-assembly or spontaneous aggregation of cells into 3D spheroids is mediated by unique cell-cell and cell-extracellular matrix (ECM) interactions, biomechanical cues and signaling pathways, which more closely simulate the *in vivo* microenvironment (Sart et al., 2014; Cesarz and Tamama, 2016). In contrast to 2D monolayers, 3D spheroid culture has been reported to enhance survival, stemness, paracrine activity, immunomodulation and multi-lineage differentiation of MSC (Follin et al., 2016; Petrenko et al., 2017) (Kale et al., 2000; Chatterjea et al., 2017). In the context of BTE applications, we have observed particular advantages of spheroid vs monolayer culture via a strong upregulation of osteogenesis-related genes in BMSC and GPC (Shanbhag et al., 2020b).

Traditional cell delivery methods involve direct seeding and attachment of cells on biomaterial scaffolds before *in vivo* transplantation. However, direct seeding may not be the optimal method for delivery of cell spheroids because the 3D structure, essential to maximize their *in vivo* effects, is lost. To preserve the 3D structure, encapsulation of spheroids in hydrogels represents an effective delivery system (Murphy et al., 2014; Murphy et al., 2015; Ho et al., 2018). Moreover, in the context of angiogenesis, when EC are cultured as spheroids in a hydrogel matrix, either alone or in coculture with MSC, 3D network formation occurs by closely mimicking *in vivo* sprouting angiogenesis (Korff and Augustin, 1999; Heiss et al., 2015). Since HPL is increasingly being used for clinical-grade MSC culture (Bieback et al., 2019b), extending its application as a hydrogel carrier represents a cost-effective strategy for tissue engineering. Furthermore, HPL gels may offer the added advantage of sustained cytokine release at regeneration sites (Robinson et al., 2016). Indeed, recent studies have demonstrated the potential of HPL hydrogels for encapsulating EC and MSC to create microvascular networks (Fortunato et al., 2016; Robinson et al., 2016).

Previous studies have investigated the capacity of MSC to support or enhance EC-mediated angiogenesis in monolayer cultures, most often in xenogeneic conditions (Steffens et al., 2009; Verseijden et al., 2010; Chen et al., 2013; Ucuzian et al., 2013; Strassburg et al., 2016). Others have studied angiogenesis-related outcomes in spheroid cocultures of MSC or fibroblasts with EC in xeno-free, i.e., human serum-supplemented, media (Eckermann et al., 2011; Bauman et al., 2018). In the former study, MSC-EC cocultures in xeno-free media (vs FBS) resulted in enhanced angiogenesis in an *in vivo* chick chorioallantoic membrane (CAM) assay. With this background, the objective of the present study was to test the *in vitro* and *in vivo* angiogenic potential of EC cocultured with GPC as 3D spheroids encapsulated in HPL hydrogels.

MATERIALS AND METHODS

Cell Culture

The use of human cells and tissues was approved by the Regional Committees for Medical Research Ethics (REK) in Norway (2016–1266, REK sør-øst C). Monolayer cultures of primary human GPC isolated from healthy donors were established in 5% HPL (Bergenlys®, Bergen, Norway). Details of isolation and characterization of GPC have been reported elsewhere (Shanbhag et al., 2020b). Early passage human umbilical vein EC (HUVEC) were purchased and cultured in EGM-2 growth medium (both from Lonza Inc., Walkersville, United States) supplemented with either 2% FBS, as per the manufacturer's recommendations, or with 5% HPL; all other media components were maintained. Cells were sub-cultured and expanded under humidified 5% CO_2 at 37°C; passages 2-4 were used in experiments. Functionality of HPL cultured HUVEC was tested in an *in vitro* tube formation assay on matrigel (Corning, NY, United States), as previously described (Fujio et al., 2017). Phase contrast images (Nikon Eclipse TS100, Tokyo, Japan) were analyzed using ImageJ software (NIH, Bethesda, United States) and angiogenesis-related parameters (tube length, branching, segments and junctions) were automatically quantified using the

Angiogenesis Analyzer plugin, as previously described (Carpentier et al., 2020).

3D Spheroid (co)Culture

3D aggregate spheroids of HUVEC were formed via guided self-assembly in microwell plates as recently described (Shanbhag et al., 2020b). Briefly, suspensions of dissociated monolayer HUVEC cultured in FBS or HPL, were seeded in microwell plates (Sphericalplate®, Kugelmeiers Ltd., Erlenbach, Switzerland) for 24 h to form spheroids of ~1000 cells each. Cell viability in spheroids was assessed via the LIVE/DEAD® kit (Invitrogen). Sprout formation in FBS and HPL cultured HUVEC spheroids was assessed using phase and confocal microscopy: for the latter, immunofluorescence (IF) staining with CD31 was performed (**Supplementary methods**). For subsequent experiments, all cell culture was performed in HPL media. For coculture spheroids, microwells were seeded with suspensions of dissociated HUVEC and GPC in two different ratios, 1:1 and 5:1 (HUVEC:GPC), based on previous work (Ma et al., 2011; Pedersen et al., 2013). After 24 h, HUVEC and HUVEC-GPC spheroids were collected by gentle pipetting and encapsulated in HPL hydrogels (HPLG).

Encapsulation in Hydrogels

Since HPL was used to establish xeno-free cultures of GPC and HUVEC, its application as a hydrogel scaffold was also investigated. Initially, HPLG were produced via addition of thrombin solution [1 IU/ml human thrombin and one TIU/ml aprotinin in 40 mM $CaCl_2$ solution (all from Sigma-Aldrich)] to sterile-filtered HPL followed by incubation at 37°C for 15 min. The resulting hydrogel was referred to as "unmodified" HPLG (0F). For encapsulation, HUVEC or coculture spheroids were suspended in HPL solution, quickly mixed with the thrombin solution, and added to culture plates with gentle shaking to ensure uniform distribution of the spheroids. The plates were transferred to the incubator for 15 min to ensure complete gelation and thereafter supplemented with EGM-2 growth medium for the indicated culture periods.

Subsequently, to improve the hydrogels mechanical properties, HPL was supplemented with fibrinogen (Sigma-Aldrich) in concentrations of 1.25 (1.25F), 2.5 (2.5F), 6.25, 12.5, and 25 mg/ml. Gelation and spheroid encapsulation was performed using the same thrombin solution as described above. These hydrogels were referred to as "modified" HPLG. Rheological properties of modified HPLG were assessed as described in the **Supplementary methods**. Only 0, 1.25 and 2.5F HPLG were used in subsequent experiments (see *Hydrogel Properties Influence HUVEC Sprouting*).

Sprouting Angiogenesis Assay

The *in vitro* angiogenic potential of mono- and coculture spheroids was tested in a sprout assay, as previously described (Nakatsu and Hughes, 2008). Briefly, HUVEC or HUVEC-GPC spheroids were encapsulated in HPLG and cultured for 72 h in EGM-2 medium to observe sprout formation. In selective experiments, HUVEC spheroids (encapsulated in 0F HPLG) were cultured with a monolayer of GPC on top of the gel, i.e., "indirect" cocultures – to test whether paracrine factors from GPC influenced HIUVEC sprouting. In "direct" cocultures, prior to spheroid formation, dissociated GPC and HUVEC were labeled with fluorescent green (DiO, 5 µL/ml) and red (Dil, 5 µL/ml) dyes (Vybrant® cell-labelling solution, Invitrogen), respectively. HUVEC-only spheroids (only red-labelled cells) were formed as controls. Spheroids of HUVEC or HUVEC-GPC (1:1 or 5:1 HUVEC:GPC) were encapsulated in modified HPLG (0, 1.25 or 2.5F), and cultured in EGM-2 for up to 72 h in 8-well µ-slides® (ibidi, Munich, Germany). Subsequently, the constructs were fixed in 4% paraformaldehyde (PFA) and permeabilized using 0.2% Triton X-100 (Sigma-Aldrich). Prior to imaging, nuclei were stained using 4′,6-diamidino-2-phenylindole (DAPI, Sigma-Aldrich).

Confocal Microscopy

Whole mount imaging of HPLG-encapsulated spheroids was performed using an Andor Dragonfly 5050 high-speed confocal microscope and Fusion software (both from Oxford Instruments, Abingdon, United Kingdom). Z-stacks were acquired from the top of each gel, with steps of 4 µm to a depth of up to 200 µm. Each image was captured with a high-speed iXon 888 Life EMCCD camera with 1024 × 1024 resolution at 100–200 × magnification. Green (GPC) and red (HUVEC) stained cells/sprouts, and their nuclei (DAPI), were scanned in the corresponding channels using 546, 647 and 405 lasers, respectively. Images were processed using the Imaris software (Oxford Instruments) and transferred to ImageJ (NIH) for analysis. Using the Sprout Morphology plugin, segmentation and thresholding of images was performed to separate GPC, HUVEC and nuclei. Images were calibrated using scale bars and sprout lengths (in µm) were automatically or manually calculated using ImageJ, as described elsewhere (Eglinger et al., 2017), on segmented images showing only HUVEC in the red-channel.

CAM Assay

The *in vivo* angiogenic potential of mono- and coculture spheroids was tested in an *ex ovo* CAM assay in developing chick embryos, in accordance with the Norwegian Animal Research Authority (Mattilsynet), where an experimental period < 14 days did not require formal ethical approval. Briefly, fertilized chicken eggs were incubated at 37°C for 72 h with intermittent rotation. On embryonic day 3, the eggs were carefully opened, their contents transferred into petri dishes and incubated in humidified air at 37°C. On day 7, HUVEC or HUVEC-GPC spheroids encapsulated in 1.25F HPLG (50 spheroids in 50 µL gel; 1:1 HPL:EGM-2) were implanted on the CAMs avoiding pre-existing blood vessels. To maintain their positions on the CAMs, the gels were contained within silicone O-rings (⌀ 10 mm). During the incubation period, some embryos were terminated as a result of embryonic death unrelated to the implants. Implants from these terminated embryos were harvested for live cell-staining using Calcein AM (Invitrogen). On day 14, the regions within the O-rings in the remaining embryos were recorded using a digital stereomicroscope (Leica Biosystems, Heerbrugg, Switzerland). Subsequently, the CAMs were fixed in 4% PFA and regions

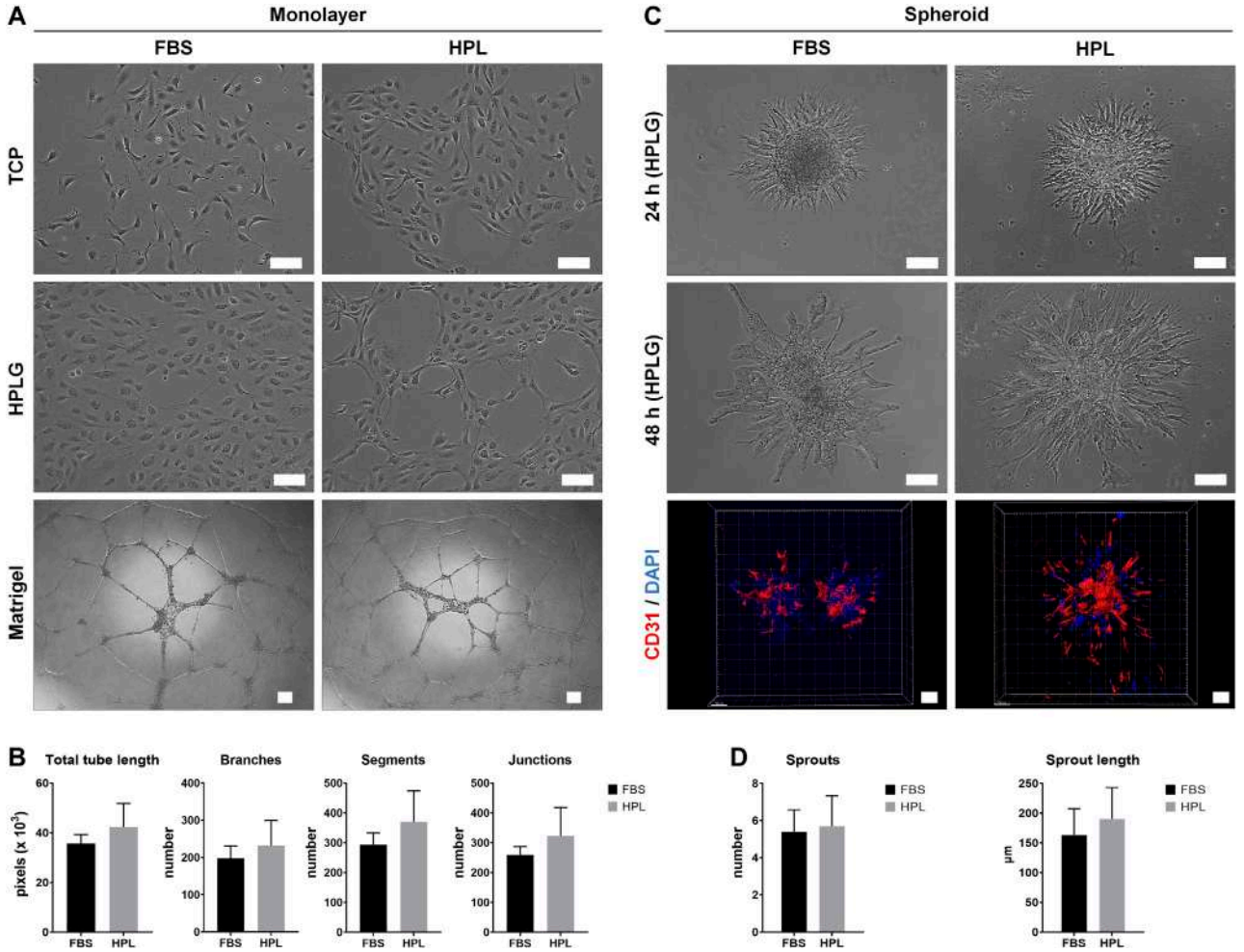

FIGURE 1 | Xeno-free HUVEC culture in HPL. **(A)** Comparison of HUVEC morphology in HPL and FBS on tissue culture plastic (TCP) and HPLG, and corresponding tube formation on Matrigel after 24 h; scale bars 100 µm. **(B)** Analysis of tube formation parameters; data represent means ± SD (n = 3). **(C)** Comparison of *in vitro* sprouting by HUVEC spheroids in HPL and FBS after 24 and 48 h in HPLG; IF staining for CD31 (HUVEC, red) and DAPI (nuclei, blue) in 48 h-spheroids; scale bars 100 µm. **(D)** Analysis of sprout formation parameters; data represent means ± SD (n = 3 or more).

around the O-rings were harvested, embedded in paraffin and analyzed histologically following hematoxylin and eosin staining. Quantification of angiogenesis-related parameters (vessel density, vessel length, segments and branching points) in CAM images was performed using the Wimasis® automated image analysis software (Onimagin Technologies, Cordoba, Spain) (Montali et al., 2017).

Statistical Analysis

Statistical analysis was performed using the Prism 9.0 software (GraphPad Software, San Diego, CA, United States). Data are presented as means ± SD, unless specified. Normality testing was performed via the Shapiro-Wilk test. The student *t* test, Mann-Whitney U test and one-way analysis of variance (ANOVA), followed by post-hoc Tukey's or Dunn's test for multiple comparisons, were applied when appropriate and $p < 0.05$ was considered statistically significant.

RESULTS

HPL Supports Xeno-free Culture of HUVEC

Monolayer HUVEC were successfully cultured by substituting 2% FBS with 5% HPL in EGM-2 media. When cultured on tissue culture plates coated with unmodified HPLG, spontaneous tube-like organization of HPL cultured HUVEC was observed (**Figure 1A**). In the matrigel assay, a trend for superior tube formation was observed in HPL vs FBS cultured HUVEC; quantification of all angiogenesis-related parameters revealed a higher trend in HPL, without significant differences ($p > 0.05$; **Figure 1B**). Spheroids of HUVEC in HPL and FBS media were formed and encapsulated in unmodified HPLG; high cell viability in the spheroids was observed after 48 h (data not shown). Sprout formation was initiated at 24 h and increased over time in both FBS and HPL cultured HUVEC; detection of CD31 in HUVEC sprouts was confirmed via IF and confocal microscopy

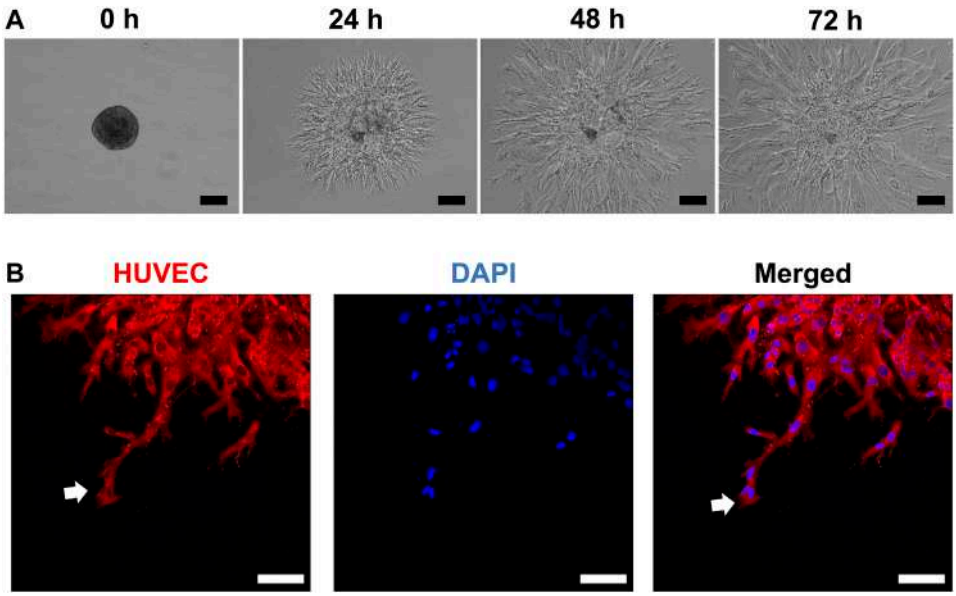

FIGURE 2 | HUVEC sprouting in HPLG. **(A)** Representative phase-contrast images showing the progression of sprout formation in xeno-free HUVEC spheroids in HPLG; scale bars 100 μm. **(B)** Representative confocal images showing sprout formation by HUVEC monoculture spheroids in unmodified HPLG; initiation by sprouting by "tip cells" (white arrows) after 24 h; scale bars 100 μm.

(**Figure 1C**). A trend for increased sprouting (sprout numbers and length) was observed in HPL vs FBS cultured HUVEC spheroids, without significant differences ($p > 0.05$; **Figure 1D**).

Spheroid Coculture Promotes Sprouting Angiogenesis

HUVEC sprouting was assessed first in unmodified (and later in modified) HPLG. Generally, sprouts appeared as narrow tube-like structures after 24 h, guided by characteristic "tip" cells, extending from the spheroid surface into the gel matrix and progressively increasing in length (**Figures 2A,B**). After 72 h, abundant network formation was observed between the sprouts of adjacent spheroids. In "indirect" cocultures, i.e., when monolayer GPC were seeded on top of HPLG encapsulating HUVEC spheroids, a trend for increased sprouting was observed in HUVEC with vs without overlying GPC ($p > 0.05$; **Supplementary Figure 1**).

In "direct" coculture spheroids, sprout formation by HUVEC was accompanied by spreading/migration of GPC within HPLG (**Figure 3A**). Both HUVEC and GPC showed high viability (**Supplementary figure 2A**). When testing different coculture ratios, spheroids of 5:1 HUVEC:GPC revealed significant increases in sprout length vs HUVEC-only spheroids ($p < 0.05$; **Figure 3B**). No significant differences were observed between 1:1 and 5:1 coculture spheroids ($p > 0.05$). Dual cell-labelling revealed GPC to be organized along, and in direct contact with, HUVEC sprouts (**Figure 3C**). GPC spreading preceded HUVEC sprouting and appeared to provide a substrate for HUVEC migration and sprouting (**Supplementary figure 2B**).

Hydrogel Properties Influence HUVEC Sprouting

Modified HPLG were produced by supplementing HPL with fibrinogen (**Figure 4A**). High cell viability and favorable sprouting of HUVEC spheroids were observed in HPLG with ≤ 2.5 mg/ml fibrinogen (**Figures 4B,C**). Spheroids in HPLG with >2.5 mg/ml fibrinogen showed no sprouting and many dead cells (**Supplementary figure 4A–C**). Therefore, only unmodified HPLG (0F) or 1.25 and 2.5F modified HPLG were used in subsequent experiments. Rheology revealed corresponding increases in storage and loss moduli of HPLG with increasing concentrations of fibrinogen (**Supplementary figure 4**). In 1:1 HUVEC:GPC cocultures, sprouting was comparable in 0F and 1.25F HPLG, and significantly greater than in 2.5F HPLG after 72 h ($p < 0.05$; **Figure 5A**). In 5:1 HUVEC:GPC cocultures, a non-significant trend for superior sprouting was observed in 1.25F HPLG ($p > 0.05$, **Figure 5B**). Thus, the combination of 5:1 HUVEC:GPC and 1.25F HPLG was considered optimal and used in the CAM assay.

Spheroid Coculture Supports Angiogenesis *in vivo*

HUVEC and HUVEC-GPC (5:1) spheroids in 1.25F HPLG were implanted on developing chicken embryo CAMs. *In vitro* sprout formation by the encapsulated spheroids was confirmed (**Supplementary figure 5**). Live cell-staining of gels harvested 24 h after implantation revealed high cell viability. While HUVEC spheroids appeared to dissociate and organize into networks, HUVEC-GPC spheroids retained their 3D structure and showed characteristic sprouting on the CAMs (**Figure 6A**).

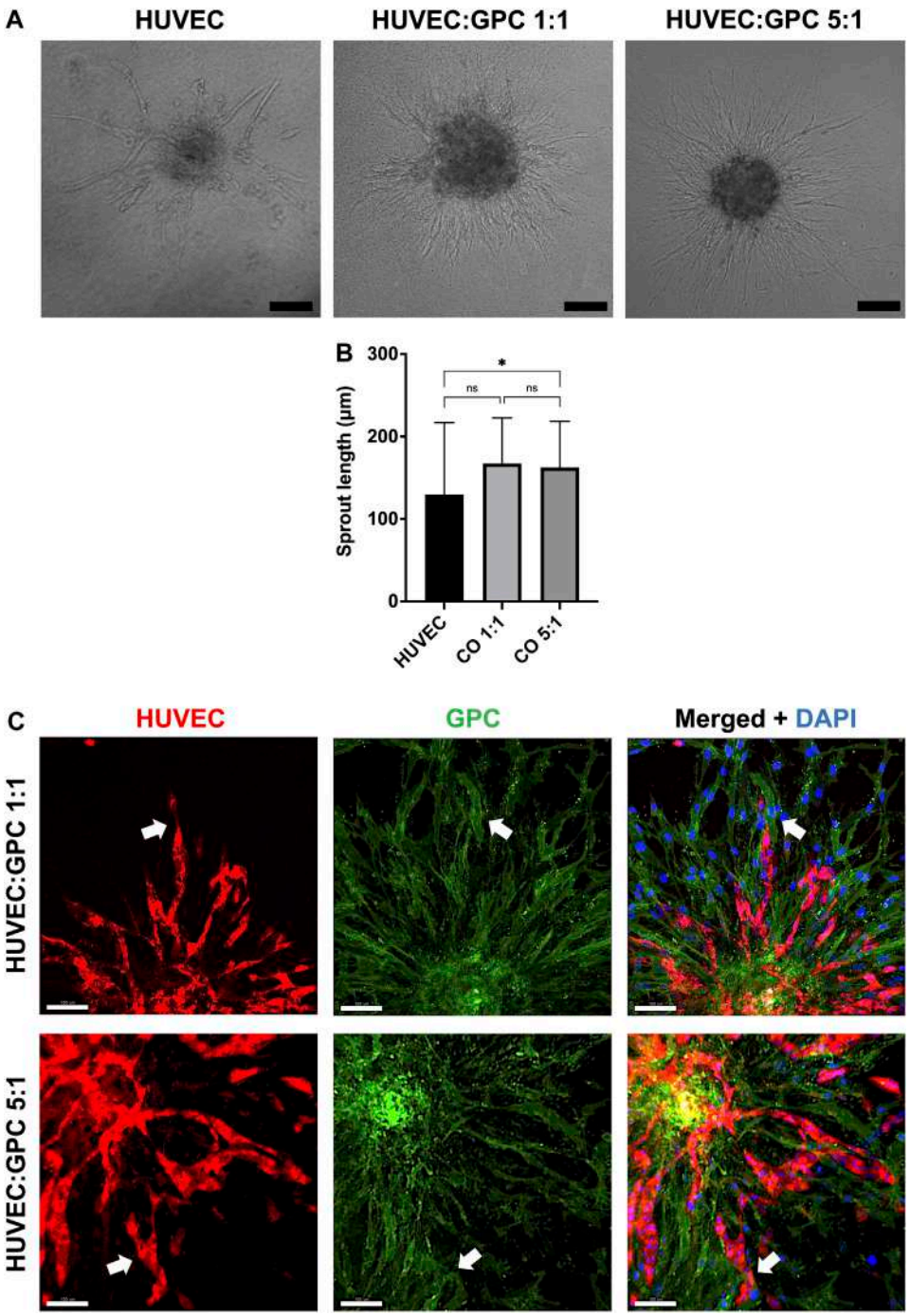

FIGURE 3 | Coculture of GPC and EC in HPLG. **(A)** Representative images of HUVEC sprouting (and GPC spreading) in HUVEC monoculture and 1:1 and 5:1 (HUVEC:GPC) coculture spheroids after 72 h in unmodified HPLG (scale bars 100 µm). **(B)** Quantification of corresponding sprout lengths based on dual-staining and confocal imaging – only red-stained HUVEC sprouts were measured; $^*p < 0.05$; data represent means ± SD of at least three experimental repeats ($n \geq 5$ spheroids per experiment). **(C)** Representative confocal images showing sprout formation in 1:1 and 5:1 HUVEC:GPC coculture spheroids; white arrows indicate GPC (green) organization along HUVEC sprouts (red;); nuclei are stained with DAPI (scale bars 100 µm).

After 7 days of implantation, active angiogenesis with dense vascular networks was observed in the regions of both HUVEC and HUVEC-GPC implants. Although the spheroids were evenly distributed in the gels at the time of implantation, after 7 days they appeared to be aggregated to one side of the O-rings and the HPLG was almost completely degraded (**Figure 6A**). Histology revealed a high density of vessels at the CAM surface, to a similar degree in both groups

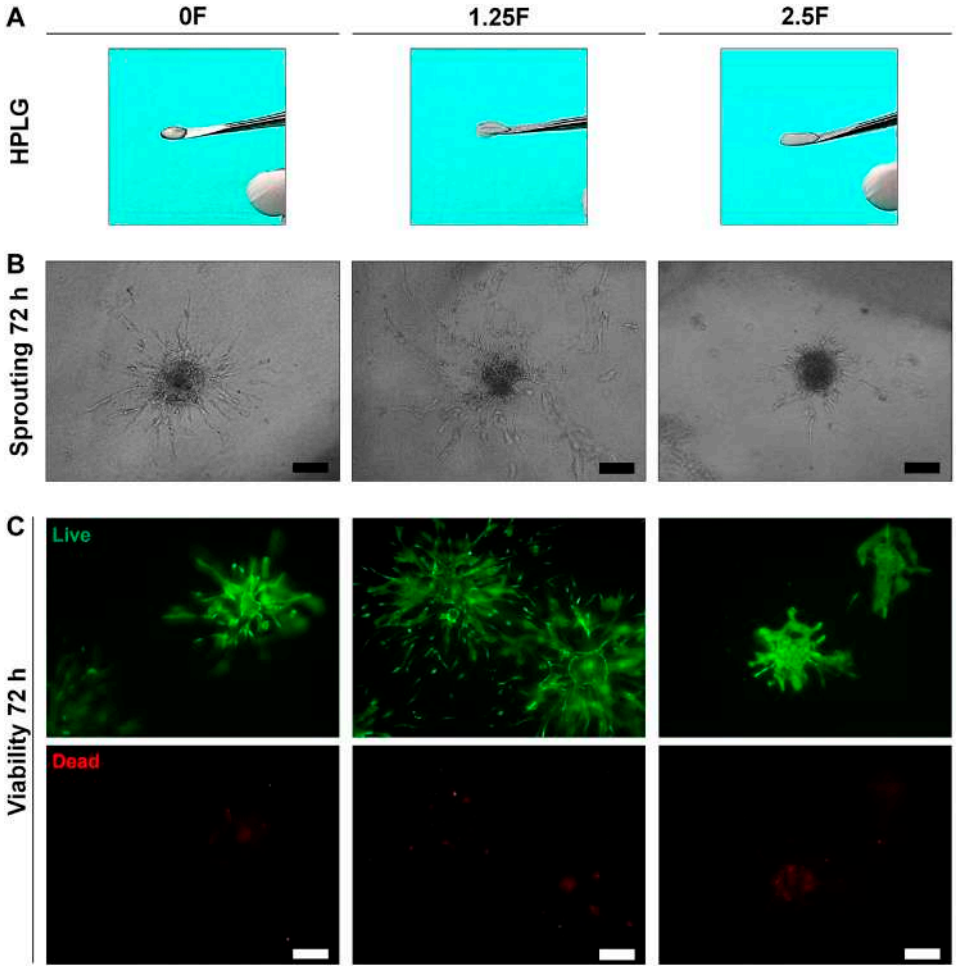

FIGURE 4 | Optimization of HPLG. **(A)** Representative photographs of unmodified (0F) and modified HPLG supplemented with 1.25 (1.25F) or 2.5 mg/ml fibrinogen (2.5F). **(B)** Representative phase contrast images of HUVEC sprouting after 72 h in the corresponding HPLG (scale bars 100 μm). **(C)** Cell viability via LIVE/DEAD assay in HUVEC spheroids after 72 h in the corresponding HPLG (scale bars 100 μm).

(**Figure 6A**). Degradation of HPLG precluded the detection of construct integration via penetration of CAM vessels into the gels. Quantification of angiogenesis revealed no significant differences between HUVEC and HUVEC-GPC spheroids for any of the tested parameters ($p > 0.05$; **Figure 6B**).

DISCUSSION

3D cocultures of MSC and EC can promote angiogenesis and potentially overcome the challenges of *in vivo* vascularization in BTE constructs (Rouwkema et al., 2006; Nguyen et al., 2012). The aim of this study was to test whether GPC, as an alternative to BMSC, supported EC-mediated sprouting angiogenesis in xeno-free HPL cultures.

HUVEC represent a feasible and frequently used model to study EC behavior in experimental settings (Morin and Tranquillo, 2013). Consistent with previous reports, tube formation and sprouting by HUVEC was improved in HPL vs FBS. Sprouting angiogenesis by 3D-cultured EC *in vitro* is considered to be a close representation of the *in vivo* angiogenic cascade, recapitulating all the key events during which quiescent EC become activated to proteolytically degrade their surrounding ECM, e.g., hydrogels, directionally migrate towards the angiogenic stimulus, proliferate, and organize into new 3D capillary networks (Korff and Augustin, 1999; Chappell et al., 2012; Nowak-Sliwinska et al., 2018). Moreover, these sprout-networks have revealed functional lumenized capillaries, which anastomose with host vasculatures when implanted *in vivo* (Alajati et al., 2008; Finkenzeller et al., 2009; Morin and Tranquillo, 2011). A recent study reported superior sprouting of EC in human serum vs FBS supplemented media (Bauman et al., 2018). Consistently, a trend for superior sprout formation by HPL vs FBS cultured HUVEC spheroids was observed herein. Thus, HPL appears to be a feasible xeno-free alternative for HUVEC culture.

The formation and stability of *in vitro* and *in vivo* capillary-like networks by EC can be enhanced via coculture with MSC

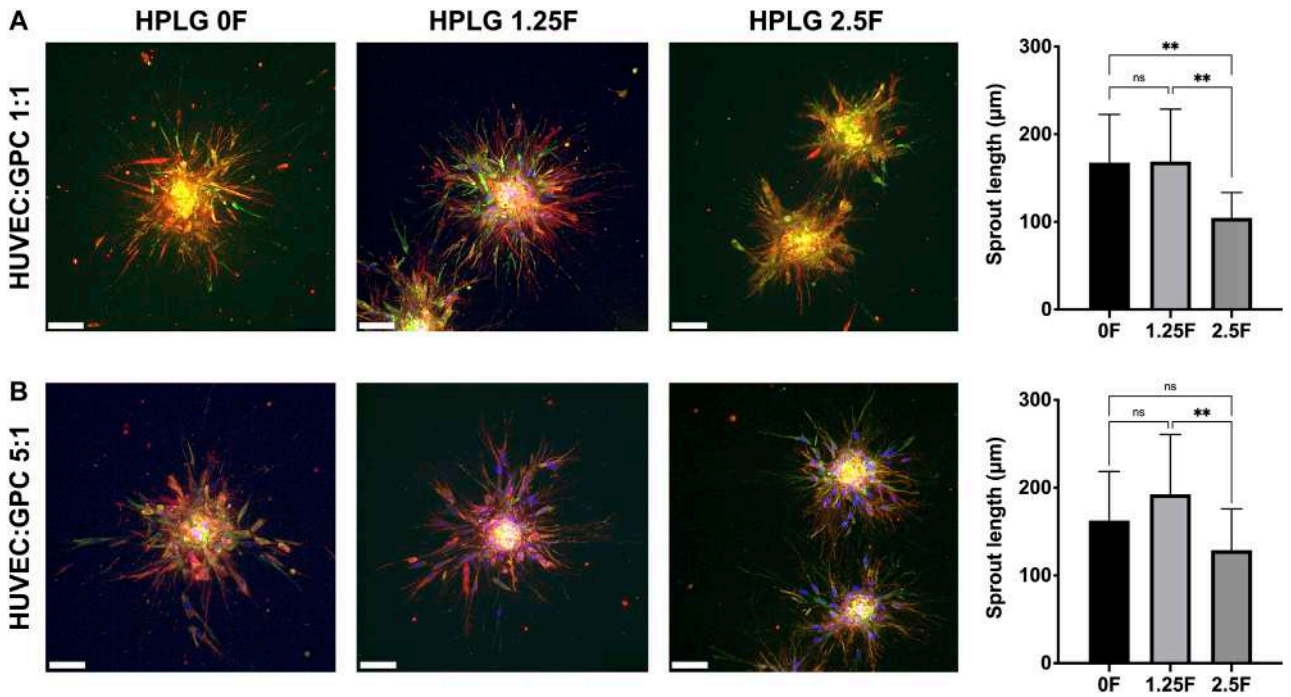

FIGURE 5 | Optimization of coculture ratios. Representative confocal images of HUVEC-sprouting (red) and GPC-spreading (green) after 72 h in 1:1 **(A)** and 5:1 **(B)** HUVEC:GPC coculture spheroids in 0, 1.25 and 2.5F HPLG (scale bars 100 μm) and corresponding quantification of sprout lengths; $^{**}p < 0.001$; data represent means ± SD of at least three experimental repeats (n = ≥ 5 spheroids per experiment).

(Pedersen et al., 2012; Pedersen et al., 2013; Ma et al., 2014). We have previously reported that GPC demonstrate MSC-like phenotype and properties in xeno-free cultures (Shanbhag et al., 2020b). Accordingly, 3D cocultures of HUVEC and GPC were established herein. To test whether GPC promoted HUVEC sprouting via cell-to-cell contact or paracrine mechanisms, direct and indirect cocultures were established, respectively. While indirect coculture with GPC revealed a trend for greater HUVEC sprouting, direct coculture with GPC in a 5:1 ratio significantly improved HUVEC sprouting. These results are consistent with previous studies of HUVEC spheroids cocultured with BMSC (Hsu et al., 2014; Robinson et al., 2016; Bauman et al., 2018), and studies highlighting the importance of direct cell-to-cell contacts, rather than paracrine interactions, in coculture settings (Ball et al., 2004; Liang et al., 2017).

To optimize the 3D cocultures, two different coculture ratios were tested. While a 1:1 ratio of MSC and EC is most frequently reported (Ma et al., 2011; Shanbhag et al., 2017a), previous studies from our group and others have suggested that higher proportions of EC may improve angiogenesis in cocultures (Verseijden et al., 2010; Pedersen et al., 2012; Pedersen et al., 2013). However, no significant differences in HUVEC sprouting were observed between high (5:1) and low (1:1) coculture ratios herein. Notably, only the 5:1 cocultures showed significantly greater sprouting vs HUVEC only spheroids. Considerably greater spreading or migration of GPC was observed in spheroids with relatively more GPC, i.e., in 1:1 spheroids. Spreading preceded HUVEC sprouting and may have provided a substrate for sprout growth and elongation. Indeed, MSC are reported to show signs of pericytic differentiation, e.g., via expression of smooth-muscle markers, in EC cocultures (Lozito et al., 2009). Similar patterns of spreading by MSC have been reported in 3D cocultures embedded in collagen gels (Shah and Kang, 2018). This is in contrast to non-embedded 3D cocultures, where MSC do not spread, and EC, in the absence of an ECM, organize into internal networks within the spheroids rather than external sprouts (Rouwkema et al., 2006; Verseijden et al., 2010; Eckermann et al., 2011; Marshall et al., 2018). In the present study, an "embedded" spheroid model was selected to recapitulate angiogenic sprouting by using HPL hydrogels as ECM scaffolds to deliver the "pre-vascularized" constructs *in vivo* (Robinson et al., 2016).

Recent studies have demonstrated the benefits of HPLG for EC-mediated angiogenesis (Fortunato et al., 2016; Robinson et al., 2016). HPLG are produced by simulating the *in vivo* coagulation cascade, i.e., via addition of thrombin and/or $CaCl_2$ to convert fibrinogen to fibrin, and thus represent highly biomimetic scaffolds for tissue engineering applications. Together with cell culture in HPL supplemented media, this would represent a fully xeno-free coculture system with a high potential for clinical translation. Although HPLG can support capillary-like network formation by EC, their mechanical properties may be considered insufficient for *in vivo* implantation, especially in non-contained bone defects. Thus, the HPLG were supplemented with fibrinogen for more predictable *in vivo* delivery. Fibrin gels are

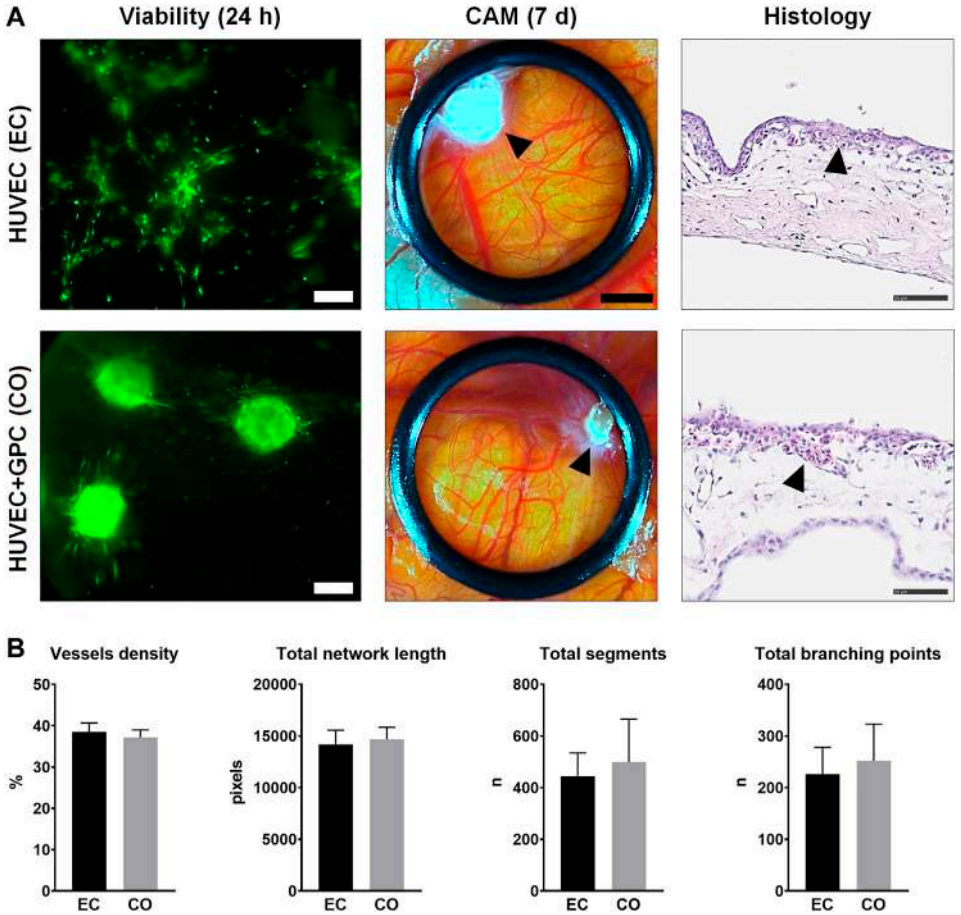

FIGURE 6 | CAM angiogenesis assay. **(A)** Comparison of HUVEC (EC) and HUVEC-GPC coculture (CO) spheroids seeded in HPLG (L to R): cell viability after 24 h [green colour indicates viable cells, note the dissociation of HUVEC (EC) spheroids into tube-like networks; scale bars 100 μm], stereomicroscope images showing neoangiogenesis in CAMs after 7 days (black arrows indicate condensed HPLG within the O-rings; scale bars 200 μm) and corresponding histological images with H & E staining (black arrows indicate newly formed vessels; scale bars 50 μm). **(B)** Analysis of angiogenesis-related parameters based on stereomicroscope images; n = number; data represent means ± SD (n = 3).

routinely used as scaffolds in a range of applications including BTE (Soffer et al., 2003). Moreover, fibrin gels have been extensively used to study EC sprouting angiogenesis (Morin and Tranquillo, 2013). Notably (unmodified) HPLG have been shown to be superior to fibrin gels in this regard (Robinson et al., 2016). However, the mechanical properties of unmodified HPLG may only allow injectable delivery due to their highly liquid nature. In the present study, it was hypothesized that supplementation of HPLG with fibrinogen would enhance the mechanical properties of the gels, while retaining the biological activity of HPL. Although the addition of fibrinogen seemingly improved the mechanical properties of HPLG, the biological activity (HUVEC viability and sprouting) declined beyond a concentration of 2.5 mg/ml. Interestingly, HUVEC sprouting in 1.25F gels was slightly enhanced vs unmodified HPLG and significantly enhanced vs 2.5F HPLG. This contrasted with a previous study comparing unmodified HPLG and 1.25 or 2.5 mg/ml fibrin gels (Robinson et al., 2016). In the context of BTE, hydrogel stiffness is also reported to influence MSC fate-determination and osteogenic differentiation (Hwang et al., 2015; Sun et al., 2018; Zigon-Branc et al., 2019). Our findings, together with previous reports (Rao et al., 2012; Hsu et al., 2014; Robinson et al., 2016), highlight the importance of ECM/scaffold properties on EC-mediated angiogenesis within tissue engineered constructs.

To test the *in vivo* angiogenic potential of spheroid-HPLG constructs, a CAM assay in the developing chick embryo was used. This offers a relatively rapid and cost-effective model for *in vivo* biomaterial/xenograft testing, particularly for angiogenesis, in a naturally immunocompromised host with a rapidly developing vascular bed (Moreno-Jimenez et al., 2016; Ribatti, 2016). Cell viability and sprouting of both HUVEC and HUVEC-GPC spheroids was confirmed after 24 h in excised CAMs. Interestingly, in the absence of GPC, HUVEC appeared to dissociate from spheroids and organize into tube-like networks as observed in monolayer cultures. Seven days after implantation, a dense network of capillaries was observed macroscopically in the CAM-regions implanted with both HUVEC and HUVEC-

GPC spheroids. This is consistent with previous studies reporting angiogenesis in CAMs implanted with xenogeneic (Steffens et al., 2009; Strassburg et al., 2016) or xeno-free coculture spheroids (Bauman et al., 2018). In the latter study, the integration of sprouts with the CAM vasculature was confirmed via immunohistochemistry (Bauman et al., 2018). However, no significant advantage of HUVEC-GPC coculture was observed in the CAM assay herein, and therefore, the benefits of coculture observed for *in vitro* sprouting were not translated *in vivo*.

Some limitations of our study must be acknowledged. While most previous studies have reported the *in ovo* "eggshell window" method for the CAM assay (Steffens et al., 2009; Liu et al., 2012; Strassburg et al., 2016; Bauman et al., 2018), a complete *ex ovo* method was used in our study. In the former, the construct is placed on the CAM through an opening in the eggshell; retention of the embryo within the egg and coverage of the window during the experimental period are advantageous in terms of hydration and reduced risk of contamination. Exposure of the CAMs in our method contributed to dehydration and faster resorption of the HPLG, which may have compromised existing sprout-networks and precluded the formation of new sprouts. Moreover, a longer observation period was used herein (7 days) compared to previous reports (3 days) (Liu et al., 2012; Bauman et al., 2018), which may also have masked any "early differences" between the groups; a single "end-point" was selected herein to minimize disturbance and exposure of the CAMs. An *in ovo* model with shorter/multiple observation periods may offer a more reliable picture in future studies. Moreover, ectopic implantation of the constructs in more relevant animal models, e.g., immunocompromised mice, may provide further clues regarding hydrogel degradation and vascular anastomosis.

It has been reported that in the absence of supporting cells, EC networks are stable for a shorter duration *in vitro* (Pedersen et al., 2012; Pill et al., 2018). When implanted *in vivo*, the engineered vessels must remain stable long enough to anastomose with the native vasculature and sustain the implanted cells (Pedersen et al., 2013). In the present study, GPC were found to be organized in close contact with HUVEC sprouts and appeared to provide a "substrate" for sprout formation/elongation. Thus, it may be hypothesized that GPC could help to stabilize EC networks in more challenging *in vivo* conditions (Zhang et al., 2020). In the context of BTE, it is unclear whether MSC/GPC in cocultures serve dual functions of supporting angiogenesis and promoting osteogenesis, i.e., osteogenic differentiation and/or paracrine stimulation. In a meta-analysis of MSC-EC co-transplantation studies *in vivo*, we observed a significant benefit of coculture for bone, but not vessel, regeneration (Shanbhag et al., 2017a). Further research is needed to clarify whether MSC, and other supporting cells, adopt a pericyte- and/or osteoblast-like phenotype when cocultured with EC. Finally, further optimization of culture conditions, e.g., cell ratios, media, ECM/scaffolds, etc., to promote both osteogenesis and angiogenesis, and not one or the other, is needed prior to clinical application.

CONCLUSION

In summary, HPL represents a suitable xeno-free alternative for HUVEC culture. HUVEC spheroids in HPL/HPLG demonstrated *in vitro* sprouting angiogenesis, which was significantly enhanced via direct coculture with GPC. A 5:1 HUVEC:GPC ratio in a specific HPLG formulation appeared to be optimal in terms of *in vitro* sprouting. Further optimizations of coculture conditions are needed to translate these *in vitro* findings in the appropriate *in vivo* models.

DATA AVAILABILITY STATEMENT

The raw data supporting the conclusions of this article will be made available by the authors, without undue reservation.

AUTHOR CONTRIBUTIONS

SSH designed the study, performed the experiments, analyzed the data, and drafted the manuscript. AR, EN, SSU, and CD contributed to the experiments, data analysis, and manuscript writing. AS, AB, and KM contributed to the design, data analysis, and manuscript writing. The authors read and approved the final manuscript.

FUNDING

This work was supported by Helse Vest Strategic Research Funding, Norway (502027), Research Council of Norway (BEHANDLING/273551), Trond Mohn Foundation, Norway (BFS-2018-TMT10) and the International Team for Implantology (ITI-117/2015). SSH. received the 2018 IADR Karring-Nyman Sunstar Guidor award (Sunstar Foundation).

ACKNOWLEDGMENTS

We thank the Bloodbank at Haukeland University Hospital for supplying the platelets and the Molecular Imaging Center (MIC), University of Bergen, for assistance with microscopy and imaging. We also thank Melina Mühlenpfordt from the Department of Physics, NTNU, for assistance with the CAM assay and Bendik Nordanger from the Department of Clinical Medicine, University of Bergen, for assistance with the histology.

SUPPLEMENTARY MATERIAL

The Supplementary Material for this article can be found online at: https://www.frontiersin.org/articles/10.3389/fbioe.2021.739225/full#supplementary-material

REFERENCES

Alajati, A., Laib, A. M., Weber, H., Boos, A. M., Bartol, A., Ikenberg, K., et al. (2008). Spheroid-based Engineering of a Human Vasculature in Mice. *Nat. Methods* 5 (5), 439–445. doi:10.1038/nmeth.1198

Ball, S. G., Shuttleworth, A. C., and Kielty, C. M. (2004). Direct Cell Contact Influences Bone Marrow Mesenchymal Stem Cell Fate. *Int. J. Biochem. Cel Biol.* 36 (4), 714–727. doi:10.1016/j.biocel.2003.10.015

Banfi, A., Muraglia, A., Dozin, B., Mastrogiacomo, M., Cancedda, R., and Quarto, R. (2000). Proliferation Kinetics and Differentiation Potential of *Ex Vivo* Expanded Human Bone Marrow Stromal Cells. *Exp. Hematol.* 28 (6), 707–715. doi:10.1016/s0301-472x(00)00160-0

Bauman, E., Feijão, T., Carvalho, D. T. O., Granja, P. L., and Barrias, C. C. (2018). Xeno-free Pre-vascularized Spheroids for Therapeutic Applications. *Sci. Rep.* 8 (1), 230. doi:10.1038/s41598-017-18431-6

Bieback, K., Fernandez-Muñoz, B., Pati, S., and Schäfer, R. (2019a). Gaps in the Knowledge of Human Platelet Lysate as a Cell Culture Supplement for Cell Therapy: a Joint Publication from the AABB and the International Society for Cell & Gene Therapy. *Int. Soc. Cel Gene TherapyTransfusion* 59, 3448–3460. doi:10.1111/trf.15483

Bieback, K., Fernandez-Muñoz, B., Pati, S., and Schäfer, R. (2019b). Gaps in the Knowledge of Human Platelet Lysate as a Cell Culture Supplement for Cell Therapy: a Joint Publication from the AABB and the International Society for Cell & Gene Therapy. *Transfusion* 59 (11), 3448–3460. doi:10.1111/trf.15483

Carpentier, G., Berndt, S., Ferratge, S., Rasband, W., Cuendet, M., Uzan, G., et al. (2020). Angiogenesis Analyzer for ImageJ - A Comparative Morphometric Analysis of "Endothelial Tube Formation Assay" and "Fibrin Bead Assay". *Sci. Rep.* 10 (1), 11568. doi:10.1038/s41598-020-67289-8

Cesarz, Z., and Tamama, K. (2016). Spheroid Culture of Mesenchymal Stem Cells. *Stem Cell Int.* 2016, 1–11. doi:10.1155/2016/9176357

Chappell, J. C., Wiley, D. M., and Bautch, V. L. (2012). How Blood Vessel Networks Are Made and Measured. *Cells Tissues Organs* 195 (1-2), 94–107. doi:10.1159/000331398

Chatterjea, A., LaPointe, V. L., LaPointe, V., Barradas, A., Garritsen, H., Yuan, H., et al. (2017). Cell Aggregation Enhances Bone Formation by Human Mesenchymal Stromal Cells. *eCM* 33, 121–129. doi:10.22203/eCM.v033a09

Chen, D.-Y., Wei, H.-J., Lin, K.-J., Huang, C.-C., Wang, C.-C., Wu, C.-T., et al. (2013). Three-dimensional Cell Aggregates Composed of HUVECs and cbMSCs for Therapeutic Neovascularization in a Mouse Model of Hindlimb Ischemia. *Biomaterials* 34 (8), 1995–2004. doi:10.1016/j.biomaterials.2012.11.045

Eckermann, C. W., Lehle, K., Schmid, S. A., Wheatley, D. N., and Kunz-Schughart, L. A. (2011). Characterization and Modulation of Fibroblast/endothelial Cell Co-cultures for Thein Vitropreformation of Three-Dimensional Tubular Networks. *Cell. Biol. Int.* 35 (11), 1097–1110. doi:10.1042/CBI20100718

Eglinger, J., Karsjens, H., and Lammert, E. (2017). Quantitative Assessment of Angiogenesis and Pericyte Coverage in Human Cell-Derived Vascular Sprouts. *Inflamm. Regener* 37, 2. doi:10.1186/s41232-016-0033-2

Fekete, N., Gadelorge, M., Fürst, D., Maurer, C., Dausend, J., Fleury-Cappellesso, S., et al. (2012). Platelet Lysate from Whole Blood-Derived Pooled Platelet Concentrates and Apheresis-Derived Platelet Concentrates for the Isolation and Expansion of Human Bone Marrow Mesenchymal Stromal Cells: Production Process, Content and Identification of Active Components. *Cytotherapy* 14 (5), 540–554. doi:10.3109/14653249.2012.655420

Finkenzeller, G., Graner, S., Kirkpatrick, C. J., Fuchs, S., and Stark, G. B. (2009). Impairedin Vivovasculogenic Potential of Endothelial Progenitor Cells in Comparison to Human Umbilical Vein Endothelial Cells in a Spheroid-Based Implantation Model. *Cell Prolif* 42 (4), 498–505. doi:10.1111/j.1365-2184.2009.00610.x

Follin, B., Juhl, M., Cohen, S., Pedersen, A. E., Kastrup, J., and Ekblond, A. (2016). Increased Paracrine Immunomodulatory Potential of Mesenchymal Stromal Cells in Three-Dimensional Culture. *Tissue Eng. B: Rev.* 22 (4), 322–329. doi:10.1089/ten.TEB.2015.0532

Fortunato, T. M., Beltrami, C., Emanueli, C., De Bank, P. A., and Pula, G. (2016). Platelet Lysate Gel and Endothelial Progenitors Stimulate Microvascular Network Formation *In Vitro*: Tissue Engineering Implications. *Sci. Rep.* 6, 25326. doi:10.1038/srep25326

Fournier, B. P. J., Ferre, F. C., Couty, L., Lataillade, J.-J., Gourven, M., Naveau, A., et al. (2010). Multipotent Progenitor Cells in Gingival Connective Tissue. *Tissue Eng. A* 16, 2891–2899. doi:10.1089/ten.tea.2009.0796

Friedenstein, A. J., Petrakova, K. V., Kurolesova, A. I., and Frolova, G. P. (1968). Heterotopic Transplants of Bone Marrow. *Transplantation* 6, 230–247. doi:10.1097/00007890-196803000-00009

Fujio, M., Xing, Z., Sharabi, N., Xue, Y., Yamamoto, A., Hibi, H., et al. (2017). Conditioned media from Hypoxic-Cultured Human Dental Pulp Cells Promotes Bone Healing during Distraction Osteogenesis. *J. Tissue Eng. Regen. Med.* 11 (7), 2116–2126. doi:10.1002/term.2109

Ghazanfari, R., Zacharaki, D., Li, H., Ching Lim, H., Soneji, S., and Scheding, S. (2017). Human Primary Bone Marrow Mesenchymal Stromal Cells and Their *In Vitro* Progenies Display Distinct Transcriptional Profile Signatures. *Sci. Rep.* 7, 10338. doi:10.1038/s41598-017-09449-x

Heiss, M., Hellström, M., Kalén, M., May, T., Weber, H., Hecker, M., et al. (2015). Endothelial Cell Spheroids as a Versatile Tool to Study Angiogenesis *In Vitro*. *FASEB j.* 29 (7), 3076–3084. doi:10.1096/fj.14-267633

Ho, S. S., Hung, B. P., Heyrani, N., Lee, M. A., and Leach, J. K. (2018). Hypoxic Preconditioning of Mesenchymal Stem Cells with Subsequent Spheroid Formation Accelerates Repair of Segmental Bone Defects. *Stem Cells* 36 (9), 1393–1403. doi:10.1002/stem.2853

Hoch, A. I., and Leach, J. K. (2015). Concise Review: Optimizing Expansion of Bone Marrow Mesenchymal Stem/stromal Cells for Clinical Applications. *Stem Cell Transl Med* 4 (4), 412. doi:10.5966/sctm.2013-0196erratum

Hsu, S.-h., Ho, T.-T., Huang, N.-C., Yao, C.-L., Peng, L.-H., and Dai, N.-T. (2014). Substrate-dependent Modulation of 3D Spheroid Morphology Self-Assembled in Mesenchymal Stem Cell-Endothelial Progenitor Cell Coculture. *Biomaterials* 35 (26), 7295–7307. doi:10.1016/j.biomaterials.2014.05.033

Hwang, J.-H., Byun, M. R., Kim, A. R., Kim, K. M., Cho, H. J., Lee, Y. H., et al. (2015). Extracellular Matrix Stiffness Regulates Osteogenic Differentiation through MAPK Activation. *PLoS One* 10 (8), e0135519. doi:10.1371/journal.pone.0135519

Jain, R. K., Au, P., Tam, J., Duda, D. G., and Fukumura, D. (2005). Engineering Vascularized Tissue. *Nat. Biotechnol.* 23, 821–823. doi:10.1038/nbt0705-821

Kale, S., Biermann, S., Edwards, C., Tarnowski, C., Morris, M., and Long, M. W. (2000). Three-dimensional Cellular Development Is Essential for *Ex Vivo* Formation of Human Bone. *Nat. Biotechnol.* 18, 954–958. doi:10.1038/79439

Kanczler, J., Oreffo, R. O. C., and Oreffo, R. (2008). Osteogenesis and Angiogenesis: the Potential for Engineering Bone. *eCM* 15, 100–114. doi:10.22203/ecm.v015a08

Keramaris, N. C., Kaptanis, S., Moss, H. L., Loppini, M., Pneumaticos, S., and Maffulli, N. (2012). Endothelial Progenitor Cells (EPCs) and Mesenchymal Stem Cells (MSCs) in Bone Healing. *Curr. Stem Cel Res Ther* 7 (293), 293–301. doi:10.2174/157488812800793081

Korff, T., and Augustin, H. G. (1999). Tensional Forces in Fibrillar Extracellular Matrices Control Directional Capillary Sprouting. *J. Cel Sci* 112 (Pt 19), 3249–3258. doi:10.1242/jcs.112.19.3249

Korff, T., and Augustin, H. G. (1998). Integration of Endothelial Cells in Multicellular Spheroids Prevents Apoptosis and Induces Differentiation. *J. Cel Biol* 143 (5), 1341–1352. doi:10.1083/jcb.143.5.1341

Levenberg, S., Rouwkema, J., Macdonald, M., Garfein, E. S., Kohane, D. S., Darland, D. C., et al. (2005). Engineering Vascularized Skeletal Muscle Tissue. *Nat. Biotechnol.* 23 (7), 879–884. doi:10.1038/nbt1109

Liang, T., Zhu, L., Gao, W., Gong, M., Ren, J., Yao, H., et al. (2017). Coculture of Endothelial Progenitor Cells and Mesenchymal Stem Cells Enhanced Their Proliferation and Angiogenesis through PDGF and Notch Signaling. *FEBS Open Bio* 7 (11), 1722–1736. doi:10.1002/2211-5463.12317

Liu, X., Wang, X., Horii, A., Wang, X., Qiao, L., Zhang, S., et al. (2012). *In Vivo* studies on Angiogenic Activity of Two Designer Self-Assembling Peptide Scaffold Hydrogels in the Chicken Embryo Chorioallantoic Membrane. *Nanoscale* 4 (8), 2720–2727. doi:10.1039/c2nr00001f

Loibl, M., Binder, A., Herrmann, M., Duttenhoefer, F., Richards, R. G., Nerlich, M., et al. (2014). Direct Cell-Cell Contact between Mesenchymal Stem Cells and Endothelial Progenitor Cells Induces a Pericyte-like Phenotype *In Vitro*. *Biomed. Res. Int.* 2014, 1–10. doi:10.1155/2014/395781

Lozito, T. P., Kuo, C. K., Taboas, J. M., and Tuan, R. S. (2009). Human Mesenchymal Stem Cells Express Vascular Cell Phenotypes upon

Interaction with Endothelial Cell Matrix. *J. Cel. Biochem.* 107 (4), 714–722. doi:10.1002/jcb.22167

Ma, J., van den Beucken, J. J. J. P., Yang, F., Both, S. K., Cui, F.-Z., Pan, J., et al. (2011). Coculture of Osteoblasts and Endothelial Cells: Optimization of Culture Medium and Cell Ratio. *Tissue Eng. C: Methods* 17, 349–357. doi:10.1089/ten.tec.2010.0215

Ma, J., Yang, F., Both, S. K., Prins, H.-J., Helder, M. N., Pan, J., et al. (2014). *In Vitro* and *In Vivo* Angiogenic Capacity of BM-MSCs/HUVECs and AT-MSCs/HUVECs Cocultures. *Biofabrication* 6 (1), 015005. doi:10.1088/1758-5082/6/1/015005

Marshall, J., Barnes, A., and Genever, P. (2018). Analysis of the Intrinsic Self-Organising Properties of Mesenchymal Stromal Cells in Three-Dimensional Co-culture Models with Endothelial Cells. *Bioengineering* 5 (4), 92. doi:10.3390/bioengineering5040092

Mitrano, T. I., Grob, M. S., Carrión, F., Nova-Lamperti, E., Luz, P. A., Fierro, F. S., et al. (2010). Culture and Characterization of Mesenchymal Stem Cells from Human Gingival Tissue. *J. Periodontol.* 81, 917–925. doi:10.1902/jop.2010.090566

Montali, M., Panvini, F. M., Barachini, S., Ronca, F., Carnicelli, V., Mazzoni, S., et al. (2017). Human Adult Mesangiogenic Progenitor Cells Reveal an Early Angiogenic Potential, Which Is Lost after Mesengenic Differentiation. *Stem Cel Res Ther* 8 (1), 106. doi:10.1186/s13287-017-0562-x

Moreno-Jiménez, I., Hulsart-Billstrom, G., Lanham, S. A., Janeczek, A. A., Kontouli, N., Kanczler, J. M., et al. (2016). The Chorioallantoic Membrane (CAM) Assay for the Study of Human Bone Regeneration: a Refinement Animal Model for Tissue Engineering. *Sci. Rep.* 6, 32168. doi:10.1038/srep32168

Morin, K. T., and Tranquillo, R. T. (2011). Guided Sprouting from Endothelial Spheroids in Fibrin Gels Aligned by Magnetic fields and Cell-Induced Gel Compaction. *Biomaterials* 32 (26), 6111–6118. doi:10.1016/j.biomaterials.2011.05.018

Morin, K. T., and Tranquillo, R. T. (2013). *In Vitro* models of Angiogenesis and Vasculogenesis in Fibrin Gel. *Exp. Cel Res.* 319 (16), 2409–2417. doi:10.1016/j.yexcr.2013.06.006

Murphy, K. C., Fang, S. Y., and Leach, J. K. (2014). Human Mesenchymal Stem Cell Spheroids in Fibrin Hydrogels Exhibit Improved Cell Survival and Potential for Bone Healing. *Cell Tissue Res* 357, 91–99. doi:10.1007/s00441-014-1830-z

Murphy, K. C., Hughbanks, M. L., Binder, B. Y. K., Vissers, C. B., and Leach, J. K. (2015). Engineered Fibrin Gels for Parallel Stimulation of Mesenchymal Stem Cell Proangiogenic and Osteogenic Potential. *Ann. Biomed. Eng.* 43 (8), 2010–2021. doi:10.1007/s10439-014-1227-x

Nakatsu, M. N., and Hughes, C. C. W. (2008). Chapter 4 an Optimized Three-Dimensional *In Vitro* Model for the Analysis of Angiogenesis. *Methods Enzymol.* 443, 65–82. doi:10.1016/S0076-6879(08)02004-1

Nguyen, L. H., Annabi, N., Nikkhah, M., Bae, H., Binan, L., Park, S., et al. (2012). Vascularized Bone Tissue Engineering: Approaches for Potential Improvement. *Tissue Eng. Part B: Rev.* 18, 363–382. doi:10.1089/ten.teb.2012.0012

Nowak-Sliwinska, P., Alitalo, K., Allen, E., Anisimov, A., Aplin, A. C., Auerbach, R., et al. (2018). Consensus Guidelines for the Use and Interpretation of Angiogenesis Assays. *Angiogenesis* 21 (3), 425–532. doi:10.1007/s10456-018-9613-x

Pedersen, T. O., Blois, A. L., Xing, Z., Xue, Y., Sun, Y., Finne-Wistrand, A., et al. (2013). Endothelial Microvascular Networks Affect Gene-Expression Profiles and Osteogenic Potential of Tissue-Engineered Constructs. *Stem Cel Res. Ther.* 4 (3), 52. doi:10.1186/scrt202

Pedersen, T. O., Blois, A. L., Xue, Y., Xing, Z., Cottler-Fox, M., Fristad, I., et al. (2012). Osteogenic Stimulatory Conditions Enhance Growth and Maturation of Endothelial Cell Microvascular Networks in Culture with Mesenchymal Stem Cells. *J. Tissue Eng.* 3 (1), 204173141244323. doi:10.1177/2041731412443236

Petrenko, Y., Syková, E., and Kubinová, Š. (2017). The Therapeutic Potential of Three-Dimensional Multipotent Mesenchymal Stromal Cell Spheroids. *Stem Cel Res. Ther.* 8, 94. doi:10.1186/s13287-017-0558-6

Pill, K., Melke, J., Mühleder, S., Pultar, M., Rohringer, S., Priglinger, E., et al. (2018). Microvascular Networks from Endothelial Cells and Mesenchymal Stromal Cells from Adipose Tissue and Bone Marrow: A Comparison. *Front. Bioeng. Biotechnol.* 6, 156. doi:10.3389/fbioe.2018.00156

Pittenger, M. F., Discher, D. E., Péault, B. M., Phinney, D. G., Hare, J. M., and Caplan, A. I. (2019). Mesenchymal Stem Cell Perspective: Cell Biology to Clinical Progress. *NPJ Regen. Med.* 4, 22. doi:10.1038/s41536-019-0083-6

Rao, R. R., Peterson, A. W., Ceccarelli, J., Putnam, A. J., and Stegemann, J. P. (2012). Matrix Composition Regulates Three-Dimensional Network Formation by Endothelial Cells and Mesenchymal Stem Cells in Collagen/fibrin Materials. *Angiogenesis* 15 (2), 253–264. doi:10.1007/s10456-012-9257-1

Ribatti, D. (2016). The Chick Embryo Chorioallantoic Membrane (CAM). A Multifaceted Experimental Model. *Mech. Develop.* 141, 70–77. doi:10.1016/j.mod.2016.05.003

Robinson, S. T., Douglas, A. M., Chadid, T., Kuo, K., Rajabalan, A., Li, H., et al. (2016). A Novel Platelet Lysate Hydrogel for Endothelial Cell and Mesenchymal Stem Cell-Directed Neovascularization. *Acta Biomater.* 36, 86–98. doi:10.1016/j.actbio.2016.03.002

Rojewski, M. T., Lotfi, R., Gjerde, C., Mustafa, K., Veronesi, E., Ahmed, A. B., et al. (2019). Translation of a Standardized Manufacturing Protocol for Mesenchymal Stromal Cells: A Systematic Comparison of Validation and Manufacturing Data. *Cytotherapy* 21 (4), 468–482. doi:10.1016/j.jcyt.2019.03.001

Rouwkema, J., Boer, J. D., and Blitterswijk, C. A. V. (2006). Endothelial Cells Assemble into a 3-dimensional Prevascular Network in a Bone Tissue Engineering Construct. *Tissue Eng.* 12, 2685–2693. doi:10.1089/ten.2006.12.2685

Sart, S., Tsai, A.-C., Li, Y., and Ma, T. (2014). Three-dimensional Aggregates of Mesenchymal Stem Cells: Cellular Mechanisms, Biological Properties, and Applications. *Tissue Eng. Part B: Rev.* 20, 365–380. doi:10.1089/ten.teb.2013.0537

Shah, S., and Kang, K.-T. (2018). Two-Cell Spheroid Angiogenesis Assay System Using Both Endothelial Colony Forming Cells and Mesenchymal Stem Cells. *Biomolecules Ther.* 26 (5), 474–480. doi:10.4062/biomolther.2018.134

Shanbhag, S., Mohamed-Ahmed, S., Lunde, T. H. F., Suliman, S., Bolstad, A. I., Hervig, T., et al. (2020a). Influence of Platelet Storage Time on Human Platelet Lysates and Platelet Lysate-Expanded Mesenchymal Stromal Cells for Bone Tissue Engineering. *Stem Cel Res Ther* 11 (1), 351. doi:10.1186/s13287-020-01863-9

Shanbhag, S., Pandis, N., Mustafa, K., Nyengaard, J. R., and Stavropoulos, A. (2017a). Cell Cotransplantation Strategies for Vascularized Craniofacial Bone Tissue Engineering: A Systematic Review and Meta-Analysis of PreclinicalIn VivoStudies. *Tissue Eng. Part B: Rev.* 23 (2), 101–117. doi:10.1089/ten.TEB.2016.0283

Shanbhag, S., Stavropoulos, A., Suliman, S., Hervig, T., and Mustafa, K. (2017b). Efficacy of Humanized Mesenchymal Stem Cell Cultures for Bone Tissue Engineering: a Systematic Review with a Focus on Platelet Derivatives. *Tissue Eng. Part B: Rev.* 23, 552–569. doi:10.1089/ten.teb.2017.0093

Shanbhag, S., Suliman, S., Bolstad, A. I., Stavropoulos, A., and Mustafa, K. (2020b). Xeno-Free Spheroids of Human Gingiva-Derived Progenitor Cells for Bone Tissue Engineering. *Front. Bioeng. Biotechnol.* 8 (968). doi:10.3389/fbioe.2020.00968

Shanbhag, S., Suliman, S., Pandis, N., Stavropoulos, A., Sanz, M., and Mustafa, K. (2019). Cell Therapy for Orofacial Bone Regeneration: A Systematic Review and Meta-Analysis. *J. Clin. Periodontol.* 46 (Suppl. 21), 162–182. doi:10.1111/jcpe.13049

Sharpe, P. T. (2016). Dental Mesenchymal Stem Cells. *Development* 143, 2273–2280. doi:10.1242/dev.134189

Soffer, E., Ouhayoun, J. P., and Anagnostou, F. (2003). Fibrin Sealants and Platelet Preparations in Bone and Periodontal Healing. *Oral Surg. Oral Med. Oral Pathol. Oral Radiol. Endodontology* 95 (5), 521–528. doi:10.1067/moe.2003.152

Stefańska, K., Mehr, K., Wieczorkiewicz, M., Kulus, M., Angelova Volponi, A., Shibli, J. A., et al. (2020). Stemness Potency of Human Gingival Cells-Application in Anticancer Therapies and Clinical Trials. *Cells* 9 (8), 1916. doi:10.3390/cells9081916

Steffens, L., Wenger, A., Stark, G. B., and Finkenzeller, G. (2009). *In Vivo* engineering of a Human Vasculature for Bone Tissue Engineering Applications. *J. Cel Mol Med* 13 (9B), 3380–3386. doi:10.1111/j.1582-4934.2008.00418.x

Strassburg, S., Nienhueser, H., Björn Stark, G., Finkenzeller, G., and Torio-Padron, N. (2016). Co-culture of Adipose-Derived Stem Cells and Endothelial Cells in Fibrin Induces Angiogenesis and Vasculogenesis in a Chorioallantoic

Membrane Model. *J. Tissue Eng. Regen. Med.* 10 (6), 496–506. doi:10.1002/term.1769

Sun, M., Chi, G., Xu, J., Tan, Y., Xu, J., Lv, S., et al. (2018). Extracellular Matrix Stiffness Controls Osteogenic Differentiation of Mesenchymal Stem Cells Mediated by Integrin α5. *Stem Cel Res Ther* 9 (1), 52. doi:10.1186/s13287-018-0798-0

Tasev, D., van Wijhe, M. H., Weijers, E. M., van Hinsbergh, V. W. M., and Koolwijk, P. (2015). Long-Term Expansion in Platelet Lysate Increases Growth of Peripheral Blood-Derived Endothelial-Colony Forming Cells and Their Growth Factor-Induced Sprouting Capacity. *PLoS One* 10 (6), e0129935. doi:10.1371/journal.pone.0129935

Ucuzian, A. A., Bufalino, D. V., Pang, Y., and Greisler, H. P. (2013). Angiogenic Endothelial Cell Invasion into Fibrin Is Stimulated by Proliferating Smooth Muscle Cells. *Microvasc. Res.* 90, 40–47. doi:10.1016/j.mvr.2013.06.012

Verseijden, F., Sluijs, S. J. P.-V., Farrell, E., van Neck, J. W., Hovius, S. E. R., Hofer, S. O. P., et al. (2010). Prevascular Structures Promote Vascularization in Engineered Human Adipose Tissue Constructs upon Implantation. *Cel Transpl.* 19 (8), 1007–1020. doi:10.3727/096368910X492571

Zhang, M., Lin, R., Wang, X., Xue, J., Deng, C., Feng, C., et al. (2020). 3D Printing of Haversian Bone-Mimicking Scaffolds for Multicellular Delivery in Bone Regeneration. *Sci. Adv.* 6 (12), eaaz6725. doi:10.1126/sciadv.aaz6725

Žigon-Branc, S., Markovic, M., Van Hoorick, J., Van Vlierberghe, S., Dubruel, P., Zerobin, E., et al. (2019). Impact of Hydrogel Stiffness on Differentiation of Human Adipose-Derived Stem Cell Microspheroids. *Tissue Eng. Part A* 25 (19-20), 1369–1380. doi:10.1089/ten.TEA.2018.0237

Conflict of Interest: The authors declare that the research was conducted in the absence of any commercial or financial relationships that could be construed as a potential conflict of interest.

Publisher's Note: All claims expressed in this article are solely those of the authors and do not necessarily represent those of their affiliated organizations, or those of the publisher, the editors and the reviewers. Any product that may be evaluated in this article, or claim that may be made by its manufacturer, is not guaranteed or endorsed by the publisher.

Copyright © 2021 Shanbhag, Rashad, Nymark, Suliman, de Lange Davies, Stavropoulos, Bolstad and Mustafa. This is an open-access article distributed under the terms of the Creative Commons Attribution License (CC BY). The use, distribution or reproduction in other forums is permitted, provided the original author(s) and the copyright owner(s) are credited and that the original publication in this journal is cited, in accordance with accepted academic practice. No use, distribution or reproduction is permitted which does not comply with these terms.

frontiers in Bioengineering and Biotechnology

ORIGINAL RESEARCH
published: 19 August 2020
doi: 10.3389/fbioe.2020.00968

Xeno-Free Spheroids of Human Gingiva-Derived Progenitor Cells for Bone Tissue Engineering

Siddharth Shanbhag[1], Salwa Suliman[1], Anne Isine Bolstad[1], Andreas Stavropoulos[2,3] and Kamal Mustafa[1]**

[1] Department of Clinical Dentistry, Faculty of Medicine, University of Bergen, Bergen, Norway, [2] Department of Periodontology, Faculty of Odontology, Malmö University, Malmö, Sweden, [3] Division of Regenerative Medicine and Periodontology, University Clinics of Dental Medicine, University of Geneva, Geneva, Switzerland

Gingiva has been identified as a minimally invasive source of multipotent progenitor cells (GPCs) for use in bone tissue engineering (BTE). To facilitate clinical translation, it is important to characterize GPCs in xeno-free cultures. Recent evidence indicates several advantages of three-dimensional (3D) spheroid cultures of mesenchymal stromal cells (MSCs) over conventional 2D monolayers. The present study aimed to characterize human GPCs in xeno-free 2D cultures, and to test their osteogenic potential in 3D cultures, in comparison to bone marrow MSCs (BMSCs). Primary GPCs and BMSCs were expanded in human platelet lysate (HPL) or fetal bovine serum (FBS) and characterized based on *in vitro* proliferation, immunophenotype and multi-lineage differentiation. Next, 3D spheroids of GPCs and BMSCs were formed via self-assembly and cultured in HPL. Expression of stemness- (SOX2, OCT4, NANOG) and osteogenesis-related markers (BMP2, RUNX2, OPN, OCN) was assessed at gene and protein levels in 3D and 2D cultures. The cytokine profile of 3D and 2D GPCs and BMSCs was assessed via a multiplex immunoassay. Monolayer GPCs in both HPL and FBS demonstrated a characteristic MSC-like immunophenotype and multi-lineage differentiation; osteogenic differentiation of GPCs was enhanced in HPL vs. FBS. $CD271^+$ GPCs in HPL spontaneously acquired a neuronal phenotype and strongly expressed neuronal/glial markers. 3D spheroids of GPCs and BMSCs with high cell viability were formed in HPL media. Expression of stemness- and osteogenesis-related genes was significantly upregulated in 3D vs. 2D GPCs/BMSCs; the latter was independent of osteogenic induction. Synthesis of SOX2, BMP2 and OCN was confirmed via immunostaining, and *in vitro* mineralization via Alizarin red staining. Finally, secretion of several growth factors and chemokines was enhanced in GPC/BMSC spheroids, while that of pro-inflammatory cytokines was reduced, compared to monolayers. In summary, monolayer GPCs expanded in HPL demonstrate enhanced osteogenic differentiation potential, comparable to that of BMSCs. Xeno-free spheroid culture further enhances stemness- and osteogenesis-related gene expression, and cytokine secretion in GPCs, comparable to that of BMSCs.

Keywords: platelet lysate, mesenchymal stromal cells, gingival stem cells, spheroid culture, bone tissue engineering, regenerative medicine

OPEN ACCESS

Edited by:
Wan-ju Li,
University of Wisconsin–Madison, United States

Reviewed by:
Francesco Grassi,
Rizzoli Orthopedic Institute (IRCCS), Italy
Zetao Chen,
Sun Yat-sen University, China

****Correspondence:***
Siddharth Shanbhag
siddharth.shanbhag@uib.no
Kamal Mustafa
kamal.mustafa@uib.no

Specialty section:
This article was submitted to Tissue Engineering and Regenerative Medicine, a section of the journal Frontiers in Bioengineering and Biotechnology

Received: *22 April 2020*
Accepted: *27 July 2020*
Published: *19 August 2020*

Citation:
Shanbhag S, Suliman S, Bolstad AI, Stavropoulos A and Mustafa K (2020) Xeno-Free Spheroids of Human Gingiva-Derived Progenitor Cells for Bone Tissue Engineering. Front. Bioeng. Biotechnol. 8:968. doi: 10.3389/fbioe.2020.00968

INTRODUCTION

Adult mesenchymal stromal cells (MSCs) are increasingly being used in bone tissue engineering (BTE) for the reconstruction of clinically challenging bone defects. MSCs were originally identified in the bone marrow (BMSCs), and these are still the most frequently tested cells in clinical studies (Friedenstein et al., 1968; Pittenger et al., 2019). However, the yield of BMSCs obtained from the marrow mononuclear cell fraction is relatively low (≤0.01%) (Pittenger et al., 1999). Moreover, considerable donor-related variations in BMSCs, in addition to the morbidity associated with bone marrow harvesting, have prompted the investigation of 'MSC-like' cells from other, relatively less invasive, tissue sources (Mohamed-Ahmed et al., 2018; Wilson et al., 2019).

Oral tissues, such as dental pulp, mucosa, periodontal ligament (PDL) and gingiva, represent alternative sources of 'MSC-like' progenitor cells (Sharpe, 2016). Gingiva, in particular, can be harvested with minimal morbidity and rapid scarless healing, and is reported to contain a subpopulation of multipotent progenitor cells (GPCs) (Fournier et al., 2010; Mitrano et al., 2010). GPCs demonstrate the characteristic MSC-phenotype, immunomodulatory properties, and multi-lineage differentiation, possibly owing to their neural crest origins (Xu et al., 2013). Notably, GPCs have demonstrated superior properties in comparison to other MSCs *in vitro* (Yang et al., 2013; Sun et al., 2019), and the ability to regenerate bone *in vivo* (Wang et al., 2011; Ge et al., 2012). However, in all of these studies, GPCs were cultured in xenogeneic media.

A critical aspect in the clinical translation of MSC-based therapies is the use of safe and standardized culture conditions. Although commonly used for MSC expansion, several limitations of xenogeneic fetal bovine serum (FBS) supplementation have been highlighted, and current recommendations from health authorities advocate the use of 'xeno-free' protocols whenever possible (Bieback et al., 2019). Accordingly, xeno-free alternatives to FBS, such as human platelet lysate (HPL), have emerged (Shanbhag et al., 2017). HPL is shown to be comparable, and often superior, to FBS for the proliferation and multi-lineage differentiation of MSCs from various tissues (Burnouf et al., 2016). Moreover, MSCs expanded in HPL demonstrate enhanced osteoblastic differentiation, suggesting particular benefits for BTE (Shanbhag et al., 2017). However, no studies have yet reported on HPL-cultured GPCs.

In order to obtain clinically relevant cell numbers, current strategies demand the large-scale *ex vivo* expansion of MSCs, most commonly via plastic adherent/monolayer culture. However, this two-dimensional (2D) culture system is not representative of the 3D *in vivo* microenvironment (Sart et al., 2014; Petrenko et al., 2017). Moreover, expansion of MSCs via serial passaging in plastic-adherent cultures may alter their phenotype and diminish their regenerative and immunomodulatory potential (Follin et al., 2016; Ghazanfari et al., 2017). In contrast, the self-assembly or spontaneous aggregation of MSCs into 3D structures, mediated by unique cell-cell and cell-extracellular matrix (ECM) interactions, biomechanical cues and signaling pathways, more closely simulates their *in vivo* microenvironment or *niche* (Ahmadbeigi et al., 2012; Sart et al., 2014). The cytoskeletal changes induced by 3D culture have also been linked to 'mesenchymal cell condensation' (MCC) – a critical event during embryonic skeletal development via endochondral ossification, which can be recapitulated *ex vivo* (Hall and Miyake, 2000; Kale et al., 2000; Facer et al., 2005; Kim and Adachi, 2019).

While a majority of the literature is focused on BMSCs, 3D cultures have also been reported to enhance the survival, stemness, paracrine/immunomodulatory activity, and multi-lineage differentiation of oral tissue-derived MSCs (Zhang et al., 2012; Lee et al., 2017; Moritani et al., 2018; Subbarayan et al., 2018). However, few studies have characterized MSC spheroids in xeno-free cultures to facilitate clinical translation (Ylostalo et al., 2017; Dong et al., 2019). Therefore, the objectives of the present study were to establish xeno-free monolayer (2D) cultures of human GPCs in HPL, and subsequently, to test their osteogenic potential in 3D spheroid cultures in comparison to BMSCs.

MATERIALS AND METHODS

Monolayer (2D) Cell Culture

GPCs were isolated as previously described (Fournier et al., 2010). Briefly, human gingival biopsies were collected after ethical approval (Regional Ethical Committee-North, Norway, 2016-1266) and informed consent from systemically healthy patients aged 18–31 years (n = 5) undergoing surgery at the Department of Clinical Dentistry, University of Bergen, Bergen, Norway. From each donor, primary connective tissue-explant cultures of GPCs were established in 5% HPL (Bergenlys®, Bergen, Norway) and 10% FBS (GE Healthcare, South Logan, UT, United States) supplemented growth media [Dulbecco's Modified Eagle's medium (DMEM, Invitrogen, Carlsbad, CA, United States) with 1% antibiotics (penicillin/streptomycin; GE Healthcare)]. BMSCs (from different patients) were isolated and cultured in HPL media as previously described (Mohamed-Ahmed et al., 2018). Details of HPL production are provided in the **Supplementary data**. Cells were sub-cultured and expanded in their respective growth media in humidified 5% CO_2 at 37°C; passage 2–4 cells from at least three different donors were used in experiments. Proliferation of GPCs in HPL and FBS over 7 days was determined via an alamar blue assay (Invitrogen); at each time point, 10% vol. dye was added to the cells, incubated for 4 h and fluorescence was measured (540 Ex/590 Em).

Immunophenotype of 2D GPCs

The immunophenotype of HPL- and FBS-cultured GPCs was assessed by flow cytometry based on expression of specific surface antigens according to the "minimal criteria" for defining MSCs (Dominici et al., 2006). Briefly, cells in HPL and FBS were incubated with conjugated antibodies against selected 'negative' (CD34, CD45, HLA-DR) and 'positive' (CD73, CD90, CD105) MSC markers, and additionally CD271 (all from BD Biosciences, San Jose, CA, United States), following the manufacturers' recommendations. Quantification was performed with a BD LSR Fortessa analyzer and fluorescence activated cell sorting (FACS)

of CD271$^+$ GPCs with a BD FACS Aria sorter (both from BD Biosciences). Data were analyzed using flow cytometry software (Flowjo v10, Flowjo, LLC, Ashland, OR, United States).

Gene Expression in 2D GPCs

The expression of adipogenesis- and osteogenesis-related genes (**Supplementary Table 1**) in HPL- and FBS-cultured GPCs after 7 days in the appropriate induction media (see below), was assessed via quantitative real-time polymerase chain reaction (qPCR) using TaqMan® real-time PCR assays (Thermo Fisher Scientific, Carlsbad, CA, United States). RNA extraction and cDNA synthesis were performed as previously described (Mohamed-Ahmed et al., 2018). The expressions of the genes of interest were normalized to that of glyceraldehyde 3-phosphate dehydrogenase (GAPDH). Data were analyzed by the $\Delta\Delta Ct$ method and results are presented as fold changes in HPL groups relative to FBS groups.

Adipogenic Differentiation of 2D GPCs

The ability of GPCs to differentiate into multiple stromal lineages was tested as previously described (Mohamed-Ahmed et al., 2018). Briefly, for adipogenic differentiation, cells in HPL and FBS were cultured in StemPro® adipogenic differentiation medium (Invitrogen) or standard growth medium (control). After 21 days, cells were fixed with 4% paraformaldehyde (PFA) for 10 min at RT and intracellular lipid formation was assessed via Oil red O staining (Sigma-Aldrich, St. Louis, MO, United States).

Osteogenic Differentiation of 2D GPCs

For osteogenic differentiation, cells in HPL and FBS were cultured in osteogenic differentiation medium prepared by adding final concentrations of 0.05 mM L-ascorbic acid 2-phosphate, 10 nM dexamethasone and 10 mM β glycerophosphate (all from Sigma-Aldrich) to the respective growth media. After 21 days, cells were fixed and extracellular calcium deposition was evaluated via Alizarin red S staining (Sigma-Aldrich). The osteogenic potential of HPL-cultured GPCs was also tested on previously validated poly(L-lactide-co-ε-caprolactone) [poly(LLA-co-CL)] copolymer scaffolds (Yassin et al., 2017) (10^6 cells/scaffold); HPL-cultured BMSCs were used as a reference. Cell attachment and spreading on the scaffolds after 24 h was observed via scanning electron microscopy (SEM; Jeol JSM 7400F, Tokyo, Japan), as previously described (Yassin et al., 2017). After 14 days of induction, Alizarin red S staining was performed as described above. In all differentiation experiments, corresponding non-induced HPL- and/or FBS-cultured cells served as controls.

Neurogenic Differentiation and Immunofluorescence (IF) Staining of 2D GPCs

Since FACS isolated CD271$^+$ GPCs showed a neuronal-like morphology, the expression of neuronal [βIII-tubulin (TUJ1)] and glial markers [glial fibrillary acidic protein (GFAP)] was assessed via IF staining. Briefly, cells were fixed with PFA, permeabilized with 0.1% Triton X-100 and blocked with 10% goat serum in phosphate-buffered saline (PBS; Invitrogen). Cells were incubated with primary antibodies; mouse monoclonal anti-TUJ1 (Abcam, Cambridge, United Kingdom, dilution 1:100) and chicken monoclonal anti-GFAP (Abcam, dilution 1:100) overnight at 4°C. Corresponding secondary antibodies were incubated for 1 h at RT (Thermo Fisher Scientific, dilution 1:200). After washing with PBS, the nuclei were stained with 4′,6-diamidino-2-phenylindole (DAPI) (Sigma-Aldrich, dilution 1:2000). Imaging was performed using a confocal microscope (Andor Dragonfly, Oxford Instruments, Abingdon, United Kingdom).

3D Spheroid Culture

Formation of GPC and BMSC spheroids was assessed via two methods: mesenspheres (Isern et al., 2013) and aggregates (Baraniak and McDevitt, 2012). Briefly, dissociated passage 1–2 monolayer GPCs and BMSCs in HPL media were seeded (1000 cells/cm^2) in low-attachment dishes (Corning®, Corning, NY, United States) for 7 days to obtain mesenspheres, or in microwell-patterned 24-well plates (Sphericalplate®, Kugelmeiers Ltd, Erlenbach, CH) for 24 h to obtain spheroid aggregates of 1000–2000 cells. The novel design of these microwell plates was optimized for embryoid body formation (Silin, 2012). Since aggregate spheroids could be formed more predictably than mesenspheres, only the former were used in subsequent experiments. Cell viability in spheroids was assessed after 7 days via a live/dead assay (Thermo Fisher Scientific). Hereafter, the terms 2D or monolayer culture and 3D or spheroid culture are used interchangeably throughout the manuscript.

Gene Expression and Osteogenic Differentiation in 3D Spheroids

The expression of pluripotency/stemness-related genes (**Supplementary Table 1**) was assessed in 3D and 2D GPCs and BMSCs after 7 days of suspension and adherent culture, respectively, via qPCR. Similarly, the expression of osteogenesis-related genes (**Supplementary Table 1**) was assessed after 7 days in standard (non-induced) and osteogenically induced cultures (as described above). Gene expression experiments were performed using spheroids and monolayers generated from both independent and pooled donor-cells and data are presented as fold changes in 3D groups relative to 2D groups. Protein expression of osteogenic markers was determined after 14 days via IF (see below). Alizarin red S staining was performed after 21 days to detect mineralization in induced and non-induced spheroids and monolayers; spheroids were stained in suspension, and following paraffin embedding and histological sectioning (3–5 μm).

IF Staining in 3D Spheroids

The protein expression of stemness [sex determining region Y-box 2 (SOX2)] and osteogenic markers [bone morphogenetic protein 2 (BMP2), osteocalcin (OCN)] was assessed in GPC and BMSC spheroids after 10 or 14 days of suspension culture via IF staining. The primary antibodies rabbit polyclonal anti-SOX2 (Abcam, dilution 1:1000), mouse monoclonal anti-BMP2 (Bio-Techne, Abingdon, United Kingdom, dilution 1:100), and rabbit polyclonal anti-OCN (Abcam, dilution 1:100) were incubated ON at 4°C. Corresponding secondary antibodies were incubated for 1 h at RT (Thermo Fisher Scientific; dilution 1:200), and

nuclei were stained with DAPI (Sigma-Aldrich; dilution 1:2000) before imaging with a confocal microscope (Andor Dragonfly). Cell autofluorescence and non-specific staining was confirmed in control samples incubated with neither or only secondary antibodies, respectively (data not shown).

Multiplex Cytokine Assay

Conditioned media (CM) from 2D and 3D GPCs and BMSCs were collected after 48 h culture in HPL-free medium and the concentrations of several cytokines (**Supplementary Table 2**) were measured using a custom multiplex assay and a Bio-Plex® 200 System (both from Bio-Rad Laboratories, CA, United States), according to the manufacturer's instructions. Although the initial number of cells seeded in 2D and 3D cultures was the same, to account for differences in the rates of cell proliferation between the conditions, cytokine concentrations (pg/mL) were normalized to the corresponding total DNA (ng/mL). DNA quantification was performed using the Quant-IT® PicoGreen dsDNA Assay Kit (Thermo Fisher Scientific) according to the manufacturer's instructions.

Statistical Analysis

Statistical analyses were performed using GraphPad Prism v 8.0 (GraphPad Software, San Diego, CA, United States). Data are presented as means (± SD), unless specified. Analyses of gene expression data are based on delta-CT values and results are presented as relative (log/non-linear) fold changes using scatter plots. Multiplex proteomic data are presented on a logarithmic ($\log_{10}$) scale. All other linear data are presented as bar graphs. Normality testing was performed via the Shapiro–Wilk test. The student *t*-test, Mann–Whitney *U*-test or one-way analysis of variance (ANOVA followed by a *post hoc* Tukey's test for multiple comparisons), were applied as appropriate, and $p < 0.05$ was considered statistically significant.

RESULTS

Characterization of 2D GPCs

GPCs demonstrating characteristic plastic adherence and fibroblastic morphology were isolated from gingiva explants in both HPL- and FBS-media. GPCs in HPL appeared smaller and more spindle-shaped, especially in early passages (**Figure 1A**), and demonstrated a higher proliferation rate ($p < 0.05$) (**Figure 1B**). Both HPL- and FBS-expanded GPCs demonstrated a characteristic MSC phenotype, i.e., > 95% of the cells were positive for CD73, CD90 and CD105, and < 5% of the cells expressed the hematopoietic markers CD34 and CD45; HLA-DR expression was < 8% (**Figure 1C**). Expression of CD271 was observed in < 5% of GPCs in both conditions.

Adipogenic Differentiation of 2D GPCs

GPCs in both HPL and FBS demonstrated the capacity to differentiate into adipocytes. The expression of genes associated with adipogenic differentiation, peroxisome proliferator-activated receptor-gamma (PPARG) and lipoprotein lipase (LPL), was significantly upregulated in HPL- vs. FBS-cultured GPCs after 7 days of adipogenic induction; LPL was also upregulated in non-induced HPL-cultured GPCs ($p < 0.05$; **Figure 1D**). Accumulation of intracellular lipid vesicles after 21 days was confirmed via Oil red O staining of GPCs in both conditions (**Figure 1E**). No differentiation of control cells was observed in the standard growth media.

Osteogenic Differentiation of 2D GPCs

GPCs in both HPL and FBS demonstrated the capacity to differentiate into osteoblasts. Genes associated with both early [runt-related transcription factor 2 (RUNX2), alkaline phosphatase (ALP)] and late osteogenic differentiation [collagen I (COL1), osteocalcin (OCN/BGLAP)] were upregulated in HPL- vs. FBS-cultured GPCs after 7 days; these genes were also upregulated in non-induced HPL-cultured GPCs ($p < 0.05$; **Figure 1D**). Extracellular calcium deposition was confirmed via Alizarin red S staining after 21 days; greater calcium deposition was observed in HPL-cultured GPCs (**Figure 1E**). Next, the osteogenic differentiation of HPL-cultured GPCs was tested on copolymer scaffolds in comparison to that of BMSCs. Cell attachment and spreading on the scaffold surface was confirmed after 24 h via SEM. After 14 days of osteogenic induction the entire scaffold surface was covered with mineralized matrix as revealed by Alizarin red S staining; staining was comparable between GPCs and BMSCs (**Supplementary Figure 1**).

Neurogenic Differentiation of 2D GPCs

To investigate whether CD271 represents a marker to enrich osteogenic cells, $CD271^+$ GPCs in HPL and FBS media were isolated via FACS. Interestingly, these cells acquired a neuronal morphology, which was more evident in HPL- than FBS-cultures (**Figure 2A**). Subsequently, IF staining revealed an abundant expression of neuronal (TUJ1) and glial markers (GFAP) in HPL-cultured $CD271^+$ GPCs, while only a few FBS-cultured cells appeared to express these markers (**Figure 2B**).

Formation and Viability of 3D Spheroids

3D spheroids of GPCs and BMSCs were formed as mesenspheres or aggregates in HPL media (**Figure 3A**). Since the former method relies on the self-renewal capacity of individual cells, the size and shape of mesenspheres varied considerably ($\phi < 100$ μm) and the frequency of sphere formation was low; sphere formation in GPCs was considerably lower than in BMSCs. In contrast to mesenspheres, highly consistent spheroids of GPCs and BMSCs were obtained via spontaneous aggregation in microwells (∼1000 cells/spheroid, ϕ 100–300 μm; **Figure 3B**). Viability of a majority of cells within the aggregate spheroids was confirmed via live/dead staining (**Figure 3C**).

Gene Expression and Osteogenic Differentiation in 3D Spheroids

The expression of stemness- and osteogenesis-related genes was assessed in 3D and 2D GPCs and BMSCs after 7 days of suspension culture. SOX2 and octamer-binding transcription factor 4 (OCT4) were significantly upregulated in GPC/BMSC spheroids vs. monolayers ($p < 0.05$); nanog homeobox factor (NANOG) was upregulated only in GPC spheroids (**Figure 4A**).

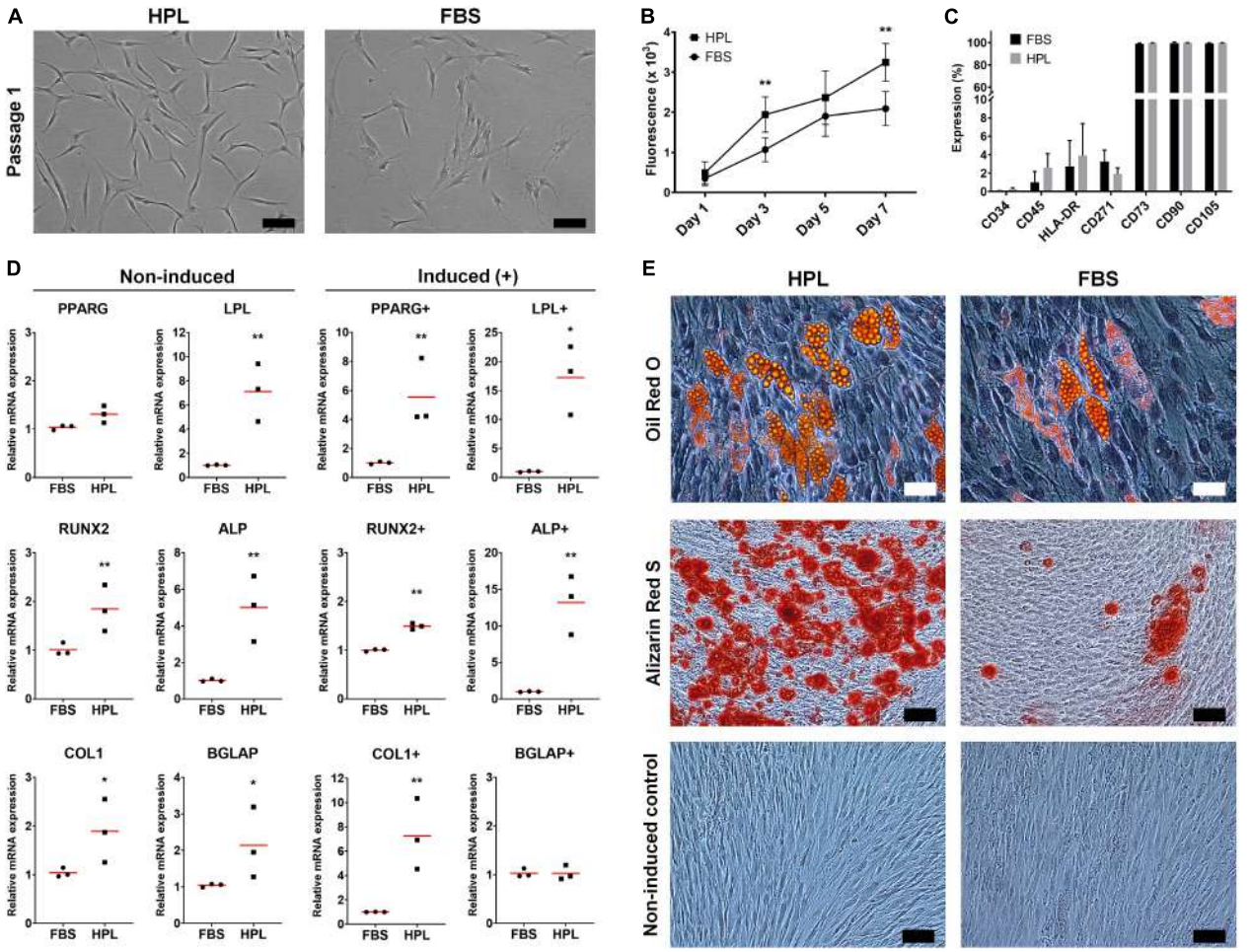

FIGURE 1 | Characterization of monolayer GPCs in HPL and FBS. **(A)** Morphology of passage 1 GPCs from one representative donor; scale bars 100 μm. **(B)** Proliferation of GPCs based on metabolic activity over 7 days; data represent means ± SD (n = 3 donors); $^{**}p < 0.001$. **(C)** Percentage expression of positive and negative surface markers based on flow cytometry; data represent means ± SD (n = 3 donors). **(D)** Relative expression (fold changes) of adipogenesis- and osteogenesis-related genes in GPCs after 7 days culture in growth or induction media (+). Data represent means; each symbol represents a single donor (n = 3 donors) based on the average of ≥ 2 experimental replicates; statistical analyses are based on delta-Ct values; $^{*}p < 0.05$; $^{**}p < 0.001$. **(E)** Representative images of Oil red O (adipogenic: scale bars 50 μm), Alizarin Red S (osteogenic) and control (non-induced) stained GPCs after 21 days; scale bars 100 μm.

A relatively higher degree of gene upregulation was observed in spheroids of GPCs as compared to BMSCs. SOX2 and OCT4 were also upregulated in independent donor GPC and BMSC spheroids (**Supplementary Figure 2A**). Expression of SOX2 in 3D GPCs and BMSCs was confirmed via IF staining (**Figure 4B**).

With regards to osteogenesis, genes associated with both early (BMP2) and late stages [OCN/BGLAP, osteopontin (OPN/SPP1)] of osteogenic differentiation were upregulated in 3D GPCs and BMSCs ($p < 0.05$) (**Figure 5A**); RUNX2 was upregulated in independent donor, but not pooled, spheroids (**Supplementary Figure 2B**). In contrast to stemness-related genes, a relatively higher degree of upregulation of osteogenesis-related genes was observed in 3D BMSCs as compared to GPCs. With regards to the effects of osteogenic induction, although BMP2, OPN and OCN were also significantly upregulated in 3D GPCs and BMSCs vs. monolayers after 7 days of osteogenic induction, upregulation of these genes was relatively higher in non-induced spheroids (**Figure 5A**). Protein expression of BMP2 and OCN after 14 days was confirmed via IF staining (**Figure 5B**, **Supplementary Figure 3**); expression of BMP2 was further confirmed via western blotting (**Supplementary Figure 4**).

After 21 days of osteogenic induction, 3D and 2D GPCs and BMSCs were positively stained for mineral deposition with Alizarin red (**Figure 6A**). In 2D cultures, the staining appeared to be marginally more intense in BMSCs, while in 3D cultures, the staining appeared comparable between GPC and BMSC spheroids. Mineral staining within the core of the spheroids was confirmed via histology, revealing a mature and organized ECM (**Figure 6B**).

Cytokine Profile of 3D Spheroids

The concentrations of various growth factors, chemokines and inflammatory cytokines (**Supplementary Table 2**) were measured in the 48 h CM of spheroid and monolayer

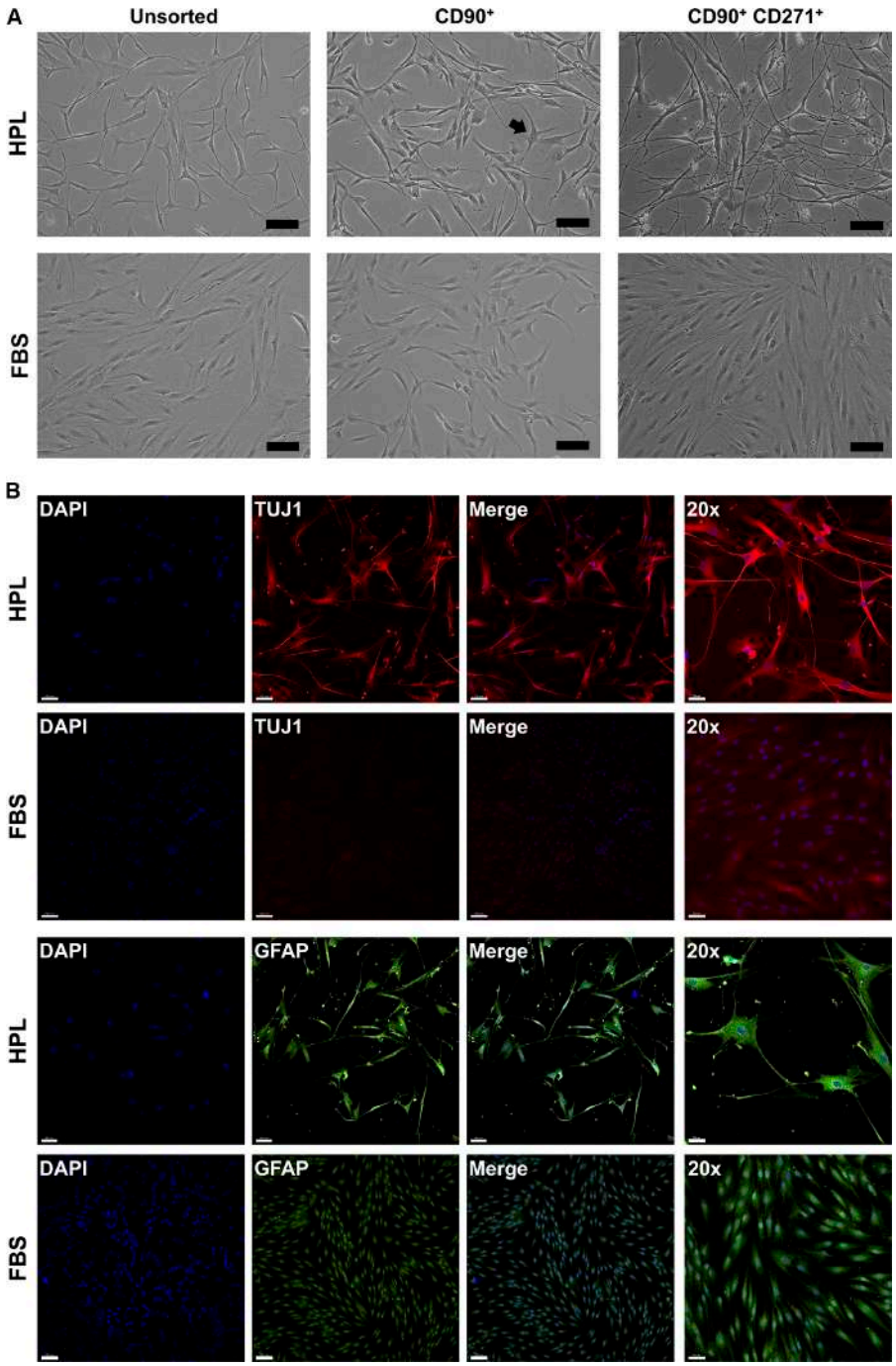

FIGURE 2 | Characterization of CD271$^+$ GPCs. **(A)** Selection of CD271$^+$ GPCs via FACS revealed a neuronal morphology in HPL-, but not FBS-cultured cells; *unsorted* cells represent the total plastic adherent gingival cell population; CD90 was used as a 'reference' marker (some cells with neuronal morphology are visible – *arrow*); scale bars 100 μm. **(B)** IF staining for βIII-tubulin (TUJ1) and GFAP in CD271$^+$ GPCs; scale bars 100 μm (50 μm for 20× images).

GPCs and BMSCs. Several growth factors (FGF2, PDGF-BB, TGF-β1, HGF, SCF, GCSF) were elevated in spheroid cultures; VEGF was elevated in GPC, but not BMSC spheroids (**Figure 6**). Notably, both spheroid and monolayer GPCs and BMSCs produced high concentrations of SCGF-β. A number of chemokines (CCL2, CCL3, CCL4, CCL5/RANTES, LIF, MIF) were also elevated in the CM of spheroid GPCs, while others (CCL11, CXCL10, CXCL12) were higher in monolayers; CXCL1 was markedly elevated in the CM of BMSC spheroids. Interestingly, several pro-inflammatory cytokines (IL-1α, 1IL-1β, IL-2, TNF-α, IFN-γ) were downregulated in the CM of GPC and BMSC spheroids, while IL-8 was markedly

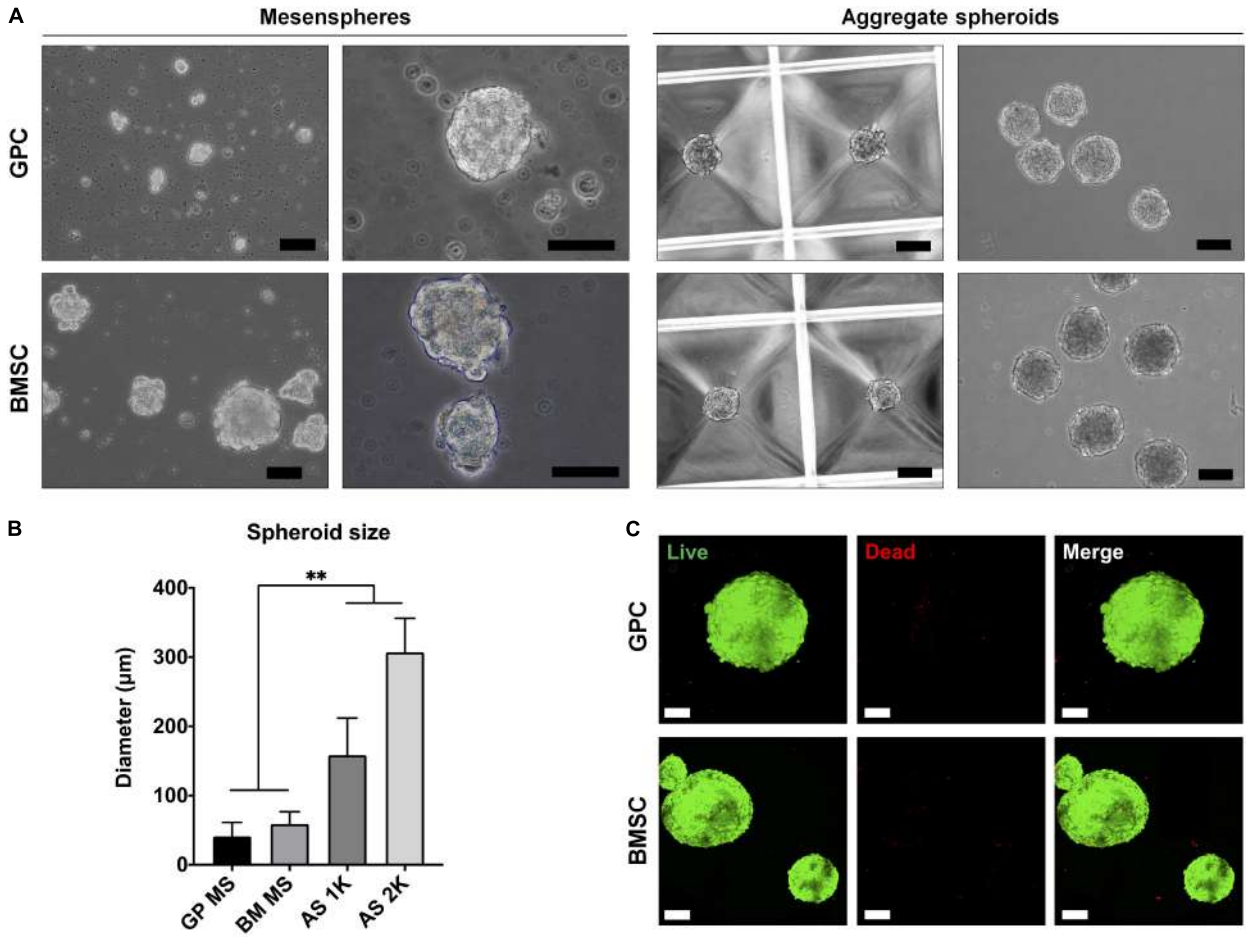

FIGURE 3 | Formation of xeno-free 3D spheroids. **(A)** Representative images of GPC and BMSC mesenspheres (scale bars 50 μm) and aggregate spheroids (scale bars 100 μm). **(B)** Quantification of spheroid size in mesenspheres (MS), and aggregate spheroids of 1000 (AS 1K) and 2000 cells (AS 2K); data represent means ± SD ($n = \geq 10$ spheres); $^{**}p < 0.001$. **(C)** Viability of GPC and BMSC aggregate spheroids represented by live (green) and dead (red) cells: scale bars 100 μm.

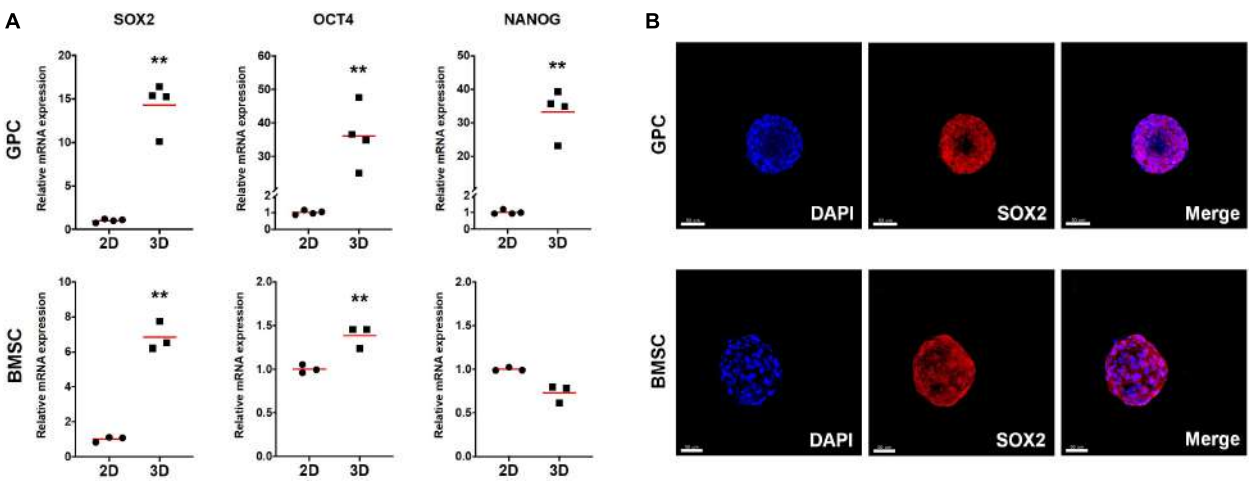

FIGURE 4 | Expression of stemness markers in xeno-free 3D spheroids. **(A)** Relative expression (fold changes) of stemness-related genes after 7 days in 2D and 3D GPCs and BMSCs. Data represent means ($n = \geq 3$ experimental replicates); statistical analyses are based on delta-Ct values; $^{*}p < 0.05$; $^{**}p < 0.001$. **(B)** IF staining of SOX2 in 3D spheroids after 10 days of suspension culture; cell nuclei are stained in DAPI: scale bars 50 μm.

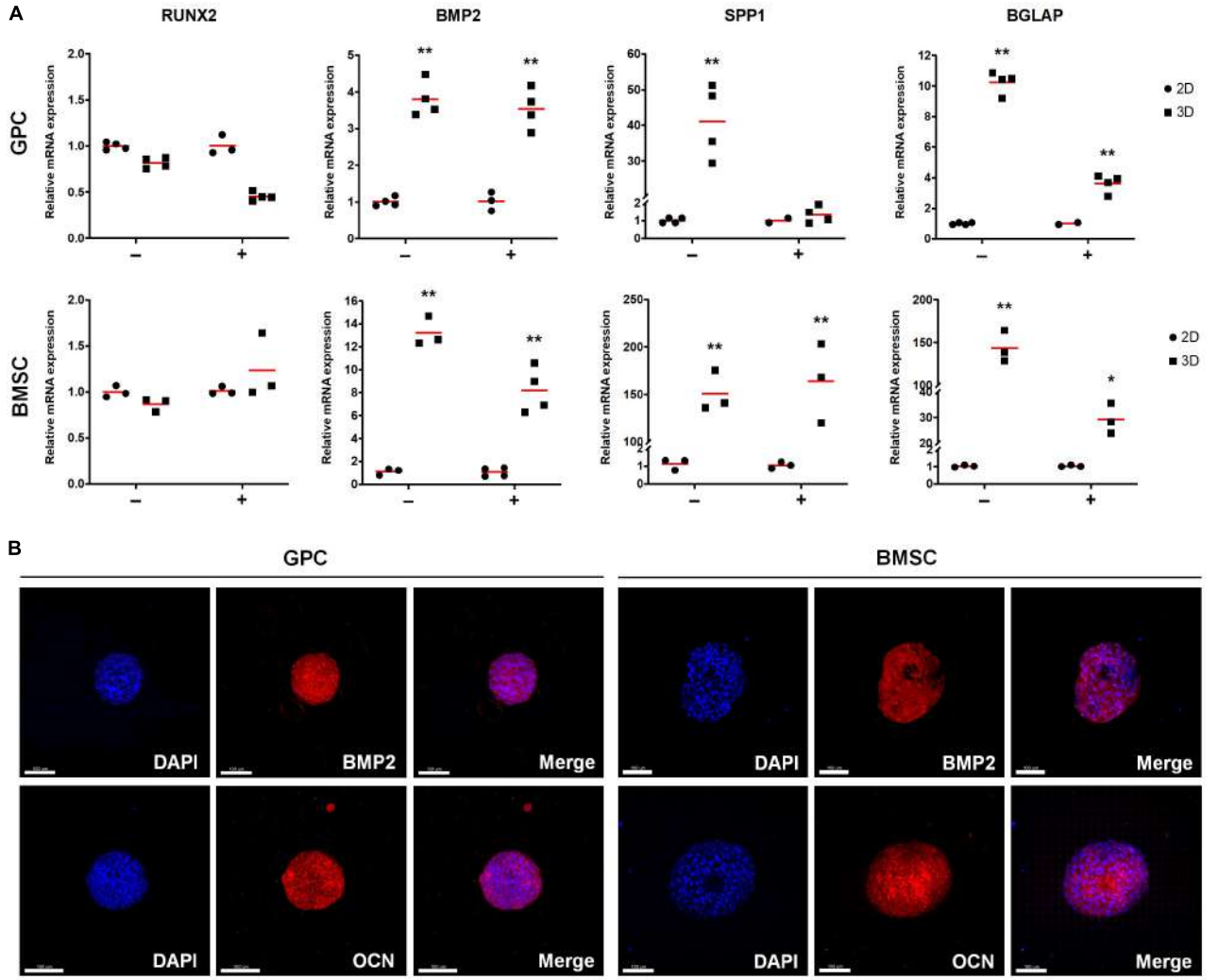

FIGURE 5 | Expression of osteogenesis markers in xeno-free 3D spheroids. **(A)** Relative expression (fold changes) of osteogenesis-related genes after 7 days in 2D and 3D GPCs and BMSCs under non-induced (–) and osteogenically induced conditions (+). Data represent means ($n = \geq 3$ experimental replicates); statistical analyses are based on delta-Ct values; $^{*}p < 0.05$; $^{**}p < 0.001$. **(B)** IF staining of BMP2 and OCN in 3D spheroids after 14 days of suspension culture; cell nuclei are stained in DAPI: scale bars 100 μm.

elevated, especially in BMSCs. The anti-inflammatory IL-10 was upregulated in monolayers in both GPCs and BMSCs (**Figure 7**).

DISCUSSION

Gingiva represents a minimally invasive source of multipotent progenitor cells (GPCs) with promising potential for BTE (Wang et al., 2011). To facilitate the clinical translation of GPCs, it is important to characterize their properties in xeno-free cultures compliant with current Good Manufacturing Practices (cGMP). Although previous studies have reported xeno-free culture of cells from other oral tissues using HPL (Naveau et al., 2011; Chen et al., 2012; Wu et al., 2017), to our knowledge, no studies have yet reported on HPL-cultured GPCs. In the present study, GPCs from matched donors were cultured in HPL- or FBS-supplemented media, thus allowing true and standardized comparisons between xeno-free and xenogeneic cultured cells. Overall, the GPCs herein demonstrated superior proliferation and osteogenic differentiation in HPL-supplemented media.

Monolayer GPCs demonstrated a 'classical' MSC-immunophenotype (Dominici et al., 2006) with no remarkable differences between HPL- and FBS-cultured cells. However, the specificity of the 'classical' surface markers to identify true MSC fractions in heterogeneous cell populations, especially those not derived from bone marrow, has been questioned (Halfon et al., 2011; Lv et al., 2014). CD271 or low-affinity nerve growth factor receptor (LNGFR) is reportedly a more specific marker for isolating a primitive subset of BMSCs with high clonogenicity and multi-lineage, specifically osteogenic, differentiation potential (Cuthbert et al., 2015). Osteogenic enrichment has also

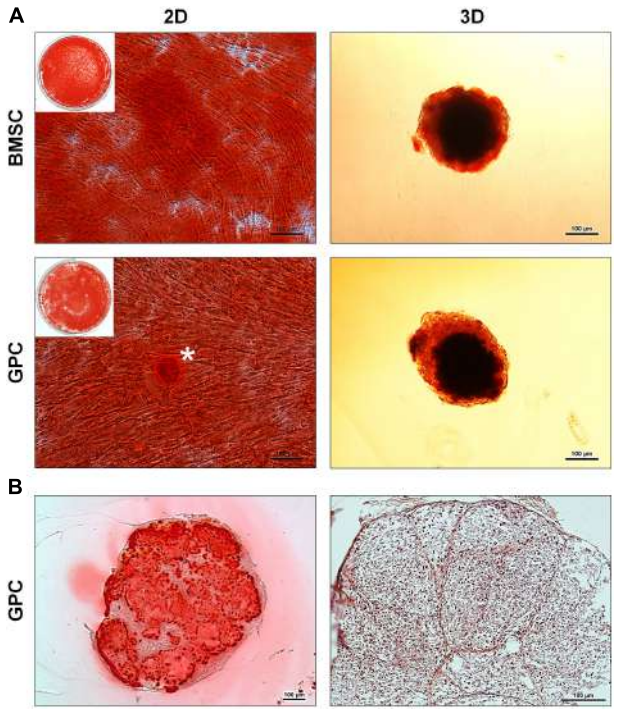

FIGURE 6 | Osteogenic differentiation of xeno-free 3D spheroids. **(A)** Alizarin red staining of 2D and 3D GPCs and BMSCs after 21 days of osteogenic induction; * indicates pronounced mineralization in an area of cellular condensation. **(B)** Histological sections of differentiated 3D GPCs showing internal mineralization (left) and ECM organization following removal of the stain (right); scale bars 100 μm.

been reported in $CD271^+$ subsets (< 5%) of dental pulp (DPCs) (Alvarez et al., 2015a) and PDL cells (PDLCs) (Alvarez et al., 2015b). Indeed, a small fraction (1–3%) of $CD271^+$ cells was identified in HPL- and FBS-cultured GPCs herein. Interestingly, these cells acquired a neuronal-like morphology; cells in HPL appeared more differentiated with limited proliferation capacity and more homogenous expression of neuronal/glial markers vs. FBS-cultured cells. Indeed, CD271 is reported to be a marker of neural stem/progenitor cells (van Strien et al., 2014). Moreover, craniofacial tissues, including gingiva, have a neural crest origin and therefore contain a subpopulation of cells with the capacity for neurogenic differentiation (Xu et al., 2013). Previous studies have reported the neuronal differentiation of unsorted GPCs when stimulated with neurogenic supplements (Subbarayan et al., 2017; Gugliandolo et al., 2019), although which fraction of the total GPC population actually differentiated, and to what extent, is unclear. Based on the findings herein, the CD271+ GPCs may represent a subpopulation with a propensity for neurogenic differentiation, which is further enhanced in HPL culture. In context, a recent study reported enhanced survival and differentiation of neuronal precursor cells in HPL (Nebie et al., 2020). However, further research is needed to confirm the phenotype and neurogenic potential of CD271+ GPCs.

Concerning multi-lineage differentiation, both HPL- and FBS-cultured monolayer GPCs could be differentiated into adipocytes and osteoblasts *in vitro*. The osteogenic differentiation of GPCs was significantly enhanced in HPL vs. FBS cultures at early and terminal stages, as revealed by gene expression and calcium deposition, respectively. Similar findings have been reported in relation to HPL-cultured DPCs (Chen et al., 2012) and PDLCs (Abuarqoub et al., 2015). Interestingly, the expression of osteogenic genes was also upregulated in non-induced HPL-cultured GPCs after 7 days. It may be hypothesized that this upregulation is related to the presence of several cytokines in HPL, which may influence MSCs' osteogenic differentiation (Shanbhag et al., 2017). HPL-cultured GPCs also demonstrated attachment and mineralization on copolymer scaffolds, in a comparable manner to BMSCs, highlighting their relevance for BTE applications. Regarding their *in vivo* mineralization capacity, previous studies have reported variable results using FBS-cultured GPCs, ranging from well- to poorly-mineralized tissues (Fournier et al., 2010; Tomar et al., 2010; Wang et al., 2011; Ge et al., 2012; Yang et al., 2013; Moshaverinia et al., 2014). Whether HPL culture enhances the *in vivo* mineralization of monolayer GPCs, remains to be determined.

To overcome the limitations of traditional 2D/monolayer cultures, several studies have demonstrated the benefits of 3D spheroid cultures in terms of promoting the self-renewal, differentiation and paracrine/immunomodulatory activity of MSCs (Murphy et al., 2014; Sart et al., 2014; Follin et al., 2016). Various methods for spheroid culture have been reported (Sart et al., 2014), and can broadly be categorized as *mesenspheres* or *aggregates*. In the *mesenspheres* approach, sphere formation occurs via self-renewal of primary non-expanded (Isern et al., 2013) or early-passage expanded MSCs (Kuroda et al., 2010) seeded in low-density non-adherent cultures. These sphere-forming cells represent 'true' stem cells with a capacity for self-renewal and differentiation both *in vitro* and *in vivo* (Basu-Roy et al., 2010; Isern et al., 2013). A small fraction of passage one GPCs herein demonstrated the capacity to form mesenspheres in HPL media. However, the frequency of sphere-forming GPCs was low and of a heterogeneous nature compared to that of BMSCs under similar conditions. One explanation for the low frequency of mesenspheres could be the media composition; mesenspheres have previously only been generated in complex media formulations (Isern et al., 2013) in comparison to the standard HPL media used herein. Nevertheless, obtaining clinically relevant MSC numbers may be challenging with this approach, especially from tissues other than bone marrow.

In contrast to mesenspheres, the more common *aggregates* approach utilizes monolayer expanded cells to form 3D spheroids, either via self-assembly (Baraniak and McDevitt, 2012; Bartosh and Ylostalo, 2014) or forced aggregation (Iwasaki et al., 2019). In the present study, aggregate spheroids were generated via 'guided' self-assembly in novel microwell-patterned tissue culture plates – no studies have yet reported this particular micro-well design to generate MSC spheroids. Spheroids with controlled size and morphology were formed after 24 h and showed favorable cell viability with few dead

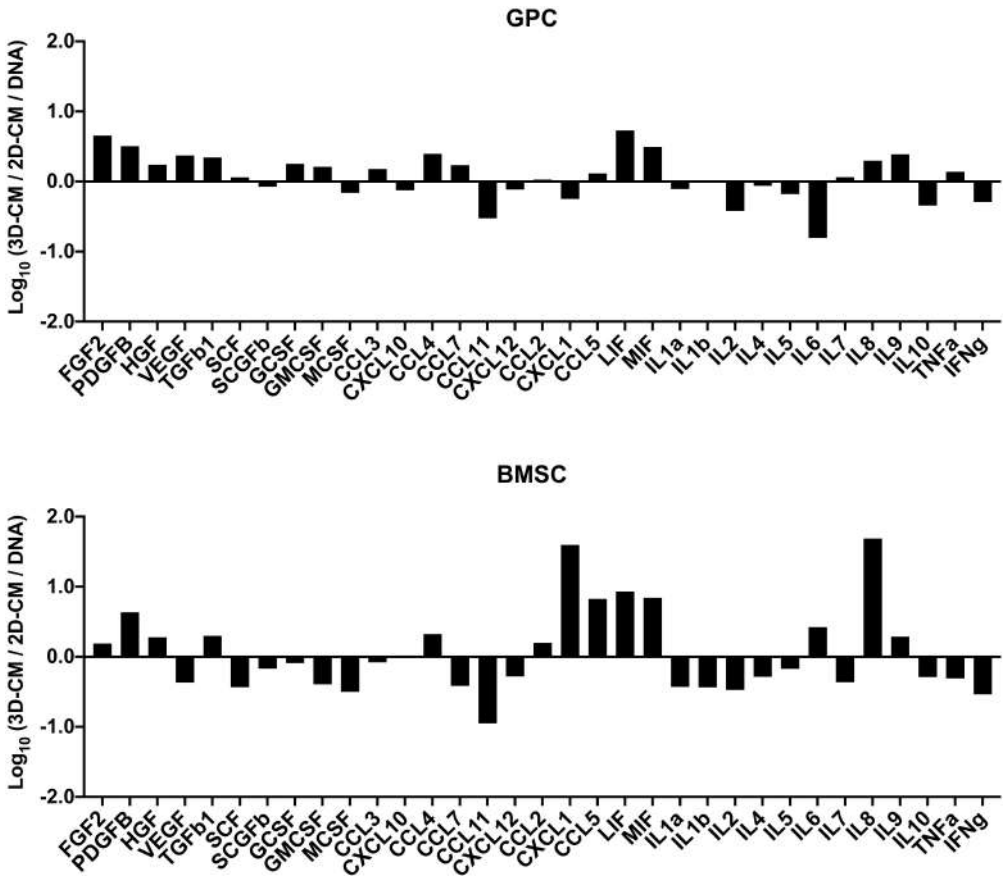

FIGURE 7 | Cytokine profile of xeno-free 3D spheroids. Cytokine concentrations (pg/mL) were measured in the 48 h CM of 2D and 3D GPCs and BMSCs and normalized to their DNA contents (ng/mL). Data are presented as the logarithm (log_{10}) of the ratio between the normalized means of 3D-CM and 2D-CM.

cells after 7 days in HPL-supplemented media. Self-assembly of cells has been linked to events during organogenesis, e.g., MCC during skeletal development (Hall and Miyake, 2000). MCC is known to be a critical event during endochondral ossification and these condensations represent "the earliest sign of the initiation of a skeletal element or elements" (Hall and Miyake, 2000). Indeed, aggregate cultures are routinely used to induce chondrogenic differentiation of MSCs *in vitro,* and often show signs of 'hypertrophy' suggestive of endochondral ossification. Even in osteogenically differentiated monolayer MSCs, mineral deposition is observed most prominently in regions of high cellular 'confluence' or condensation (**Figure 6**), after prolonged (2–4 weeks) *in vitro* culture (Kaul et al., 2015). Aggregates of MSCs/osteoprogenitors are reported to mimic such condensations *in vitro,* thereby recapitulating embryonic events during endochondral ossification (Kale et al., 2000; Kim and Adachi, 2019). Moreover, the cytoskeletal changes induced by self-assembly of MSCs into 3D structures, as reviewed elsewhere (Sart et al., 2014), induce "epigenetic" changes which enhance their self-renewal and differentiation potential (Guo et al., 2014).

In *pluripotent* embryonic stem cells (ESCs), self-renewal and maintenance of pluripotency are regulated by three main transcription factors – SOX2, OCT4 and NANOG (He et al., 2009). In *multipotent* cells, such as MSCs, these factors are associated with self-renewal (or 'stemness') and maintenance of an undifferentiated cellular state, even in 2D/monolayer cultures (Kolf et al., 2007). In more differentiated 2D cells, e.g., fibroblasts, *ectopic* (over)expression of pluripotency factors triggers cellular reprogramming back to a pluripotent state, as in induced pluripotent stem cells (iPSCs) (He et al., 2009). However, simply changing the microenvironment from 2D to 3D/spheroid culture is known to cause an *intrinsic* upregulation of pluripotency factors in MSCs/osteoprogenitors, suggesting enhanced self-renewal and differentiation potential (Basu-Roy et al., 2010; Guo et al., 2014). Consistently, a significant upregulation of pluripotency factors was observed in 3D vs. 2D GPCs and BMSCs herein. Interestingly, similar observations were recently reported in PDLCs (Moritani et al., 2018) and dermal fibroblasts (Lo et al., 2019). In the latter study, transcriptome analyses revealed differential regulation of 3304 genes in 3D vs. 2D cultures, and the authors concluded that even in naturally heterogeneous populations, such as fibroblasts, the mere shift from a 2D to 3D microenvironment induces gene expression patterns suggestive of "dedifferentiation" or "reprogramming" towards pluripotency

(Lo et al., 2019). Both PDL and gingiva are connective tissues with large fibroblast populations. Indeed, fibroblasts from various tissues, including gingiva, are reportedly indistinguishable from MSCs *in vitro*, based on the current "minimal criteria" (Mostafa et al., 2011; Denu et al., 2016). This identical pattern of pluripotency gene-upregulation further supports the evidence for a certain plasticity between 'MSCs' and more differentiated cells (Ichim et al., 2018). However, whether upregulation of pluripotency factors in 3D spheroids of GPCs directly translates to enhanced *in vivo* survival, requires further investigation.

In addition to pluripotency markers, an upregulation of early (RUNX2, BMP2) and late osteogenesis-related genes (OPN, OCN) was observed in GPC/BMSC spheroids, even in the absence of osteogenic supplements. As already discussed, a similar upregulation of osteogenic genes was observed in non-induced *HPL*-cultured 2D GPCs. However, *post hoc* analyses of *FBS*-cultured GPC spheroids revealed a similar pattern of osteogenic gene upregulation (**Supplementary Figure 5**), suggesting that this was primarily an effect of 3D culture. In context, a recent study reported upregulation of osteogenesis-related genes in FBS-cultured spheroids of murine pre-osteoblastic (MC3T3-E1) cells, where a stronger effect of "cell condensation" than osteogenic induction was highlighted, and attributed to recapitulation of 'MCC-like' events (Kim and Adachi, 2019). BMPs, including BMP2, are known to mediate MCC during skeletal development *in vivo* (Hall and Miyake, 2000), and are also well-established regulators of MSC osteogenic differentiation *in vitro*, via both extrinsic and autocrine signaling (Phimphilai et al., 2006). BMP2 is also reported to be among the most strongly upregulated genes in 3D spheroids of MSCs (Potapova et al., 2007; Cesarz et al., 2016) and other cells, e.g., fibroblasts (Lo et al., 2019). A previous study reported the 'early' *intrinsic* upregulation of BMP2 in FBS-cultured BMSC spheroids, independent of osteogenic induction, which translated to superior *in vitro* ECM production and mineralization vs. 2D BMSCs (Kabiri et al., 2012). The spontaneous upregulation of other bone-related markers (OPN, OCN), along with BMP2, as observed in the GPC/BMSC spheroids herein, further compliments these reports. OPN and OCN are important bone ECM proteins which subsequently undergo mineralization, and their expression is typically associated with later stages of osteogenic differentiation (Liu and Lee, 2013). However, positive staining (Alizarin red) for mineral deposits was only observed in osteogenically induced GPC/BMSC spheroids herein. Indeed, previous studies have reported superior *in vivo* bone regeneration by osteogenically induced spheroids of human BMSCs (Suenaga et al., 2015), DPCs (Lee et al., 2017) and PDLCs (Moritani et al., 2018), vs. monolayers. Thus, it may be hypothesized that MCC-like assemblies induced by spheroid culture *intrinsically* 'prime' MSCs towards osteoblastic commitment, although *extrinsic* signals/supplements may be necessary for terminal differentiation and/or matrix mineralization (Kale et al., 2000; Facer et al., 2005).

It is of relevance to discuss the simultaneous upregulation of pluripotency and osteogenesis-related genes in *in vitro* 3D spheroids, in the context of other literature. A similar observation was reported in a previous study comparing the transcriptome of 2D and 3D BMSCs – genes related to pluripotency (SOX2, OCT4, NANOG) and osteogenesis (BMP2, RUNX2, OPN) were upregulated in 3D BMSCs after 3 days of *in vitro* culture (Potapova et al., 2007). The pluripotency factors SOX2, OCT4 and NANOG are known to meditate somatic cell-reprogramming, and intrinsic BMP-signaling is also involved in the early stages this process (Samavarchi-Tehrani et al., 2010). With regard to 2D MSCs, SOX2 and BMP2 were found to be upregulated in subsets of BMSCs with high self-renewal and differentiation potential (Mareddy et al., 2010). Moreover, in 'reprogrammed' BMSCs (via forced expression of SOX2 or NANOG), osteogenic differentiation is enhanced, reportedly via BMP-signaling (Go et al., 2008; Ogasawara et al., 2013). In 3D MSCs, the switch to spheroid culture (without extrinsic supplements) leads to an epigenetic upregulation of not only the pluripotency factors, but also BMP2. BMPs, including BMP2, are known to mediate MCC *in vivo,* and MSC spheroids are considered to be the *in vitro* counterparts of 'MCC-like' condensations. In the MSC osteogenic differentiation cascade, BMP2 is a potent autocrine regulator of RUNX2, which in turn regulates the downstream expression of osteoblast-specific markers, e.g., OPN and OCN (Liu and Lee, 2013). Indeed, RUNX2, OPN and OCN were found to be upregulated in 3D GPCs and BMSCs herein. Thus, based on the literature, it may be hypothesized that BMP-signaling may act as a 'link' between these two distinct processes, i.e., self-renewal and (osteogenic) lineage commitment (**Supplementary Figure 6**). The co-existence of self-renewing *stem* cells and more-committed *progenitor* cells is a characteristic feature of the stem cell-*niche* (Kolf et al., 2007; He et al., 2009), which appears to be recapitulated in 3D spheroids. However, the role of BMP2 as hypothesized above was not experimentally confirmed herein, and demands further investigation.

Another advantage of 3D culture is the reported enhancement of MSCs' paracrine and immunomodulatory activity (Follin et al., 2016). Emerging concepts in BTE highlight paracrine- and immune-modulation as primary mechanisms for MSC-mediated bone regeneration (Pittenger et al., 2019). Consistent with previous reports (Zhang et al., 2012; Miranda et al., 2019), the secretome of GPC/BMSC spheroids was enriched in terms of upregulation of several growth factors and chemokines/immune-modulatory cytokines, and downregulation of several pro-inflammatory cytokines. This could, at least partly, explain the observed *in vivo* benefits of spheroid MSCs in regeneration and inflammation models (Zhang et al., 2012; Miranda et al., 2019). Moreover, the enrichment of several cytokines implicated in MSC recruitment and osteogenic differentiation, suggests that transplantation of HPL-cultured 3D GPCs, or their CM, may induce a favorable *in vivo* host-response. Indeed, the CM of 2D GPCs expanded in FBS (Qiu et al., 2020) or defined serum-free medium (Diomede et al., 2018) has recently been shown to promote *in vivo* bone regeneration. Interestingly, both 2D and 3D GPCs (and BMSCs) herein, secreted high concentrations of

stem cell growth factor (SCGF) – a protein encoded by the CLEC11A gene, which has been shown to promote osteogenic differentiation and *in vivo* fracture healing in murine MSC-models (Yue et al., 2016). Since high concentrations of SCGF were also detected in HPL (data not shown), this could be another benefit of HPL supplementation for BTE applications. Finally, whether the combination of HPL supplementation and 3D culture enhances the *in vivo* bone regeneration capacity of GPCs, should be investigated in future studies.

CONCLUSION

Monolayer GPCs expanded in HPL vs. FBS demonstrate enhanced *in vitro* osteogenic differentiation, comparable to that of BMSCs. When cultured as 3D spheroids in HPL, both GPCs and BMSCs express significantly higher levels of pluripotency genes as compared to monolayers, suggesting a higher potential for self-renewal. Simultaneously, the expression of osteogenesis-related genes is also significantly increased in GPC and BMSC spheroids, independent of osteogenic induction; *in vitro* mineralization was comparable between GPCs and BMSCs Finally, the secretome of GPC and BMSC spheroids is enriched, in terms of several growth factors, chemokines and immune-modulatory cytokines, in comparison to that of monolayers. In summary, while xeno-free cultured spheroids of GPCs are comparable to BMSCs *in vitro*, GPCs offer the advantage of less-invasive tissue harvesting and are thus promising candidates for BTE applications.

DATA AVAILABILITY STATEMENT

All datasets presented in this study are included in the article/**Supplementary Material**. Additional data can be made available by the authors upon request.

AUTHOR CONTRIBUTIONS

SSh designed the study, performed the experiments, analyzed the data, and drafted the manuscript. SSu contributed to the design, experiments, data analysis, and manuscript writing. AIB, AS, and KM contributed to the design, data analysis, and manuscript writing. All authors read and approved the final manuscript.

FUNDING

This work was supported by Helse Vest Strategic Research Funding, Norway (502027), Research Council of Norway (BEHANDLING/273551), Trond Mohn Foundation, Norway (BFS2018TMT10), and International Team for Implantology grant (ITI-1117/2015). SSh received the 2018 IADR/Karring-Nyman Sunstar Guidor award (Sunstar Foundation).

ACKNOWLEDGMENTS

We thank the Bloodbank at Haukeland University Hospital for supplying the platelets, Dr. Cecilie Gjerde and Dr. Torbjørn Ø Pedersen for the dental biopsies, and the Molecular Imaging Center (MIC), University of Bergen, for assistance with the confocal imaging. We also thank Niyaz Al-Sharabi and Neha Rana from the Department of Clinical Dentistry, and Harsh Dongre, Ridhima Das and Prof. Daniela Elena Costea from the Department of Clinical Medicine, University of Bergen, for assistance with the protein analysis and histology.

SUPPLEMENTARY MATERIAL

The Supplementary Material for this article can be found online at: https://www.frontiersin.org/articles/10.3389/fbioe.2020.00968/full#supplementary-material

REFERENCES

Abuarqoub, D., Awidi, A., and Abuharfeil, N. (2015). Comparison of osteo/odontogenic differentiation of human adult dental pulp stem cells and stem cells from apical papilla in the presence of platelet lysate. *Arch. Oral Biol.* 60, 1545–1553. doi: 10.1016/j.archoralbio.2015.07.007

Ahmadbeigi, N., Soleimani, M., Babaeijandaghi, F., Mortazavi, Y., Gheisari, Y., Vasei, M., et al. (2012). The aggregate nature of human mesenchymal stromal cells in native bone marrow. *Cytotherapy* 14, 917–924. doi: 10.3109/14653249.2012.689426

Alvarez, R., Lee, H. L., Hong, C., and Wang, C. Y. (2015a). Single CD271 marker isolates mesenchymal stem cells from human dental pulp. *Int. J. Oral Sci.* 7, 205–212. doi: 10.1038/ijos.2015.29

Alvarez, R., Lee, H. L., Wang, C. Y., and Hong, C. (2015b). Characterization of the osteogenic potential of mesenchymal stem cells from human periodontal ligament based on cell surface markers. *Int. J. Oral Sci.* 7, 213–219. doi: 10.1038/ijos.2015.42

Baraniak, P. R., and McDevitt, T. C. (2012). Scaffold-free culture of mesenchymal stem cell spheroids in suspension preserves multilineage potential. *Cell Tissue Res.* 347, 701–711. doi: 10.1007/s00441-011-1215-5

Bartosh, T. J., and Ylostalo, J. H. (2014). Preparation of anti-inflammatory mesenchymal stem/precursor cells (MSCs) through sphere formation using hanging-drop culture technique. *Curr. Protoc. Stem Cell Biol.* 28:Unit2B.6. doi: 10.1002/9780470151808.sc02b06s28

Basu-Roy, U., Ambrosetti, D., Favaro, R., Nicolis, S. K., Mansukhani, A., and Basilico, C. (2010). The transcription factor Sox2 is required for osteoblast self-renewal. *Cell Death Diff.* 17, 1345–1353. doi: 10.1038/cdd.2010.57

Bieback, K., Fernandez-Munoz, B., Pati, S., and Schafer, R. (2019). Gaps in the knowledge of human platelet lysate as a cell culture supplement for cell therapy: a joint publication from the AABB and the International Society for Cell & Gene Therapy. *Transfusion* 59, 3448–3460. doi: 10.1111/trf.15483

Burnouf, T., Strunk, D., Koh, M. B., and Schallmoser, K. (2016). Human platelet lysate: replacing fetal bovine serum as a gold standard for human cell propagation? *Biomaterials* 76, 371–387. doi: 10.1016/j.biomaterials.2015.10.065

Cesarz, Z., Funnell, J. L., Guan, J., and Tamama, K. (2016). Soft elasticity-associated signaling and bone morphogenic protein 2 are key regulators of mesenchymal stem cell spheroidal aggregates. *Stem Cells Dev.* 25, 622–635. doi: 10.1089/scd.2015.0356

Chen, B., Sun, H. H., Wang, H. G., Kong, H., Chen, F. M., and Yu, Q. (2012). The effects of human platelet lysate on dental pulp stem cells derived from impacted human third molars. *Biomaterials* 33, 5023–5035. doi: 10.1016/j.biomaterials.2012.03.057

Cuthbert, R. J., Giannoudis, P. V., Wang, X. N., Nicholson, L., Pawson, D., Lubenko, A., et al. (2015). Examining the feasibility of clinical grade CD271+

enrichment of mesenchymal stromal cells for bone regeneration. *PLoS One* 10:e0117855. doi: 10.1371/journal.pone.0117855

Denu, R. A., Nemcek, S., Bloom, D. D., Goodrich, A. D., Kim, J., Mosher, D. F., et al. (2016). Fibroblasts and mesenchymal stromal/stem cells are phenotypically indistinguishable. *Acta Haematol.* 136, 85–97. doi: 10.1159/000445096

Diomede, F., Gugliandolo, A., Scionti, D., Merciaro, I., Cavalcanti, M. F., Mazzon, E., et al. (2018). Biotherapeutic effect of gingival stem cells conditioned medium in bone tissue restoration. *Int. J. Mol. Sci.* 19:39. doi: 10.3390/ijms19020329

Dominici, M., Le Blanc, K., Mueller, I., Slaper-Cortenbach, I., Marini, F., Krause, D., et al. (2006). Minimal criteria for defining multipotent mesenchymal stromal cells. The International Society for Cellular Therapy position statement. *Cytotherapy* 8, 315–317. doi: 10.1080/14653240600855905

Dong, G., Wang, S., Ge, Y., Deng, Q., Cao, Q., Wang, Q., et al. (2019). Serum-free culture system for spontaneous human mesenchymal stem cell spheroid formation. *Stem Cells Int.* 2019:6041816. doi: 10.1155/2019/6041816

Facer, S. R., Zaharias, R. S., Andracki, M. E., Lafoon, J., Hunter, S. K., and Schneider, G. B. (2005). Rotary culture enhances pre-osteoblast aggregation and mineralization. *J. Dent. Res.* 84, 542–547. doi: 10.1177/154405910508400611

Follin, B., Juhl, M., Cohen, S., Pedersen, A. E., Kastrup, J., and Ekblond, A. (2016). Increased paracrine immunomodulatory potential of mesenchymal stromal cells in three-dimensional culture. *Tissue Eng. Part B Rev.* 22, 322–329. doi: 10.1089/ten.TEB.2015.0532

Fournier, B. P., Ferre, F. C., Couty, L., Lataillade, J. J., Gourven, M., Naveau, A., et al. (2010). Multipotent progenitor cells in gingival connective tissue. *Tissue Eng. Part A* 16, 2891–2899. doi: 10.1089/ten.TEA.2009.0796

Friedenstein, A. J., Petrakova, K. V., Kurolesova, A. I., and Frolova, G. P. (1968). Heterotopic of bone marrow. Analysis of precursor cells for osteogenic and hematopoietic tissues. *Transplantation* 6, 230–247.

Ge, S., Mrozik, K. M., Menicanin, D., Gronthos, S., and Bartold, P. M. (2012). Isolation and characterization of mesenchymal stem cell-like cells from healthy and inflamed gingival tissue: potential use for clinical therapy. *Regen. Med.* 7, 819–832. doi: 10.2217/rme.12.61

Ghazanfari, R., Zacharaki, D., Li, H., Ching Lim, H., Soneji, S., and Scheding, S. (2017). Human primary bone marrow mesenchymal stromal cells and their in vitro progenies display distinct transcriptional profile signatures. *Sci. Rep.* 7:10338. doi: 10.1038/s41598-017-09449-x

Go, M. J., Takenaka, C., and Ohgushi, H. (2008). Forced expression of Sox2 or Nanog in human bone marrow derived mesenchymal stem cells maintains their expansion and differentiation capabilities. *Exp. Cell Res.* 314, 1147–1154. doi: 10.1016/j.yexcr.2007.11.021

Gugliandolo, A., Diomede, F., Scionti, D., Bramanti, P., Trubiani, O., and Mazzon, E. (2019). The role of hypoxia on the neuronal differentiation of gingival mesenchymal stem cells: a transcriptional study. *Cell Transplant* 28, 538–552. doi: 10.1177/0963689718814470

Guo, L., Zhou, Y., Wang, S., and Wu, Y. (2014). Epigenetic changes of mesenchymal stem cells in three-dimensional (3D) spheroids. *J. Cell. Mol. Med.* 18, 2009–2019. doi: 10.1111/jcmm.12336

Halfon, S., Abramov, N., Grinblat, B., and Ginis, I. (2011). Markers distinguishing mesenchymal stem cells from fibroblasts are downregulated with passaging. *Stem Cells Dev.* 20, 53–66. doi: 10.1089/scd.2010.0040

Hall, B. K., and Miyake, T. (2000). All for one and one for all: condensations and the initiation of skeletal development. *Bioessays* 22, 138–147. doi: 10.1002/(sici)1521-1878(200002)22:2<138::aid-bies5>3.0.co;2-4

He, S., Nakada, D., and Morrison, S. J. (2009). Mechanisms of stem cell self-renewal. *Annu. Rev. Cell Dev. Biol.* 25, 377–406. doi: 10.1146/annurev.cellbio.042308.113248

Ichim, T. E., O'Heeron, P., and Kesari, S. (2018). Fibroblasts as a practical alternative to mesenchymal stem cells. *J. Transl. Med.* 16:212. doi: 10.1186/s12967-018-1536-1

Isern, J., Martin-Antonio, B., Ghazanfari, R., Martin, A. M., Lopez, J. A., del Toro, R., et al. (2013). Self-renewing human bone marrow mesenspheres promote hematopoietic stem cell expansion. *Cell Rep.* 3, 1714–1724. doi: 10.1016/j.celrep.2013.03.041

Iwasaki, K., Nagata, M., Akazawa, K., Watabe, T., and Morita, I. (2019). Changes in characteristics of periodontal ligament stem cells in spheroid culture. *J. Periodontal Res.* 54, 364–373. doi: 10.1111/jre.12637

Kabiri, M., Kul, B., Lott, W. B., Futrega, K., Ghanavi, P., Upton, Z., et al. (2012). 3D mesenchymal stem/stromal cell osteogenesis and autocrine signalling. *Biochem. Biophys. Res. Commun.* 419, 142–147. doi: 10.1016/j.bbrc.2012.01.017

Kale, S., Biermann, S., Edwards, C., Tarnowski, C., Morris, M., and Long, M. W. (2000). Three-dimensional cellular development is essential for ex vivo formation of human bone. *Nat. Biotechnol.* 18, 954–958. doi: 10.1038/79439

Kaul, H., Hall, B. K., Newby, C., and Ventikos, Y. (2015). Synergistic activity of polarised osteoblasts inside condensations cause their differentiation. *Sci. Rep.* 5:11838. doi: 10.1038/srep11838

Kim, J., and Adachi, T. (2019). Cell condensation triggers the differentiation of osteoblast precursor cells to osteocyte-like cells. *Front. Bioeng. Biotechnol.* 7:288. doi: 10.3389/fbioe.2019.00288

Kolf, C. M., Cho, E., and Tuan, R. S. (2007). Mesenchymal stromal cells. Biology of adult mesenchymal stem cells: regulation of niche, self-renewal and differentiation. *Arthritis Res. Ther.* 9:204. doi: 10.1186/ar2116

Kuroda, Y., Kitada, M., Wakao, S., Nishikawa, K., Tanimura, Y., Makinoshima, H., et al. (2010). Unique multipotent cells in adult human mesenchymal cell populations. *Proc. Natl. Acad. Sci. U.S.A.* 107, 8639–8643. doi: 10.1073/pnas.0911647107

Lee, S. H., Inaba, A., Mohindroo, N., Ganesh, D., Martin, C. E., Chugal, N., et al. (2017). Three-dimensional sphere-forming cells are unique multipotent cell population in dental pulp cells. *J. Endod.* 43, 1302–1308. doi: 10.1016/j.joen.2017.03.016

Liu, T. M., and Lee, E. H. (2013). Transcriptional regulatory cascades in Runx2-dependent bone development. *Tissue Eng. B Rev.* 19, 254–263. doi: 10.1089/ten.TEB.2012.0527

Lo, L. M., Raghunath, M., and Lee, K. K. H. (2019). Growing human dermal fibroblasts as spheroids renders them susceptible for early expression of pluripotency genes. *Adv. Biosyst.* 3:1900094. doi: 10.1002/adbi.201900094

Lv, F. J., Tuan, R. S., Cheung, K. M., and Leung, V. Y. (2014). Concise review: the surface markers and identity of human mesenchymal stem cells. *Stem Cells* 32, 1408–1419. doi: 10.1002/stem.1681

Mareddy, S., Dhaliwal, N., Crawford, R., and Xiao, Y. (2010). Stem cell-related gene expression in clonal populations of mesenchymal stromal cells from bone marrow. *Tissue Eng. A* 16, 749–758. doi: 10.1089/ten.TEA.2009.0307

Miranda, J. P., Camoes, S. P., Gaspar, M. M., Rodrigues, J. S., Carvalheiro, M., Barcia, R. N., et al. (2019). The secretome derived from 3D-cultured umbilical cord tissue MSCs counteracts manifestations typifying rheumatoid arthritis. *Front. Immunol.* 10:18. doi: 10.3389/fimmu.2019.00018

Mitrano, T. I., Grob, M. S., Carrion, F., Nova-Lamperti, E., Luz, P. A., Fierro, F. S., et al. (2010). Culture and characterization of mesenchymal stem cells from human gingival tissue. *J. Periodontol.* 81, 917–925. doi: 10.1902/jop.2010.090566

Mohamed-Ahmed, S., Fristad, I., Lie, S. A., Suliman, S., Mustafa, K., Vindenes, H., et al. (2018). Adipose-derived and bone marrow mesenchymal stem cells: a donor-matched comparison. *Stem Cell. Res. Ther.* 9:168. doi: 10.1186/s13287-018-0914-1

Moritani, Y., Usui, M., Sano, K., Nakazawa, K., Hanatani, T., Nakatomi, M., et al. (2018). Spheroid culture enhances osteogenic potential of periodontal ligament mesenchymal stem cells. *J. Periodontal. Res.* 53, 870–882. doi: 10.1111/jre.12577

Moshaverinia, A., Chen, C., Xu, X., Akiyama, K., Ansari, S., Zadeh, H. H., et al. (2014). Bone regeneration potential of stem cells derived from periodontal ligament or gingival tissue sources encapsulated in RGD-modified alginate scaffold. *Tissue Eng. A* 20, 611–621. doi: 10.1089/ten.TEA.2013.0229

Mostafa, N. Z., Uludağ, H., Varkey, M., Dederich, D. N., Doschak, M. R., and El-Bialy, T. H. (2011). In vitro osteogenic induction of human gingival fibroblasts for bone regeneration. *Open Dent. J.* 5, 139–145. doi: 10.2174/1874210601105010139

Murphy, K. C., Fang, S. Y., and Leach, J. K. (2014). Human mesenchymal stem cell spheroids in fibrin hydrogels exhibit improved cell survival and potential for bone healing. *Cell Tissue Res.* 357, 91–99. doi: 10.1007/s00441-014-1830-z

Naveau, A., Lataillade, J. J., Fournier, B. P., Couty, L., Prat, M., Ferre, F. C., et al. (2011). Phenotypic study of human gingival fibroblasts in a medium enriched with platelet lysate. *J. Periodontol.* 82, 632–641. doi: 10.1902/jop.2010.100179

Nebie, O., Barro, L., Wu, Y. W., Knutson, F., Buee, L., Devos, D., et al. (2020). Heat-treated human platelet pellet lysate modulates microglia activation, favors wound healing and promotes neuronal differentiation in vitro. *Platelets* [Epub ahead of print]. doi: 10.1080/09537104.2020.1732324

Ogasawara, T., Ohba, S., Yano, F., Kawaguchi, H., Chung, U. I., Saito, T., et al. (2013). Nanog promotes osteogenic differentiation of the mouse mesenchymal cell line C3H10T1/2 by modulating bone morphogenetic protein (BMP) signaling. *J. Cell Physiol.* 228, 163–171. doi: 10.1002/jcp.24116

Petrenko, Y., Sykova, E., and Kubinova, S. (2017). The therapeutic potential of three-dimensional multipotent mesenchymal stromal cell spheroids. *Stem Cell Res. Ther.* 8:94. doi: 10.1186/s13287-017-0558-6

Phimphilai, M., Zhao, Z., Boules, H., Roca, H., and Franceschi, R. T. (2006). BMP signaling is required for RUNX2-dependent induction of the osteoblast phenotype. *J. Bone Miner. Res.* 21, 637–646. doi: 10.1359/jbmr.060109

Pittenger, M. F., Discher, D. E., Péault, B. M., Phinney, D. G., Hare, J. M., and Caplan, A. I. (2019). Mesenchymal stem cell perspective: cell biology to clinical progress. *NPJ Regen. Med.* 4:22. doi: 10.1038/s41536-019-0083-6

Pittenger, M. F., Mackay, A. M., Beck, S. C., Jaiswal, R. K., Douglas, R., Mosca, J. D., et al. (1999). Multilineage potential of adult human mesenchymal stem cells. *Science* 284, 143–147. doi: 10.1126/science.284.5411.143

Potapova, I. A., Gaudette, G. R., Brink, P. R., Robinson, R. B., Rosen, M. R., Cohen, I. S., et al. (2007). Mesenchymal stem cells support migration, extracellular matrix invasion, proliferation, and survival of endothelial cells in vitro. *Stem Cells* 25, 1761–1768. doi: 10.1634/stemcells.2007-0022

Qiu, J., Wang, X., Zhou, H., Zhang, C., Wang, Y., Huang, J., et al. (2020). Enhancement of periodontal tissue regeneration by conditioned media from gingiva-derived or periodontal ligament-derived mesenchymal stem cells: a comparative study in rats. *Stem Cell Res. Ther.* 11:42. doi: 10.1186/s13287-019-1546-9

Samavarchi-Tehrani, P., Golipour, A., David, L., Sung, H. K., Beyer, T. A., Datti, A., et al. (2010). Functional genomics reveals a BMP-driven mesenchymal-to-epithelial transition in the initiation of somatic cell reprogramming. *Cell Stem Cell* 7, 64–77. doi: 10.1016/j.stem.2010.04.015

Sart, S., Tsai, A. C., Li, Y., and Ma, T. (2014). Three-dimensional aggregates of mesenchymal stem cells: cellular mechanisms, biological properties, and applications. *Tissue Eng. B Rev.* 20, 365–380. doi: 10.1089/ten.TEB.2013.0537

Shanbhag, S., Stavropoulos, A., Suliman, S., Hervig, T., and Mustafa, K. (2017). Efficacy of humanized mesenchymal stem cell cultures for bone tissue engineering: a systematic review with a focus on platelet derivatives. *Tissue Eng. Part B Rev.* 23, 552–569. doi: 10.1089/ten.TEB.2017.0093

Sharpe, P. T. (2016). Dental mesenchymal stem cells. *Development* 143, 2273–2280. doi: 10.1242/dev.134189

Silin, S. (2012). Round-bottomed honeycomb microwells: embryoid body shape correlates with stem cell fate. *J. Dev. Biol. Tissue Eng.* 4, 12–22. doi: 10.5897/jdbte11.025

Subbarayan, R., Murugan Girija, D., Mukherjee, J., Mamidanna, S. R. R., and Ranga Rao, S. (2017). Comparision of gingival and umbilical cord stem cells based on its modulus and neuronal differentiation. *J. Cell. Biochem.* 118, 2000–2008. doi: 10.1002/jcb.25918

Subbarayan, R., Murugan Girija, D., and Ranga Rao, S. (2018). Gingival spheroids possess multilineage differentiation potential. *J. Cell. Physiol.* 233, 1952–1958. doi: 10.1002/jcp.25894

Suenaga, H., Furukawa, K. S., Suzuki, Y., Takato, T., and Ushida, T. (2015). Bone regeneration in calvarial defects in a rat model by implantation of human bone marrow-derived mesenchymal stromal cell spheroids. *J. Mater. Sci. Mater. Med.* 26:254. doi: 10.1007/s10856-015-5591-3

Sun, Q., Nakata, H., Yamamoto, M., Kasugai, S., and Kuroda, S. (2019). Comparison of gingiva-derived and bone marrow mesenchymal stem cells for osteogenesis. *J. Cell. Mol. Med.* 23, 7592–7601. doi: 10.1111/jcmm.14632

Tomar, G. B., Srivastava, R. K., Gupta, N., Barhanpurkar, A. P., Pote, S. T., Jhaveri, H. M., et al. (2010). Human gingiva-derived mesenchymal stem cells are superior to bone marrow-derived mesenchymal stem cells for cell therapy in regenerative medicine. *Biochem. Biophys. Res. Commun.* 393, 377–383. doi: 10.1016/j.bbrc.2010.01.126

van Strien, M. E., Sluijs, J. A., Reynolds, B. A., Steindler, D. A., Aronica, E., and Hol, E. M. (2014). Isolation of neural progenitor cells from the human adult subventricular zone based on expression of the cell surface marker CD271. *Stem Cells Transl. Med.* 3, 470–480. doi: 10.5966/sctm.2013-0038

Wang, F., Yu, M., Yan, X., Wen, Y., Zeng, Q., Yue, W., et al. (2011). Gingiva-derived mesenchymal stem cell-mediated therapeutic approach for bone tissue regeneration. *Stem Cells Dev.* 20, 2093–2102. doi: 10.1089/scd.2010.0523

Wilson, A., Hodgson-Garms, M., Frith, J. E., and Genever, P. (2019). Multiplicity of mesenchymal stromal cells: finding the right route to therapy. *Front. Immunol.* 10:1112. doi: 10.3389/fimmu.2019.01112

Wu, R. X., Yu, Y., Yin, Y., Zhang, X. Y., Gao, L. N., and Chen, F. M. (2017). Platelet lysate supports the in vitro expansion of human periodontal ligament stem cells for cytotherapeutic use. *J. Tissue Eng. Regen. Med.* 11, 2261–2275. doi: 10.1002/term.2124

Xu, X., Chen, C., Akiyama, K., Chai, Y., Le, A. D., Wang, Z., et al. (2013). Gingivae contain neural-crest- and mesoderm-derived mesenchymal stem cells. *J. Dent. Res.* 92, 825–832. doi: 10.1177/0022034513497961

Yang, H., Gao, L. N., An, Y., Hu, C. H., Jin, F., Zhou, J., et al. (2013). Comparison of mesenchymal stem cells derived from gingival tissue and periodontal ligament in different incubation conditions. *Biomaterials* 34, 7033–7047. doi: 10.1016/j.biomaterials.2013.05.025

Yassin, M. A., Mustafa, K., Xing, Z., Sun, Y., Fasmer, K. E., Waag, T., et al. (2017). A copolymer scaffold functionalized with nanodiamond particles enhances osteogenic metabolic activity and bone regeneration. *Macromol. Biosci.* 17:1600427. doi: 10.1002/mabi.201600427

Ylostalo, J. H., Bazhanov, N., Mohammadipoor, A., and Bartosh, T. J. (2017). Production and administration of therapeutic mesenchymal stem/stromal cell (MSC) spheroids primed in 3-D cultures under xeno-free conditions. *J. Vis. Exp.* 121:55126. doi: 10.3791/55126

Yue, R., Shen, B., and Morrison, S. J. (2016). Clec11a/osteolectin is an osteogenic growth factor that promotes the maintenance of the adult skeleton. *eLife* 5:e18782. doi: 10.7554/eLife.18782

Zhang, Q., Nguyen, A. L., Shi, S., Hill, C., Wilder-Smith, P., Krasieva, T. B., et al. (2012). Three-dimensional spheroid culture of human gingiva-derived mesenchymal stem cells enhances mitigation of chemotherapy-induced oral mucositis. *Stem Cells Dev.* 21, 937–947. doi: 10.1089/scd.2011.0252

Conflict of Interest: The authors declare that the research was conducted in the absence of any commercial or financial relationships that could be construed as a potential conflict of interest.

Copyright © 2020 Shanbhag, Suliman, Bolstad, Stavropoulos and Mustafa. This is an open-access article distributed under the terms of the Creative Commons Attribution License (CC BY). The use, distribution or reproduction in other forums is permitted, provided the original author(s) and the copyright owner(s) are credited and that the original publication in this journal is cited, in accordance with accepted academic practice. No use, distribution or reproduction is permitted which does not comply with these terms.

Shanbhag et al. Stem Cell Research & Therapy (2020) 11:351
https://doi.org/10.1186/s13287-020-01863-9

Stem Cell Research & Therapy

RESEARCH Open Access

Influence of platelet storage time on human platelet lysates and platelet lysate-expanded mesenchymal stromal cells for bone tissue engineering

Siddharth Shanbhag[1], Samih Mohamed-Ahmed[1], Turid Helen Felli Lunde[2], Salwa Suliman[1], Anne Isine Bolstad[1], Tor Hervig[2,3,4] and Kamal Mustafa[1*]

Abstract

Background: Human platelet lysate (HPL) is emerging as the preferred xeno-free supplement for the expansion of mesenchymal stromal cells (MSCs) for bone tissue engineering (BTE) applications. Due to a growing demand, the need for standardization and scaling-up of HPL has been highlighted. However, the optimal storage time of the source material, i.e., outdated platelet concentrates (PCs), remains to be determined. The present study aimed to determine the optimal storage time of PCs in terms of the cytokine content and biological efficacy of HPL.

Methods: Donor-matched bone marrow (BMSCs) and adipose-derived MSCs (ASCs) expanded in HPL or fetal bovine serum (FBS) were characterized based on in vitro proliferation, immunophenotype, and multi-lineage differentiation. Osteogenic differentiation was assessed at early (gene expression), intermediate [alkaline phosphatase (ALP) activity], and terminal stages (mineralization). Using a multiplex immunoassay, the cytokine contents of HPLs produced from PCs stored for 1–9 months were screened and a preliminary threshold of 4 months was identified. Next, HPLs were produced from PCs stored for controlled durations of 0, 1, 2, 3, and 4 months, and their efficacy was compared in terms of cytokine content and BMSCs' proliferation and osteogenic differentiation.

Results: BMSCs and ASCs in both HPL and FBS demonstrated a characteristic immunophenotype and multi-lineage differentiation; osteogenic differentiation of BMSCs and ASCs was significantly enhanced in HPL vs. FBS. Multiplex network analysis of HPL revealed several interacting growth factors, chemokines, and inflammatory cytokines. Notably, stem cell growth factor (SCGF) was detected in high concentrations. A majority of cytokines were elevated in HPLs produced from PCs stored for ≤ 4 months vs. > 4 months. However, no further differences in PC storage times between 0 and 4 months were identified in terms of HPLs' cytokine content or their effects on the proliferation, ALP activity, and mineralization of BMSCs from multiple donors.

(Continued on next page)

* Correspondence: kamal.mustafa@uib.no
[1]Department of Clinical Dentistry, Faculty of Medicine, University of Bergen, Årstadveien 19, 5008 Bergen, Norway
Full list of author information is available at the end of the article

© The Author(s). 2020 **Open Access** This article is licensed under a Creative Commons Attribution 4.0 International License, which permits use, sharing, adaptation, distribution and reproduction in any medium or format, as long as you give appropriate credit to the original author(s) and the source, provide a link to the Creative Commons licence, and indicate if changes were made. The images or other third party material in this article are included in the article's Creative Commons licence, unless indicated otherwise in a credit line to the material. If material is not included in the article's Creative Commons licence and your intended use is not permitted by statutory regulation or exceeds the permitted use, you will need to obtain permission directly from the copyright holder. To view a copy of this licence, visit http://creativecommons.org/licenses/by/4.0/. The Creative Commons Public Domain Dedication waiver (http://creativecommons.org/publicdomain/zero/1.0/) applies to the data made available in this article, unless otherwise stated in a credit line to the data.

(Continued from previous page)
Conclusions: MSCs expanded in HPL demonstrate enhanced osteogenic differentiation, albeit with considerable donor variation. HPLs produced from outdated PCs stored for up to 4 months efficiently supported the proliferation and osteogenic differentiation of MSCs. These findings may facilitate the standardization and scaling-up of HPL from outdated PCs for BTE applications.

Keywords: Platelet lysate, Mesenchymal stromal cells, Bone tissue engineering, Regenerative medicine

Background

Adult mesenchymal stromal cells (MSCs) from various tissue sources, most frequently bone marrow (BMSCs) and adipose tissue (ASCs), are increasingly being used in bone tissue engineering (BTE) strategies for reconstruction of clinically challenging bone defects [1]. Although the use of whole tissue fractions, such as bone marrow concentrates and adipose stromal vascular fractions (SVFs), offers the feasibility of minimum cell manipulation and cost-effectiveness, the yield of MSCs obtained is relatively low. MSCs represent < 1% of the mononuclear cell fraction in the bone marrow and approximately 1.4% in adipose SVF [2]. This has encouraged ex vivo expansion strategies, which aim to exponentially amplify the number of BMSCs or ASCs available for implantation and thereby improve clinical outcomes.

The use of safe, standardized, and efficacious culture conditions is a critical aspect of Good Manufacturing Practice (GMP)-grade MSC expansion. Supplements providing growth factors (GFs), proteins, and enzymes for ex vivo MSC expansion are broadly categorized as xenogeneic (animal-derived), xeno-free (human-derived), or chemically defined [3, 4]. Although fetal bovine serum (FBS) is commonly used for MSC expansion [5], several limitations of FBS supplementation have been highlighted [3, 6]. European guidelines advocate the use of "non-ruminant" over "ruminant materials" for the manufacture of human medicinal products [7]. Accordingly, an increase in the use of "xeno-free" supplements, such as human platelet lysate (HPL), to develop GMP-compliant MSC expansion protocols has recently been reported [4, 8].

HPL is defined as a cell-free, protein- and GF-rich biological material produced from platelet concentrates (PCs) initially intended for transfusion [9]. Platelets release a wide range of physiological GFs and cytokines, which can significantly enhance cell growth and function. Pooled- and/or single-donor apheresis PCs are routinely prepared by blood establishments for transfusion and, depending on local regulations, stored for a maximum of 4–7 days before being discarded [9]. It is estimated that 5–20% of PCs produced in transfusion centers become "outdated" and utilizing these for HPL production is reported to be an ethically and economically optimal strategy, due to comparable efficacy of HPL produced from "fresh" and outdated PCs [6]. The current literature consistently demonstrates that HPL is at least comparable, and often superior, to FBS in supporting MSC proliferation, stromal phenotype, chromosomal stability, and multi-lineage differentiation potential [10]. Interestingly, MSCs expanded in HPL have been reported to demonstrate enhanced osteoblastic differentiation potential, suggesting particular benefits of HPL expansion for BTE applications [4]. A clinically validated protocol for MSC expansion in HPL for BTE applications has recently been published [11].

The importance of HPL in GMP-grade MSC production is highlighted by the publication of several recent consensus statements [9, 12–14]. The most common themes in these reports are the need to scale-up HPL production by blood establishments and, more urgently, the need for standardization of HPL products. There is currently considerable large variation in the methods used to produce HPL, which is further complicated by the availability of several inadequately defined commercial HPL products. A need for standardization has been described at various levels of the HPL production process, such as the source material (pooled buffy coats vs. apheresis PCs and fresh vs. outdated PCs) and storage medium [plasma vs. platelet additive solution (PAS) or a combination]. Moreover, the pool sizes, i.e., the number of PC units or individual donations that are pooled to produce a single HPL product, method of platelet lysis, use of pathogen inactivation strategies, and quality control/release criteria for the final product vary between manufacturers [14].

Nevertheless, there is a clear consensus that the use of outdated pooled PCs as the source material is the optimal strategy for large-scale HPL production. Although the storage time of PCs varies between blood centers based on national regulations, recent recommendations call for immediate freezing of outdated PCs, i.e., within 7 days after collection, for subsequent HPL production—this represents an efficient use of resources and minimizes waste [9]. However, for many blood centers, it may not always be possible to initiate HPL production on the day of (or soon after) PC expiry, and the maximum duration for which PCs can be stored before being used to prepare an efficient HPL remains unknown. If outdated PCs can be stored for a standardized period to produce an optimal HPL product, it would facilitate logistical solutions and encourage more blood establishments to incorporate HPL production into their protocols. Thus, optimizing the storage time of PCs

would be a step towards addressing *both* the standardization *and* scaling-up of HPL production.

In the context of BTE, a recent study demonstrated differential effects of commercial HPL products on the mineralization capacity of BMSCs, although the mechanisms and HPL components contributing to these differences were not studied [15]. It would be of interest to investigate the effects of PC storage times on the cytokine contents of HPL, and subsequently the proliferation kinetics and osteogenic differentiation potential of HPL-expanded MSCs. Therefore, the objectives of this study were to characterize HPL in terms of its cytokine content and efficacy for MSC expansion (vs. FBS), particularly for BTE applications, and to investigate the effect of PC storage time on the cytokine content and efficacy of HPL in terms of MSC proliferation and osteogenic differentiation.

Materials and methods

Production of HPL

PC preparation and storage

The HPL herein (Bergenlys®, Bergen, Norway) is prepared from outdated pooled whole blood-derived PCs. The PCs are prepared at the Department of Immunology and Transfusion Medicine, Haukeland University Hospital, Bergen, Norway, according to established procedures and in line with national and EU quality requirements. Briefly, written informed consent is obtained from volunteer, healthy blood donors (aged 18–70 years) complying with national guidelines for blood donation. Whole blood is processed with the Reveos® Automated Blood Processing Unit (Terumo BCT, Lakewood, CO, USA). All donations are tested for ABO and RhD blood groups, infectious disease markers (HIV1/2, HBV, HCV), and sterility (aerobic bacteria). Donor information and manufacturing details are stored to ensure traceability of the final product. PCs (~ 300 mL) are generated by manually pooling five interim platelet units (IPUs) in 30% plasma and 70% platelet additive solution (Terumo BCT) and subsequently leukocyte-filtered (Immuflex®, Terumo BCT). Pooled PCs containing $> 2 \times 10^{11}$ platelets (and $< 1 \times 10^{6}$ leukocytes) are X-ray irradiated at a dose of 25 Gy and stored at 22 °C ± 2 °C under agitation for no longer than 7 days for use as transfusion units. All unused (or outdated) 7-day-old PCs are frozen at − 80 °C within 24 h for subsequent HPL production.

HPL production

Unused 7-day-old PCs were used for HPL production via the freeze/thaw lysis method [16]. Briefly, four different PCs (each PC containing buffy coats from five donors = 4 × 5 = 20 donors per HPL product) were exposed to multiple freezing (− 80 °C for at least 3 h) and thawing cycles [+ 37 °C in a plasma thawer (Plasmatherm®, Barkey GmbH Co. KG, Leoppoldshoehe, Germany) for 15 min] to ensure platelet lysis before pooling. Pooled PCs were then centrifuged at 3000×*g* (4 °C, 15 min) to remove platelet fragments and aliquoted as the final HPL product. No fibrinogen depletion step was performed. HPL aliquots were stored at − 80 °C and thawed overnight at 4 °C for subsequent use in experiments.

Cell culture with HPL

Isolation and expansion of donor-matched BMSCs and ASCs

The biological efficacy of HPL was tested in various cellular assays using human BMSCs and ASCs. Donor-matched BMSCs and ASCs were isolated and expanded according to established protocols [17]. Briefly, human adipose tissue and bone marrow aspirates were obtained after informed parental consent and ethical approval (2013-1248/Regional Ethical Committee, South East, Norway) from patients aged 8–14 years undergoing surgery at the Department of Plastic Surgery, Haukeland University Hospital. For each donor, BMSCs and ASCs were isolated in 5% HPL and 10% FBS (GE Healthcare, South Logan, UT, USA) supplemented growth media [Dulbecco's modified Eagle's medium (DMEM, Invitrogen, Carlsbad, CA, USA) with 1% antibiotics (penicillin/streptomycin; GE Healthcare)]. In HPL-supplemented media, 1 IU/mL of heparin was added to prevent gelation and the medium was sterile filtered (0.2 μm) before use. Cells were sub-cultured and expanded according to a clinically validated protocol with a seeding density of 4000 cells/cm^2 [11]; passage 2–4 cells from at least three different donors were used in experiments. Cell number and viability were assessed using 0.4% Trypan blue stain (Invitrogen) and a Countess® Automated Cell Counter (Invitrogen).

Immunophenotype of BMSCs and ASCs

The immunophenotype of BMSCs and ASCs in HPL and FBS was assessed by flow cytometry based on the expression of specific surface antigens, as previously described [17] according to the "minimal criteria" for defining MSCs [18]. Briefly, the cells in HPL and FBS were incubated with conjugated antibodies against selected "negative" (CD34, CD45, HLA-DR) and "positive" (CD73, CD90, CD105) MSC markers (all from BD Biosciences, San Jose, CA, USA) and STRO-1 (Santa Cruz Biotechnology, Dallas, TX, USA) following the manufacturers' recommendations. Quantification was performed with a BD LSR Fortessa cell analyzer (BD Biosciences), and data were analyzed using flow cytometry software (FlowJo V10, Flowjo, LLC, Ashland, OR, USA).

Cell proliferation based on DNA quantification

BMSCs and ASCs in HPL and FBS were seeded in 24-well plates at a density of 4000 cells/cm^2. After 1, 7, and

14 days of culture, DNA quantification was performed using the Quant-IT® PicoGreen dsDNA Assay Kit (Thermo Fisher Scientific, Carlsbad, CA, USA) according to the manufacturer's instructions. Briefly, cells were lysed in 0.1% Triton X-100 and the PicoGreen staining solution was added and incubated for 5 min at RT protected from light, before fluorescence was measured at 480 nm (Ex)/520 nm (Em) with a microplate reader. DNA concentrations (ng/mL) were calculated based on known standards.

Multi-lineage differentiation of BMSCs and ASCs

The ability of BMSCs and ASCs to differentiate into multiple stromal lineages was tested as previously described [17]. Briefly, for adipogenic differentiation, cells in HPL and FBS were cultured in StemPro® adipogenic differentiation medium (Invitrogen) or standard growth medium (control). After 14 days, intracellular lipid formation was assessed via Oil red O (Sigma-Aldrich) staining. For quantification, the stain was extracted using 99% isopropanol (Sigma-Aldrich) and absorbance was measured at 540 nm using a microplate reader. For osteogenic differentiation, cells in HPL and FBS were cultured in osteogenic differentiation medium prepared by adding final concentrations of 0.05 mM L-ascorbic acid 2-phosphate, 10 nM dexamethasone, and 10 mM β glycerophosphate (all from Sigma-Aldrich) to the respective growth media. Cells in standard growth medium served as controls. After 21 days, extracellular calcium deposition was evaluated via Alizarin red S staining (Sigma-Aldrich). For quantification, the stain was dissolved in cetylpyridinium chloride (Sigma-Aldrich) and absorbance was measured at 540 nm using the microplate reader.

Gene expression

After 7 days of osteogenic induction, the expression of osteogenesis-related genes (Supplementary Table 1) was assessed in BMSCs and ASCs in HPL and FBS via quantitative real-time polymerase chain reaction (qPCR) using TaqMan® real-time PCR assays (Thermo Fisher Scientific). RNA extraction and cDNA synthesis were performed as previously described [17]. The expressions of the genes of interest were normalized to that of glyceraldehyde 3-phosphate dehydrogenase (GAPDH). Data were analyzed by the $\Delta\Delta Ct$ method, and results are presented as fold changes in HPL groups relative to FBS groups.

Alkaline phosphatase (ALP) activity

After 7 and 14 days, ALP activity in the cells was measured using the SIGMAFAST BCIP/NBT assay (Sigma-Aldrich). Following manufacturer's instructions, cells were lysed in 0.1% Triton-X100 buffer, mixed with a working solution containing a phosphatase substrate and alkaline buffer solution, and incubated at 37 °C for 15 min, and absorbance was measured at 405 nm using a microplate reader.

Cytokine content in HPL

Multiplex assay and cytokine network analysis

The concentrations of 48 cytokines (Supplementary Table 2) in HPL were measured using a multiplex immunoassay—Bio-Plex® Pro 48-plex Human Cytokine Screening Panel (Bio-Rad Laboratories, CA, USA) and a Bio-Plex® 200 System (Bio-Rad), according to the manufacturer's instructions. The cytokines included various GFs, inflammatory mediators, and chemokines involved in regulating MSC growth and function. To validate the multiplex data, concentrations of three selected GFs, namely platelet-derived growth factor BB (PDGF-BB), transforming growth factor-β1 (TGF-β1), and vascular endothelial growth factor (VEGF), were measured in representative batches of HPL via enzyme-linked immunosorbent assay (ELISA) kits (R&D Diagnostics, Wiesbaden, Germany) following the manufacturer's protocols. Interactions between cytokines were analyzed using the Search Tool for the Retrieval of Interacting Genes/Proteins (STRING) database and online software [19]. Cytokines were clustered according to the Markov Cluster algorithm and the STRING global score as previously reported [20].

Screening of different storage times to identify a threshold

The first multiplex assay included several HPL batches produced from PCs with different storage times (range 1–9 months). These HPLs, and corresponding PC units, were identified and screened retrospectively from a biobank, i.e., not collected and intentionally frozen for specific periods of time (as performed later in the study). In order to determine whether the duration of frozen storage of PCs affects the cytokine content of subsequently produced HPL, the storage times were divided into two categories: storage ≤ 4 months and > 4 months. Categorization was based on (a) recommendations regarding "quarantine storage" of GMP-grade blood products which state that the product must only be released if the donors have been tested negative for transmissible diseases twice, i.e., at the time of blood donation and re-tested as negative 4 months (or longer) thereafter [13, 21], and (b) current practices at the HPL production site (Haukeland Hospital Bloodbank), which are in line with the above recommendations.

Identifying a specific threshold for PC storage time

Since a preliminary threshold of 4 months was identified in the screening assay, a more focused custom-designed multiplex assay with 16 selected cytokines was performed to identify a specific threshold, if any, between 0 and 4 months. For this purpose, HPL batches were

specially produced from PCs frozen for controlled durations of 1, 2, 3, and 4 months. A reference HPL batch of PCs frozen and processed immediately ("0 months") was also included. The custom assay was a modification of the 48-plex panel (Bio-Rad) previously described. For both multiplex assays, data was analyzed using the Bio-Plex Manager Software (Bio-Rad) and final cytokine concentrations were derived in pg/mL.

Effect of frozen PC storage time on HPL efficacy

MSC morphology and proliferation kinetics

To investigate whether PC storage times affected the biological performance of HPL, cellular assays were performed using BMSCs. Previously cryopreserved passage 1 BMSCs were expanded for three additional passages in HPL produced from 0-, 1-, 2-, 3-, or 4-month PCs. At approximately 80% sub-confluence, cells from all conditions were harvested, counted, and re-seeded at 4000 cells/cm^2, following the same clinically validated protocol [11]. The population doubling (PD) rate was determined using the following formula [22]:

$$X = \frac{\log10(N_H) - \log10(N_1)}{\log10(2)}$$

N_H is the harvested cell number and N_1 is the plated cell number. The PD for each passage was calculated and added to the PD of the previous passages to generate data for cumulative population doublings (CPD). Additionally, the population doubling time (PDT), i.e., the average time between two doublings, was calculated using the following formula [22]:

$$X = \frac{\log2 \times \Delta t}{\log10(N_H) - \log10(N_1)}$$

MSC osteogenic differentiation

To investigate whether PC freezing times affected the osteogenic differentiation potential of BMSCs, cells expanded for two passages with HPL produced from 0-, 1-, 2-, 3-, or 4-month PCs were plated for osteogenic differentiation assays. The differentiation medium was prepared by adding osteogenic supplements (as described above) to the respective growth media. Osteogenic differentiation was assessed via an ALP assay after 7 and 14 days (as described above) and via Alizarin red S staining of extracellular calcium deposits after 21 days (as described above) in osteogenically induced and non-induced BMSCs. Additionally, quantification of DNA per sample in the ALP experiment was performed as previously described. ALP activity was normalized to the amount of DNA per corresponding sample (ng/mL).

Statistical analysis

Statistical analyses were performed using the IBM SPSS version 17.0 software package (SPSS Inc., Chicago, IL, USA). Data are represented as arithmetic means ± SD, unless specified. For gene expression, statistical analyses are based on delta-Ct values and data are presented as relative fold changes. The student t test and one-way analysis of variance (ANOVA), followed by a post hoc Tukey's test for multiple comparisons, were applied when appropriate and $p < 0.05$ was considered statistically significant.

Results

Characterization of HPL efficacy

Isolation and characterization of BMSCs and ASCs

Donor-matched BMSCs and ASCs demonstrating characteristic plastic adherence and fibroblastic morphology were successfully expanded in both HPL- and FBS-supplemented media. Distinct morphological differences were observed between cells in HPL and FBS—the former being smaller and more spindle-shaped; these differences were more apparent at earlier passages (Fig. 1a). BMSCs and ASCs in both HPL and FBS demonstrated the characteristic MSC phenotype, i.e., > 95% of the cells were positive for the stromal markers CD73, CD90, and CD105, while < 5% of the cells expressed HLA-DR or the hematopoietic markers CD34 and CD45 (Fig. 1b, Supplementary figure 1). A trend for higher expression of STRO-1 was observed in HPL-cultured BMSCs and ASCs (Fig. 1c). Cell proliferation over 14 days was significantly greater in HPL-cultured BMSCs and ASCs based on DNA quantification (Fig. 1c).

Multi-lineage differentiation of BMSCs and ASCs

BMSCs and ASCs in both HPL- and FBS-supplemented media demonstrated the capacity to differentiate into adipocytes and osteoblasts, with some differences. Osteogenic differentiation in HPL and FBS was assessed at the gene, protein, and functional levels. Expression of early osteogenesis-related genes RUNX2 and BMP2 was significantly upregulated in HPL-cultured BMSCs and ASCs after 7 days (Fig. 3a). Interestingly, expressions of SPP1 and BGLAP, typically associated with later stages of osteogenesis, were also upregulated in HPL-cultured cells; BGLAP was significantly upregulated in ASCs. Intracellular ALP activity after 7 and 14 days was higher in HPL- vs. FBS-cultured BMSCs and ASCs; these differences were more pronounced in ASCs (Fig. 3b). While BMSCs generally presented higher ALP activity compared to ASCs at 7 days, the activity at 14 days was comparable between the two cell types. Significantly greater mineral deposition via Alizarin red S staining was observed in HPL- vs. FBS-cultured BMSCs and ASCs after 21 days, suggesting an enhanced osteogenic differentiation capacity of these cells (Fig. 3c). A trend for superior

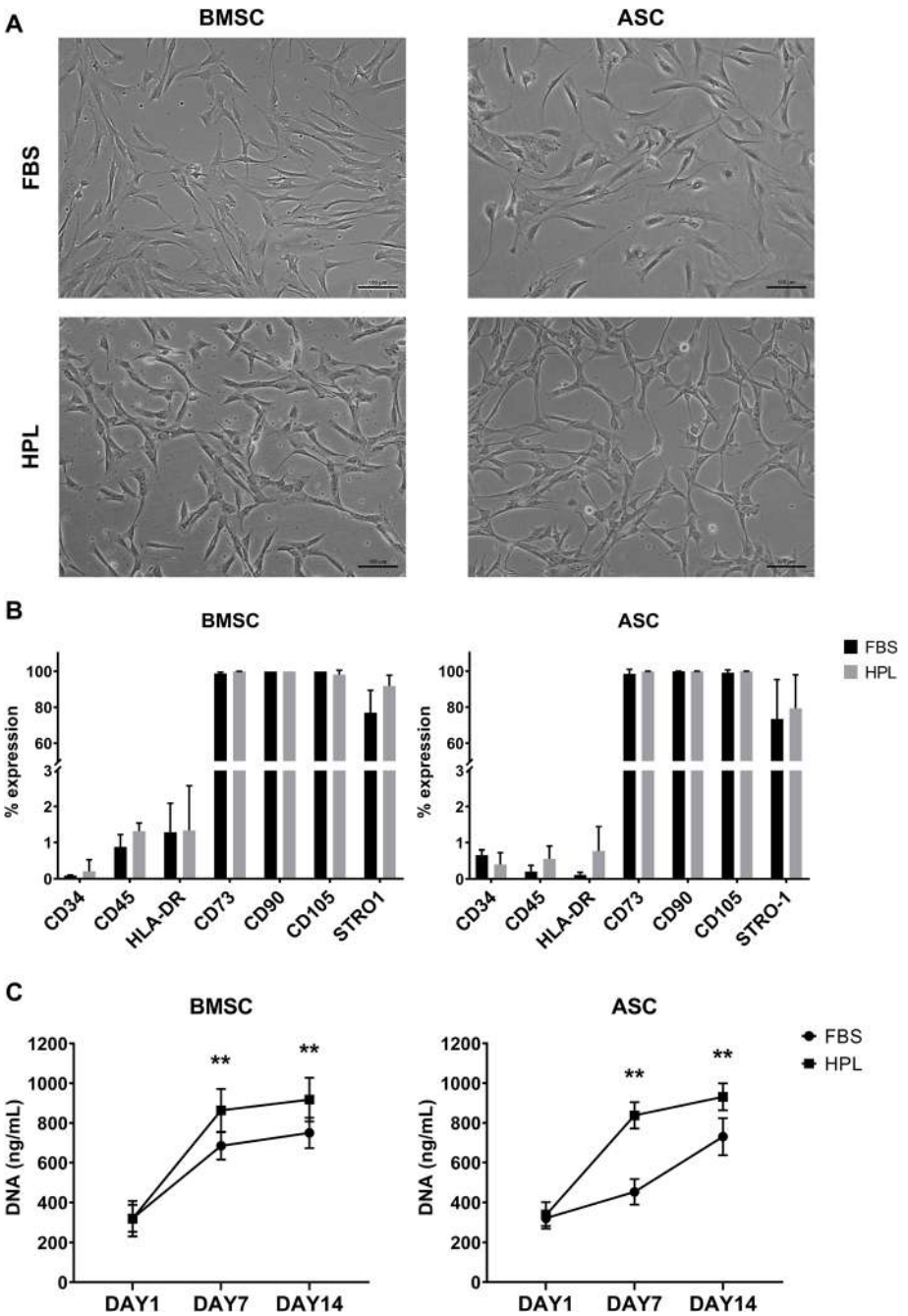

Fig. 1 Characterization of BMSCs and ASCs in HPL. **a** Morphology of BMSCs and ASCs from one representative donor (scale bar 100 μm). **b** Surface marker expression of BMSCs and ASCs based on flow cytometry; data represent means ± SD ($n = 3$ donors). **c** Proliferation of BMSCs and ASCs over 14 days based on DNA quantification; data represent means ± SD ($n = 3$ donors); $^{**}p < 0.001$

mineralization was observed in BMSCs as compared to ASCs. After 14 days of induction, ASCs demonstrated superior adipogenic differentiation, i.e., greater accumulation of intracellular lipid vesicles, compared to BMSCs, as revealed by quantification of Oil red O staining (Fig. 2e). HPL-cultured ASCs and BMSCs demonstrated similar adipogenic differentiation vs. their FBS-cultured counterparts (Fig. 2f). No adipogenic or osteogenic differentiation of cells was observed in the standard growth media (data not shown).

Characterization of HPL cytokine content

Multiplex assay and cytokine network analysis

A multiplex immunoassay was performed using HPLs produced from frozen PCs stored for 1–9 months. Thirty

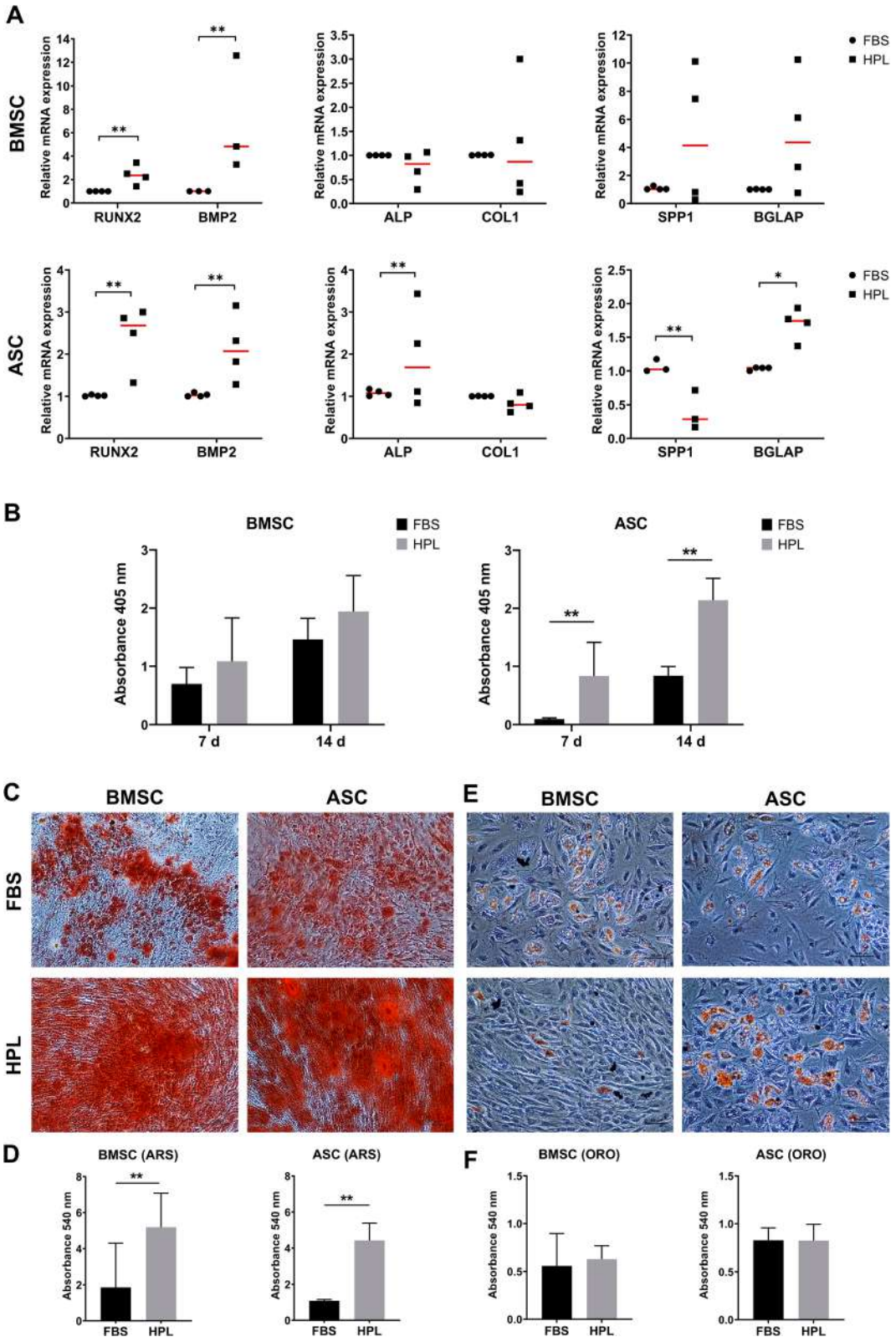

Fig. 2 (See legend on next page.)

(See figure on previous page.)
Fig. 2 Multi-lineage differentiation of BMSCs and ASCs in HPL. **a** Osteogenic differentiation: relative expression (fold changes) of early, intermediate, and late osteogenic gene markers in BMSCs and ASCs after 7 days of induction. Data represent means; each symbol represents a single donor ($n = \geq 3$ donors) based on the average of ≥ 2 experimental replicates; statistical analyses are based on delta-Ct values; $^{*}p < 0.05$; $^{**}p < 0.001$. **b** ALP activity in BMSCs and ASCs after 7 and 14 days of osteogenic induction. Data represent means ± SD ($n = 3$ donors); $^{**}p < 0.001$. Representative images of Alizarin Red S (ARS) staining (**c**) and quantification (**d**) after 21 days. **e** Adipogenic differentiation: representative images of Oil red O (ORO) staining and quantification (**f**) after 14 days. Scale bars 100 μm. Data represent means ± SD ($n = 3$ donors); $^{**}p < 0.001$

of the 48 cytokines tested, including various GFs ($n = 11$), chemokines ($n = 9$), and inflammatory mediators ($n = 10$), were reliably detected in all tested HPLs. Cytokine concentrations, in comparison to previous studies, are reported in Table 1. Concentrations of three selected GFs, i.e., PDGF-BB, TGF-1, and VEGF, were validated via ELISA (Supplementary figure 2). The cytokine network analysis identified two major clusters of GFs, and chemokine/inflammatory mediators; stem cell growth factor (SCGF/CLEC11A) and stem cell factor (SCF/KITLG) were clustered separately (Fig. 3). Clear and abundant interactions were identified between the clusters including synergistic relations between several proteins that contribute to MSC proliferation, chemotaxis, and osteogenic differentiation.

Screening of different storage times to identify a threshold

Of these 30 cytokines, the concentrations of 27 cytokines were significantly reduced in the > 4-month group while only one cytokine, i.e., regulated upon activation, normal T cell expressed and secreted (RANTES), was significantly increased vs. the ≤ 4-month group. In addition to the known predominant cytokines PDGF-BB and TGF-β1, high levels of SCGF and macrophage inhibitory factor (MIF) were detected in HPL. Other GFs, such as basic fibroblast growth factor (b-FGF), hepatocyte growth factor (HGF), SCF, VEGF, and all inflammatory mediators [various interleukins (IL), tumor necrosis factor-α (TNF-α), and TNF-β] were present in relatively lower concentrations (Fig. 4).

Identifying a specific threshold for PC storage time

After a preliminary threshold of 4 months was identified, a second multiplex immunoassay with 16 selected cytokines was performed to identify a specific threshold, if any, for cytokine degradation between 0 and 4 months. Significantly lower concentrations were detected at 0 and 1 months for SCF and at 2 months for GCSF (Fig. 5). No significant differences were observed between the different storage times for any of the other tested cytokines, and no definitive threshold below 4 months could be identified.

Effect of frozen PC storage time on HPL efficacy

MSC morphology and proliferation kinetics

PC storage time did not seem to affect the biological performance of HPL; no differences in BMSC morphology were observed between the different storage times over three serial passages (Fig. 6a). The proliferation data revealed lower PD rate (fewer doublings) and higher PDT with increasing passages. No significant differences were observed with regard to kinetics-related variables (PD, CPD, PDT) or absolute DNA amounts between the different PC storage times (Fig. 6b).

MSC osteogenic differentiation

To investigate whether PC storage times affected the osteogenic differentiation potential of BMSCs, ALP activity (7, 14 days) and mineralization (21 days) were assessed. When combining data from all donors, no significant differences in ALP (Fig. 7a) or mineralization (Fig. 7b) were observed between the different PC storage times. Considerable variation was observed between the different BMSC donors in all groups—a trend for higher mean ALP activity (at 7 days) and mineralization, with lower inter-donor variation, was observed in the 3-month storage group. When analyzing data from individual donors, some differences in ALP activity and mineralization were observed, i.e., BMSCs from the same donor showed different activities in HPLs from different PC storage times, although these differences did not reach statistical significance for any of the donors. Overall, donor-related properties rather than PC storage time seemed to influence the osteogenic potential of HPL-cultured BMSCs.

Discussion

HPL is emerging as the preferred xeno-free supplement for the GMP-grade expansion of MSCs for BTE applications [1, 11]. Accordingly, there is a growing need for standardization and scaling-up of HPL production [12, 14]. Current GMP guidelines call for HPL release criteria to include testing for specific cytokines and biological efficacy based on cellular assays [9, 12]. In the present study, a scalable and GMP-compliant HPL was produced based on previously published methods and characterized for its cytokine content and efficacy for MSC expansion. Consistent with previous reports, HPL supported the expansion, stromal phenotype, and multilineage, particularly osteogenic, differentiation of MSCs in comparison to FBS [17].

A strength of the present study was the comparison of donor-matched cells from two different tissue sources,

Table 1 Multiplex-based measurements of cytokine concentrations (pg/mL) in HPL

Reference	(21)*	(39)	(41)	(42)	(43)	(44)**	Present study
Starting material	< 5 d BC or AP	< 24 h AP	Fresh BC	Exp BC	7 d BC (3 w at − 80C), pathogen inactivated	5–7 d BC	7 d BC
Donors (*n*)	< 12 (BC) or 1 (AP)	1	16	245 + 16	16	40	20
Lysis method	1–2× F/T	2× F/T	3× F/T	1× F/T	3× F/T	3× F/T	3× F/T
Cytokines (*n*)	23	12	27	22	37	45	48
PDGF-AA	239,412 ± 53,690			10,287 + 1820	11,433.75 + 3083.45		
PDGF-AB/BB	571,730 + 381,036	1244 + 478.46	13,534.4 + 326.9	27,407 + 5365	25,941.5 + 1891.06	11,121 + 1126	11,783.482 + 917.39
TGF-β1	139,029 + 18,854						306,801.77 + 81,171.87
b-FGF	495 + 27	77.09 + 21.33	256.6 + 7.6		407 + 105	569 + 10	56.48 + 9.85
HGF			1594.7 + 172.3			2631 + 204	542.39 + 42.21
VEGF-A/D	325 + 34	660.88 + 221.90	421.9 + 1.9		424.5 + 88.91	1742 + 133/398 + 60	440.175 + 40.35
EGF			754.9 + 89.9		997.5 + 825.58	1104 + 224	
IGF						1122 + 54	
b-NGF		85.55 + 24.27				936 + 28	19.05 + 9.29
BDNF						3169 + 213	
SCGF/CLEC11a							186,005.65 + 12,463.91
SCF/KITLG						260 + 35	30.45 + 4.35
G-CSF	74 + 19		131.4 + 9.4		40 + 15.36		108.68 + 13.17
GM-CSF	34 + 16		98.1 + 3.8		22 + 6.27	2423 + 0	7.42 + 2.28
M-CSF				129,689 + 14,654			129.65 + 55.04
MCP1/CCL2		585.75 + 200.47	64.5 + 5.0		152.5 + 30.65	1060 + 73	16.00 + 3.26
MIP-1α/CCL3	47 + 4		12.5 + 0.5	29,337 + 2030	27.25 + 5.12	531 + 37	1.59 + 0.24
MIP-1β/CCL4	51 + 5		134.9 + 2.3	17,087 + 2385	124.25 + 33.93	1641 + 289	169.77 + 13.01
RANTES/CCL5	2,705,600 + 496,076	67.71 + 18.33	15,810.8 + 717.7	376,730 + 56,734		1453 + 24	8788.00 + 644.50
MCP3/CCL7					397 + 126.25		OOR<
Eotaxin/CCL11			72.6 + 3.3		91.5 + 31.2	196 + 64	44.68 + 5.86
CTACK/CCL27							311.83 + 44.73
MSP/MST1				688,589 + 132,037			
MDC					470.25 + 300.42		
MIF				287,188 + 51,282			6645.36 + 768.15
LIF						1473 + 114	79.47 + 18.88
GROa/CXCL1	11,126 + 6480			40,947 + 3148		866 + 109	1203.04 + 98.03
IL-8/CXCL8	80 + 6	17.15 + 5.22	112.5 + 5.3		57 + 16.53	ND	21.98 + 3.82
MIG/CXCL9							96.33 + 8.36
IP-10/CXCL10			284.7 + 3.1		82.5 + 33.37	527 + 65	384.76 + 11.42
SDF1α/CXCL12						16,102 + 1506	753.49 + 49.21
Fractalkine/CX3CL1					174.75 + 54.59		

Table 1 Multiplex-based measurements of cytokine concentrations (pg/mL) in HPL *(Continued)*

Reference	(21)*	(39)	(41)	(42)	(43)	(44)**	Present study
IL-1α	41 + 6	88.78 + 33.30		4854 + 533	39.25 + 18.44	ND	
IL-1β	3 + 2	24.89 + 9.22	6.7 + 0.4		4.47 + 1.77	ND	2.82 + 0.39
IL-1ra			235.3 + 4.8	3997 + 589	717.25 + 283.94	10,580 + 605	
IL-2	OOR<		OOR<		4.92 + 2.59	ND	OOR<
IL-2ra							209.18 + 81.59
IL-3					4.97 + 1.55		OOR<
IL-4			14.2 + 0.5	3840 + 639	30.75 + 12.91	ND	OOR<
IL-5			OOR <		53.25 + 26.34	ND	180.33 + 67.29
IL-6	3 + 0	159.75 + 61.57	22.5 + 0.6		9 + 4.42	1847 + 178	54.19 + 21.40
IL-7	32 + 16		41.8 + 1.1		27 + 7.39	145 + 24	31.43 + 5.57
IL-9			129.9 + 6.3		6.9 + 2.5	942 + 49	208.42 + 20.72
IL-10	3 + 2		60.2 + 2.4		10.85 + 7.74	186 + 25	OOR <
IL-12(p40)					51.5 + 13.91		135.82 + 25.12
IL-12(p70)			113.9 + 5.1		8.85 + 3.08	ND	12.85 + 4.61
IL-13			7.7 + 1.1		291 + 131.16	ND	OOR<
IL-15			OOR <		7.7 + 3.52	568 + 29	689.27 + 228.99
IL-17			1022.5 + 56.4		10.87 + 4.04	622 + 91	11.25 + 1.76
IL-18						2466 + 349	34.37 + 11.56
IL-21						ND	
IL-22						ND	
IL-23						ND	
IL-27						2658 + 1053	
IL-31						ND	
TNF-α	8 + 2	427.25 + 167.01	133.3 + 10.4		20.25 + 5.56	2942 + 0	46.97 + 5.8
TNF-β					390.5 + 164.81	ND	246.03 + 25.05
TRAIL/TNFSF10							86.28 + 5.33
IFN-γ	14 + 4	6.61 + 2.27	154.6 + 7.4		12.125 + 2.59	ND	23.41 + 3.19
IFN-a2					63.25 + 19.72	64 + 40	8.44 + 1.29
VCAM-1	1,789,695 + 1,108,320						
ICAM-1	137,300 + 93,670						
Angiopoietin-1				121,156 + 22,164			
Angiogenin				102,085 + 17,627			
IGFBP3				530,240 + 75,663			
CD40L	29,738 + 8361			151,662 + 17,153			
TIMP-1				231,407 + 39,966			

BC buffy coats, *AP* apheresis, *PI* pathogen inactivated, *F/T* freeze/thaw cycles, *d* days, *w* weeks, *OOR* out of range
Data represent means ± SD
*No significant differences between buffy coat- and apheresis-derived HPL
**Cytokine concentrations in medium supplemented with 10% HPL

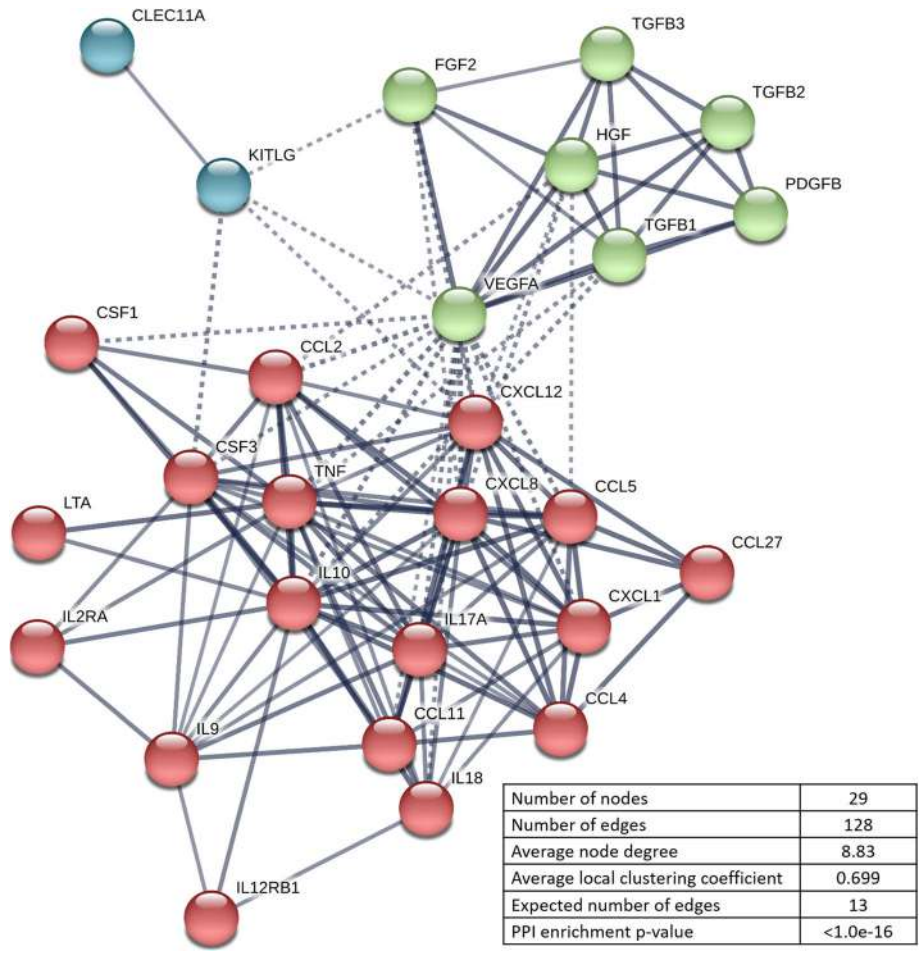

Fig. 3 Protein–protein interaction network visualized by STRING. The nodes indicate proteins, and edges indicate the number of interactions. Color saturation of the edges represents the confidence score of a functional association. The number of average interactions per node is indicated by the node degree. The clustering coefficient specifies the average node density of the map. Disconnected nodes are hidden, and only interactions with a high confidence score of ≥ 0.7 are shown

i.e., BMSCs and ASCs, to evaluate HPL efficacy. Moreover, MSCs from each tissue type were cultured in HPL- and FBS-supplemented media from the time of isolation (passage 0), thus allowing true and standardized comparisons between xeno-free and xenogeneic-cultured cells [23]. Since the focus herein was BTE, the in vitro osteogenic differentiation of BMSCs and ASCs was studied in detail and was shown to be significantly enhanced in HPL vs. FBS at the early (expression of osteogenic genes), intermediate (ALP activity) and late stages (mineral deposition). Moreover, a trend for higher expression of STRO-1, a marker associated increased osteogenic potential [24], was observed in HPL- vs. FBS-cultured BMSCs and ASCs. When comparing the two cell types, osteogenic differentiation appeared to be accelerated in HPL-cultured BMSCs vs. ASCs, based on gene expression and ALP activity during the "early" differentiation stages, while adipogenic differentiation of HPL-cultured ASCs was superior to that of BMSCs. One possible explanation could be the "tissue source variability" of BMSCs and ASCs [17, 25]. In context, previous studies have reported similar or enhanced differentiation of ASCs compared to BMSCs in vitro, but inferior bone formation in vivo, in both xenogeneic [26, 27] and HPL-supplemented cultures [28].

A substantial body of evidence points to the enhanced osteogenic potential of MSCs cultured in HPL [29–36], although the specific components contributing to this phenomenon are unknown. In the present study, the cytokine content of HPL was analyzed via a quantitative multiplex immunoassay to identify potentially relevant cytokines contributing to MSC osteogenesis. Although previous studies have measured cytokines in HPL via semi-quantitative assays [22, 36–40], to our knowledge, only five studies have reported quantitative multiplex-based assessments [21, 39, 41–44]. Considerable

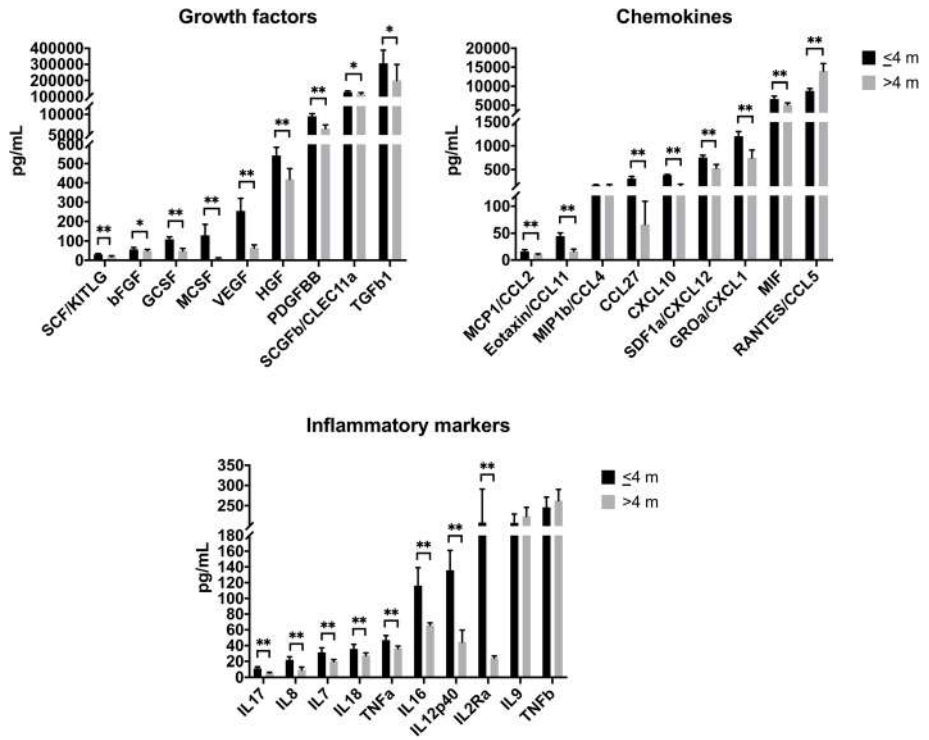

Fig. 4 Cytokine concentrations in HPL from PCs stored for ≤ 4 or > 4 [5–9] months (m). Data represent means ± SD ($n = 12$ HPL batches per group). *$p < 0.05$, **$p < 0.001$

differences in cytokine concentrations are observed across the different studies (Table 1). Moreover, it is presently unclear which cytokines in HPL are most important, what are the optimal (minimum and/or maximum) concentrations of specific cytokines, and what are the effects of HPL preparation methods on individual cytokine concentrations [10]. Nevertheless, some cytokines such as PDGF-BB, TGF-β1, and b-FGF have been consistently identified in HPL in substantial quantities. A previous study identified PDGF-BB, TGF-β1, and b-FGF to be necessary for the optimal proliferation of MSCs in HPL [21]. However, these three factors on their own were not sufficient to promote MSC proliferation [21]. These data are consistent with findings that combinations of cytokines, rather than single GFs, are important to exert maximal effects on MSC migration and proliferation [45]. However, in another study, even the use of defined combinations of several recombinant GFs and chemokines was inferior to HPL supplementation for MSC expansion [46]. Since measurement of selected cytokine concentrations has been cited as a "quality control" measure for GMP-grade HPL [12], further information is needed on which cytokines (for specific MSC applications, e.g., BTE) should be tested along with "target" concentration ranges.

In addition to established factors such as PDGF-BB and TGF-β1, high concentrations of stem cell growth factor (SCGF)—a cytokine not previously identified in HPL—were detected in the multiplex analysis herein. SCGF is a protein encoded by the CLEC11A gene (C-type lectin domain family 11, member A) and is associated with the growth of hematopoietic progenitor cells [47]. In the context of the bone, SCGF/CLEC11A is reportedly expressed in the bone marrow by a variety of stromal cells [47, 48]. Interestingly, CLEC11A was recently shown to be expressed by murine BMSCs, and its overexpression promoted their in vitro osteogenic differentiation and in vivo osteogenesis in a fracture healing model [47]. However, a more recent study showed contrasting results in human BMSCs, where silencing, rather than overexpression, of CLEC11A promoted their in vitro osteogenic differentiation [49]. In another study, SCGF was detected in the secretome of BMSCs undergoing osteogenic differentiation and was found to be downregulated on days 1, 7, and 14 compared to day 0 [50]. Thus, in addition to PDGF-BB and TGF-β1, SCGF/CLEC11A signaling may be involved in the regulation of osteogenic differentiation of HPL-cultured MSCs.

Consistent with results from the above study [49], the in silico network analysis herein identified only a single interaction for SCGF/CLEC11A, which was with the chemokine stem cell factor (SCF), a ligand for the c-kit receptor (KITLG) [51]. Like SCGF, SCF is also typically associated with hematopoietic cell proliferation [51].

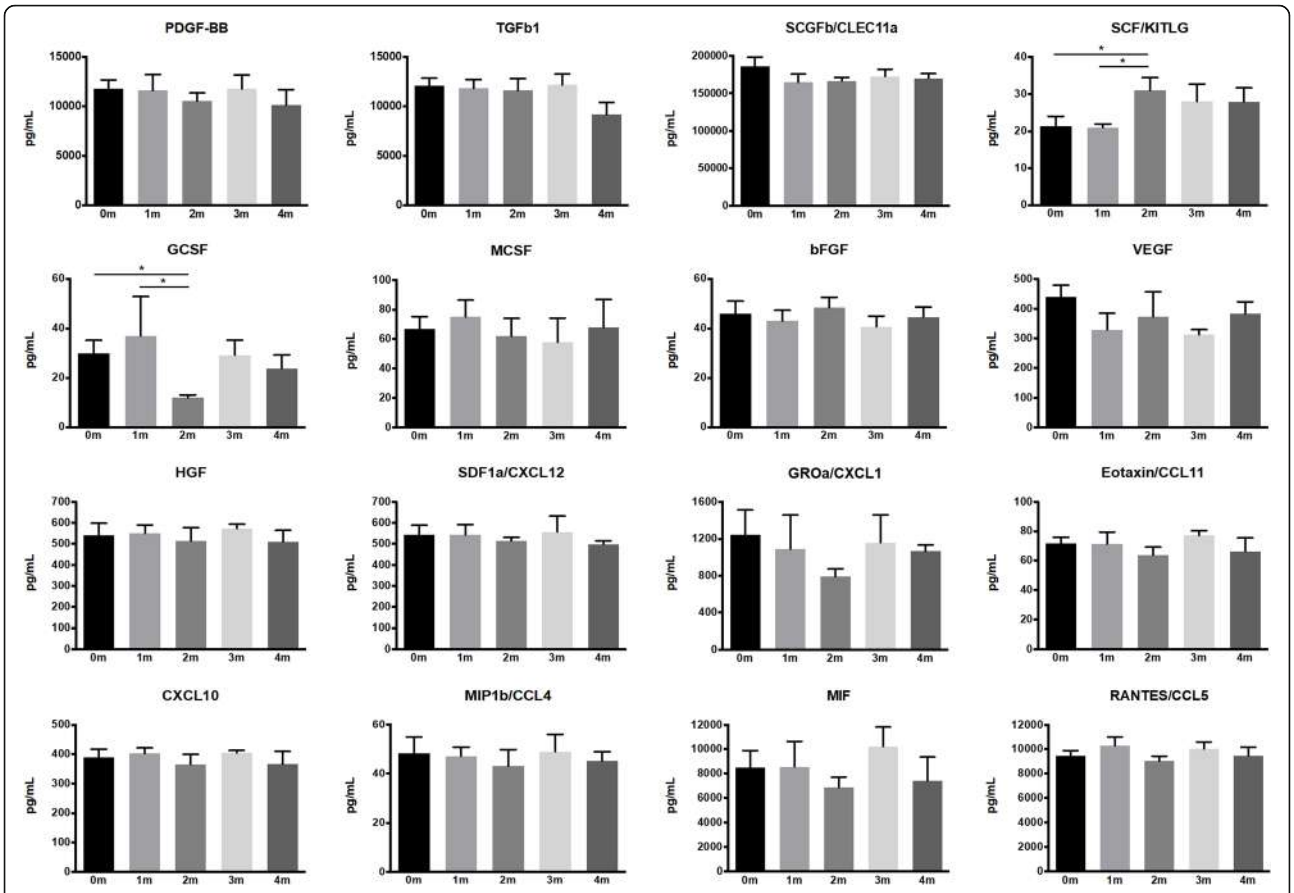

Fig. 5 Cytokine concentrations in HPL from PCs stored for 0–4 months (m). Data represent means ± SD ($n = \geq 3$ HPL batches per group). *$p < 0.05$

Although SCF was detected at a relatively lower concentration compared to SCGF, the network analysis revealed several interactions with the cytokine/chemokine and GF clusters. Recently, SCF signaling has been implicated in the mobilization, and subsequent osteogenic differentiation, of BMSCs in vitro and in in vivo models of fracture healing [52] and dental pulp/dentin regeneration [53]. Further studies are needed to elucidate the nature of the interaction(s) between SCGF, SCF, and other cytokines in the context of MSCs' osteogenic differentiation.

In addition to GFs, HPL also contains a wide range of chemokines, which regulate MSC migration, proliferation, and differentiation. Several chemokines of the CCL and CXCL families have been identified in HPL (Table 1). Of these, stromal derived factor-1 (SDF-1/CXCL12) is the most extensively studied and is involved in the recruitment of endogenous BMSCs to injury sites [54]. Platelets have been shown to release SDF1 and recruit progenitor cells to initiate wound healing at sites of vascular injury [55]. In the context of the bone, SDF1 was shown to play a critical role in the recruitment of murine BMSCs to the injury site during the early stages of fracture healing, and inhibition of SDF1 led to reduced in vivo bone formation [56]. Moreover, SDF1 regulated BMP2-induced osteogenic differentiation of mouse and human BMSCs; blocking SDF1 signaling led to significantly reduced ALP activity and mineralization of the cells [57]. Recent studies have also demonstrated enhanced in vivo bone regeneration following delivery of SDF1 via recruitment of endogenous MSCs to regeneration sites [58–61], thus highlighting the role of SDF1 in regulating MSCs' osteogenic differentiation.

Emerging evidence suggests that MSCs exert their regenerative effects primarily via paracrine mechanisms and modulation of immune cells, including osteoclasts [62]. Osteoblast-osteoclast interactions are known to be critical for bone regeneration. This is especially relevant in BTE, where MSCs are often delivered using biomaterial scaffolds, which elicits an initial inflammatory/resorptive response by macrophages/osteoclasts prior to bone formation by MSCs/osteoblasts [63]. It is therefore also of interest to consider the cytokines in HPL that may be involved in the regulation of osteoclastic activity. The most consistently reported of these are RANTES/CCL5 and associated cytokines, monocyte chemotactic protein-1 (MCP-1/CCL2), macrophage inflammatory protein 1 (MIP-1α/CCL3 and MIP-β/CCL4), and macrophage migration inhibitory factor (MIF). All of these

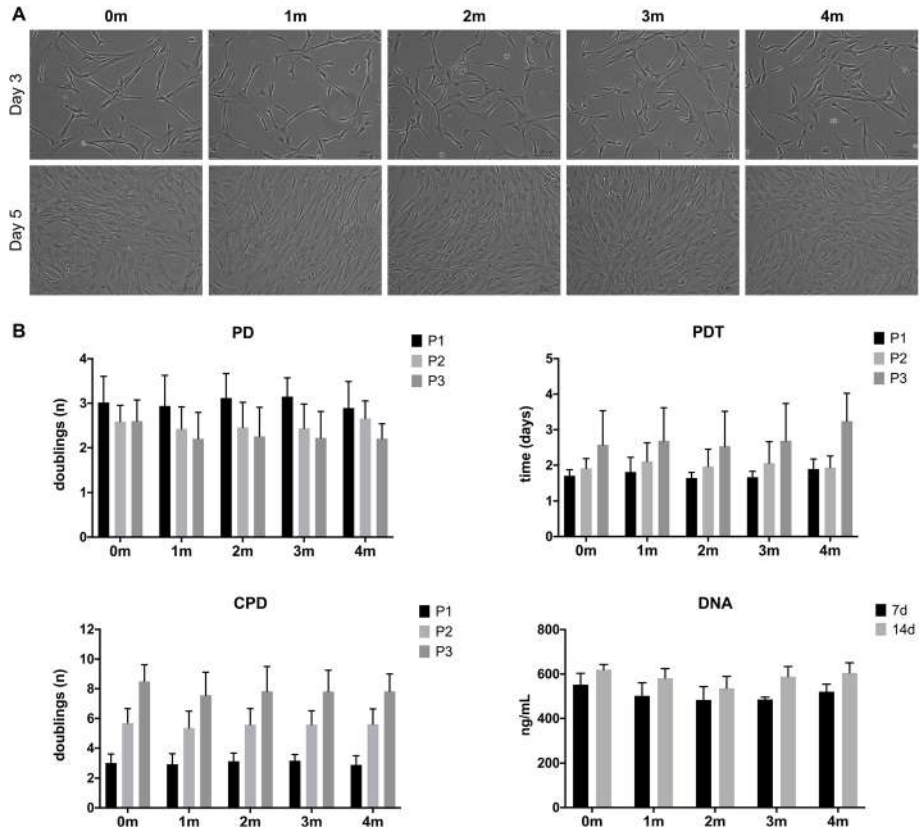

Fig. 6 Morphology and proliferation kinetics of BMSCs in HPL from PCs stored for 0–4 months (m). **a** Morphology of BMSCs at passage 2 (representative images from one donor), scale bar 100 μm. **b** Proliferation kinetics over three serial passages (P1–3) and DNA content after 7 and 14 days (d). Data represent means ± SD ($n = \geq 4$ donors). PD, population doubling rate; CPD, cumulative population doublings; PDT, population doubling time

have been implicated in the recruitment and differentiation of osteoclasts and/or their precursors [64–66]. Moreover, it has been demonstrated that RANTES secreted by osteoclasts promotes the migration of osteoblasts and MSCs in vitro [64, 67, 68] and mineralization in vivo [68, 69].

In addition to GFs and chemokines, a number of inflammatory cytokines were identified in the HPL herein. The evidence for the effects of inflammatory cytokines on MSCs is conflicting since these effects appear to be (a) tissue/site-specific, (b) MSC type-specific, and (c) dose-dependent, based on which a particular cytokine may exert pro- or anti-inflammatory and pro- or anti-osteogenic effects [54]. The most commonly reported of these are TNF-α and IL-1, predominant during the acute inflammatory phase of healing. The combination of HPL and exogenous IL-1α was shown to result in a transient increase in the inflammatory response accompanied by an increase in proliferation, without loss of differentiation potential, in human osteoblasts [70] and ASCs [71]. Interferon-γ (IFN-γ), another major pro-inflammatory cytokine, has consistently more anti-osteogenic effects [54]. Nevertheless, several studies have reported advantages of "pre-conditioning" MSCs with IFN-γ, either alone or in combination with other cytokines such as TNF-α and IL-1, in terms of their immunomodulatory and regenerative potential [72].

Recent studies have reported differences in MSC proliferation and osteogenic differentiation when cultured in different HPL formulations, expressing differences in their protein compositions [15, 73]. MSC proliferation, i.e., PD rate/time, is considered a "key parameter" during ex vivo expansion [11], and ALP and mineralization assays are routinely used to test the in vitro osteogenic capacity of MSCs. In the context of BTE, the in vitro PD time and ALP activity of MSCs are reported to most likely correlate with their in vivo mineralization capacity [74]. Accordingly, in the present study, the growth kinetics and osteogenic potential of BMSCs were tested in HPLs produced from the different PC storage times; BMSCs from multiple donors were used to account for donor-related variations. No significant differences were observed between the different PC storage times in terms of either BMSC proliferation or ALP activity/mineralization. However, considerable donor-related variation was observed in relation to the latter. Notably, the highest relative mean ALP activity and mineralization, with the

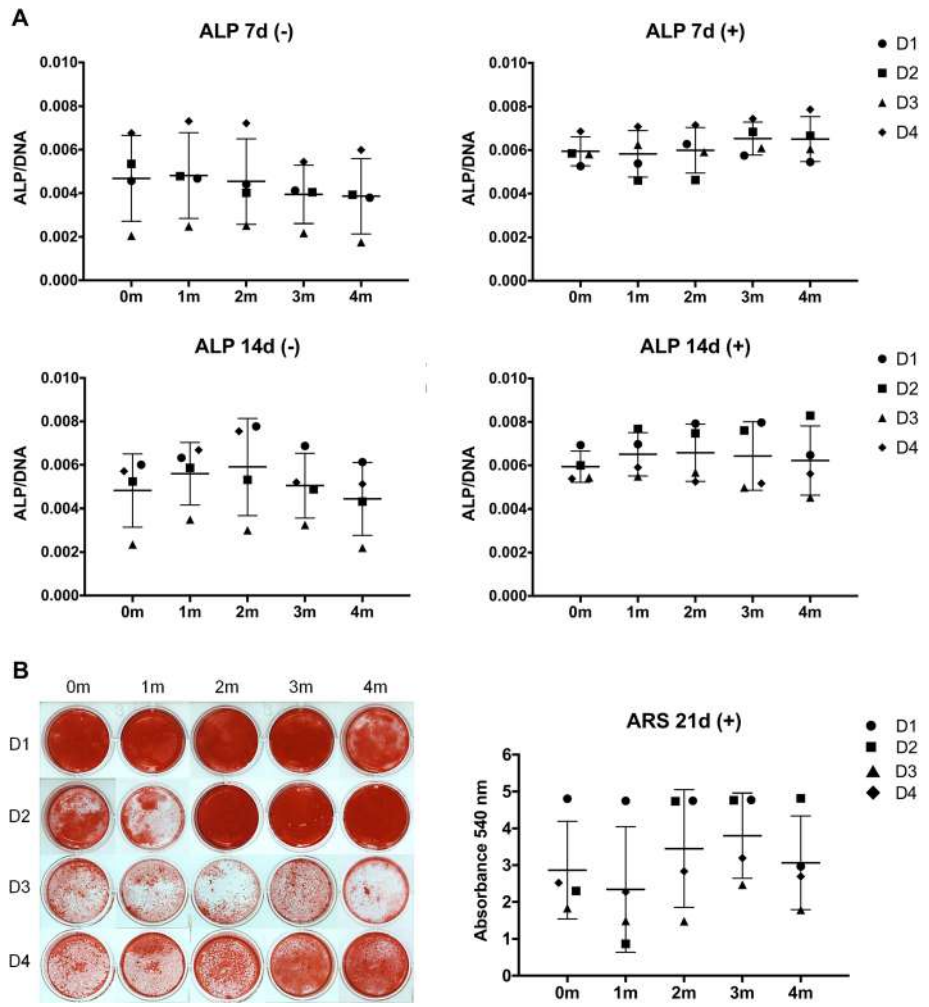

Fig. 7 Osteogenic differentiation of BMSCs in HPL from PCs stored for 0–4 months (m). **a** ALP activity at 7 and 14 days (d) in osteogenic (+) and standard (–) HPL media. ALP activity (absorbance) was normalized to the corresponding DNA content (ng/mL). **b** Representative images and quantification of Alizarin Red S (ARS)-stained cells after 21 days of induction. Data represent means ± SD; each symbol represents a single donor (D, $n = 4$ donors) based on the average of 3 experimental replicates

least inter-donor variation, was observed in the 3-month PC storage group. The results herein are consistent with a recent study reporting on MSCs from a similar donor cohort (healthy young patients), which reported large inter-donor variations in xenogeneic MSCs [17]. It is well-known that several biological (age, sex), behavioral (alcohol/tobacco use), and disease-related (obesity, diabetes) factors influence MSC properties including proliferation and osteogenic differentiation [75]. Nevertheless, it must be acknowledged that the observed donor variation may have confounded the detection of significant differences between PC storage times in the present study.

Among various aspects of HPL production which require standardization is the storage time of the source material, i.e., PCs produced by blood establishments. Current recommendations call for blood centers to freeze outdated PCs (within 7 days of collection) for later HPL production, although "the maximum period time that PCs can be used after expiry to prepare an efficient HPL for cell expansion is unknown" [9]. International blood authorities advise a minimum interval of 3 months between blood donations to allow for repeated viral testing to minimize the risk of disease transmission via platelet products. In the context of HPL, this is especially relevant when smaller PC-pool sizes are used (≤ 16 donors) and where pathogen reduction is not applied [6]. In the present study, HPL produced from PCs stored for > 4 months showed a significant deterioration of several cytokines relevant for MSCs. No significant differences between PC storage times < 4 months were observed in terms of HPL cytokine concentrations, i.e., a clear trend for cytokine deterioration with time, or corresponding MSC proliferation and osteogenic differentiation. Thus, the data herein did not allow for the

detection of any statistical associations between specific HPL cytokines and the degree of MSC osteogenic differentiation. Nevertheless, our observation that outdated PCs can be safely frozen for up to 4 months (preferably 3 months when the focus is BTE) may facilitate the implementation of routines enabling more blood banks to produce HPL. This would address the need for standardization and scaling-up of HPL production, while also benefiting blood bank economies.

Conclusions

The expansion of human MSCs in HPL represents a favorable strategy for BTE. MSCs expanded in HPL demonstrate a high in vitro osteogenic differentiation potential, albeit with considerable donor variation. Exactly which components of HPL contribute to enhancing the osteogenic potential of MSCs is unclear, since HPL contains a complex mixture of cytokines, chemokines, and inflammatory mediators presenting with synergistic effects. Based on the proteomic analysis herein, further investigation of the role of certain cytokines, particularly SCGF, in the regulation of MSCs' osteogenic differentiation is warranted. Finally, a maximum frozen storage time of 4 months is recommended for outdated PCs assigned for HPL production at blood establishments.

Supplementary information

Supplementary information accompanies this paper at https://doi.org/10.1186/s13287-020-01863-9.

Additional file 1 : Supplementary Table 1. Real-time PCR assays. **Supplementary Table 2**. Multiplex human cytokine screening panel. **Supplementary Figure 1**. Immunophenotype of BMSCs and ASCs in FBS and HPL. **Supplementary Figure 2**. Cytokine concentrations in HPL.

Abbreviations

BTE: Bone tissue engineering; MSCs: Mesenchymal stromal cells; BMSCs: Bone marrow-derived mesenchymal stromal cells; ASCs: Adipose tissue-derived mesenchymal stromal cells; SVF: Stromal vascular fraction; GMP: Good manufacturing practice; FBS: Fetal bovine serum; HPL: Human platelet lysate; PCs: Platelet concentrates; qPCR: Quantitative real-time polymerase chain reaction; ELISA: Enzyme-linked immunosorbent assay; ALP: Alkaline phosphatase; GFs: Growth factors; PD: Population doubling rate; PDT: Population doubling time; CPD: Cumulative population doubling

Acknowledgements

We thank the Bloodbank at Haukeland University Hospital for supplying the platelet concentrates, the technical staff at the Department of Clinical Dentistry for assisting in the preparation of platelet lysates, and Prof. Stein Atle Lie for the statistical assistance with the study.

Authors' contributions

S.S. designed the study, performed the experiments, analyzed the data, and drafted the manuscript. S.M.A., T.H.F.L., and S.S. contributed to the design, experiments, data analysis, and manuscript writing. A.I.B., T.H., and K.M. contributed to the design, data analysis, and manuscript writing. The authors read and approved the final manuscript.

Funding

This work was supported by Helse Vest Strategic Research Funding, Norway (502027); Research Council of Norway (BEHANDLING/273551); and the Trond Mohn Foundation, Norway (BFS2018TMT10).

Availability of data and materials

Additional data can be made available by the authors upon request.

Ethics approval and consent to participate

Ethical approval for the collection and use of the human tissue samples was obtained from the Regional Committees for Medical and Health Research Ethics (REK) in Norway (reference number 2013/1248/REK sør-øst C).

Consent for publication

Not applicable.

Competing interests

The authors confirm that there are no known conflicts of interest associated with this publication and there has been no significant financial support for this work that could have influenced its outcome.

Author details

[1]Department of Clinical Dentistry, Faculty of Medicine, University of Bergen, Årstadveien 19, 5008 Bergen, Norway. [2]Department of Immunology and Transfusion Medicine, Haukeland University Hospital, Bergen, Norway. [3]Laboratory of Immunology and Transfusion Medicine, Haugesund Hospital, Fonna Health Trust, Haugesund, Norway. [4]Department of Clinical Science, University of Bergen, Bergen, Norway.

Received: 3 March 2020 Revised: 25 June 2020
Accepted: 29 July 2020 Published online: 23 September 2020

References

1. Shanbhag S, Suliman S, Pandis N, Stavropoulos A, Sanz M, Mustafa K. Cell therapy for orofacial bone regeneration: a systematic review and meta-analysis. J Clin Periodontol. 2019;46(Suppl 21):162–82.
2. Prins HJ, Schulten EAJM, Ten Bruggenkate CM, Klein-Nulend J, Helder MN. Bone regeneration using the freshly isolated autologous stromal vascular fraction of adipose tissue in combination with calcium phosphate ceramics. Stem Cell Transl Med. 2016;5(10):1362–74.
3. Karnieli O, Friedner OM, Allickson JG, Zhang N, Jung S, Fiorentini D, et al. A consensus introduction to serum replacements and serum-free media for cellular therapies. Cytotherapy. 2017;19(2):155–69.
4. Shanbhag S, Stavropoulos A, Suliman S, Hervig T, Mustafa K. Efficacy of humanized mesenchymal stem cell cultures for bone tissue engineering: a systematic review with a focus on platelet derivatives. Tissue Eng Part B Rev. 2017;23(6):552–69.
5. Mendicino M, Bailey AM, Wonnacott K, Puri RK, Bauer SR. MSC-based product characterization for clinical trials: an FDA perspective. Cell Stem Cell. 2014;14(2):141–5.
6. Bieback K, Fernandez-Munoz B, Pati S, Schafer R. Gaps in the knowledge of human platelet lysate as a cell culture supplement for cell therapy: a joint publication from the AABB and the International Society for Cell & Gene Therapy. Transfusion. 2019;59(11):3448–60.
7. European Medicines Agency. Guideline on the use of bovine serum in the manufacture of human biological medicinal products. EMA/CHMP/BWP/457920/2012 rev 1. Amsterdam: European Medicines Agency; 2013.
8. Phinney DG, Galipeau J, Msc Committee of the International Society of C, Gene T. Manufacturing mesenchymal stromal cells for clinical applications: a survey of good manufacturing practices at U.S. academic centers. Cytotherapy. 2019;21(7):782–92.
9. Schallmoser K, Henschler R, Gabriel C, Koh MBC, Burnouf T. Production and quality requirements of human platelet lysate: a position statement from the working party on cellular therapies of the International Society of Blood Transfusion. Trends Biotechnol. 2020;38(1):13–23.
10. Burnouf T, Strunk D, Koh MB, Schallmoser K. Human platelet lysate: replacing fetal bovine serum as a gold standard for human cell propagation? Biomaterials. 2016;76:371–87.
11. Rojewski MT, Lotfi R, Gjerde C, Mustafa K, Veronesi E, Ahmed AB, et al. Translation of a standardized manufacturing protocol for mesenchymal

stromal cells: a systematic comparison of validation and manufacturing data. Cytotherapy. 2019;21(4):468–82.
12. Henschler R, Gabriel C, Schallmoser K, Burnouf T, Koh MBC. Human platelet lysate current standards and future developments. Transfusion. 2019;59(4): 1407–13.
13. Strunk D, Lozano M, Marks DC, Loh YS, Gstraunthaler G, Schennach H, et al. International Forum on GMP-grade human platelet lysate for cell propagation. Vox Sang. 2018;113(1):e1–e25.
14. Strunk D, Lozano M, Marks DC, Loh YS, Gstraunthaler G, Schennach H, et al. International Forum on GMP-grade human platelet lysate for cell propagation: summary. Vox Sang. 2018;113(1):80–7.
15. Boraldi F, Burns JS, Bartolomeo A, Dominici M, Quaglino D. Mineralization by mesenchymal stromal cells is variously modulated depending on commercial platelet lysate preparations. Cytotherapy. 2018;20(3):335–42.
16. Schallmoser K, Strunk D. Generation of a pool of human platelet lysate and efficient use in cell culture. Methods Mol Biol. 2013;946:349–62.
17. Mohamed-Ahmed S, Fristad I, Lie SA, Suliman S, Mustafa K, Vindenes H, et al. Adipose-derived and bone marrow mesenchymal stem cells: a donor-matched comparison. Stem Cell Res Ther. 2018;9(1):168.
18. Dominici M, Le Blanc K, Mueller I, Slaper-Cortenbach I, Marini F, Krause D, et al. Minimal criteria for defining multipotent mesenchymal stromal cells. The International Society for Cellular Therapy position statement. Cytotherapy. 2006;8:315–7.
19. Szklarczyk D, Gable AL, Lyon D, Junge A, Wyder S, Huerta-Cepas J, et al. STRING v11: protein-protein association networks with increased coverage, supporting functional discovery in genome-wide experimental datasets. Nucleic Acids Res. 2019;47(D1):D607–D13.
20. Munir A, Døskeland A, Avery SJ, Fuoco T, Mohamed-Ahmed S, Lygre H, et al. Efficacy of copolymer scaffolds delivering human demineralised dentine matrix for bone regeneration. J Tissue Eng. 2019;10: 2041731419852703.
21. Fekete N, Gadelorge M, Furst D, Maurer C, Dausend J, Fleury-Cappellesso S, et al. Platelet lysate from whole blood-derived pooled platelet concentrates and apheresis-derived platelet concentrates for the isolation and expansion of human bone marrow mesenchymal stromal cells: production process, content and identification of active components. Cytotherapy. 2012;14(5):540–54.
22. Bieback K, Hecker A, Kocaomer A, Lannert H, Schallmoser K, Strunk D, et al. Human alternatives to fetal bovine serum for the expansion of mesenchymal stromal cells from bone marrow. Stem Cells. 2009;27(9):2331–41.
23. Suliman S, Ali HRW, Karlsen TA, Amiaud J, Mohamed-Ahmed S, Layrolle P, et al. Impact of humanised isolation and culture conditions on stemness and osteogenic potential of bone marrow derived mesenchymal stromal cells. Sci Rep. 2019;9(1):16031.
24. Gronthos S, Graves SE, Ohta S, Simmons PJ. The STRO-1+ fraction of adult human bone marrow contains the osteogenic precursors. Blood. 1994; 84(12):4164–73.
25. Xu L, Liu Y, Sun Y, Wang B, Xiong Y, Lin W, et al. Tissue source determines the differentiation potentials of mesenchymal stem cells: a comparative study of human mesenchymal stem cells from bone marrow and adipose tissue. Stem Cell Res Ther. 2017;8(1):275.
26. Fennema EM, Tchang LAH, Yuan H, van Blitterswijk CA, Martin I, Scherberich A, et al. Ectopic bone formation by aggregated mesenchymal stem cells from bone marrow and adipose tissue: a comparative study. J Tissue Eng Regen Med. 2018;12(1):e150–e8.
27. Brocher J, Janicki P, Voltz P, Seebach E, Neumann E, Mueller-Ladner U, et al. Inferior ectopic bone formation of mesenchymal stromal cells from adipose tissue compared to bone marrow: rescue by chondrogenic pre-induction. Stem Cell Res. 2013;11(3):1393–406.
28. Brennan MA, Renaud A, Guilloton F, Mebarki M, Trichet V, Sensebé L, et al. Inferior in vivo osteogenesis and superior angiogenesis of human adipose-derived stem cells compared with bone marrow-derived stem cells cultured in xeno-free conditions. Stem Cell Transl Med. 2018;7(3):315.
29. Castren E, Sillat T, Oja S, Noro A, Laitinen A, Konttinen YT, et al. Osteogenic differentiation of mesenchymal stromal cells in two-dimensional and three-dimensional cultures without animal serum. Stem Cell Res Ther. 2015;6:167.
30. Li CY, Wu XY, Tong JB, Yang XX, Zhao JL, Zheng QF, et al. Comparative analysis of human mesenchymal stem cells from bone marrow and adipose tissue under xeno-free conditions for cell therapy. Stem Cell Res Ther. 2015;6:55.
31. Xia W, Li H, Wang Z, Xu R, Fu Y, Zhang X, et al. Human platelet lysate supports ex vivo expansion and enhances osteogenic differentiation of human bone marrow-derived mesenchymal stem cells. Cell Biol Int. 2011; 35(6):639–43.
32. Chevallier N, Anagnostou F, Zilber S, Bodivit G, Maurin S, Barrault A, et al. Osteoblastic differentiation of human mesenchymal stem cells with platelet lysate. Biomaterials. 2010;31(2):270–8.
33. Kuterbekov M, Machillot P, Baillet F, Jonas AM, Glinel K, Picart C. Design of experiments to assess the effect of culture parameters on the osteogenic differentiation of human adipose stromal cells. Stem Cell Res Ther. 2019; 10(1):256.
34. Shansky YD, Sergeeva NS, Sviridova IK, Karalkin PA, Kirsanova VA, Akhmedova SA, et al. Human platelet lysate sustains the osteogenic/adipogenic differentiation potential of adipose-derived mesenchymal stromal cells and maintains their DNA integrity in vitro. Cells Tissues Organs. 2019;207(3–4):149–64.
35. Cowper M, Frazier T, Wu X, Curley L, Ma MH, Mohuiddin OA, et al. Human platelet lysate as a functional substitute for fetal bovine serum in the culture of human adipose derived stromal/stem cells. Cells. 2019;8(7):724.
36. Mangum LH, Natesan S, Stone R 2nd, Wrice NL, Larson DA, Florell KF, et al. Tissue source and cell expansion condition influence phenotypic changes of adipose-derived stem cells. Stem Cells Int. 2017;2017:7108458.
37. Horn P, Bokermann G, Cholewa D, Bork S, Walenda T, Koch C, et al. Impact of individual platelet lysates on isolation and growth of human mesenchymal stromal cells. Cytotherapy. 2010;12(7):888–98.
38. Copland IB, Garcia MA, Waller EK, Roback JD, Galipeau J. The effect of platelet lysate fibrinogen on the functionality of MSCs in immunotherapy. Biomaterials. 2013;34(32):7840–50.
39. Renn TY, Kao YH, Wang CC, Burnouf T. Anti-inflammatory effects of platelet biomaterials in a macrophage cellular model. Vox Sang. 2015;109(2):138–47.
40. Canestrari E, Steidinger HR, McSwain B, Charlebois SJ, Dann CT. Human platelet lysate media supplement supports lentiviral transduction and expansion of human T lymphocytes while maintaining memory phenotype. J Immunol Res. 2019;2019:3616120.
41. Sovkova V, Vocetkova K, Rampichova M, Mickova A, Buzgo M, Lukasova V, et al. Platelet lysate as a serum replacement for skin cell culture on biomimetic PCL nanofibers. Platelets. 2018;29(4):395–405.
42. Viau S, Lagrange A, Chabrand L, Lorant J, Charrier M, Rouger K, et al. A highly standardized and characterized human platelet lysate for efficient and reproducible expansion of human bone marrow mesenchymal stromal cells. Cytotherapy. 2019;21(7):738–54.
43. Christensen C, Jonsdottir-Buch S, Sigurjonsson O. Effects of amotosalen treatment on human platelet lysate bioactivity; 2019.
44. Laner-Plamberger S, Oeller M, Mrazek C, Hartl A, Sonderegger A, Rohde E, et al. Upregulation of mitotic bookmarking factors during enhanced proliferation of human stromal cells in human platelet lysate. J Transl Med. 2019;17(1):432.
45. Ozaki Y, Nishimura M, Sekiya K, Suehiro F, Kanawa M, Nikawa H, et al. Comprehensive analysis of chemotactic factors for bone marrow mesenchymal stem cells. Stem Cells Dev. 2007;16(1):119–29.
46. Fekete N, Rojewski MT, Lotfi R, Schrezenmeier H. Essential components for ex vivo proliferation of mesenchymal stromal cells. Tissue Eng Part C Methods. 2014;20(2):129–39.
47. Yue R, Shen B, Morrison SJ. Clec11a/osteolectin is an osteogenic growth factor that promotes the maintenance of the adult skeleton. Elife. 2016;5:e18782.
48. Ito C, Sato H, Ando K, Watanabe S, Yoshiba F, Kishi K, et al. Serum stem cell growth factor for monitoring hematopoietic recovery following stem cell transplantation. Bone Marrow Transpl. 2003;32(4):391–8.
49. Chaboya C. Elucidating the signaling pathways for the c-type lectin clec11a in human mesenchymal stromal cells. Sacramento: California State University; 2019.
50. Kristensen LP, Chen L, Nielsen MO, Qanie DW, Kratchmarova I, Kassem M, et al. Temporal profiling and pulsed SILAC labeling identify novel secreted proteins during ex vivo osteoblast differentiation of human stromal stem cells. Mol Cell Proteomics. 2012;11(10):989–1007.
51. Grabarek J, Groopman JE, Lyles YR, Jiang S, Bennett L, Zsebo K, et al. Human kit ligand (stem cell factor) modulates platelet activation in vitro. J Biol Chem. 1994;269(34):21718–24.
52. Matsumoto T, Ii M, Nishimura H, Shoji T, Mifune Y, Kawamoto A, et al. Lnk-dependent axis of SCF-cKit signal for osteogenesis in bone fracture healing. J Exp Med. 2010;207(10):2207–23.
53. Ruangsawasdi N, Zehnder M, Patcas R, Ghayor C, Siegenthaler B, Gjoksi B, et al. Effects of stem cell factor on cell homing during functional pulp

regeneration in human immature teeth. Tissue Eng Part A. 2017;23(3–4):115–23.
54. Deshpande S, James AW, Blough J, Donneys A, Wang SC, Cederna PS, et al. Reconciling the effects of inflammatory cytokines on mesenchymal cell osteogenic differentiation. J Surg Res. 2013;185(1):278–85.
55. Massberg S, Konrad I, Schurzinger K, Lorenz M, Schneider S, Zohlnhoefer D, et al. Platelets secrete stromal cell-derived factor 1alpha and recruit bone marrow-derived progenitor cells to arterial thrombi in vivo. J Exp Med. 2006;203(5):1221–33.
56. Kitaori T, Ito H, Schwarz EM, Tsutsumi R, Yoshitomi H, Oishi S, et al. Stromal cell-derived factor 1/CXCR4 signaling is critical for the recruitment of mesenchymal stem cells to the fracture site during skeletal repair in a mouse model. Arthritis Rheum. 2009;60(3):813–23.
57. Hosogane N, Huang Z, Rawlins BA, Liu X, Boachie-Adjei O, Boskey AL, et al. Stromal derived factor-1 regulates bone morphogenetic protein 2-induced osteogenic differentiation of primary mesenchymal stem cells. Int J Biochem Cell Biol. 2010;42(7):1132–41.
58. Liu H, Li M, Du L, Yang P, Ge S. Local administration of stromal cell-derived factor-1 promotes stem cell recruitment and bone regeneration in a rat periodontal bone defect model. Mater Sci Eng C Mater Biol Appl. 2015;53:83–94.
59. Yang F, Xue F, Guan J, Zhang Z, Yin J, Kang Q. Stromal-cell-derived factor (SDF) 1-alpha overexpression promotes bone regeneration by osteogenesis and angiogenesis in osteonecrosis of the femoral head. Cell Physiol Biochem. 2018;46(6):2561–75.
60. Ando Y, Ishikawa J, Fujio M, Matsushita Y, Wakayama H, Hibi H, et al. Stromal cell-derived factor-1 accelerates bone regeneration through multiple regenerative mechanisms. J Oral Maxillofac Surg Med Pathol. 2019;31(4):245–50.
61. Huang J, Chi H, Chi H, Qiu L, Wang Y, Qiu Z, et al. Stromal cell-derived factor 1 promotes cell migration to enhance bone regeneration after hypoxic preconditioning. Tissue Eng Part A. 2019;25(17–18):1300–9.
62. Haumer A, Bourgine PE, Occhetta P, Born G, Tasso R, Martin I. Delivery of cellular factors to regulate bone healing. Adv Drug Deliv Rev. 2018;129:285–94.
63. Gamblin AL, Brennan MA, Renaud A, Yagita H, Lezot F, Heymann D, et al. Bone tissue formation with human mesenchymal stem cells and biphasic calcium phosphate ceramics: the local implication of osteoclasts and macrophages. Biomaterials. 2014;35(36):9660–7.
64. Yano S, Mentaverri R, Kanuparthi D, Bandyopadhyay S, Rivera A, Brown EM, et al. Functional expression of beta-chemokine receptors in osteoblasts: role of regulated upon activation, normal T cell expressed and secreted (RANTES) in osteoblasts and regulation of its secretion by osteoblasts and osteoclasts. Endocrinology. 2005;146(5):2324–35.
65. Kim MS, Magno CL, Day CJ, Morrison NA. Induction of chemokines and chemokine receptors CCR2b and CCR4 in authentic human osteoclasts differentiated with RANKL and osteoclast like cells differentiated by MCP-1 and RANTES. J Cell Biochem. 2006;97(3):512–8.
66. Onodera S, Sasaki S, Ohshima S, Amizuka N, Li M, Udagawa N, et al. Transgenic mice overexpressing macrophage migration inhibitory factor (MIF) exhibit high-turnover osteoporosis. J Bone Miner Res. 2006;21(6):876–85.
67. Ponte AL, Marais E, Gallay N, Langonne A, Delorme B, Herault O, et al. The in vitro migration capacity of human bone marrow mesenchymal stem cells: comparison of chemokine and growth factor chemotactic activities. Stem Cells. 2007;25(7):1737–45.
68. Liu YC, Kao YT, Huang WK, Lin KY, Wu SC, Hsu SC, et al. CCL5/RANTES is important for inducing osteogenesis of human mesenchymal stem cells and is regulated by dexamethasone. Biosci Trends. 2014;8(3):138–43.
69. Lee JS, Lee JB, Cha JK, Choi EY, Park SY, Cho KS, et al. Chemokine in inflamed periodontal tissues activates healthy periodontal-ligament stem cell migration. J Clin Periodontol. 2017;44(5):530–9.
70. Ruggiu A, Ulivi V, Sanguineti F, Cancedda R, Descalzi F. The effect of platelet lysate on osteoblast proliferation associated with a transient increase of the inflammatory response in bone regeneration. Biomaterials. 2013;34(37):9318–30.
71. Romaldini A, Mastrogiacomo M, Cancedda R, Descalzi F. Platelet lysate activates human subcutaneous adipose tissue cells by promoting cell proliferation and their paracrine activity toward epidermal keratinocytes. Front Bioeng Biotechnol. 2018;6:203.
72. Noronha NC, Mizukami A, Caliári-Oliveira C, Cominal JG, JLM R, Covas DT, et al. Priming approaches to improve the efficacy of mesenchymal stromal cell-based therapies. Stem Cell Res Ther. 2019;10(1):131.
73. Juhl M, Tratwal J, Follin B, Sondergaard RH, Kirchhoff M, Ekblond A, et al. Comparison of clinical grade human platelet lysates for cultivation of mesenchymal stromal cells from bone marrow and adipose tissue. Scand J Clin Lab Invest. 2016;76(2):93–104.
74. Janicki P, Boeuf S, Steck E, Egermann M, Kasten P, Richter W. Prediction of in vivo bone forming potency of bone marrow-derived human mesenchymal stem cells. Eur Cell Mater. 2011;21:488–507.
75. Widholz B, Tsitlakidis S, Reible B, Moghaddam A, Westhauser F. Pooling of patient-derived mesenchymal stromal cells reduces inter-individual confounder-associated variation without negative impact on cell viability, proliferation and osteogenic differentiation. Cells. 2019;8(6):633.

Publisher's Note

Springer Nature remains neutral with regard to jurisdictional claims in published maps and institutional affiliations.

Ready to submit your research? Choose BMC and benefit from:

- fast, convenient online submission
- thorough peer review by experienced researchers in your field
- rapid publication on acceptance
- support for research data, including large and complex data types
- gold Open Access which fosters wider collaboration and increased citations
- maximum visibility for your research: over 100M website views per year

At BMC, research is always in progress.

Learn more biomedcentral.com/submissions

International Journal of Implant Dentistry

RESEARCH Open Access

Patient experience following iliac crest-derived alveolar bone grafting and implant placement

Cecilie G. Gjerde[1,2*], Siddharth Shanbhag[2], Evelyn Neppelberg[1,3], Kamal Mustafa[2] and Harald Gjengedal[4]

Abstract

Background: The objective of this study was to assess patient-reported outcomes such as satisfaction and quality of life after advanced alveolar bone augmentation with anterior iliac crest grafting and implant treatment in orally compromised patients.

Methods: This cross-sectional retrospective cohort study included 59 patients (29 women and 30 men) with major functional problems, who underwent advanced alveolar augmentation with autologous iliac bone grafts during a 100-year period (2002–2012).
The self-administered questionnaire included 36 validated questions related to (1) demographics, (2) perceived general and oral health, (3) donor site and hospitalization, (4) status of implants and/or prosthesis, and (5) oral health-related quality of life (OHRQoL).

Results: Questionnaires were completed by 44 patients: 24 women and 20 men (response rate, 74.6%). Most patients reported good tolerance of the operative iliac bone harvesting (85%) and implant (90%) procedures. Post-operative pain at the donor site was reported by 38%, lasting 18.1 ± 16.1 days. An average of 4.3 ± 3.5 days of hospitalization and 20.2 ± 18.5 days of sick leave was reported. The overall satisfaction with prosthetic reconstruction was 90.5%. OHRQoL was reported with a mean Oral Health Impact Profile-14 (OHIP-14) score of 8.4.

Conclusion: Favorable OHRQoL and satisfaction were reported after advanced reconstruction of alveolar ridges with iliac crest-derived grafting and implants in severely compromised patients. However, this treatment requires substantial resources including hospitalization and sick leave.

Keywords: Dental implants, Reconstruction, Quality of life, Bone graft, Iliac crest, Donor site morbidity, PROMs

Background

Insufficient alveolar bone volume, as a result of periodontal disease, trauma, congenital anomalies and/or resorption atrophy, often presents a clinical challenge for optimal placement of dental implants for prosthetic rehabilitation. In such cases, augmentation of alveolar bone, with either autologous bone, allogeneic, xenogeneic, or alloplastic biomaterials, is a prerequisite for placing implants in restoratively and esthetically acceptable positions.

Limited alveolar ridge defects are solved by local grafting. In cases of larger defects and extreme resorption, larger grafts are necessary. The most common donor site for large autologous bone grafts is the iliac crest, due to its accessibility, comparatively abundant bone volume, and high bone quality [1].

Autologous bone is still considered as a "gold standard" for alveolar reconstruction, according to systematic reviews [2–5]. Intra-oral donor sites, like mandibular ramus and symphysis, allow harvesting of limited volumes of autologous bone. The anterior iliac crest is the preferred extra-oral donor site for alveolar augmentation for larger bone volumes [1, 6, 7]. However, complications are reported, including pain, gait disturbance, hematomas, paranesthesia, and infections [8–15].

* Correspondence: cecilie.gjerde@uib.no
[1]Department of Oral and Maxillofacial Surgery, Institute of Clinical Dentistry, University of Bergen, Årstadveien 19, 5009 Bergen, Norway
[2]Centre for Clinical Dental Research, Institute of Clinical Dentistry, University of Bergen, Bergen, Norway
Full list of author information is available at the end of the article

Springer Open

© The Author(s). 2020 **Open Access** This article is distributed under the terms of the Creative Commons Attribution 4.0 International License (http://creativecommons.org/licenses/by/4.0/), which permits unrestricted use, distribution, and reproduction in any medium, provided you give appropriate credit to the original author(s) and the source, provide a link to the Creative Commons license, and indicate if changes were made.

Traditionally, objective clinical variables, like the amount of bone gain (in millimeters) after augmentation, are reported as outcome measures after surgical procedures in clinical studies [16]. Patients' experiences like patient-reported outcome measures (PROMs) have been increasingly used as a measure of treatment effect after medical and dental therapies [17, 18]. Importantly, these measures reflect the patients' perceptions of the treatment outcome in addition to conventional clinical measures. Nowadays, Norwegian authorities address clinicians to include patients' perspective in decisions regarding different treatment modalities [19]. It has been suggested that PROMs such as treatment satisfaction, perceived cost-effectiveness, and quality of life (QoL) may be more important and relevant to patients' daily lives than objective clinical measures [16, 20]. Patient satisfaction is an important outcome measure, related to, although not synonymous with QoL, as satisfaction tends to reflect the process, rather than the outcome, of care [21]. Thus, an increase in the use of PROMs has been highlighted in dental implant research [22].

Health-related QoL (HRQoL) is a dynamic concept referring to an individual's subjective assessment and perspective of current general health condition as well as functional, social, and emotional well-being [23, 24]. Most people regard oral health as important for QoL, and this is mediated through the concept of oral health-related QoL (OHRQoL) [25]. In this regard, OHRQoL is an important PROM in dental research, as oral health is an integral part of general health and well-being [26].

Different instruments to assess OHRQoL may be utilized to detect changes in physical, functional, and psychosocial impacts of oral disorders and have been validated for use in clinical studies [27–29]. The Oral Health Impact Profile-14 (OHIP-14) questionnaire is a widely used OHRQoL instrument [27]. It includes 14 questions covering seven domains of oral health and attempts to assess their impact on patients' OHRQoL [30, 31]. OHIP-14 has previously been translated into Norwegian and used in a large study ($n = 3538$) with a calculated Norwegian national norm value [32]. Although previous studies have reported PROMs in relation to bone grafting [9, 33–42], to our knowledge, only one previous study has systematically assessed impact of donor site harvesting on OHRQoL, where (a) a postoperative lowering of OHRQoL was observed following bone grafting from both intra-oral and extra-oral sites and (b) iliac crest grafts compared to intraoral donor sites had a negative impact on postoperative QoL [37]. Moreover, to our knowledge, only one study has previously assessed the cost-effectiveness of autologous iliac crest grafting [43].

The aim of this study was to assess PROMs such as satisfaction and OHRQoL after advanced reconstruction of alveolar bone by anterior iliac crest-derived grafting and implant treatment.

Methods

Study population

This cross-sectional retrospective cohort study was based on records from all patients ($n = 69$) who underwent advanced alveolar augmentation with autologous iliac bone grafts at the Department of Oral and Maxillofacial Surgery, Haukeland University Hospital, Bergen, Norway, over 10 years (2002–2012). These patients were orally compromised with severe chewing problems as well as speech difficulties and had previously undergone several unsuccessful rehabilitation methods, prior to referral. At the time of this survey, seven patients had passed away, two had moved to unknown addresses, and one was hospitalized in a psychiatric institution. Thus, the study sample included 59 patients: 29 women and 30 men.

The Norwegian Committee for Medical Research Ethics ("REK," Health Region West), acknowledged this study as a treatment quality control study.

Treatment protocol—operative procedure

Bone graft surgeries were performed under general anesthesia and sterile conditions. Cortico-cancellous bone blocks were harvested from the anterior superior iliac crest. Reconstructions in the maxilla ($N = 57$) or mandible ($N = 2$) were performed in one operation by two teams using an onlay bone graft fixated with titanium micro-screws (1.5 mm Ø). The surgical procedure was performed according to the protocol commonly used at Haukeland University Hospital. In brief, the harvesting of autogenous bones from the anterior iliac crests started with a skin incision following the skin lines in a posterolateral direction starting from 3 to 4 cm medial to the iliac crests. The superior surfaces of the iliac crests are exposed after a sharp dissection through the periosteum following the crests. The dissections are performed with great attention to avoid laceration of the fascia lata. Both cortical and spongious bone are harvested. The donor sites are closed in layers with special attention to the first layer—the fascia lata. This layer is sutured close to avoid marrowbone bleeding. Activated vacuum drainages are positioned between the fascia lata and the muscles until the patients are mobilized. The skin incisions are closed with continuous intracutaneous resorbable sutures. All patients included in the study were hospitalized 2–3 days postoperatively. Patients received phenoxymethylpenicillin (1 g × 3) or clindamycin (300 mg × 3) for 5 days following the operation. Vacuum drainage at the donor site was used until the patient was mobilized the morning after surgery. Analgesics (paracetamol or non-steroid anti-inflammatory drugs) were prescribed 7–10 days postoperatively.

Implants were placed 4–6 months after the grafting procedure. The implant installations were performed by different oral surgeons (not in the hospital) and different implant systems were used. The implants installed into the augmented bone were allowed to heal for an additional 4–6 months before loading.

Data collection

Medical records

The records of the original 69 patients were examined with regard to (1) grafting site (2), "graft-survival" determined by the ability to place implants in the grafted site(s) and (3) "implant survival" determined by the presence of functional implant-supported prostheses at the most recent follow-up. Reasons for implant failure were recorded when available.

Questionnaire

A self-administered questionnaire (Additional file 1) was sent by post to all 59 patients, together with an information leaflet about the survey, a return envelope with prepaid postage and an informed consent form. Reminder letters were sent after 2 and 4 weeks if no response was received.

The questionnaire contained 36 previously validated questions, which were categorized and related to (1) demographic and lifestyle, (2) perceived general and oral health, (3) donor site and hospitalization, (4) implant and prosthesis, and (5) OHRQoL (OHIP-14) (Table 1). Responses to questions in categories 1–2 were recorded as "yes/no" or graded on a 3- to 5-point Likert scale [44]. Category 3 included information on the duration of hospitalization and sick leave. Category 4 included information on "graft survival," i.e., whether implants (and prostheses) were delivered in the augmented site(s), and "implant survival," i.e., the presence or "loss/loosening" of any implants after surgery. OHRQoL was assessed using a Norwegian version of the OHIP-14 [32]. These 14 questions addressed seven domains of OHRQoL and their responses were graded on a 5-point Likert scale ranging from "at no time" (0) to "all of the time" (4) (Table 1).

Table 1 Summary of questions

Category	Response
Question	
(1) Perceived health-status	
General health	"Very good" to "bad"
Oral health	"Very good" to "bad"
Overall quality of life	"Excellent" to "bad"
(2) Lifestyle-related	
Smoking	"Yes," "no," or "sometimes"
Appetite	"Good" to "bad"
(3) Donor site-related	
Pain	"Yes" and "no"
Infection	"Yes" and "no"
Presence of a scar	"Yes" and "no"
Reduced sensitivity	"No" to "total loss of sensitivity"
Problems walking	"No" to "a lot"
Satisfaction	"Very satisfied" to "dissatisfied"
(4) Implant-related	
Intraoral pain	"No" to "strong pain"
Installation of implants and prosthetic	"Yes", "no" or "just implants"
Loss of implants	"Yes" and "no"
Satisfaction with prosthesis	"Very satisfied" to "dissatisfied"
(5) OHIP-14	"At no time" to "all of the time"

Statistical analysis

Data were anonymized and analyzed using SPSS v 24 (SPSS Inc., Chicago, IL, USA). Descriptive analyses were applied. Statistical significance was set at 5% level.

Results

The final sample consisted of 44 patients that responded and completed the questionnaire, giving a response rate of 74.6%: 24 women and 20 men, mean age of 61.2 years ± 13.1 (range 27–82 years). The mean time from augmentation surgery until completing the questionnaire was 7.8 years ± 2.65 (range 1.9–12 years).

Summary of demographic and lifestyle-related data is presented (Table 2).

Descriptive findings

Health-related PROMs

Most patients reported "good" or "very good" levels of general health (81.4%), oral health (83.7%), and overall quality of life (90.7%). Less than 5% reported "bad" levels for either of these variables. Most patients reported better general (86%) and oral health (78%) after treatment. Only two patients (4.7%) reported their oral health to be worse after treatment.

Donor site- and hospitalization-related PROMs

Most patients (85.4%) were satisfied with the hip surgery procedure. Pain at the donor site was reported by 38% of patients, lasting for an average of 18.1 ± 16.1 days and measuring 43.6 ± 27 on the VAS (0–100) scale. Only two patients (4.7%) reported post-operative infection at the donor site. Scar formation on skin (hip) was reported in 49% of patients, by majority esthetically acceptable (90.4%). Four (9.5%) and two (4.7%) patients reported "a little" or "a lot" of reduced sensitivity at the donor site, respectively. Three patients (7.3%) reported problems in

Table 2 Patients' demographic and lifestyle-related data

Variable	Frequency	
	N or Mean ± SD	%
Patients		
Female	24	54.5
Male	20	45.5
Age (years)	61.16 ± 13.10	
Age at operation	53.73 ± 13.07	
Time from augmentation to completing questionnaire (months)	93.55 ± 31.75	
Civil status		
Married	30	68.2
Single	11	25.0
Widow(er)	3	6.8
Housing		
Alone	12	27.3
With another person	23	52.3
> two persons	9	20.5
Education		
Up to primary	7	11.3
Up to secondary	23	53.5
"Artium"	1	2.3
High school	9	20.9
University	3	7.0
Smoking		
Yes	8	19.0
No	33	78.6
Sometimes	1	2.4
Cigarettes/day	13.65 ± 7.22	
Years of smoking	26.52 ± 11.63	

walking (Table 3). The average time of hospitalization was 4.3 ± 3.5 days and sick leave 20.2 ± 18.5 days.

Implant-/prostheses-related PROMs

Most patients ($n = 40$, 90.9%) reported to have implants placed and received prostheses in the augmentation site(s). This was interpreted as graft survival, indicating a graft survival rate of 90.9% on the patient level. Two patients received implants, although without further prosthetic rehabilitation. Implants could not be installed in two patients. However, 29.3% of patients reported "loosening or loss" of implants in the post-operative period (1 year), indicating an implant survival rate on the patient level of 70.7%, and most patients (8 out of 11) received new implants.

No pain was reported in 39 patients (82.9%) following implant surgery and a majority of patients (90.2%) were satisfied/very satisfied with the implant therapy overall and in terms of overall satisfaction with teeth (90.5%).

The correlation analyses performed did not show a significant correlation between the complications at the donor site and implant loss (Table 4).

OHRQoL

The mean OHIP-14 score (Table 5) was 8.4 ± 9.7 (range 0–56) in 44 patients of whom 35 patients scored 14 or less. Nine patients scored a total sum of 1 [1], i.e. "hardly ever" impact on any single item and "at no time" on the remaining 13 items. The functional limitation domain had the highest score (2.34) and the social disability domain the lowest score (0.61).

Discussion

An important finding in this study is that a majority of patients were very satisfied after iliac crest-derived alveolar bone grafting and implant therapy. Although 90% of the patients in our study had successful bone grafting, only 70.1% reported implant survival together with prosthetic rehabilitation after 1 year. These figures are lower than those reported in previous studies [2, 3, 9]. A review by Chiapasco et al. showed that the mean graft failure in 16 studies was 1.6% and partial loss of graft of 3.3% [45]. The same review showed that the overall survival rate of dental implants in transplanted bone was 87%. However, it must be kept in mind that the patients in our study were orally compromised and very challenging to reconstruct. Moreover, the patients in our study did not report on the number of implants lost, and we do not have reliable records of the exact number of implants each patient had got installed. This could indicate differences in survival on implant or patient levels—a variable of clinical importance as the number of lost implants may be higher.

Another important finding is that patients reported to tolerate the augmentation procedure well; 85% of patients were satisfied with the hip operation (performed under general anesthesia), comparable to a previous report [46]. However, 40% of the patients reported pain for 18 ± 16 days after augmentation, which is in accordance with other studies [37, 46] and which should be considered during the treatment planning of patients scheduled to received iliac crest-derived bone grafts [33]. Two patients reported infection at the donor site. All operations were performed by a strict sterile regime and protocol at the university hospital.

The level of OHRQoL reported by the patients was favorable with an OHIP-14 value of 8.4. In a previous study, Dahl et al. reported an OHIP-14 score of 4.1 in the Norwegian adult population (2441 patients), with 35% of the sample reporting "no oral health problems" [32]. If the study sample in the study of Dahl et al. is considered to be representative of the general population, patients in our study reported poorer OHRQoL than the general population. Thus, even though the participants in this study report good oral health and better than before operation on the single questions, they

Table 3 Patient-reported outcomes

Question	Response	Frequency
Oral health	Very good/good	81.8%
Quality of Life	Very good/good	90.9%
General health	Very good/good	81.8%
Pain after hip operation	Excessive	35.0%
Satisfaction hip operation	Very	85.7%
Post op infection in hip site	No	95.3%
Visible scar on hip	Yes	48.8%
Acceptable scar	Yes	20 of 21[a]
Reduced sensibility on hip site	No	86.0%
Problem walking	No	92.9%
Augmented bone block still present	No	6.8%
New augmentation	Yes	1 of 4[a]
Oral pain after augmentation	No/some	83.3%
Implant/teeth in augmented bone	Yes	90.9%
Lost implants	Yes	28.6%
Time lost after installation	0–3 months	42.9%
	7–12 months	28.6%
New implants installed	Yes	8 of 11[a]
Satisfaction with implant-retained teeth	Very satisfied/satisfied	90.5%

[a]Incomplete or missing data

still report having problems related to their oral condition. This is to be expected as the patients in our study were orally compromised before augmentation with almost no alveolar ridge to retain or support a prosthetic construction. Since the patients had extensive alveolar bone loss rendering them orally handicapped, any improvement in function would be likely to have a positive impact on satisfacation and OHR-QoL. However, it is difficult to relate their reported level of

Table 4 Correlation analyses

Outcome variables	Correlations	Spearman's rho	*P* value
OHRQoL	Oral health compared	0.596	< 0.0001
	General health now	0.369	0.014
	General health compared	0.412	0.005
	Implants placed/teeth installed	0.317	0.036
	Lost implants	− 0.372	0.015
	Smoking	− 0.334	0.005
	Speaking	0.572	< 0.0001
	Chewing	0.375	0.014
Implants placed	General health	− 0.314	0.038
	Oral pain post op	0.334	0.031
	Oral health	0.305	0.044
	General health compared	0.314	0.038
	Satisfaction hip operation	− 0.439	0.004
	OHRQoL	0.317	0.036
Lost implants	General health	− 0.328	0.034
	QoL	− 0.342	0.027
	OHRQoL	− 0.372	0.015
	Satisfied teeth	− 0.328	0.034

Table 5 Summary of OHIP-14 ($N = 44$ and response range 0–8)

OHIP domain	Minimum	Maximum	Mean	SD
Functional limitation	0	7	2.34	1.70
Physical pain	0	7	1.16	1.51
Psychological discomfort	0	8	1.64	2.27
Physical disability	0	8	0.75	1.77
Psychological disability	0	8	1.18	2.11
Social disability	0	8	0.61	1.40
Handicap	0	8	0.70	1.71
Total	0	64	8.4	9.7

OHRQoL to the augmentation and implant installation per se, as this was performed up to 12 years prior to completing the questionnaire (mean 7 years and 10 months). So, patients' present oral situation with fixed teeth could/may alter the "reference" for the patients regarding OHRQoL. However, we cannot reliably ascribe the level of OHRQoL to the treatment performed years ago, since we have no such data either before or soon after the prosthetic rehabilitation, and therefore, cannot estimate the influence the effect of response shift on the study outcomes. Previous reports show a significant influence of implant-retained prosthetic treatment on OHRQoL, but these reports are based on before-and-after registrations [47].

Patients in our study reported satisfaction with the augmentation and implant installation, and as these patients were orally compromised before the operation, their satisfaction with getting fixed teeth most likely improved their perceived oral health condition. This might also, in part, explain why they reported good OHRQoL. Thus, our findings indicate that a majority of patients tolerate the augmentation and implantation procedures very well and with minor long-term sequelae.

The treatment protocol described in this study, i.e., advanced bone reconstructions under general anesthetics, hospitalization, and sick leave, is considered expensive in a public health services. In the present study, an average of 4.3 days of hospitalization and 20.2 days of sick leave was reported, which is costly for the health service and inconvenient for the patient [33, 43]. When comparing iliac bone graft as a treatment to bone substitutes, a previous study clearly demonstrated that iliac bone graft procedure demands more resources and more than three times the costs of bone substitutes [43]. Although the patients reported good satisfaction and OHRQoL after iliac bone grafting, this treatment is demanding for patients as well as health services, indicating the need for alternative treatment modalities [37, 43, 46].

Conclusions

Favorable OHRQoL and satisfaction were reported after advanced reconstruction with iliac crest-derived grafts and implant treatment in orally compromised patients. However, this treatment requires substantial resources including hospitalization and sick leave.

Supplementary information

Supplementary information accompanies this paper at https://doi.org/10.1186/s40729-019-0200-8.

Additional file 1. A self-administered questionnaire.

Abbreviations

HRQoL: Health-related quality of life; OHIP-14: Oral Health Impact Profile-14; OHRQoL: Oral health-related quality of life; PROMs: Patient-reported outcome measures; QoL: Quality of life

Acknowledgements

The staff and surgeons at the Department of Oral and Maxillofacial Surgery, Head and Neck Clinic, Haukeland University Hospital, Bergen. Randi Aursland, master student, who helped collecting data. The patients included in this study.

Authors' contributions

CG contributed to the design of the trial, acquisition of the data, follow-up of the patient-reported data, and analysis and interpretation of the data and drafted the manuscript. SS contributed to the design of the trial, statistical analysis, and analysis and interpretation of the data and drafted the manuscript. EN contributed to the conception and design and critically revised the manuscript. KM contributed to the conception and design and critically revised the manuscript. HG contributed to the design of the trial, statistical analysis, and analysis and interpretation of the data and drafted the manuscript. All authors gave final approval and agreed to be accountable for all aspects of the work.

Funding

This work was partially funded by the Research Council of Norway through the BEHANDLING project (grant no. 273551) and TROND MOHN Foundation, Norway (BFS2018TMT10).

Availability of data and materials

The datasets used and/or analyzed during the current study are available from the corresponding author on reasonable request.

Ethics approval and consent to participate

The Ethics Committee was contacted in 2015, and no ethical approval was needed since this was then considered a quality control study. Written consent was obtained from all participants.

Consent for publication

Not applicable.

Competing interests

Cecilie G Gjerde, Siddharth Shanbhag, Evelyn Neppelberg, Kamal Mustafa, and Harald Gjengedal declare that they have no competing interests.

Author details

[1]Department of Oral and Maxillofacial Surgery, Institute of Clinical Dentistry, University of Bergen, Årstadveien 19, 5009 Bergen, Norway. [2]Centre for Clinical Dental Research, Institute of Clinical Dentistry, University of Bergen, Bergen, Norway. [3]Department of Oral and Maxillofacial Surgery, Head and Neck Clinic, Haukeland University Hospital, Bergen, Norway. [4]Department of Prosthodontics, Institute of Clinical Dentistry, University of Bergen, Bergen, Norway.

Received: 10 October 2019 Accepted: 11 December 2019
Published online: 05 February 2020

References

1. Schaaf H, Lendeckel S, Howaldt HP, Streckbein P. Donor site morbidity after bone harvesting from the anterior iliac crest. Oral Surg Oral Med Oral Pathol Oral Radiol Endod. 2010;109(1):52–8.

2. Sakkas A, Wilde F, Heufelder M, Winter K, Schramm A. Autogenous bone grafts in oral implantology-is it still a "gold standard"? A consecutive review of 279 patients with 456 clinical procedures. Int J Implant Dent. 2017;3(1):23.
3. Aghaloo TL, Moy PK. Which hard tissue augmentation techniques are the most successful in furnishing bony support for implant placement? Int J Oral Maxillofac Implants. 2007;22(Suppl):49–70.
4. Jensen SS, Terheyden H. Bone augmentation procedures in localized defects in the alveolar ridge: clinical results with different bone grafts and bone-substitute materials. Int J Oral Maxillofac Implants. 2009;24(Suppl):218–36.
5. Rocchietta I, Fontana F, Simion M. Clinical outcomes of vertical bone augmentation to enable dental implant placement: a systematic review. J Clin Periodontol. 2008;35(8 Suppl):203–15.
6. Kalk WW, Raghoebar GM, Jansma J, Boering G. Morbidity from iliac crest bone harvesting. J Oral Maxillofac Surg. 1996;54(12):1424–9 discussion 30.
7. Seiler JG 3rd, Johnson J. Iliac crest autogenous bone grafting: donor site complications. J South Orthop Assoc. 2000;9(2):91–7.
8. Eufinger H, Leppanen H. Iliac crest donor site morbidity following open and closed methods of bone harvest for alveolar cleft osteoplasty. J Craniomaxillofac Surg. 2000;28(1):31–8.
9. Nkenke E, Weisbach V, Winckler E, Kessler P, Schultze-Mosgau S, Wiltfang J, et al. Morbidity of harvesting of bone grafts from the iliac crest for preprosthetic augmentation procedures: a prospective study. Int J Oral Maxillofac Surg. 2004;33(2):157–63.
10. Dawson KH, Egbert MA, Myall RW. Pain following iliac crest bone grafting of alveolar clefts. J Craniomaxillofac Surg. 1996;24(3):151–4.
11. Swan MC, Goodacre TE. Morbidity at the iliac crest donor site following bone grafting of the cleft alveolus. Br J Oral Maxillofac Surg. 2006;44(2):129–33.
12. Jessop ZM, Al-Himdani S, Clement M, Whitaker IS. The challenge for reconstructive surgeons in the twenty-first century: manufacturing tissue-engineered solutions. Front Surg. 2015;2:52.
13. Hill NM, Horne JG, Devane PA. Donor site morbidity in the iliac crest bone graft. Aust N Z J Surg. 1999;69(10):726–8.
14. Finkemeier CG. Bone-grafting and bone-graft substitutes. J Bone Joint Surg Am. 2002;84-A(3):454–64.
15. Hernigou P, Desroches A, Queinnec S, Flouzat Lachaniette CH, Poignard A, Allain J, et al. Morbidity of graft harvesting versus bone marrow aspiration in cell regenerative therapy. Int Orthop. 2014;38(9):1855–60.
16. Chow A, Mayer EK, Darzi AW, Athanasiou T. Patient-reported outcome measures: the importance of patient satisfaction in surgery. Surgery. 2009;146(3):435–43.
17. Marshall S, Haywood K, Fitzpatrick R. Impact of patient-reported outcome measures on routine practice: a structured review. J Eval Clin Pract. 2006;12(5):559–68.
18. McGrath C, Lam O, Lang N. An evidence-based review of patient-reported outcome measures in dental implant research among dentate subjects. J Clin Periodontol. 2012;39(Suppl 12):193–201.
19. Helsedepartement DKOo. Oppdragsdokument Helse Vest 2017.
20. Wiklund I. Assessment of patient-reported outcomes in clinical trials: the example of health-related quality of life. Fundam Clin Pharmacol. 2004;18(3):351–63.
21. Newsome PR, McGrath C. Patient-centred measures in dental practice: 1. An overview. Dent Update. 2006;33(10):596–8 600.
22. Lang NP, Zitzmann NU, Working Group 3 of the VEWoP. Clinical research in implant dentistry: evaluation of implant-supported restorations, aesthetic and patient-reported outcomes. J Clin Periodontol. 2012;39(Suppl 12):133–8.
23. Waldron D, O'Boyle CA, Kearney M, Moriarty M, Carney D. Quality-of-life measurement in advanced cancer: assessing the individual. J Clin Oncol. 1999;17(11):3603–11.
24. Browne JP, O'Boyle CA, McGee HM, Joyce CR, McDonald NJ, O'Malley K, et al. Individual quality of life in the healthy elderly. Qual Life Res. 1994;3(4):235–44.
25. McGrath C, Bedi R. A national study of the importance of oral health to life quality to inform scales of oral health related quality of life. Qual Life Res. 2004;13(4):813–8.
26. John MT, Hujoel P, Miglioretti DL, LeResche L, Koepsell TD, Micheelis W. Dimensions of oral-health-related quality of life. J Dent Res. 2004;83(12):956–60.
27. Slade GD. Derivation and validation of a short-form oral health impact profile. Community Dent Oral Epidemiol. 1997;25(4):284–90.
28. Locker D, Allen F. What do measures of 'oral health-related quality of life' measure? Community Dent Oral Epidemiol. 2007;35(6):401–11.
29. Sischo L, Broder HL. Oral health-related quality of life: what, why, how, and future implications. J Dent Res. 2011;90(11):1264–70.
30. Slade GD. Assessing change in quality of life using the Oral Health Impact Profile. Community Dent Oral Epidemiol. 1998;26(1):52–61.
31. Locker D, Allen PF. Developing short-form measures of oral health-related quality of life. J Public Health Dent. 2002;62(1):13–20.
32. Dahl KE, Wang NJ, Skau I, Ohrn K. Oral health-related quality of life and associated factors in Norwegian adults. Acta Odontol Scand. 2011;69(4):208–14.
33. Joshi A, Kostakis GC. An investigation of post-operative morbidity following iliac crest graft harvesting. Br Dent J. 2004;196(3):167–71 discussion 55.
34. Kessler P, Thorwarth M, Bloch-Birkholz A, Nkenke E, Neukam FW. Harvesting of bone from the iliac crest--comparison of the anterior and posterior sites. Br J Oral Maxillofac Surg. 2005;43(1):51–6.
35. Nkenke E, Schultze-Mosgau S, Radespiel-Troger M, Kloss F, Neukam FW. Morbidity of harvesting of chin grafts: a prospective study. Clin Oral Implants Res. 2001;12(5):495–502.
36. Nkenke E, Radespiel-Troger M, Wiltfang J, Schultze-Mosgau S, Winkler G, Neukam FW. Morbidity of harvesting of retromolar bone grafts: a prospective study. Clin Oral Implants Res. 2002;13(5):514–21.
37. Reissmann DR, Dietze B, Vogeler M, Schmelzeisen R, Heydecke G. Impact of donor site for bone graft harvesting for dental implants on health-related and oral health-related quality of life. Clin Oral Implants Res. 2013;24(6):698–705.
38. Vu DD, Schmidt BL. Quality of life evaluation for patients receiving vascularized versus nonvascularized bone graft reconstruction of segmental mandibular defects. J Oral Maxillofac Surg. 2008;66(9):1856–63.
39. Truedsson A, Hjalte K, Sunzel B, Warfvinge G. Maxillary sinus augmentation with iliac autograft - a health-economic analysis. Clin Oral Implants Res. 2013;24(10):1088–93.
40. Papi P, Giardino R, Sassano P, Amodeo G, Pompa G, Cascone P. Oral health related quality of life in cleft lip and palate patients rehabilitated with conventional prostheses or dental implants. J Int Soc Prev Community Dent. 2015;5(6):482–7.
41. Landes CA, Bundgen L, Laudemann K, Ghanaati S, Sader R. Patient satisfaction after prosthetic rehabilitation of bone-grafted alveolar clefts with nonsubmerged ITI Straumann dental implants loaded at three months. Cleft Palate Craniofac J. 2012;49(5):601–8.
42. Reisine S, Freilich M, Ortiz D, Pendrys D, Shafer D, Taxel P. Quality of life improves among post-menopausal women who received bone augmentation during dental implant therapy. Int J Oral Maxillofac Surg. 2012;41(12):1558–62.
43. Dahlin C, Johansson A. Iliac crest autogenous bone graft versus alloplastic graft and guided bone regeneration in the reconstruction of atrophic maxillae: a 5-year retrospective study on cost-effectiveness and clinical outcome. Clin Implant Dent Relat Res. 2011;13(4):305–10.
44. Gjengedal H, Berg E, Gronningsaeter AG, Dahl L, Malde MK, Boe OE, et al. The influence of relining or implant retaining existing mandibular dentures on health-related quality of life: a 2-year randomized study of dissatisfied edentulous patients. Int J Prosthodont. 2013;26(1):68–78.
45. Chiapasco M, Casentini P, Zaniboni M. Bone augmentation procedures in implant dentistry. Int J Oral Maxillofac Implants. 2009;24(Suppl):237–59.
46. Barone A, Ricci M, Mangano F, Covani U. Morbidity associated with iliac crest harvesting in the treatment of maxillary and mandibular atrophies: a 10-year analysis. J Oral Maxillofac Surg. 2011;69(9):2298–304.
47. Hara M, Matsumoto T, Yokoyama S, Higuchi D, Baba K. Location of implant-retained fixed dentures affects oral health-related quality of life. Clin Implant Dent Relat Res. 2017;19(4):710–6.

Publisher's Note

Springer Nature remains neutral with regard to jurisdictional claims in published maps and institutional affiliations.

Submit your manuscript to a SpringerOpen journal and benefit from:

- ► Convenient online submission
- ► Rigorous peer review
- ► Open access: articles freely available online
- ► High visibility within the field
- ► Retaining the copyright to your article

Submit your next manuscript at ► springeropen.com

Received: 6 August 2018 | Revised: 17 October 2018 | Accepted: 26 October 2018

DOI: 10.1111/jcpe.13049

SUPPLEMENT ARTICLE

WILEY Journal of Clinical Periodontology

Cell therapy for orofacial bone regeneration: A systematic review and meta-analysis

Siddharth Shanbhag[1] | Salwa Suliman[1] | Nikolaos Pandis[2] | Andreas Stavropoulos[3] | Mariano Sanz[4] | Kamal Mustafa[1]

[1]Department of Clinical Dentistry, Center for Clinical Dental Research, University of Bergen, Bergen, Norway

[2]Department of Orthodontics and Dentofacial Orthopedics, University of Bern, Bern, Switzerland

[3]Department of Periodontology, Faculty of Odontology, Malmö University, Malmö, Sweden

[4]Section of Periodontology, Faculty of Odontology, University Complutense of Madrid, Madrid, Spain

Correspondence
Kamal Mustafa, Department of Clinical Dentistry – Tissue Engineering group, Faculty of Medicine, University of Bergen, Bergen, Norway.
Email: kamal.mustafa@uib.no

Funding information
This review was supported by funding from Helse Vest, Norway (project number: 912048 K.M.), and the Bergen Stem Cell Consortium (project number: 502027, K.M.)

Abstract

Aim: The objective of the present review was to answer the focused question: what is the effect of cell therapy in terms of orofacial bone regeneration compared to grafting with only biomaterial scaffolds and/or autogenous bone?

Methods: Electronic databases were searched for relevant controlled clinical and pre-clinical (large-animal) studies. Separate meta-analyses of quantitative data regarding histological or radiographic new bone formation were performed.

Results: Forty-seven eligible clinical and 57 pre-clinical studies were included. Clinical studies were categorized based on the use of "minimally manipulated" whole tissues (e.g., bone marrow) or ex vivo expanded cells from "uncommitted" (bone marrow, adipose tissue) or "committed" sources (periosteum, bone). Based on limited and heterogeneous clinical evidence, implantation of cells (mostly whole bone marrow), in combination with biomaterial scaffolds results in bone regeneration which is (a) superior compared to implantation of scaffolds alone in sinus and horizontal ridge augmentation, and (b) comparable to autogenous bone in alveolar cleft repair.

Conclusions: Although current evidence points to the benefits of cell therapy in certain clinical indications, it is unclear whether the use of ex vivo expanded cells, either uncommitted or committed, is superior to whole tissue fractions in terms of bone regeneration. The relatively larger effect sizes in favour of cell therapy observed in pre-clinical studies are diminished in clinical trials. Future controlled studies should include cost-effectiveness analyses to guide clinical decision-making.

KEYWORDS
bone grafting, bone tissue engineering, cell therapy, mesenchymal stem cells, meta-analysis, systematic review

1 | INTRODUCTION

Reconstruction of oral and maxillofacial bone deficiencies is often a clinical challenge. Ridge remodelling following tooth loss is the most common cause for alveolar bone deficiencies in the horizontal and/or vertical dimensions (Chiapasco & Casentini, 2018; Rocchietta, Ferrantino, & Simion, 2018), and in the posterior edentulous maxilla, this is further complicated by pneumatization of the maxillary sinus(es) (Corbella, Weinstein, Francetti, Taschieri, & Del Fabbro, 2017; Danesh-Sani, Engebretson, & Janal, 2017). More challenging segmental defects, which include the inferior mandibular border, often result from trauma, tumour resection, or radiation-related osteonecrosis (Chanchareonsook, Junker, Jongpaiboonkit, & Jansen, 2014). Further, congenital anomalies are frequently associated with alveolar defects such as orofacial clefts involving the maxilla (Janssen, Weijs, Koole, Rosenberg, & Meijer, 2014).

Several regenerative surgical approaches have been proposed to prevent and/or reconstruct alveolar defects, most commonly,

 © 2019 John Wiley & Sons A/S. Published by John Wiley & Sons Ltd

alveolar ridge/socket preservation (SP) following dental extraction (Avila-Ortiz et al., 2016), vertical and horizontal ridge augmentation (RA) (Daugela, Cicciu, & Saulacic, 2016; Elnayef et al., 2017, 2018), maxillary sinus-floor augmentation (SA) (Danesh-Sani et al., 2017), and alveolar cleft (AC) repair in the palatal aspect of the maxilla (Wu et al., 2017). All of these techniques mainly involve the use of autogenous bone (AB) grafts and/or bone substitute materials, and often in combination with barrier membranes, that is the guided bone regeneration (GBR) principle (Elgali, Omar, Dahlin, & Thomsen, 2017); in the case of more advanced (e.g., segmental) defects, vascularized tissue flaps are used (Hayden, Mullin, & Patel, 2012). Although AB transplantation is still considered the gold standard, larger defects may require volumes of bone locally unavailable, leading to the need for harvesting from a second surgical site, usually involving general anaesthesia, hospitalization and significantly increased costs (Dahlin & Johansson, 2011). Thus, the morbidity associated with invasive AB harvesting and flap transfer, especially from a remote donor site, along with its unpredictable resorption rate, are major limiting factors (Nkenke & Neukam, 2014; Shanbhag, Shanbhag, & Stavropoulos, 2014). Alternatives have included a range of allogeneic, xenogeneic and alloplastic AB substitutes, but no consensus currently exists on the effectiveness of one material over the other, in comparison with AB, or for specific clinical indications (Al-Nawas & Schiegnitz, 2014; Milinkovic & Cordaro, 2014; Sanz-Sánchez, Ortiz-Vigón, Sanz-Martín, Figuero, & Sanz, 2015).

Adult or postnatal stem cells represent promising candidates for regenerative therapy, since they have the potential to replicate in an undifferentiated state as well as to differentiate along committed lineages. Although adult stem cells are utilised in the clinic since many decades as haematopoietic stem cell (HSC) therapy through bone marrow transplantation (Mohty, Richardson, McCarthy, & Attal, 2015), more recently, a multipotent population of mesenchymal stromal or "stem" cells (MSCs) was identified in the non-haematopoietic fraction of bone marrow (Friedenstein, Chailakhjan, & Lalykina, 1970). These MSCs have been defined by various characteristics, such as plastic adherence, self-renewal or colony forming unit (CFU)-potential, stromal phenotype and surface marker expression ($CD73^+CD90^+CD105^+CD34^-CD45^-HLA\text{-}DR^-$), and the ability to differentiate into at least three stromal lineages, that is bone, fat and cartilage (Dominici et al., 2006). In addition to their differentiation capacity, MSCs also exert paracrine or trophic effects, via secretion of soluble bioactive molecules, which "empower" host progenitor cells and modulate immune cells (and thereby the immune response), to promote regeneration (Wang, Chen, Cao, & Shi, 2014). In fact, recent observations point to trophic activity as the primary mechanism of MSC-mediated regeneration, rather than direct differentiation (Caplan, 2017; Haumer et al., 2018).

In this context, tissue engineering aims to combine and deliver the cellular (progenitor cells), extracellular (scaffolds) and/or molecular elements (growth factors) involved in physiological regenerative processes, for therapeutic applications. Specifically, regarding bone tissue engineering (BTE), this usually involves harvesting osteogenic cells from an autologous source (e.g., bone marrow, adipose tissue), their "chair-side" manipulation or ex vivo amplification, and combination with an appropriate biomaterial scaffold for in vivo implantation (Evans et al., 2007; Oryan, Kamali, Moshiri, & Baghaban Eslaminejad, 2017). Thus, the "triad" of *osteogenic* cells, *osteoinductive* signals (growth factors released by cells), and *osteoconductive* scaffolds, aims to replicate the properties of AB, and alleviate the need for invasive harvesting (Oppenheimer, Mesa, & Buchman, 2012). The cells can be harvested by minimally, and relatively less, invasive techniques (compared to AB harvesting) from various tissues, most commonly bone marrow and adipose tissues, under local anaesthesia, and without the need for hospitalization. Thus, BTE strategies are indeed emerging as promising alternatives to AB and/or biomaterial-based grafting, as demonstrated by several pre-clinical and some clinical studies (for reviews, see Janssen et al., 2014; Padial-Molina et al., 2015; Shanbhag et al., 2015; Shanbhag, Pandis, Mustafa, Nyengaard, & Stavropoulos, 2016, 2018; Miguita, Mantesso, Pannuti, & Deboni, 2017). Among these BTE strategies, three main interventions using cell therapies have been tested: (a) use of "minimally manipulated" whole tissue fractions; (b) use of more-than-minimally manipulated or ex vivo expanded *uncommitted* stem/progenitor cells; and (c) use of ex vivo expanded *committed* bone-derived cells.

Minimally manipulated whole tissue fractions have mainly included bone marrow aspirates—either whole (BMA) or concentrated (BMAC), adipose stromal vascular fraction (A-SVF), and tissue "micrografts." The rationale for using whole tissue fractions are (a) feasibility of a chair-side protocol, (b) minimum cell manipulation, (c) cost-effectiveness, and (d) delivery of a heterogeneous cell population. In addition to minimizing the time and costs associated with clinical-grade cell culture—which requires expensive Good Manufacturing Practice (GMP)–grade facilities, this approach generates a population of cells that is not comprised solely of MSCs, but also includes a number of other cell types with therapeutic potential, including HSCs, endothelial cells (ECs), and immune cells (monocytes, macrophages, etc.) (Fraser et al., 2014). This preserves the physiological microenvironment or "niche," with all cells in their natural ratios, including those which produce paracrine signals to induce host osteoprogenitors and MSCs (Jager et al., 2011).

Clinical relevance

Scientific rationale for study: Although cell therapy has shown the potential to enhance bone regeneration, there are several aspects regarding the source(s) of cells, their manipulation, mode of application, as well as the cost-benefit that need further elaboration.*Principal findings:* Cell therapy may enhance alveolar bone regeneration in specific clinical indications.*Practical implications:* Further clinical trials are needed before cell therapy can become a routine clinical procedure.

Bone marrow is known to contain a heterogeneous population of progenitor cells (including MSCs, HSCs, and endothelial progenitor cells), and supporting growth factors and cytokines (Chahla et al., 2016; Patterson et al., 2017). Concentration of the mononuclear cell fraction (MNC) of bone marrow (which includes MSCs) via density gradient centrifugation steps to remove red blood cells, granulocytes, immature myeloid precursors, and platelets, represents an attractive clinical strategy, since it is currently FDA-approved and shown to be efficacious as a point-of-care method of autologous cell delivery (Chahla et al., 2017; Jager et al., 2011). Moreover, since self-renewing, plastic-adherent MSCs represent only a small fraction (0.001%–0.01%) of MNC within the bone marrow, it may be hypothesized that a concentrate (BMAC) could increase the likelihood of attachment of these cells when loaded onto biomaterial scaffolds, and thereby ensure successful delivery to the defect site (El-Jawhari, Sanjurjo-Rodriguez, Jones, & Giannoudis, 2016).

An emerging and relatively less invasive alternative tissue source for minimally manipulated cell fractions is A-SVF, which, like bone marrow, contains a sub-population of adipose stem/stromal cells (ASCs) in addition to hematopoietic and ECs. Since the frequency of ASCs in A-SVF is reportedly much higher than that of BMSCs in BMA(C), the direct use of A-SVF, without culture-expansion, has been advocated (Fraser et al., 2014). However, although the use of minimally manipulated whole tissue fractions may be time- and cost-effective, the yield of progenitor cells obtained is relatively low. MSCs represent <1% of the MNC in BMA, and approximately 1.4% in A-SVF, based on CFU potential (Prins, Schulten, Ten Bruggenkate, Klein-Nulend, & Helder, 2016). This has encouraged ex vivo expansion strategies, which aim to exponentially increase the number of cells of a specific phenotype, that is *committed* or *uncommitted*, available for implantation, and thereby improve clinical outcomes (Petite et al., 2000).

The use of expanded *uncommitted* cells is based on the fact that MSCs, originally identified in bone marrow (BMSCs), are the most commonly reported cells in autologous regenerative therapies. MSCs have also been isolated from less invasive sources such as adipose tissue (ASCs), dental tissues and a range of adnexal gestational tissues, among others (Nancarrow-Lei, Mafi, Mafi, & Khan, 2017). Although MSCs from different tissue sources share biological characteristics, they have been reported to show functional differences in their properties, such as surface phenotype and differentiation potential (Al-Nbaheen et al., 2013). However, whether or not the tissue of origin regulates the epigenetics of MSCs and affects their subsequent in vivo differentiation potential remains to be determined in a comparative clinical study.

The use of expanded *committed* cells is based on obtaining as tissue source the alveolar bone itself—specifically, the periosteum and cancellous bone/marrow. The periosteum has been described as an osteoprogenitor cell-containing bone envelope with high regenerative potential (Hutmacher & Sittinger, 2003), while marrow-resident osteoblasts (OBs) are the fundamental cells of bone tissue involved in its formation, function, repair, and maintenance (Jayakumar & Di Silvio, 2010). Although multipotent MSC-like cells have been identified in both periosteum (Olbrich, Rieger, Reinert, & Alexander, 2012) and alveolar bone (Mason, Tarle, Osibin, Kinfu, & Kaigler, 2014), for the purpose of this review, cells obtained from these tissues were considered to be more osteogenically "committed" than those from other tissues (Akintoye et al., 2006; Pettersson, Kingham, Wiberg, & Kelk, 2017).

It was therefore the primary objective of the present review to systematically assess the literature to answer the focused question: in clinical studies, what is the effect of cell therapy in terms of orofacial bone regeneration compared to grafting with only biomaterial scaffolds and/or AB? Secondary objectives were (a) to assess the preclinical to clinical translation of cell therapy by comparing preclinical and clinical data, and (b) to determine which is the most suitable cell therapy approach for regenerating bone deficiencies.

2 | MATERIALS AND METHODS

Following Cochrane (Higgins & Green, 2011) and Preferred Reporting Items for Systematic Reviews guidelines (Moher, Liberati, Tetzlaff, & Altman, 2009), an electronic literature search based on pre-defined inclusion criteria was performed in 3 repositories (PubMed, Embase and Cochrane library) up to May 2018 (Figure 1). Sampling of the clinical evidence was focused on controlled trials—either randomized (RCT) or non-randomized (CT). Uncontrolled studies (UT) and cases reports (with ≥3 patients) of cell-based BTE were also identified to capture possible relevant information regarding cell sources, delivery strategies, and adverse events, although data regarding bone regeneration from these studies were not considered for the meta-analyses. Sampling of pre-clinical data was limited to large-animal models and regards mainly an update of our previously published reviews (Shanbhag et al., 2016, 2018). These data were only included to compare with the clinical data, which is the focus of the present review. Quantitative data regarding histomorphometric or radiographic bone regeneration was included in meta-analyses. Separate analyses were performed for clinical (grouped by indication/defect-type and method of outcome evaluation) and pre-clinical studies (grouped by species and defect-type). Details of the review methodology are reported in the Appendix.

3 | RESULTS

3.1 | Summary of included studies

After screening, 47 controlled clinical studies were included, of which 22 were RCTs, mostly with a low to unclear risk of bias (Supporting Information Figure S8). Additionally, 30 UT and case series were identified (Supporting Information Tables S1–S3). A majority of the evidence was derived from studies of SA and horizontal RA (30 controlled studies). Additionally, studies of SP, AC and cranial defect (CD) repair, and reconstruction following fracture, cystectomy or tumour resection, were identified (Table 1). Most studies included a "split-mouth" design, utilized a

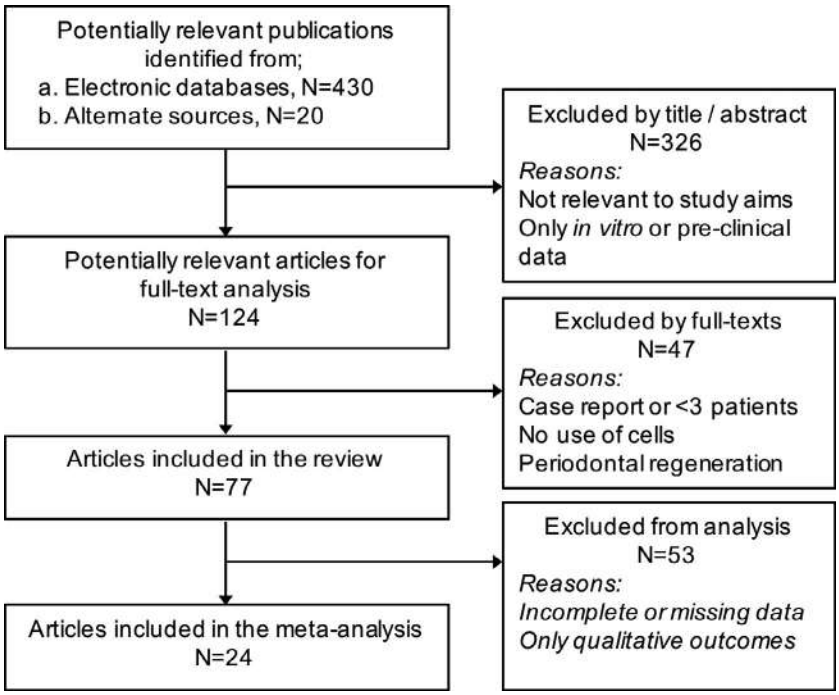

FIGURE 1 Flow chart for study inclusion (n = number of articles)

TABLE 1 Distribution of included clinical studies according to indications

Indication	Uncontrolled	Controlled
SA	7	25
RA	4	6
SA and/or RA (in the same patients or in different patients in the same study)	10	–
Ridge/SP	–	5
AC	3	7
CD	3	–
Other (fracture, cyst, tumour resection)	3	4
Total	30	47

SA: sinus augmentation; RA: ridge augmentation; SP: socket preservation; AC: alveolar cleft; CD: cranial defect.

GBR approach for augmentation, that is a membrane to cover the cell-scaffold construct, and reported the placement of implants in regenerated sites. Outcomes were assessed via in situ clinical examination and/or radiography [computed tomography (CT) or cone-beam CT (CBCT)], or via histological and/or micro-CT (μ-CT) assessments of biopsy specimens. The primary outcome measure was quantitative assessments of new bone formation (NBF) via histomorphometry or μ-CT of biopsies, or in situ CT-based assessments of "bone fill" (BF) within the treated defects.

Scaffolds used (xenogeneic and alloplastic) to deliver cells to the regeneration sites were: (a) *ceramic* scaffolds, such as deproteinized bovine bone mineral (DBBM), hydroxyl-apatite (HA), beta-tricalcium phosphate (β-TCP), biphasic HA/β-TCP (BCP) and freeze-dried bone allograft (FDBA); (b) *polymeric* scaffolds, such as collagen (COL) or gelatin sponges, platelet-rich/poor plasma (PRP/PPP) or fibrin (PRF), and polylactic–polyglycolic acid copolymer (PLGA); or (c) *composite* scaffolds, including various combinations of the above (Lee, Cuddihy, & Kotov, 2008).

Cell therapy approaches were categorized according to US Food and Drug Administration (FDA) guidelines on the use of Human Cells, Tissues, and cellular and tissue-based Products (HCT/P; Code of Federal Regulation Title 21-CFR-1271) and the European Medicines Agency (EMA) guidelines on the use Advanced Therapy Medicinal Products (ATMP; European Regulation 1394/2007), as: (1) "minimally manipulated" whole tissue fractions, usually involving a point-of-care or chair-side procedure, or (2) "more-than-minimally manipulated", that is ex vivo culture-expanded cells, further categorized (for the purpose of this review) as (a) uncommitted stem/progenitor cells, and (b) committed bone-derived cells (Supporting Information Figure S1). Summaries of the included clinical studies in each category are presented in Tables 2–4.

TABLE 2 Summary of controlled studies using whole tissue fractions

Study (design)	Site	Patients (sex, age)	Cell therapy group		Control group	Follow-up	Method	Outcome
			Cell source (culture)	Scaffold				
BMA or BMAC (n = 19)								
Wojtowicz et al., 2003; Wojtowicz, Chaberek, Urbanowska, & Ostrowski, 2007 (CC)	Cyst—max or man (15–21 mm)	17 (17M, 27–44 y)	Iliac BMA (*whole*, 1.4 ± 0.1 x10^8 MNC + 0.9 ± 0.1 × 10^6 CD34 + cells/transplant) *or* BMA (*Ficoll*, 0.6 ± 0.1 × 10^8 MNC + 1.9 ± 0.2 × 10^6 CD34 + cells/transplant)	DBBM (Bio-Oss®) + PRF/Col mem	PRP + DBBM + PRF/Col mem	3 m	Radio	PRP > BMA
Gimbel et al., 2007 (CC)	AC—uni	69 (6–12 y)	Iliac BMA (40 ml, passed through heparinized column)	Col sponge (Healos®)	Iliac AB (conventional *or* minimal invasive)	6w, 6 m, 2y	Clinical Patient-reported	+ (pain, cost T<C)
Sauerbier et al., 2010 (CT); *Duttenhoefer* et al., *2014*	SA (<3 mm) —uni/bi	11 (47–69 y)	Iliac BMAC (Harvest®, 3 ml)	DBBM (Bio-Oss®)	*BMA (Ficoll)* + DBBM	3 m 2.5 y	Histo IS	NS NS
Sauerbier et al., 2011 (RCT)	SA (<3 mm) —uni/bi	26 (38–68 y)	Iliac BMAC (Harvest®, 3 ml)	DBBM (Bio-Oss®)	DBBM + Man AB (70:30)	3–4 m	Histo	NS
Rickert et al., 2011 (RCT); *Rickert* et al., *2014*	SA (<4 mm) —bi	12 (48–69 y)	Iliac BMAC (Harvest®, 3 ml)	DBBM (Bio-Oss®)	DBBM + Man AB (70:30)	13–16 w 12 m	Histo IS	*S* C>T
Wildburger et al., 2014 (RCT), *Kuhl* et al., *2014*	SA (<3 mm) —bi	7 (47–72 y)	Iliac BMAC (Harvest®, 3 ml)	DBBM (Bio-Oss®)	DBBM only	3, 6 m 0.5, 6 m	Histo CT (V)	NS NS
Payer et al., 2014 (RCT), *Kuhl* et al., *2014*	SA (<3 mm) —bi	6 (3M, 43–70 y)	Tibial BMA (8 ml)	DBBM (Bio-Oss®)	DBBM only	3, 6 m 0.5, 6 m	Histo CT (V)	NS NS
Sununliganon (2013) (RCT)	SA (<5 mm) —uni/bi ± impl	4 (bi, 2F, 30–71 y); 9 (uni, 6M, 23–72 y)	Iliac BMAC (MarrowStim®, 3 ml)	BBM (Endobon®)	BBM only *or* Iliac AB	7 m 3, 6 m, 1, 2y	Histo (qual) µCT (BV/TV%)	NS NS
Bertolai et al., 2015 (RCT)	SA (<5 mm) —bi	20 (10M, 55.2 y)	Iliac BMAC (Regen®, 14–15 ml)	FDBA + PRP	FDBA only	3 m	Histo (qual)	T>C
Pasquali et al., 2015 (RCT)	SA (<4 mm) —bi	8 (~55y)	Iliac BMAC (Harvest®, 4 ml)	DBBM (Bio-Oss®)	DBBM only	6 m	Histo	*S*
De Oliveira et al., 2016 (RCT)	SA (<4 mm) —uni/bi	15 (12F, ~55y)	Iliac BMA—single *or* double centrifugation	DBBM (Bio-Oss®)	DBBM only	6 m	Histo	NS
Pelegrine, da Costa, Correa, & Marques, 2010 (RCT)	SP	13 (7M, 28–70 y)	Iliac BMA (4–5 ml)	None	Empty (clot)	6 m	Histo	NS
Da Costa, Pelegrine, Fagundes, Simoes Mde, & Taha, 2011 (RCT)	RA—ant max (hor; <5 mm)	10 (8F, 40–55 y)	Iliac BMAC (Harvest® 4 ml)	Allograft block	Allograft only	6 m	Histo	*S*
Pelegrine et al., 2016 (RCT)	RA—ant max (hor; <3 mm)	8 (~52y)	Iliac BMAC (Harvest® 4 ml)	EBM (Bio-Gen®)	EBM only	4 m 4, 8 m	Histo CBCT (BG)	NS

(Continues)

TABLE 2 (Continued)

Study (design)	Site	Patients (sex, age)	Cell therapy group		Control group	Follow-up	Method	Outcome
			Cell source (culture)	Scaffold				
Lavareda Correa et al., 2017 (RCT)	RA—ant max (hor; 2–4 mm)	10 (8F, 36–52 y)	Iliac BMAC (Harvest® 4 ml)	Allograft block + granules	Allograft only	6 m	Histo CBCT (BV, BD)	NS NS
Marx & Harrell, 2014 (RCT)	RA—man SD (6–8 cm)	40 (22M, 19–78 y)	Iliac BMA (10 ml; 15.5 × 10^6/ml TNC + 54 ± 38/ml CD34 +) *or* BMAC (Harvest® 10 ml; 98 × 10^6/ml TNC + 1000 ± 750/mL CD34 + cells)	Allograft + rhBMP-2/Col sponge	*BMA* + scaffold	6 m	Histo CT	*S* *S*
Talaat, Ghoneim, Salah, & Adly, 2018 (RCT)	Cyst—mand	20 (13M, 18–50 y)	Iliac BMAC (Harvest® 6–9 ml)	PRP + Col sponge	Empty defects	3, 6, 12 m	Panoramic	*S*
Du et al., 2017 (CT)	AC—uni	20 (12F, 8–28 y)	Iliac BMAC (TBD® 1 ml)	β-TCP (Bio-lu®)	Iliac AB	6, 12 m	CT (BV/TV%)	NS
Al-Ahmady et al., 2018 (RCT)	AC—uni	20 (12F, 8–18 y)	Iliac BMA (*Ficoll* 2 ml)	Col sponge-nHA + PRF	Iliac AB	6, 12 m	CBCT (grade)	T>C
Adipose SVF (n = 1)								
Prins et al., 2016 (CT); *Farre-Guasch* et al., *2018*	SA (4–8 mm) —uni/bi	10 (6F, 46–69 y)	Abdominal SVF (Celution®, 5 ml cell susp., mixed pop., 83% CD90 + , 67% CD34 +), 2 × 10^7 cells/2 g scaffold/SA (1.4 × 10^5 CFU-F/g)	β-TCP (Ceros®) or BCP (Bone Ceramic®)	β-TCP *or* BCP only	6 m 6 m 2.5y	Histo μCT IHC (CD34, SMA) IS	NS *S* NS 100%
Micrografts (n = 4)								
d'Aquino et al., 2009 (CT); *Giuliani* et al., *2013*	SP—bi	7	Dental pulp-derived (Rigenera®)	Col sponge (Gingistat®)	Col sponge only	3 m 36 m	Histo (qual) Histo	T>C *S*
Monti et al., (2016) (CT)	SP—bi	6 (4F, 22–60 y)	Dental pulp-derived (Rigenera®)		Col sponge only	45–70 days	Histo (qual)	T>C
D'Aquino et al. (2016) (CT)	SP (multi-rooted) —bi	35 (21F, 25–64 y)	Max periosteum-derived (Rigenera®)	Col sponge (Gingistat®)	Col sponge only	45–90 days	Clinical Histo (qual)	*S* T>C
Rodriguez et al. (2017) (CT)	SA—uni	24 (12F, 45–64 y)	Max periosteum-derived (Rigenera®)	PLGA/HA	PLGA/HA *or* DBBM (Bio-Oss®)	4 m	Histo	*S*

CT: controlled trial; RCT: randomized CT; CC: case–control; SA: sinus augmentation; RA: ridge augmentation/GBR; SP: socket preservation; AC: alveolar cleft; SD: segmental or continuity defects; CD: cranial defect; ORN: osteoradionecrosis; uni: unilateral; bi: bilateral; imp: simultaneous implant placement; man: mandible; max: maxilla; hor: horizontal; M: male; F: female; y: years; m: months; w: weeks; Histo: histomorphometry; Histo (qual): qualitative histology; IHC: immunohistochemistry; Radio: radiographic; CT: computed tomography; V: volume; μCT; micro-CT; BV/TV: bone volume/total volume; BG: bone gain; T: test group; C: control group; Comp: complications; IS: implant survival; +: favourable bone regeneration outcomes; BMA: bone marrow aspirate; BMAC: bone marrow aspirate concentrate; AB: autogenous bone; HA: hydroxyl-apatite; β-TCP: beta-tricalcium phosphate; BCP: biphasic calcium phosphate; BAG: bioactive glass; GAG: glycosaminoglycans; Col: collagen; DBBM: demineralized bovine bone mineral; ABB: anorganic bovine bone; Pep: PepGen; PRP: platelet-rich plasma; PRF: platelet-rich fibrin; rhBMP-2: recombinant human bone morphogenetic protein-2; FD: freeze-dried; PLA: polylactide; PLGA: polylactic-co-glycolic acid; *study/year in italics*: follow-up study reporting on the same patient sample; *S*: statistically significant differences between T and C groups; NS: no statistically significant differences between T and C groups.

Fifty-seven eligible pre-clinical in vivo studies in large-animal models [dogs, minipigs and small-ruminants (sheep and goats)] were also identified (Supporting Information Tables S4–S6). These studies represented SA, RA [in the form of critical size defects (CSD)], and AC models. The following section is focused on results of the meta-analyses. Details of the included clinical studies, along with relevant supporting literature, are presented in the discussion.

3.2 | Meta-analyses: Effect sizes of cell therapy

The clinical evidence is mostly based on randomized (SA, RA) and non-randomized controlled trials (AC repair). Twenty-six studies reporting quantitative outcomes of bone regeneration based on histomorphometry (NBF), μ-CT [regenerated bone volume/total volume (BV/TV)] or CT (BF) were included in separate meta-analyses. Pooled estimates of treatment effect [effect sizes (ES)] were calculated for the outcomes NBF, BV/TV and BF in SA/RA, SA and AC repair, respectively. For SA studies, sub-group analyses were performed according to the time of biopsy, that is at 3–4 months or 6 months after augmentation. Additionally, regression analyses were performed to evaluate the effect of time (</≥6 months) and types of cells used (whole tissue, uncommitted or committed) on bone regeneration. Overall, the clinical meta-analyses revealed:

a). in SA, significantly greater bone regeneration was observed after cell therapy in 1 meta-analysis of histomorphometric results (ES: 4.12% NBF, 6 studies, vs. scaffolds, 6 months) and in 1 meta-analysis of μ-CT results (ES: 4.76% BV/TV, 3 studies, vs. scaffolds, 4–7 months), while in 1 meta-analysis of histomorphometric results no benefit was observed (12 studies, vs. scaffolds, 3–4 months). Based on a meta-regression analysis of histomorphometric data from 15 studies, there were no differences between the various cell therapy strategies, that is whole tissues vs. expanded uncommitted cells vs. expanded committed cells, in terms of the amount of bone regeneration (Supporting Information Table S7).
b). in horizontal RA, significantly greater bone regeneration was observed after cell therapy in 1 meta-analysis of histomorphometric results (ES: 13.42% NBF, 3 studies, vs. scaffolds; 1 study, vs. scaffold + AB, 4–6 months).
c). in AC defects, 1 meta-analysis failed to show a benefit of cell therapy over AB, as evaluated with CT (3 studies, 6 months).

Overall, the clinical meta-analyses revealed moderate to high heterogeneity (I^2 70%–99%), and wide predictive intervals, often crossing the line of no effect (Table 5, Supporting Information Figures S2–S4).

A meta-analysis of 57 eligible preclinical studies was also performed to compare the preclinical and clinical evidence for cell therapy and thereby assess its translation. To allow comparison with clinical data, similar pooled estimates (ES) were calculated for histomorphometric NBF. Sub-group analyses according to species and observation times were performed; analysis according to cell types (whole tissue, uncommitted or committed) could not be performed due to insufficient numbers of studies/comparisons in each sub-group. Overall, the pre-clinical meta-analyses revealed:

a). in SA models, significantly greater bone regeneration was observed after cell therapy in dogs (ES: 10.21% NBF, 5 studies, vs. scaffolds, <6 months) and small-ruminants (ES: 11.11% NBF, 3 studies, vs. AB, 2–4 months).
b). in CSD models, significantly greater bone regeneration was observed after cell therapy in dogs (ES: 12.14/20.11% NBF, 12 studies, vs. scaffolds, 1–2/2–4 months and ES: 48.73%, 3 studies, vs. scaffolds, 12 months), pigs (ES: 14.84% NBF, 4 studies, vs. scaffolds, 2–3 months) and small-ruminants (25.78% NBF, 3 studies, vs. scaffolds, 3–5 months).
c). in AC defect models, no significant benefit of cell therapy over AB was observed in dogs (3 studies, 2–5 months).

Similar to clinical studies, the pre-clinical meta-analyses also revealed moderate to high heterogeneity (I^2 60%–99%) with wide predictive intervals (Table 5, Supporting Information Figures S5–S7). However, for all comparisons, larger ES were observed in the pre-clinical vs. clinical meta-analyses.

4 | DISCUSSION

The primary objective of the present review was to assess the current clinical evidence on the effectiveness of cell therapy for orofacial bone regeneration, compared to grafting with only biomaterial scaffolds and/or AB. Based on limited data from 26 (of 47 included) controlled studies, implantation of cells in combination with scaffolds seems to be (a) superior to implantation of scaffolds alone in SA (based on histological and μ-CT outcomes) and horizontal RA (based on histological outcomes), and (b) comparable to AB grafts in AC repair (based on CT outcomes). Although the meta-analyses revealed statistically significant outcomes for these comparisons, heterogeneity in the studies was high as evidenced by the wide prediction intervals (Table 5). While the current available evidence is insufficient to determine the best strategy in terms of cell–types and –sources (whole tissue, uncommitted or committed), a discussion around this topic seems to be clinically important and is presented herein.

4.1 | Use of minimally manipulated whole tissue fractions

A majority of included studies reported the use of minimally manipulated whole tissue fractions, particularly bone marrow—as either whole (BMA) or concentrated (BMAC) aspirates (Table 2, Supploring Information Table S1). In several studies, significantly greater NBF was observed when using autologous BMAC-loaded vs. cell-free scaffolds (most commonly DBBM) in SA and RA. While a majority of studies reported harvesting from the iliac crest, one study each reported harvesting from the femur (Ibanez, Agustina, Ibanez, & Ibanez, 2012) and tibia (Payer et al., 2014). Regarding the

TABLE 3 Summary of controlled studies using "uncommitted" culture-expanded cells

Study (design)	Site	Patients (sex, age)	Cell therapy group			Control group	Follow-up	Method	Outcome
			Cell source (culture)	Cell number	Scaffold				
BMSCs (n = 5)									
Hernandez Alfero et al. (2005) (RCT)	SA (3–13 mm) —bilat	5 (5F, 37–75 y)	Replicell® or Ixymyelocel-t® Iliac "TRCs" (IMDM + 10% FBS + 10% HS, 12–14 days)	7–20 × 10^7 cells/SA	DBBM (Bio-Oss®) + PPF	DBBM+ PPF	4 m	Histo CT	NS
Kaigler et al. (2015) (RCT)	SA (2–6.2 mm) —unilat	26 (10F, 26–66 y)	Replicell® or Ixymyelocel-t® Iliac "TRCs"	1.6–15 × 10^7 cells/SA	β-TCP (Cerasorb®)	β-TCP only	4 m	Histo µCT	*Unclear* NS overall
Kaigler et al. (2013) (RCT)	SP—unilat	24 (13F, 31–63 y)	Replicell® or Ixymyelocel-t® Iliac "TRCs"	1.5 × 10^7 cells/SP	Gelatin sponge (Gelfoam®)	Gelatin sponge only	6, 12 w	Histo µCT	NS *S 6w*, NS 12w
Bajestan et al. (2017) (RCT)	RA (hor; 2° to AC or trauma)	17 (12M, 18–54 y)	Replicell® or Ixymyelocel-t® Iliac "TRCs"	1.5–4.4 × 10^7 cells/cc (2–5 cc/pt)	β-TCP (Cerasorb®)	Man AB	4 m	Re-entry	NS Comp
Khalifa and Gomaa (2017) (CT)	AC	16 (7–12 y)	Iliac BMSCs (DMEM + 20% AS, pass. 3)	5 × 10^5 cells/scaffold	HA-Si (Nanobone®)	Man AB	3, 6 m	CT	*S*
ASCs (n = 5)									
Alekseeva, Kulakov et al. (2012) (CT)	SA (<5 mm) —uni/bilat	25 (29–60 y)	Abdominal ASCs (DMEM/F12 + 10% AS, osteo+ 7d)	5–7 × 10^6 cells/cm^3 scaffold	HA-Col/GAG + PRP	DBBM (Bio-Oss®) + PRP	4–6 m	Histo CBCT	T>C
Khojasteh and Sadeghi (2016) (CC)	RA—max/man (hor)	8 (5M, 25–60 y)	Buccal fat pad ASCs (DMEM + 10% AS, pass. 3–4)	10^6 cells/scaffold	Iliac AB + FDBA granules	Iliac AB + FDBA only	5 m	Histo CBCT	T>C NS
Khojasteh et al. (2017) (CT)	AC—uni	10 (3F, 8–14 y + 4 adults)	Buccal fat pad ASCs (DMEM + 10% AS, pass. 3–4)	10^6 cells/scaffold	Man AB + BBM (Cerabone®) *or* Iliac AB + BBM, + Col mem	Iliac AB + Col mem	6 m	CBCT Histo (n=2)	NS
Soliman, Ismail, Shouman, Bahaaeldin, and El-Hadidy (2018) (CC)	AC—uni/bi	24 (15M, 7–27 y)	Abdominal ASCs (DMEM + 10%–13% FBS)	3 × 10^6 cells/ml	Allograft *or* iliac AB	Iliac AB only	6 m	Radio	NS
Castillo-Cardiel et al. (2017) (RCT)	Man condyle fractures	20 (~29–31 y)	Abdominal ASCs (DMEM + 10% FBS, 24 h)	NR	Open reduction	Open reduction	4, 12 w	CT (BD)	*S*

CT: controlled trial; RCT: randomized CT; CC: case–control; SA: sinus augmentation; RA: ridge augmentation/GBR; SP: socket preservation; AC: alveolar cleft; SD: segmental or continuity defects; CD: cranial defect; ORN: osteoradionecrosis; uni: unilateral; bi: bilateral; imp: simultaneous implant placement; man: mandible; max: maxilla; hor: horizontal; M: male; F: female; y: years; m: months; w: weeks; Histo: histomorphometry; Histo (qual): qualitative histology; IHC: immunohistochemistry; Radio: radiographic; CT: computed tomography; µCT; micro-CT; V: volume; BV/TV: bone volume/total volume; BG: bone gain; T: test group; C: control group; Comp: complications; IS: implant survival; +: favourable bone regeneration outcomes; BMSC: bone marrow MSC; ASC: adipose tissue-derived MSC; TRCs: tissue repair cells; FBS: foetal bovine serum; HS: horse serum; AS: autologous serum; osteo+: osteogenic induction; pass.: passage; AB: autogenous bone; HA: hydroxyl-apatite; Si: silica; β-TCP: beta-tricalcium phosphate; BCP: biphasic calcium phosphate; BAG: bioactive glass; GAG: glycosaminoglycans; Col: collagen; DBBM: demineralized bovine bone mineral; ABB: anorganic bovine bone; Pep: PepGen; PRP: platelet-rich plasma; PRF: platelet-rich fibrin; *S*: statistically significant differences between T and C groups; NS: no statistically significant differences between T and C groups.

TABLE 4 Summary of controlled studies using "committed" culture-expanded cells

Study (design)	Site	Patients (sex, age)	Cell therapy group			Control group	Follow-up	Method	Outcome
			Cell source (culture)	Cell number	Scaffold				
POCs (n = 6)									
Springer et al. (2006) (CC)	SA—uni/bilat	8 (4F, 43–65 y)	Man POCs (aMEM + 20% AS, osteo+, 21d)	6×10^6 cells/scaffold + 1 w culture	Col fleece (Lyostypt®)	DBBM (Bio-Oss®)	6–8 m	Histo (qual) Radio	*S*
Zizelmann et al. (2007) (CT)	SA (<5 mm) —uni/bilat ± impl	20	Man POCs (Bioseed-Oralbone®, DMEM/F12 + 10% AS, pass. 3–4, osteo+, 6w, +fibrinogen)	1.5×10^6 cells/disc + 6–9 days culture	PLGA (Ethisorb®) discs	Iliac AB	3 m	CT (V-loss%)	T 90%, C 29%
Voss et al. (2010) (CC)	SA (class 4,5) —uni/bilat ± impl	35 (21F, 35–69 y) (41C pts 38–73 y)	Man POCs (Bioseed-Oralbone®)	1.5×10^6 cells/disc + 6–9 days culture	PLGA (Ethisorb®) discs	Iliac AB	15 w	Histo (qual)	Comp T > C
Mangano et al. (2009) (CT)	SA (2–10 mm) —bilat	5 (3F, 45–64 y)	Man POCs (Bioseed-Oralbone®)	1.5×10^6 cells/disc + 6–9 days culture	PLGA (Ethisorb®) discs	CaP (Coral)	6 m	Histo CT (BD)	C > T C > T
Nagata et al. (2012) (CC)	SA (<2 mm) —uni/bi (n = 15) or RA (hor + ver; n = 14)	25[a] (+15C pts) (13F, 18–76 y)	Man POC sheet (M199 + 10% FBS + AA, 6w)	NR	Man AB + PRP	Man AB + PRP	4 m 3, 12 m	IHC CT (V)	*S* NS
Ogawa et al. (2016) (CC)	SA (<2 mm) —uni/bilat	23[a] (+15C pts) (10M, 40–70 y)	Man POC sheet	NR	Man AB + PRP	Man AB + PRP	4, 12 m	CT (V%)	NS
OBs (n = 6)									
Pradel et al. (2006) (CC)	Man cysts	8 (7M, 8–16 y)	Max/man OBs (Exp, DMEM + 10% AS, osteo+, pass. 2, 8–12w)	5×10^5 cells/scaffold	DBBM (Osteovit®)	Iliac AB	3, 6, 12 m	Radio (BD)	NS
Pradel and Lauer (2012) (CC)	AC—uni/bi	20 (15M, 16–72 y)	Max/man OBs	5×10^5 cells/scaffold	DBBM (Osteovit®)	Iliac AB	6 m	CBCT (%fill)	T 40.9%, C 36.6%
Pradel, Mai, Manolo Hagedorn, Lauer, and Allegrini (2008) (CC)	SA (mod-sev) —uni/bi	6 (6F, 38–52 y)	Max/man OBs	5×10^5 cells/scaffold	DBBM (Osteovit®)	OBs + S-BBM (Tutobon®)	5 m	Histo (qual)	S-BBM>BBM
Gonshor et al. (2011) (RCT)	SA (<6 mm) —uni/bilat	18 (12F, 42–79 y)	Cellular allograft (Osteocel®)	$>5 \times 10^4$ cells/cm^3	Allograft	Allograft only	3–4 m	Histo	*S*
Springer et al. (2006) (CC)	SA—uni/bilat	5 (4F, 43–65 y)	Max tuberosity OBs (Exp, DMEM + 20% AS)	3.3×10^6 cells/cm^2 scaffold (+40 days cult)	DBBM (Bio-Oss®)	DBBM only	6–8 m	Histo (qual) Radio	*S*
Hermund, Stavropoulos, (2012), *Hermund et al., (2013)* (RCT)	SA (<3 mm)—uni	20 (11F, ~58–60 y)	Max tuberosity OBs (Exp, DMEM/F12 + 20% FBS + AA, 10% AS 1w, 1 m)	2×10^6 cells/ml	DBBM (Bio-Oss®) + Max AB (1:1)	DBBM + Max AB (1:1)	4 m	Histo *IS*	NS NS

CT: controlled trial; RCT: randomized CT; CC: case–control; SA: sinus augmentation; RA: ridge augmentation/GBR; SP: socket preservation; AC: alveolar cleft; SD: segmental or continuity defects; CD: cranial defect; ORN: osteoradionecrosis; uni: unilateral; bi: bilateral; imp: simultaneous implant placement; man: mandible; max: maxilla; hor: horizontal; ver: vertical; mod-sev: moderate-severe; M: male; F: female; y: years; m: months; w: weeks; Histo: histomorphometry; Histo (qual): qualitative histology; IHC: immunohistochemistry; Radio: radiographic; CT: computed tomography; V: volume; BD: bone density; T: test group; C: control group; Comp: complications; IS: implant survival; +: favourable bone regeneration outcomes; POCs: periosteal cells; OBs: osteoblasts; Exp: explant culture; FBS: foetal bovine serum; HS: horse serum; AS: autologous serum; osteo+: osteogenic induction; pass.: passage; AB: autogenous bone; HA: hydroxyl-apatite; Si: silica; β-TCP: beta-tricalcium phosphate; BCP: biphasic calcium phosphate; BAG: bioactive glass; GAG: glycosaminoglycans; Col: collagen; DBBM: demineralized bovine bone mineral; ABB: anorganic bovine bone; Pep: PepGen; PRP: platelet-rich plasma; PRF: platelet-rich fibrin; *S*: statistically significant differences between T and C groups; NS: no statistically significant differences between T and C groups; a: overlapping patient samples.

TABLE 5 Comparison of cell therapy effect sizes in preclinical and clinical meta-analyses

	Preclinical					Clinical				
	Category	*n*	ES	95% CI	PI	Category	*n*	ES	95% CI	PI
Sinus augmentation										
Dogs	vs. Scaffolds (<6 m)	5	10.21	4.00, 16.42	−12.17, 32.59	vs. Scaffolds (6 m)	6	4.12	0.25, 7.98	−7.42, 15.65
Sheep/goats	vs. AB (2–4 m)	3	11.11	5.33, 16.90	−13.37, 35.60	vs. Scaffolds[b] (4–7 m)	3	4.76	2.80, 6.71	0.47, 9.04
Pigs, sheep/goats	vs. Scaffolds (2–4 m)	2, 5	NS	–	–	vs. Scaffolds (3–4 m)	12	NS	–	–
Ridge augmentation (CSD[a])										
Dogs	vs. Scaffolds (1–2 m)	5	12.14	6.16, 18.11	−8.73, 33	vs. Scaffolds (4–6 m)	4	13.42	7.75, 19.09	−2.09, 28.93
Dogs	vs. Scaffolds (2–4 m)	9	20.11	11.65, 28.56	−15.17, 55.39					
Dogs	vs. Scaffolds (12 m)	3	48.73	43.87, 53.60	17.20, 80.26					
Pigs	vs. Scaffolds (2–3 m)	4	14.84	9.66, 20.01	−2.50, 32.19					
Sheep	vs. Scaffolds (3–5 m)	3	25.78	18.55, 33.01	−52.77, 104.32					
Dogs	vs. AB (12 m)	3	NS	–	–					
Alveolar cleft repair										
Dogs	vs. AB (2–5 m)	3	NS	–	–	vs. AB (6 m)	3	NS	–	–

Numbers indicate Effect Sizes (ES), 95% Confidence Intervals (CI) and estimated Prediction Intervals (PI); n: number of studies; NS: non-significant effects; AB: autogenous bone; m: months; CSD: critical size defects

[a]In preclinical studies; all comparisons are based on histomorphometric outcomes, except [b]Based on micro-CT.

morbidity associated with BMA harvesting, lower donor site morbidity and donor site pain-intensity and -frequency were reported in patients treated with BMA/scaffolds vs. iliac AB grafting for AC repair (Gimbel et al., 2007). In one RCT of mandibular segmental defect-repair (Marx & Harrell, 2014), significantly greater NBF was observed when using BMAC—containing a higher fraction of $CD34^+$ cells (1012 ± 752 cells/ml) compared to un-concentrated BMA (54 ± 38 cells/ml), although both groups had similar concentrations of $CD90^+CD105^+$ MSCs (15×10^6 cells/ml) and were delivered in combination with rhBMP-2-loaded COL and allograft scaffolds. Interestingly, the NBF was higher when BMAC (67% ± 13%), but not BMA (36% ± 10%), was added to the constructs compared to only rhBMP-2 (+PRP; 59% ± 12%) or AB (54% ± 10%), as reported by the group in a previous study (Marx, Armentano, Olavarria, & Samaniego, 2013). The authors highlighted an important complimentary role of $CD34^+$ HSCs in MSC-mediated bone regeneration, and the benefits of implanting heterogeneous cell populations at regeneration sites (Marx & Harrell, 2014).

One controlled trial (Prins et al., 2016) reported the application of autologous A-SVF for SA via enzymatic digestion of abdominal adipose tissues using a chair-side isolation system (Celution®, Cytori Therapeutics, San Diego, CA, USA). Significantly greater NBF was observed in six patients treated with A-SVF-loaded vs. cell-free β-TCP or BCP scaffolds after 6 months—most markedly in the "cranial" portion of the augmentation sites distant from the native residual ridge (Prins et al., 2016). Interestingly, subsequent immunohistochemical analyses of biopsy specimens also revealed a higher quantity and quality/maturity of blood vessels in the areas of active bone formation (Farre-Guasch et al., 2018). Similar results were observed in a phase I clinical study of orthopaedic fracture treatment with A-SVF (Saxer et al., 2016). Indeed, previous studies have demonstrated the angiogenic and vasculogenic potential of A-SVF, attributed to the

presence of ECs and perivascular cells (Jin, Chae, Son, & Kim, 2017; Zakhari, Zabonick, Gettler, & Williams, 2018). However, whether the in vivo bone-forming potential of A-SVF may be enhanced by prior osteogenic stimulation, remains to be clinically determined (Scherberich, Muller, Schafer, Banfi, & Martin, 2010). Nevertheless, the expected surge in clinical use of A-SVF may be hampered by recent US and European guidelines, which seek to classify A-SVF as "more-than-minimally manipulated" cells (Raposio & Ciliberti, 2017).

One research group has reported the use of a proprietary chairside mechanical tissue disaggregation system (Rigenera®, Human Brain Wave srl, Turin, Italy) to isolate cell fractions termed "autologous micrografts" from dental pulp (d'Aquino et al., 2009; Monti et al. 2016) and periosteal tissues (D'Aquino et al., 2016; Rodriguez et al., 2017). Significantly greater histological and/or radiographic bone regeneration was observed with dental pulp or periosteum micrograft-loaded versus cell-free scaffolds in SP and SA. The protocol involves simultaneous mechanical disaggregation (using a micro-blade grid) of a small tissue sample and filtering of the solution through a 50-μm strain, to yield a suspension of "side population" progenitor cells, which is then loaded onto a biomaterial prior to implantation. Characterization of this "side population" following in vitro culture revealed a heterogeneous population including MSC-like cells ($CD73^+CD90^+CD105^+CD45^-CD14^-$) with multi-lineage differentiation potential (Trovato et al., 2015).

Although the use of minimally manipulated whole tissue fractions is time- and cost-effective, the yield of progenitor cells obtained is relatively low. MSCs represent <1% of the MNC in BMA, and approximately 1.4% in A-SVF, based on CFU potential (Prins et al., 2016). This has encouraged ex vivo expansion strategies, which aim to exponentially increase the number of cells of a specific phenotype, that is *committed* or *uncommitted*, available for implantation, and thereby improve clinical outcomes.

4.2 | Use of expanded uncommitted cells

Ten controlled (and 18 uncontrolled) studies reported the implantation of autologous MSCs from bone marrow or adipose tissues (Table 3, Supporting Information Table S2). Culture-expanded BMSCs were used in SA (Hernandez Alfero et al., 2005; Kaigler et al., 2013, 2015), RA (Bajestan et al., 2017) or AC repair (Khalifa & Gomaa, 2017). Of these, the former four studies reported the use of a commercial automated bioreactor system (Replicell® or Ixymyelocel-t®, Aastrom Biosciences Inc., Ann Arbor, MI, USA) for isolation of a mixed population of $CD90^+$ MSCs, HSCs, endothelial and inflammatory cells, termed "tissue repair cells" (TRCs), from the MNC-fraction of bone marrow (Bartel et al., 2012). TRCs were obtained via a single-step process following a 12–14 day-expansion period in a "single-pass perfusion" bioreactor, in which, unlike typical MSC cultures, the non-adherent (i.e., hematopoietic, endothelial and inflammatory) cell fractions were retained and the adherent cells were not passaged. The authors hypothesize that these accessory cells may serve to enhance tissue regeneration by promoting vascularization and modulating the inflammatory response in the regenerating tissues (Dennis et al., 2007). However, no significant differences in NBF were observed when comparing TRC-scaffold constructs with scaffolds alone (Hernandez Alfero et al., 2005; Kaigler et al., 2013, 2015) or AB (Bajestan et al., 2017).

One strategy to enhance the regenerative efficacy of MSCs is via osteogenic induction and pre-differentiation (Oryan et al., 2017). In the present review, the evidence for osteogenic pre-differentiation of BMSCs prior to clinical application was conflicting. Among the UT, one group reported the application of osteogenically pre-induced MSCs seeded on HA scaffolds for RA/SA. The authors reported successful bone regeneration, suggestive of "osteogenesis" by the implanted cells, in only one of six patients (Meijer, de Bruijn, Koole, & van Blitterswijk, 2008). Two other groups reported favourable bone regeneration in RA (Wojtowicz, Jodko, Perek, & Popowski, 2014; Wojtowicz et al., 2013), AC (Chai et al., 2006) and CD repair (Chai, Zhang, Liu, Cui, & Cao, 2003) when using osteogenically pre-differentiated cells. Conversely, another group has reported extensively on the application of autologous non-induced BMSCs mixed with PRP, termed "injectable tissue engineered bone" for successful SA and RA (Ueda, Yamada, Kagami, & Hibi, 2008; Ueda, Yamada, Ozawa, & Okazaki, 2005; Yamada et al., 2008; Yamada, Nakamura, Ito, et al., 2013; Yamada, Nakamura, Ueda, & Ito, 2013). Other studies also reported favourable outcomes when using non-induced BMSCs seeded on BCP scaffolds for SA (Shayesteh et al., 2008) and AC repair (Behnia, Khojasteh, Soleimani, Tehranchi, & Atashi, 2012). Moreover, one recent controlled study reported superior bone regeneration following AC repair with non-induced BMSC-loaded HA scaffolds, compared to the gold standard, that is AB grafts (Khalifa & Nowair, 2017). Nevertheless, since the current pre-clinical evidence from large-animal models is also conflicting (Adamzyk et al., 2016; Corbella et al., 2017), no clear conclusions can be drawn regarding the benefits of osteogenic pre-differentiation of MSCs.

A majority of the included studies (and all studies in the meta-analysis) of cell therapy for RA reported augmentation in the horizontal dimension, as a treatment for "narrow ridges." It is well accepted that different types of ridge deficiencies, that is horizontal, vertical and segmental (in ascending order of complexity), have different regenerative potentials, and thus, may require different treatment strategies (Esposito et al., 2009). In context, a recent phase I feasibility study reported the use of autologous BMSCs to regenerate deficient ridges in the posterior mandible (Gjerde et al., 2018). Regeneration in the atrophic posterior mandible is reported to be especially challenging due to difficulties in achieving optimal flap closure and graft stabilization, and the local microarchitecture of dense cortical bone with limited vascularity (Elnayef et al., 2017). Nevertheless, successful regeneration in both horizontal and vertical dimensions was reported in 11 patients treated with BMSC-loaded BCP scaffolds contained by a titanium-reinforced membrane (Gjerde et al., 2018). A similar strategy was successfully applied in the treatment of orthopaedic non-unions in a recent multicenter trial (Gómez-Barrena et al., 2018). Both studies included a highly standardized laboratory protocol for cell manufacturing and provide examples of successful regeneration in challenging bone deficiencies.

In the case of mandibular defects (Gjerde et al., 2018), the authors also reported an unexpected additional benefit on soft tissue healing, that is increased keratinized mucosa, at the augmented sites, attributed to the well-documented paracrine effects of MSCs (Vizoso, Eiro, Cid, Schneider, & Perez-Fernandez, 2017). Interestingly, this was the only study in which ex vivo MSC-expansion was performed using human platelet lysate (HPL)—an emerging alternative to animal- and human-derived serum supplements for cell culture (Shanbhag, Stavropoulos, Suliman, Hervig, & Mustafa, 2017). A majority of the included studies reported the use of autologous or animal-derived serum [foetal bovine serum (FBS)] for cell expansion. Several advantages of HPL over FBS and human serum have been documented, owing largely to the wide range of growth factors released by platelets, which can enhance the osteogenic potential and paracrine efficacy of MSCs (Shanbhag et al., 2017). Indeed, the authors of the present study acknowledged that expansion in HPL may have resulted in osteogenic "pre-conditioning" of the BMSCs, leading to bone formation, and the observed paracrine effects on soft tissues (Gjerde et al., 2018).

In the context of MSCs paracrine effects, it is relevant to mention the emerging "cell-free" strategies, which exploit the secretome or "conditioned media" from MSCs, that is the secreted bioactive molecules including extracellular vesicles, to promote regeneration (Vizoso et al., 2017). This concept is based on observations that a very small fraction of implanted MSCs survives long enough in vivo to differentiate, suggesting that MSCs mainly exert their regenerative effects via paracrine mechanisms (Haumer et al., 2018). Following promising pre-clinical results, one group has recently reported the clinical application of allogeneic MSCs conditioned medium, in combination with β-TCP or COL sponge scaffolds, for bone regeneration in SA, RA and SP, in nine patients with favourable outcomes and no adverse events (Katagiri, Osugi, Kawai, & Hibi, 2016; Katagiri et al., 2017). The safety and efficacy of allogeneic MSCs secretome (lyophilised) as an "off-the-shelf" therapy for bone regeneration should be investigated in future clinical trials.

As previously discussed, abdominal adipose tissue represents a promising alternative to iliac bone marrow, since; (a) it is relatively less invasive to harvest, and (b) the average yield of MSC-like cells are reportedly greater compared to bone marrow (Bajek et al., 2016; Qadan et al., 2018). However, previous studies have suggested a lower intrinsic osteogenic potential of ASCs versus BMSCs in vitro and in vivo (Brennan et al., 2017; Liao & Chen, 2014). Moreover, the in vivo bone-forming potential of ASCs has been demonstrated only when pre-cultured in the presence of additional osteogenic stimulating factors (Scherberich et al., 2010). In this context, one research group reported the use of osteogenically pre-induced ASCs together with HA-COL scaffolds and PRP for treatment of various alveolar defects (Alekseeva, Kulakov, Gol'dshteĭn, & Kulakov, 2012; Alekseeva, Rachinskaia, Volkov, Kulakov, & Gol'dshteĭn, 2012; Alekseeva, Volkov, Kulakov, & Gol'dshteĭn, 2012; Kulakov et al., 2008) . In one controlled study of SA, the authors reported greater histological NBF with the ASC-constructs compared to DBBM alone (Alexeeva et al., 2012). Another research group reported the use of non-induced autologous ASCs and ceramic scaffolds, with or without additional recombinant human bone morphogenetic protein-2 (rhBMP-2) to treat challenging segmental mandibular (Sandor et al., 2014; Wolff et al., 2013) or CDs (Thesleff et al., 2011, 2017), respectively. While uneventful healing and successful reconstruction ("bridging") of segmental defects was reported in three patients treated with ASCs *with* rhBMP-2 (average follow-up of 35 months), late complications (6–7 years post-operative) such as infection and partial or total graft resorption were observed in the cranial reconstructions of 4/5 patients receiving ASCs *without* rhBMP-2. The authors attributed the compromised results to large defect sizes, rapid resorption of the ceramic scaffolds, and possibly the lack of osteoinductive signals in the form of rhBMP-2. In context, a recent study demonstrated enhanced osteogenic differentiation of cells from "whole adipose tissue" stimulated by rhBMP-2 compared to stimulation by osteogenic medium alone (Bondarava et al., 2017).

An alternative source of ASCs identified in the present review was the intra-oral buccal fat pad (BFP). Similar to abdominal adipose tissue, BFP is reported to harbour a SVF with a sub-population of ASCs with osteogenic differentiation potential (Farre-Guasch et al., 2018), which can be enhanced by additional stimulation with rhBMP-2 (Shiraishi, Sumita, Wakamastu, Nagai, & Asahina, 2012). Moreover, BFP shows limited donor-variation in size and is independent of body weight and fat distribution, thereby making it an attractive source of ASCs for orofacial BTE (Salehi-Nik & Rezai Rad, 2017). In the present review, one research group reported RA (Khojasteh & Sadeghi, 2016) and AC repair (Khojasteh et al., 2017) using autologous BFP-ASCs compared to AB. Superior NBF was observed in both studies when AB scaffolds were supplemented with BFP-ASCs compared the gold standard of AB grafts alone (Khojasteh & Sadeghi, 2016; Khojasteh et al., 2017).

One completed single-arm trial has reported the use of autologous dental pulp stem cells (DPSCs) to treat unilateral AC defects in five 7–12-year-old patients (Bueno, 2015). A sub-population of multipotent progenitor cells has been identified in the dental pulp of both permanent (DPSCs) and deciduous teeth [stem cells from human exfoliated deciduous teeth (SHED)] (Ducret et al., 2015). The proposed benefits of DPSCs and SHED include the ease of accessibility from unerupted third molars or exfoliated deciduous teeth, respectively, and their high proliferation and osteogenic differentiation potential, both in vitro and in vivo (Leyendecker Junior, Gomes Pinheiro, Lazzaretti Fernandes, & Franco Bueno, 2018; Nakajima et al., 2018). In particular, SHED might represent a promising strategy for AC repair, since patients are usually treated with secondary bone grafts, most frequently iliac AB, between 6 and 11 years of age (Kang, 2017; Pinheiro, de Pinho, Aranha, Fregnani, & Bueno, 2018). In the included study, a substantial amount of regeneration (89% BF) was observed in AC defects, 6 months after treatment with autologous SHED-loaded DBBM scaffolds (Bueno, 2015). However, whether DPSCs and SHED represent a feasible alternative to the gold standard (AB grafts) in AC repair remains to be determined.

4.3 | Use of expanded committed cells

The rationale for using committed cells is to circumvent the possible limitation of differences in degrees of osteogenic potential found in heterogeneous cell populations, for example bone marrow and adipose tissues. However, these cells may not possess self-renewal capacity and multipotency to the same extent as MSCs (Akintoye et al., 2006; Pettersson et al., 2017). Nine studies (six controlled) reported the use of ex vivo expanded periosteal cells (POCs) for SA (Table 4, Supporitng Information Table S3). Six studies reported the use of a commercial POC-seeded bone graft (BioSeed–Oralbone®, Biotissue Technologies, Freiburg, Germany) with conflicting results. The graft consists of autologous ex vivo expanded POCs seeded on PLGA scaffolds and osteogenically induced for 1 week. While promising results were observed in preliminary reports (Beaumont, Schmidt, Tatakis, & Zafiropoulos, 2008; Trautvetter, Kaps, Schmelzeisen, Sauerbier, & Sittinger, 2011), other studies frequently reported complications and/or graft failure, especially when extensive sinus grafting was performed, that is in patients with the most compromised residual ridges (Mangano et al., 2009; Schimming & Schmelzeisen, 2004; Voss et al., 2010; Zizelmann et al., 2007). In three controlled studies, inferior outcomes of the POC-autograft were observed in comparison to ceramic scaffolds (Mangano et al., 2009) or AB (Voss et al., 2010; Zizelmann et al., 2007). The authors attributed the compromised outcomes to (a) poor vascularization of the constructs upon implantation in vivo, and (b) the degradation profile of the PLGA scaffolds, which creates an acidic local microenvironment unconducive to cell survival and function (Liu, Slamovich, & Webster, 2006). In contrast, when a similar strategy for ex vivo expansion and pre-differentiation of POCs was used in combination with collagen scaffolds, based on preliminary in vitro screening (Petrovic, Schlegel, Schultze-Mosgau, & Wiltfang, 2006), superior bone regeneration was observed after SA in comparison to cell-free NBBM scaffolds (Springer et al., 2006).

One group reported the use periosteal "cell-sheets" formed by ex vivo expanded POCs, in combination with AB and PRP for SA and RA (Nagata et al., 2012; Ogawa et al., 2016). The cell sheet technique is based on implantation of cells grown as single or multiple layers together with their secreted extracellular matrix (ECM), as opposed to conventional single-cell suspensions. Proposed advantages of this technique include preservation of the cell-to-cell connections and ECM components along with a high cell-seeding efficacy (Yorukoglu, Kiter, Akkaya, Satiroglu-Tufan, & Tufan, 2017). Superior NBF after 4 months and comparable volumetric stability of augmented sites after 6–12 months were observed in the POC-seeded AB (+PRP) grafts compared to conventional AB (+PRP) grafts (Nagata et al., 2012; Ogawa et al., 2016). The authors suggested that inclusion of POCs in tissue-engineered constructs could reduce the volume of AB needed by up to 40%, thereby reducing donor site morbidity (Nagata et al., 2012). However, whether POC sheets used in combination with a biomaterial could entirely eliminate the need for AB harvesting remains to be determined.

Six studies reported the use of autologous OBs for SA, RA or AC repair (Table 4). As previously stated, OBs are the fundamental cells involved in the function, repair, and maintenance of bone (Jayakumar & Di Silvio, 2010). In the present review, OBs were isolated via enzymatic digestion or explant culture of intra-oral bone biopsies and usually cultured in osteogenic induction medium. The observed pre-clinical benefits of autologous OB-seeded DBBM scaffolds were favourably translated in an early patient case series (Fuerst et al., 2009). In three controlled studies, comparable bone regeneration in SA and RA was observed with autologous ex vivo expanded OB-seeded DBBM scaffolds versus cell-free DBBM scaffolds (Springer et al., 2006), AB (Pradel, Eckelt, & Lauer, 2006), or their 50–50 combination (Hermund, Donatsky, Nielsen, Clausen, and Holmstrup, 2012). Interestingly, one study reported comparable bone regeneration in SA using POC-seeded collagen and OB-seeded DBBM scaffolds (both superior to cell-free scaffolds), suggesting a comparable degree of osteogenic commitment in the two cell types (Springer et al., 2006). In one study, superior BF was observed when using autologous OB-seeded DBBM scaffolds versus the gold standard, iliac AB, for AC repair (Pradel & Lauer, 2012). Since the OBs were isolated from a small (3–4 mm) biopsy of maxillary bone, the authors proposed the cell-based strategy as a feasible alternative to more invasive AB grafting (Pradel & Lauer, 2012).

While all of the above studies reported the use of autologous cells, two SA studies (one controlled) reported the use of a commercial "allogeneic cellular bone matrix" (Osteocel®, NuVasive Biologics, CA, USA) containing viable osteoprogenitor cells (Gonshor, McAllister, Wallace, & Prasad, 2011; McAllister, Haghighat, & Gonshor, 2009). Although, the clinical use of allografts has been limited by safety concerns with regards to disease transmission and lack of osteogenic properties comparable to autologous bone, recent advances in donor screening and viral testing have greatly improved allograft safety. Moreover, novel tissue processing methods which selectively remove immune cells and preserve osteogenic cells, have been applied to allografts. Osteocel® is obtained from cadaveric cancellous bone of screened donors following selective cell preservation. Previous studies have identified MSC-like cells in Osteocel® at a higher frequency than those found in freshly isolated iliac bone or BMA (Baboolal et al., 2014; Skovrlj et al., 2014). In one RCT, significantly greater NBF was observed following SA with Osteocel® compared to cell-free allograft (Gonshor et al., 2011). Nevertheless, the need for further studies to investigate the mechanism of action of osteoprogenitors in cellular allografts, that is whether these cells participate directly in NBF via differentiation or whether they act as immunoregulators of host MSCs, has been highlighted (Baboolal et al., 2014).

4.4 | Clinical relevance of findings

While significant overall benefit of cell therapy (BTE) was observed in most pre-clinical in vivo studies and for most indications, in general, this benefit was not translated in the clinical studies included herein, that is the ES were much smaller in patients than large-animals and

did not extent to all indications, but only to SA and horizontal RA (no studies of vertical RA were eligible for the meta-analysis). In this context, the model used is critical when interpreting the results regarding the potential of a therapeutic intervention to enhance bone regeneration. In particular, the maxillary sinus represents a *spontaneously healing defect*, in the sense that space provided, that is the Schneiderian membrane is elevated and kept at a distance to the sinus bone wall, and in the absence of infection, bone regeneration occurs in the sinus cavity in a predicable fashion—even without the need for any grafting (Duan et al., 2017; Lundgren, Andersson, Gualini, & Sennerby, 2004; Riben & Thor, 2016). The major bulk of bone regeneration in an augmented sinus forms within the first 4–5 months post-operatively, and thereafter only relatively smaller increases in bone formation may be observed (Handschel et al., 2009; Klijn, Meijer, Bronkhorst, & Jansen, 2010). Thus, it appears that the regenerative potential of the sinus is "exhausted" after a certain amount of bone formation is achieved and no intervention can produce larger amounts of bone regeneration within the sinus. This view appears supported by the circumstantial evidence indicating that even application of growth factors, including BMPs—highly potent growth factors for bone regeneration, does not result in considerably different bone densities compared with any other type of augmentation material (Schliephake, 2015). Even in the present analysis, the significant effect of BTE in SA (after 6 months) was largely due to a single study (Pasquali et al., 2015), showing a large positive effect over the control intervention. Thus, in retrospect, it may come as no surprise that BTE failed to show similarly remarkable potential in enhancing bone formation in human sinuses, comparing with animals. A similar concern regards the use of the extraction socket model, representing also a largely spontaneously healing defect; remarkable differences in terms of histological outcome of healing within the socket may not be expected among various types of treatments with similar mechanical stability and space provision capacities, in the absence of infection (MacBeth, Trullenque-Eriksson, Donos, & Mardas, 2017).

The lack of similarly remarkable effects of BTE in the clinic compared with those observed in pre-clinical in vivo models, may also be related to dimensional (size) differences in human and animal defects. In particular, "diffusion distances," important aspects for characterization of mass transport limitations (e.g., diffusion of oxygen and removal of metabolic waste) relevant to the survival of transplanted cells, are usually smaller in animals compared with humans (Muschler, Raut, Patterson, Wenke, & Hollinger, 2010); this in turn may have allowed a better performance of the transplanted cells in animals compared with humans. In this context, it is also worth discussing the different outcome measures employed in the studies. Histomorphometry of biopsy specimens is considered the "gold standard" method for quantitative evaluation of bone structure (Vidal et al., 2012), and was therefore considered as the primary outcome measure in the meta-analyses. More recently, micro-CT has been proposed as a less-destructive and –time/-labour intensive method for assessing 3-D bone microarchitecture (Hedberg et al., 2005). In the present review, histological and radiographic data were analysed separately. However, it must be acknowledged that obtaining biopsy specimens of regenerated tissues is considerably easier in animals (usually following euthanasia) than in clinical situations. Loss or damage to clinical specimens during harvesting and/or processing cannot be excluded and may be a further contributing factor to the differences in outcomes. Moreover, variation between the studies regarding processing methods, difficulty in differentiating between mineralized scaffolds and regenerated mineralized bone and investigator-related factors (inter-observer variation, lack of blinding, etc.), may have contributed to heterogeneity in the observed results (Shanbhag et al., 2017).

It is relevant to discuss the results herein, in the context of future studies. Although statistically significant benefits of BTE were observed in certain indications, the prediction intervals in both the clinical and pre-clinical meta-analyses were generally quite large and often crossing the line of no effect, that is the "zero line." Prediction intervals reflect the heterogeneity in the current studies and provide a range for the expected effect of the intervention in a future study under a different setting. Thus, although statistically significant effects of BTE were observed in certain indications in the current analysis, the wide prediction intervals suggest that future studies in different settings may show no, or even opposite, effects, that is in the favour of scaffolds alone (IntHout, Ioannidis, Rovers, & Goeman, 2016). Only in the case of clinical SA (vs. scaffolds, 4–7 months) evaluated by μ-CT, did BTE show a significant effect with a narrow prediction interval.

Finally, the cost of BTE, in comparison to current alternatives, is an important factor in clinical decision-making. One included study, reporting the use of autologous ASCs to treat extensive mandibular defects, estimated the cost of GMP-grade cell expansion alone to be 12,000 USD (Wolff et al., 2013). In this context, the use of whole tissue [BMA(C) or SVF] would considerably reduce costs in comparison to expanded cells. However, the per-patient costs associated with the "gold standard" treatment, that is iliac crest-derived AB grafting, are also reported to be considerably high, primarily due to the need for hospitalization and general anaesthesia (Dahlin & Johansson, 2011; Francis et al., 2013; Mehta et al., 2018). Indeed, one included study reported significantly greater costs (in addition to higher complications and morbidity) associated with AB grafting versus BTE (BMA + scaffolds) for AC repair (Gimbel et al., 2007). Thus, in addition to clinical efficacy, future controlled studies should evaluate the cost-effectiveness of cell therapy for bone regeneration to guide clinical decision-making.

5 | CONCLUSIONS

Based on the reviewed evidence, the following conclusions may be drawn:

1. Based on limited and heterogeneous evidence from clinical studies, transplantation of cells, most commonly whole BMA or BMAC, in combination with biomaterial scaffolds results in superior bone regeneration compared to implantation of

scaffolds alone in SA and horizontal RA, and comparable bone regeneration to the gold standard (AB grafts) in AC repair.
2. It is unclear whether implantation of ex vivo expanded cells is superior to minimally manipulated whole tissue fractions (BMA/C or A-SVF). In the case of ex vivo expanded cells, it is unclear whether implantation of committed cells (POCs or OBs) is superior to uncommitted cells (BMSCs or ASCs) in terms of bone regeneration.
3. In the case of BMSCs, it is unclear whether osteogenic pre-differentiation is beneficial. In the case of ASCs, additional osteogenic stimulation, via osteogenic pre-differentiation or addition of osteoinductive factors, for example BMP-2, may be beneficial.
4. The relatively larger ES in favour of cell therapy observed in pre-clinical studies are diminished in clinical trials, suggesting a gap in translation.

ACKNOWLEDGEMENT

The authors acknowledge the support of the authors of the primary studies who provided additional information and data for the review.

CONFLICT OF INTEREST

The authors have stated explicitly that there are no conflicts of interest in connection with this article.

ORCID

Andreas Stavropoulos https://orcid.org/0000-0001-8161-3754
Mariano Sanz https://orcid.org/0000-0002-6293-5755
Kamal Mustafa https://orcid.org/0000-0002-2968-2856
Siddharth Shanbhag http://orcid.org/0000-0003-0056-8379

REFERENCES

Adamzyk, C., Kachel, P., Hoss, M., Gremse, F., Modabber, A., Holzle, F., … Lethaus, B. (2016). Bone tissue engineering using polyetherketoneketone scaffolds combined with autologous mesenchymal stem cells in a sheep calvarial defect model. *Journal of Cranio-Maxillo-Facial Surgery*, *44*, 985–994. https://doi.org/10.1016/j.jcms.2016.04.012

Akintoye, S. O., Lam, T., Shi, S., Brahim, J., Collins, M. T., & Robey, P. G. (2006). Skeletal site-specific characterization of orofacial and iliac crest human bone marrow stromal cells in same individuals. *Bone*, *38*, 758–768. https://doi.org/10.1016/j.bone.2005.10.027

Alekseeva, I. S., Kulakov, A. A., Gol'dshteĭn, D. V., & Kulakov, A. V. (2012). Bone tissue restoration after tooth removal by means of tissue-engineering construction based on multipotent stromal adipose cells. *Stomatologiia (Mosk)*, *91*, 32–35.

Alekseeva, I. S., Rachinskaia, O. A., Volkov, A. V., Kulakov, A. A., & Gol'dshteĭn, D. V. (2012). A comparative evaluation of bone tissue formation by tissue scaffold and osteoplastic material «Bio-Oss» transplantation in the maxillary sinus floor. *Stomatologiia (Mosk)*, *91*, 41–44.

Alekseeva, I. S., Volkov, A. V., Kulakov, A. A., & Gol'dshteĭn, D. V. (2012). Clinical and experimental study on the use of combined cell transplant on the basis of multipotent mesenchymal stromal cells of adipose tissue in patients with severe deficiency of jaws bone tissue. *Cellular Transplantation and Tissue Engineering*, *7*, 97–105.

Al-Ahmady, H. H., Abd Elazeem, A. F., Bellah Ahmed, N. E., Shawkat, W. M., Elmasry, M., Abdelrahman, M. A., & Abderazik, M. A. (2018). Combining autologous bone marrow mononuclear cells seeded on collagen sponge with Nano Hydroxyapatite, and platelet-rich fibrin: Reporting a novel strategy for alveolar cleft bone regeneration. *J Craniomaxillofac Surg.*, *46*, 1593–1600.

Al-Nawas, B., & Schiegnitz, E. (2014). Augmentation procedures using bone substitute materials or autogenous bone - a systematic review and meta-analysis. *European Journal of Oral Implantology*, *7*(Suppl 2), S219–S234.

Al-Nbaheen, M., Vishnubalaji, R., Ali, D., Bouslimi, A., Al-Jassir, F., Megges, M., … Aldahmash, A. (2013). Human stromal (mesenchymal) stem cells from bone marrow, adipose tissue and skin exhibit differences in molecular phenotype and differentiation potential. *Stem Cell Reviews*, *9*, 32–43. https://doi.org/10.1007/s12015-012-9365-8

d'Aquino, R., De Rosa, A., Lanza, V., Tirino, V., Laino, L., Graziano, A., … Papaccio, G. (2009). Human mandible bone defect repair by the grafting of dental pulp stem/progenitor cells and collagen sponge biocomplexes. *European Cells and Materials*, *18*, 75–83. https://doi.org/10.22203/eCM

Avila-Ortiz, G., Bartold, P. M., Giannobile, W., Katagiri, W., Nares, S., Rios, H., … Wikesjo, U. M. (2016). Biologics and cell therapy tissue engineering approaches for the management of the edentulous maxilla: A systematic review. *International Journal of Oral and Maxillofacial Implants*, *31*(Suppl), s121–s164.

Baboolal, T. G., Boxall, S. A., El-Sherbiny, Y. M., Moseley, T. A., Cuthbert, R. J., Giannoudis, P. V., … Jones, E. (2014). Multipotential stromal cell abundance in cellular bone allograft: Comparison with fresh age-matched iliac crest bone and bone marrow aspirate. *Regenerative Medicine*, *9*, 593–607. https://doi.org/10.2217/rme.14.17

Bajek, A., Gurtowska, N., Olkowska, J., Kazmierski, L., Maj, M., & Drewa, T. (2016). Adipose-derived stem cells as a tool in cell-based therapies. *Archivum Immunolgiae et Therapiae Experimentalis*, *64*, 443–454. https://doi.org/10.1007/s00005-016-0394-x

Bajestan, M. N., Rajan, A., Edwards, S. P., Aronovich, S., Cevidanes, L. H. S., Polymeri, A., … Kaigler, D. (2017). Stem cell therapy for reconstruction of alveolar cleft and trauma defects in adults: A randomized controlled, clinical trial. *Clinical Implant Dentistry and Related Research*, *19*, 793–801. https://doi.org/10.1111/cid.12506

Bartel, R. L., Cramer, C., Ledford, K., Longcore, A., Parrish, C., Stern, T., … Zeigler, F. (2012). The Aastrom experience. *Stem Cell Research & Therapy*, *3*, 26. https://doi.org/10.1186/scrt117

Beaumont, C., Schmidt, R. J., Tatakis, D. N., & Zafiropoulos, G. G. (2008). Use of engineered bone for sinus augmentation. *Journal of Periodontology*, *79*, 541–548. https://doi.org/10.1902/jop.2008.070255

Behnia, H., Khojasteh, A., Soleimani, M., Tehranchi, A., & Atashi, A. (2012). Repair of alveolar cleft defect with mesenchymal stem cells and platelet derived growth factors: A preliminary report. *Journal of Cranio-Maxillo-Facial Surgery*, *40*, 2–7. https://doi.org/10.1016/j.jcms.2011.02.003

Bertolai, R., Catelani, C., Aversa, A., Rossi, A., Giannini, D., & Bani, D. (2015). Bone graft and mesenchimal stem cells: Clinical observations and histological analysis. *Clinical cases in mineral and Bone Metabolism*, *12*, 183–187. https://doi.org/10.11138/ccmbm/2015.12.2.183

Bondarava, M., Cattaneo, C., Ren, B., Thasler, W. E., Jansson, V., Muller, P. E., & Betz, O. B. (2017). Osseous differentiation of human fat tissue grafts: From tissue engineering to tissue differentiation. *Scientific Reports*, *7*, 39712. https://doi.org/10.1038/srep39712

Brennan, M. A., Renaud, A., Guilloton, F., Mebarki, M., Trichet, V., Sensebé, L., … Layrolle, P. (2017). Inferior in vivo osteogenesis and superior angiogeneis of human adipose tissue: A comparison with bone marrow-derived stromal stem cells cultured in xeno-free conditions. *Stem Cells Translational Medicine*, *6*, 2160–2172. https://doi.org/10.1002/sctm.17-0133

Bueno, D. F. (2015). Use of mesenchymal stem cells for alveolar bone tissue engineering for cleft lip and palate patients. Clinical-Trials.gov Identifier: NCT01932164. Retreived from https://clinicaltrials.gov/ct2/show/NCT01932164

Caplan, A. I. (2017). Mesenchymal stem cells: Time to change the name!. *Stem Cells Translational Medicine*, *6*, 1445–1451. https://doi.org/10.1002/sctm.17-0051

Castillo-Cardiel, G., Lopez-Echaury, A. C., Saucedo-Ortiz, J. A., Fuentes-Orozco, C., Michel-Espinoza, L. R., Irusteta-Jimenez, L., … Gonzalez-Ojeda, A. (2017). Bone regeneration in mandibular fractures after the application of autologous mesenchymal stem cells, a randomized clinical trial. *Dental Traumatology*, *33*, 38–44. https://doi.org/10.1111/edt.12303

Chahla, J., Dean, C. S., Moatshe, G., Pascual-Garrido, C., Serra Cruz, R., & LaPrade, R. F. (2016). Concentrated bone marrow aspirate for the treatment of chondral injuries and osteoarthritis of the knee: A systematic review of outcomes. *Orthopaedic Journal of Sports Medicine*, *4*, 2325967115625481. https://doi.org/10.1177/2325967115625481

Chahla, J., Mannava, S., Cinque, M. E., Geeslin, A. G., Codina, D., & LaPrade, R. F. (2017). Bone marrow aspirate concentrate harvesting and processing technique. *Arthroscopy Techniques*, *6*, e441–e445. https://doi.org/10.1016/j.eats.2016.10.024

Chai, G., Zhang, Y., Hu, X. J., Wang, M., Liu, W., Cui, L., & Cao, Y. L. (2006). Repair alveolar cleft bone defects with bone marrow stromal cells. *Zhonghua Zheng Xing Wai Ke Za Zhi*, *22*, 409–411.

Chai, G., Zhang, Y., Liu, W., Cui, L., & Cao, Y. L. (2003). Clinical application of tissue engineered bone repair of human craniomaxillofacial bone defects. *Zhonghua Yi Xue Za Zhi*, *83*, 1676–1681.

Chanchareonsook, N., Junker, R., Jongpaiboonkit, L., & Jansen, J. A. (2014). Tissue-engineered mandibular bone reconstruction for continuity defects: A systematic approach to the literature. *Tissue Engineering Part B Reviews*, *20*, 147–162. https://doi.org/10.1089/ten.teb.2013.0131

Chiapasco, M., & Casentini, P. (2018). Horizontal bone-augmentation procedures in implant dentistry: Prosthetically guided regeneration. *Periodontology 2000*, *77*, 213–240. https://doi.org/10.1111/prd.12219

Corbella, S., Weinstein, R., Francetti, L., Taschieri, S., & Del Fabbro, M. (2017). Periodontal regeneration in aggressive periodontitis patients: A systematic review of the literature. *Journal of Investigative and Clinical Dentistry*, *8*, e12245. https://doi.org/10.1111/jicd.12245

da Costa, C. E., Pelegrine, A. A., Fagundes, D. J., Simoes Mde, J., & Taha, M. O. (2011). Use of corticocancellous allogeneic bone blocks impregnated with bone marrow aspirate: A clinical, tomographic, and histomorphometric study. *General Dentistry*, *59*, e200–e205.

Dahlin, C., & Johansson, A. (2011). Iliac crest autogenous bone graft versus alloplastic graft and guided bone regeneration in the reconstruction of atrophic maxillae: A 5-year retrospective study on cost-effectiveness and clinical outcome. *Clinical Implant Dentistry and Related Research*, *13*, 305–310. https://doi.org/10.1111/j.1708-8208.2009.00221.x

Danesh-Sani, S. A., Engebretson, S. P., & Janal, M. N. (2017). Histomorphometric results of different grafting materials and effect of healing time on bone maturation after sinus floor augmentation: A systematic review and meta-analysis. *Journal of Periodontal Research*, *52*, 301–312. https://doi.org/10.1111/jre.12402

D'Aquino, R., Trovato, L., Graziano, A., Ceccarelli, G., Cusella de Angelis, G., Marangini, A., … Rodriguez y Baena, R. (2016). Periosteum-derived micro-grafts for tissue regeneration of human maxillary bone. *Journal of Translational Science*, *2*, 125–129.

Daugela, P., Cicciu, M., & Saulacic, N. (2016). Surgical regenerative treatments for peri-implantitis: Meta-analysis of recent findings in a systematic literature review. *Journal of Oral and Maxillofacial Research*, *7*, e15. https://doi.org/10.5037/jomr.2029.283X

de Oliveira, T. A., Aloise, A. C., Orosz, J. E., de Mello, E. O. R., de Carvalho, P., & Pelegrine, A. A. (2016). Double centrifugation versus single centrifugation of bone marrow aspirate concentrate in sinus floor elevation: A pilot study. *International Journal of Oral and Maxillofacial Implants*, *31*, 216–222. https://doi.org/10.11607/jomi.4170

Dennis, J. E., Esterly, K., Awadallah, A., Parrish, C. R., Poynter, G. M., & Goltry, K. L. (2007). Clinical-scale expansion of a mixed population of bone-marrow-derived stem and progenitor cells for potential use in bone-tissue regeneration. *Stem Cells*, *25*, 2575–2582. https://doi.org/10.1634/stemcells.2007-0204

Dominici, M., Le Blanc, K., Mueller, I., Slaper-Cortenbach, I., Marini, F., Krause, D., … Horwitz, E. (2006). Minimal criteria for defining multipotent mesenchymal stromal cells. The International Society for Cellular Therapy position statement. *Cytotherapy*, *8*, 315–317. https://doi.org/10.1080/14653240600855905

Du, F., Wu, H., Li, H., Cai, L., Wang, Q., Liu, X., … Cao, Y. (2017). Bone marrow mononuclear cells combined with beta-tricalcium phosphate granules for alveolar cleft repair: A 12-month clinical study. *Scientific Reports*, *7*, 13773. https://doi.org/10.1038/s41598-017-12602-1

Duan, D. H., Fu, J. H., Qi, W., Du, Y., Pan, J., & Wang, H. L. (2017). Graft-free maxillary sinus floor elevation: A systematic review and meta-analysis. *Journal of Periodontology*, *88*, 550–564. https://doi.org/10.1902/jop.2017.160665

Ducret, M., Fabre, H., Degoul, O., Atzeni, G., McGuckin, C., Forraz, N., … FARGES, J.-C. (2015). Manufacturing of dental pulp cell-based products from human third molars: Current strategies and future investigations. *Frontiers in Physiology*, *6*, 213. https://doi.org/10.3389/fphys.2015.00213

Duttenhoefer, F., Hieber, S. F., Stricker, A., Schmelzeisen, R., Gutwald, R., & Sauerbier, S. (2014). Follow-up of implant survival comparing ficoll and bone marrow aspirate concentrate methods for hard tissue regeneration with mesenchymal stem cells in humans. *BioResearch Open Access*, *3*, 75–76. https://doi.org/10.1089/biores.2014.0003

Elgali, I., Omar, O., Dahlin, C., & Thomsen, P. (2017). Guided bone regeneration: Materials and biological mechanisms revisited. *European Journal of Oral Sciences*, *125*, 315–337. https://doi.org/10.1111/eos.12364

El-Jawhari, J. J., Sanjurjo-Rodriguez, C., Jones, E., & Giannoudis, P. V. (2016). Collagen-containing scaffolds enhance attachment and proliferation of non-cultured bone marrow multipotential stromal cells. *Journal of Orthopaedic Research*, *34*, 597–606. https://doi.org/10.1002/jor.23070

Elnayef, B., Monje, A., Gargallo-Albiol, J., Galindo-Moreno, P., Wang, H. L., & Hernandez-Alfaro, F. (2017). Vertical ridge augmentation in the atrophic mandible: A systematic review and meta-analysis. *International Journal of Oral and Maxillofacial Implants*, *32*, 291–312. https://doi.org/10.11607/jomi.4861

Elnayef, B., Porta, C., Suarez-Lopez Del Amo, F., Mordini, L., Gargallo-Albiol, J., & Hernandez-Alfaro, F. (2018). The fate of lateral ridge augmentation: A systematic review and meta-analysis. *International Journal of Oral and Maxillofacial Implants*, *33*, 622–635. https://doi.org/10.11607/jomi.6290

Esposito, M., Grusovin, M. G., Felice, P., Karatzopoulos, G., Worthington, H. V., & Coulthard, P. (2009). Interventions for replacing missing teeth: Horizontal and vertical bone augmentation techniques for dental implant treatment. *Cochrane Database Systematic Review*, *4*, CD003607.

Evans, C. H., Palmer, G. D., Pascher, A., Porter, R., Kwong, F. N., Gouze, E., … Ghivizzani, S. C. (2007). Facilitated endogenous repair: Making tissue engineering simple, practical, and economical. *Tissue Engineering*, *13*, 1987–1993. https://doi.org/10.1089/ten.2006.0302

Farre-Guasch, E., Bravenboer, N., Helder, M. N., Schulten, E., Ten Bruggenkate, C. M., & Klein-Nulend, J. (2018). Blood vessel formation and bone regeneration potential of the stromal vascular fraction seeded on a calcium phosphate scaffold in the human maxillary sinus floor elevation model. *Materials (Basel)*, *11*, pii:E161. https://doi.org/10.3390/ma11010161

Francis, C. S., Mobin, S. S., Lypka, M. A., Rommer, E., Yen, S., Urata, M. M., & Hammoudeh, J. A. (2013). rhBMP-2 with a demineralized bone matrix scaffold versus autologous iliac crest bone graft for alveolar cleft reconstruction. *Plastic and Reconstructive Surgery*, *131*, 1107–1115. https://doi.org/10.1097/PRS.0b013e3182865dfb

Fraser, J. K., Hicok, K. C., Shanahan, R., Zhu, M., Miller, S., & Arm, D. M. (2014). The Celution® system: Automated processing of adipose-derived regenerative cells in a functionally closed system. *Advance in Wound Care (New Rochelle)*, *3*, 38–45. https://doi.org/10.1089/wound.2012.0408

Friedenstein, A. J., Chailakhjan, K. R., & Lalykina, K. S. (1970). The development of fibroblast colonies in monolayer cultures of guinea-pig bone marrow and spleen cells. *Cell and Tissue Kinetics*, *3*, 393–403. https://doi.org/10.1111/j.1365-2184.1970.tb00347.x

Fuerst, G., Strbac, G. D., Vasak, C., Tangl, S., Leber, J., Gahleitner, A., … Watzek, G. (2009). Are culture-expanded autogenous bone cells a clinically reliable option for sinus grafting? *Clinical Oral Implants Research*, *20*, 135–139. https://doi.org/10.1111/j.1600-0501.2008.01624.x

Giuliani, A., Manescu, A., Langer, M., Rustichelli, F., Desiderio, V., Paino, F., De Rosa, A., Laino, L., d'Aquino, R., Tirino, V., & Papaccio, G. (2013). *Stem Cells Transl Med.*, *2*, 316–24.

Gimbel, M., Ashley, R. K., Sisodia, M., Gabbay, J. S., Wasson, K. L., Heller, J., … Bradley, J. P. (2007). Repair of alveolar cleft defects: Reduced morbidity with bone marrow stem cells in a resorbable matrix. *The Journal of Craniofacial Surgery*, *18*, 895–901. https://doi.org/10.1097/scs.0b013e3180a771af

Gjerde, C., Mustafa, K., Hellem, S., Rojewski, M., Gjengedal, H., Yassin, M. A., …. Layrolle, P. (2018). Cell therapy induced regeneration of severely atrophied mandibular bone in a clinical trial. *Stem Cell Research & Therapy*, *9*, 213. https://doi.org/10.1186/s13287-018-0951-9

Gómez-Barrena, E., Rosset, P., Gebhard, F., Hernigou, P., Baldini, N., Rouard, H., … Layrolle, P. (2018). Feasibility and safety of treating non-unions in tibia, femur and humerus with autologous, expanded, bone marrow-derived mesenchymal stromal cells associated with biphasic calcium phosphate biomaterials in a multicentric, non-comparative trial. *Biomaterials*, *S0142–9612*(18), 30205–30209.

Gonshor, A., McAllister, B. S., Wallace, S. S., & Prasad, H. (2011). Histologic and histomorphometric evaluation of an allograft stem cell-based matrix sinus augmentation procedure. *International Journal of Oral and Maxillofacial Implants*, *26*, 123–131.

Handschel, J., Simonowska, M., Naujoks, C., Depprich, R. A., Ommerborn, M. A., Meyer, U., & Kubler, N. R. (2009). A histomorphometric meta-analysis of sinus elevation with various grafting materials. *Head and Face Medicine*, *5*, 12. https://doi.org/10.1186/1746-160X-5-12

Haumer, A., Bourgine, P. E., Occhetta, P., Born, G., Tasso, R., & Martin, I. (2018). Delivery of cellular factors to regulate bone healing. *Advanced Drug Delivery Reviews*, *129*, 285–294. https://doi.org/10.1016/j.addr.2018.01.010

Hayden, R. E., Mullin, D. P., & Patel, A. K. (2012). Reconstruction of the segmental mandibular defect: Current state of the art. *Current opinion in otolaryngology and head and neck surgery*, *20*, 231–236. https://doi.org/10.1097/MOO.0b013e328355d0f3

Hedberg, E. L., Kroese-Deutman, H. C., Shih, C. K., Lemoine, J. J., Liebschner, M. A., Miller, M. J., … Jansen, J. A. (2005). Methods: A comparative analysis of radiography, microcomputed tomography, and histology for bone tissue engineering. *Tissue Engineering*, *11*, 1356–1367. https://doi.org/10.1089/ten.2005.11.1356

Hermund, N. U., Donatsky, O., Nielsen, H., Clausen, C., & Holmstrup, P. (2013). Long-term changes in graft height after sinus floor augmentation with mesenchymal stem cells in a randomised clinical trial: Radiographic evaluation with a minimum followup of 2.5 years. *Journal of Medical and Dental Sciences*, *2*, 5–14.

Hermund, N. U., Stavropoulos, A., Donatsky, O., Nielsen, H., Clausen, C., Reibel, J., … Holmstrup, P. (2012). Reimplantation of cultivated human bone cells from the posterior maxilla for sinus floor augmentation. Histological results from a randomized controlled clinical trial. *Clinical Oral Implants Research*, *23*, 1031–1037. https://doi.org/10.1111/j.1600-0501.2011.02251.x

Hernandez Alfero, F., Marti, C., Orozco, L., Marinoso, M. L., Rodriguez, L., Torrico, C., … Hock, J. M. (2005). Aastrom Biosciences, Inc., Clinical Feasibility Study: The Use of Autologous Bone Marrow-Derived Tissue Repair Cells (TRC) for Maxillary Sinus Floor Augmentation in Edentulous Humans [press release]. Retrieved from http://investors.vcel.com/static-files/f8394516-dfc8-45b8-bda6-ceca0c7eae71.

Higgins, J. P. T., & Green, S. (eds). (2011). Cochrane handbook for systematic reviews of interventions Version 5.1.0 [updated March 2011]. The Cochrane Collaboration, 2011. Retrieved from www.handbook.cochrane.org

Hutmacher, D. W., & Sittinger, M. (2003). Periosteal cells in bone tissue engineering. *Tissue Engineering*, *9*(Suppl 1), S45–S64. https://doi.org/10.1089/10763270360696978

Ibanez, J. C., Agustina, J. M., Ibanez, M. C., & Ibanez, M. I. (2012). Bio-Oss and stem cells from bone marrow obtained from the distal femur for sinus grafting. Abstract from the 20th Annual Scientific Meeting of the European Association of Osseointegration, 10-13 October 2012, Copenhagen, Denmark (additional information obtained via personal communication). Retreived from https://www.researchgate.net/publication/285055976.

IntHout, J., Ioannidis, J. P., Rovers, M. M., & Goeman, J. J. (2016). Plea for routinely presenting prediction intervals in meta-analysis. *British Medical Journal Open*, *6*, e010247. https://doi.org/10.1136/bmjopen-2015-010247

Jager, M., Herten, M., Fochtmann, U., Fischer, J., Hernigou, P., Zilkens, C., … Krauspe, R. (2011). Bridging the gap: Bone marrow aspiration concentrate reduces autologous bone grafting in osseous defects. *Journal of Orthopaedic Research*, *29*, 173–180. https://doi.org/10.1002/jor.21230

Janssen, N. G., Weijs, W. L., Koole, R., Rosenberg, A. J., & Meijer, G. J. (2014). Tissue engineering strategies for alveolar cleft reconstruction: A systematic review of the literature. *Clin Oral Investigations*, *18*, 219–226. https://doi.org/10.1007/s00784-013-0947-x

Jayakumar, P., & Di Silvio, L. (2010). Osteoblasts in bone tissue engineering. *Proceedings of the Institution of Mechanical Engineers. Part H*, *224*, 1415–1440. https://doi.org/10.1243/09544119JEIM821

Jin, E., Chae, D. S., Son, M., & Kim, S. W. (2017). Angiogenic characteristics of human stromal vascular fraction in ischemic hindlimb. *International Journal of Cardiology*, *234*, 38–47. https://doi.org/10.1016/j.ijcard.2017.02.080

Kaigler, D., Avila-Ortiz, G., Travan, S., Taut, A. D., Padial-Molina, M., Rudek, I., … Giannobile, W. V. (2015). Bone engineering of maxillary sinus bone deficiencies using enriched CD90 + stem cell therapy: A randomized clinical trial. *Journal of Bone and Mineral Research*, *30*, 1206–1216. https://doi.org/10.1002/jbmr.2464

Kaigler, D., Pagni, G., Park, C. H., Braun, T. M., Holman, L. A., Yi, E., … Giannobile, W. V. (2013). Stem cell therapy for craniofacial bone regeneration: A randomized, controlled feasibility trial. *Cell Transplantation*, *22*, 767–777. https://doi.org/10.3727/096368912X652968

Kang, N. H. (2017). Current methods for the treatment of alveolar cleft. *Archives of Plastic Surgery*, *44*, 188–193. https://doi.org/10.5999/aps.2017.44.3.188

Katagiri, W., Osugi, M., Kawai, T., & Hibi, H. (2016). First-in-human study and clinical case reports of the alveolar bone regeneration with the

secretome from human mesenchymal stem cells. *Head and Face Medicine*, *12*, 5. https://doi.org/10.1186/s13005-016-0101-5

Katagiri, W., Watanabe, J., Toyama, N., Osugi, M., Sakaguchi, K., & Hibi, H. (2017). Clinical study of bone regeneration by conditioned medium from mesenchymal stem cells after maxillary sinus floor elevation. *Implant Dentistry*, *26*, 607–612. https://doi.org/10.1097/ID.0000000000000618

Khalifa, M. E., & Gomaa, N. E. (2017). Dental Arch Expansion after Alveolar Cleft Repair using Autogenous Bone Marrow Derived Mesenchymal Stem Cells Versus Autogenous Chin Bone Graft. *The Journal of Dental Treatment Oral Care*, *2*, 103.

Khalifa, M. E., & Nowair, I. M. (2017). Alveolar cleft repair using autogenous bone marrow-derived mesenchymal stem cells. *Egyptian Journal of Oral & Maxillofacial Surgery*, *8*, 46–51. https://doi.org/10.1097/01.OMX.0000515464.02298.bb

Khojasteh, A., Kheiri, L., Behnia, H., Tehranchi, A., Nazeman, P., Nadjmi, N., & Soleimani, M. (2017). Lateral ramus cortical bone plate in alveolar cleft osteoplasty with concomitant use of buccal fat pad derived cells and autogenous bone: Phase I clinical trial. *BioMed Research International*, *2017*, 6560234. https://doi.org/10.1155/2017/6560234

Khojasteh, A., & Sadeghi, N. (2016). Application of buccal fat pad-derived stem cells in combination with autogenous iliac bone graft in the treatment of maxillomandibular atrophy: A preliminary human study. *International Journal of Oral and Maxillofacial Surgery*, *45*, 864–871. https://doi.org/10.1016/j.ijom.2016.01.003

Klijn, R. J., Meijer, G. J., Bronkhorst, E. M., & Jansen, J. A. (2010). A meta-analysis of histomorphometric results and graft healing time of various biomaterials compared to autologous bone used as sinus floor augmentation material in humans. *Tissue Engineering Part B Reviews*, *16*, 493–507. https://doi.org/10.1089/ten.teb.2010.0035

Kuhl, S., Payer, M., Kirmeier, R., Wildburger, A., Wegscheider, W., & Jakse, N. (2014). The influence of bone marrow aspirates and concentrates on the early volume stability of maxillary sinus grafts with deproteinized bovine bone mineral - first results of a RCT. *Clinical Oral Implants Research*, *25*, 221–225. https://doi.org/10.1111/clr.12101

Kulakov, A. A., Goldshtein, D. V., Grigoryan, A. S., Rzhaninova, A. A., Alekseeva, I. S., Arutyunyan, I. V., & Volkov, A. V. (2008). Clinical study of the efficiency of combined cell transplant on the basis of multipotent mesenchymal stromal adipose tissue cells in patients with pronounced deficit of the maxillary and mandibulary bone tissue. *Bulletin of Experimental Biology and Medicine*, *146*, 522–525. https://doi.org/10.1007/s10517-009-0322-8

Lavareda Correa, S. C., Elias de Sousa, J., Pasquali, P. J., Scavone de Macedo, L. G., Aloise, A. C., Teixeira, M. L., & Pelegrine, A. A. (2017). Use of bone allograft with or without bone marrow aspirate concentrate in appositional reconstructions: A tomographic and histomorphometric study. *Implant Dentistry*, *26*, 915–921. https://doi.org/10.1097/ID.0000000000000669

Lee, J., Cuddihy, M. J., & Kotov, N. A. (2008). Three-dimensional cell culture matrices: State of the art. *Tissue Engineering Part B Reviews*, *14*, 61–86. https://doi.org/10.1089/teb.2007.0150

Leyendecker Junior, A., Gomes Pinheiro, C. C., Lazzaretti Fernandes, T., & Franco Bueno, D. (2018). The use of human dental pulp stem cells for in vivo bone tissue engineering: A systematic review. *Journal of Tissue Engineering*, *9*, 2041731417752766.

Liao, H. T., & Chen, C. T. (2014). Osteogenic potential: Comparison between bone marrow and adipose-derived mesenchymal stem cells. *World Journal of Stem Cells*, *6*, 288–295. https://doi.org/10.4252/wjsc.v6.i3.288

Liu, H., Slamovich, E. B., & Webster, T. J. (2006). Less harmful acidic degradation of poly(lacticco-glycolic acid) bone tissue engineering scaffolds through titania nanoparticle addition. *International Journal of Nanomedicine*, *1*, 541–545. https://doi.org/10.2147/nano.2006.1.4.541

Lundgren, S., Andersson, S., Gualini, F., & Sennerby, L. (2004). Bone reformation with sinus membrane elevation: A new surgical technique for maxillary sinus floor augmentation. *Clinical Implant Dentistry and Related Research*, *6*, 165–173. https://doi.org/10.1111/j.1708-8208.2004.tb00224.x

MacBeth, N., Trullenque-Eriksson, A., Donos, N., & Mardas, N. (2017). Hard and soft tissue changes following alveolar ridge preservation: A systematic review. *Clinical Oral Implants Research*, *28*, 982–1004. https://doi.org/10.1111/clr.12911

Mangano, C., Piattelli, A., Mangano, A., Mangano, F., Mangano, A., Iezzi, G., … Shibli, J. A. (2009). Combining scaffolds and osteogenic cells in regenerative bone surgery: A preliminary histological report in human maxillary sinus augmentation. *Clinical Implant Dentistry and Related Research*, *11*(Suppl 1), e92–e102. https://doi.org/10.1111/j.1708-8208.2009.00227.x

Marx, R. E., Armentano, L., Olavarria, A., & Samaniego, J. (2013). rhBMP-2/ACS grafts versus autogenous cancellous marrow grafts in large vertical defects of the maxilla: An unsponsored randomized open-label clinical trial. *International Journal of Oral and Maxillofacial Implants*, *28*, e243–e251. https://doi.org/10.11607/jomi.te04

Marx, R. E., & Harrell, D. B. (2014). Translational research: The CD34 + cell is crucial for large-volume bone regeneration from the milieu of bone marrow progenitor cells in craniomandibular reconstruction. *International Journal of Oral and Maxillofacial Implants*, *29*, e201–e209. https://doi.org/10.11607/jomi.te56

Mason, S., Tarle, S. A., Osibin, W., Kinfu, Y., & Kaigler, D. (2014). Standardization and safety of alveolar bone-derived stem cell isolation. *Journal of Dental Research*, *93*, 55–61. https://doi.org/10.1177/0022034513510530

McAllister, B. S., Haghighat, K., & Gonshor, A. (2009). Histologic evaluation of a stem cell-based sinus-augmentation procedure. *Journal of Periodontology*, *80*, 679–686. https://doi.org/10.1902/jop.2009.080345

Mehta, S., Blagg, R., Willcockson, J., Gociman, B., Yamashiro, D., & Siddiqi, F. (2018). Cost-effectiveness analysis of demineralized bone matrix and rhBMP-2 versus autologous iliac crest bone grafting in alveolar cleft patients. *Plastic and Reconstructive Surgery*, *142*, 737–743. https://doi.org/10.1097/PRS.0000000000004646

Meijer, G. J., de Bruijn, J. D., Koole, R., & van Blitterswijk, C. A. (2008). Cell based bone tissue engineering in jaw defects. *Biomaterials*, *29*, 3053–3061. https://doi.org/10.1016/j.biomaterials.2008.03.012

Miguita, L., Mantesso, A., Pannuti, C. M., & Deboni, M. C. Z. (2017). Can stem cells enhance bone formation in the human edentulous alveolar ridge? A systematic review and meta-analysis. *Cell and Tissue Banking*, *18*, 217–228. https://doi.org/10.1007/s10561-017-9612-y

Milinkovic, I., & Cordaro, L. (2014). Are there specific indications for the different alveolar bone augmentation procedures for implant placement? A systematic review. *International Journal of Oral and Maxillofacial Surgery*, *43*, 606–625. https://doi.org/10.1016/j.ijom.2013.12.004

Moher, D., Liberati, A., Tetzlaff, J., & Altman, D. G.; PRISMA Group. (2009). Preferred reporting items for systematic reviews and meta-analyses: The PRISMA statement. *BMJ 339*, b2535. https://doi.org/10.1136/bmj.b2535

Mohty, M., Richardson, P. G., McCarthy, P. L., & Attal, M. (2015). Consolidation and maintenance therapy for multiple myeloma after autologous transplantation: Where do we stand? *Bone Marrow Transplantation*, *50*, 1024–1029. https://doi.org/10.1038/bmt.2015.83

Monti, M., Graziano, A., Rizzo, S., Perotti, C., Del Fante, C., d'Aquino, R., & Redi, C. A. (2017). Rodriguez Y Baena R. *J Cell Physiol.*, *232*, 548–555.

Muschler, G. F., Raut, V. P., Patterson, T. E., Wenke, J. C., & Hollinger, J. O. (2010). The design and use of animal models for translational research in bone tissue engineering and regenerative medicine. *Tissue*

Engineering Part B Reviews, *16*, 123–145. https://doi.org/10.1089/ten.teb.2009.0658

Nagata, M., Hoshina, H., Li, M., Arasawa, M., Uematsu, K., Ogawa, S., … Takagi, R. (2012). A clinical study of alveolar bone tissue engineering with cultured autogenous periosteal cells: Coordinated activation of bone formation and resorption. *Bone*, *50*, 1123–1129. https://doi.org/10.1016/j.bone.2012.02.631

Nakajima, K., Kunimatsu, R., Ando, K., Ando, T., Hayashi, Y., Kihara, T., … Tanimoto, K. (2018). Comparison of the bone regeneration ability between stem cells from human exfoliated deciduous teeth, human dental pulp stem cells and human bone marrow mesenchymal stem cells. *Biochemical and Biophysical Research Communications*, *497*, 876–882. https://doi.org/10.1016/j.bbrc.2018.02.156

Nancarrow-Lei, R., Mafi, P., Mafi, R., & Khan, W. (2017). A systemic review of adult mesenchymal stem cell sources and their multilineage differentiation potential relevant to musculoskeletal tissue repair and regeneration. *Current Stem Cell Research & Therapy*, *12*, 601–610. https://doi.org/10.2174/1574888x12666170608124303

Nkenke, E., & Neukam, F. W. (2014). Autogenous bone harvesting and grafting in advanced jaw resorption: Morbidity, resorption and implant survival. *European Journal of Oral Implantology*, *7*(Suppl 2), S203–S217.

Ogawa, S., Hoshina, H., Nakata, K., Yamada, K., Uematsu, K., Kawase, T., … Nagata, M. (2016). High-resolution three-dimensional computed tomography analysis of the clinical efficacy of cultured autogenous periosteal cells in sinus lift bone grafting. *Clinical Implant Dentistry and Related Research*, *18*, 707–716. https://doi.org/10.1111/cid.12356

Olbrich, M., Rieger, M., Reinert, S., & Alexander, D. (2012). Isolation of osteoprogenitors from human jaw periosteal cells: A comparison of two magnetic separation methods. *PLoS ONE*, *7*, e47176. https://doi.org/10.1371/journal.pone.0047176

Oppenheimer, A. J., Mesa, J., & Buchman, S. R. (2012). Current and emerging basic science concepts in bone biology: Implications in craniofacial surgery. *The Journal of Craniofacial Surgery*, *23*, 30–36. https://doi.org/10.1097/SCS.0b013e318240c6d9

Oryan, A., Kamali, A., Moshiri, A., & Baghaban Eslaminejad, M. (2017). Role of mesenchymal stem cells in bone regenerative medicine: What is the evidence? *Cells Tissues Organs*, *204*, 59–83. https://doi.org/10.1159/000469704

Padial-Molina, M., O'Valle, F., Lanis, A., Mesa, F., Dohan Ehrenfest, D. M., Wang, H. L., & Galindo-Moreno, P. (2015). Clinical application of mesenchymal stem cells and novel supportive therapies for oral bone regeneration. *BioMed Research International*, *2015*, 341327. https://doi.org/10.1155/2015/341327

Pasquali, P. J., Teixeira, M. L., de Oliveira, T. A., de Macedo, L. G., Aloise, A. C., & Pelegrine, A. A. (2015). Maxillary sinus augmentation combining bio-oss with the bone marrow aspirate concentrate: A histomorphometric study in humans. *International Journal of Biomaterials*, *2015*, 121286. https://doi.org/10.1155/2015/121286

Patterson, T. E., Boehm, C., Nakamoto, C., Rozic, R., Walker, E., Piuzzi, N. S., & Muschler, G. F. (2017). The efficiency of bone marrow aspiration for the harvest of connective tissue progenitors from the human iliac crest. *Journal of Bone and Joint Surgery. American Volume*, *99*, 1673–1682. https://doi.org/10.2106/JBJS.17.00094

Payer, M., Lohberger, B., Strunk, D., Reich, K. M., Acham, S., & Jakse, N. (2014). Effects of directly autotransplanted tibial bone marrow aspirates on bone regeneration and osseointegration of dental implants. *Clinical Oral Implants Research*, *25*, 468–474. https://doi.org/10.1111/clr.12172

Pelegrine, A. A., da Costa, C. E., Correa, M. E., & Marques, J. F. Jr (2010). Clinical and histomorphometric evaluation of extraction sockets treated with an autologous bone marrow graft. *Clinical Oral Implants Research*, *21*, 535–542. https://doi.org/10.1111/j.1600-0501.2009.01891.x

Pelegrine, A. A., Teixeira, M. L., Sperandio, M., Almada, T. S., Kahnberg, K. E., Pasquali, P. J., & Aloise, A. C. (2016). Can bone marrow aspirate concentrate change the mineralization pattern of the anterior maxilla treated with xenografts? A preliminary study. *Contemporary Clinical Dentistry*, *7*, 21–26. https://doi.org/10.4103/0976-237X.177112

Petite, H., Viateau, V., Bensaïd, W., Meunier, A., de Pollak, C., Bourguignon, M., … Guillemin, G. (2000). Tissue-engineered bone regeneration. *Nature Biotechnology*, *18*, 959–963. https://doi.org/10.1038/79449

Petrovic, L., Schlegel, A. K., Schultze-Mosgau, S., & Wiltfang, J. (2006). Different substitute biomaterials as potential scaffolds in tissue engineering. *International Journal of Oral and Maxillofacial Implants*, *21*, 225–231.

Pettersson, L. F., Kingham, P. J., Wiberg, M., & Kelk, P. (2017). In vitro osteogenic differentiation of human mesenchymal stem cells from jawbone compared with dental tissue. *Tissue Engineering and Regenerative Medicine*, *14*, 763–774. https://doi.org/10.1007/s13770-017-0071-0

Pinheiro, C. C. G., de Pinho, M. C., Aranha, A. C., Fregnani, E., & Bueno, D. F. (2018). Low power laser therapy: A strategy to promote the osteogenic differentiation of deciduous dental pulp stem cells from cleft lip and palate patients. *Tissue Engineering Part A*, *24*, 569–575. https://doi.org/10.1089/ten.tea.2017.0115

Pradel, W., Eckelt, U., & Lauer, G. (2006). Bone regeneration after enucleation of mandibular cysts: Comparing autogenous grafts from tissue-engineered bone and iliac bone. *Oral Surgery, Oral Medicine, Oral Pathology, Oral Radiology and Endodontics*, *101*, 285–290. https://doi.org/10.1016/j.tripleo.2005.06.001

Pradel, W., & Lauer, G. (2012). Tissue-engineered bone grafts for osteoplasty in patients with cleft alveolus. *Annual of Anatomy*, *194*, 545–548. https://doi.org/10.1016/j.aanat.2012.06.002

Pradel, W., Mai, R., Manolo Hagedorn, G., Lauer, G., & Allegrini, S. Jr (2008). The biomaterial influences the ossification after sinus floor elevation using tissue-engineered bone grafts. *Biomedizinische Technik/Biomedical Engineering*, *53*, 224–228. https://doi.org/10.1515/BMT.2008.034

Prins, H. J., Schulten, E. A., Ten Bruggenkate, C. M., Klein-Nulend, J., & Helder, M. N. (2016). Bone regeneration using the freshly isolated autologous stromal vascular fraction of adipose tissue in combination with calcium phosphate ceramics. *Stem Cells Translational Medicine*, *5*, 1362–1374. https://doi.org/10.5966/sctm.2015-0369

Qadan, M. A., Piuzzi, N. S., Boehm, C., Bova, W., Moos, M. Jr, Midura, R. J., … Muschler, G. F. (2018). Variation in primary and culture-expanded cells derived from connective tissue progenitors in human bone marrow space, bone trabecular surface and adipose tissue. *Cytotherapy*, *20*, 343–360. https://doi.org/10.1016/j.jcyt.2017.11.013

Raposio, E., & Ciliberti, R. (2017). Clinical use of adipose-derived stem cells: European legislative issues. *Annals of Medicine and Surgery (London)*, *24*, 61–64. https://doi.org/10.1016/j.amsu.2017.11.002

Riben, C., & Thor, A. (2016). Follow-up of the sinus membrane elevation technique for maxillary sinus implants without the use of graft material. *Clinical Implant Dentistry and Related Research*, *18*, 895–905. https://doi.org/10.1111/cid.12360

Rickert, D., Sauerbier, S., Nagursky, H., Menne, D., Vissink, A., & Raghoebar, G. M. (2011). Maxillary sinus floor elevation with bovine bone mineral combined with either autogenous bone or autogenous stem cells: A prospective randomized clinical trial. *Clinical Oral Implants Research*, *22*, 251–258. https://doi.org/10.1111/j.1600-0501.2010.01981.x

Rickert, D., Vissink, A., Slot, W. J., Sauerbier, S., Meijer, H. J., & Raghoebar, G. M. (2014). Maxillary sinus floor elevation surgery with BioOss(R) mixed with a bone marrow concentrate or autogenous bone: Test of principle on implant survival and clinical performance. *International Journal of Oral and Maxillofacial Surgery*, *43*, 243–247. https://doi.org/10.1016/j.ijom.2013.09.006

Rocchietta, I., Ferrantino, L., & Simion, M. (2018). Vertical ridge augmentation in the esthetic zone. *Periodontology 2000*, *77*, 241–255. https://doi.org/10.1111/prd.12218

Rodriguez, Y. B. R., D'Aquino, R., Graziano, A., Trovato, L., Aloise, A. C., Ceccarelli, G., … Lupi, S. M. (2017). Autologous periosteum-derived micrografts and PLGA/HA enhance the bone formation in sinus lift augmentation. *Frontiers in Cell and Developmental Biology*, *5*, 87. https://doi.org/10.3389/fcell.2017.00087

Salehi-Nik, N., & Rezai Rad, M. (2017). Buccal fat pad as a potential source of stem cells for bone regeneration: A literature review. *Stem Cell International*, *2017*, 8354640. https://doi.org/10.1155/2017/8354640

Sandor, G. K., Numminen, J., Wolff, J., Thesleff, T., Miettinen, A., Tuovinen, V. J., … Ohman, J. (2014). Adipose stem cells used to reconstruct 13 cases with cranio-maxillofacial hard-tissue defects. *Stem Cells Translational Medicine*, *3*, 530–540. https://doi.org/10.5966/sctm.2013-0173

Sanz-Sánchez, I., Ortiz-Vigón, A., Sanz-Martín, I., Figuero, E., & Sanz, M. (2015). Effectiveness of lateral bone augmentation on the alveolar crest dimension: A systematic review and meta-analysis. *Journal of Dental Research*, *94*(9 Suppl), 128S–142S. https://doi.org/10.1177/0022034515594780

Sauerbier, S., Rickert, D., Gutwald, R., Nagursky, H., Oshima, T., Xavier, S. P., … Koch, F. P. (2011). Bone marrow concentrate and bovine bone mineral for sinus floor augmentation: A controlled, randomized, single-blinded clinical and histological trial–per-protocol analysis. *Tissue Engineering Part A*, *17*, 2187–2197. https://doi.org/10.1089/ten.tea.2010.0516

Sauerbier, S., Stricker, A., Kuschnierz, J., Buhler, F., Oshima, T., Xavier, S. P., … Gutwald, R. (2010). In vivo comparison of hard tissue regeneration with human mesenchymal stem cells processed with either the FICOLL method or the BMAC method. *Tissue Engineering Part C Methods*, *16*, 215–223. https://doi.org/10.1089/ten.tec.2009.0269

Saxer, F., Scherberich, A., Todorov, A., Studer, P., Miot, S., Schreiner, S., … Jakob, M. (2016). Implantation of stromal vascular fraction progenitors at bone fracture sites: From a rat model to a first-in-man study. *Stem Cells*, *34*, 2956–2966. https://doi.org/10.1002/stem.2478

Scherberich, A., Muller, A. M., Schafer, D. J., Banfi, A., & Martin, I. (2010). Adipose tissue-derived progenitors for engineering osteogenic and vasculogenic grafts. *Journal of Cellular Physiology*, *225*, 348–353. https://doi.org/10.1002/jcp.22313

Schimming, R., & Schmelzeisen, R. (2004). Tissue-engineered bone for maxillary sinus augmentation. *Journal of Oral and Maxillofacial Surgery*, *62*, 724–729. https://doi.org/10.1016/j.joms.2004.01.009

Schliephake, H. (2015). Clinical efficacy of growth factors to enhance tissue repair in oral and maxillofacial reconstruction: A systematic review. *Clinical Implant Dentistry and Related Research*, *17*, 247–273. https://doi.org/10.1111/cid.12114

Shanbhag, S., Pandis, N., Mustafa, K., Nyengaard, J. R., & Stavropoulos, A. (2016). Alveolar bone tissue engineering in critical-size defects of experimental animal models: A systematic review and meta-analysis. *Journal of Tissue Engineering and Regenerative Medicine*, *11*, 2935–2949. https://doi.org/10.1002/term.2198

Shanbhag, S., Pandis, N., Mustafa, K., Nyengaard, J. R., & Stavropoulos, A. (2018). Bone tissue engineering in oral peri-implant defects in preclinical in vivo research: A systematic review and meta-analysis. *J Tissue Eng Regen Med*, *12*, e336–e349. https://doi.org/10.1002/term.2412

Shanbhag, S., Shanbhag, V., & Stavropoulos, A. (2014). Volume changes of maxillary sinus augmentations over time: A systematic review. *International Journal of Oral and Maxillofacial Implants*, *29*, 881–892. https://doi.org/10.11607/jomi.3472

Shanbhag, S., Stavropoulos, A., Suliman, S., Hervig, T., & Mustafa, K. (2017). Efficacy of humanized mesenchymal stem cell cultures for bone tissue engineering: A systematic review with a focus on platelet derivatives. *Tissue Engineering Part B Reviews*, *23*, 552–569. https://doi.org/10.1089/ten.teb.2017.0093

Shayesteh, Y. S., Khojasteh, A., Soleimani, M., Alikhasi, M., Khoshzaban, A., & Ahmadbeigi, N. (2008). Sinus augmentation using human mesenchymal stem cells loaded into a beta-tricalcium phosphate/hydroxyapatite scaffold. *Oral Surgery, Oral Medicine, Oral Pathology, Oral Radiology and Endodontics*, *106*, 203–209. https://doi.org/10.1016/j.tripleo.2007.12.001

Shiraishi, T., Sumita, Y., Wakamastu, Y., Nagai, K., & Asahina, I. (2012). Formation of engineered bone with adipose stromal cells from buccal fat pad. *Journal of Dental Research*, *91*, 592–597. https://doi.org/10.1177/0022034512445633

Skovrlj, B., Guzman, J. Z., Al Maaieh, M., Cho, S. K., Iatridis, J. C., & Qureshi, S. A. (2014). Cellular bone matrices: Viable stem cell-containing bone graft substitutes. *Spine Journal*, *14*, 2763–2772. https://doi.org/10.1016/j.spinee.2014.05.024

Soliman, H. A., Ismail, H. E. A., Shouman, O. O., Bahaaeldin, A. M., & El-Hadidy, M. R. (2018). Stem cells assisted cancellous bone graft versus stem cells with demineralized bone matrix for alveolar cleft reconstruction. *Egypt Journal of Plastic Reconstructive Surgery*, *42*, 93–101.

Springer, I. N., Nocini, P. F., Schlegel, K. A., De Santis, D., Park, J., Warnke, P. H., … Wiltfang, J. (2006). Two techniques for the preparation of cell-scaffold constructs suitable for sinus augmentation: Steps into clinical application. *Tissue Engineering*, *12*, 2649–2656. https://doi.org/10.1089/ten.2006.12.2649

Sununliganon, L. (2013). Stem cell approach for maxillary sinus grafting in atrophic maxilla. (Thesis). University of Hong Kong, Pokfulam, Hong Kong SAR. Retrieved from https://doi.org/10.5353/th_b5089951

Talaat, W. M., Ghoneim, M. M., Salah, O., & Adly, O. A. (2018). Autologous bone marrow concentrates and concentrated growth factors accelerate bone regeneration after enucleation of mandibular pathologic lesions. *The Journal of Craniofacial Surgery*, *29*, 992–997. https://doi.org/10.1097/SCS.0000000000004371

Thesleff, T., Lehtimaki, K., Niskakangas, T., Huovinen, S., Mannerstrom, B., Miettinen, S., … Ohman, J. (2017). Cranioplasty with Adipose-derived stem cells, beta-tricalcium phosphate granules and supporting mesh: Six-year clinical follow-up results. *Stem Cells Translational Medicine*, *6*, 1576–1582. https://doi.org/10.1002/sctm.16-0410

Thesleff, T., Lehtimaki, K., Niskakangas, T., Mannerstrom, B., Miettinen, S., Suuronen, R., & Ohman, J. (2011). Cranioplasty with adipose-derived stem cells and biomaterial: A novel method for cranial reconstruction. *Neurosurgery*, *68*, 1535–1540. https://doi.org/10.1227/NEU.0b013e31820ee24e

Trautvetter, W., Kaps, C., Schmelzeisen, R., Sauerbier, S., & Sittinger, M. (2011). Tissue-engineered polymer-based periosteal bone grafts for maxillary sinus augmentation: Five-year clinical results. *Journal of Oral and Maxillofacial Surgery*, *69*, 2753–2762. https://doi.org/10.1016/j.joms.2011.02.096

Trovato, L., Monti, M., Del Fante, C., Cervio, M., Lampinen, M., Ambrosio, L., … Graziano, A. (2015). A new medical device rigeneracons allows to obtain viable micro-grafts from mechanical disaggregation of human tissues. *Journal of Cellular Physiology*, *230*, 2299–2303. https://doi.org/10.1002/jcp.24973

Ueda, M., Yamada, Y., Kagami, H., & Hibi, H. (2008). Injectable bone applied for ridge augmentation and dental implant placement: Human progress study. *Implant Dentistry*, *17*, 82–90. https://doi.org/10.1097/ID.0b013e31815cd591

Ueda, M., Yamada, Y., Ozawa, R., & Okazaki, Y. (2005). Clinical case reports of injectable tissue-engineered bone for alveolar augmentation with simultaneous implant placement. *The International Journal of Periodontics and Restorative Dentistry*, *25*, 129–137.

Vidal, B., Pinto, A., Galvão, M. J., Santos, A. R., Rodrigues, A., Cascão, R., et al. (2012). Bone histomorphometry revisited. *Acta Reumatológica Portuguesa*, *37*, 294–300.

Vizoso, F. J., Eiro, N., Cid, S., Schneider, J., & Perez-Fernandez, R. (2017). Mesenchymal stem cell secretome: Toward cell-free therapeutic strategies in regenerative medicine. *International Journal of Molecular Sciences*, *18*, 1852. https://doi.org/10.3390/ijms18091852

Voss, P., Sauerbier, S., Wiedmann-Al-Ahmad, M., Zizelmann, C., Stricker, A., Schmelzeisen, R., & Gutwald, R. (2010). Bone regeneration in

sinus lifts: Comparing tissue-engineered bone and iliac bone. *British Journal of Oral and Maxillofacial Surgery*, *48*, 121–126. https://doi.org/10.1016/j.bjoms.2009.04.032

Wang, Y., Chen, X., Cao, W., & Shi, Y. (2014). Plasticity of mesenchymal stem cells in immunomodulation: Pathological and therapeutic implications. *Nature Immunology*, *15*, 1009–1016. https://doi.org/10.1038/ni.3002

Wildburger, A., Payer, M., Jakse, N., Strunk, D., Etchard-Liechtenstein, N., & Sauerbier, S. (2014). Impact of autogenous concentrated bone marrow aspirate on bone regeneration after sinus floor augmentation with a bovine bone substitute–a split-mouth pilot study. *Clinical Oral Implants Research*, *25*, 1175–1181. https://doi.org/10.1111/clr.12228

Wojtowicz, A., Chaberek, S., Kisłowska-Syryczyńska, M., Urbanowska, E., Wiktor-Jędrzejczak, W., & Ostrowski, K. (2003). Jaw bone augmentation using autologous bone marrow hematopoietic stem cells and platelets: Fractal analysis of X-ray. *Post Biol Komórki*, *30*(Suppl. 21), 115–126.

Wojtowicz, A., Chaberek, S., Urbanowska, E., & Ostrowski, K. (2007). Comparison of efficiency of platelet rich plasma, hematopoieic stem cells and bone marrow in augmentation of mandibular bone defects. *New York State Dental Journal*, *73*, 41–45.

Wojtowicz, A., Jodko, M., Perek, J., & Popowski, W. (2014). Interactive 3D imaging technologies: Application in advanced methods of jaw bone reconstruction using stem cells/pre-osteoblasts in oral surgery. *Wideochirurgia i Inne Techniki Małoinwazyjne*, *9*, 441–448. https://doi.org/10.5114/wiitm.2014.43126

Wojtowicz, A., Perek, J., Urbanowska, E., Kaminski, A., Olender, E., & Jodko, M. (2013). The treatment of maxillary bone defects used autologic pre-osteoblsts on allogenic bone scaffolds. *Dental and Medical Problems*, *50*, 20–29.

Wolff, J., Sandor, G. K., Miettinen, A., Tuovinen, V. J., Mannerstrom, B., Patrikoski, M., & Miettinen, S. (2013). GMP-level adipose stem cells combined with computer-aided manufacturing to reconstruct mandibular ameloblastoma resection defects: Experience with three cases. *Annals of Maxillofacial Surgery*, *3*, 114–125. https://doi.org/10.4103/2231-0746.119216

Wu, C., Pan, W., Feng, C., Su, Z., Duan, Z., Zheng, Q., … Li, C. (2017). Grafting materials for alveolar cleft reconstruction: A systematic review and best-evidence synthesis. *International Journal of Oral and Maxillofacial Surgery*, *47*, 345–356.

Yamada, Y., Nakamura, S., Ito, K., Kohgo, T., Hibi, H., Nagasaka, T., & Ueda, M. (2008). Injectable tissue-engineered bone using autogenous bone marrow-derived stromal cells for maxillary sinus augmentation: Clinical application report from a 2-6-year follow-up. *Tissue Engineering Part A*, *14*, 1699–1707. https://doi.org/10.1089/ten.tea.2007.0189

Yamada, Y., Nakamura, S., Ito, K., Umemura, E., Hara, K., Nagasaka, T., … Wakabayashi, T. (2013). Injectable bone tissue engineering using expanded mesenchymal stem cells. *Stem Cells*, *31*, 572–580. https://doi.org/10.1002/stem.1300

Yamada, Y., Nakamura, S., Ueda, M., & Ito, K. (2013). Osteotome technique with injectable tissue-engineered bone and simultaneous implant placement by cell therapy. *Clinical Oral Implants Research*, *24*, 468–474. https://doi.org/10.1111/j.1600-0501.2011.02353.x

Yorukoglu, A. C., Kiter, A. E., Akkaya, S., Satiroglu-Tufan, N. L., & Tufan, A. C. (2017). A concise review on the use of mesenchymal stem cells in cell sheet-based tissue engineering with special emphasis on bone tissue regeneration. *Stem Cells International*, *2017*, 2374161. https://doi.org/10.1155/2017/2374161

Zakhari, J. S., Zabonick, J., Gettler, B., & Williams, S. K. (2018). Vasculogenic and angiogenic potential of adipose stromal vascular fraction cell populations in vitro. *In Vitro Cellular & Developmental Biology – Animal*, *54*, 32–40. https://doi.org/10.1007/s11626-017-0213-7

Zizelmann, C., Schoen, R., Metzger, M. C., Schmelzeisen, R., Schramm, A., Dott, B., … Gellrich, N. C. (2007). Bone formation after sinus augmentation with engineered bone. *Clinical Oral Implants Research*, *18*, 69–73. https://doi.org/10.1111/j.1600-0501.2006.01295.x

SUPPORTING INFORMATION

Additional supporting information may be found online in the Supporting Information section at the end of the article.

How to cite this article: Shanbhag S, Suliman S, Pandis N, et al. Cell therapy for orofacial bone regeneration: A systematic review and meta-analysis. *J Clin Periodontol*. 2019;46(Suppl. 21):162–182. https://doi.org/10.1111/jcpe.13049

TISSUE ENGINEERING: Part B
Volume 00, Number 00, 2017
© Mary Ann Liebert, Inc.
DOI: 10.1089/ten.teb.2017.0093

termis
Tissue Engineering
& Regenerative Medicine
International Society

Downloaded by Mary Ann Liebert, Inc., publishers from online.liebertpub.com at 08/03/17. For personal use only.

REVIEW ARTICLE

Efficacy of Humanized Mesenchymal Stem Cell Cultures for Bone Tissue Engineering: A Systematic Review with a Focus on Platelet Derivatives

Siddharth Shanbhag, DDS, MSc,[1] Andreas Stavropoulos, DDS, PhD,[2] Salwa Suliman, DDS, PhD,[1] Tor Hervig, MD, PhD,[3] and Kamal Mustafa, DDS, PhD[1]

Fetal bovine serum (FBS) is the most commonly used supplement for *ex vivo* expansion of human mesenchymal stem cells (hMSCs) for bone tissue engineering applications. However, from a clinical standpoint, it is important to substitute animal-derived products according to current good manufacturing practice (cGMP) guidelines. Humanized alternatives to FBS include three categories of products: human serum (HS), human platelet derivatives (HPDs)—including platelet lysate (PL) or platelet releasate (PR), produced by freeze/thawing or chemical activation of platelet concentrates, respectively, and chemically defined media (serum-free) (CDM). In this systematic literature review, the *in vitro* and *in vivo* osteogenic potential of hMSCs expanded in humanized (HS-, HPD-, or CDM-supplemented) media versus hMSCs expanded in FBS-supplemented media, was compared. In addition, PL and PR were compared in terms of their growth factor (GF)/cytokine-content and cell-culture efficacy. When using either 10–20% autologous or pooled HS, 3–10% pooled HPDs or CDM supplemented with GFs, in comparison with 10–20% FBS, a majority of studies reported similar or superior *in vitro* proliferation and osteogenic differentiation, and *in vivo* bone formation in ectopic or orthotopic rodent models. Moreover, a trend for higher GF content was observed in PL versus PR, although evidence for cell culture efficacy is limited. In summary, humanized supplements seem at least equally effective as FBS for hMSC expansion and osteogenic differentiation. Although pooled HPDs appear to be the most favorable supplement for large-scale hMSC expansion, further efforts are needed to standardize the preparation and composition of these products in compliance with cGMP standards.

Keywords: serum-free media, human serum, platelet-rich plasma, platelet lysate, platelet releasate, mesenchymal stem cells, good manufacturing practices

Background

Reconstruction of maxillofacial bone deficiencies, resulting from trauma, pathology, or ablative surgery, often poses a clinical challenge.[1] Although autologous bone transplantation is still considered the ''gold standard'' for maxillofacial bone regeneration, large defects may require volumes of bone locally unavailable.[2] Moreover, the morbidity associated with bone harvesting is often a major limiting factor.[3] Alternatives to autologous bone include allogeneic, xenogeneic, and synthetic bone substitutes, but no consensus currently exists on the effectiveness of one material over the other, in comparison with autologous bone, or in various indications.[4,5]

The bone tissue engineering (BTE) approach involves harvesting of osteogenic cells, commonly mesenchymal stem cells (MSCs), usually from an autologous source (bone marrow, adipose tissue, dental tissues, etc.), their *in vitro* expansion, and combination with an appropriate carrier scaffold for *in vivo* implantation.[6] More recently, the use of allogeneic or ''off-the-shelf'' MSC-based products has been proposed,[7] although several concerns still exist around their clinical safety.[8] Nevertheless, the ''triad'' of (autologous or allogeneic) *osteogenic* cells, *osteoinductive* signals (growth factors [GFs] released by cells), and *osteoconductive* scaffolds may replicate the properties of autologous bone, without the need for invasive harvesting.[9] The prospects of BTE are very promising as demonstrated by several

[1]Department of Clinical Dentistry, Centre for Clinical Dental Research, University of Bergen, Bergen, Norway.
[2]Department of Periodontology, Faculty of Odontology, Malmö University, Malmö, Sweden.
[3]Department of Immunology and Transfusion Medicine, Haukeland University Hospital, Bergen, Norway.

Downloaded by Mary Ann Liebert, Inc., publishers from online.liebertpub.com at 08/03/17. For personal use only.

preclinical (see review[10]) and some clinical studies (see reviews[6,11]).

Strategies for using human MSCs (hMSCs) in regenerative therapy may involve either (1) the direct clinical use of tissue fractions containing these cells (along with other supporting cells), for example, whole or concentrated bone marrow, or adipose stromal vascular fractions (SVFs), usually performed through a ''chair-side'' procedure without the need for current good manufacturing practice (cGMP)-grade laboratories, or, more commonly, (2) the *ex vivo* expansion of hMSCs from harvested tissues, for example, bone marrow or adipose tissues, in cGMP-grade conditions before clinical application, to achieve relevant number of cells. Traditionally, *ex vivo* expansion of hMSCs has been performed using basal culture media plus supplements to provide GFs, proteins, and enzymes to support cell growth.[12] Fetal bovine serum (FBS) (or fetal calf serum) is most commonly used to supplement hMSC cultures, because the fetal milieu is enriched with GFs and poor in antibodies. However, for clinical use it is important to substitute animal-derived products, because hMSCs can internalize xenogeneic proteins, and thus carry the risk of infection (through viral or prion agents) and immunoreaction; it has been reported that a single injection of 100 million hMSCs expanded in 20% FBS-supplemented media is associated with $\sim$7–30 mg of calf serum proteins.[13] In addition, there are concerns regarding FBS sample-to-sample inconsistency, and animal welfare in terms of the ''3 R's'' principle (replacement, reduction, refinement).[14,15]

Although use of clinical-grade FBS may be permitted by regulatory health agencies in phase-1 clinical studies—>80% of proposals submitted to the FDA for MSC-based products report expansion in FBS,[16] later phase trials involving larger patient groups demand the use of culture conditions free of animal-derived products, according to cGMP guidelines.[14,17,18] Such ''xeno-free'' or humanized alternatives to FBS broadly include three categories of products: (1) autologous or allogeneic human serum (HS), (2) pooled human platelet derivatives (HPDs), and (3) chemically defined media (serum-free) (CDM).[19] HPDs are of particular interest, given the wide range of physiological GFs and cytokines released by platelets, which can significantly enhance cell growth and function.[20–23] HPDs include (1) *platelet-rich plasma* (PRP): a concentration of platelets in a small volume of plasma and a starting point for the other platelet products, which, depending on the method of releasing GFs, are either (2) *platelet lysate* (PL): produced by physical disruption of platelets in PRP through one or more freezing/thawing cycle(s) or (3) *platelet releasate* (PR): produced by chemical activation of platelets in PRP through coagulation, most commonly with thrombin and/or calcium compounds.[23]

When using new culture conditions for hMSC expansion, it is important to characterize the cells in different stages, to rule out significant changes in their properties, for example, phenotype, proliferation, and differentiation potential, both *in vitro* and *in vivo*.[24,25] Preclinical *in vivo* testing of new regenerative therapies in relevant animal models is an important aspect of translational research, and in most cases a requirement of regulatory health agencies, before initiating human clinical trials.[26,27] In BTE research, implantation of cells or cell-based constructs in ectopic, that is, nonosseous sites (e.g., subcutaneous or intramuscular), usually constitutes a starting point for *proof-of-principle* or feasibility studies, whereas implantation in orthotopic sites (e.g., ''critical size'' defects (CSDs) in calvarial or alveolar bone) aims to simulate clinical conditions, especially in large animal models (dogs, sheep, etc.), and predict potential for therapeutic efficacy.[28,29]

The primary aim of this study was to systematically review the available literature to answer the focused question: do hMSCs expanded in humanized (HS-, HPD-, or CDM-supplemented) media possess superior osteogenic potential *in vitro* and enhance bone formation *in vivo* in ectopic or orthotopic animal models, compared with hMSCs expanded in FBS-supplemented media? A secondary aim of the review was to compare different HPDs in terms of their GF/cytokine content and efficacy for use in cell culture.

Materials and Methods

Study design

A review protocol was developed based on the preferred reporting items for systematic reviews and meta-analyses (PRISMA) guidelines,[30] and predetermined inclusion/exclusion criteria.

Inclusion criteria

(1) Studies reporting both *in vitro* and *in vivo* outcomes of humanized hMSC cultures.
(2) (a) Inclusion of randomized or nonrandomized controlled animal experimental studies with two or more experimental groups and (b) use of ectopic (subcutaneous or intramuscular) and/or orthotopic (bone defect) models in small or large animals.
(3) Transplantation of human-derived cells (MSCs or osteoblasts) expanded in FBS-free cultures in at least one experimental group.
(4) A control group receiving FBS-supplemented culture-expanded cells.
(5) Reporting of qualitative and/or quantitative histological data, or quantitative three-dimensional (3D) radiographic data (through computed tomography [CT] or micro-CT), regarding new bone formation (NBF).

Exclusion criteria. Absence of an FBS-supplemented culture group, that is, studies reporting *in vivo* comparisons of scaffolds and cells expanded in humanized media versus scaffolds alone (without cells).

Search strategy, screening, and study selection

Electronic databases of MEDLINE (through PubMed) and EMBASE were searched for relevant English language literature up to and including October 2016. ''Gray'' literature was searched through the Google and Google Scholar search engines. Bibliographies of the selected studies and relevant review articles were checked for cross references. A specific search strategy was developed for MEDLINE (Supplementary Table S1; Supplementary Data are available online at www.liebertpub.com/teb) and adapted for other databases. Titles and abstracts of the search-identified studies were screened by two authors (S.S. and A.S.) and full

Downloaded by Mary Ann Liebert, Inc., publishers from online.liebertpub.com at 08/03/17. For personal use only.

texts of all eligible studies were obtained. Uncertainty in the determination of eligibility was resolved by discussion with the other authors. Two authors (S.S. and A.S.) reviewed the selected full texts independently and final inclusion was based on the aforementioned inclusion criteria. A summary of the screening process is presented in Figure 1.

Data extraction

Data were extracted from the full texts of selected articles on author(s), study design, *in vitro* evaluations (hMSC proliferation, characterization/phenotype, differentiation), *in vivo* evaluations (animal species, model type [ectopic/orthotopic], number of animals/procedures, observation time(s), and method(s) of outcome evaluation), main findings, and conclusions. Descriptive summaries of studies were entered into tables. Quantitative data regarding NBF were extracted for possible meta-analysis. Authors were contacted in cases of incomplete or unclear data.

Risk of bias

Risk of bias (RoB) assessment was performed using a modification of the *SY*stematic *R*eview *C*entre for *L*aboratory animal *E*xperimentation (SYRCLE) RoB tool for animal studies and judged as ''high,'' ''low,'' or ''unclear''[31,32] (Supplementary Table S2). Any disagreement between the reviewers during study selection, data extraction, and quality assessment was resolved by discussion and consensus.

Results

Search results and study characteristics

Of the 128 search-identified studies, 15 studies[33–47] reporting both *in vitro* and *in vivo* comparisons of FBS-free and FBS-supplemented hMSC cultures were included in the review (Tables 1 and 2). A list of excluded studies along with reasons for exclusion—most commonly absence of an FBS control group—is reported in Supplementary Table S3. All included studies reported the use of rodent models, that is, rats and mice. Thirteen studies reported on subcutaneous, that is, ectopic, implantation models, three studies reported on orthotopic, that is, bone defect, models, and one study[44] reported on both ectopic and orthotopic models. Observation times ranged from 4 to 9 weeks and 5 to 12 weeks for ectopic and orthotopic models, respectively.

Risk of bias

Random allocation of animals or defects to different treatment groups, to minimize ''selection bias,'' was not reported in any of the studies. Similarly, no studies reported blinding of outcome assessors to treatment groups, to minimize ''detection bias.'' All studies reported outcome evaluation, including statistical analyses in case of quantitative outcomes, but few reported any information on adverse reactions or complications. Overall, RoB in most studies was judged to be ''high'' (Supplementary Table S2).

Characteristics of humanized culture strategies

Cells. All studies reported the use of human-derived cells, most commonly bone marrow-derived MSCs (BMSCs). Other types of cells used were periosteum-derived cells,[39] umbilical cord-derived MSCs (UCMSCs),[44] dental pulp-derived MSCs (DPSCs),[38] and adipose tissue-derived MSCs (ASCs)[47] or SVFs.[42,45] The number of implanted cells ranged from 1×10^5 to 2.5×10^6 per implant. One study[34] reported cryopreservation (at passage 2) and revival of BMSCs after 3 months for *in vivo* implantation.

Media supplements. Humanized supplements could be broadly categorized as HS, HPDs (PRP, PL, or PR), and CDM. HS (5–20%) was derived from peripheral blood and used in autologous (same donor(s) as MSCs) or allogeneic forms (pooled from multiple donors). One study[40] reported the use of 3% pooled PRP with additional GFs (epidermal growth factor [EGF], platelet-derived growth factor-BB [PDGF-BB]). Four studies[41–44] used 5% pooled PL, whereas one study[45] used 10% pooled thrombin-activated PR. All studies using PL or PR reported the addition of heparin to the medium (usually 2 U/mL) to prevent clot formation.

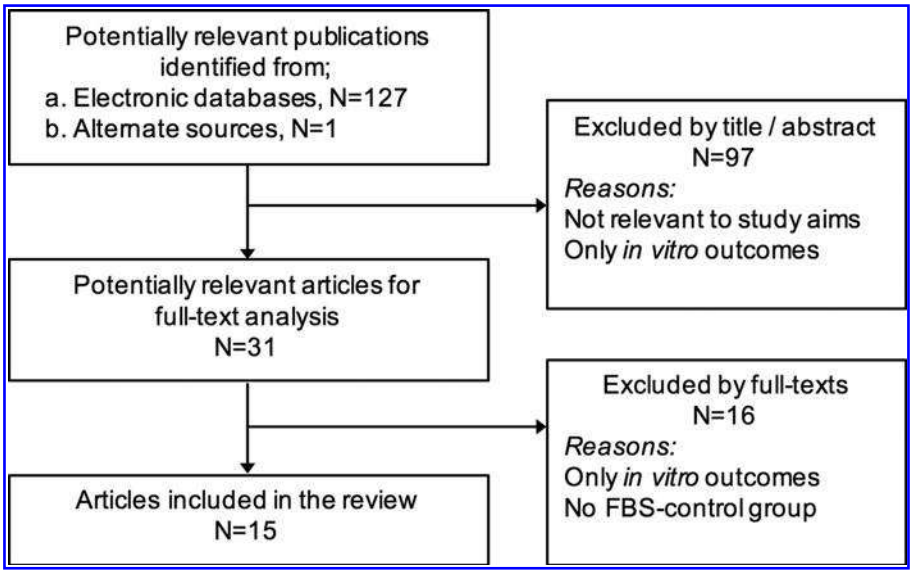

FIG. 1. Flowchart for study screening and selection; *n*, number of articles.

Downloaded by Mary Ann Liebert, Inc., publishers from online.liebertpub.com at 08/03/17. For personal use only.

Table 1. Summary of *In Vitro* Outcomes in the Included Studies

Study	*Cells, donor's age*	*Media supplements*	In vitro		
			Phenotype	*Proliferation*	*Osteogenic differentiation*
Human serum					
Kuznetsov *et al.*[33]	BMSC, $N=6$; 0.5–15 years	20% HS (commercial) 20% FBS	NR	*n* at pass-2, CFU-F at 11 days: FBS>HS[a]	NR
Matsuo *et al.*[34]	BMSC, $N=7$; 6–32 years; cryo	10% auto HS+bFGF 10% FBS	NR	NR	ARS: ND
Pytlik *et al.*[35]	BMSC, $N=105$; 21–86 years	10% pooled HS (5 donors)±rh-GF (Dex, FGF-2, EGF, PDGF-BB, M-CSF) 10% FBS	hMSC ($CD45^-$, $CD235a^-$): FBS>HS^-, but = HS^+ Other markers[b]	*n* at 14 days: HS^+>FBS[a] CFU-F at 14 days: FBS>HS/HS^+[a]	VKS, IHC (ALP, Col-I): ND
Stehlik *et al.*[36]	BMSC, $N=$NR	10% pooled HS (5 donors)+rh-GF (Dex, FGF-2, EGF, PDGF-BB, M-CSF) 10% FBS	hMSC (CD45-, CD235a-): ND Other markers[b]	*n* at 14 days: HS^+>FBS	VKS, ALP-a: ND
Takeda *et al.*[37]	BMSC, $N=8$; 7–11 years	10% auto HS 10% FBS	NR	*n* at pass-2: FBS>HS[a]	ALP-a: HS>FBS[a] PCR (ALP, OC): ND
Pisciotta *et al.*[38]	DPSC, $N=$NR; teen	10% pooled HS (NR) 10% FBS	Stro-1^+, c-Kit^+, $CD34^+$: ND	*n* for 7 days, PD for 5 passes: HS>FBS[a] CFU-F: ND	ALP-a, ARS: HS>FBS[a] IHC (OC, OP, *Osx*, *Runx-2*, Col-I): ND
Roberts *et al.*[39]	POC, $N=6$; 18 ± 8 years	10% pooled HS (15 donors) 10% FBS	NR	*n* for 14 days: HS>FBS[a]	ALP-a, PCR (*Runx-2*, ALP), ARS: HS>FBS[a]
Platelet derivatives					
Vogel *et al.*[40]	BMSC, $N=6$; 12–75 years	3% pooled PRP [5 donor buffy coats (1.5×10^6/μL), stirring for clot formation]+EGF, PDGF-BB 2% FBS+EGF, PDGF-BB	NR	*n* at pass-4: PRP>FBS	ALP-a: ND ARS: FBS>PRP[a]
Prins *et al.*[41]	BMSC, $N=9$; 4–74 years	5% pooled PL [4 donor buffy coats (1×10^9/mL), 1 FT at −80°C, 10 U/mL Heparin] 10% FBS	$CD73^+$, $CD90^+$, $CD105^+$; $CD14^-$, $CD31^-$, $CD34^-$, $CD45^-$: ND	*n* at pass-3: PL>FBS[a] CFU-F at 10 days: ND	ALP-a: ND
Muller *et al.*[42]	SVFs, $N=16$; 47 ± 23 years	5% pooled PL [7 donor apheresis (1×10^9/mL), 1 FT at −80°C, 2 U/mL heparin] 10% FBS+FGF-2 (3D dynamic culture, 5 days)[c]	$CD90^+$, $CD105^+$, $CD45^-$: ND $CD31^+$, $CD34^+$: PL>FBS $CD146^+$: FBS>PL[d]	*n* at pass-3: FBS>PL CFU-F at 14 days: ND	ARS: ND
Chevallier *et al.*[43]	BMSC, $N=10$; 36–54 years	5% pooled PL [4 donor apheresis (1×10^9/mL), 1 FT at −80°C, 2 U/mL heparin] 10% FBS	$CD73^+$, $CD90^+$, $CD105^+$, $CD45^-$: ND	PD at 7 days: PL>FBS[a]	ARS: ND PCR (ALP, OP, BSP, BMP-2): PL>FBS[a] PCR (*Runx-2*, OC): ND

(*continued*)

Downloaded by Mary Ann Liebert, Inc., publishers from online.liebertpub.com at 08/03/17. For personal use only.

Table 1. (Continued)

Study	*Cells, donor's age*	*Media supplements*	In vitro		
			Phenotype	*Proliferation*	*Osteogenic differentiation*
Todeschi *et al.*[44]	UCMSC (N=NR), *BMSC as control*	UCMSC: 5% pooled PL [5 donor buffy coats ($1–2\times10^6$/μL), 3 FT at −30°C, 2 U/mL heparin] BMSC: 10% FBS	NR	NR	NR
Tchang *et al.*[45]	SVFs, N=13	10% pooled tPR [8 donor buffy coats ($2–3\times10^6$/μL), 1 U/mL h-T, 2 U/mL heparin] 10% FBS+FGF-2 (3D dynamic culture, 5 days)[c]	In 3D; $CD73^+$, Runx-2^+, OC^+, $CD31^+$: ND	In 3D; n at 5 days: tPR>FBS[a] CFU-F at 14 days: tPR>FBS	In 2-D; FC (OC^+): ND ARS: ND IHC (CD31): ND[e] In 3D; PCR (*Runx-2*, ON, VEGF): tPR>FBS
Chemically defined media					
Agata *et al.*[46]	BMSC, N=4; 26–37 years	CDM (commercial) 10% FBS	$CD73^+$, $CD90^+$, $CD34^-$, $CD45^-$, HLA-DR^- $CD105^+$: CDM>FBS $CD146^+$: FBS>CDM[f]	Yield, n: CDM>FBS	ALP-a: FBS>CDM[g]
Sato *et al.*[47]	ASC, N=26; 49–84 years	CDM+rh-GF (bFGF, PDGF-BB, TGF-β1), BSA 10% FBS	$CD73^+$, $CD90^+$, $CD34^-$, $CD45^-$: ND At pass-5; $CD74^+$, $CD90^+$, $CD105^+$, $CD14^-$, $CD31^-$, $CD34^-$, $CD45^-$, HLA-DR^-: ND	Rate, PD for 30 days: CDM>FBS[a]	ARS: ND PCR (*Runx-2*, OC, OP, ALP, Col-I): ND PCR (CCL2, CCL5, BMP-2): CDM>FBS[a] ELISA (CCL2, CCL5, BMP-2): CDM>FBS[a] (only for CCL2)[h]

[a]Statistically significant differences.
[b]HS-supplemented cultures had significantly higher expression of $CD29^+$, $CD49c^+$, $CD49d^+$, $CD106^+$, and/or $CD71^+$ cells.
[c]SVF cells were directly seeded and cultured inside a porous HA scaffold in a bioreactor system with either 10% FBS or tPR for 5 days.
[d]PL cultures had significantly higher proportion of $CD31^+/CD34^+$ cells, whereas FBS cultures had higher proportion of $CD146^+$ cells.
[e]SVF cells cultured for 1 week inside fibrin gels formed $CD31^+$ tubular structures.
[f]CDM cultures had significantly higher proportion of $CD105^+$ cells, whereas FBS cultures had higher proportion of $CD146^+$ cells.
[g]Absolute ALP-a of BMSC expanded in FBS was higher than in CDM; however, the ratio of ALP-a (ALP-a of induced cells/noninduced cells) was higher in CDM than in FBS.
[h]Although CCL2 was higher in CDM-cultured cells than in FBS-cultured cells, CCL5 and BMP-2 were equally stimulated by TNF-α in both conditions.

3D, three dimensional; (non)induced, osteogenically (non)induced; ALP-a, alkaline phosphatase activity; ASCs, adipose tissue-derived MSCs; ARS, alizarin red staining; auto, autologous; blood, peripheral blood; bFGF, basic fibroblast growth factor; BMP, bone morphogenetic protein; BMSC, bone marrow-derived MSC; BSP, bone sialoprotein; CFU-F, colony forming unit-fibroblast efficiency; CDM, chemically defined media (serum-free); Col-I, collagen-I; cryo, cryopreserved; DPSCs, dental pulp-derived MSCs; EGF, epidermal growth factor; FBS, fetal bovine serum; FC, flow cytometry; FGF, fibroblast growth factor; FT, freeze/thaw cycles; GF, growth factor; HA, hydroxyapatite; HS, human serum; hMSC, human MSC; hT, human thrombin; IHC, immunohistochemistry; M-CSF, macrophage colony-stimulating factor; MSC, mesenchymal stem cell; n, number of cells/counts; n, number of animals; N, number of donors; ND, no significant differences; NR, not reported; OC, osteocalcin; OP, osteopontin; pass-, passage (number); PCR, polymerase chain reaction (gene expression); PD, population doubling; PDGF, platelet-derived growth factor; PL, platelet lysate; PRP, platelet-rich plasma; rh-GF, recombinant human growth factor; SVFs, stromal vascular fractions; TGF, transforming growth factor; TNF, tumor necrosis factor; tPR, thrombin-activated platelet releasate; UCMSCs, umbilical cord-derived MSCs; VEGF, vascular endothelial growth factor; VKS, von Kossa staining; yield, initial cell yield.

Downloaded by Mary Ann Liebert, Inc., publishers from online.liebertpub.com at 08/03/17. For personal use only.

Table 2. Summary of *In Vivo* Outcomes in the Included Studies

Study	*Cells, induction, no. of cells*	*Media supplements*	In vivo			
			Model	*Animals observation*	*Scaffold*	*Outcomes*
Human serum						
Kuznetsov *et al.*[33]	BMSC, noninduced, 2.5×10^6	20% HS 20% FBS SF media	Subcutaneous	ID mice (female, 15 weeks, $n=$NR) 8 weeks	HA-TCP	Semi-quan histo: FBS>HS FBS changed to HS>HS
Matsuo *et al.*[34]	BMSC, induced, 1×10^5	10% auto HS+bFGF 10% FBS	Subcutaneous	ID mice (male, 5 weeks, $n=$NR) 6, 9 weeks	HA	Quan histo: HS=FBS
Pytlik *et al.*[35]	BMSC, induced, 2×10^5	10% pooled HS±rh-GF 10% FBS	Subcutaneous	ID mice ($n=$NR) 6–9 weeks	PLA	Qual histo: HS=FBS
Stehlik *et al.*[36]	BMSC, induced, 2×10^5	10% pooled HS+rh-GF 10% FBS	Subcutaneous	ID mice 6 weeks	PLA	Qual histo: HS>FBS
Takeda *et al.*[37]	BMSC, noninduced, 1×10^5	10% auto HS 10% FBS	Subcutaneous	ID mice (male, 5 weeks, $n=$NR) 4 weeks	HA	Qual histo: HS>FBS
Pisciotta *et al.*[38]	DPSC, induced, 1×10^6	10% pooled HS 10% FBS	Calvarial CSD (5×8 mm)	SD rats (male, 14 weeks) 6 weeks	Collagen sponge	Quan histo: HS>FBS
Roberts *et al.*[39]	POC, noninduced, 1×10^6	10% pooled HS 10% FBS	Subcutaneous	ID mice 8 weeks	CP	Quan histo, μ-CT: HS>FBS
Platelet derivatives						
Vogel *et al.*[40]	BMSC, noninduced, 2×10^5 or 10^6	3% pooled PRP 2% FBS +EGF, PDGF-BB	Subcutaneous	ID mice ($n=6$) 8 weeks	TCP, CDHA	Semi-quan histo: PRP=FBS
Prins *et al.*[41]	BMSC, induced, 2×10^5	5% pooled PL 10%FBS	Subcutaneous	ID mice (male, $n=10$) 6 weeks	BCP	Quan histo: PL=FBS
Muller *et al.*[42]	SVFs, noninduced, 3×10^6	5% pooled PL 10% FBS +FGF-2 (3D dynamic culture, 5 days)[a]	Subcutaneous	ID mice (1 month, $n=$NR) 8 weeks	HA	Quan histo: PL=FBS (bone) FBS>PL (vessel)

(*continued*)

Downloaded by Mary Ann Liebert, Inc., publishers from online.liebertpub.com at 08/03/17. For personal use only.

Table 2. (Continued)

Study	Cells, induction, no. of cells	Media supplements	In vivo			
			Model	Animals observation	Scaffold	Outcomes
Chevallier *et al.* 2010[43]	BMSC, noninduced, 3×10^5	5% pooled PL 10% FBS	Subcutaneous	ID mice (7 weeks, $n=6$) 7 weeks	HA-TCP	Qual histo: PL>FBS
Todeschi *et al.*[44]	UCMSC, noninduced, 2.5×10^6, *BMSC as control*	5% pooled PL (UCMSC) 10% FBS (BMSC)	Subcutaneous	ID mice (NR) 60 days	HA-Si-TCP+fibrin	Qual histo, quan vessels BMSC>UCMSC (bone) UCMSC>BMSC (vessels)
			Calvarial CSD (5 mm)	ID mice ($n=9$) 90 days	HA-PU+fibrin	Quan histo: UCMSC = BMSC
Tchang *et al.*[45]	SVFs, induced, 5×10^6	10% pooled tPR 10% FBS+FGF-2 (3D dynamic culture, 5 days)[a]	Subcutaneous	ID mice (NR) 8 weeks	HA	Quan histo: tPR>FBS (bone) tPR = FBS (vessels)
Chemically defined media						
Agata *et al.*[46]	BMSC, induced, 5×10^5	CDM (commercial) 10% FBS	Subcutaneous	ID mice (female, 6 weeks, $n=$NR) 4 weeks	TCP	Quan histo: CDM = FBS
Sato *et al.*[47]	ASC, noninduced, 5×10^5	CDM+rh-GF, BSA 10% FBS	Femur fracture	ID mice (12 weeks, $n=100$) 20, 30, 40 days	Gelfoam	Qual histo, μ-CT Histo: CDM>FBS μ-CT: CDM>FBS

[a]SVF cells were directly seeded and cultured inside a porous HA scaffold in a bioreactor system with either 10% FBS or tPR for 5 days. For details of cells and media supplements, see Table 2.

μ-CT, micro-computed tomography; BCP, biphasic calcium phosphate; BSA, bovine serum albumin; CDHA, calcium-deficient HA; CP, calcium phosphate; CSDs, critical size defects; HA, hydroxyapatite; histo, histological bone formation; ID, immunodeficient; *n*, number of animals; PLA, poly(L-lactide); PU, polyurethane; qual, qualitative; quan, quantitative; SD, Sprague Dawley; Si, silica; TCP, tricalcium phosphate; vessels, vessel formation.

Downloaded by Mary Ann Liebert, Inc., publishers from online.liebertpub.com at 08/03/17. For personal use only.

Two studies used serum-free CDM: (1) a commercial MSC expansion medium (STEMPRO® MSC SFM basal medium+supplement; Invitrogen)[46] and (2) a specifically defined medium for ASC, containing growth factors (fibroblast growth factor-2 [FGF-2]/basic fibroblast growth factor [bFGF], transforming growth factor [TGF]-β, PDGF-BB), and bovine serum albumin[47]—this medium was not humanized in the true sense, as it was not *completely* free of animal products. In seven studies,[34–36,38,41,45,46] cells were osteogenically induced before *in vivo* implantation.

In vitro *outcomes*

A summary of the *in vitro* outcomes in the included studies is presented in Table 1. A majority of studies reported no differences between the immunophenotype of hMSCs expanded in humanized or FBS-based cultures, based on surface antigen expression using fluorescence-activated cell sorting. Seven of the 13 studies reported significantly greater MSC proliferation in humanized cultures, that is, HS,[38,39] PRP,[40] PL,[43] PR,[45] or CDM,[46,47] versus FBS-supplemented cultures. Two studies[33,37] reported significantly greater proliferation in FBS-supplemented versus HS-supplemented cultures. Osteogenic differentiation of hMSCs, assessed through alkaline phosphatase activity (ALP-a), gene expression of osteogenic markers, and/or mineralization assays, was reported to be comparable or greater in humanized versus FBS-based cultures. Detailed *in vitro* results from the included studies are presented in Supplementary Data.

In vivo *outcomes*

Qualitative outcomes. Seven studies[35–37,42–44,47] reported only qualitative histological outcomes after ectopic (six studies) or orthotopic (one study) implantation of cells grown in FBS-free or FBS-supplemented media (Table 2). In most cases, more favorable histological outcomes were reported in implants of FBS-free (HS or PL) cultured cells, for example, enhanced cellular response, better organization of collagen fibers, more osteoid and extracellular matrix formation, and superior mineralization. In one study,[44] more mature bone formation was observed in implants of BMSCs cultured in FBS media than in those of UCMSCs in PL media, whereas in another study,[42] limited bone formation was observed in implants of both FBS- and PL-cultured cells after 3D dynamic culture.

Quantitative outcomes. Nine studies reported quantitative (or semiquantitative) histomorphometric outcomes, most commonly, estimation of NBF within ectopic implants[33,34,39–41,45,46] or calvarial defects[38,44] (Table 2). One study[47] reported radiographic bone density measurements, through micro-CT, in a rat femur ''fracture model.'' Mineral phase (hydroxyapatite [HA], beta-tricalcium phosphate [β-TCP], biphasic [HA-TCP]) or collagen scaffolds were used as cell carriers for implantation.

In ectopic models, a majority of studies reported either similar or significantly greater NBF by cells cultured in FBS-free media than by cells cultured in FBS-supplemented media after 4–8 weeks. In one study,[33] maximum NBF was observed in implants of BMSCs cultured in FBS-supplemented media changed to serum-free CDM (supplemented with insulin–transferrin–sodium selenite), compared with BMSCs cultured continuously in FBS-supplemented media, BMSCs cultured continuously in HS-supplemented media, or BMSCs cultured in FBS-supplemented media changed to HS-supplemented media, 3 days before implantation. In two studies, adipose-derived SVF cells were directly cultured on 3D scaffolds under dynamic conditions in either 5% pooled PL[42] or 10% pooled PR[45] before implantation, and similar[42] or superior[45] NBF in comparison with cells cultured dynamically in 10% FBS (+FGF-2) was observed. However, no blood vessels of human origin could be detected in implants of PL-supplemented cells (as compared with FBS-supplemented cells),[42] but similar vessel densities were reported in implants of PR-supplemented cells and FBS-supplemented cells.[45] In another study,[44] significantly greater vessel formation was observed in implants of UCMSCs cultured in PL-supplemented media than in those of BMSCs in FBS-supplemented media (although a reverse trend for orthotopic bone formation was observed). Further analysis revealed that vessel formation resulted from the paracrine angiogenic effects of UCMSCs rather than their direct endothelial differentiation.[44]

In calvarial defect models, one study[44] reported similar NBF by UCMSCs cultured in PL-supplemented media and BMSCs in FBS-supplemented media, and seeded on HA-copolymer scaffolds. However, *in situ* hybridization revealed that in the latter, NBF resulted from direct osteogenic differentiation of implanted BMSCs, whereas in the UCMSC implants, NBF resulted primarily through recruitment of host cells.[44] In another study,[38] significantly greater NBF and vessel formation were observed in implants of osteogenically differentiated DPSCs cultured in HS-supplemented versus FBS-supplemented media. Finally, in one study of a mouse femur fracture model,[47] similar biomechanical quality (''bending strength'') but greater radiographic bone density was observed in implants of ASCs cultured in CDM supplemented with GFs (bFGF, PDGF-BB, and TGF-β) versus ASCs in FBS-supplemented media; histology revealed a better healing response, with more osteoblastic activity, in the FBS-free ASC implants.

Discussion

A majority of the evidence for BTE is based on *in vitro* evaluation; however, it is important that these *in vitro* findings are eventually confirmed *in vivo* to facilitate clinical translation.[48] Recent reviews of preclinical *in vivo* studies have revealed favorable outcomes of BTE approaches for periodontal[32] and alveolar bone defect regeneration.[10] However, a translational limitation of traditional BTE strategies is the use of mostly animal-derived serum supplements, such as FBS, for *ex vivo* cell expansion. FBS substitutes are increasingly being used to develop cGMP-compliant hMSC expansion protocols according to international regulations (European Directives for EU countries, 2007/1394/EC)—to ensure reproducibility, efficacy, and safety of the therapeutic products.[25,49] Human blood components (plasma, serum, platelet derivatives, etc.) represent safe and pragmatic FBS substitutes for clinical-grade hMSC expansion.[14] Moreover, commercial CDM are increasingly being proposed for hMSC expansion to minimize the risk of pathogen transfer. The type of material used for medium supplementation can largely influence cellular responses, the concentration and nature of GFs released, and, ultimately, the clinical outcomes.[50–54]

Downloaded by Mary Ann Liebert, Inc., publishers from online.liebertpub.com at 08/03/17. For personal use only.

Summary of in vivo *outcomes*

The majority of reviewed studies reported ectopic models of bone formation. Ectopic models allow the evaluation of bone regeneration in nonosseous (e.g., subcutaneous or intramuscular) sites, usually in small animals.[29] The lack of endogenous osteogenic cells, cytokines, and mechanical factors (all of which can potentially stimulate bone formation) within the local intradermal environment ensures that, theoretically, any resulting bone formation after cell transplantation is of exogenous origin.[29] Overall, the majority of reviewed studies reported either similar or superior ectopic bone formation in implants of hMSCs expanded in HS- (5/6 studies), HPD- (5/6 studies), or CDM-supplemented media (1/1 study), than in those of FBS-supplemented media.

Orthotopic bone models, which involve surgically created defects in osseous sites, for example, CSDs in rodent calvaria, allow for testing of exogenous agents (e.g., cells) in the presence of endogenous osteogenic factors.[28] Rodent calvaria are considered as a challenging environment for bone regeneration because of poor blood supply and limited bone marrow and, therefore, it may be inferred that regeneration in this context is largely caused by the direct and/or indirect effects of exogenous transplanted cells.[28] All reviewed studies reported similar or superior orthotopic bone regeneration in implants of hMSCs expanded in HS-, HPD-, or CDM-supplemented media (one study each) than that in FBS-supplemented media, suggesting that hMSCs expanded in humanized media demonstrate adequate osteogenic and/or osteoinductive potential *in vivo*.

Characteristics of Humanized Media Supplements

Human serum

A majority of studies in this review investigated HS in comparison with FBS for hMSC expansion. In two studies,[35,36] HS was further supplemented with insulin and recombinant human GFs—EGF, PDGF-BB, FGF-2, and macrophage colony-stimulating factor (M-CSF). Optimal results were observed only when HS-based cultures were supplemented, for example, a significantly lower proportion of hMSCs was observed in nonsupplemented HS-based cultures versus FBS-based cultures, but addition of supplements enhanced the hMSC yield beyond that of FBS-based cultures.[35] Regarding the concentration of HS, a majority of studies reported the use of 10% HS, whereas one study used 20% HS.[33] A previous study[55] found 10% HS to be equally or more effective than 10% FBS for large-scale expansion of human BMSCs, but 1% and 3% HS were found to be inferior. The authors did not include concentrations >10% because of significantly larger quantities of blood needed.[55] Therefore, although 10% HS appears to be effective for hMSC expansion, it is unclear whether superior hMSC growth can be achieved with higher concentrations.

Use of both autologous (i.e., hMSCs and blood derived from the same donors) and allogeneic HS (i.e., prepared from pooled whole blood of multiple donors) was reported. Autologous HS appears to be a suitable FBS substitute for clinical applications, whereas allogeneic HS is reported to be inferior to autologous HS with regard to hMSC survival and proliferation.[56] However, the amount of serum needed for large-scale MSC expansion is a potential limiting factor. Considering a 2- to 3-week expansion period (2L of medium with 10% HS), 200 mL of serum would require at least one 500 mL blood donation.[57] The lack of availability of HS from blood establishments also limits its large-scale use as an allogeneic product.[20] Furthermore, previous studies have reported lower proliferation of hMSCs in media supplemented with HS versus platelet derivatives, which have emerged as the preferred supplement for clinical-grade hMSC expansion.[14,58]

Chemically defined media

To circumvent the risks of pathogen transmission and difficulty of standardized preparation of HS-derived supplements, synthetic serum-free CDM have been developed. These CDM are usually supplemented with recombinant human GF combinations (PDGF, FGF, TGF-β, EGF, etc.), although the exact content and formulations of commercial media are rarely disclosed.[20] In this review, two studies reported the use of CDM for expansion of BMSCs[46] or ASCs.[47] In both studies, superior *in vitro* proliferation and/or *in vivo* osteogenesis of hMSCs were reported in CDM versus 10% FBS. However, the feasibility of using CDM for large-scale hMSC expansion has been questioned, given that (1) the inherent variability and specificity of primary cell cultures may complicate the use of CDM, (2) a specific mix of GFs will have to be developed to adjust to different hMSC sources (bone marrow, adipose tissue, cord blood, dental pulp, etc.), and (3) several recombinant GFs and their combinations required to develop certain CDM would need to be approved for therapeutic use by regulatory authorities.[20] In one study,[59] defined combinations of several recombinant GFs (TGF-β1, activin-A, bFGF, EGF, PDGF-BB, insulin-like growth factor [IGF]-1, and vascular endothelial growth factor [VEGF]) and chemokines (CCL21, CCL25, CXCL12, and RANTES) in a serum-free medium failed to achieve hMSC proliferation compared with 5% or 10% PL. Conversely, a recent study[60] reported significantly shorter expansion times to achieve clinically relevant number of hMSCs, when using a commercial CDM versus 10% PL. However, the PL-based system was found to be significantly more cost-effective than CDM (total cost of CDM was 200% that of PL) for large-scale MSC expansion.[60]

Platelet derivatives

Platelet concentrates. Platelet derivatives are attractive supplements for cell culture, because platelets contain high concentrations of physiological GFs. These are usually prepared from platelet concentrates, obtained as apheresis products or whole blood-derived buffy coat units.[21] Platelet derivatives may be used as autologous or ''pooled'' products. Autologous products eliminate the risk of disease transmission, although obtaining a sufficient quantity, and quality in terms of GF contents, of autologous concentrates for clinical-grade hMSC expansion may be highly dependent on the donor and method of platelet isolation.[61] Alternatively, pooling platelets from multiple donors can provide larger volumes of concentrates, and also reduce donor-based variations in terms of platelet counts, GF contents, and effects on hMSCs.[62–67] Studies have reported pooling of platelet concentrates from 4 up to 40 donors (Supplementary Table S4). Pooled platelet concentrates are routinely prepared by blood establishments for transfusion,[21] whereas safety practices

Downloaded by Mary Ann Liebert, Inc., publishers from online.liebertpub.com at 08/03/17. For personal use only.

such as donor screening and pathogen inactivation reduce the risk of transmitting infectious diseases through pooled products.[20] Together, these efforts could allow the large-scale, cost-effective, and standardized manufacturing of ''off-the-shelf'' humanized cell culture supplements.

Pooling can also help to enhance platelet concentrations in these products. A platelet concentration of $1 \times 10^6/\mu L$ is considered to be of therapeutic value.[68] Allogeneic platelet concentrates with a minimum platelet content of 2×10^{11}/unit in ~ 300 mL are routinely prepared for platelet transfusion by blood banks in Europe.[69] A significant advantage is the ability to use ''expired'' platelet concentrates (older than 5 days) that are no longer suitable for transfusion, but are equally effective as fresh platelets, in supporting hMSC growth and osteogenic differentiation.[17,70] However, platelet concentrations cannot solely predict GF levels,[71] because the method of preparation, specifically the method of platelet ''activation,'' can largely affect the content and efficacy of the final product, that is, the lysate (PL) or releasate (PR).[72]

Platelet lysate and platelet releasate. PL is usually prepared from pooled PRP units by one or more freezing and thawing cycle(s) to *mechanically* disrupt the platelet membranes, whereas PR is prepared by *chemical* activation of platelets in PRP, most commonly by addition of thrombin and/or calcium chloride.[45,73] Although PL contains the entire intracellular contents released from platelets, activation with thrombin or calcium in PR closely mimics physiological platelet activation and GF release that occurs during wound healing.[74] Moreover, activation with exogenous thrombin causes a rapid release of platelet GFs (a majority of the stored GFs are released within the first 1–4 h[75,76]), whereas activation with calcium causes a more gradual GF release (for 7 days) through the formation of endogenous thrombin and ''partial'' platelet activation.[77,78] Recent studies have identified optimal GF release profiles after PRP activation with solely calcium,[79] or calcium with a low dose of thrombin.[78]

Growth factors. Platelets contain large quantities of GFs, such as platelet-derived growth factor isoforms (PDGF-AA, -AB, and -BB), TGF-β, EGF, FGF-2, VEGF, brain-derived neurotrophic factor, hepatocyte growth factor, connective tissue growth factor, and bone morphogenetic protein (BMP)-2, -4, and -6.[21] Of these, PDGF-BB and FGF-2 have been identified to be particularly important for the hMSC growth-promoting effects of platelet derivatives.[80] However, it is challenging to compare platelet derivatives (or other humanized supplements) with FBS in terms of their GF contents, given the differences in their origins, and also because of the scarcity of literature regarding the GF contents of FBS. To our knowledge, only one published study has compared GF contents in PL and FBS and reported significantly higher concentrations of PDGF-AA, -AB, -BB, TGF-β, IGF, and VEGF in PL.[81]

Recent studies[82,83] have also highlighted the role of platelet-derived extracellular vesicles (EVs), also known as microparticles or exosomes, which may be internalized by hMSCs, thereby functioning as an efficient mechanism for GF delivery. These EVs, present in PL and PR, have been shown to contain a high concentration of GFs, for example, FGF, VEGF, PDGF-BB, and TGF-β1, and are thus mediators of platelet-stimulated hMSC proliferation and osteogenic differentiation.[83,84]

A number of studies have compared GF contents in PL and PR, and between PL/PR and HS (Supplementary Table S4). The most commonly evaluated GFs were PDGF-AA, -AB, -BB, TGF-β1, FGF, EGF, IGF-1, and VEGF; these GFs are commonly associated with favorable hMSC proliferation and osteogenic differentiation.[85,86] However, because of large differences between studies in terms of protocols for preparation of the products, and methods for evaluating GF concentrations, specific values of GF concentrations could not be reliably compared. Nevertheless, these studies demonstrated that both PR and PL contained high concentrations of multiple GFs and equally promoted proliferation and differentiation of various cell types, including hMSCs. Most commonly, high concentrations of PDGF isoforms, TGF-β1 and FGF, were identified in PL and PR, all of which are considered important for hMSC recruitment, proliferation, and osteogenic differentiation.[87–90] Other bone-related proteins such as osteocalcin and osteopontin have also been identified in PL.[91] Interestingly, no studies compared the release of BMPs from platelet products. BMPs are members of the TGF-β superfamily, and important regulators of skeletal development and bone formation.[92] BMP-2, -4, -6, -7, and -9, which are reported to be the most potent inducers of osteogenic differentiation,[93,94] have been identified in PL.[95,96] Moreover, platelets may contain potentiators of BMP-mediated osteogenic differentiation.[97] However, further research is needed to determine whether the presence of these GFs in culture media indeed ''primes'' hMSC differentiation toward an osteoblastic lineage.[86]

It is currently inconclusive whether PL is superior to PR, or vice versa, because of differences in the methods of PL/PR preparation and platelet concentrations, which do not allow direct interstudy comparisons. However, a trend for reporting of higher GF concentrations in PL was observed, and the number of freeze/thaw cycles and/or freezing temperatures seemed to affect GF release in PL—2–5 cycles were reported to be adequate for achieving optimal platelet lysis[56,98–100] and lower freezing temperatures were beneficial when using fewer cycles.[101]

Inflammatory cytokines. In addition to GFs, platelet products contain physiological levels of a range of inflammatory cytokines, including interleukin (IL)-1α, IL-6, IL-7, IL-8, tumor necrosis factor (TNF)-α, granulocyte-colony stimulating factor, granulocyte macrophage colony-stimulating factor, macrophage inflammatory protein (MIP)-1α, MIP-1β, and interferon-γ, among others.[20] These cytokines play important roles in chemotaxis, cell proliferation, differentiation, and angiogenesis. Evidence for the effects of inflammatory cytokines on MSC osteogenic differentiation is conflicting, with several cytokines reported to have both pro- and antiosteogenic effects (see review[102]). However, recent studies have suggested that controlled delivery of certain inflammatory cytokines may enhance hMSC proliferation and osteogenic differentiation.[103–105] Indeed, these findings can be correlated with *in vivo* observations of osseous wound healing, which is characterized by an initial ''inflammatory phase'' during which several proinflammatory cytokines are upregulated to recruit and guide the proliferation and differentiation of MSCs at the injury site and initiate the regenerative process.[106]

Downloaded by Mary Ann Liebert, Inc., publishers from online.liebertpub.com at 08/03/17. For personal use only.

Differential expression of bioactive factors and consequent effects on hMSC proliferation have been reported in PR and PL.[107] In a detailed comparison of 174 cytokines (and GFs), Bieback *et al.*[58] reported similar expression of a majority of cytokines in PL and thrombin-activated platelet releasate (tPR), including IL-1α, IL-1β, and TNF-α, although higher concentrations of PDGF-AA, -BB, -AB, and VEGF were reported in PL. Conversely, another study[108] reported significantly higher levels of IL-1α, IL-1β, IL-6, monocyte chemoattractant protein (MCP)-1, INF-γ, TNF-α, and M-CSF in PL versus PR. Interestingly, in one study,[109] significantly higher levels of IL-1β were detected in tPR 1–6 days after thrombin activation (mean 425 pg/mL) versus PL (i.e., total intracellular IL-1β content, mean 1.4 pg/mL), suggesting *de novo* synthesis.[110] This finding was supported by a more recent study,[78] which reported a 10-fold increase in IL-1β levels in PRP (vs. baseline) after calcium or thrombin activation. Similarly, another recent study[76] identified a number of proinflammatory cytokines, most prominently chemokine CCL5/RANTES, to be upregulated in tPR for 5 days, which is in agreement with a previous report.[58] In context, results from a number of studies suggest a possible negative effect of thrombin activation on PRP-mediated *in vivo* bone regeneration.[111–114] Indeed, high levels of RANTES have also been identified in PL preparations.[58,80,115] Interestingly, in one of these studies,[80] inhibition of RANTES (or other cytokines, e.g., PDGF-AA and VEGF) in 10% PL-supplemented medium had no effect on hMSC proliferation. Nevertheless, when considering platelet products for clinical-grade MSC expansion, use of exogenous products for platelet activation, such as thrombin (especially of nonhuman origin[116]), may complicate the regulatory approval process.[21]

In vitro and *in vivo* osteogenic efficacy. In this review, studies reported the use of either 5% PL or 10% tPR. A lower concentration of PL (5–10%) than FBS (usually 10–20%) may be adequate for cell culture because of a higher concentration of GFs in PL[81]; an optimal media composition of alpha-minimal essential medium supplemented with 10% PL has been reported for hMSC expansion.[54] This is consistent with current literature, which suggests that PL in concentrations of 5–10% can enhance the growth of several cell types compared with 10% FBS,[20,21,98,117,118] and effectively support the clinical-grade expansion of hMSCs from different sources *in vitro*.[119,120] The efficacy of 5–8% PL-expanded hMSCs to regenerate bone in calvarial CSD of nude mice has previously been reported.[121] This expansion protocol is currently being applied in an ongoing clinical trial of alveolar bone regeneration with autologous BMSCs.[122]

Vascularization of bone constructs is an important determinant of their *in vivo* success, and is considered to be a translational limitation of current BTE strategies.[123,124] The proangiogenic effects of platelet products have been well studied, both *in vitro* and *in vivo*,[125] and it could be hypothesized that culturing hMSCs in platelet-supplemented medium could enhance their proangiogenic properties through paracrine mechanisms. This was confirmed in one included study,[44] wherein a significantly higher number of blood vessels were detected in ectopic implants of UCMSCs cultured in 5% PL versus BMSCs in 10% FBS; the vessels were determined to be of host origin, confirming that the observed angiogenesis was a result of the paracrine effects of implanted UCMSCs, rather than direct endothelial differentiation.[44] In contrast, two studies, in which adipose-derived SVF cells containing distinct subpopulations of endothelial cells ($CD31^+/CD34^+$) were cultured under dynamic conditions in either 5% pooled PL[42] or 10% pooled tPR,[45] in comparison with 10% FBS (+FGF-2), identified *in vivo* blood vessels of human origin in implants of tPR- and FBS-cultured cells, suggesting direct endothelial differentiation, but not in PL-cultured cells.[42,45] Possible explanations for these observations could be differences in PL, PR, and FBS, in terms of (1) GF profiles (as previously discussed), (2) their ability to support the growth and differentiation of endothelial cells, and (c) their effects on hMSC secretory profiles. Although both PL[126] and PR[127] have been shown to independently stimulate angiogenesis *in vitro*, their effects on hMSCs, particularly on their *in vitro* and *in vivo* angiogenic and osteogenic secretory/paracrine profiles, are currently unclear.

In the context of (bone) tissue engineering, implantation of *exogenous* hMSCs is expected to induce regeneration through direct (osteogenic) differentiation and/or through paracrine mechanisms, that is, secretory molecules stimulating *endogenous* cells (see reviews[128,129]). Paracrine effects of hMSCs can also have anti-inflammatory and immunomodulatory functions, that is, suppression of the host immune response. Results from previous *in vitro* studies suggest that secretory profiles of hMSCs may vary depending on culture conditions, in the contexts of both regeneration, for example, between PL- and PR-supplemented medium,[58,107] and immunomodulation, for example, between PL- and FBS-supplemented medium.[130,131] However, whether humanized cultures enhance the paracrine and/or immunomodulatory functions of hMSCs *in vivo* remains to be determined.

Long-term expanded hMSCs undergo reduction in their proliferation and differentiation potential as a result of ''aging'' or replicative senescence,[132,133] which may be influenced by culture conditions.[134] However, studies that have investigated the influence of humanized media reported significantly higher proliferation (population doublings), but similar senescence-associated changes, in hMSCs cultured in either HS-[135] or PL-supplemented media,[136] compared with FBS-supplemented media, with no evidence of chromosomal transformations, suggesting that senescence-associated changes in hMSCs may be independent of culture supplements. Interestingly, changing to PL-supplemented media has been reported to attenuate senescence in late-passage FBS-expanded hMSCs and induce ''cellular rejuvenation'' by enhancing, or at least maintaining, their proliferation and differentiation potential.[137] These findings further support the substitution of FBS in hMSC cultures with humanized supplements, particularly PL.

Few published reports exist regarding the clinical applications of PL-expanded MSCs for bone regeneration. In contrast, PRP has been extensively used for this application, alone, in combination with bone substitute materials,[138] or as a scaffold for hMSCs,[139] although the evidence regarding its clinical efficacy is inconclusive.[140] The use of autologous BMSCs expanded in 10–20% autologous PL has been reported for various orthopedic indications in a large patient sample ($n = 339$)[141]—BMSCs were mixed with autologous PL or PRP and injected into peripheral joints or intervertebral disks. No evidence of tumor formation at the injection sites or major adverse events related to the procedure were

Downloaded by Mary Ann Liebert, Inc., publishers from online.liebertpub.com at 08/03/17. For personal use only.

identified after up to 3 years.[141] Finally, one ongoing clinical study[122] is investigating the use of autologous BMSCs expanded in 5–8% pooled PL-supplemented media, in combination with biphasic calcium phosphate scaffolds, for alveolar bone regeneration.

Although a majority of clinical trials of hMSC-based therapy report the use of autologous cells—most often expanded in FBS media—the use of allogeneic hMSCs is emerging as a promising alternative.[18] Allogeneic MSCs, often ''pooled'' from multiple donors, have been applied in the treatment of graft-versus-host disease (GVHD),[142] osteogenesis imperfecta,[143] and, more recently, in osteoarthritis.[144] To our knowledge, no published clinical trials have reported the use of allogeneic hMSCs for bone regeneration. Nevertheless, recent trials[145–147] have demonstrated the effectiveness of pooled allogeneic hMSCs (8–12 donors) expanded in PL-supplemented (5–10%) media for treatment of GVHD, in both adults and children. It has previously been suggested that variability of observed clinical success rates may be attributed to donor-based variations in hMSCs, and ''xenocontamination'' through FBS cultures,[148] which may lead to hyperimmunogenicity, improper trafficking, and poor engraftment of implanted hMSCs.[149] Variations in hMSC properties, including osteogenic differentiation potential, between donors[150] and tissue sources,[120] even when cultured in PL-supplemented media,[120,151] have been reported. An interesting avenue for future research could be to determine whether optimization of humanized supplement production can attenuate donor-based variations in allogeneic hMSC cultures.

Methodological issues and quality of reporting

In this review, no meta-analysis of data regarding *in vivo* bone regeneration from individual studies could be performed, because of large inconsistencies (heterogeneity) in the nature of the animal models used, therapies tested, and outcomes evaluated. Furthermore, the review identified a lack of studies comparing humanized alternatives and FBS as hMSC culture supplements for *in vivo* bone regeneration. Therefore, an overall ''pooled estimate'' of the efficacy of FBS-based and FBS-free hMSC cultures could not be obtained.[152] Since the reliability of results of systematic reviews directly depends on the quality of the primary studies, RoB within the included studies was assessed through compliance with the SYRCLE tool, which addresses particular aspects of bias that play a role in animal experimental studies.[31] Studies were judged to be of a high RoB, and a clear need for more standardized reporting of studies was identified, to allow reliable future reproduction and synthesis.

Conclusions

Based on the results of 15 studies in rodents, mostly using ectopic (subcutaneous) models, implantation of hMSCs cultured in humanized media results in similar, if not superior, *in vivo* bone formation compared with that of hMSCs cultured in FBS-supplemented media. In a majority of studies, the *in vitro* benefits of humanized cultures were translated *in vivo*. Pooled platelet derivatives currently represent the most feasible alternative to FBS for clinical-grade hMSC expansion. Based on limited evidence, a trend for reporting higher concentrations of GFs was observed in PL versus thrombin- and/or calcium-activated PR. However, further well-designed studies are needed to validate the preclinical and clinical *in vivo* efficacy of platelet derivatives, in addition to their cost-effectiveness, in comparison with that of other FBS substitutes. Moreover, standardization of preparation protocols, in compliance with cGMP standards, is needed to facilitate their large scale use for hMSC expansion.

Acknowledgments

This review was supported by funding from Helse Vest, Norway (project number: 912048, K.M.), and the Bergen Stem Cell Consortium (project number: 502027, K.M.).

Disclosure Statement

No competing financial interests exist.

References

1. Götz, C., Warnke, P.H., and Kolk, A. Current and future options of regeneration methods and reconstructive surgery of the facial skeleton. Oral Surg Oral Med Oral Pathol Oral Radiol **120,** 315, 2015.
2. Fretwurst, T., Gad, L.M., Nelson, K., and Schmelzeisen, R. Dentoalveolar reconstruction. Curr Opin Otolaryngol Head Neck Surg **23,** 316, 2015.
3. Nkenke, E., and Neukam, F.W. Autogenous bone harvesting and grafting in advanced jaw resorption: morbidity, resorption and implant survival. Eur J Oral Implantol **7 Suppl 2,** S203, 2014.
4. Al-Nawas, B., and Schiegnitz, E. Augmentation procedures using bone substitute materials or autogenous bone—a systematic review and meta-analysis. Eur J Oral Implantol **7,** 219, 2014.
5. Milinkovic, I., and Cordaro, L. Are there specific indications for the different alveolar bone augmentation procedures for implant placement? A systematic review. Int J Oral Maxillofac Surg **43,** 606, 2014.
6. Shanbhag, S., and Shanbhag, V. Clinical applications of cell-based approaches in alveolar bone augmentation: a systematic review. Clin Implant Dent Relat Res **17,** e17, 2015.
7. Hanley, P.J., Mei, Z., da Graca Cabreira-Hansen, M., Klis, M., Li, W., Zhao, Y., Durett, A.G., Zheng, X., Wang, Y., Gee, A.P., and Horwitz, E.M. Manufacturing mesenchymal stromal cells for phase I clinical trials. Cytotherapy **15,** 416, 2013.
8. Lohan, P., Coleman, C.M., Murphy, J.M., Griffin, M.D., Ritter, T., and Ryan, A.E. Changes in immunological profile of allogeneic mesenchymal stem cells after differentiation: should we be concerned? Stem Cell Res Ther **5,** 99, 2014.
9. Oppenheimer, A.J., Mesa, J., and Buchman, S.R. Current and emerging basic science concepts in bone biology: implications in craniofacial surgery. J Craniofac Surg **23,** 30, 2012.
10. Shanbhag, S., Pandis, N., Mustafa, K., Nyengaard, J., and Stavropoulos, A. Alveolar bone tissue engineering in critical-size defects of experimental animal models: a systematic review and meta-analysis. J Tissue Eng Regen Med 2016, doi: 10.1002/term.2198.
11. Padial-Molina, M., Valle, F., Lanis, A., Mesa, F., Dohan Ehrenfest, D.M., Wang, H.-L., and Galindo-Moreno, P.

Downloaded by Mary Ann Liebert, Inc., publishers from online.liebertpub.com at 08/03/17. For personal use only.

Clinical application of mesenchymal stem cells and novel supportive therapies for oral bone regeneration. Biomed Res Int **2015,** 16, 2015.

12. Bieback, K., Schallmoser, K., Klüter, H., and Strunk, D. Clinical protocols for the isolation and expansion of mesenchymal stromal cells. Transfus Med Hemother **35,** 286, 2008.
13. Spees, J.L., Gregory, C.A., Singh, H., Tucker, H.A., Peister, A., Lynch, P.J., Hsu, S.C., Smith, J., and Prockop, D.J. Internalized antigens must be removed to prepare hypoimmunogenic mesenchymal stem cells for cell and gene therapy. Mol Ther **9,** 747, 2004.
14. Bieback, K. Platelet lysate as replacement for fetal bovine serum in mesenchymal stromal cell cultures. Transfus Med Hemother **40,** 326, 2013.
15. Russel, W.M.S., and Burch, R.L. The Principles of Humane Experimental Technique. London: Methuen & Co., 1959. [Special edition published by Universities Federation for Animal Welfare (UFAW), 1992].
16. Mendicino, M., Bailey, A.M., Wonnacott, K., Puri, R.K., and Bauer, S.R. MSC-based product characterization for clinical trials: an FDA perspective. Cell Stem Cell **14,** 141, 2014.
17. Hemeda, H., Giebel, B., and Wagner, W. Evaluation of human platelet lysate versus fetal bovine serum for culture of mesenchymal stromal cells. Cytotherapy **16,** 170, 2014.
18. Ikebe, C., and Suzuki, K. Mesenchymal stem cells for regenerative therapy: optimization of cell preparation protocols. Biomed Res Int **2014,** 951512, 2014.
19. Tekkatte, C., Gunasingh, G.P., Cherian, K.M., and Sankaranarayanan, K. ''Humanized'' stem cell culture techniques: the animal serum controversy. Stem Cells Int **2011,** 504723, 2011.
20. Shih, D.T.B., and Burnouf, T. Preparation, quality criteria, and properties of human blood platelet lysate supplements for ex vivo stem cell expansion. N Biotechnol **32,** 199, 2015.
21. Burnouf, T., Strunk, D., Koh, M.B., and Schallmoser, K. Human platelet lysate: replacing fetal bovine serum as a gold standard for human cell propagation? Biomaterials **76,** 371, 2016.
22. Foss, B., Bruserud, O., and Hervig, T. Platelet-released supernatants enhance hematopoietic stem cell proliferation in vitro. Platelets **19,** 155, 2008.
23. Rubio-Azpeitia, E., and Andia, I. Partnership between platelet-rich plasma and mesenchymal stem cells: in vitro experience. Muscles Ligaments Tendons J **4,** 52, 2014.
24. Astori, G., Amati, E., Bambi, F., Bernardi, M., Chieregato, K., Schafer, R., Sella, S., and Rodeghiero, F. Platelet lysate as a substitute for animal serum for the ex-vivo expansion of mesenchymal stem/stromal cells: present and future. Stem Cell Res Ther **7,** 93, 2016.
25. Mannello, F., and Tonti, G.A. Concise review: no breakthroughs for human mesenchymal and embryonic stem cell culture: conditioned medium, feeder layer, or feeder-free; medium with fetal calf serum, human serum, or enriched plasma; serum-free, serum replacement nonconditioned medium, or ad hoc formula? All that glitters is not gold! Stem Cells **25,** 1603, 2007.
26. Pellegrini, G., Seol, Y.J., Gruber, R., and Giannobile, W.V. Pre-clinical models for oral and periodontal reconstructive therapies. J Dent Res **88,** 1065, 2009.
27. Halme, D.G., and Kessler, D.A. FDA regulation of stem-cell-based therapies. N Engl J Med **355,** 1730, 2006.
28. Muschler, G.F., Raut, V.P., Patterson, T.E., Wenke, J.C., and Hollinger, J.O. The design and use of animal models for translational research in bone tissue engineering and regenerative medicine. Tissue Eng Part B Rev **16,** 123, 2010.
29. Scott, M.A., Levi, B., Askarinam, A., Nguyen, A., Rackohn, T., Ting, K., Soo, C., and James, A.W. Brief review of models of ectopic bone formation. Stem Cells Dev **21,** 655, 2012.
30. Moher, D., Liberati, A., Tetzlaff, J., and Altman, D.G. Preferred reporting items for systematic reviews and meta-analyses: the PRISMA statement. PLoS Med **6,** e1000097, 2009.
31. Hooijmans, C.R., Rovers, M.M., de Vries, R.B.M., Leenaars, M., Ritskes-Hoitinga, M., and Langendam, M.W. SYRCLE's risk of bias tool for animal studies. BMC Med Res Methodol **14,** 43, 2014.
32. Yan, X.-Z., Yang, F., Jansen, J.A., de Vries, R.B.M., and van den Beucken, J.J.J.P. Cell-based approaches in periodontal regeneration: a systematic review and meta-analysis of periodontal defect models in animal experimental work. Tissue Eng Part B Rev **21,** 411, 2015.
33. Kuznetsov, S.A., Mankani, M.H., and Robey, P.G. Effect of serum on human bone marrow stromal cells: ex vivo expansion and in vivo bone formation. Transplantation **70,** 1780, 2000.
34. Matsuo, A., Yamazaki, Y., Takase, C., Aoyagi, K., and Uchinuma, E. Osteogenic potential of cryopreserved human bone marrow-derived mesenchymal stem cells cultured with autologous serum. J Craniofac Surg **19,** 693, 2008.
35. Pytlik, R., Stehlik, D., Soukup, T., Kalbacova, M., Rypacek, F., Trc, T., Mulinkova, K., Michnova, P., Kideryova, L., Zivny, J., Klener, P., Jr., Vesela, R., Trneny, M., and Klener, P. The cultivation of human multipotent mesenchymal stromal cells in clinical grade medium for bone tissue engineering. Biomaterials **30,** 3415, 2009.
36. Stehlik, D., Pytlik, R., Rychtrmocova, H., Vesela, R., Kopecny, Z., and Trc, T. [Xenogeneic protein free cultivation of mesenchymal multipotent stromal cells]. Acta Chir Orthop Traumatol Cech **78,** 537, 2011.
37. Takeda, A., Yamazaki, Y., Baba, K., Ishiguro, M., Aoyagi, K., Ikemoto, S., and Uchinuma, E. Osteogenic potential of human bone marrow-derived mesenchymal stromal cells cultured in autologous serum: a preliminary study. J Oral Maxillofac Surg **70,** e469, 2012.
38. Pisciotta, A., Riccio, M., Carnevale, G., Beretti, F., Gibellini, L., Maraldi, T., Cavallini, G.M., Ferrari, A., Bruzzesi, G., and De Pol, A. Human serum promotes osteogenic differentiation of human dental pulp stem cells in vitro and in vivo. PLoS One **7,** e50542, 2012.
39. Roberts, S.J., Owen, H.C., Tam, W.L., Solie, L., Van Cromphaut, S.J., Van den Berghe, G., and Luyten, F.P. Humanized culture of periosteal progenitors in allogeneic serum enhances osteogenic differentiation and in vivo bone formation. Stem Cells Transl Med **3,** 218, 2014.
40. Vogel, J.P., Szalay, K., Geiger, F., Kramer, M., Richter, W., and Kasten, P. Platelet-rich plasma improves expansion of human mesenchymal stem cells and retains differentiation capacity and in vivo bone formation in calcium phosphate ceramics. Platelets **17,** 462, 2006.
41. Prins, H.J., Rozemuller, H., Vonk-Griffioen, S., Verweij, V.G., Dhert, W.J., Slaper-Cortenbach, I.C., and Martens, A.C. Bone-forming capacity of mesenchymal stromal

Downloaded by Mary Ann Liebert, Inc., publishers from online.liebertpub.com at 08/03/17. For personal use only.

cells when cultured in the presence of human platelet lysate as substitute for fetal bovine serum. Tissue Eng Part A **15,** 3741, 2009.
42. Muller, A.M., Davenport, M., Verrier, S., Droeser, R., Alini, M., Bocelli-Tyndall, C., Schaefer, D.J., Martin, I., and Scherberich, A. Platelet lysate as a serum substitute for 2D static and 3D perfusion culture of stromal vascular fraction cells from human adipose tissue. Tissue Eng Part A **15,** 869, 2009.
43. Chevallier, N., Anagnostou, F., Zilber, S., Bodivit, G., Maurin, S., Barrault, A., Bierling, P., Hernigou, P., Layrolle, P., and Rouard, H. Osteoblastic differentiation of human mesenchymal stem cells with platelet lysate. Biomaterials **31,** 270, 2010.
44. Todeschi, M.R., El Backly, R., Capelli, C., Daga, A., Patrone, E., Introna, M., Cancedda, R., and Mastrogiacomo, M. Transplanted umbilical cord mesenchymal stem cells modify the in vivo microenvironment enhancing angiogenesis and leading to bone regeneration. Stem Cells Dev **24,** 1570, 2015.
45. Tchang, L.A., Pippenger, B.E., Todorov, A., Jr., Wolf, F., Burger, M.G., Jaquiery, C., Bieback, K., Martin, I., Schaefer, D.J., and Scherberich, A. Pooled thrombin-activated platelet-rich plasma: a substitute for fetal bovine serum in the engineering of osteogenic/vasculogenic grafts. J Tissue Eng Regen Med **11,** 1542, 2015.
46. Agata, H., Watanabe, N., Ishii, Y., Kubo, N., Ohshima, S., Yamazaki, M., Tojo, A., and Kagami, H. Feasibility and efficacy of bone tissue engineering using human bone marrow stromal cells cultivated in serum-free conditions. Biochem Biophys Res Commun **382,** 353, 2009.
47. Sato, K., Itoh, T., Kato, T., Kitamura, Y., Kaul, S.C., Wadhwa, R., Sato, F., and Ohneda, O. Serum-free isolation and culture system to enhance the proliferation and bone regeneration of adipose tissue-derived mesenchymal stem cells. In Vitro Cell Dev Biol Anim **51,** 515, 2015.
48. Cousin, M.A., Greenberg, A.J., Koep, T.H., Angius, D., Yaszemski, M.J., Spinner, R.J., and Windebank, A.J. The value of systematic reviews in estimating the cost and barriers to translation in tissue engineering. Tissue Eng Part B Rev **22,** 430, 2016.
49. Chimenti, I., Gaetani, R., Forte, E., Angelini, F., De Falco, E., Zoccai, G.B., Messina, E., Frati, G., and Giacomello, A. Serum and supplement optimization for EU GMP-compliance in cardiospheres cell culture. J Cell Mol Med **18,** 624, 2014.
50. Kurita, M., Aiba-Kojima, E., Shigeura, T., Matsumoto, D., Suga, H., Inoue, K., Eto, H., Kato, H., Aoi, N., and Yoshimura, K. Differential effects of three preparations of human serum on expansion of various types of human cells. Plast Reconstr Surg **122,** 438, 2008.
51. Muraglia, A., Todeschi, M.R., Papait, A., Poggi, A., Spano, R., Strada, P., Cancedda, R., and Mastrogiacomo, M. Combined platelet and plasma derivatives enhance proliferation of stem/progenitor cells maintaining their differentiation potential. Cytotherapy **17,** 1793, 2015.
52. Zimmermann, R., Arnold, D., Strasser, E., Ringwald, J., Schlegel, A., Wiltfang, J., and Eckstein, R. Sample preparation technique and white cell content influence the detectable levels of growth factors in platelet concentrates. Vox Sang **85,** 283, 2003.
53. Weibrich, G., Hansen, T., Kleis, W., Buch, R., and Hitzler, W.E. Effect of platelet concentration in platelet-rich plasma on peri-implant bone regeneration. Bone **34,** 665, 2004.
54. Kawasumi, M., Kitoh, H., Siwicka, K.A., and Ishiguro, N. The effect of the platelet concentration in platelet-rich plasma gel on the regeneration of bone. J Bone Joint Surg Br **90,** 966, 2008.
55. Stute, N., Holtz, K., Bubenheim, M., Lange, C., Blake, F., and Zander, A.R. Autologous serum for isolation and expansion of human mesenchymal stem cells for clinical use. Exp Hematol **32,** 1212, 2004.
56. Shahdadfar, A., Fronsdal, K., Haug, T., Reinholt, F.P., and Brinchmann, J.E. In vitro expansion of human mesenchymal stem cells: choice of serum is a determinant of cell proliferation, differentiation, gene expression, and transcriptome stability. Stem Cells **23,** 1357, 2005.
57. Perez-Ilzarbe, M., Diez-Campelo, M., Aranda, P., Tabera, S., Lopez, T., del Canizo, C., Merino, J., Moreno, C., Andreu, E.J., Prosper, F., and Perez-Simon, J.A. Comparison of ex vivo expansion culture conditions of mesenchymal stem cells for human cell therapy. Transfusion (Paris) **49,** 1901, 2009.
58. Bieback, K., Hecker, A., Kocaomer, A., Lannert, H., Schallmoser, K., Strunk, D., and Kluter, H. Human alternatives to fetal bovine serum for the expansion of mesenchymal stromal cells from bone marrow. Stem Cells **27,** 2331, 2009.
59. Fekete, N., Rojewski, M.T., Lotfi, R., and Schrezenmeier, H. Essential components for ex vivo proliferation of mesenchymal stromal cells. Tissue Eng Part C Methods **20,** 129, 2014.
60. Wuchter, P., Vetter, M., Saffrich, R., Diehlmann, A., Bieback, K., Ho, A.D., and Horn, P. Evaluation of GMP-compliant culture media for in vitro expansion of human bone marrow mesenchymal stromal cells. Exp Hematol **44,** 508, 2016.
61. Horn, P., Bokermann, G., Cholewa, D., Bork, S., Walenda, T., Koch, C., Drescher, W., Hutschenreuther, G., Zenke, M., Ho, A.D., and Wagner, W. Impact of individual platelet lysates on isolation and growth of human mesenchymal stromal cells. Cytotherapy **12,** 888, 2010.
62. Weibrich, G., Kleis, W.K., Hafner, G., and Hitzler, W.E. Growth factor levels in platelet-rich plasma and correlations with donor age, sex, and platelet count. J Craniomaxillofac Surg **30,** 97, 2002.
63. Weibrich, G., Buch, R.S., Kleis, W.K., Hafner, G., Hitzler, W.E., and Wagner, W. Quantification of thrombocyte growth factors in platelet concentrates produced by discontinuous cell separation. Growth Factors **20,** 93, 2002.
64. Cho, H.S., Song, I.H., Park, S.Y., Sung, M.C., Ahn, M.W., and Song, K.E. Individual variation in growth factor concentrations in platelet-rich plasma and its influence on human mesenchymal stem cells. Korean J Lab Med **31,** 212, 2011.
65. Lohmann, M., Walenda, G., Hemeda, H., Joussen, S., Drescher, W., Jockenhoevel, S., Hutschenreuter, G., Zenke, M., and Wagner, W. Donor age of human platelet lysate affects proliferation and differentiation of mesenchymal stem cells. PLoS One **7,** e37839, 2012.
66. Evanson, J.R., Guyton, M.K., Oliver, D.L., Hire, J.M., Topolski, R.L., Zumbrun, S.D., McPherson, J.C., and Bojescul, J.A. Gender and age differences in growth factor concentrations from platelet-rich plasma in adults. Mil Med **179,** 799, 2014.

Downloaded by Mary Ann Liebert, Inc., publishers from online.liebertpub.com at 08/03/17. For personal use only.

67. Gomez, L.A., Escobar, M., and Penuela, O. Standardization of a protocol for obtaining platelet rich plasma from blood donors; a tool for tissue regeneration procedures. Clin Lab **61,** 973, 2015.
68. Marx, R.E. Platelet-rich plasma: evidence to support its use. J Oral Maxillofac Surg **62,** 489, 2004.
69. European Directorate for the Quality of Medicines & Healthcare. Guide to the Preparation, Use and Quality Assurance of Blood Components. Strasbourg, France: Council of Europe. Recommendation No. R (95) 15, 2015.
70. Jonsdottir-Buch, S.M., Lieder, R., and Sigurjonsson, O.E. Platelet lysates produced from expired platelet concentrates support growth and osteogenic differentiation of mesenchymal stem cells. PLoS One **8,** e68984, 2013.
71. Zimmermann, R., Jakubietz, R., Jakubietz, M., Strasser, E., Schlegel, A., Wiltfang, J., and Eckstein, R. Different preparation methods to obtain platelet components as a source of growth factors for local application. Transfusion (Paris) **41,** 1217, 2001.
72. Wasterlain, A.S., Braun, H.J., and Dragoo, J.L. Contents and formulations of platelet-rich plasma. Oper Tech Orthop **22,** 33, 2012.
73. Schallmoser, K., and Strunk, D. Generation of a pool of human platelet lysate and efficient use in cell culture. Methods Mol Biol **946,** 349, 2013.
74. Kocaoemer, A., Kern, S., Kluter, H., and Bieback, K. Human AB serum and thrombin-activated platelet-rich plasma are suitable alternatives to fetal calf serum for the expansion of mesenchymal stem cells from adipose tissue. Stem Cells **25,** 1270, 2007.
75. Marx, R.E. Platelet-rich plasma (PRP): what is PRP and what is not PRP? Implant Dent **10,** 225, 2001.
76. Jalowiec, J.M., D'Este, M., Bara, J.J., Denom, J., Menzel, U., Alini, M., Verrier, S., and Herrmann, M. An in vitro investigation of platelet-rich plasma-gel as a cell and growth factor delivery vehicle for tissue engineering. Tissue Eng Part C Methods **22,** 49, 2016.
77. Foster, T.E., Puskas, B.L., Mandelbaum, B.R., Gerhardt, M.B., and Rodeo, S.A. Platelet-rich plasma: from basic science to clinical applications. Am J Sports Med **37,** 2259, 2009.
78. Roh, Y.H., Kim, W., Park, K.U., and Oh, J.H. Cytokine-release kinetics of platelet-rich plasma according to various activation protocols. Bone Joint Res **5,** 37, 2016.
79. Amable, P.R., Carias, R.B., Teixeira, M.V., da Cruz Pacheco, I., Correa do Amaral, R.J., Granjeiro, J.M., and Borojevic, R. Platelet-rich plasma preparation for regenerative medicine: optimization and quantification of cytokines and growth factors. Stem Cell Res Ther **4,** 67, 2013.
80. Fekete, N., Gadelorge, M., Furst, D., Maurer, C., Dausend, J., Fleury-Cappellesso, S., Mailander, V., Lotfi, R., Ignatius, A., Sensebe, L., Bourin, P., Schrezenmeier, H., and Rojewski, M.T. Platelet lysate from whole blood-derived pooled platelet concentrates and apheresis-derived platelet concentrates for the isolation and expansion of human bone marrow mesenchymal stromal cells: production process, content and identification of active components. Cytotherapy **14,** 540, 2012.
81. Shanskii, Y.D., Sergeeva, N.S., Sviridova, I.K., Kirakozov, M.S., Kirsanova, V.A., Akhmedova, S.A., Antokhin, A.I., and Chissov, V.I. Human platelet lysate as a promising growth-stimulating additive for culturing of stem cells and other cell types. Bull Exp Biol Med **156,** 146, 2013.
82. Aatonen, M.T., Ohman, T., Nyman, T.A., Laitinen, S., Gronholm, M., and Siljander, P.R. Isolation and characterization of platelet-derived extracellular vesicles. J Extracell Vesicles **3,** 2014. doi: 10.3402/jev.v3.24692.
83. Torreggiani, E., Perut, F., Roncuzzi, L., Zini, N., Baglio, S.R., and Baldini, N. Exosomes: novel effectors of human platelet lysate activity. Eur Cell Mater **28,** 137, 2014.
84. Gruber, R., Varga, F., Fischer, M.B., and Watzek, G. Platelets stimulate proliferation of bone cells: involvement of platelet-derived growth factor, microparticles and membranes. Clin Oral Implants Res **13,** 529, 2002.
85. Rodrigues, M., Griffith, L.G., and Wells, A. Growth factor regulation of proliferation and survival of multipotential stromal cells. Stem Cell Res Ther **1,** 32, 2010.
86. Hughes, F.J., Turner, W., Belibasakis, G., and Martuscelli, G. Effects of growth factors and cytokines on osteoblast differentiation. Periodontol 2000 **41,** 48, 2006.
87. Donovan, J., Abraham, D., and Norman, J. Platelet-derived growth factor signaling in mesenchymal cells. Front Biosci (Landmark Ed) **18,** 106, 2013.
88. Ng, F., Boucher, S., Koh, S., Sastry, K.S., Chase, L., Lakshmipathy, U., Choong, C., Yang, Z., Vemuri, M.C., Rao, M.S., and Tanavde, V. PDGF, TGF-beta, and FGF signaling is important for differentiation and growth of mesenchymal stem cells (MSCs): transcriptional profiling can identify markers and signaling pathways important in differentiation of MSCs into adipogenic, chondrogenic, and osteogenic lineages. Blood **112,** 295, 2008.
89. Eom, Y.W., Oh, J.E., Lee, J.I., Baik, S.K., Rhee, K.J., Shin, H.C., Kim, Y.M., Ahn, C.M., Kong, J.H., Kim, H.S., and Shim, K.Y. The role of growth factors in maintenance of stemness in bone marrow-derived mesenchymal stem cells. Biochem Biophys Res Commun **445,** 16, 2014.
90. Crane, J.L., and Cao, X. Bone marrow mesenchymal stem cells and TGF-beta signaling in bone remodeling. J Clin Invest **124,** 466, 2014.
91. Leotot, J., Coquelin, L., Bodivit, G., Bierling, P., Hernigou, P., Rouard, H., and Chevallier, N. Platelet lysate coating on scaffolds directly and indirectly enhances cell migration, improving bone and blood vessel formation. Acta Biomater **9,** 6630, 2013.
92. Urist, M.R. Bone morphogenetic protein: the molecularization of skeletal system development. J Bone Miner Res **12,** 343, 1997.
93. Cheng, H., Jiang, W., Phillips, F.M., Haydon, R.C., Peng, Y., Zhou, L., Luu, H.H., An, N., Breyer, B., Vanichakarn, P., Szatkowski, J.P., Park, J.Y., and He, T.C. Osteogenic activity of the fourteen types of human bone morphogenetic proteins (BMPs). J Bone Joint Surg Am **85-A,** 1544, 2003.
94. Luu, H.H., Song, W.X., Luo, X., Manning, D., Luo, J., Deng, Z.L., Sharff, K.A., Montag, A.G., Haydon, R.C., and He, T.C. Distinct roles of bone morphogenetic proteins in osteogenic differentiation of mesenchymal stem cells. J Orthop Res **25,** 665, 2007.
95. Sipe, J.B., Zhang, J., Waits, C., Skikne, B., Garimella, R., and Anderson, H.C. Localization of bone morphogenetic proteins (BMPs)-2, -4, and -6 within megakaryocytes and platelets. Bone **35,** 1316, 2004.

Downloaded by Mary Ann Liebert, Inc., publishers from online.liebertpub.com at 08/03/17. For personal use only.

96. Kalen, A., Wahlstrom, O., Linder, C.H., and Magnusson, P. The content of bone morphogenetic proteins in platelets varies greatly between different platelet donors. Biochem Biophys Res Commun **375,** 261, 2008.
97. Tomoyasu, A., Higashio, K., Kanomata, K., Goto, M., Kodaira, K., Serizawa, H., Suda, T., Nakamura, A., Nojima, J., Fukuda, T., and Katagiri, T. Platelet-rich plasma stimulates osteoblastic differentiation in the presence of BMPs. Biochem Biophys Res Commun **361,** 62, 2007.
98. Baik, S.Y., Lim, Y.A., Kang, S.J., Ahn, S.H., Lee, W.G., and Kim, C.H. Effects of platelet lysate preparations on the proliferation of HaCaT cells. Ann Lab Med **34,** 43, 2014.
99. Nugraha, Y., Sari, P., Purwoko, R.Y., Luviah, E., and Pawitan, J.A. Effect of lysed platelet count in platelet concentrates on various growth factor levels after freeze rhaw cycles. Int J PharmTech Res **6,** 2036, 2014.
100. Strandberg, G., Sellberg, F., Sommar, P., Ronaghi, M., Lubenow, N., Knutson, F. and Berglund, D. Standardizing the freeze-thaw preparation of growth factors from platelet lysate. Transfusion **57,** 1058, 2017.
101. Mojica-Henshaw, M.P., Jacobson, P., Morris, J., Kelley, L., Pierce, J., Boyer, M., and Reems, J.A. Serum-converted platelet lysate can substitute for fetal bovine serum in human mesenchymal stromal cell cultures. Cytotherapy **15,** 1458, 2013.
102. Deshpande, S., James, A.W., Blough, J., Donneys, A., Wang, S.C., Cederna, P.S., Buchman, S.R., and Levi, B. Reconciling the effects of inflammatory cytokines on mesenchymal cell osteogenic differentiation. J Surg Res **185,** 278, 2013.
103. Li, C., Li, G., Liu, M., Zhou, T., and Zhou, H. Paracrine effect of inflammatory cytokine-activated bone marrow mesenchymal stem cells and its role in osteoblast function. J Biosci Bioeng **121,** 213, 2016.
104. Pourgholaminejad, A., Aghdami, N., Baharvand, H., and Moazzeni, S.M. The effect of pro-inflammatory cytokines on immunophenotype, differentiation capacity and immunomodulatory functions of human mesenchymal stem cells. Cytokine **85,** 51, 2016.
105. Croes, M., Oner, F.C., Kruyt, M.C., Blokhuis, T.J., Bastian, O., Dhert, W.J., and Alblas, J. Proinflammatory mediators enhance the osteogenesis of human mesenchymal stem cells after lineage commitment. PLoS One **10,** e0132781, 2015.
106. Mountziaris, P.M., and Mikos, A.G. Modulation of the inflammatory response for enhanced bone tissue regeneration. Tissue Eng Part B Rev **14,** 179, 2008.
107. Kinzebach, S., Dietz, L., Kluter, H., Thierse, H.J., and Bieback, K. Functional and differential proteomic analyses to identify platelet derived factors affecting ex vivo expansion of mesenchymal stromal cells. BMC Cell Biol **14,** 48, 2013.
108. Renn, T.Y., Kao, Y.H., Wang, C.C., and Burnouf, T. Anti-inflammatory effects of platelet biomaterials in a macrophage cellular model. Vox Sang **109,** 138, 2015.
109. Frechette, J.P., Martineau, I., and Gagnon, G. Platelet-rich plasmas: growth factor content and roles in wound healing. J Dent Res **84,** 434, 2005.
110. Hartwig, D., Hartel, C., Hennig, H., Muller-Steinhardt, M., Schlenke, P., and Kluter, H. Evidence for de novo synthesis of cytokines and chemokines in platelet concentrates. Vox Sang **82,** 182, 2002.
111. Karp, J.M., Sarraf, F., Shoichet, M.S., and Davies, J.E. Fibrin-filled scaffolds for bone-tissue engineering: an in vivo study. J Biomed Mater Res A **71,** 162, 2004.
112. Nikolidakis, D., van den Dolder, J., Wolke, J.G., Stoelinga, P.J., and Jansen, J.A. The effect of platelet-rich plasma on the bone healing around calcium phosphate-coated and non-coated oral implants in trabecular bone. Tissue Eng **12,** 2555, 2006.
113. Roussy, Y., Bertrand Duchesne, M.P., and Gagnon, G. Activation of human platelet-rich plasmas: effect on growth factors release, cell division and in vivo bone formation. Clin Oral Implants Res **18,** 639, 2007.
114. Han, B., Woodell-May, J., Ponticiello, M., Yang, Z., and Nimni, M. The effect of thrombin activation of platelet-rich plasma on demineralized bone matrix osteoinductivity. J Bone Joint Surg Am **91,** 1459, 2009.
115. Ben Azouna, N., Jenhani, F., Regaya, Z., Berraeis, L., Ben Othman, T., Ducrocq, E., and Domenech, J. Phenotypical and functional characteristics of mesenchymal stem cells from bone marrow: comparison of culture using different media supplemented with human platelet lysate or fetal bovine serum. Stem Cell Res Ther **3,** 6, 2012.
116. Lawson, J.H. The clinical use and immunologic impact of thrombin in surgery. Semin Thromb Hemost **32 Suppl 1,** 98, 2006.
117. Altaie, A., Owston, H., and Jones, E. Use of platelet lysate for bone regeneration—are we ready for clinical translation? World J Stem Cells **8,** 47, 2016.
118. Mohammadi, S., Nikbakht, M., Malek Mohammadi, A., Zahed Panah, M., Ostadali, M.R., Nasiri, H., and Ghavamzadeh, A. Human platelet lysate as a xeno free alternative of fetal bovine serum for the in vitro expansion of human mesenchymal stromal cells. Int J Hematol Oncol Stem Cell Res **10,** 161, 2016.
119. Fazzina, R., Iudicone, P., Fioravanti, D., Bonanno, G., Totta, P., Zizzari, I.G., and Pierelli, L. Potency testing of mesenchymal stromal cell growth expanded in human platelet lysate from different human tissues. Stem Cell Res Ther **7,** 122, 2016.
120. Li, C.Y., Wu, X.Y., Tong, J.B., Yang, X.X., Zhao, J.L., Zheng, Q.F., Zhao, G.B., and Ma, Z.J. Comparative analysis of human mesenchymal stem cells from bone marrow and adipose tissue under xeno-free conditions for cell therapy. Stem Cell Res Ther **6,** 55, 2015.
121. Brennan, M.A., Renaud, A., Amiaud, J., Rojewski, M.T., Schrezenmeier, H., Heymann, D., Trichet, V., and Layrolle, P. Pre-clinical studies of bone regeneration with human bone marrow stromal cells and biphasic calcium phosphate. Stem Cell Res Ther **5,** 114, 2014.
122. University of Bergen, Jaw Bone Reconstruction Using a Combination of Autologous Mesenchymal Stem Cells and Biomaterial Prior to Dental Implant Placement. ClinicalTrials.gov. Bethesda (MD): National Library of Medicine (US) 2000–2016. Available at: https://clinicaltrialsgov/ct2/show/NCT027511252016 Accessed January 20, 2017.
123. Amini, A.R., Laurencin, C.T., and Nukavarapu, S.P. Bone tissue engineering: recent advances and challenges. Crit Rev Biomed Eng **40,** 363, 2012.
124. Nguyen, L.H., Annabi, N., Nikkhah, M., Bae, H., Binan, L., Park, S., Kang, Y., Yang, Y., and Khademhosseini, A. Vascularized bone tissue engineering: approaches for potential improvement. Tissue Eng Part B Rev **18,** 363, 2012.

Downloaded by Mary Ann Liebert, Inc., publishers from online.liebertpub.com at 08/03/17. For personal use only.

125. Martinez, C.E., Smith, P.C., and Palma Alvarado, V.A. The influence of platelet-derived products on angiogenesis and tissue repair: a concise update. Front Physiol **6,** 290, 2015.
126. Barsotti, M.C., Losi, P., Briganti, E., Sanguinetti, E., Magera, A., Al Kayal, T., Feriani, R., Di Stefano, R., and Soldani, G. Effect of platelet lysate on human cells involved in different phases of wound healing. PLoS One **8,** e84753, 2013.
127. Etulain, J., Fondevila, C., Negrotto, S., and Schattner, M. Platelet-mediated angiogenesis is independent of VEGF and fully inhibited by aspirin. Br J Pharmacol **170,** 255, 2013.
128. Hofer, H.R., and Tuan, R.S. Secreted trophic factors of mesenchymal stem cells support neurovascular and musculoskeletal therapies. Stem Cell Res Ther **9,** 131, 2016.
129. Madrigal, M., Rao, K.S., and Riordan, N.H. A review of therapeutic effects of mesenchymal stem cell secretions and induction of secretory modification by different culture methods. J Transl Med **11,** 260, 2014.
130. Abdelrazik, H., Spaggiari, G.M., Chiossone, L., and Moretta, L. Mesenchymal stem cells expanded in human platelet lysate display a decreased inhibitory capacity on T- and NK-cell proliferation and function. Eur J Immunol **41,** 3281, 2011.
131. Ulivi, V., Tasso, R., Cancedda, R., and Descalzi, F. Mesenchymal stem cell paracrine activity is modulated by platelet lysate: induction of an inflammatory response and secretion of factors maintaining macrophages in a proinflammatory phenotype. Stem Cells Dev **15,** 1858, 2014.
132. Wagner, W., Ho, A.D., and Zenke, M. Different facets of aging in human mesenchymal stem cells. Tissue Eng Part B Rev **16,** 445, 2010.
133. Turinetto, V., Vitale, E., and Giachino, C. Senescence in human mesenchymal stem cells: functional changes and implications in stem cell-based therapy. Int J Mol Sci **17,** pii:E1164, 2016.
134. Cholewa, D., Stiehl, T., Schellenberg, A., Bokermann, G., Joussen, S., Koch, C., Walenda, T., Pallua, N., Marciniak-Czochra, A., Suschek, C.V., and Wagner, W. Expansion of adipose mesenchymal stromal cells is affected by human platelet lysate and plating density. Cell Transplant **20,** 1409, 2011.
135. Bieback, K., Hecker, A., Schlechter, T., Hofmann, I., Brousos, N., Redmer, T., Besser, D., Klüter, H., Müller, A.M., and Becker, M. Replicative aging and differentiation potential of human adipose tissue-derived mesenchymal stromal cells expanded in pooled human or fetal bovine serum. Cytotherapy **14,** 570, 2012.
136. Schallmoser, K., Bartmann, C., Rohde, E., Bork, S., Guelly, C., Obenauf, A.C., Reinisch, A., Horn, P., Ho, A.D., Strunk, D., and Wagner, W. Replicative senescence-associated gene expression changes in mesenchymal stromal cells are similar under different culture conditions. Haematologica **95,** 867, 2010.
137. Griffiths, S., Baraniak, P.R., Copland, I.B., Nerem, R.M., and McDevitt, T.C. Human platelet lysate stimulates high-passage and senescent human multipotent mesenchymal stromal cell growth and rejuvenation in vitro. Cytotherapy **12,** 1469, 2013.
138. Plachokova, A.S., Nikolidakis, D., Mulder, J., Jansen, J.A., and Creugers, N.H. Effect of platelet-rich plasma on bone regeneration in dentistry: a systematic review. Clin Oral Implants Res **19,** 539, 2008.
139. Yamada, Y., Nakamura, S., Ito, K., Umemura, E., Hara, K., Nagasaka, T., Abe, A., Baba, S., Furuichi, Y., Izumi, Y., Klein, O.D., and Wakabayashi, T. Injectable bone tissue engineering using expanded mesenchymal stem cells. Stem cells (Dayton, Ohio) **31,** 572, 2013.
140. Pocaterra, A., Caruso, S., Bernardi, S., Scagnoli, L., Continenza, M.A., and Gatto, R. Effectiveness of platelet-rich plasma as an adjunctive material to bone graft: a systematic review and meta-analysis of randomized controlled clinical trials. Int J Oral Maxillofac Surg **45,** 1027, 2016.
141. Centeno, C.J., Schultz, J.R., Cheever, M., Freeman, M., Faulkner, S., Robinson, B., and Hanson, R. Safety and complications reporting update on the re-implantation of culture-expanded mesenchymal stem cells using autologous platelet lysate technique. Curr Stem Cell Res Ther **6,** 368, 2011.
142. Zhang, J., Huang, X., Wang, H., Liu, X., Zhang, T., Wang, Y., and Hu, D. The challenges and promises of allogeneic mesenchymal stem cells for use as a cell-based therapy. Stem Cell Res Ther **6,** 234, 2015.
143. Otsuru, S., Gordon, P.L., Shimono, K., Jethva, R., Marino, R., Phillips, C.L., Hofmann, T.J., Veronesi, E., Dominici, M., Iwamoto, M., and Horwitz, E.M. Transplanted bone marrow mononuclear cells and MSCs impart clinical benefit to children with osteogenesis imperfecta through different mechanisms. Blood **120,** 1933, 2012.
144. Gupta, P.K., Chullikana, A., Rengasamy, M., Shetty, N., Pandey, V., Agarwal, V., Wagh, S.Y., Vellotare, P.K., Damodaran, D., Viswanathan, P., Thej, C., Balasubramanian, S., and Majumdar, A.S. Efficacy and safety of adult human bone marrow-derived, cultured, pooled, allogeneic mesenchymal stromal cells (Stempeucel®): preclinical and clinical trial in osteoarthritis of the knee joint. Arthritis Res Ther **18,** 301, 2016.
145. von Bonin, M., Stölzel, F., Goedecke, A., Richter, K., Wuschek, N., Hölig, K., Platzbecker, U., Illmer, T., Schaich, M., Schetelig, J., Kiani, A., Ordemann, R., Ehninger, G., Schmitz, M., and Bornhäuser, M. Treatment of refractory acute GVHD with third-party MSC expanded in platelet lysate-containing medium. Bone Marrow Transplant **43,** 245, 2009.
146. Lucchini, G., Introna, M., Dander, E., Rovelli, A., Balduzzi, A., Bonanomi, S., Salvadè, A., Capelli, C., Belotti, D., Gaipa, G., Perseghin, P., Vinci, P., Lanino, E., Chiusolo, P., Orofino, M.G., Marktel, S., Golay, J., Rambaldi, A., Biondi, A., D'Amico, G., and Biagi, E. Platelet-lysate-expanded mesenchymal stromal cells as a salvage therapy for severe resistant graft-versus-host disease in a pediatric population. Biol Blood Marrow Transplant **16,** 1293, 2010.
147. Kuçi, Z., Bönig, H., Kreyenberg, H., Bunos, M., Jauch, A., Janssen, J.W., Škifić, M., Michel, K., Eising, B., Lucchini, G., Bakhtiar, S., Greil, J., Lang, P., Basu, O., von Luettichau, I., Schulz, A., Sykora, K.W., Jarisch, A., Soerensen, J., Salzmann-Manrique, E., Seifried, E., Klingebiel, T., Bader, P., and Kuçi, S. Mesenchymal stromal cells from pooled mononuclear cells of multiple bone marrow donors as rescue therapy in pediatric severe steroid-refractory graft-versus-host disease: a multicenter survey. Haematologica **101,** 985, 2016.

148. Sakamoto, N., Tsuji, K., Muul, L.M., Lawler, A.M., Petricoin, E.F., Candotti, F., Metcalf, J.A., Tavel, J.A., Lane, H.C., Urba, W.J., Fox, B.A., Varki, A., Lunney, J.K., and Rosenberg, A.S. Bovine apolipoprotein B-100 is a dominant immunogen in therapeutic cell populations cultured in fetal calf serum in mice and humans. Blood **110,** 501, 2007.
149. Haque, N., Abu Kasim, N.H., and Rahman, M.T. Optimization of pre-transplantation conditions to enhance the efficacy of mesenchymal stem cells. Int J Biol Sci **11,** 324, 2015.
150. Siddappa, R., Licht, R., van Blitterswijk, C., and de Boer, J. Donor variation and loss of multipotency during in vitro expansion of human mesenchymal stem cells for bone tissue engineering. J Orthop Res **25,** 1029, 2007.
151. Fazzina, R., Iudicone, P., Fioravanti, D., Bonanno, G., Totta, P., Zizzari, I.G., and Pierelli, L. Potency testing of mesenchymal stromal cell growth expanded in human platelet lysate from different human tissues. Stem Cell Res Ther **6,** 55, 2015.
152. Deeks, J.J., Higgins, J.P.T., and Altman, D.G. Analysing data and undertaking meta-analyses. In: Higgins, J.P., and Green S., eds. Cochrane Handbook for Systematic Reviews of Interventions: Cochrane Book Series. Chichester, United Kingdom: John Wiley & Sons, Ltd, 2008, pp. 243.

Address correspondence to:
Kamal Mustafa, DDS, PhD
Department of Clinical Dentistry
Centre for Clinical Dental Research
University of Bergen
Årstadveien 19
5009 Bergen
Norway

E-mail: kamal.mustafa@uib.no

Received: February 28, 2017
Accepted: May 22, 2017
Online Publication Date: July 28, 2017

Downloaded by Mary Ann Liebert, Inc., publishers from online.liebertpub.com at 08/03/17. For personal use only.

TISSUE ENGINEERING: Part B
Volume 23, Number 2, 2017
© Mary Ann Liebert, Inc.
DOI: 10.1089/ten.teb.2016.0283

termis
Tissue Engineering
& Regenerative Medicine
International Society

REVIEW ARTICLE

Cell Cotransplantation Strategies for Vascularized Craniofacial Bone Tissue Engineering: A Systematic Review and Meta-Analysis of Preclinical *In Vivo* Studies

Siddharth Shanbhag, DDS, MSc,[1,2] Nikolaos Pandis, DDS, PhD,[3] Kamal Mustafa, DDS, PhD,[1] Jens R. Nyengaard, MD, PhD,[4] and Andreas Stavropoulos, DDS, PhD[2]

The regenerative potential of tissue-engineered bone constructs may be enhanced by *in vitro* coculture and *in vivo* cotransplantation of vasculogenic and osteogenic (progenitor) cells. The objective of this study was to systematically review the literature to answer the focused question: In animal models, does cotransplantation of osteogenic and vasculogenic cells enhance bone regeneration in craniofacial defects, compared with solely osteogenic cell-seeded constructs? Following PRISMA (Preferred Reporting Items for Systematic Reviews and Meta-Analyses) guidelines, electronic databases were searched for controlled animal studies reporting cotransplantation of endothelial cells (ECs) with mesenchymal stem cells (MSCs) or osteoblasts in craniofacial critical size defect (CSD) models. Twenty-two studies were included comparing outcomes of MSC/scaffold versus MSC+EC/scaffold (co)transplantation in calvarial ($n=15$) or alveolar ($n=7$) CSDs of small (rodents, rabbits) and large animal (minipigs, dogs) models. On average, studies presented with an unclear to high risk of bias. MSCs were derived from autologous, allogeneic, xenogeneic, or human (bone marrow, adipose tissue, periosteum) sources; in six studies, ECs were derived from MSCs by endothelial differentiation. In most studies, MSCs and ECs were cocultured *in vitro* (2–17 days) before implantation. Coculture enhanced MSC osteogenic differentiation and an optimal MSC:EC seeding ratio of 1:1 was identified. Alloplastic copolymer or composite scaffolds were most often used for *in vivo* implantation. Random effects meta-analyses were performed for histomorphometric and radiographic new bone formation (%NBF) and vessel formation in rodents' calvarial CSDs. A statistically significant benefit in favor of cotransplantation versus MSC-only transplantation for radiographic %NBF was observed in rat calvarial CSDs (weighted mean difference 7.80% [95% confidence interval: 1.39–14.21]); results for histomorphometric %NBF and vessel formation were inconclusive. Overall, heterogeneity in the meta-analyses was high ($I^2 > 80\%$). In summary, craniofacial bone regeneration is enhanced by cotransplantation of vasculogenic and osteogenic cells. Although the direction of treatment outcome is in favor of cotransplantation strategies, the magnitude of treatment effect does not seem to be of relevance, unless proven otherwise in clinical studies.

Keywords: bone tissue engineering, coculture, endothelial cells, mesenchymal stem cells, meta-analysis, vascularization

Introduction

Reconstruction of maxillofacial bone deficiencies, resulting from aging, trauma, pathology, or ablative surgery, remains a clinical challenge.[1] Although autologous bone transplantation is still considered the gold standard for maxillofacial bone regeneration,[2,3] large defects may require volumes of bone locally unavailable. Moreover, the morbidity associated with bone harvesting can be a major limiting factor.[4] Alternatives have included allogeneic, xenogeneic, and alloplastic bone substitutes, but no consensus currently exists on the effectiveness of one material over the other, in comparison with autogenous bone, or for any particular indication.[5,6]

[1]Department of Clinical Dentistry, Centre for Clinical Dental Research, University of Bergen, Bergen, Norway.
[2]Department of Periodontology, Faculty of Odontology, Malmö University, Malmö, Sweden.
[3]Department of Orthodontics and Dentofacial Orthopedics, School of Dental Medicine, University of Bern, Bern, Switzerland.
[4]Stereology and Electron Microscopy Laboratory, Department of Clinical Medicine, Aarhus University, Aarhus, Denmark.

The bone tissue engineering (BTE) approach involves harvesting of osteogenic cells (most commonly mesenchymal stem cells [MSCs]) from an autologous source (e.g., bone marrow, adipose tissue), their *in vitro* expansion, and, in combination with an appropriate carrier scaffold, their *in vivo* implantation.[7] Thus, the triad of *osteogenic* cells, *osteoinductive* signals (growth factors [GFs] released by cells), and *osteoconductive* scaffolds replicates the properties of autogenous bone, without the need for invasive harvesting.[8] The prospects of BTE for alveolar bone repair are very promising, as demonstrated by several preclinical and some clinical studies (for reviews, see Shanbhag and Shanbhag,[7] Shanbhag et al.,[9] and Padial-Molina et al.[10]).

The promising results of preclinical BTE studies have not yet translated into significantly improved clinical outcomes in human trials.[11–13] A major limitation of traditional BTE approaches is the reported lack of adequate and timely vascularization of the implanted construct—which is essential for oxygenation, nutrition, and waste elimination to/from the cells.[14] Absence of adequate vascular supply can result in premature cell death in regions of the construct distant from the host vasculature since diffusion of oxygen and nutrients is only limited to a distance of 150–200 μm.[15,16] One strategy to overcome this limitation is to co*culture* (*in vitro*) and co*transplant* (*in vivo*) osteogenic cells along with endothelial cells (ECs) or endothelial progenitor cells (EPCs) to simultaneously stimulate osteogenesis and *vasculogenesis*, that is, *de novo* formation of blood vessels, within bone constructs.[17,18]

EPCs and ECs are hematopoietic cells, which contribute directly to the process of new vessel formation,[17] and can be easily isolated from peripheral blood, bone marrow, and other tissues.[19] These cells also play a central role in emerging prevascularization strategies, which aim to generate primitive vessels within tissue constructs *in vitro* that functionally anastomose with the host vasculature when implanted *in vivo*.[20,21] Recent studies have demonstrated enhanced performance of osteogenic cells (MSCs or osteoblasts [OBs]) when cocultured with EPCs or ECs in terms of *in vitro* gene expression and *in vivo* bone formation, suggesting a synergistic effect of vasculogenesis and osteogenesis—as discussed in several recent review articles.[22–25]

Preclinical testing of new regenerative therapies in clinically relevant animal models is an important aspect of translational research and, in most cases, a requirement of regulatory health agencies before initiating human clinical trials.[26,27] Commonly reported animal models of relevance to craniofacial bone regeneration involve calvarial and alveolar critical size defects (CSDs). A CSD is the smallest size experimental defect in the cranial or alveolar bone of the animal that will not spontaneously and extensively regenerate with bone within a defined time frame without intervention.[28,29]

Following the PRISMA (Preferred Reporting Items for Systematic Reviews and Meta-analyses) guidelines,[30] the aim of the present study was to systematically review the available literature to answer the focused PICO (population, intervention, comparison, outcome) question: In CSDs of experimental animals, does a cotransplantation approach, that is, implanting osteogenic *and* vasculogenic cells seeded on biomaterial scaffolds, enhance bone regeneration compared with implanting *only* osteogenic cell-seeded scaffolds?

Materials and Methods

Inclusion and exclusion criteria

Inclusion criteria

(1) English-language articles.
(2) Randomized or nonrandomized, controlled preclinical studies with two or more experimental groups.
(3) Involving CSDs in the calvaria, maxillae, or mandibles of small or large animals.
(4) Cotransplantation of cultured autologous, allogeneic, or human-derived MSCs (or OBs) and EPCs (or ECs) seeded on biomaterial scaffolds in at least one experimental group.
(5) A control group receiving transplantation of only MSC- or OB-seeded scaffolds.
(6) Quantitative assessment of new bone formation (%NBF)[29] through (a) histomorphometry or (b) three-dimensional (3D) computed tomography (CT) or micro-CT. Quantitative histological or immunohistochemical assessment of new vessel formation (vasculogenesis) was considered as a secondary outcome.

Exclusion criteria

(1) Solely *in vitro* studies.
(2) *In vivo* studies reporting CSDs in other anatomical sites (e.g., long bones), ectopic models (e.g., subcutaneous), or systemic cell delivery.
(3) Absence of a cotransplantation group or an MSC-only group.

Search strategy, screening, and study selection

Electronic databases of MEDLINE (via PubMed) and EMBASE were searched for relevant English-language literature up to and including April 2016. Unpublished literature was searched through the Google and Google Scholar search engines. Bibliographies of the selected studies and relevant review articles were checked for cross-references. A specific search strategy was developed for MEDLINE (Table 1) and adapted for other databases. Titles and abstracts of the search-identified studies were screened by two authors (S.S. and A.S.) and full texts of all eligible studies were obtained. Uncertainty in the determination of eligibility was resolved by discussion with the other authors. Two authors (S.S. and A.S.) reviewed the selected full texts independently, and final inclusion was based on the aforementioned inclusion criteria. A summary of the screening process is presented in Figure 1.

Data extraction

Data were extracted from full texts of included articles on author(s), study design, animal species, model characteristics, number of animals, number of procedures, inclusion criteria, outcome(s), method(s) of outcome evaluation, main findings, and conclusions. Descriptive summaries of studies were entered into tables. Quantitative data regarding NBF, that is, regenerated bone volume as a percentage, and vessel formation, that is, vessel numbers/density per unit area, were extracted from studies for possible meta-analyses. When data were presented as ratios or volumes (mm^3), they

Table 1. Search Strategy for MEDLINE

Search	*Keywords*	*Result*
#6	((((((mesenchymal OR stem OR stromal OR MSC* OR osteogenic OR osteoprogenitor* OR osteoblast*) AND (endothelial OR ''endothelial progenitor'' OR EC* OR EPC*) AND cells))) AND ((coculture OR ''co culture'' OR ''co transplantation'')))) AND ((bone OR osteogenesis OR regeneration))) AND ((cranial OR craniofacial OR calvarial OR calvarium OR skull OR mandibular OR mandible OR maxilla OR maxillary OR jaw OR alveolar))	109
#5	(((mesenchymal OR stem OR stromal OR MSC* OR osteogenic OR osteoprogenitor* OR osteoblast*) AND (endothelial OR ''endothelial progenitor'' OR EC* OR EPC*) AND cells))) AND ((coculture OR ''co culture'' OR ''co transplantation''))	2998
#4	(cranial OR craniofacial OR calvarial OR calvarium OR skull OR mandibular OR mandible OR maxilla OR maxillary OR jaw OR alveolar)	450582
#3	((bone OR osteogenesis OR regeneration))	1295834
#2	((coculture OR ''co culture'' OR ''co transplantation''))	33502
#1	(((mesenchymal OR stem OR stromal OR MSC* OR osteogenic OR osteoprogenitor* OR osteoblast*) AND (endothelial OR ''endothelial progenitor'' OR EC* OR EPC*) AND cells)))	84697

were converted to percentages using total defect volume data. Standard errors of means, when reported, were converted to standard deviations for analysis. If data were only expressed graphically, numerical values were requested from the authors, and if a response was not received, digital ruler software was used to measure graphical data (ImageJ; National Institutes of Health, Bethesda, MD). When studies reported outcomes at multiple time points, data from similar time points of different studies were pooled for meta-analysis.

Quality assessment and risk of bias

Reporting quality assessment of all studies was performed based on a modification of the ARRIVE (Animal Research: Reporting *In Vivo* Experiments) guidelines regarding relevant items.[31,32] Compliance with the guidelines was evaluated using a predefined grading system applied to each of the 20 items[33] (Supplementary Table S1; Supplementary Data are available online at www.liebertpub.com/teb). Reporting quality was judged as high, moderate, or low. Risk of bias (RoB) assessment was performed using a modification of the SYstematic Review Centre for Laboratory animal Experimentation (SYRCLE) RoB tool for animal studies[34] and judged as high, low, or unclear[35] (Supplementary Table S2). Any disagreement between the reviewers during study selection, data extraction, and quality assessment was resolved by discussion and consensus.

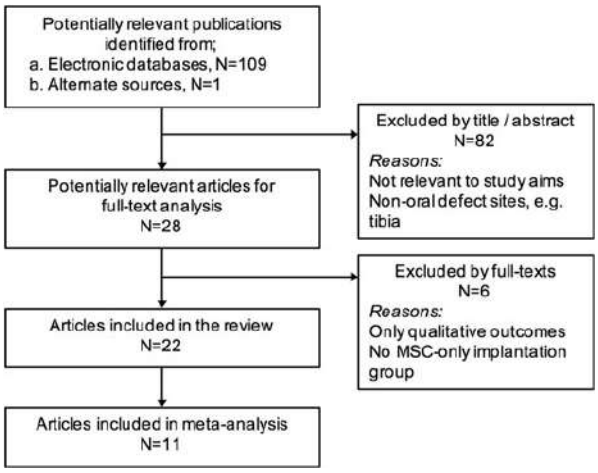

FIG. 1. Flowchart for study screening and selection. *N*, number of articles.

Meta-analysis

Meta-analysis was performed to compare the effectiveness of MSC/EC cotransplantation (experimental [Ex]) and MSC-only transplantation (control [Co]) using histomorphometric and micro-CT data (mean and standard deviation of %NBF and number of animals/defects [*n*] per group). Studies were pooled based on homogeneity regarding PICO and observation time. Subgroup analyses were performed at the level of animals and observation time(s), using the DerSimonian and Laird random effects model[36] and STATA Statistical Software (StataCorp LP, College Station, TX). In one study,[37] the design included multiple interventions per animal, that is, bilateral calvarial defects, for which a correlation coefficient (*r*) was calculated for between treatment-group measurements.[38] An *r*-value of 0.5 was used for this study; for parallel group studies, the *r*-value was set at 0 and thus both study types were included in the same analysis.[39] Pooled estimates of treatment effect (weighted mean differences [WMDs]) were calculated along with 95% confidence intervals (CIs), and the I^2 statistic was used as a measure of inconsistency of results across studies.[36]

Results

Search results and study characteristics

Of the 110 search-identified titles, 22 studies reporting quantitative histomorphometric and/or radiographic (CT/micro-CT) outcomes from 5 different species and 474 animals were included in the review (Table 2). A list of excluded studies along with reasons for exclusion is provided in Supplementary Table S5. Small animal models included rats (number of animals [*n*] = 356), mice ($n = 77$), and rabbits ($n = 27$). Large animal models included minipigs ($n = 6$) and

Table 2. Summary of Study Characteristics

Study	*Strain, age*	*Model, defect size (mm)*	n	*Time (weeks)*	*Cells*	*Source; induction*	*Cells, coratio, time*	*Scaffold*	*Outcome(s)*
Rats									
Kaigler *et al.*[41]	Nude SD, NR	CCSD, 8.5	30	6, 12	BMSC DMEC	Human; no	5×10^5, 1:1, 1 h	PLGA	μCT Vessels
Xing *et al.*[37]	Lewis, 3 months	CCSD (b), 6	12	5	BMSC BMSC-EC	Allo; yes	5×10^5, 5:1, 7 days	Poly(LLA-co-DXO)	Histo Vessels
Kim *et al.*[45]	SD, adult	CCSD, 8	30	8, 12	ASC HUVEC	Human; yes	2×10^5, 2:1, 2 days	PCL/PLGA/TCP	μCT
Cornejo *et al.*[54]	Lewis, 8 weeks	CCSD, 8	37	8	ASC ASC-EC	Auto; yes	1×10^5, 1:1, 2 days	Allograft	μCT Vessels
He *et al.*[43]	Nude, 10 weeks	CCSD, 8	40	4, 12	BMSC UCB-EC	Human; no	5×10^5, 1:1, NR	HA-PLGA	μCT Vessels
He *et al.*[52]	SD, 8 weeks	CCSD, 8	30	5	BMSC *BMSC-BMP2* BMSC-EPC *EPC-BMP2*	Allo; no	1×10^6, 1:1, NR	Nano-CS/alginate	Histo, μCT Vessels
Ma *et al.*[47]	Nude, 9 weeks	CCSD (b), 5	10	8	ASC HUVEC	Human; no	24×10^6, 1:1, 7 days	Ti-mesh	Histo
Shah *et al.*[56]	Lewis, 2 months	CCSD, 8	28	8	ASC ASC-EC	Allo; yes	1×10^5, 1:1, NR	PLA	μCT Vessels
Sathy *et al.*[59]	Fischer, 12 weeks	CCSD, 8	64	4, 12	BMSC EC, MSC-PC	Allo; yes	2×10^5, NR, ON	HA-PLA-Col/Fn (ML)	μCT Vessels
Johari *et al.*[48]	Wistar (IS), 8 weeks	CCSD, 5	36	4, 12	HOB HUVEC	Human; yes	3×10^5, 1:1, 3 days	Gelatin-HA	Histo
Liang *et al.*[57]	SD, 8 weeks	MxCSD (b), 4×3×3	27	6	BMSC BM-EPC	Allo; yes	3×10^5, 1:1, 17 days	Cell sheets (no scaffold)	Histo, μCT Vessels
Wen *et al.*[58]	SD, 8 weeks	MxCSD (b), 4×3×3	12	4, 6	BMSC BM-EPC	Allo; yes	5×10^6, 1:1, 7 days[a]	Fibrin glue	μCT Vessels
Mice									
Kim *et al.*[53]	SCID, 7 weeks	CCSD, 4	8	8	BMSC BMSC-EC	Dog; yes	4×10^5, 1:1, 30 months	HA-PLGA	Histo Vessels
Koob *et al.*[42]	SCID, 8 weeks	CCSD, 4.3	27	6	BMSC HUVEC	Human; yes	1×10^6 (MSC), 3×10^5 (EC), 1 h	DBBM/fibrin/ matrigel	Histo Vessels
Goerke *et al.*[44]	SCID, 8 weeks	CCSD, 4.3	22	6	BMSC-SMC PB-EPC	Human; yes	3×10^5,1:1, ON	DBBM/collagen	Histo Vessels
Kim *et al.*[46]	Nude, 7 weeks	CCSD (b), 3	20	10	BMSC ASC	Human; no	1×10^5, 2:1, NR	HA-β-TCP	μCT

(*continued*)

Table 2. (Continued)

Study	*Strain, age*	*Model, defect size (mm)*	n	*Time (weeks)*	*Cells*	*Source; induction*	*Cells, coratio, time*	*Scaffold*	*Outcome(s)*
Rabbits									
Li *et al.*[55]	NZ, 3 months	CCSD, 15	15	8	BMSC PB-EPC	Auto; no	Cell sheets, NR	HA	Histo, μCT
Liu *et al.*[73]	NZ, NR	MCSD (b), 10×15	12	4, 8	BMSC BMSC-EC	Auto; yes (in ctrl grp)	2×10^4, 1:1, 14 days	PLGA	Histo
Minipigs									
Lee *et al.*[49]	0.5–1 years	MCSD, 15×5	2	4, 7, 10, 12	POC AT-EC	Human; yes	2×10^5, 2:1, 7 days	PDO/PLF	CT
Lee *et al.*[50]	0.5–1 years	MCSD, 15×5	2	12	POC PO-EC	Human; yes	2×10^5, 2:1, 7 days	PDO/PLF	CT
Lee *et al.*[51]	0.5–1 years	MCSD, 15×5	2	4, 8, 12	POC UCB-EPC	Human; yes	2×10^5, 2:1, 7 days	PDO/PLF	CT
Dogs									
Khojasteh *et al.*[60]	Mongrel	MCSD (b), 10	8	8	BMSC BM-EPC	Auto; no	5×10^5, 1:1, 48 h	β-TCP-PLGA±*VEGF*	Histo

[a]Indirect coculture of MSCs and EPCs, that is, MSCs cultured in the presence or absence of EPCs were implanted.

μCT, microcomputed tomography; Allo, allogeneic; Auto, autologous; (b), bilateral CSD; CCSD, calvarial CSD; Cells, number of implanted MSCs; coratio, time, coculture (MSC:EC) ratio and coculture time; CSD, critical size defect; CT, computed tomography; EPCs, endothelial progenitor cells; Histo, histomorphometry; Human, human-derived; induction, osteogenic induction; IS, immune suppressed; MCSD, mandibular CSD; MxCSD, maxillary CSD; *n*, number of animals; NR, not reported; NZ, New Zealand; ON, overnight; SCID, severe combined immunodeficiency; SD, Sprague-Dawley; Vessels, vessel regeneration.

Cells (osteogenic): ASC, adipose tissue-derived MSC; BMSC, bone marrow-derived mesenchymal stem cell; HOB, human osteoblast; POC, periosteal cell.

Cells (vasculogenic): ASC-EC, ASC-differentiated EC; AT-EC, adipose tissue-derived EC; BMSC, bone marrow-derived MSC; BMSC-BMP2, BMP2 gene-modified BMSC; BMSC-EPC/EC, BMSC-differentiated EPC/EC; BMSC-SMC, BMSC-differentiated smooth muscle cell; DMEC, dermal microvascular EC; EC, endothelial cell; EPC-BMP2, BMP2 gene-modified EPC; HUVEC, human umbilical vein EC; PB-EPC, peripheral blood EPC; PO-EC, periosteum-derived EC; UCB-EPC, umbilical cord blood-derived EPC.

Scaffolds: DBBM, demineralized bovine bone mineral; HA-PLA-Col/Fn (ML), HA-PLA-collagen/fibronectin (multilayered scaffold); HA-PLGA, hydroxyapatite-PLGA; Nano-CS/Alginate, nano-calcium sulfate/alginate; PCL/PLGA/TCP, polycaprolactone/PLGA/tricalcium phosphate; PDO/PLF, polydioxanone/pluronic F127 copolymer; PLGA, poly-lactide-co-glycolide; Poly(LLA-co-DXO), poly(L-lactide-co-1,5-dioxepan-2-one) copolymer; Ti-mesh, titanium mesh; VEGF, vascular endothelial growth factor.

dogs ($n=8$; Table 2). Sample sizes in individual studies ranged from 2 to 64, and observation times ranged from 4 to 12 weeks. Fifteen studies used calvarial CSD models, while seven studies used maxillary (two studies) or mandibular CSDs (five studies). No studies included a positive control group treated with gold standard autogenous bone.

Quality assessment and RoB

Overall, the included studies were of unclear to high RoB and moderate reporting quality (Supplementary Tables S2 and S3). Most studies provided adequate information regarding title, abstract, introduction, study objectives, ethical approval, experimental design, and procedures. However, information regarding experimental animals and their housing and husbandry was generally inadequate. No studies provided information on sample size calculation or baseline characteristics of the animals. In seven studies, animals (or defects) were randomly allocated to treatment groups to minimize selection bias, although no details of the randomization procedure were reported. Four studies reported blinding of outcome assessors to treatment groups to minimize detection bias. All studies reported detailed outcome evaluation, including statistical analyses. Finally, information regarding study limitations and implications for translation to human models was limited. None of the studies reported implications for the 3Rs principle (replacement, refinement, and reduction) of animals in research.[31,40]

Characteristics of cell cotransplantation strategies

Osteogenic cells. Included studies reported on the use of autologous, allogeneic, xenogeneic, or human bone marrow-derived MSCs (BMSCs), adipose tissue-derived MSCs (ASCs), periosteal cells (POCs), or human osteoblasts (HOBs) as the osteogenic cell population. Eleven studies reported the use of human-derived cells, that is, BMSCs,[41–44] ASCs,[45–47] HOBs,[48] or POCs.[49–51] MSCs were used in early passages (2–5) and most often osteogenically induced before implantation (66% studies). One study[52] reported the use of bone morphogenetic protein-2 (BMP-2) gene-modified allogeneic BMSCs in rats.

Vasculogenic cells. ECs and EPCs in the included studies were obtained from commercial, autologous, allogeneic, or human sources—most commonly, bone marrow. Commercially obtained human umbilical vein endothelial cells (HUVECs) were reported in three studies,[42,45,47] while EPC isolation from human umbilical cord blood was reported in two studies.[43,51] In six studies, ECs were differentiated from a fraction of the isolated MSCs by endothelial induction.[37,52–56] EC/EPCs were characterized by expression of endothelial-specific markers, CD31, CD146, or CD34, through flow cytometry, immunostaining, or polymerase chain reaction (PCR) analysis.

Coculture. A majority (60%) of studies reported *in vitro* coculture of MSCs and EPC/ECs overnight or for 2–17 days before implantation; in three studies,[41,42,53] MSCs and ECs were coseeded on scaffolds only 0.5–1.5 h before implantation. One study[57] reported cell sheet preparation through BMSC-EPC coculture for 10 days, while another study (by the same group)[58] reported indirect coculture of BMSCs and EPCs using a transwell system—to investigate the influence of EPC secretory products on BMSCs. Coculture conditions varied between studies; MSCs and EPC/ECs were cocultured in standard, osteogenic, endothelial, or combination culture media. In two studies,[47,52] the optimal seeding ratio of MSC:ECs and the influence of coculture on *in vitro* osteogenic potential of MSCs were evaluated by alkaline phosphatase (ALP) activity or calcium staining assay after 7 or 28 days, respectively. Coculture enhanced MSC osteogenic differentiation compared with MSC-only culture, and an MSC:EC seeding ratio of 1:1 (vs. 1:2, 2:1, 5:1, etc.) was identified as being most optimal. The number of implanted cells ranged from 1×10^3 to 12×10^6 each for MSCs and EPC/ECs. In one study,[52] coculture of BMP-2-modified BMSCs and EPCs enhanced ALP activity and OB and endothelial marker expression compared with monoculture of BMP-2-modified BMSCs or unmodified BMSCs. *In vitro* prevascularization, that is, formation of primitive capillary-like networks, following 1-week dynamic coculture of BMSCs and ECs on copolymer scaffolds was reported in one study.[37]

Scaffolds. In most studies, alloplastic copolymer or composite scaffolds were used as carriers for cells. Other common biomaterials such as β-tricalcium phosphate (β-TCP), hydroxyapatite (HA), and bovine bone mineral (BBM) were also used as scaffolds. One study reported the use of (rat) calvarial allografts.[54] One study[59] reported the use of a multilayered composite (HA-copolymer) scaffold comprising MSCs and ECs in a layered construct design. Another study[60] reported incorporation of vascular endothelial growth factor (VEGF) within β-TCP scaffolds in some experimental groups. Scaffolds were prepared according to defect dimensions and seeded with cells either well before (2–14 days) or shortly before (1–1.5 h) surgery.

Qualitative outcomes

Overall, minimal signs of inflammatory response, infection, or adverse reactions were observed across all studies, even after transplantation of allogeneic, xenogeneic, or human-derived cells. Detection of newly formed vessels was performed through immunohistochemical staining for endothelial-specific markers such as CD31, CD34, von Willebrand factor (vWF), VEGF, and so on. One study[45] reported PCR analysis of retrieved tissues to identify endothelial marker genes (CD31, vWF, and vascular endothelial-cadherin). A general observation across studies was the detection of vascular structures consistently in areas of NBF. In four studies,[41,42,44,45] detection of human-specific endothelial markers in retrieved tissues confirmed the contribution of implanted ECs in vasculogenesis.

Meta-analyses

Meta-analysis was performed if there were three or more studies in each comparison group. Eleven studies reporting histomorphometric or micro-CT-based %NBF following MSC/EC cotransplantation versus MSC-only transplantation, in calvarial CSDs of rats and mice, were included in two separate meta-analyses (Fig. 2). A comparison was also made between cotransplantation and EC-only transplantation (Fig. 3). Finally, vessel regeneration was compared between cotransplantation and MSC-only groups (Fig. 4).

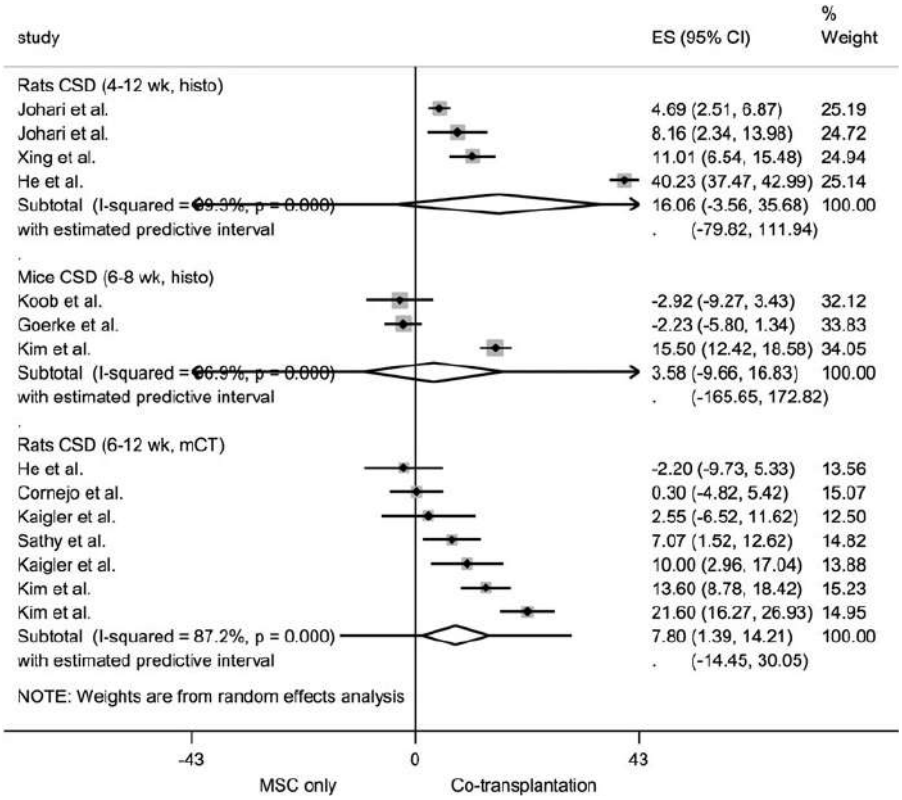

FIG. 2. Forest plot for the comparison cotransplantation versus MSC-only transplantation for bone formation in rodent CSD models. The forest plot displays relative weight of the individual studies, the estimates of treatment effect (ES, effect size) expressed as WMDs, 95% CIs, and a predictive interval for the outcome %NBF. The *diamond* indicates the pooled estimate and its 95% CI. μCT, microcomputed tomography-based %NBF; CI, confidence interval; CSD, critical size defect; histo, histomorphometric new bone formation (%NBF); MSC, mesenchymal stem cell; wk, weeks; WMDs, weighted mean differences.

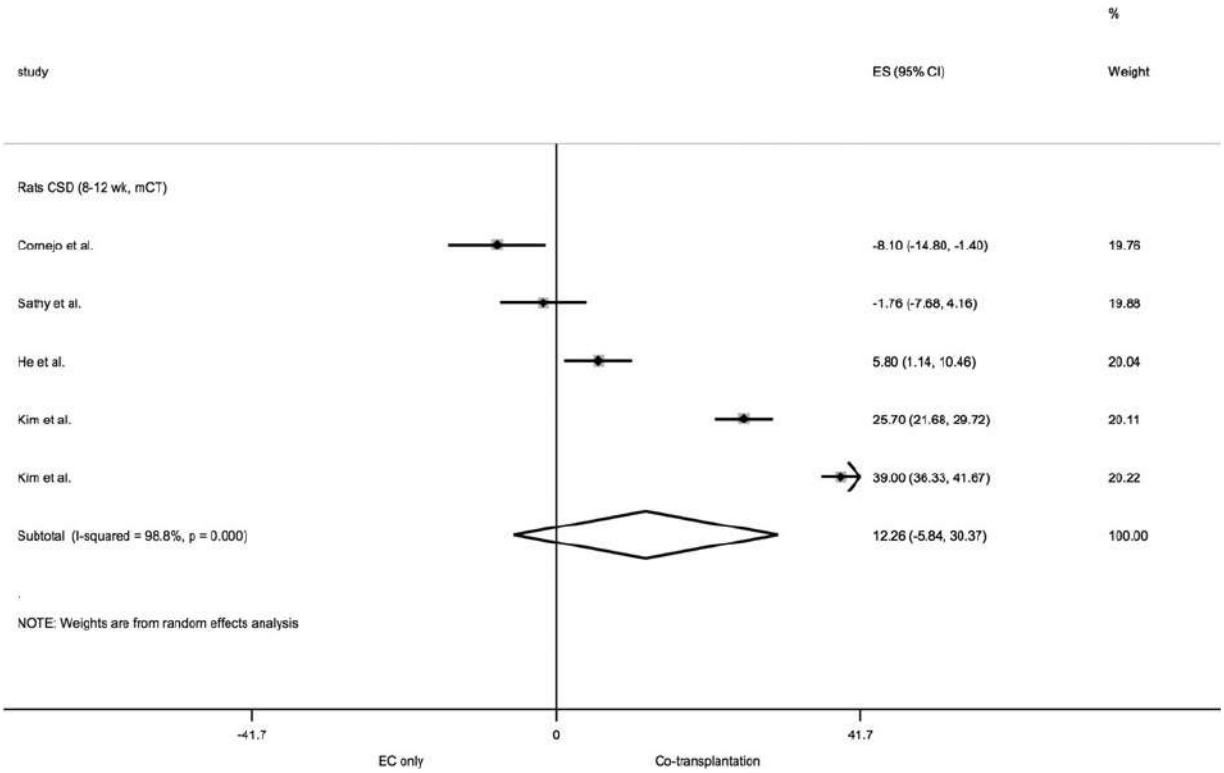

FIG. 3. Forest plot for the comparison cotransplantation versus EC-only transplantation for bone formation in rat CSD models. The forest plot displays relative weight of the individual studies, the estimates of treatment effect (ES) expressed as WMDs, 95% CIs, and a predictive interval for the outcome %NBF. The *diamond* indicates the pooled estimate and its 95% CI. EC, endothelial cell.

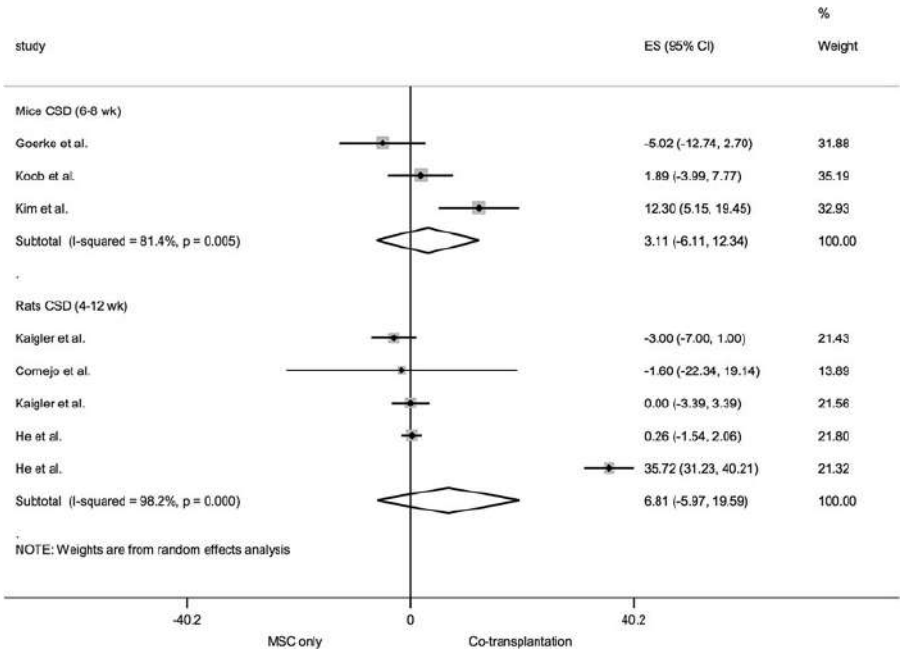

FIG. 4. Forest plot for the comparison cotransplantation versus MSC-only transplantation for vessel formation in rodent CSD models. The forest plot displays relative weight of the individual studies, the estimates of treatment effect (ES) expressed as WMDs, 95% CIs, and a predictive interval for the outcome vessel density per unit area. The *diamond* indicates the pooled estimate and its 95% CI.

To minimize any confounding influence of exogenous GFs, experimental groups receiving gene-modified cells and/or GFs were excluded. Since there were fewer than 10 studies in each meta-analysis, publication bias through funnel plots or statistical testing was not assessed due to the lack of power to distinguish chance from real asymmetry.[61]

The meta-analyses revealed a statistically significant effect in favor of cotransplantation versus MSC-only transplantation for radiographic bone regeneration in rat calvarial CSDs—pooled estimate (WMDs): 7.80% NBF (95% CI 1.39–14.21). Results for histomorphometric bone regeneration and vessel regeneration were inconclusive. Heterogeneity in most cases was very high ($I^2 > 80\%$, $p < 0.05$). Pooled WMDs with 95% CI and measures of heterogeneity for each of the subgroups are presented in Supplementary Table S4, along with an example for interpretation.

Discussion

The aim of this study was to systematically review the preclinical *in vivo* evidence for cell cotransplantation strategies for craniofacial BTE. Recent reviews of preclinical *in vivo* studies have revealed favorable outcomes of BTE approaches for periodontal[35] and alveolar bone defect regeneration.[9] However, a translational limitation of traditional BTE strategies, including implantation of osteogenic cells seeded on biomaterial scaffolds, is the inadequate vascularization of constructs in human clinical defects.[62] Preclinical studies have demonstrated benefits of coculturing and cotransplanting osteogenic and vasculogenic cells in experimental animal defects to overcome this limitation. For the present review, the most commonly reported animal models of relevance to maxillofacial bone regeneration, that is, calvarial and alveolar CSDs, employing cotransplantation strategies, were considered.

Animal models

Small animal models. A majority of studies included in the present review reported on small animal models, that is, rodents and rabbits. Generally, small animal models constitute a starting point for proof-of-principle or *feasibility* studies before clinical modeling and *efficacy testing* in larger animals.[26,63] Rodent models are often preferred over larger animals due to significantly lower costs, easier housing and handling, and minimal social concern.[64] The calvarial CSD model has been well characterized in rodents—a circular defect of 5 mm diameter is generally considered to be of critical size.[29,65] The present meta-analysis revealed significantly higher radiographic bone regeneration following cotransplantation versus MSC-only or EC-only transplantation in calvarial CSDs of rats; results for histomorphometry were inconclusive. Calvarial bone is reported to physiologically resemble the mandible and therefore calvarial CSDs represent a reliable experimental model to test regenerative therapies for maxillofacial applications.[66,67] Moreover, rodent calvaria are considered as a challenging environment for bone regeneration due to poor blood supply and limited bone marrow[68]; thus, the role of vascularization in bone graft healing is even more critical in this zone.[69] In context, recent studies demonstrated that cotransplantation of EPCs with MSCs enhances vertical bone regeneration, compared with cell-free β-TCP scaffolds, in a rat calvarial dome model—corresponding to the guided bone regeneration (GBR) technique.[70,71]

Rabbits, like rodents, provide advantages of small size and easy handling; additionally, they provide larger volumes of bone tissue and creation of more reliable CSDs than in rodents.[72] The included rabbit studies reported significantly greater histomorphometric %NBF in cotransplantation versus MSC-only groups in either calvarial[55] or mandibular[73] CSD models. However, the significant differences in structure,

composition, and physiology of rodent, rabbit, and human bone (e.g., trabecular content, metabolic rate, remodeling) must be considered when extrapolating results from these studies to avoid, for example, overestimation of clinical performance.[74,75]

Large animal models. Large animal models are especially pertinent in BTE research as defects with relevant diffusion distances simulating the clinical setting can be generated, which allows evaluation of the influence of mass transport, hypoxia, and vascularization on transplanted cell survival.[75] Four studies included in the present review reported data from large animal models—minipigs and dogs. Dogs and pigs, due to the similarities in structure, composition, and physiology between canine/porcine and human bones, are extensively used in musculoskeletal research[76]; the rate of remodeling in pigs (1.2–1.5 μm/day) is comparable with that in humans (1.0–1.5 μm/day), but slower compared with that in dogs (1.5–2.0 μm/day).[74] Minipigs are often preferred due to easier handling than domestic pigs and morphological similarities to human bone.[77] In the present review, all three minipig studies reported superior radiographic bone regeneration in mandibular CSDs augmented with copolymer scaffolds loaded with human POCs and ECs (derived from adipose tissue, periosteum, or umbilical cord blood) versus scaffolds loaded with only POCs after 12 weeks.[49–51] Interestingly, no immunological reactions were reported following implantation of human-derived cells in pigs. The biocompatibility of MSCs within and across species can be attributed to their hypoimmunogenic, immunomodulatory, and anti-inflammatory properties, which have been discussed in detail elsewhere.[78]

A single included study[60] in dogs reported significantly greater histomorphometric %NBF following 8 weeks of coimplantation of autologous MSCs and EPCs in composite (β-TCP-PLGA) scaffolds versus only MSC-seeded scaffolds ($45.21\% \pm 0.16\%$ vs. $34.59\% \pm 1.49\%$). Interestingly, the investigators also included VEGF—a key regulator of angiogenesis, in some of the experimental groups. The highest %NBF was observed in the MSC/VEGF group ($63.42\% \pm 1.6\%$). However, no significant differences were observed between the MSC/EPC/VEGF ($47.80\% \pm 1.87\%$) and MSC/EPC groups ($45.21\% \pm 0.16\%$), suggesting that no additional benefit of VEGF could be expected when EPCs were used.[60] In context, a recent study reported significantly greater %NBF in femoral defects of sheep, following cotransplantation of dynamically cultured autologous BMSC-derived OBs and ECs ($\sim 88.10\% \pm 5.22\%$) versus solely OBs on β-TCP scaffolds ($\sim 17.65\% \pm 4.50\%$) after 16 weeks.[79]

In the present review, only studies employing craniofacial defects were included; due to differences in the embryonic development, structure, biomechanics/chemistry, and regenerative capacity between craniofacial and long bones, findings from studies using long bone models are not directly transferable to the craniofacial skeleton.[80,81] In context, similar to the findings of the present review, several studies using long bone defects in both small[82–87] and large animal models[79,88] have reported significantly greater bone and vessel regeneration following MSC-EC cotransplantation versus MSC-only transplantation (including human-derived cells).

Coculture: translational considerations

MSCs and EPCs represent the most favorable progenitor cell populations for osteogenic and vasculogenic differentiation within a coculture system. Bone marrow has traditionally been considered the gold standard source for MSCs and EPCs (a fraction of the hematopoietic stem cell population); however, the morbidity and procedural burden associated with marrow harvesting have led to identification of relatively less invasive sources of MSCs (adipose tissue, oral tissues, etc.) and EPCs (peripheral blood, umbilical cord blood, endothelial-induced MSCs, etc.). The *ex vivo* differentiation of MSCs into functional ECs by endothelial induction—as reported by six included studies—represents a particularly attractive strategy since both cell types are obtained from the same primary source, minimizing the need for additional tissue harvesting.[89]

Predifferentiation or induction of progenitor cells before implantation is considered to enhance their *in vivo* efficacy.[47] The choice of culture media plays an important role in determining the optimal conditions for inducing osteogenic and endothelial differentiation of MSCs and EPC/ECs, respectively, without exerting negative effects on either cell type.[22] In the present review, coculture of MSC-EPC/ECs was performed for 2–14 days before implantation in standard culture medium (SM), osteogenic medium (OM), a 1:1 mixture of SM or OM and endothelial medium (EM), or sequential culture first in EM and then in OM. In one study,[58] a transwell indirect coculture system was used, in which MSCs were exposed to the secretome of EPCs before implantation. Although all studies reported favorable *in vivo* outcomes, no studies correlated *in vivo* outcomes with different *in vitro* culture conditions. However, recent evidence suggests that optimal results may be achieved with coculture of MSC-ECs in purely OM in terms of both *in vitro* and *in vivo* bone formation and vascularization.[90–92]

MSC expansion is commonly performed using basal culture media plus supplements to provide GFs, proteins, and enzymes to support cell growth. Fetal bovine serum (FBS) is commonly used to supplement culture media because the fetal milieu is enriched with growth factors and poor in antibodies.[93] However, for clinical-grade therapy, it is important to substitute animal-derived products because MSCs can internalize xenogeneic proteins and thus there is a risk of infection and immunoreactions.[93] In addition, there are concerns regarding sample-to-sample inconsistency and ethics of animal welfare. Alternatives to FBS include chemically defined media or human blood platelet-derived supplements (e.g., platelet lysate [PL]) to provide the necessary factors for cell growth and function.[93] One study[47] reported on the use of human PL for ASC and ASC/HUVEC cultures and that significantly improved *in vitro* mineralization (osteogenesis) in PL- versus FBS-supplemented cultures was observed. These results are consistent with reports of BMSC/HUVEC cocultures with PL supplementation.[94]

Only one study[37] reported the use of a dynamic coculture system for rat BMSCs and ECs seeded on copolymer scaffolds, with formation of capillary-like structures *in vitro* after 1 week, suggesting a possible strategy for prevascularization.[95] In context, a recent study[79] in a large animal (sheep) model reported bone regeneration in femoral defects following dynamic coculture of autologous OBs and ECs in

a perfusion bioreactor system. Bioreactor systems (spinner flasks, perfusion systems, etc.) are reported to enhance the proliferation, homogeneous distribution, and differentiation of MSCs in scaffolds compared with conventional, static two-dimensional (2D) culture by providing the appropriate inductive and mechanical cues in a controlled environment.[96,97] Additionally, bioreactors ensure more homogeneous distribution and perfusion of cells and culture media throughout the scaffold and can reportedly overcome the problems associated with nutrient gradients that develop in static cultures, that is, when cells nearer to the scaffold surface consume more nutrients than cells in the center, resulting in internal cell death.[96]

Scaffold materials chosen to deliver cells and/or GFs play a critical role in the performance of BTE constructs. Biocompatible and biodegradable scaffolds can support and facilitate the attachment, proliferation, and differentiation of progenitor cells, ingrowth of vascular structures, and mass transfer while also providing structural stability, space maintenance, and osteoconductivity at the regeneration site.[16,22] Commercial bone substitute materials, for example, β-TCP, HA, BBM, and so on, have been shown to be clinically effective scaffolds for MSCs.[7] However, alloplastic copolymer scaffolds have gained significant importance since each of their properties integral to performance (architecture, biodegradability, porosity, pore size, etc.) can be optimized during the fabrication process.[98] Especially in cotransplantation strategies—where the presence of multiple cell types and complex simultaneous processes demand differential scaffold design, copolymer scaffolds provide several advantages.[99] In the present review, a majority of studies reported the use of copolymer composite scaffolds to support MSC monocultures and MSC-EC cocultures with adequate *in vitro* efficacy and subsequently successful *in vivo* outcomes.

Efficacy of human-derived cells

The main translational implication of the *in vitro* findings is that cotransplantation of previously cocultured osteogenic and vasculogenic cells could enhance *in vivo* bone regeneration either by directly inducing osteogenic differentiation of MSCs or by enhancing neovascularization and cell survival within the constructs.[47,86] In the present review, significantly better *in vitro* cell survival, metabolic activity, and differentiation were observed in human-derived MSC and EC cocultures compared with MSC or EC monocultures. This is consistent with recent reports of the contribution of ECs to enhanced osteogenic differentiation of MSCs.[92,100] Cotransplantation of human BMSCs or ASCs with EPC/ECs (with or without prior coculture) in rodent calvarial CSDs yielded significantly greater bone formation in two studies,[41,45] while others[42–44] observed no differences between cotransplantation and MSC-only groups. In one study,[47] human ASC monocultures demonstrated superior *in vitro* activity and *in vivo* bone formation than 1-week ASC-HUVEC cocultures on titanium mesh scaffolds. Therefore, the evidence for bone regeneration by cotransplantation of human MSCs and ECs is conflicting. Interestingly, one study,[101] excluded from the current review due to lack of quantitative outcomes, reported a codifferentiation strategy where human ASCs cultured in a combination of osteogenic and vasculogenic induction media acquired both phenotypes—positive for CD31 and osteopontin. These codifferentiated ASCs, when seeded on HA scaffolds and implanted into rat calvarial CSDs, resulted in superior (qualitative) bone and vessel formation than scaffold-only controls.[101]

It is of relevance to consider the sources and types of vasculogenic cells used in a coculture/cotransplantation system. EPCs, under physiological conditions, are largely restricted to bone marrow and peripheral blood and consist of a heterogeneous population of cells.[102,103] Recent evidence suggests that EPCs may also be isolated from umbilical cord blood.[104] ECs are an EPC subtype committed to EC differentiation.[102] In the included studies, relatively less variation in human EPC/EC sources was observed compared with osteogenic cell sources (Table 2). EPCs were derived from bone marrow, peripheral blood, or umbilical cord blood, while ECs were most often derived through endothelial differentiation of MSCs. The contribution of implanted human EPCs or ECs to vessel formation was confirmed by identification of human-specific endothelial markers in regenerating tissues.[41,42,44,45] Vessel counting was generally performed on stained histological sections of the central region of tissue explants and therefore represents vasculogenesis in the central part of the construct. This finding is of clinical relevance since a limitation of traditional BTE constructs is the lack of vascularization within the central regions.[16,22]

Vascularization in BTE

Implanted EPC/ECs are reported to contribute to neovascularization through direct endothelial differentiation (vasculogenesis) and/or stimulation of the host regenerative response, for example, by release of trophic factors to recruit host EPC/ECs.[86] Recent evidence suggests that exogenous EPCs are also involved in homing of MSCs to defect sites,[105] while MSCs, in turn, may stimulate EPC differentiation through release of trophic factors.[106] Moreover, a fraction of MSCs exposed to endothelial factors reportedly differentiate into *pericytes*, which line and stabilize newly forming vessels.[92,95] One study reported differentiation of human BMSCs into smooth muscle cells (SMCs) before coculture and cotransplantation with EPCs—the hypothesis was that SMCs would support EPC survival and stabilize the regenerating vessels, thus improving vascularization.[44] However, no significant additional benefit of cotransplantation versus MSC-SMC-only or EPC-only transplantation was observed in terms of bone and vessel regeneration.[44]

Initiating *prevascularization* within BTE constructs before implantation is another emerging strategy.[107] One included study[37] reported the identification of nascent microvascular networks *in vitro* following 1-week dynamic coculture of rat BMSCs and ECs on copolymer scaffolds. Upon implantation into rat CSDs for 8 weeks, slightly higher amount of vessel formation was observed in the regenerating tissues of cocultures than MSC-only implants.[37] In context, a recent study[79] in a sheep model investigated bone regeneration in femoral defects implanted with prevascularized (MSC+EC) constructs dynamically cultured for 14 days in a perfusion bioreactor. Histological analysis of the prevascularized constructs at 16 weeks revealed microvessel-like structures containing red blood cells, suggesting a functional connection of primitive networks with host vasculature.[79] The ability of primitive vessels in prevascularized constructs

to anastomose with host vasculature has previously been demonstrated.[20,108–110]

In the present review, one study[59] reported the use of a radiopaque contrast agent to quantify vessel regeneration within rat calvarial CSDs through micro-CT. At 4 weeks, infiltration of the contrast agent revealed vessel formation and/or infiltration (from the periphery) throughout the defect—no significant differences in vessel quantity (%) were observed between the central and peripheral regions.[59] Such novel imaging techniques, which can assist in tracking the *in vivo* behavior of primitive vessels in prevascularized constructs, should be utilized in future studies of vascularized BTE in orthotopic defect models.

The primary rationale for cell cotransplantation is that ECs can form primitive microvascular networks and improve cell survival in BTE constructs.[111] Although the presence of ECs may enhance vascularization in CSDs, transplantation of solely ECs (vs. solely MSCs) does not appear to enhance bone formation; indeed, the presence of an osteogenic cell population within the construct is reportedly necessary for osteogenesis.[112] In the present review, three studies[42,43,45] included a control group of solely human EC transplantation and observed significantly lower bone formation compared with MSC-only or MSC+EC groups, while one study[44] reported no differences between groups. A similar trend was observed for vessel formation. However, in one study,[54] transplantation of rat ASC-derived ECs yielded significantly greater bone and vessel formation than MSC-only or MSC+EC transplantation. Therefore, the combination of MSCs with ECs, at least for human-derived cells, appears to be the most optimal strategy for vascularized BTE than any one cell type alone.

Alternative strategies

Alternative strategies to enhance vascularization in BTE constructs have been proposed, of which local delivery of exogenous osteogenic and/or angiogenic GFs has been extensively documented.[16] GFs are molecular signals that coordinate wound healing and regeneration. Local delivery of exogenous (recombinant) or autologous GFs can direct cellular behavior by initiating specific osteogenic cell signaling cascades and mobilizing host progenitor cells (MSC, EPC) to the regeneration site.[113,114] Delivery of pooled (e.g., autologous platelet concentrates) or single GF (e.g., recombinant human bone morphogenetic protein-2 [rhBMP-2] or growth and differentiation factor-5 [rhGDF-5]) combined with biomaterial scaffolds has been shown to significantly enhance bone regeneration in clinical studies of contained or limited bone defects, for example, sinus augmentation, saddle defects, and extraction sockets.[114,115] However, for larger defects, combined delivery of osteogenic and angiogenic GFs may be more beneficial.[116] VEGF plays a critical role in angiogenesis during bone formation and is an ideal candidate for combination GF delivery strategies.[14] Recent preclinical studies have reported conflicting results of bone and vessel regeneration, following implantation of scaffolds loaded with BMP-2 or VEGF either alone or in combination, in calvarial CSD models.[117–119] In the present review, delivery of VEGF through β-TCP-PLGA scaffolds resulted in significantly lower %NBF than delivery of VEGFs with MSCs and/or EPCs in canine mandibular CSDs,[60] suggesting that GF delivery may compliment, but not substitute, the regenerative action of implanted cells. Recent studies, however, have shown that by using an appropriate delivery mode, it could be possible to lower the dose and delivery of GFs and minimize adverse reactions.[120,121] Determination of the optimal dosage, delivery method, temporospatial release profile, and reliance on host cell responses are some of the reported limitations of current GF delivery strategies.[16,22]

Another proposed strategy is the implantation of genetically modified MSCs encoding for angiogenic and/or osteogenic GFs.[122] MSCs are modified *ex vivo*, most commonly through adenoviral transduction, to express favorable GFs (e.g., BMP-2, VEGF) or transcription factors (e.g., HIF-1α) and have been shown to enhance bone regeneration in craniofacial CSDs compared with unmodified MSCs.[123–126] In the present review, one study[52] reported significantly greater bone and vessel formation in rat calvarial CSDs following coculture and cotransplantation of BMP-2-transduced MSCs and ECs compared with unmodified cocultures or unmodified MSCs after 5 weeks. However, additional sensitive *in vitro* procedures relating to GF gene transduction must be considered in these strategies.

Meta-analyses and heterogeneity

A random effects model was chosen for the present meta-analysis to account for the expected between-study variance.[127] Heterogeneity (I^2) was found to be very high within all categories in the meta-analyses. This could be due to *biological* factors related to the animals and/or *methodological* differences between the studies. *Biological* factors may include the animals' species, gender, age, immunological status, or the sources of MSCs and ECs used, and so on. In particular, sex and age of animals are reported to affect morphological, physiological, immunological, and behavioral parameters and thereby influence the outcomes of experiments.[128] *Methodological* differences in the study design (e.g., sample sizes, randomization), nature of interventions (e.g., use of autologous vs. allogeneic or human cells, osteogenic induction of cells before implantation), and outcome evaluation (e.g., methods of bone histomorphometry or micro-CT) may have also contributed to heterogeneity.

Although histomorphometry is considered the gold standard method for evaluation of 2D bone structure, micro-CT is emerging as a reliable alternative for assessing 3D microarchitecture with high resolution and accuracy in a fast and nondestructive manner. Several studies have reported high correlation between micro-CT and histomorphometry.[129–131] However, to minimize heterogeneity in the present meta-analyses, results of micro-CT and histomorphometry studies were analyzed separately.

Quality of reporting

The reliability of results of meta-analyses directly depends on the quality of the primary studies.[127] As assessed by compliance with the ARRIVE guidelines and SYRCLE RoB tool, the included studies were judged to be of moderate reporting quality, but an unclear to high RoB. The ARRIVE guidelines aim to improve the reporting quality of animal studies and have been widely used for assessment of

preclinical research in implant dentistry,[32] while the SYRCLE tool addresses particular aspects of bias that play a role in animal experimental studies.[34] Nevertheless, a clear need for more standardized reporting of animal studies was identified herein to allow reliable future reproduction and synthesis.

Clinical relevance

Although no clinical studies have reported direct coculture or cotransplantation of cells for bone regeneration in humans, one study[132] evaluated the efficacy of bone marrow aspirate containing populations of both hematopoietic ($CD34^+$ HSC) and mesenchymal ($CD44^+$, $CD90^+$, $CD105^+$ MSC) progenitor cells for mandibular reconstruction. Patients ($n=20$ per group) received bone marrow grafts with either standard (54 ± 38 cells/mL) or high (1012 ± 752 cells/mL) concentrations of $CD34^+$ HSCs and similar concentrations of MSCs (15×10^6 cells) together with rhBMP-2 in an allograft scaffold. Significantly higher %NBF was observed in patients receiving higher concentrations of $CD34^+$ HSCs ($67\%\pm13\%$ vs. $36\%\pm10\%$) after 6 months, suggesting an important and complimentary role of HSC to MSC in alveolar bone regeneration and the benefits of implanting heterogeneous cell populations at regeneration sites.[132,133]

Due to the large inherent variation in animal studies, preclinical meta-analyses aim to disclose the direction rather than size of the effect of an intervention.[127,134] Fundamental limitations of animal models that must be considered when interpreting the findings are (1) the *underestimation of clinical variation*, with regard to both local (defect size, morphology, mass transfer, etc.) and systemic (age, comorbidities, etc.) aspects; and (2) the *overestimation of clinical performance* since the CSDs utilized are uniform surgically created defects with sound surrounding tissues and generally uncompromised blood supply and most often involve healthy animals, which is often not the case in clinical scenarios.[75] Moreover, the dimensional differences between experimental defects in small animals and the clinical situation must be considered, especially with regard to vasculogenesis. Although it may be inferred that bone and vessel regeneration observed within calvarial CSDs in the included studies was largely due to the direct and/or indirect regenerative effects of exogenous cells functioning in a truly demanding environment (due to the highly cortical structure [low bone marrow] and poor local vascularity [absence of a primary nutrient artery] of the calvarium[28,135,136]), the numerical values or magnitude of response from the present meta-analysis cannot be directly translated to the human situation. Thus, the $\sim8\%$ additional NBF observed in defects augmented with cotransplanted cells would not translate to 8% (or x-times 8%) more bone if the same procedure was performed in humans.[27] Moreover, considering the magnitude of estimates of treatment effect, the clinical relevance (benefit) of cotransplantation procedures for oral and maxillofacial indications may be questioned.

Conclusions

The reviewed preclinical *in vivo* evidence can be summarized as follows:

(1) Based on the results of small animal (rodent) models, cotransplantation of osteogenic (MSCs or OBs) and vasculogenic cells (EPCs or ECs) seeded on biomaterial scaffolds results in greater radiographic bone regeneration than transplantation of solely MSC-/OB-seeded constructs.
(2) Coculture of MSCs and EPC/ECs under specific conditions *in vitro* can enhance their regenerative potential when cotransplanted *in vivo*.
(3) MSCs and ECs from human sources demonstrate synergistic activity when cocultured *in vitro*. However, the evidence for bone and vessel regeneration following *in vivo* cotransplantation of human cells is inconclusive.
(4) The magnitude of estimates of treatment effect was relatively small and thus the clinical relevance (benefit) of cotransplantation procedures for oral and maxillofacial indications may be questioned.
(5) The results should be interpreted with caution due to large heterogeneity between studies as a result of biological and methodological factors.
(6) There is a need for more standardized reporting of well-designed and adequately powered animal studies to allow reliable future reproduction and synthesis.

Acknowledgments

The authors would like to thank all the corresponding authors of the primary studies who provided additional information for the review.

Disclosure Statement

No competing financial interests exist.

References

1. Götz, C., Warnke, P.H., and Kolk, A. Current and future options of regeneration methods and reconstructive surgery of the facial skeleton. Oral Surg Oral Med Oral Pathol Oral Radiol **120,** 315, 2015.
2. Fretwurst, T., Gad, L.M., Nelson, K., and Schmelzeisen, R. Dentoalveolar reconstruction. Curr Opin Otolaryngol Head Neck Surg **23,** 316, 2015.
3. Corbella, S., Taschieri, S., Weinstein, R., and Del Fabbro, M. Histomorphometric outcomes after lateral sinus floor elevation procedure: a systematic review of the literature and meta-analysis. Clin Oral Implants Res **27,** 1106, 2016.
4. Nkenke, E., and Neukam, F.W. Autogenous bone harvesting and grafting in advanced jaw resorption: morbidity, resorption and implant survival. Eur J Oral Implantol **7** Suppl 2**,** S203, 2014.
5. Al-Nawas, B., and Schiegnitz, E. Augmentation procedures using bone substitute materials or autogenous bone – a systematic review and meta-analysis. Eur J Oral Implantol **7,** 219, 2014.
6. Milinkovic, I., and Cordaro, L. Are there specific indications for the different alveolar bone augmentation procedures for implant placement? A systematic review. Int J Oral Maxillofac Surg **43,** 606, 2014.
7. Shanbhag, S., and Shanbhag, V. Clinical applications of cell-based approaches in alveolar bone augmentation: a systematic review. Clin Implant Dent Relat Res **17,** e17, 2015.

8. Oppenheimer, A.J., Mesa, J., and Buchman, S.R. Current and emerging basic science concepts in bone biology: implications in craniofacial surgery. J Craniofac Surg **23,** 30, 2012.
9. Shanbhag, S., Pandis, N., Mustafa, K., Nyengaard, J., and Stavropoulos, A. Alveolar bone tissue engineering in critical-size defects of experimental animal models: a systematic review and meta-analysis. J Tissue Eng Regen Med 2016 [Epub ahead of print]; DOI: 10.1002/term.2198
10. Padial-Molina, M., Valle, F., Lanis, A., Mesa, F., Dohan Ehrenfest, D.M., Wang, H.-L., and Galindo-Moreno, P. Clinical application of mesenchymal stem cells and novel supportive therapies for oral bone regeneration. Biomed Res Int **2015,** 16, 2015.
11. Meijer, G.J., de Bruijn, J.D., Koole, R., and van Blitterswijk, C.A. Cell-based bone tissue engineering. PLoS Med **4,** e9, 2007.
12. Zuk, P.A. Tissue engineering craniofacial defects with adult stem cells: are we ready yet? Pediatr Res **63,** 478, 2008.
13. Dawson, J.I., Kanczler, J., Tare, R., Kassem, M., and Oreffo, R.O.C. Concise review: bridging the gap: bone regeneration using skeletal stem cell-based strategies – where are we now? Stem Cells **32,** 35, 2014.
14. Kanczler, J.M., and Oreffo, R.O.C. Osteogenesis and angiogenesis: the potential for engineering bone. Eur Cell Mater **15,** 100, 2008.
15. Jain, R.K., Au, P., Tam, J., Duda, D.G., and Fukumura, D. Engineering vascularized tissue. Nat Biotechnol **23,** 821, 2005.
16. Nguyen, L.H., Annabi, N., Nikkhah, M., Bae, H., Binan, L., Park, S., Kang, Y., Yang, Y., and Khademhosseini, A. Vascularized bone tissue engineering: approaches for potential improvement. Tissue Eng Part B Rev **18,** 363, 2012.
17. Kalka, C., Masuda, H., Takahashi, T., Kalka-Moll, W.M., Silver, M., Kearney, M., Li, T., Isner, J.M., and Asahara, T. Transplantation of ex vivo expanded endothelial progenitor cells for therapeutic neovascularization. Proc Natl Acad Sci U S A **97,** 3422, 2000.
18. Balaji, S., King, A., Crombleholme, T.M., and Keswani, S.G. The role of endothelial progenitor cells in postnatal vasculogenesis: implications for therapeutic neovascularization and wound healing. Adv Wound Care **2,** 283, 2013.
19. Keramaris, N.C., Kaptanis, S., Moss, H.L., Loppini, M., Pneumaticos, S., and Maffulli, N. Endothelial progenitor cells (EPCs) and mesenchymal stem cells (MSCs) in bone healing. Curr Stem Cell Res Ther **7,** 293, 2012.
20. Chen, X., Aledia, A.S., Ghajar, C.M., Griffith, C.K., Putnam, A.J., Hughes, C.C.W., and George, S.C. Prevascularization of a fibrin-based tissue construct accelerates the formation of functional anastomosis with host vasculature. Tissue Eng Part A **15,** 1363, 2009.
21. Kaigler, D., Pagni, G., Park, C.-H., Tarle, S.A., Bartel, R.L., and Giannobile, W.V. Angiogenic and osteogenic potential of bone repair cells for craniofacial regeneration. Tissue Eng Part A **16,** 2809, 2010.
22. Liu, Y., Chan, J.K., and Teoh, S.H. Review of vascularised bone tissue-engineering strategies with a focus on co-culture systems. J Tissue Eng Regen Med **9,** 85, 2015.
23. Mercado-Pagán, Á.E., Stahl, A.M., Shanjani, Y., and Yang, Y. Vascularization in bone tissue engineering constructs. Ann Biomed Eng **43,** 718, 2015.
24. Roux, B.M., Cheng, M.H., and Brey, E.M. Engineering clinically relevant volumes of vascularized bone. J Cell Mol Med **19,** 903, 2015.
25. Unger, R.E., Dohle, E., and Kirkpatrick, C.J. Improving vascularization of engineered bone through the generation of pro-angiogenic effects in co-culture systems. Adv Drug Deliv Rev **94,** 116, 2015.
26. Pellegrini, G., Seol, Y.J., Gruber, R., and Giannobile, W.V. Pre-clinical models for oral and periodontal reconstructive therapies. J Dent Res **88,** 1065, 2009.
27. Stavropoulos, A., Sculean, A., Bosshardt, D.D., Buser, D., and Klinge, B. Pre-clinical in vivo models for the screening of bone biomaterials for oral/craniofacial indications: focus on small-animal models. Periodontol 2000 **68,** 55, 2015.
28. Schmitz, J.P., and Hollinger, J.O. The critical size defect as an experimental model for craniomandibulofacial nonunions. Clin Orthop Relat Res 299, 1986.
29. Vajgel, A., Mardas, N., Farias, B.C., Petrie, A., Cimões, R., and Donos, N. A systematic review on the critical size defect model. Clin Oral Implants Res **25,** 879, 2014.
30. Moher, D., Liberati, A., Tetzlaff, J., and Altman, D.G. Preferred reporting items for systematic reviews and meta-analyses: the PRISMA statement. PLoS Med **6,** e1000097, 2009.
31. Kilkenny, C., Browne, W.J., Cuthill, I.C., Emerson, M., and Altman, D.G. Improving bioscience research reporting: the ARRIVE guidelines for reporting animal research. PLoS Biol **8,** e1000412, 2010.
32. Berglundh, T., and Stavropoulos, A. Preclinical in vivo research in implant dentistry. Consensus of the eighth European workshop on periodontology. J Clin Periodontol **39** Suppl 1**,** 1, 2012.
33. Schwarz, F., Iglhaut, G., and Becker, J. Quality assessment of reporting of animal studies on pathogenesis and treatment of peri-implant mucositis and peri-implantitis. A systematic review using the ARRIVE guidelines. J Clin Periodontol **39** Suppl 1**,** 63, 2012.
34. Hooijmans, C.R., Rovers, M.M., de Vries, R.B.M., Leenaars, M., Ritskes-Hoitinga, M., and Langendam, M.W. SYRCLE's risk of bias tool for animal studies. BMC Med Res Methodol **14,** 43, 2014.
35. Yan, X.-Z., Yang, F., Jansen, J.A., de Vries, R.B.M., and van den Beucken, J.J.J.P. Cell-based approaches in periodontal regeneration: a systematic review and meta-analysis of periodontal defect models in animal experimental work. Tissue Eng Part B Rev **21,** 411, 2015.
36. Deeks, J.J., Higgins, J.P.T., and Altman, D.G. Analysing data and undertaking meta-analyses. In: Higgins, J.P.T., and Green, S., eds. Cochrane Handbook for Systematic Reviews of Interventions. Chichester: John Wiley & Sons Ltd., 2008, p. 243.
37. Xing, Z., Xue, Y., Dånmark, S., Schander, K., Ostvold, S., Arvidson, K., Hellem, S., Finne-Wistrand, A., Albertsson, A.-C., and Mustafa, K. Effect of endothelial cells on bone regeneration using poly(L-lactide-co-1,5-dioxepan-2-one) scaffolds. J Biomed Mater Res A **96,** 349, 2011.
38. Higgins, J.P.T., and Deeks, J.J. Selecting Studies and Collecting Data. In: Higgins, J.P.T., and Green, S., eds. Cochrane Handbook for Systematic Reviews of Interventions. Chichester: John Wiley & Sons Ltd., 2008, p. 151.
39. Higgins, J.P.T., Deeks, J.J., and Altman, D.G. Special topics in statistics. In: Higgins, J.P.T., and Green, S., eds. Cochrane Handbook for Systematic Reviews of Interventions. Chichester: John Wiley & Sons Ltd., 2008, p. 481.

40. Russel, W.M.S., and Burch, R.L. The Principles of Humane Experimental Technique. London: Methuen & Co., 1959.
41. Kaigler, D., Krebsbach, P.H., Wang, Z., West, E.R., Horger, K., and Mooney, D.J. Transplanted endothelial cells enhance orthotopic bone regeneration. J Dent Res **85,** 633, 2006.
42. Koob, S., Torio-Padron, N., Stark, G.B., Hannig, C., Stankovic, Z., and Finkenzeller, G. Bone formation and neovascularization mediated by mesenchymal stem cells and endothelial cells in critical-sized calvarial defects. Tissue Eng Part A **17,** 311, 2011.
43. He, J., Decaris, M.L., and Leach, J.K. Bioceramic-mediated trophic factor secretion by mesenchymal stem cells enhances in vitro endothelial cell persistence and in vivo angiogenesis. Tissue Eng Part A **18,** 1520, 2012.
44. Goerke, S.M., Obermeyer, J., Plaha, J., Stark, G.B., and Finkenzeller, G. Endothelial progenitor cells from peripheral blood support bone regeneration by provoking an angiogenic response. Microvasc Res **98,** 40, 2015.
45. Kim, J.Y., Jin, G.-Z., Park, I.S., Kim, J.-N., Chun, S.Y., Park, E.K., Kim, S.-Y., Yoo, J., Kim, S.-H., Rhie, J.-W., and Cho, D.-W. Evaluation of solid free-form fabrication-based scaffolds seeded with osteoblasts and human umbilical vein endothelial cells for use in vivo osteogenesis. Tissue Eng Part A **16,** 2229, 2010.
46. Kim, K.-I., Park, S., and Im, G.-I. Osteogenic differentiation and angiogenesis with cocultured adipose-derived stromal cells and bone marrow stromal cells. Biomaterials **35,** 4792, 2014.
47. Ma, J., Both, S.K., Ji, W., Yang, F., Prins, H.J., Helder, M.N., Pan, J., Cui, F.Z., Jansen, J.A., and van den Beucken, J.J. Adipose tissue-derived mesenchymal stem cells as monocultures or cocultures with human umbilical vein endothelial cells: performance in vitro and in rat cranial defects. J Biomed Mater Res A **102,** 1026, 2014.
48. Johari, B., Ahmadzadehzarajabad, M., Azami, M., Kazemi, M., Soleimani, M., Kargozar, S., Hajighasemlou, S., Farajollahi, M.M., and Samadikuchaksaraei, A. Repair of rat critical size calvarial defect using osteoblast-like and umbilical vein endothelial cells seeded in gelatin/hydroxyapatite scaffolds. J Biomed Mater Res A **104,** 1770, 2016.
49. Lee, J.-H., Kim, J.-H., Oh, S.-H., Kim, S.-J., Hah, Y.-S., Park, B.-W., Kim, D.R., Rho, G.-J., Maeng, G.-H., Jeon, R.-H., Lee, H.-C., Kim, J.-R., Kim, G.-C., Kim, U.-K., and Byun, J.-H. Tissue-engineered bone formation using periosteal-derived cells and polydioxanone/pluronic F127 scaffold with pre-seeded adipose tissue-derived CD146 positive endothelial-like cells. Biomaterials **32,** 5033, 2011.
50. Lee, J.H., Kim, S.W., Kim, U.K., Oh, S.H., June-Kim, S., Park, B.W., Kim, J.H., Hah, Y.S., Kim, D.R., Rho, G.J., Maeng, G.H., Jeon, R.H., Lee, H.C., Kim, J.R., Kim, G.C., and Byun, J.H. Generation of osteogenic construct using periosteal-derived osteoblasts and polydioxanone/pluronic F127 scaffold with periosteal-derived CD146 positive endothelial-like cells. J Biomed Mater Res A **101,** 942, 2013.
51. Lee, J.-H., Hah, Y.-S., Cho, H.-Y., Kim, J.-H., Oh, S.-H., Park, B.-W., Kang, Y.-H., Choi, M.-J., Shin, J.-K., Rho, G.-J., Jeon, R.-H., Lee, H.-C., Kim, G.-C., Kim, U.-K., Kim, J.-R., Lee, C.-I., and Byun, J.-H. Human umbilical cord blood-derived CD34-positive endothelial progenitor cells stimulate osteoblastic differentiation of cultured human periosteal-derived osteoblasts. Tissue Eng Part A **20,** 940, 2014.
52. He, X., Dziak, R., Yuan, X., Mao, K., Genco, R., Swihart, M., Sarkar, D., Li, C., Wang, C., Lu, L., Andreadis, S., and Yang, S. BMP2 genetically engineered MSCs and EPCs promote vascularized bone regeneration in rat critical-sized calvarial bone defects. PLoS One **8,** e60473, 2013.
53. Kim, S.S., Park, M.S., Cho, S.W., Kang, S.W., Ahn, K.M., Lee, J.H., and Kim, B.S. Enhanced bone formation by marrow-derived endothelial and osteogenic cell transplantation. J Biomed Mater Res A **92,** 246, 2010.
54. Cornejo, A., Sahar, D.E., Stephenson, S.M., Chang, S., Nguyen, S., Guda, T., Wenke, J.C., Vasquez, A., Michalek, J.E., Sharma, R., Krishnegowda, N.K., and Wang, H.T. Effect of adipose tissue-derived osteogenic and endothelial cells on bone allograft osteogenesis and vascularization in critical-sized calvarial defects. Tissue Eng Part A **18,** 1552, 2012.
55. Li, G., Wang, X., Cao, J., Ju, Z., Ma, D., Liu, Y., and Zhang, J. Coculture of peripheral blood $CD34^+$ cell and mesenchymal stem cell sheets increase the formation of bone in calvarial critical-size defects in rabbits. Br J Oral Maxillofac Surg **52,** 134, 2014.
56. Shah, A.R., Cornejo, A., Guda, T., Sahar, D.E., Stephenson, S.M., Chang, S., Krishnegowda, N.K., Sharma, R., and Wang, H.T. Differentiated adipose-derived stem cell cocultures for bone regeneration in polymer scaffolds in vivo. J Craniofac Surg **25,** 1504, 2014.
57. Liang, Y., Wen, L., Shang, F., Wu, J., Sui, K., and Ding, Y. Endothelial progenitors enhanced the osteogenic capacities of mesenchymal stem cells in vitro and in a rat alveolar bone defect model. Arch Oral Biol **68,** 123, 2016.
58. Wen, L., Wang, Y., Wen, N., Yuan, G., Wen, M., Zhang, L., Liu, Q., Liang, Y., Cai, C., Chen, X., and Ding, Y. Role of endothelial progenitor cells in maintaining stemness and enhancing differentiation of mesenchymal stem cells by indirect cell-cell interaction. Stem Cells Dev **25,** 123, 2016.
59. Sathy, B.N., Watson, B.M., Kinard, L.A., Spicer, P.P., Dahlin, R.L., Mikos, A.G., and Nair, S. Bone tissue engineering with multilayered scaffolds-Part II: combining vascularization with bone formation in critical-sized bone defect. Tissue Eng Part A **21,** 2495, 2015.
60. Khojasteh, A., Fahimipour, F., Jafarian, M., Sharifi, D., Jahangir, S., Khayyatan, F., and Baghaban Eslaminejad, M. Bone engineering in dog mandible: coculturing mesenchymal stem cells with endothelial progenitor cells in a composite scaffold containing vascular endothelial growth factor. J Biomed Mater Res B Appl Biomater 2016. [Epub ahead of print]; DOI: 10.1002/jbm.b.33707
61. Sterne, J.A.C., Egger, M., and Moher, D. Addressing reporting biases. In: Higgins, J.P.T., and Green, S., eds. Cochrane Handbook for Systematic Reviews of Interventions. Chichester: John Wiley & Sons Ltd., 2008, p. 297.
62. Amini, A.R., Laurencin, C.T., and Nukavarapu, S.P. Bone tissue engineering: recent advances and challenges. Crit Rev Biomed Eng **40,** 363, 2012.
63. Li, Y., Chen, S.-K., Li, L., Qin, L., Wang, X.-L., and Lai, Y.-X. Bone defect animal models for testing efficacy of bone substitute biomaterials. J Orthop Translat **3,** 95, 2015.

64. Gomes, P.S., and Fernandes, M.H. Rodent models in bone-related research: the relevance of calvarial defects in the assessment of bone regeneration strategies. Lab Anim **45,** 14, 2011.
65. Cooper, G.M., Mooney, M.P., Gosain, A.K., Campbell, P.G., Losee, J.E., and Huard, J. Testing the critical size in calvarial bone defects: revisiting the concept of a critical-size defect. Plast Reconstr Surg **125,** 1685, 2010.
66. Bays, R.A. Current concepts in bone grafting. In: Irby W.B., and Shelton D.W., eds. Current Advances in Oral and Maxillofacial Surgery. St. Louis, MO: CV Mosby, 1983, p. 109.
67. Slotte, C., Lundgren, D., and Sennerby, L. Bone morphology and vascularization of untreated and guided bone augmentation-treated rabbit calvaria: evaluation of an augmentation model. Clin Oral Implants Res **16,** 228, 2005.
68. Conn, P.M. Sourcebook of Models for Biomedical Research. Totowa, NJ: Humana Press, 2008.
69. Power, S.M., Matic, D.B., and Holdsworth, D.W. The effects of nonvascularized versus vascularized bone grafting on calvarial defect healing. J Craniofac Surg **26,** 290, 2015.
70. Zigdon-Giladi, H., Bick, T., Lewinson, D., and Machtei, E.E. Mesenchymal stem cells and endothelial progenitor cells stimulate bone regeneration and mineral density. J Periodontol **85,** 984, 2014.
71. Zigdon-Giladi, H., Bick, T., Lewinson, D., and Machtei, E.E. Co-transplantation of endothelial progenitor cells and mesenchymal stem cells promote neovascularization and bone regeneration. Clin Implant Dent Relat Res **17,** 353, 2015.
72. Stübinger, S., and Dard, M. The rabbit as experimental model for research in implant dentistry and related tissue regeneration. J Invest Surg **26,** 266, 2013.
73. Liu, J., Liu, C., Sun, B., Shi, C., Qiao, C., Ke, X., Liu, S., Liu, X., and Sun, H. Differentiation of rabbit bone mesenchymal stem cells into endothelial cells in vitro and promotion of defective bone regeneration in vivo. Cell Biochem Biophys **68,** 479, 2014.
74. Pearce, A.I., Richards, R.G., Milz, S., Schneider, E., and Pearce, S.G. Animal models for implant biomaterial research in bone: a review. Eur Cell Mater **13,** 1, 2007.
75. Muschler, G.F., Raut, V.P., Patterson, T.E., Wenke, J.C., and Hollinger, J.O. The design and use of animal models for translational research in bone tissue engineering and regenerative medicine. Tissue Eng Part B Rev **16,** 123, 2010.
76. Aerssens, J., Boonen, S., Lowet, G., and Dequeker, J. Interspecies differences in bone composition, density, and quality: potential implications for in vivo bone research 1. Endocrinology **139,** 663, 1998.
77. Mardas, N., Dereka, X., Donos, N., and Dard, M. Experimental model for bone regeneration in oral and cranio-maxillo-facial surgery. J Invest Surg **27,** 32, 2014.
78. Ryan, J.M., Barry, F.P., Murphy, J.M., and Mahon, B.P. Mesenchymal stem cells avoid allogeneic rejection. J Inflamm (Lond) **2,** 8, 2005.
79. Li, D.Q., Li, M., Liu, P.L., Zhang, Y.K., Lu, J.X., and Li, J.M. Improved repair of bone defects with prevascularized tissue-engineered bones constructed in a perfusion bioreactor. Orthopedics **37,** 685, 2014.
80. Garland, C.B., and Pomerantz, J.H. Regenerative strategies for craniofacial disorders. Front Physiol **3,** 453, 2012.
81. Matsuura, T., Tokutomi, K., Sasaki, M., Katafuchi, M., Mizumachi, E., and Sato, H. Distinct characteristics of mandibular bone collagen relative to long bone collagen: relevance to clinical dentistry. Biomed Res Int **2014,** 769414, 2014.
82. Yu, H., Vandevord, P.J., Gong, W., Wu, B., Song, Z., Matthew, H.W., Wooley, P.H., and Yang, S.Y. Promotion of osteogenesis in tissue-engineered bone by pre-seeding endothelial progenitor cells-derived endothelial cells. J Orthop Res **26,** 1147, 2008.
83. Yu, H., VandeVord, P.J., Mao, L., Matthew, H.W., Wooley, P.H., and Yang, S.Y. Improved tissue-engineered bone regeneration by endothelial cell mediated vascularization. Biomaterials **30,** 508, 2009.
84. Seebach, C., Henrich, D., Kahling, C., Wilhelm, K., Tami, A.E., Alini, M., and Marzi, I. Endothelial progenitor cells and mesenchymal stem cells seeded onto beta-TCP granules enhance early vascularization and bone healing in a critical-sized bone defect in rats. Tissue Eng Part A **16,** 1961, 2010.
85. Hao, Z., Feng, W., Hao, T., andYu, B. Study on bone marrow mesenchymal stem cells derived osteoblasts and endothelial cells compound with chitosan/hydroxyapatite scaffold to construct vascularized tissue engineered bone [Chinese]. Zhongguo Xiu Fu Chong Jian Wai Ke Za Zhi **26,** 489, 2012.
86. Seebach, C., Henrich, D., Wilhelm, K., Barker, J.H., and Marzi, I. Endothelial progenitor cells improve directly and indirectly early vascularization of mesenchymal stem cell-driven bone regeneration in a critical bone defect in rats. Cell Transplant **21,** 1667, 2012.
87. Pang, H., Wu, X.H., Fu, S.L., Luo, F., Zhang, Z.H., Hou, T.Y., Li, Z.Q., Chang, Z.Q., Yu, B., and Xu, J.Z. Prevascularisation with endothelial progenitor cells improved restoration of the architectural and functional properties of newly formed bone for bone reconstruction. Int Orthop **37,** 753, 2013.
88. Lu, Y.M., Cheng, L.M., Pei, G.X., Cai, Z., Pan, L., Su, J., Zhang, K.H., Guo, L.L., Yu, Q.S., and Guo, Y.R. Experimental study of repairing femoral bone defects with nHA/RHLC/PLA scaffold composite with endothelial cells and osteoblasts in canines [Chinese]. Zhonghua Yi Xue Za Zhi **93,** 1335, 2013.
89. Janeczek Portalska, K., Leferink, A., Groen, N., Fernandes, H., Moroni, L., van Blitterswijk, C., and de Boer, J. Endothelial differentiation of mesenchymal stromal cells. PLoS One **7,** e46842, 2012.
90. Correia, C., Grayson, W.L., Park, M., Hutton, D., Zhou, B., Guo, X.E., Niklason, L., Sousa, R.A., Reis, R.L., and Vunjak-Novakovic, G. In vitro model of vascularized bone: synergizing vascular development and osteogenesis. PLoS One **6,** e28352, 2011.
91. Ma, J., van den Beucken, J.J.J.P., Yang, F., Both, S.K., Cui, F.-Z., Pan, J., and Jansen, J.A. Coculture of osteoblasts and endothelial cells: optimization of culture medium and cell ratio. Tissue Eng Part C Methods **17,** 349, 2011.
92. Pedersen, T.O., Blois, A.L., Xing, Z., Xue, Y., Sun, Y., Finne-Wistrand, A., Akslen, L.A., Lorens, J.B., Leknes, K.N., Fristad, I., and Mustafa, K. Endothelial microvascular networks affect gene-expression profiles and osteogenic potential of tissue-engineered constructs. Stem Cell Res Ther **4,** 52, 2013.
93. Shih, D.T.B., and Burnouf, T. Preparation, quality criteria, and properties of human blood platelet lysate supplements

for ex vivo stem cell expansion. N Biotechnol **32,** 199, 2015.
94. Ma, J., van den Beucken, J.J., Both, S.K., Prins, H.J., Helder, M.N., Yang, F., and Jansen, J.A. Osteogenic capacity of human BM-MSCs, AT-MSCs and their cocultures using HUVECs in FBS and PL supplemented media. J Tissue Eng Regen Med **9,** 779, 2015.
95. Brennan, M.A., Davaine, J.-M., and Layrolle, P. Prevascularization of bone tissue-engineered constructs. Stem Cell Res Ther **4,** 96, 2013.
96. Yeatts, A.B., and Fisher, J.P. Bone tissue engineering bioreactors: dynamic culture and the influence of shear stress. Bone **48,** 171, 2011.
97. Gardel, L.S., Serra, L.A., Reis, R.L., and Gomes, M.E. Use of perfusion bioreactors and large animal models for long bone tissue engineering. Tissue Eng Part B Rev **20,** 126, 2014.
98. Santos, M.I., and Reis, R.L. Vascularization in bone tissue engineering: physiology, current strategies, major hurdles and future challenges. Macromol Biosci **10,** 12, 2010.
99. Stoppato, M., Stevens, H.Y., Carletti, E., Migliaresi, C., Motta, A., and Guldberg, R.E. Influence of scaffold properties on the inter-relationship between human bone marrow derived stromal cells and endothelial cells in pro-osteogenic conditions. Acta Biomater **25,** 16, 2015.
100. Gershovich, J.G., Dahlin, R.L., Kasper, F.K., and Mikos, A.G. Enhanced osteogenesis in cocultures with human mesenchymal stem cells and endothelial cells on polymeric microfiber scaffolds. Tissue Eng Part A **19,** 2565, 2013.
101. Gardin, C., Bressan, E., Ferroni, L., Nalesso, E., Vindigni, V., Stellini, E., Pinton, P., Sivolella, S., and Zavan, B. In vitro concurrent endothelial and osteogenic commitment of adipose-derived stem cells and their genomical analyses through comparative genomic hybridization array: novel strategies to increase the successful engraftment of tissue-engineered bone grafts. Stem Cells Dev **21,** 767, 2011.
102. Fuchs, S., Dohle, E., Kolbe, M., and Kirkpatrick, C.J. Outgrowth endothelial cells: sources, characteristics and potential applications in tissue engineering and regenerative medicine. Adv Biochem Eng Biotechnol **123,** 201, 2010.
103. Salingova, B., Madarasova, M., Stejskal, S., Tesarova, L., Simara, P., and Koutna, I. From endothelial progenitor cells to tissue engineering: how far have we come? J Stem Cell Res Ther **4,** 3, 2014.
104. Mead, L.E., Prater, D., Yoder, M.C., and Ingram, D.A. Isolation and characterization of endothelial progenitor cells from human blood. Curr Protoc Stem Cell Biol **Chapter 2,** Unit 2C.1, 2008.
105. Wei, H., Zhao, X., Yuan, R., Dai, X., Li, Y., and Liu, L. Effects of PB-EPCs on homing ability of rabbit BMSCs via endogenous SDF-1 and MCP-1. PLoS One **10,** e0145044, 2015.
106. Kamprom, W., Kheolamai, P., U-Pratya, Y., Supokawej, A., Wattanapanitch, M., Laowtammathron, C., and Issaragrisil, S. Effects of mesenchymal stem cell-derived cytokines on the functional properties of endothelial progenitor cells. Eur J Cell Biol **95,** 153, 2016.
107. Eman, R.M., Meijer, H.A.W., Oner, F.C., Dhert, W.J.A., and Alblas, J. Establishment of an early vascular network promotes the formation of ectopic bone. Tissue Eng Part A **22,** 253, 2016.
108. Rouwkema, J., de Boer, J., and Van Blitterswijk, C.A. Endothelial cells assemble into a 3-dimensional prevascular network in a bone tissue engineering construct. Tissue Eng **12,** 2685, 2006.
109. Scherberich, A., Galli, R., Jaquiery, C., Farhadi, J., and Martin, I. Three-dimensional perfusion culture of human adipose tissue-derived endothelial and osteoblastic progenitors generates osteogenic constructs with intrinsic vascularization capacity. Stem Cells **25,** 1823, 2007.
110. Rouwkema, J., Westerweel, P.E., de Boer, J., Verhaar, M.C., and van Blitterswijk, C.A. The use of endothelial progenitor cells for prevascularized bone tissue engineering. Tissue Eng Part A **15,** 2015, 2009.
111. Matsumoto, T., Kuroda, R., Mifune, Y., Kawamoto, A., Shoji, T., Miwa, M., Asahara, T., and Kurosaka, M. Circulating endothelial/skeletal progenitor cells for bone regeneration and healing. Bone **43,** 434, 2008.
112. Sahar, D.E., Walker, J.A., Wang, H.T., Stephenson, S.M., Shah, A.R., Krishnegowda, N.K., and Wenke, J.C. Effect of endothelial differentiated adipose-derived stem cells on vascularity and osteogenesis in poly(D,L-lactide) scaffolds in vivo. J Craniofac Surg **23,** 913, 2012.
113. Chenard, K.E., Teven, C.M., He, T.-C., and Reid, R.R. Bone morphogenetic proteins in craniofacial surgery: current techniques, clinical experiences, and the future of personalized stem cell therapy. J Biomed Biotechnol **2012,** 601549, 2012.
114. Schliephake, H. Clinical efficacy of growth factors to enhance tissue repair in oral and maxillofacial reconstruction: a systematic review. Clin Implant Dent Relat Res **17,** 247, 2015.
115. Lee, J., and Wikesjö, U.M.E. Growth/differentiation factor-5: pre-clinical and clinical evaluations of periodontal regeneration and alveolar augmentation – review. J Clin Periodontol **41,** 797, 2014.
116. Cui, Q., Dighe, A.S., and Irvine, J.N. Combined angiogenic and osteogenic factor delivery for bone regenerative engineering. Curr Pharm Des **19,** 3374, 2013.
117. Patel, Z.S., Young, S., Tabata, Y., Jansen, J.A., Wong, M.E.K., and Mikos, A.G. Dual delivery of an angiogenic and an osteogenic growth factor for bone regeneration in a critical size defect model. Bone **43,** 931, 2008.
118. Young, S., Patel, Z.S., Kretlow, J.D., Murphy, M.B., Mountziaris, P.M., Baggett, L.S., Ueda, H., Tabata, Y., Jansen, J.A., Wong, M., and Mikos, A.G. Dose effect of dual delivery of vascular endothelial growth factor and bone morphogenetic protein-2 on bone regeneration in a rat critical-size defect model. Tissue Eng Part A **15,** 2347, 2009.
119. Zhang, W., Zhu, C., Wu, Y., Ye, D., Wang, S., Zou, D., Zhang, X., Kaplan, D.L., and Jiang, X. VEGF and BMP-2 promote bone regeneration by facilitating bone marrow stem cell homing and differentiation. Eur Cell Mater **27,** 1, 2014.
120. Suliman, S., Xing, Z., Wu, X., Xue, Y., Pedersen, T.O., Sun, Y., Doskeland, A.P., Nickel, J., Waag, T., Lygre, H., Finne-Wistrand, A., Steinmuller-Nethl, D., Krueger, A., and Mustafa, K. Release and bioactivity of bone morphogenetic protein-2 are affected by scaffold binding techniques in vitro and in vivo. J Control Release **197,** 148, 2015.
121. Suliman, S., Sun, Y., Pedersen, T.O., Xue, Y., Nickel, J., Waag, T., Finne-Wistrand, A., Steinmuller-Nethl, D., Krueger, A., Costea, D.E., and Mustafa, K. In vivo host

response and degradation of copolymer scaffolds functionalized with nanodiamonds and bone morphogenetic protein 2. Adv Healthc Mater **5,** 730, 2016.
122. Kofron, M.D., and Laurencin, C.T. Bone tissue engineering by gene delivery. Adv Drug Deliv Rev **58,** 555, 2006.
123. Peng, H., Wright, V., Usas, A., Gearhart, B., Shen, H.-C., Cummins, J., and Huard, J. Synergistic enhancement of bone formation and healing by stem cell-expressed VEGF and bone morphogenetic protein-4. J Clin Invest **110,** 751, 2002.
124. Xiao, C., Zhou, H., Liu, G., Zhang, P., Fu, Y., Gu, P., Hou, H., Tang, T., and Fan, X. Bone marrow stromal cells with a combined expression of BMP-2 and VEGF-165 enhanced bone regeneration. Biomed Mater **6,** 015013, 2011.
125. Zou, D., Zhang, Z., Ye, D., Tang, A., Deng, L., Han, W., Zhao, J., Wang, S., Zhang, W., Zhu, C., Zhou, J., He, J., Wang, Y., Xu, F., Huang, Y., and Jiang, X. Repair of critical-sized rat calvarial defects using genetically engineered bone marrow-derived mesenchymal stem cells overexpressing hypoxia-inducible factor-1alpha. Stem Cells **29,** 1380, 2011.
126. Lin, C.-Y., Chang, Y.-H., Kao, C.-Y., Lu, C.-H., Sung, L.-Y., Yen, T.-C., Lin, K.-J., and Hu, Y.-C. Augmented healing of critical-size calvarial defects by baculovirus-engineered MSCs that persistently express growth factors. Biomaterials **33,** 3682, 2012.
127. Hooijmans, C.R., IntHout, J., Ritskes-Hoitinga, M., and Rovers, M.M. Meta-analyses of animal studies: an introduction of a valuable instrument to further improve healthcare. ILAR J **55,** 418, 2014.
128. Florez-Vargas, O., Brass, A., Karystianis, G., Bramhall, M., Stevens, R., Cruickshank, S., and Nenadic, G. Bias in the reporting of sex and age in biomedical research on mouse models. Elife **5,** e13615, 2016.
129. Müller, R., Van Campenhout, H., Van Damme, B., Van Der Perre, G., Dequeker, J., Hildebrand, T., and Rüegsegger, P. Morphometric analysis of human bone biopsies: a quantitative structural comparison of histological sections and micro-computed tomography. Bone **23,** 59, 1998.
130. Thomsen, J.S., Laib, A., Koller, B., Prohaska, S., Mosekilde, L., and Gowin, W. Stereological measures of trabecular bone structure: comparison of 3D micro computed tomography with 2D histological sections in human proximal tibial bone biopsies. J Microsc **218,** 171, 2005.
131. Duke, P.J., Doan, L., Luong, H., Kelley, C., LeBoeuf, W., Diep, Q., Johnson, E., and Cody, D.D. Correlation between micro-ct sections and histological sections of mouse skull defects implanted with engineered cartilage. Gravit Space Biol Bull **22,** 45, 2009.
132. Marx, R.E., and Harrell, D.B. Translational research: the $CD34^{+}$ cell is crucial for large-volume bone regeneration from the milieu of bone marrow progenitor cells in craniomandibular reconstruction. Int J Oral Maxillofac Implants **29,** e201, 2014.
133. Guerrero, J., Oliveira, H., Catros, S., Siadous, R., Derkaoui, S.-M., Bareille, R., Letourneur, D., and Amédée, J. The use of total human bone marrow fraction in a direct three-dimensional expansion approach for bone tissue engineering applications: focus on angiogenesis and osteogenesis. Tissue Eng Part A **21,** 861, 2015.
134. Vesterinen, H.M., Sena, E.S., Egan, K.J., Hirst, T.C., Churolov, L., Currie, G.L., Antonic, A., Howells, D.W., and Macleod, M.R. Meta-analysis of data from animal studies: a practical guide. J Neurosci Methods **221,** 92, 2014.
135. Sirola, K. Regeneration of defects in the calvaria. An experimental study. Ann Med Exp Biol Fenn **38** Suppl 2**,** 1, 1960.
136. Hussain, I., Moharamzadeh, K., Brook, I.M., José de Oliveira Neto, P., and Salata, L.A. Evaluation of osteoconductive and osteogenic potential of a dentin-based bone substitute using a calvarial defect model. Int J Dent **2012,** 396316, 2012.
137. Eldesoqi, K., Henrich, D., El-Kady, A.M., Arbid, M.S., Abd El-Hady, B.M., Marzi, I., and Seebach, C. Safety evaluation of a bioglass-polylactic acid composite scaffold seeded with progenitor cells in a rat skull critical-size bone defect. PLoS One **9**, e87642, 2014.
138. Eldesoqi, K., Henrich, D., El-Kady, A.M., El-Hady, B.M.A., Sweify, K.M., Relja, B., Nau, C., Marzi, I., and Seebach, C. Improved bone formation by differentiated mesenchymal stem cells and endothelial progenitor cells seeded on high concentrated bioglass-polylactic acid composite in calvarial rat bone defect. J Stem Cell Res Dev Ther **2,** 4, 2015.

Address correspondence to:
Andreas Stavropoulos, DDS, PhD
Department of Periodontology
Faculty of Odontology
Malmö University
Carl Gustafs väg
20506 Malmö
Sweden

E-mail: andreas.stavropoulos@mah.se

Received: July 8, 2016
Accepted: September 26, 2016
Online Publication Date: November 1, 2016

JOURNAL OF TISSUE ENGINEERING AND REGENERATIVE MEDICINE
J Tissue Eng Regen Med 2017.
Published online in Wiley Online Library (wileyonlinelibrary.com) **DOI:** 10.1002/term.2412

REVIEW

Bone tissue engineering in oral peri-implant defects in preclinical *in vivo* research: A systematic review and meta-analysis

Siddharth Shanbhag[1,2], Nikolaos Pandis[3], Kamal Mustafa[2], Jens R. Nyengaard[4] and Andreas Stavropoulos[1]*

[1]*Department of Clinical Dentistry, Centre for Clinical Dental Research, University of Bergen, Norway*
[2]*Department of Periodontology, Faculty of Odontology, Malmö University, Malmö, Sweden*
[3]*Department of Orthodontics and Dentofacial Orthopedics, University of Bern, Bern, Switzerland*
[4]*Stereology and Electron Microscopy Laboratory, Department of Clinical Medicine, Aarhus University, Aarhus, Denmark*

Abstract

The regeneration and establishment of osseointegration within oral peri-implant bone defects remains a clinical challenge. Bone tissue engineering (BTE) is emerging as a promising alternative to autogenous and/or biomaterial-based bone grafting. The objective of this systematic review was to answer the focused question: in animal models, do cell-based BTE strategies enhance bone regeneration and/or implant osseointegration in experimental peri-implant defects, compared with grafting with autogenous bone or only biomaterial scaffolds? Electronic databases were searched for controlled animal studies reporting on peri-implant defects and implantation of mesenchymal stem cells (MSC) or other cells seeded on biomaterial scaffolds, following Preferred Reporting Items for Systematic reviews and Meta-Analyses (PRISMA) guidelines. Random effects meta-analyses were performed for the outcomes histomorphometric bone area fraction (BA) and bone-to-implant contact (BIC). Nineteen studies reporting on large animal models (dogs and sheep) were included. Experimental defects were created surgically (16 studies) or via ligature-induced peri-implantitis (LIPI, three studies). In general, studies presented with an unclear to high risk of bias. In most studies, MSC were used in combination with alloplastic mineral phase or polymer scaffolds; no study directly compared cell-loaded scaffolds vs. autogenous bone. In three studies, cells were also modified by *ex vivo* gene transfer of osteoinductive factors. The meta-analyses indicated statistically significant benefits in favour of: (a) cell-loaded vs. cell-free scaffolds [weighted mean differences (WMD) of 10.73–12.30% BA and 11.77–15.15% BIC] in canine surgical defect and LIPI models; and (b) gene-modified vs. unmodified cells (WMD of 29.44% BA and 16.50% BIC) in canine LIPI models. Overall, heterogeneity in the meta-analyses was high (I^2 70–88%); considerable variation was observed among studies regarding the nature of cells and scaffolds used. In summary, bone regeneration and osseointegration in peri-implant defects are enhanced by the addition of osteogenic cells to biomaterial scaffolds. Although the direction of treatment outcome is clearly in favour of BTE strategies, due to the limited magnitude of treatment effect observed, no conclusive statements regarding the clinical benefit of such procedures for oral indications can yet be made. Copyright © 2017 John Wiley & Sons, Ltd.

Received 14 June 2016; Revised 23 October 2016; Accepted 13 January 2017

Keywords **dental implants; osseointegration; bone tissue engineering; mesenchymal stem cells; scaffolds; meta-analysis**

1. Background

Osseointegrated implants are an integral part of modern reconstructive dentistry and are associated with favourable long-term therapeutic outcomes (Moraschini *et al.,* 2015). Adequate bone volume allowing placement of implants in functionally and/or aesthetically optimal positions is an important prerequisite for success (Albrektsson *et al.,* 1981). However, insufficient alveolar bone volume, as a result of periodontal disease, trauma, and/or resorption atrophy, often presents a clinical challenge for implant installation. Furthermore, implant placement in deficient bone or in extraction sockets with compromised bone walls may result in horizontal and/or vertical defects exposing the implant body and potentially compromising short- and long-term outcomes (Chiapasco *et al.,* 2009). Progressive bone loss around implants as a result of infection, i.e. peri-implantitis, also compromises osseointegration, i.e. the direct bone-to-implant contact (BIC) (Renvert *et al.,* 2009). In all these cases, bone reconstructive procedures are often employed with the aim to reconstruct the resulting peri-implant defects and, ideally, to restore the compromised or lost BIC.

Regenerative procedures to repair peri-implant defects mainly follow the principle of guided bone regeneration, using barrier membranes most often in combination with bone grafts and/or bone substitute materials (Chiapasco and Zaniboni, 2009). A substantial body of preclinical evidence supports the effectiveness of these procedures, including the establishment of BIC or 'osseointegration', even in cases of previously microbially contaminated implant surfaces (Berglundh and Stavropoulos, 2012).

*Correspondence to: Andreas Stavropoulos, Department of Periodontology, Faculty of Odontology, Malmö University, Carl Gustafs väg, 20506 Malmö, Sweden. E-mail: andreas.stavropoulos@mah.se

Copyright © 2017 John Wiley & Sons, Ltd.

Furthermore, the existing clinical evidence suggests that such regenerative surgical procedures are generally effective in regenerating bone defects around implants, but no consensus exists on the effectiveness of one technique over the other (Sanz *et al.,* 2015; Sicilia *et al.,* 2015).

Bone tissue engineering (BTE) aims to combine and deliver the cellular (cells), extracellular (scaffolds) and/or molecular elements (cues/signals, growth factors) involved in physiological regenerative processes, for therapeutic applications. This usually involves harvesting osteogenic cells from an autologous source (e.g. bone marrow, adipose tissue), their *in vitro* culture expansion and combination with an appropriate carrier scaffold for *in vivo* implantation (Shanbhag and Shanbhag, 2015). BTE strategies are emerging as promising alternatives to autogenous bone and/or biomaterial-based grafting, as demonstrated by several recent clinical studies (Kaigler *et al.,* 2013). Nevertheless, no conclusive evidence regarding their efficacy exists in the literature, due to large variation in the methodology of studies, and a need for further, more standardized, preclinical research has been highlighted (Li *et al.,* 2015). Preclinical *in vivo* testing of new regenerative therapies in clinically relevant animal models is indeed an important aspect of translational research, and in most cases a regulatory requirement prior to initiating human trials (Pellegrini *et al.,* 2009; Stavropoulos *et al.,* 2015).

In this context, the aim of this study was to systematically review the available literature reporting the use of BTE strategies for reconstructing oral peri-implant bone defects in animal experimental models. Based on the nature of the retrieved data, the aim was to perform a meta-analysis of the efficacy of BTE vs. autogenous- and/or biomaterial-based grafting approaches.

2. Materials and methods

2.1. Focused question

A review protocol was developed based on the Preferred Reporting Items for Systematic reviews and Meta-Analyses (PRISMA) guidelines (Moher *et al.,* 2009). The focused 'PICO' (population, intervention, comparison, outcome) question was: in peri-implant defects in experimental animals, does a BTE approach, i.e. implantation of osteogenic cells seeded on biomaterial scaffolds, enhance histomorphometric bone regeneration and BIC, compared with grafting with only autogenous bone or biomaterials?

2.2. Inclusion and exclusion criteria

Inclusion criteria:

English language studies.
Randomized or non-randomized controlled animal experimental studies with two or more experimental groups.
Use of experimental peri-implant defects in the maxillae or mandibles of small or large animals.
Transplantation of cultured autologous, allogeneic or human-derived osteogenic cells seeded on biomaterial scaffolds in at least one experimental group.

Exclusion criteria:

In vitro studies.
Animal studies reporting ectopic (e.g. subcutaneous) models or systemic cell delivery.
Absence of a control group, i.e. a group with no cell, i.e. scaffold-only, transplantation.

2.3. Outcome measures

The histomorphometric parameters most frequently reported in preclinical implant research were selected as primary outcomes: (1) percentage bone area fraction (% BA), considered as the relative amount (as a percentage) of the total area of new bone within the defect area or within an area of interest within the defect, and (2) percentage BIC (%BIC), considered as the relative amount (as a percentage) of direct BIC to the total implant surface within the defect area or within an area of interest within the defect.

2.4. Search strategy, screening and study selection

Electronic databases of MEDLINE (via PubMed) and EMBASE were searched for relevant English-language literature up to and including August 2015. Unpublished literature was searched via the Google and Google Scholar search engines. Bibliographies of the selected studies and relevant review articles were checked for cross-references. A specific search strategy was developed for MEDLINE (Table 1) and adapted for other databases. Titles and abstracts of the search-identified studies were screened by two authors (S.S. and A.S.) and full texts of all eligible studies were obtained. Uncertainty in the determination of eligibility was resolved by discussion with other authors. Two authors (S.S. and A.S.) reviewed the selected full texts independently and final inclusion was based on the aforementioned inclusion criteria. A summary of the screening process is presented in Figure 1.

2.5. Data extraction

The following data were extracted from the full texts of selected articles: author(s), study design, animal species, model type, number of animals/defects, number of procedures, inclusion criteria, observation time(s), outcome(s), method(s) of outcome evaluation, main findings and conclusions. Descriptive summaries of included studies were entered into tables. Quantitative histomorphometric data regarding %BA and %BIC were

Copyright © 2017 John Wiley & Sons, Ltd.

DOI: 10.1002/term

Table 1. Summary of study characteristics: surgical defect models

Reference	Strain, age, gender	Extraction site, healing time	Implant size, surface Defect type, dimensions (mm)	*N*/*n*	Time	Cells	Source; induction	Cell number	Membrane	Scaffold Outcome (cells vs. scaffold)
Dogs										
Ito *et al.* (2006)	Hybrid, adult	Mandible (b) P1–4, M1 1 month	3.75 × 7; Branemark Circum. 10(W)	12/ 72	2, 4, 8 weeks	BMSC	Iliac, auto; yes	1×10^7	Goretex	Fibrin glue ± PRP Cells*
Sparks *et al.* (2007)	Foxhound, male, 2 years	Mandible (b) P1–4, M1 5 months	2.8 × 10; SA Circum. 1.5(W) × 4(H)	5/50	10 weeks	HDF	Dermal, human; no	Unclear	No	PLGA Empty ND
Mizuno *et al.* (2008)	Beagle, female	Mandible (b) P1–4 12 weeks	3.75 × 7; Machined Buccal dehis. 4(W) × 4(H)	4/14	12 weeks	POC	Mandible, auto;	Cell sheets	No	PRP ND
Kim *et al.* (2009)	Beagle, adult male	Mandible (b) P1–4, M1 3 months	3.3 × 10; SA Circum. saddle 10(W) × 5(H)	4/24	8, 16 weeks	BMSC, PDLSC	Iliac, auto	1×10^6	Collagen	HA-βTCP Cells*
Ribeiro *et al.* (2010b)	Beagle, 1.5 years	Mandible (b) P3, P4, M1 3 months	4 × 8.5; Machined Buccal dehis. 4(W) × 5(H)	6/24	3 months	POC	Mandible, auto; yes	2×10^7	Ti-ePFTE	Collagen sponge Empty ND
Ribeiro *et al.* (2010a)	Beagle, 1.5 years	Mandible (b) P3, P4 3 months	4 × 8.5; Machined Buccal dehis. 4(W) × 5(H)	7/14	3 months	POC, BMSC	Mandible, iliac, auto; yes	2×10^7	No	Collagen sponge † NR
Wang *et al.* (2011)	Beagle, 1.5 years	Mandible (b) Unclear 3 months	3.75 × 10; Branemark Supra-alveolar 7(W) × 4(H)	5/30	12 weeks	BMSC	Iliac, auto	6×10^5	No	CP cement ± BMP-2, FGF Empty Cells*
Ribeiro *et al.* (2012)	Beagle, 1.5 years	Mandible (b) P3, P4 3 months	4 × 8.5; Machined Buccal dehis. 4(W) × 5(H)	8/24	3 months	BMSC	Iliac, auto; yes	2×10^7	Ti-ePFTE	Collagen sponge † Empty NR
Zou *et al.* (2012)	Labrador, adult, male	Mandible (b) P1–4 Immediate	3.5 × 12; Unclear Mesial 5(MD) × 4(BL) × 6(H)	5/30	12 weeks	BMSC-GFP, BMSC-HIF-1α, BMSC-cHIF-1α	Iliac, auto	2×10^5 /ml	No	CMP cement Empty Cells*
Han *et al.* (2013)	Mongrel, adult male	Mandible (b) P2–4 Immediate	3 × 10; Oxidized Distal 5(MD) × 4(BL) × 6(H)	4/24	12 weeks	PBMSC	Blood, auto; yes	2×10^6 /ml	Collagen	CSH-nHA-Col Cells*
Hao *et al.* (2014)	Beagle, 2 years male	Mandible (b) P2–4 Immediate	3.6 × 8; SA Mesial 4(MD) × 3.5(BL) × 4(H)	8/48	2, 4, 8 weeks	UCMSC	Human	2×10^8	No	PRF Cells*
Yun *et al.* (2014)	Mongrel adult male	Mandible (b) P1–4, M1 3 months	4 × 8.5; RBM Mesial intrabony 4 × 4 × 4	4/32	6, 12 weeks	BMSC	Human	2×10^5 /ml	No	HA ± PRP ND
Echeto *et al.* (2014)	Beagle	Mandible (b) P2, P4 6 weeks	3.5 × 8; TiOBlast Saddle 7(W) × 3(H)	6/24	6 weeks	BMSC	Iliac, allo	1×10^7 /ml	No	HA-βTCP Mandible AB Empty NR
Xu *et al.* (2015)	Labrador, adult male	Mandible (b) P1–4 Immediate	3.75 × 10; Unclear Mesial 6(H) × 4(BL) × 5(MD)	6/24	12 weeks	BMSC	Femur, auto	2×10^7 /ml	No	β-TCP ± PDGF Cells*
Bressan *et al.* (2015)	Labrador, 1 year	Mandible (b) P1–4, M1 3 months	3.3 × 10; SA Circum. 5.4(W) × 5(H)	6/72	4 weeks	ASC	Bichat bulla, auto	1×10^6	No	DBBM Cells*
Sheep										
Hoşgör *et al.* (2013)	Adult male	Mandible (b) Unclear	3.3 × 8; SA Circum. 4.1(W) × 4(H)	5/30	8 weeks	BMSC/ OB	Iliac; auto; yes	Unclear	No	PRP Cells*

N, number of animals; *n*, number of implants/defects; (b), bilateral defects or 'split-mouth' design; P, pre-molar; M, molar; SA, sand-blasted acid-etched surface; RBM, resorbable blast media surface; (W), width; (H), height; (BL), buccolingual dimension; (MD), mesiodistal dimension; Circum., circumferential defect; dehis., dehiscence defect; BMSC, bone marrow mesenchymal stem cells; HDF, human dermal fibroblasts; POC, periosteal cells; PDLSC, periodontal ligament stem cells; GFP, green fluorescent protein; HIF-1α, hypoxia inducible factor-1α; cHIF-1α, consecutively active form of HIF-1α; PBMSC, peripheral blood-derived mesenchymal stem cells; UCMSC, umbilical cord blood-derived mesenchymal stem cells; BMP-2, bone morphogenetic protein-2; OB, osteoblasts; ASC, adipose tissue-derived stem cells; auto, autologous; allo, allogeneic; Ti-ePFTE, titanium-expanded polytetrafluoroethylene membrane; Empty, inclusion of an 'empty defect' or no-treatment control group; PRP, platelet-rich plasma; PLGA, polylactic-co-glycolic acid; HA-βTCP, hydroxyapatite-β-tricalcium phosphate; CP, calcium phosphate; CMP, calcium mono-phosphate; CSH-nHA-Col, calcium sulphate-hemihydrate nano-HA collagen; PRF, platelet-rich fibrin; AB, autogenous bone; PDGF, platelet-derived growth factor; DBBM, deproteinized bovine bone mineral; Outcome (cells vs. scaffold), study outcomes (%BA/BIC) in favour of cell-based or scaffold-only group; ND, no significant differences between groups ($p > 0.05$); NR, not reported.

*Statistically significant result ($p < 0.05$).

†Absence of a 'scaffold-only' or a 'cell-free' control group.

Copyright © 2017 John Wiley & Sons, Ltd.

DOI: 10.1002/term

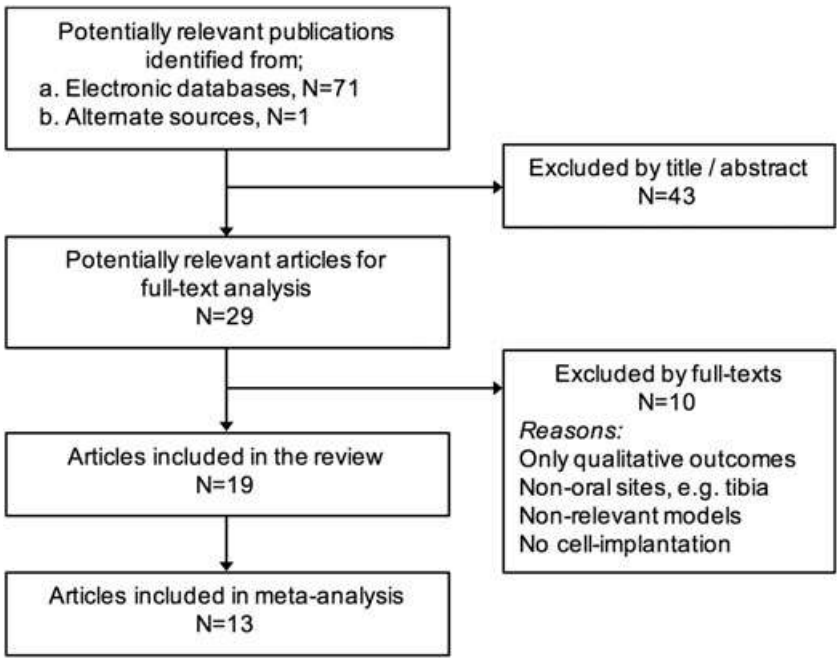

Figure 1. Flowchart for study screening and selection (N = number of articles)

extracted for possible meta-analysis. Standard errors of means, when reported, were converted to standard deviations for analysis. If data were only expressed graphically, numerical values were requested from the authors, and if a response was not received, digital ruler software was used to measure graphical data (ImageJ, National Institutes of Health, Bethesda, MD, USA). When studies reported outcomes at multiple time points, data from similar time points of different studies were pooled for the meta-analysis.

2.6. Risk of bias and quality assessment

Risk of bias assessment of the included studies was performed using the SYRCLE risk of bias tool for animal studies (Hooijmans *et al.,* 2014). Risk of bias was assessed as being 'high', 'low' or 'unclear' in each of the tool's 10 items. Items 9 and 10 were modified to include information on whether the study was randomized or blinded at any level. Item 8 was always judged as 'yes' when all animals were included in the analysis or numbers of excluded animals, together with reasons for exclusion, were provided.

Reporting quality of the studies was assessed based on a modification of the ARRIVE (Animal Research: Reporting *In Vivo* Experiments) guidelines, regarding relevant items (Berglundh and Stavropoulos, 2012; Kilkenny *et al.,* 2010). Compliance with the guidelines was evaluated using a predefined grading system applied to each of the 20 items (Schwarz *et al.,* 2012) (Table S2). Reporting quality was judged as 'high', 'moderate' or 'low'. Any disagreement between the reviewers during study selection, data extraction and quality assessment was resolved by discussion and consensus.

2.7. Meta-analysis

A meta-analysis was performed to compare the effectiveness of cell-loaded (experimental) and cell-free (control) approaches using histomorphometric data [means ± standard deviation and number of animals/defects (n) per group] for the outcomes %BA and %BIC in surgically created defects. Studies were pooled based on homogeneity regarding 'PICO'. The DerSimonian and Laird random effects model (Deeks *et al.*, 2008) was applied using STATA Statistical Software (StataCorp LP, College Station, TX, USA). When studies included multiple experimental groups and one control group, n in the control group was divided by the number of experimental groups (Vesterinen *et al.,* 2014). As the design in all studies included multiple interventions per animal, i.e. a 'split-mouth' design, a correlation coefficient (r-value of 0.50) was used for between-treatment group measurements. To explore the influence of different variables on the outcomes, meta-regression analyses were performed for the variables 'implant placement' (delayed or immediate), 'implant surface' (rough or machined), 'membrane barrier' (used or not), 'defect morphology' (studies were grouped into categories based on similar morphology to take into account defect type and/or dimensions; see Table 3) and 'observation time' ($<$12 weeks or $\geq$12 weeks). Pooled estimates of treatment effect (weighted mean differences; WMD) were calculated together with 95% confidence intervals (CI), and the I^2 statistic was used as a measure of inconsistency of results across studies (Deeks *et al.,* 2008).

Copyright © 2017 John Wiley & Sons, Ltd.

DOI: 10.1002/term

3. Results

3.1. Search results and study characteristics

Of the 72 search-identified studies, 19 studies reporting treatment of alveolar peri-implant defects in large animal models, i.e. dogs [18 studies, number of animals (n) = 107] and sheep (one study, n = 5), were included (Tables 2 and 3). Observation times ranged between 2 and 16 weeks for dogs (average, 9 weeks), whereas it was 8 weeks for sheep. Sixteen studies reported surgically created peri-implant defects, whereas three studies in dogs reported ligature-induced peri-implantitis (LIPI) models (Machtei *et al.,* 2016; Park *et al.,* 2015; Xu *et al.,* 2016). In the majority of studies, implants were placed in healed extraction sites after an average healing period of 3 months, and defects with a circumferential, dehiscence, intrabony or supra-alveolar component were prepared (Table 4). In four studies, implants were placed 'immediately' in canine extraction sockets to allow the creation of mesial or distal defects. Sixteen studies reported histomorphometric %BIC as the primary outcome; 14 of these studies also reported % BA. One study reported histomorphometric 'mineral apposition rate' [bone formation (μm)/day] as the primary outcome (Wang *et al.,* 2011), whereas one study only reported qualitative histological findings, and the use of autogenous bone in one of the control groups (Echeto *et al.,* 2014).

3.2. Risk of bias and quality assessment

Overall, the included studies were of unclear to high risk of bias and moderate reporting quality (Tables 4 and 5). Most studies provided adequate information regarding title, abstract, introduction, study objectives, ethical approval, experimental design and procedures (Table 5). Information regarding experimental animals and their housing and husbandry was generally inadequate – the majority of studies lacked complete information regarding the animals' age and gender (Table 1). Only one study provided information on the sample size calculation and baseline characteristics of the animals (Machtei *et al.,* 2016). In 11 studies (58%), animals or defects were randomly allocated to different treatment groups to minimize 'selection bias'. Five studies (26%) reported blinding of outcome assessors to treatment groups, to minimize 'detection bias'. All studies reported a detailed outcome evaluation, including statistical analyses.

3.3. Clinical observations

The majority of studies reported uneventful healing outcomes with no adverse reactions, remarkable inflammation, postoperative infection, wound dehiscence or other peri- and/or postoperative complications at the surgical sites. One study reported the exclusion of six of 14 defect sites (three sites each in experimental

Table 2. Summary of study characteristics: ligature-induced peri-implantitis models

Reference	Strain, age, gender	Extraction site, healing time	Implant size, surface Defect type, dimensions (mm)	*N/n*	Time	Cells	Source; induction	Cell number	Membrane	Scaffold Outcome (cells vs. scaffold)
Park *et al.* (2015)	Beagle, adult	Mandible (b) P1–4, M1 3 months	3.5 × 8.5; SA 3 months healing 4 months ligatures Circum. infra-bony, 40% bone loss	6/24	3 months	PDLSC, PDLSC-BMP-2	Pre-molars, molars, auto	1×10^6	Collagen	HA-Col Cells* (BMP-2)
Xu *et al.* (2016)	Beagle, 18 month male	Mandible (b) P1–4 3 months	3.8 × 10; cpTi 2 months healing 3 months ligatures 40% bone loss	6/24	6 months	ASC, ASC-BMP-2, ASC-GFP	Inguinal fat, auto	2×10^7 /ml	No	β-TCP Cells* (BMP-2)
Machtei *et al.* (2016)	Foxhound, 12 month male	Mandible (b) P1–4 3 months	3.75 × 10; SA 2 months healing 2 months ligatures Circum. infra-bony, 3-5(H) × 2-4(W)	5/30	3 months	EPC	Peripheral blood, auto	1×10^6	Collagen	β-TCP Empty Cells*

N, number of animals; *n*, number of implants/defects; (b), bilateral defects or 'split-mouth' design; P, pre-molar; M, molar; SA, sand-blasted acid-etched surface; (W), width; (H), height; Circum., circumferential defect; PDLSC, periodontal ligament stem cells; GFP, green fluorescent protein; BMP-2, bone morphogenetic protein-2; ASC, adipose tissue-derived stem cells; Auto, autologous; β-TCP, β-tricalcium phosphate; cpTi commercial pure titanium; EPC, endothelial progenitor cells; HA-Col, hydroxyapatite-collagen scaffold; 'healing', duration of implant healing time before placement of 'ligatures'; Outcome (cells vs. scaffold), study outcomes (%BA/BIC) in favour of cell-based or scaffold-only group.
*Statistically significant result ($p < 0.05$).

Copyright © 2017 John Wiley & Sons, Ltd.

DOI: 10.1002/term

Table 3. Categorization of studies according to defect morphology

Category	Defect type	Description	Studies
1	Circumferential saddle	Circumferential 'through-and-through' defect involving the alveolar crest	Echeto *et al.* (2014); Ito *et al.* (2006); Kim *et al.* (2009)
2	Circumferential intrabony	Circular defect resulting in a contained 'marginal gap' around the implant	Bressan *et al.* (2015); Hoşgör *et al.* (2013); Sparks *et al.* (2007)
3	Mesial or distal intrabony	Semi-circular defect resulting in a marginal gap on either the mesial or distal aspect of the implant	Han *et al.* (2013); Hao *et al.* (2014); Xu *et al.* (2015); Yun *et al.* (2014); Zou *et al.* (2012)
4	Buccal dehiscence	Linear defect involving only the buccal aspect of the alveolar bone exposing the implant	Mizuno *et al.* (2008); Ribeiro *et al.* (2010a, b, 2012)
5	Ligature-induced peri-implantitis (LIPI)	Supra-alveolar defect resulting in ~40% bone loss around implant	Machtei *et al.* (2016); Park *et al.* (2015); Xu *et al.* (2016)

All studies provided illustrations and/or clinical pictures of their respective defect models in the original manuscripts.

and control groups) from histological analysis as a result of membrane exposure and possible infection (Mizuno *et al.,* 2008).

3.4. Characteristics of tissue engineering strategies

3.4.1. Cells

All but four studies reported the use of autologous cells; of these four studies, one study each reported the use of human dermal (Sparks *et al.,* 2007), bone marrow (Yun *et al.,* 2014) or umbilical cord-derived cells (Hao *et al.,* 2014) in dogs, whereas one study reported on the use of allogeneic cells in dogs (Echeto *et al.,* 2014). Notably, no immunological reactions related to the use of allogeneic or human cells were reported in these studies. Most studies reported on the use of bone marrow mesenchymal stem cells (BMSC); three studies used periosteal cells (POC) (Mizuno *et al.,* 2008; Ribeiro *et al.,* 2010a, b), two studies used periodontal ligament stem cells (PDLSC) (Kim *et al.,* 2009; Park *et al.,* 2015), two studies used adipose tissue-derived MSC (Bressan *et al.,* 2015; Xu *et al.,* 2016) and one study used endothelial progenitor cells (Machtei *et al.,* 2016). MSC were used in early (one to six) passages, with (seven studies) or without osteogenic pre-induction. Primary cell cultures were expanded *ex vivo*; seeding densities ranged from 2×10^5 to 2×10^8 cells per scaffold. Cells were cultured on scaffolds for a specified period (average 24 h), in basal or osteogenic media prior to implantation.

Three studies reported the use of 'gene-modified' cells; cells were altered via adenoviral vector-mediated gene transfer of the growth factor bone morphogenetic protein-2 (BMP-2) (Park *et al.,* 2015; Xu *et al.,* 2016) or the transcription factor hypoxia inducible factor-1α (HIF-1α) (Zou *et al.,* 2012). Gene-modified cell groups were compared with 'control gene-modified' cells (cells infected with adenovirus expressing enhanced green fluorescent protein; EGFP), unmodified cells and/or scaffold-only groups.

3.4.2. Scaffolds

A majority of studies reported on the use of mineral phase alloplastic scaffolds [hydroxyapatite, alpha-/beta-tricalcium-phosphate (β-TCP), calcium phosphate cement] used in block, disc or particulate form. Seven studies used non-mineral phase scaffolds [platelet-rich plasma (PRP), platelet-rich fibrin or collagen]. Two studies reported the addition to the scaffolds of growth factors known to stimulate osteogenesis – BMP-2 and fibroblast growth factor (Wang *et al.,* 2011) and platelet-derived growth factor-BB (Xu *et al.,* 2015) – in at least one experimental group.

3.5. Meta-analysis

Histomorphometric data from 13 studies in dogs comparing cell-loaded vs. cell-free scaffolds were pooled for the outcomes %BA and %BIC (Figures 2 and 3); studies employing the LIPI model were analysed separately (Figures 4 and 5). For each outcome, a comparative analysis of gene-modified vs. 'unmodified' cells was also performed. Overall, the meta-analyses revealed statistically significant effects in favour of (a) cell-loaded vs. cell-free scaffolds in canine peri-implant defect models, with pooled estimates (WMD) of 12.30% BA (95% CI: 6.02, 18.58) and 15.15% BIC (95% CI: 12.05, 18.25); (b) cell-loaded vs. cell-free scaffolds in canine LIPI models, with WMD of 10.73% BA (95% CI: 4.02, 17.44) and 11.77% BIC (95% CI: 5.68, 17.86); and (c) BMP gene-modified vs. unmodified cells in canine LIPI models, with WMD of 29.44% BA (95% CI: 7.55, 51.32) and 16.50% BIC (95% CI: 12.89, 20.10). Moderate to high heterogeneity (I^2 70–87.8%) was observed in the analyses.

Meta-regression analyses showed no association between any of the tested variables and %BA, but revealed statistically significant effects on %BIC in favour of defects created in native bone vs. defects associated with extraction sockets, and nearly statistically significant effects in favour of longer observation times, i.e. ≥12 weeks vs. <12 weeks (Table S3).

4. Discussion

4.1. Overall

The aim of this study was to systematically review the preclinical *in vivo* evidence for BTE strategies to regenerate oral peri-implant bone defects in experimental

Copyright © 2017 John Wiley & Sons, Ltd.

DOI: 10.1002/term

Table 4. Assessment of risk of bias using a modified SYRCLE risk of bias tool

Risk of bias domain	1. Was the allocation sequence adequately generated and applied?	2. Were the groups similar at baseline or adjusted for confounders?	3. Was the allocation adequately concealed?	4. Were the animals randomly housed during the experiment?	5. Were the caregivers and/or investigators blinded?	6. Were animals selected at random for outcome assessment?	7. Was the outcome assessor blinded?	8. Were incomplete outcome data adequately addressed?	9. Was it stated that the experiment was randomized at any level?	10. Was it stated that the experiment was blinded at any level?
Ito *et al.* (2006)	U	Y	U	U	U	U	U	Y	Y	N
Sparks *et al.* (2007)	U	Y	U	U	U	Y	Y	Y	Y	Y
Mizuno *et al.* (2008)	U	Y	U	U	U	Y	U	Y	Y	N
Kim *et al.* (2009)	U	Y	U	U	U	Y	U	Y	Y	N
Ribeiro *et al.* (2010a)	Y	Y	U	U	U	Y	Y	Y	Y	Y
Ribeiro *et al.* (2010b)	U	Y	U	U	U	Y	Y	Y	Y	Y
Wang *et al.* (2011)	N	Y	N	U	U	Y	U	Y	N	N
Ribeiro *et al.* (2012)	Y	Y	U	U	U	Y	Y	Y	Y	Y
Zou *et al.* (2012)	U	Y	U	U	U	Y	U	Y	Y	N
Han *et al.* (2013)	U	Y	U	U	U	Y	Y	Y	Y	Y
Hao *et al.* (2014)	N	U	N	U	U	Y	U	Y	N	N
Yun *et al.* (2014)	U	Y	U	U	U	U	U	Y	Y	N
Echeto *et al.* (2014)	U	Y	U	U	U	Y	U	Y	Y	N
Xu *et al.* (2015)	U	Y	U	U	U	Y	U	Y	Y	N
Hosgör *et al.* (2013)	N	Y	N	U	U	Y	U	Y	N	N
Park *et al.* (2015)	N	Y	N	U	U	Y	U	Y	N	N
Bressan *et al.* (2015)	N	U	N	U	N	Y	U	U	N	N
Xu *et al.* (2016)	N	Y	N	U	N	Y	U	Y	N	N
Machtei *et al.* (2016)	N	Y	N	Y	N	Y	U	Y	N	N

Responses to 'signalling questions' in each domain were judged as 'yes' (Y; low risk of bias), 'no' (N; high risk of bias) or 'unclear' (U; unclear risk of bias).

animal models. Overall, the results showed that BTE approaches result in significantly better outcomes in terms of regenerated bone area (BA) and direct bone-to-implant contact (BIC) than biomaterials alone. These results are in agreement with a recent systematic review of BTE for alveolar bone regeneration (Shanbhag *et al.,* 2016). In this study, the results of meta-analyses showed that significantly greater bone regeneration was observed in favour of cell-based vs. cell-free approaches in alveolar bone critical-size defects (CSD) in small (rats, rabbits) and large animals (dogs, mini-pigs) (Shanbhag *et al.,* 2016). The results are also in line with other recent meta-analyses on the effectiveness of BTE with regards to periodontal regeneration (Yan *et al.,* 2015) and in terms of histological bone regeneration in all anatomical skeletal defects in large animal models (Liao *et al.,* 2014). In context, a beneficial effect of BTE has been further described in systematic review (SR) of human clinical trials evaluating the effectiveness of this type of technology for alveolar bone regeneration (Padial-Molina *et al.,* 2015; Shanbhag and Shanbhag, 2015). Nevertheless, it has to be stressed that due to considerable variation among studies with regards to the nature of cells, biomaterial scaffolds and type/dimensions of defects used in the various reports, no conclusive statements regarding the clinical effectiveness of BTE can yet be made. Moreover, no studies directly compared the effectiveness of BTE strategies with the 'gold standard', i.e. autogenous bone, for peri-implant defect repair. In context, a recent study reported comparable new bone formation (NBF) in peri-implant defects of rabbit tibia treated with BTE (autologous BMSC or adipose tissue-derived stem cells in β-TCP/collagen scaffolds) or autogenous bone (Erdogan *et al.,* 2015).

4.2. Factors influencing study outcomes

Based on previous evidence, the influence of the following factors on osseointegration surrogate outcomes (%BA, %BIC) was analysed herein: defect morphology/dimensions (Polyzois *et al.,* 2007; Schwarz *et al.,* 2010), implant placement time (Mainetti *et al.,* 2014), implant surface characteristics (Barfeie *et al.,* 2015) and the use of membranes to contain the grafted sites (Chiapasco and Zaniboni, 2009; Lorenzoni *et al.,* 1998). Only the timing of implant placement demonstrated a statistically significant effect on %BIC, with 11% greater BIC observed in implants placed in association with defects surgically created in healed sites compared with the BIC in immediate implants placed in large extraction sockets. Nevertheless, the relatively small number of studies and large heterogeneity in the current meta-analysis complicate the interpretation of this finding. In context, a recent study reported similar sequential healing patterns around implants placed in extraction sockets vs. healed sites in dogs, with no significant differences in BIC at early (1 week) or later (3 months) time points (Mainetti *et al.,* 2014).

Copyright © 2017 John Wiley & Sons, Ltd.

DOI: 10.1002/term

Table 5. Assessment of reporting quality using a modified ARRIVE checklist

ARRIVE item	Introduction				Methods										Results				Discussion		
	1	2	3	4	5	6a	6b	7	8	9	10	11	12	13	14	15	16	17	18	19	20
Ito *et al.* (2006)	1	2	2	1	1	1	1	2	1	0	1	1	2	2	0	1	2	1	1	1	2
Sparks *et al.* (2007)	1	2	2	1	2	1	1	2	1	1	1	1	2	2	0	2	2	2	1	2	2
Mizuno *et al.* (2008)	1	2	2	1	2	1	0	2	1	0	1	1	2	2	0	2	2	2	1	2	2
Kim *et al.* (2009)	1	2	2	1	2	1	0	2	1	0	1	1	2	2	0	2	2	2	1	2	2
Ribeiro *et al.* (2010b)	1	2	2	1	2	1	1	2	1	0	1	1	2	2	0	2	2	2	1	2	2
Ribeiro *et al.* (2010a)	1	2	2	1	2	1	1	2	1	0	1	1	2	2	0	2	2	2	1	2	2
Wang *et al.* (2011)	0	2	2	1	2	1	1	2	1	0	1	0	2	2	0	2	2	2	1	1	1
Ribeiro *et al.* (2012)	1	2	2	1	2	1	1	2	1	0	1	1	2	2	0	2	2	2	1	2	2
Zou *et al.* (2012)	1	2	2	1	2	1	1	2	2	2	1	1	2	2	0	2	2	2	1	2	2
Han *et al.* (2013)	1	2	2	1	2	1	1	2	1	0	1	1	2	2	0	2	2	2	1	2	2
Hao *et al.* (2014)	1	2	2	1	0	1	0	2	2	2	1	0	2	2	0	2	2	2	1	1	0
Yun *et al.* (2014)	1	2	2	1	2	1	0	2	2	2	1	1	2	2	0	2	2	2	1	2	2
Echeto *et al.* (2014)	1	2	2	1	2	1	1	2	1	0	1	0	2	2	0	2	2	2	1	1	0
Xu *et al.* (2015)	1	1	2	1	2	1	0	2	2	0	1	1	2	2	0	2	2	2	1	2	2
Hoşgör *et al.* (2013)	0	2	1	1	2	1	1	2	1	0	1	0	2	2	0	2	2	2	1	1	2
Park *et al.* (2015)	1	2	2	1	2	1	0	2	1	0	1	0	2	2	0	2	2	2	1	2	2
Bressan *et al.* (2015)	0	1	1	1	1	1	0	1	1	1	1	1	1	1	0	1	1	0	1	1	2
Xu *et al.* (2016)	1	2	2	1	2	1	0	2	1	0	1	1	2	2	0	2	2	2	1	2	2
Machtei *et al.* (2016)	1	2	2	1	2	1	1	2	2	1	2	1	2	2	0	2	2	2	1	2	2

A detailed list of ARRIVE items 1–20, together with scoring criteria, is provided in Table S2.

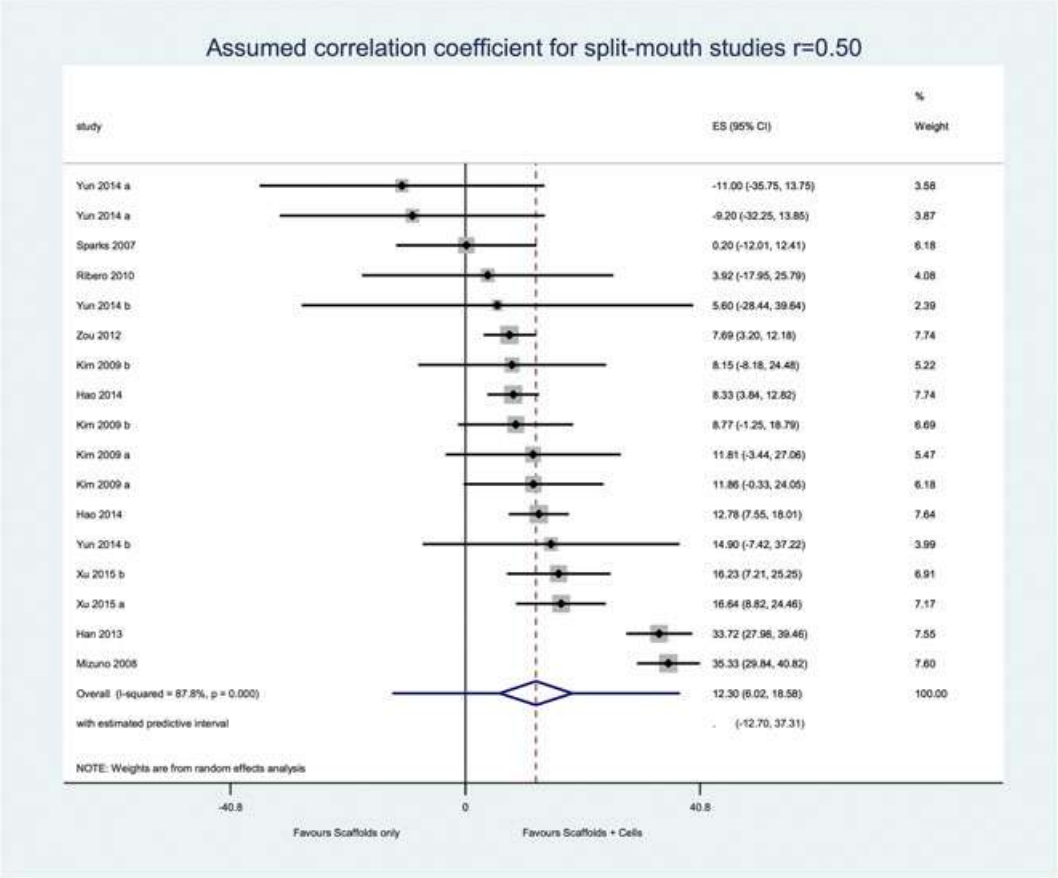

Figure 2. Forest plot for the comparison cell-loaded vs. cell-free scaffolds for percentage bone area (%BA) in surgical defect models. The forest plot displays the relative weight of the individual studies, the estimates of treatment effect (ES) expressed as weighted mean differences (WMD), 95% confidence intervals (CI) and a predictive interval, for the outcome percentage bone-to-implant contact (%BIC). The diamond indicates the pooled estimate and its 95% CI. The letters a and b represent different comparison groups within the same study [Colour figure can be viewed at wileyonlinelibrary.com]

4.3. Use of gene-modified cells

Gene transfer is a method by which osteogenic regulators can be introduced, either directly or via cells, into defect sites to enhance *in vivo* bone regeneration (Kofron and Laurencin, 2006). Three studies reported the *ex vivo* gene transfer of a growth factor, BMP-2 (Park *et al.,* 2015; Xu *et al.,* 2016) or transcription factor, HIF-1α (Zou *et al.,* 2012), into cells prior to implantation in canine peri-implant defects. BMPs, which are potent osteoinductive

Copyright © 2017 John Wiley & Sons, Ltd.

DOI: 10.1002/term

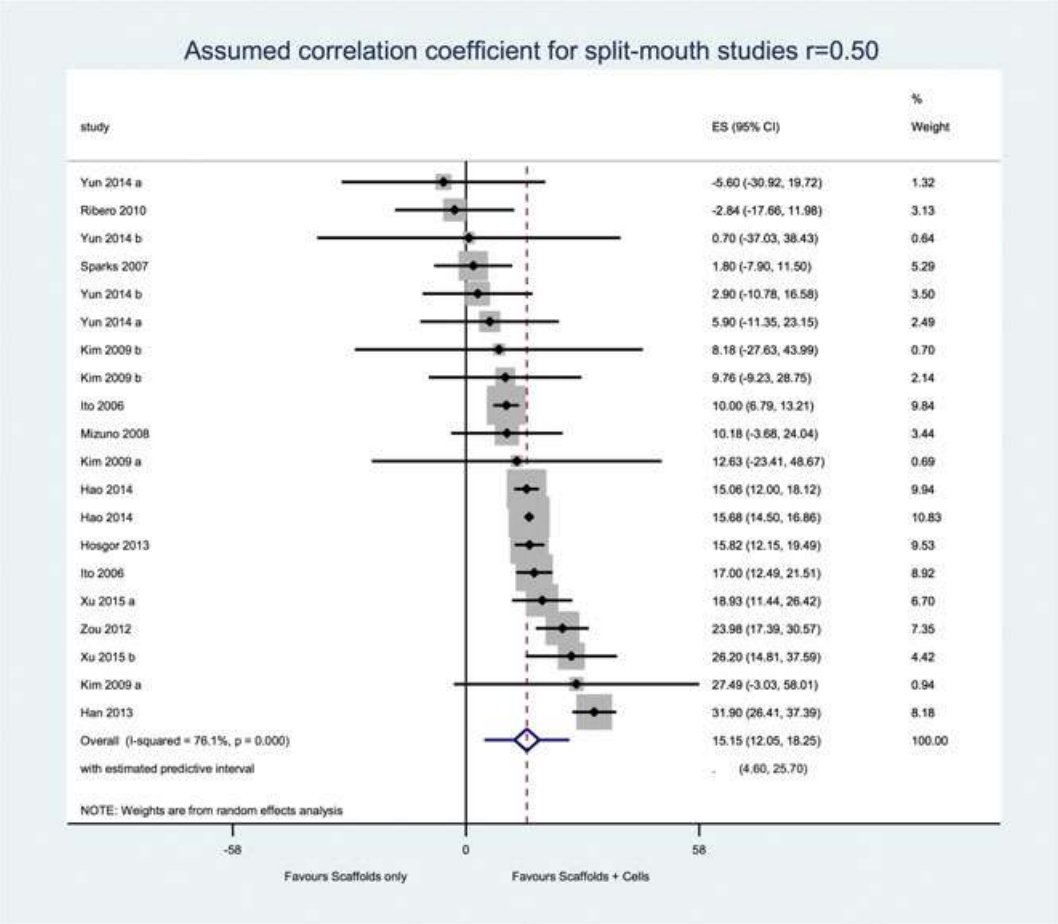

Figure 3. Forest plot for the comparison cell-loaded vs. cell-free scaffolds for percentage bone-to-implant contact (%BIC) in surgical defect models. The forest plot displays the relative weight of the individual studies, the estimates of treatment effect (ES) expressed as weighted mean differences (WMD), 95% confidence intervals (CI) and a predictive interval, for the outcome percentage bone area (%BA). The diamond indicates the pooled estimate and its 95% CI. The letters a and b represent different comparison groups within the same study [Colour figure can be viewed at wileyonlinelibrary.com]

agents, have been well established to regenerate bone *in vivo* (Khojasteh *et al.,* 2013). HIF-1α is a key regulator of angiogenesis, a process synergistic and inter-dependent with osteogenesis at regeneration sites (Drager *et al.,* 2015). In the present meta-analysis (two studies), statistically significant effects for %BA and %BIC were observed in favour of BMP-modified cells over unmodified and control (EGFP) gene-modified cells. These results are in agreement with previous *in vivo* studies reporting superior outcomes of BMP gene-modified cells in maxillofacial bone regeneration (Castro-Govea *et al.,* 2012; Chang *et al.,* 2003; Chung *et al.,* 2011), whereas HIF gene-modified cells have been shown to enhance regeneration in calvarial CSD (Zou *et al.,* 2011).

4.4. Implantation of human-derived cells in experimental animals

Three studies reported the use of human dermal fibroblasts (Sparks *et al.,* 2007), BMSC (Yun *et al.,* 2014) or umbilical cord-derived MSC (Hao *et al.,* 2014) in dogs. No immunological reactions were reported in relation to xenogeneic cell transplantation. Similarly, a recent study reported the use of stem cells from human exfoliated deciduous teeth for regeneration of canine mandibular CSD (Behnia *et al.,* 2014). The biocompatibility of MSC across species can be attributed to their hypoimmunogenic, immunomodulatory and anti-inflammatory properties. MSC are reported to exert these effects via three broad mechanisms: (1) their lack or limited expression of major histocompatibility complex (MHC)-I and MHC-II molecules; (2) via direct and indirect modulation of T-cell responses; and (3) secretion of various anti-inflammatory cytokines, making them a promising resource for allogeneic transplantation in regenerative therapies (Ryan *et al.,* 2005).

4.5. Meta-analyses and heterogeneity

A random effects model was chosen for the present meta-analysis to account for the expected between-study variance (Hooijmans *et al.,* 2014). The distribution of effect sizes was provided by WMDs and I^2. I^2 is a measure of 'true# inconsistency between the study results, due to between-study differences and not simply due to chance (Hooijmans *et al.,* 2014). I^2 was found herein to be significantly high, despite the fact that attempts were made to minimize heterogeneity when performing the present meta-analyses, i.e. care was taken to pool studies

Copyright © 2017 John Wiley & Sons, Ltd.

DOI: 10.1002/term

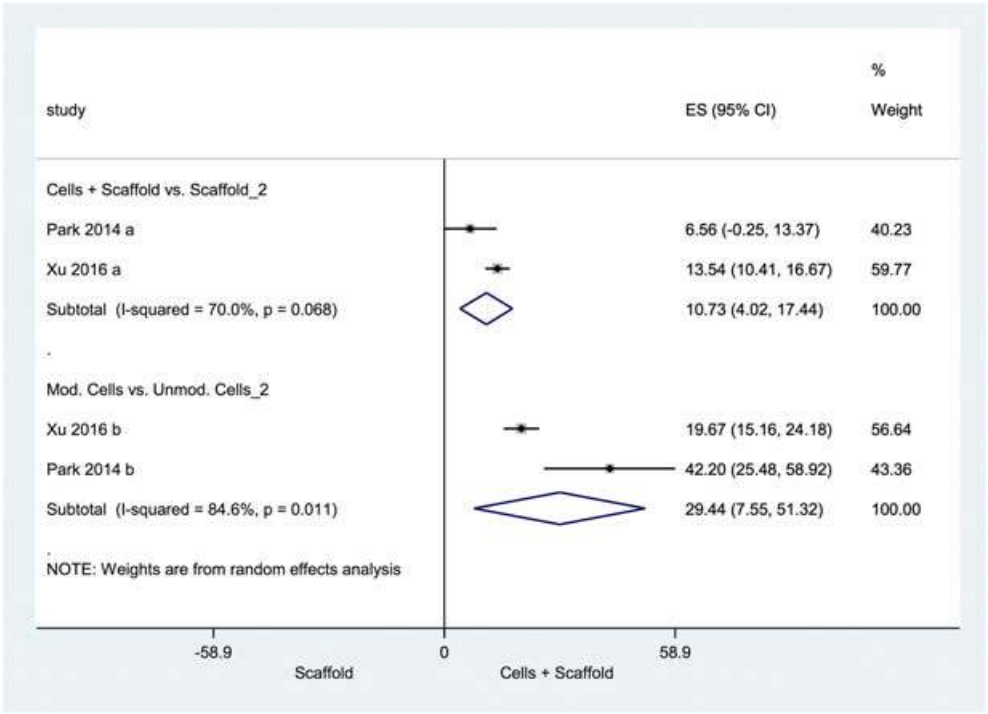

Figure 4. Forest plot for the comparisons cell-loaded vs. cell-free scaffolds and gene-modified vs. unmodified cells for percentage bone area (%BA) in ligature-induced peri-implantitis (LIPI) models. The forest plot displays the relative weight of the individual studies, the estimates of treatment effect (ES) expressed as weighted mean differences (WMD), 95% confidence intervals (CI) and a predictive interval, for the outcome percentage bone-to-implant contact (%BIC). The diamond indicates the pooled estimate and its 95% CI; Mod. Cells, bone morphogenetic protein-2 (BMP-2) gene-modified cells; Unmod. Cells; unmodified cells. In the second comparison (Mod. Cells vs. Unmod. Cells.) the forest plot labels 'cells + scaffold' and 'scaffold' are replaced by 'BMP2-modified cells' and 'unmodified cells', respectively. The letters a and b represent different comparison groups within the same study [Colour figure can be viewed at wileyonlinelibrary.com]

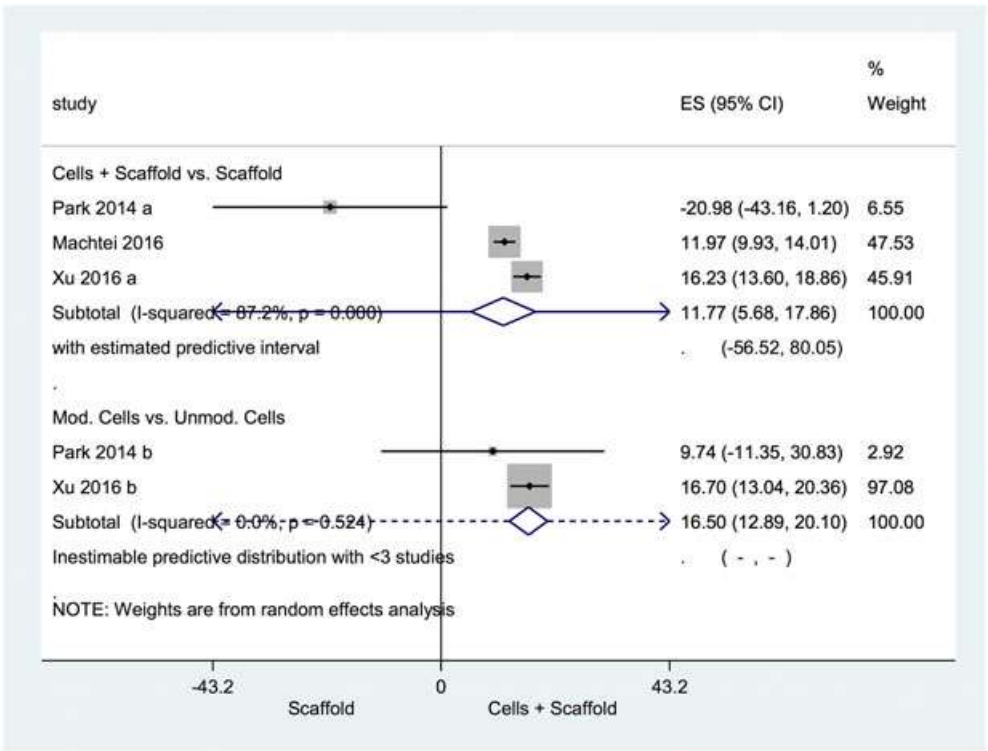

Figure 5. Forest plot for the comparison cell-loaded vs. cell-free scaffolds and gene-modified vs. unmodified cells for percentage bone-to-implant contact (%BIC) in ligature-induced peri-implantitis (LIPI) models. The forest plot displays the relative weight of the individual studies, the estimates of treatment effect (ES) expressed as weighted mean differences (WMD), 95% confidence intervals (CI) and a predictive interval, for the outcome percentage bone area (%BA). The diamond indicates the pooled estimate and its 95% CI; Mod. Cells, bone morphogenetic protein-2 (BMP-2) gene-modified cells; Unmod. Cells; unmodified cells. In the second comparison (Mod. Cells vs. Unmod. Cells.) forest plot labels 'cells + scaffold' and 'scaffold' are replaced by 'BMP2-modified cells' and 'unmodified cells', respectively. The letters a and b represent different comparison groups within the same study [Colour figure can be viewed at wileyonlinelibrary.com]

Copyright © 2017 John Wiley & Sons, Ltd.

DOI: 10.1002/term

with similar characteristics in terms of 'PICO', surgical and ligature-induced models were analysed separately, meta-regression analyses were performed for some variables potentially influencing the outcomes and the use of multiple treatments in the same animal was adjusted for in the analyses using recommended statistical methods (Higgins *et al.,* 2008). This wide variation in data could be due to biological factors related to the animals and/or methodological differences between the studies. Biological factors may include the animals' gender, age, immunological status, etc., whereas methodological differences in the study design (e.g. sample sizes, randomization), nature of interventions (e.g. use of autologous vs. allogeneic or human cells, osteogenic induction of cells prior to implantation) and outcome evaluation (e.g. methods of bone histomorphometry) could possibly explain the large heterogeneity observed in the meta-analyses.

In particular, the source and origin of the progenitor cells used for implantation may be a relevant source of heterogeneity, as it has been previously shown that the osteogenic potential of cells vary according to their source (Liao and Chen, 2014; Robey, 2011). Indeed, two included studies reported no significant differences in peri-implant bone regeneration when comparing cells from different autologous sources, i.e. BMSC vs. PDLSC (Kim *et al.,* 2009) and BMSC vs. POC (Ribeiro *et al.,* 2010b). However, variation in the sources of cells used across several studies could possibly explain the large heterogeneity observed in the meta-analyses. Similarly, differences in the number of implanted cells per defect, i.e. seeding density, may have influenced the results. Previous studies have identified 'optimal' seeding densities of 1–2 $\times$ 10^6 cells (per 40–50 mg of scaffold) (Brennan *et al.,* 2014; Mankani *et al.,* 2007) and 8 $\times$ 10^6 cells (per cm^3 of scaffold) (Kruyt *et al.,* 2008), in terms of bone formation, in ectopic implantation models of small and large animals, respectively. Although all included studies in the present review reported cell numbers corresponding to these values, it was not always clear in what ratio, i.e. cells:scaffolds, the cells were implanted. Further studies are needed to determine optimal seeding densities for specific animal models of BTE.

4.6. Outcome measures

Histomorphometry is considered the 'gold standard' method for the evaluation of bone structure (Rentsch *et al.,* 2014; Vidal *et al.,* 2012) and of the bone–implant interface in osseointegration research. Conventional histomorphometry is considered to be destructive, time-consuming and limited to two-dimensional assessment of tissue sections; a third dimension can be added on the basis of stereology (Müller *et al.,* 1998). All studies included in the meta-analysis reported relatively consistent methods for calculating the main parameters of interest, i.e. %BA and %BIC. However, inconsistencies in the processing methods (e.g. choice of staining, section thickness, number of sections analysed per implant, software used for analysis, etc.) (Chappard *et al.,* 1999; Kopp *et al.,* 2012; Stewart *et al.,* 2013) and investigator-related factors (e.g. inter-observer and inter-method variation, lack of blinding, etc.) (Wright *et al.,* 1992) may have introduced bias in the results and heterogeneity in the meta-analysis.

Recently, micro-computed tomography (micro-CT) has been proposed as an alternative method for assessing three-dimensional peri-implant bone microarchitecture with high resolution and accuracy, in a fast and non-destructive manner. Only one study in the present review reported micro-CT assessment of peri-implant bone regeneration (Zou *et al.,* 2012). A high correlation between micro-CT and histomorphometry for assessing peri-implant bone regeneration has been reported in recent preclinical (Kang *et al.,* 2015; Vandeweghe *et al.,* 2013) and clinical studies (de Lange *et al.,* 2014; Johansson *et al.,* 2013). A potential limitation, in some cases, is the presence of metal artefacts (beam hardening) around the implant periphery, which may complicate accurate assessment of BIC (Vandeweghe *et al.,* 2013). Moreover, micro-CT techniques may allow visualization of angiogenesis during bone regeneration (Udagawa *et al.,* 2013) and should be considered as an additional analytical tool in future studies.

4.7. Clinical relevance

The application of BTE for the reconstruction of oral peri-implant defects has been reported only in a clinical case series (Yamada *et al.,* 2013). 'Injectable tissue engineered bone' comprising of autologous BMSC (5 $\times$ 10^6 cells; osteogenically induced) and PRP were delivered into peri-implant defects of 36 patients and covered with a non-resorbable membrane. Radiographic evaluation revealed complete bone fill within all defects, comparable bone density (CT) to adjacent native bone and stable marginal bone levels, after 6–12 months (Yamada *et al.,* 2013). However, further well-designed controlled studies are needed to confirm the clinical effectiveness of BTE for peri-implant bone regeneration.

The results of the present meta-analysis have thus to be seen in the context of preclinical *in vivo* modelling. Advantages of large animal models include the ability to create standardized experimental conditions on both sides of the alveolar bones, i.e. having both experimental and control groups within the same animal (thus limiting the inter-animal variation and then the number of animals required) and to use clinically relevant sizes of defects and standard dental implants (Schwarz *et al.,* 2015). Dogs are widely used animal models in bone/implant research, given the similarities in structure, composition and physiology between canine and human bone (Aerssens *et al.,* 1998; Muschler *et al.,* 2010). Especially in BTE, where the influence of the limitations of mass transport, hypoxia and vascularization on the survival of transplanted cells must be evaluated in a clinically relevant setting, large animal models allow the

Copyright © 2017 John Wiley & Sons, Ltd.

DOI: 10.1002/term

preparation of defects with clinically relevant diffusion distances (Muschler *et al.,* 2010). In all included studies, the exposed implant surfaces were covered with biomaterials (with or without cells) and/or additional membranes, as is commonly performed in clinical practice (Chiapasco and Zaniboni, 2009). Moreover, the canine LIPI models in the three included studies closely simulate naturally occurring human peri-implantitis lesions, with several morphological and histological similarities being reported between the two (Schwarz *et al.,* 2015). Nevertheless, when interpreting the results of the present meta-analysis, the following limitation, inherent of preclinical *in vivo* modelling, should be considered: there is often an underestimation of clinical variation, with regards to both local (defect morphology and size, mass transfer, soft tissues, etc.) and systemic (age, comorbidities, etc.) biological environments. Specifically, in the context of experimental defects, these are uniformly surgically created, with sound surrounding soft tissues and generally uncompromised blood supply, and most often in young and healthy animals; this is often not the case in clinical scenarios, and in turn may often lead to the overestimation of clinical performance (Muschler *et al.,* 2010). Standardization of peri-implant defect models to better represent the clinical scenario, as well as standardization of study reporting, should be important considerations in future preclinical investigations.

Clinical meta-analyses aim to obtain a combined estimate or size of treatment effect, while meta-analyses of preclinical *in vivo* studies aim to summarize the effect of an intervention, in terms of the direction rather than the size (Hooijmans *et al.,* 2014). Thus, from the results of the present meta-analysis, it can be inferred that a similar positive response after BTE protocols for the treatment of implant-associated bone defects could also be expected in humans (Stavropoulos *et al.,* 2015). On the other hand, the numerical values or magnitude of response from the present meta-analysis cannot be directly translated to the human situation, i.e. the ~15% additional BIC observed in defects augmented with cell-loaded biomaterial scaffolds compared with scaffolds alone, would not translate to 15% (or '*x*-times' 15%) more bone, if the same procedure was performed in humans. In perspective, considering the magnitude of estimates of treatment effect, the clinical relevance (benefit) of such procedures for oral indications may be questioned.

5. Conclusions

The reviewed preclinical *in vivo* evidence can be summarized as follows:

1. Based on the results of large animal (canine) models, the addition of osteogenic cells to biomaterial scaffolds can enhance histomorphometric bone regeneration and osseointegration in surgical and ligature-induced oral peri-implant defects.
2. Based on limited evidence, *ex vivo* gene modification of cells with BMP-2 further enhances their capacity to repair LIPI defects.
3. Evidence for a comparison of tissue-engineered constructs with the 'gold standard', i.e. autogenous bone, with repair of oral peri-implant defects, is lacking.
4. The results should be interpreted with caution due to large heterogeneity between studies as a result of biological and methodological factors.

Conflict of interest

The authors declare no conflict of interest and no external funding was obtained for performing the current review.

References

Aerssens J, Boonen S, Lowet G *et al.* 1998; Interspecies differences in bone composition, density, and quality: potential implications for in vivo bone research. *Endocrinology* **139**: 663–670.

Albrektsson T, Brånemark P, Hansson H *et al*. 1981; Osseointegrated titanium implants: requirements for ensuring a long-lasting, direct bone-to-implant anchorage in man. *Acta Odontol Scand* **52**: 155–170.

Barfeie A, Wilson J, Rees J. 2015; Implant surface characteristics and their effect on osseointegration. *Br Dent J* **218**: E9.

Behnia A, Haghighat A, Talebi A *et al.* 2014; Transplantation of stem cells from human exfoliated deciduous teeth for bone regeneration in the dog mandibular defect. *World J Stem Cells* **6**: 505–510.

Berglundh T, Stavropoulos A. 2012; Preclinical in vivo research in implant dentistry. Consensus of the eighth European workshop on periodontology. *J Clin Periodontol* **39**(Suppl 1): 1–5.

Brennan MA, Renaud A, Amiaud J *et al.* 2014; Pre-clinical studies of bone regeneration with human bone marrow stromal cells and biphasic calcium phosphate. *Stem Cell Res Ther* **5**: 114.

Bressan E, Botticelli D, Sivolella S *et al.* 2015; Adipose-derived stem cells as a tool for dental implant osseointegration: an experimental study in the dog. *Int J Mol Cell Med* **4**: 197–208.

Castro-Govea Y, Cervantes-Kardasch VH, Borrego-Soto G *et al.* 2012; Human bone morphogenetic protein 2-transduced mesenchymal stem cells improve bone regeneration in a model of mandible distraction surgery. *J Craniofac Surg* **23**: 392–396.

Chang SC-N, Chuang HL, Chen YR *et al.* 2003; Ex vivo gene therapy in autologous bone marrow stromal stem cells for tissue-engineered maxillofacial bone regeneration. *Gene Ther* **10**: 2013–2019.

Chappard D, Legrand E, Pascaretti C *et al.* 1999; Comparison of eight histomorphometric methods for measuring trabecular bone architecture by image analysis on histological sections. *Microsc Res Tech* **45**: 303–312.

Chiapasco M, Casentini P, Zaniboni M. 2009; Bone augmentation procedures in implant dentistry. *Int J Oral Maxillofac Implants* **24**(Suppl.): 237–259.

Chiapasco M, Zaniboni M. 2009; Clinical outcomes of GBR procedures to correct peri-implant dehiscences and fenestrations: a systematic review. *Clin Oral Implants Res* **20**(Suppl. 4): 113–123.

Chung VH-Y, Chen AY-L, Kwan C-C *et al.* 2011; Mandibular alveolar bony defect repair using bone morphogenetic protein 2-expressing autologous mesenchymal stem cells. *J Craniofac Surg* **22**: 450–454.

Deeks JJ, Higgins JPT, Altman DG. 2008; Analysing data and undertaking meta-analyses. In Cochrane Handbook for Systematic Reviews of Interventions. John Wiley & Sons: Chichester: 243–296.

Drager J, Harvey EJ, Barralet J. 2015; Hypoxia signalling manipulation for bone regeneration. *Expert Rev Mol Med* **17**: e6.

Echeto L, De Kok I, Sacco D *et al.* 2014; Peri-implant alveolar bone augmentation using allogeneic marrow-derived stem cells; a pilot study in the canine mandible. *J Genet Mol Cell Biol* **1**: 1–9.

Erdogan Ö, Supachawaroj N, Soontornvipart K *et al.* 2015; Treatment of peri-implant defects in the rabbit's tibia with adipose or bone marrow-derived mesenchymal stem cells. *Clin Implant Dent Relat Res* doi: https://doi.org/10.1111/cid.12378.

Han X, Liu H, Wang D *et al.* 2013; Alveolar bone regeneration around immediate implants using an injectable nHAC/CSH loaded with autogenic blood-acquired mesenchymal progenitor cells: an experimental study in the dog mandible. *Clin Implant Dent Relat Res* **15**: 390–401.

Copyright © 2017 John Wiley & Sons, Ltd.

Hao P, Wang Z, Xu Q *et al.* 2014; Effect of umbilical cord mesenchymal stem cell in peri-implant bone defect after immediate implant : an experiment study in beagle dogs. *Int J Clin Exp Pathol* **7**: 8271–8278.

Higgins JPT, Deeks JJ, Altman DG. 2008; Special topics in statistics. In Cochrane Handbook for Systematic Reviews of Interventions. John Wiley & Sons: Chichester: 481–529.

Hooijmans CR, IntHout J, Ritskes-Hoitinga M *et al.* 2014; Meta-analyses of animal studies: an introduction of a valuable instrument to further improve healthcare. *ILAR J* **55**: 418–426.

Hooijmans CR, Rovers MM, de Vries RB *et al.* 2014; SYRCLE's risk of bias tool for animal studies. *BMC Med Res Methodol* **14**: 43.

Hoşgör F, Yilmaz N, Senyurt O *et al.* 2013; Effect of osteoblast cell culture on the bone implant contact. *Acta Odontol Scand* **71**: 626–631.

Ito K, Yamada Y, Naiki T *et al.* 2006; Simultaneous implant placement and bone regeneration around dental implants using tissue-engineered bone with fibrin glue, mesenchymal stem cells and platelet-rich plasma. *Clin Oral Implants Res* **17**: 579–586.

Johansson L-A, Isaksson S, Bryington M *et al.* 2013; Evaluation of bone regeneration after three different lateral sinus elevation procedures using micro-computed tomography of retrieved experimental implants and surrounding bone: a clinical, prospective, and randomized study. *Int J Oral Maxillofac Implants* **28**: 579–586.

Kaigler D, Pagni G, Park CH *et al.* 2013; Stem cell therapy for craniofacial bone regeneration: a randomized, controlled feasibility trial. *Cell Transplant* **22**: 767–777.

Kang S-W, Lee W-J, Choi S-C *et al.* 2015; Volumetric quantification of bone-implant contact using micro-computer tomography analysis based on region-based segmentation. *Imaging Sci Dent* **45**: 7–13.

Khojasteh A, Behnia H, Naghdi N *et al.* 2013; Effects of different growth factors and carriers on bone regeneration: a systematic review. *Oral Surg Oral Med Oral Pathol Oral Radiol* **116**: e405–e423.

Kilkenny C, Browne WJ, Cuthill IC *et al.* 2010; Improving bioscience research reporting: the ARRIVE guidelines for reporting animal research. *PLoS Biol* **8**: e1000412.

Kim SH, Kim KH, Seo BM *et al.* 2009; Alveolar bone regeneration by transplantation of periodontal ligament stem cells and bone marrow stem cells in a canine peri-implant defect model: a pilot study. *J Periodontol* **80**: 1815–1823.

Kofron MD, Laurencin CT. 2006; Bone tissue engineering by gene delivery. *Adv Drug Deliv Rev* **58**: 555–576.

Kopp S, Warkentin M, Öri F *et al.* 2012; Section plane selection influences the results of histomorphometric studies: the example of dental implants. *Biomed Tech (Berl)* **57**: 365–370.

Kruyt M, De Bruijn J, Rouwkema J *et al.* 2008; Analysis of the dynamics of bone formation, effect of cell seeding density, and potential of allogeneic cells in cell-based bone tissue engineering in goats. *Tissue Eng Part A* **14**: 1081–1088.

de Lange GL, Overman JR, Farré-Guasch E *et al.* 2014; A histomorphometric and micro-computed tomography study of bone regeneration in the maxillary sinus comparing biphasic calcium phosphate and deproteinized cancellous bovine bone in a human split-mouth model. *Oral Surg Oral Med Oral Pathol Oral Radiol* **117**: 8–22.

Li Y, Chen S-K, Li L *et al.* 2015; Bone defect animal models for testing efficacy of bone substitute biomaterials. *J Orthop Transl* **3**: 95–104.

Liao HT, Chen CT. 2014; Osteogenic potential: comparison between bone marrow and adipose-derived mesenchymal stem cells. *World J Stem Cells* **6**: 288–295.

Liao Y, Zhang X-L, Li L *et al.* 2014; Stem cell therapy for bone repair: a systematic review and meta-analysis of preclinical studies with large animal model. *Br J Clin Pharmacol* **78**: 718–726

Lorenzoni M, Pertl C, Keil C *et al.* 1998; Treatment of peri-implant defects with guided bone regeneration: a comparative clinical study with various membranes and bone grafts. *Int J Oral Maxillofac Implants* **13**: 639–646.

Machtei EE, Kim DM, Karimbux N *et al.* 2016; The use of endothelial progenitor cells combined with barrier membrane for the reconstruction of peri-implant osseous defects: an animal experimental study. *J Clin Periodontol* **43**: 289–297.

Mainetti T, Lang NP, Bengazi F *et al.* 2014; Sequential healing at implants installed immediately into extraction sockets. An experimental study in dogs. *Clin Oral Implants Res* **27**: 130–138.

Mankani MH, Kuznetsov SA, Robey PG. 2007; Formation of hematopoietic territories and bone by transplanted human bone marrow stromal cells requires a critical cell density. *Exp Hematol* **35**: 995–1004.

Mizuno D, Kagami H, Mizuno H *et al.* 2008; Bone regeneration of dental implant dehiscence defects using a cultured periosteum membrane. *Clin Oral Implants Res* **19**: 289–294.

Moher D, Liberati A, Tetzlaff J *et al.* 2009; Preferred reporting items for systematic reviews and meta-analyses: the PRISMA statement. *PLoS Med* **6**: e1000097.

Moraschini V, Poubel LADC, Ferreira VF *et al.* 2015; Evaluation of survival and success rates of dental implants reported in longitudinal studies with a follow-up period of at least 10 years: a systematic review. *Int J Oral Maxillofac Surg* **44**: 377–388.

Müller R, Van Campenhout H, Van Damme B *et al.* 1998; Morphometric analysis of human bone biopsies: a quantitative structural comparison of histological sections and micro-computed tomography. *Bone* **23**: 59–66.

Muschler GF, Raut VP, Patterson TE *et al.* 2010; The design and use of animal models for translational research in bone tissue engineering and regenerative medicine. *Tissue Eng Part B Rev* **16**: 123–145.

Padial-Molina M, O'Valle F, Lanis A, Mesa F, Dohan Ehrenfest DM, Wang HL, Galindo-Moreno P. 2015; Clinical Application of Mesenchymal Stem Cells and Novel Supportive Therapies for Oral Bone Regeneration. *Biomed Research International*: https://doi.org/10.1155/2015/341327.

Park S-Y, Kim K-H, Gwak E-H *et al.* 2015; Ex vivo bone morphogenetic protein 2 gene delivery using periodontal ligament stem cells for enhanced re-osseointegration in the regenerative treatment of peri-implantitis. *J Biomed Mater Res Part A* **103**: 38–47.

Pellegrini G, Seol YJ, Gruber R *et al.* 2009; Pre-clinical models for oral and periodontal reconstructive therapies. *J Dent Res* **88**: 1065–1076.

Polyzois I, Renvert S, Bosshardt DD *et al.* 2007; Effect of Bio-Oss on osseointegration of dental implants surrounded by circumferential bone defects of different dimensions: an experimental study in the dog. *Clin Oral Implants Res* **18**: 304–310.

Rentsch C, Schneiders W, Manthey S *et al.* 2014. Comprehensive histological evaluation of bone implants. *Biomatter* **4**: e27993.

Renvert S and Persson R.. 2009; Periodontitis as a Potential Risk Factor for Peri-Implantitis. *J Clin Periodontol* **36**: 9–14.

Ribeiro FV, Suaid FF, Ruiz KGS *et al.* 2010a; Periosteum-derived cells as an alternative to bone marrow cells for bone tissue engineering around dental implants. A histomorphometric study in beagle dogs. *J Periodontol* **81**: 907–916.

Ribeiro FV, Suaid FF, Ruiz KGS *et al.* 2010b. Peri-implant reconstruction using autologous periosteum-derived cells and guided bone regeneration. *J Clin Periodontol* **37**: 1128–1136.

Ribeiro FV, Suaid FF, Ruiz KGS *et al.* 2012; Effect of autologous bone marrow-derived cells associated with guided bone regeneration or not in the treatment of peri-implant defects. *Int J Oral Maxillofac Surg* **41**: 121–127.

Robey PG. 2011; Cell sources for bone regeneration: the good, the bad, and the ugly (but promising). *Tissue Eng Part B Rev* **17**: 423–430.

Ryan JM, Barry FP, Murphy JM *et al.* 2005; Mesenchymal stem cells avoid allogeneic rejection. *J Inflamm (Lond)* **2**: 8.

Sanz M, Donos N, Alcoforado G *et al.* 2015; Therapeutic concepts and methods for improving dental implant outcomes. Summary and consensus statements. The 4th EAO Consensus Conference 2015. *Clin Oral Implants Res* **26**: 202–206.

Schwarz F, Iglhaut G, Becker J. 2012; Quality assessment of reporting of animal studies on pathogenesis and treatment of peri-implant mucositis and peri-implantitis. A systematic review using the ARRIVE guidelines. *J Clin Periodontol* **39**(Suppl. 1): 63–72.

Schwarz F, Sahm N, Schwarz K *et al.* 2010; Impact of defect configuration on the clinical outcome following surgical regenerative therapy of peri-implantitis. *J Clin Periodontol* **37**: 449–455.

Schwarz F, Sculean A, Engebretson SP *et al.* 2015; Animal models for peri-implant mucositis and peri-implantitis. *Periodontol* **68**: 168–181.

Shanbhag S, Pandis N, Nyengaard JR *et al.* 2016; Alveolar bone tissue engineering in critical-size defects of experimental animal models: a systematic review and meta-analysis. *J Tissue Eng Regen Med* doi: https://doi.org/10.1002/term.2198

Shanbhag S, Shanbhag V. 2015; Clinical applications of cell-based approaches in alveolar bone augmentation: a systematic review. *Clin Implant Dent Relat Res* **17**: e17–e34.

Sicilia A, Quirynen M, Fontolliet A *et al.* 2015; Long-term stability of peri-implant tissues after bone or soft tissue augmentation. Effect of zirconia or titanium abutments on peri-implant soft tissues. Summary and consensus statements. The 4th EAO Consensus Conference 2015. *Clin Oral Implants Res* **26**: 148–152.

Sparks MS, Kerns DG, Wilson TG *et al.* 2007; Bone regeneration around implants in the canine mandible with cultured fibroblasts in polyglactin mesh. *J Periodontol* **78**: 1276–1287.

Stavropoulos A, Sculean A, Bosshardt DD *et al.* 2015; Pre-clinical in vivo models for the screening of bone biomaterials for oral/craniofacial indications: focus on small-animal models. *Periodontol* **68**: 55–65.

Stewart MC, McCormick LE, Goliath JR *et al.* 2013; A comparison of histomorphometric data collection methods. *J Forensic Sci* **58**: 109–113.

Udagawa A, Sato S, Hasuike A *et al.* 2013; Micro-CT observation of angiogenesis in bone regeneration. *Clin Oral Implants Res* **24**: 787–792.

Vandeweghe S, Coelho PG, Vanhove C *et al.* 2013; Utilizing micro-computed tomography to evaluate bone structure surrounding dental implants: a comparison with histomorphometry. *J Biomed Mater Res Part B Appl Biomater* **101**: 1259–1266.

Vesterinen HM, Sena ES, Egan KJ *et al.* 2014; Meta-analysis of data from animal studies: a practical guide. *J Neurosci Methods* **221**: 92–102.

Vidal B, Pinto A, Galvão MJ *et al.* 2012; Bone histomorphometry revisited. *Acta Reumatol Port* **37**: 294–300.

Wang L, Zou D, Zhang S *et al.* 2011; Repair of bone defects around dental implants with bone morphogenetic protein/fibroblast growth factor-loaded porous calcium phosphate cement: a pilot study in a canine model. *Clin Oral Implants Res* **22**: 173–181.

Wright CD, Vedi S, Garrahan NJ *et al.* 1992; Combined inter-observer and inter-method variation in bone histomorphometry. *Bone* **13**: 205–208.

Xu L, Sun X, Bai J *et al.* 2016; Reosseointegration following regenerative therapy of tissue-engineered bone in a canine model of experimental peri-implantitis. *Clin Implant Dent Relat Res* **18**: 379–391.

Xu L, Zhang W, Lv K *et al.* 2015; Peri-implant bone regeneration using rhPDGF-BB, BMSCs, and β-TCP in a canine model. *Clin Implant Dent Relat Res* **18**: 241–252.

Yamada Y, Nakamura S, Ito K *et al.* 2013; Injectable bone tissue engineering using expanded mesenchymal stem cells. *Stem Cells* **31**: 572–580.

Yan X-Z, Yang F, Jansen JA *et al.* 2015; Cell-based approaches in periodontal regeneration: a systematic review and meta-analysis of periodontal defect models in animal experimental work. *Tissue Eng Part B Rev* **21**: 411–426.

Yun J-H, Han S-H, Choi S-H *et al.* 2014; Effects of bone marrow-derived mesenchymal stem cells and platelet-rich plasma on bone regeneration for osseointegration of dental implants: preliminary study in canine three-wall intrabony defects. *J Biomed Mater Res Part B Appl Biomater* **102**: 1021–1030.

Zou D, He J, Zhang K *et al.* 2012; The bone-forming effects of HIF-1α-transduced BMSCs promote osseointegration with dental implant in canine mandible. *PLoS One* **7**: e0032355.

Zou D, Zhang Z, Ye D *et al.* 2011; Repair of critical-sized rat calvarial defects using genetically engineered bone marrow-derived mesenchymal stem cells overexpressing hypoxia-inducible factor-1alpha. *Stem Cells* **29**: 1380–1390.

Copyright © 2017 John Wiley & Sons, Ltd.

Supporting information

Additional Supporting Information may be found online in the supporting information tab for this article.

Table S1. Search strategy for MEDLINE
Table S2. Checklist for quality assessment of studies according to modified ARRIVE guidelines and a predefined grading system
Table S3. Meta-regression analysis for the influence of different variables on %BIC
Table S4. Monte Carlo permutation test for meta-regression on %BIC (permutations = 1000)

Copyright © 2017 John Wiley & Sons, Ltd.

DOI: 10.1002/term

JOURNAL OF TISSUE ENGINEERING AND REGENERATIVE MEDICINE
J Tissue Eng Regen Med 2016.
Published online in Wiley Online Library (wileyonlinelibrary.com) **DOI:** 10.1002/term.2198

REVIEW

Alveolar bone tissue engineering in critical-size defects of experimental animal models: a systematic review and meta-analysis

Siddharth Shanbhag[1,2], Nikolaos Pandis[3], Kamal Mustafa[1], Jens R. Nyengaard[4] and Andreas Stavropoulos[2]*
[1]*Department of Clinical Dentistry, Centre for Clinical Dental Research, University of Bergen, Bergen, Norway*
[2]*Department of Periodontology, Faculty of Odontology, Malmö University, Malmö, Sweden*
[3]*Department of Orthodontics and Dentofacial Orthopedics, University of Bern, Bern, Switzerland*
[4]*Stereology and Electron Microscopy Laboratory, Department of Clinical Medicine, Aarhus University, Aarhus, Denmark*

Abstract

Regeneration of large, 'critical-size' bone defects remains a clinical challenge. Bone tissue engineering (BTE) is emerging as a promising alternative to autogenous, allogeneic and biomaterial-based bone grafting. The objective of this systematic review was to answer the focused question: in animal models, do cell-based BTE strategies enhance regeneration in alveolar bone critical-size defects (CSDs), compared with grafting with only biomaterial scaffolds or autogenous bone? Following PRISMA guidelines, electronic databases were searched for controlled animal studies reporting maxillary or mandibular CSD and implantation of mesenchymal stem cells (MSCs) or osteoblasts (OBs) seeded on biomaterial scaffolds. A random effects meta-analysis was performed for the outcome histomorphometric new bone formation (%NBF). Thirty-six studies were included that reported on large- (monkeys, dogs, sheep, minipigs) and small-animal (rabbits, rats) models. On average, studies presented with an unclear-to-high risk of bias and short observation times. In most studies, MSCs or OBs were used in combination with alloplastic mineral-phase scaffolds. In five studies, cells were modified by *ex vivo* gene transfer of bone morphogenetic proteins (BMPs). The meta-analysis indicated statistically significant benefits in favour of: (1) cell-loaded vs. cell-free scaffolds [weighted mean difference (WMD) 15.59–49.15% and 8.60–13.85% NBF in large- and small-animal models, respectively]; and (2) BMP-gene-modified vs. unmodified cells (WMD 10.06–20.83% NBF in small-animal models). Results of cell-loaded scaffolds vs. autogenous bone were inconclusive. Overall, heterogeneity in the meta-analysis was high ($I^2 > 90\%$). In summary, alveolar bone regeneration is enhanced by addition of osteogenic cells to biomaterial scaffolds. The direction and estimates of treatment effect are useful to predict therapeutic efficacy and guide future clinical trials of BTE. Copyright © 2016 John Wiley & Sons, Ltd.

Received 16 November 2015; Revised 7 January 2016; Accepted 14 March 2016

Keywords **bone tissue engineering; bone regeneration; mesenchymal stem cells; scaffolds; meta-analysis**

1. Introduction

Reconstruction of alveolar bone deficiencies, resulting from ageing, trauma, ablative surgery or pathology, remains a clinical challenge (Götz *et al*., 2015). Although autologous bone transplantation is still considered the 'gold standard' for maxillofacial bone regeneration (Corbella *et al*., 2015; Fretwurst *et al*., 2015), large defects may require volumes of bone that are locally unavailable. Moreover, the morbidity associated with bone harvesting can be a major limiting factor (Nkenke and Neukam, 2014). Alternatives have included allogeneic, xenogeneic and alloplastic bone substitutes, but no consensus currently exists on the effectiveness of one material over the other in comparison with autogenous bone, or for all indications (Al-Nawas and Schiegnitz, 2014; Milinkovic and Cordaro, 2014).

The bone tissue engineering approach involves harvesting of osteogenic cells [most commonly mesenchymal stem cells (MSCs)] from an autologous source (e.g. bone marrow, adipose tissue etc.), their *in vitro* culture expansion and combination with an appropriate carrier scaffold for implantation *in vivo* (Shanbhag and Shanbhag, 2015). Thus, the 'triad' of osteogenic cells, osteoinductive signals (growth factors released by cells), and osteoconductive scaffolds, replicates the properties of autogenous bone, without the need for invasive harvesting (Oppenheimer *et al*., 2012). The prospects for use of such tissue-engineered products for alveolar bone repair are very promising, as demonstrated by recent clinical studies (Padial-Molina *et al*., 2015; Shanbhag and Shanbhag, 2015).

Preclinical testing of new regenerative therapies in clinically relevant animal models is an important aspect of translational research and, in most cases, a requirement of regulatory health agencies before initiating human clinical trials (Pellegrini *et al*., 2009; Stavropoulos *et al*., 2015). The advantage of animal models, in addition to

*Correspondence to: A. Stavropoulos, Department of Periodontology, Faculty of Odontology, Malmö University, Carl Gustafs väg, 20506 Malmö, Sweden. E-mail: andreas.stavropoulos@mah.se

Copyright © 2016 John Wiley & Sons, Ltd.

testing therapeutic safety and efficacy, is the possibility of better understanding of the underlying biological processes via methods that may be considered too invasive for human application (e.g., repeated harvesting of biological samples, biopsies, etc.) (Peric *et al*., 2015). Small-animal models (rodents and rabbits) usually constitute a starting point for proof-of-principle or feasibility studies, while studies in large-animal models (dogs, pigs, sheep, and non-human primates) attempt to simulate clinical conditions more closely and predict therapeutic efficacy (Stavropoulos *et al*., 2015).

The 'calvarial critical-size defect' (CCSD) is a widely used experimental model for screening bone biomaterials in small and large animals. This is the smallest-size experimental defect in the cranium of the animal that will not spontaneously and completely regenerate with bone in a defined time-frame without intervention (Schmitz and Hollinger, 1986; Vajgel *et al*., 2014). However, CCSD may reflect poorly the clinical scenario of alveolar bone defects, given the variation in development and healing pattern between different skeletal sites (Quarto *et al*., 2010; Ichikawa *et al*., 2015), and the additional influence of dental and masticatory factors on alveolar bone physiology (Liebschner, 2004; Bagi *et al*., 2011).

For this reason, critical-size defect (CSD) models have been developed involving the maxillary and mandibular bones of small and large animals. The aim of the present study was to systematically review the available literature to answer the focused 'PICO' (population, intervention, comparison, outcome) question: In alveolar CSD of experimental animals, does a tissue engineering approach (implantation of osteogenic cells seeded on biomaterial scaffolds), enhance histomorphometric bone regeneration, compared with grafting with only biomaterial scaffolds or autogenous bone? Based on the nature of the data retrieved, it was also aimed to perform a meta-analysis of the efficacy of 'cell-based' vs. 'cell-free' approaches, to determine the estimates and, more importantly, the direction of treatment effect for guiding future human clinical trials.

2. Material and methods

2.1. Study design

A review protocol was developed based on the Preferred Reporting Items for Systematic reviews and Meta-Analyses (PRISMA) guidelines (Moher *et al*., 2009), and predetermined inclusion/exclusion criteria.

Inclusion criteria were:

1. English language studies.
2. Randomized or non-randomized controlled animal experimental studies with two or more experimental groups.
3. Use of experimental CSD in the maxillae or mandibles of small- or large-animal models (CSD were defined by the inclusion of an untreated or 'empty defect' control group in which the defects did not heal throughout the observation period, or if the reported model was based on a referenced previous confirmatory study).
4. Transplantation of cultured autologous, allogeneic or human-derived osteogenic cells [MSCs or osteoblasts (OBs)] seeded on biomaterial scaffolds in at least one experimental group.
5. A control group receiving 'cell-free' biomaterial scaffolds or autogenous bone.
6. Reporting of quantitative histomorphometric new bone formation (%NBF), which was selected as the primary outcome (Vajgel *et al*., 2014). Studies reporting quantitative radiographic assessments of bone formation via computerized tomography (CT) or micro-CT were considered separately.

Exclusion criteria were:

1. *In vitro* studies.
2. *In vivo* animal studies reporting CSD in other anatomical sites (calvarial or non-craniofacial), ectopic (e.g. subcutaneous) models or systemic cell-delivery.
3. Absence of a control group.
4. *In vivo* animal studies reporting alveolar bone CSD with only qualitative or semiquantitative histological analyses.

2.2. Search strategy, screening and study selection

Electronic databases of MEDLINE (via PubMed) and EMBASE were searched for relevant English-language literature up to and including June 2015. Unpublished literature was searched via the Google and Google Scholar search engines. Bibliographies of the studies selected and relevant review articles were checked for cross-references. A specific search strategy was developed for MEDLINE (see the Supplementary material online) and adapted for other databases.

Titles and abstracts of the search-identified studies were screened by two authors (S.S. and A.S.) and full texts of all eligible studies were obtained. Uncertainty in the determination of eligibility was resolved by discussion with the other authors. Two authors (S.S. and A.S.) reviewed the selected full texts independently and final inclusion was based on the aforementioned inclusion criteria. A summary of the screening process is presented in Figure 1.

2.3. Data extraction

Data was extracted from the full texts of selected articles on: author(s), study design, animal species, model type, number of animals/defects, number of procedures, inclusion criteria, observation time(s), outcome(s), method (s) of outcome evaluation, main findings and conclusions. Descriptive summaries of studies included were entered into tables. Quantitative histomorphometric data regarding %NBF was extracted for possible meta-analysis. Standard errors of mean, when reported, were converted

Copyright © 2016 John Wiley & Sons, Ltd.

DOI: 10.1002/term

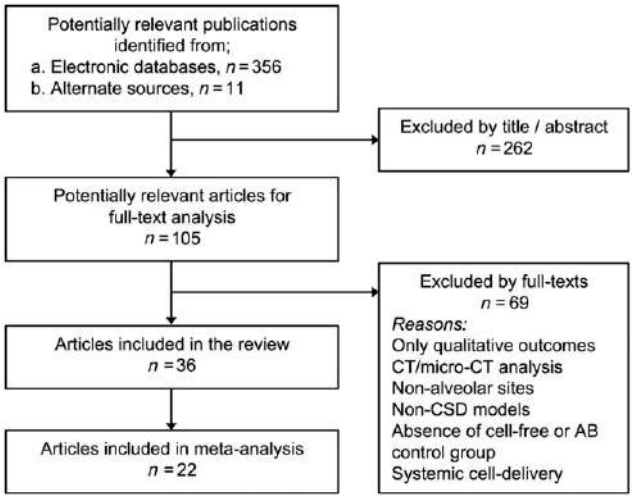

Figure 1. Flowchart for study screening and selection. AB, autogenous bone; CSD, critical-size defect; CT, computed tomography; 'n', number of articles.

to standard deviation (SD) for analysis. If data were only expressed graphically, numerical values were requested from the authors, and if no response was received digital ruler software was used to measure graphical data (ImageJ; National Institutes of Health, Bethesda, MD, USA). When studies reported outcomes at multiple time-points, data from similar time-points of different studies were pooled for meta-analysis.

2.4. Quality assessment and risk of bias

Reporting quality assessment of all studies was performed based on a modification of the ARRIVE (Animal Research: Reporting *In Vivo* Experiments) guidelines, regarding relevant items (Kilkenny *et al*., 2010; Berglundh and Stavropoulos, 2012). Compliance with the guidelines was evaluated using a predefined grading system applied to each of the 20 items (Schwarz *et al*., 2012; Supporting information). Reporting quality was judged as 'high', 'moderate' or 'low'. Risk of bias (RoB) assessment was performed using a modification of SYstematic Review Centre for Laboratory animal Experimentation (SYRCLE) RoB tool for animal studies, and judged as 'high', 'low' or 'unclear' (Hooijmans *et al*., 2014b; Yan *et al*., 2015; see the Supplementary material online). Any disagreement between the reviewers during study selection, data extraction, and quality assessment was resolved by discussion and consensus.

2.5. Meta-analysis

Meta-analysis was performed to compare the effectiveness of cell-loaded [experimental (Ex)] and cell-free [control (Co)] scaffolds using histomorphometric data [means and SD of %NBF and number of animals/defects (n) per group]. Studies were pooled based on homogeneity regarding PICO and observation time. Subgroup analyses were performed at the level of animals and observation time, using the DerSimonian and Laird random effects model (Deeks *et al*., 2008) and STATA Statistical Software (StataCorp LP, College Station, TX, USA). When studies included multiple Ex-groups and one Co-group, the number of animals/defects (n) in the Co-group was divided by the number of Ex-groups (Vesterinen *et al*., 2014). In several studies, the design included multiple interventions per animal (e.g., 'split-mouth' design), for which a correlation coefficient (r) was calculated for between treatment group measurements. The r-value, calculated from one split-mouth study (Haghighat *et al*., 2011) using the p-value provided (Higgins and Deeks, 2008), was close to 0.80 and this was used for the meta-analysis. For parallel group studies, the r-value was set at 0, and thus, both parallel and split-mouth studies were included in the same analysis, if appropriate (Higgins *et al*., 2008). To assess robustness of the findings, sensitivity analyses were performed using r-values of 0.50 and 0.20. Pooled estimates of treatment effect [weighted mean differences (WMD)] were calculated along with 95% confidence interval (CI), and the I^2 statistic was used as a measure of inconsistency of results across studies (Deeks *et al*., 2008).

3. Results

3.1. Search results and study characteristics

Of the 367 search-identified studies, 36 studies reporting quantitative histomorphometric outcomes from 6 different species and 636 animals were included in the review. A list of studies excluded along with reasons for exclusion is reported in the Supplementary material online. Large-animal models included monkeys (one study, n = 24), dogs (14 studies, n = 94), sheep (one study, n = 8) and minipigs (four studies, n = 38) (Table 1). Small-animal models included rabbits (eight studies, n = 179) and rats (eight studies, n = 293) (Table 2). Sample sizes ranged from 2–24 and 9–75 for the large- and small-animal models, respectively. Observation times varied between species: monkeys (6 months), dogs (4 weeks to 12 months), sheep (5 months), minipigs (8–12 weeks), rabbits (4–24 weeks) and rats (4–8 weeks). Nine studies – six in dogs, one in pigs, and one each in rabbits and rats – included a control group receiving autogenous bone.

3.2. Quality assessment and risk of bias

Most studies provided adequate information regarding title, abstract, introduction, study objectives, ethical approval, experimental design and procedures (Figure 2). Information regarding experimental animals, and their housing and husbandry, was generally inadequate; the majority of studies lacked complete information regarding animals' age and gender (Tables 1 and 2). No studies provided information on sample-size calculation or baseline characteristics of the animals. In 19 studies (52.7%), animals or defects were randomly allocated to different treatment groups to minimize 'selection bias', although no

Copyright © 2016 John Wiley & Sons, Ltd.

DOI: 10.1002/term

Table 1. Summary of study characteristics in large-animal models

Study	Strain, age, gender	Defect model, dimensions	*n*	Time	Cells	Source, induction	Cell number	Scaffold, AB if used
Monkeys								
Chanchareonsook *et al*. 2014b	*Macaca fascicularis*, adult male	Mandible SD, 15 mm, length	24	6 months	BMSC	Femur, auto; no	5×10^6	PCL–HA ± BMP-2
Dogs								
De Kok *et al*. 2003	Beagle, adult	Mandible CSD (s), 20 × 6.5 mm	14	4 weeks, 9 weeks	BMSC	Iliac, auto or allo	1×10^6	HAβ–TCP
Yamada *et al*. 2004	Hybrid, adult	Mandible CSD (s), 10× 10 mm	4	8 weeks	BMSC	Iliac, auto; yes	1×10^7/ml	PRP gel, iliac AB
Yoshimi *et al*. 2009	Hybrid, adult	Mandible CSD (s), 10× 10 mm	Unclear	8 weeks	BMSC	Iliac, auto; yes	1×10^7/ml	Peptide ECM ± PRP
Yamada *et al*. 2011	Hybrid, adult	Mandible CSD (s), 10× 10 mm	Unclear	8 weeks	BMSC or DPSC	Iliac, auto; auto or puppy; yes	1×10^7/ml	PRP gel
Jafarian *et al*. 2008	Mongrel, adult	Mandible CSD (s), 10 mm, diameter	4	6 weeks	BMSC	Humerus, auto; no	5×10^5	HAβ–TCP–Col or Bio–Oss–Col®
Vahabi *et al*. 2012	Hybrid, 1 year, male	Mandible CSD (s), 10 mm, diameter	5	8 weeks	BMSC	Iliac, auto; no	5×10^5	HAβ-TCP
Khojasteh *et al*. 2013	Mongrel, adult male	Mandible CSD (s), 20× 10× 10 mm	4	8 weeks	BMSC	Humerus, auto; no	5×10^5	PCL-TCP
Haghighat *et al*. 2011	NR, 3y	Mandible CSD (s), 9 mm, diameter	4	6 weeks	ADSC	Thoracic, auto; no	5×10^6	Collagen
Behnia *et al*. 2014	Mixed, adult male	Mandible CSD (s), 9 mm, diameter	4	12 weeks	SHED	Human; no	1×10^6	Collagen
Zhao *et al*. 2009	Mongrel, adult male	Mandible SD (s), 20× 10 mm	14	12 months	BMSC	Iliac, auto; yes	5×10^7	Silk-polymer ± apatite, mandible AB
Wang *et al*. 2015	Beagle, adult, male	Mandible SD, 30 mm, length	16	12 mo	OB, fresh or cryo	Mandible, auto; yes	2×10^7	β-TCP, mandible AB
Zhang *et al*. 2011	Beagle, 24 weeks, male	Maxilla cleft (s), 10× 5× 15 mm, ortho. Movement	7	20 weeks	BMSC	Iliac, auto; yes	2×10^7	β-TCP, iliac AB
Pourebrahim *et al*. 2013	Mongrel, adult	Maxilla cleft (s) 15 mm, width, 2 months' healing	4	15 days, 60 days	ADSC	Scapula, auto; no	5×10^6	HAβ–TCP (no scaffold only) tibial AB
Huang *et al*. 2015	Beagle, 24 weeks, male	Maxilla cleft, 15 mm, width, RME	14	12 weeks	BMSC	Iliac, auto; yes	Unclear	β-TCP, Iliac AB
Sheep								
Schliephake *et al*. 2001	NR, adult female	Mandible SD, 35 mm, length	8	5 months	OB	Iliac bone, auto; no	$1–5 \times 10^6$	Bovine bone
Minipigs								
Zheng *et al*. 2009	Inbred, 4–6 months, female	Mandible CSD, 25× 15× 15 mm	16	6 months	DPSC	Deciduous, auto; no	4×10^8	β-TCP
Pieri *et al*. 2009	NR, adult	Mandible CSD (s), 3.5× 8 mm	8	3 months	BMSC	Iliac, auto; no	4×10^7	HA-PRP, mandible AB
Konopnicki *et al*. 2015	Yucatan	Mandible CSD (s), 20 × 20 mm	2	8 weeks	BMSC	Iliac, auto; yes	30×10^6	PCL–TCP
Kuo *et al*. 2015	Lanyu, 3 months	Mandible CSD (s), 6 mm, diameter	12	8 weeks	DPSC	Commercial, human; no	2×10^6	α-CSH, α-CSH/ACP or α-CSH/β-TCP

CSD, critical-size defect; SD, segmental defect; (s), split-mouth design; n, number of animals; ortho. Movement, orthodontic tooth movement; RME, rapid maxillary expansion; AB, autogenous bone; BMSC, bone marrow MSC; ADSC, adipose tissue-derived MSC; OB cryo, cryopreserved osteoblasts; DPSC, dental pulp stem cells; SHED, stem cells from human exfoliated deciduous teeth; Auto, autologous; Allo, allogeneic; Human, human-derived; PRP, platelet-rich plasma; HA, hydroxyl-apatite; β-TCP, beta-tricalcium phosphate; Col, collagen; PCL, poly-caprolactone; ECM, extracellular matrix; CSH, calcium sulphate hemihydrate.

details of the randomization procedure were reported. Ten studies (27.7%) reported blinding of outcome assessors to treatment groups, to minimize 'detection bias'. All studies reported detailed outcome evaluation, including statistical analyses, but few reported any information on adverse reactions or complications. Overall, RoB in most studies was judged to be 'unclear' (Figure 3). Information regarding study limitations and implications for translation to human models was limited, and none of the studies referred to the '3R's' principle (replacement, refinement and reduction) for experimental animals (Kilkenny *et al*., 2010).

3.3. Characteristics of animal models

Studies reported the use of CSD more frequently in the mandible (83.3%) than the maxilla. A majority of studies included bilateral CSD or a 'split-mouth' design (55.5%). Dental extraction was commonly performed in large-animal models and adequate healing time allowed before defect preparation. Following general anaesthesia, irrigated trephine drills were used to prepare unilateral or bilateral CSD, most often in the mandibular body or ramus, using either an intra-oral (large animals) or extra-oral (small animals) approach. The CSD ranged from 4 mm in diameter (rats) to 15 mm in length (rabbits) in small animals, and from 6 mm in diameter (pigs) to 20 mm in length (dogs) in large animals. Four studies reported the use of 'segmental' defects in monkeys (15 mm; Chanchareonsook *et al*., 2014b), dogs (20–30 mm; Zhao *et al*., 2009; Wang *et al*., 2015) or sheep (35 mm; Schliephake *et al*., 2001), where a portion of the mandibular body was resected by either disrupting or preserving mandibular continuity. When continuity was disrupted a titanium plate was fixed with screws on either end for stabilization. Three studies reported the repair of experimental maxillary 'clefts' in dogs, with

Copyright © 2016 John Wiley & Sons, Ltd.

DOI: 10.1002/term

Table 2. Summary of study characteristics in small-animal models

Study	Strain, age, gender	Defect model, dimensions	*n*	Time	Cells	Source, induction	Cell number	Scaffold, AB if used
Rabbits								
Jiang *et al*. 2006	NZ, female	Mandible CSD (s), 15 × 6 mm	14	4 weeks	BMSC, BMSC-BMP-4, or BMSC-EGFP	Femur, auto; yes	50×10^6	Porcine bone
Li *et al*. 2010	NZ	Mandible CSD, 12 × 8 mm	54	4, 8, 16 weeks	BMSC, BMSC-BMP-7	Tibia, allo; yes	2×10^6	nHA–PA
Liu *et al*. 2011	NZ, mature female	Mandible CSD, 10 × 4 × 3 mm	36	12 weeks	DPSC	Permanent, allo; yes	1×10^8	nHA–PLA ± BMP-2, Iliac AB
Sun *et al*. 2013	NZ, adult	Mandible CSD (s), 10 × 6 mm	18	4, 8, 12 weeks	POC or POC-BMP-2	Mandible, allo; yes	1×10^7	Bioglass–ceramic
Park *et al*. 2013	NZ	Mandible CSD; 5-week healing, 6 × 4 × 3 mm	9	4 weeks	ABMSC	Mandible, Auto; No	1×10^6	Bio-Oss®
Saad *et al*. 2015	NZ, adult male	Mandible CSD, 15 × 10 mm	16	4, 12, 24 weeks	BMSC	Femur, auto; no	$5–7 \times 10^6$	β-TCP
Su *et al*. 2015	NZ, male	Mandible CSD, 10 × 5 × 4 mm	20	12 weeks	PDLSC or PDLSC-OPG	Impacted, allo; no	5×10^6	β-TCP
Wei *et al*. 2015	NZ, male	Mandible CSD (s), 8 mm, diameter	12	4 weeks, 12 weeks	ADSC	Inguinal pad, auto; no	1.5×10^6	Antler cancellous bone
Rats								
Arosarena *et al*. 2003	Fischer, male	Mandible CSD, 4 mm, diameter	37	8 weeks	BMSC	Femur, allo; no	1×10^7	HA–collagen ± BMP-3, TGFβ-2
Jiang *et al*. 2009	Fischer, 12 weeks male	Mandible CSD, 5 mm, diameter	24	8 weeks	BMSC, BMSC-BMP-2, or BMSC-LacZ	Femur, allo; yes	2×10^7	HA–Silk polymer
Schliephake *et al*. 2009	Athymic nude, 5–7 weeks	Mandible CSD (s), 5 mm, diameter	30	6 weeks	OB	Femur, Human; No	5×10^6	Biocoral®, HA-Collagen or TCP
Zhao *et al*. 2010	Fischer, 6 weeks male	Mandible CSD (s), 5 mm, diameter	11	8 weeks	BMSC, BMSC-BMP-2, or BMSC-EGFP	Femur, allo; yes	2×10^7	β-TCP
Mohammadi & Amini 2015	Wistar, male	Mandible CSD, 4 mm, diameter	75	1, 2, 3, 4 weeks	ADSC (SVF)	Omentum, allo; no	2×10^7	Chitosan
Raposo-Amaral *et al*. 2014	Wistar, adult male	Maxilla CSD, 5 mm, diameter	28	8 weeks	MMSC	Muscle, human; no	1×10^6	Bio-Oss-Col® or α-TCP, calvarial AB
Jiawen *et al*. 2014	Sprague–Dawley, 6–8 weeks	Maxilla CSD, 4 × 4 × 3 mm	16	4 weeks, 8 weeks	AESC	Amnion, human; no	$2–3 \times 10^8$	β-TCP
Korn *et al*. 2014	Lewis, female	Maxilla CSD, 3 mm, diameter	72	1, 3, 6 weeks	BMSC, induced or non-induced	Femur, allo; yes	5×10^4	HAβ–TCP–Silica

CSD, critical-size defect; (s), split-mouth design; *n*, number of animals; AB, autogenous bone; NZ, New Zealand; BMSC, bone marrow MSC; BMSC-BMP-4/7/2, bone morphogenetic protein-4/7/2-modified BMSC; EGFP, enhanced green fluorescent protein; DPSC, dental pulp stem cells; POC, periosteal stem cells; PDLSC, periodontal ligament stem cells; LacZ, beta-galactosidase; ADSC, adipose tissue-derived MSC; SVF, stromal vascular fraction; MMSC, muscle-derived MSC; AESC, amniotic epithelial stem cells; Auto, autologous; Allo, allogeneic; Human, human-derived; HA, hydroxyl-apatite; nHA, nano-HA; β-TCP, beta-tricalcium phosphate; TGFβ-2, transforming growth factor beta-2; Col, collagen.

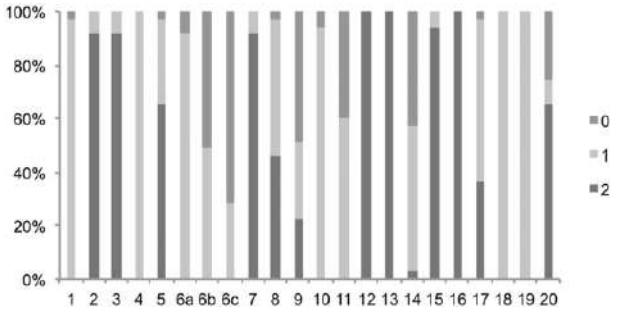

Figure 2. Frequency distribution (%) of the scores assessed for each item of the modified ARRIVE guidelines in all studies included. Items 2, 3, 5, 7–10, 12, 13 and 15–20 were scored 0, 1 or 2 (clearly inadequate, possibly adequate or clearly adequate). All other items scored 0 or 1 (no or yes).

(Zhang *et al*., 2011; Huang *et al*., 2015) or without (Pourebrahim *et al*., 2013) additional orthodontic procedures.

3.4. Characteristics of tissue engineering strategies

3.4.1. Cells

All but four studies in large-animal models reported the use of autologous cells; two studies reported either the use of allogeneic adult (De Kok *et al*., 2003) or puppy-derived cells (Yamada *et al*., 2011) in dogs and two studies reported the use of human dental-derived cells [dental pulp stem cells (DPSCs) or stem cells from human exfoliated deciduous teeth (SHED)] in dogs (Behnia *et al*., 2014) or minipigs (Kuo *et al*., 2015). Among the small-animal models, nine studies reported the use of allogeneic cells, including DPSCs (Liu *et al*., 2011), periosteal- (Sun *et al*., 2013) or periodontal-ligament-derived stem cells (PDLSCs) (Su *et al*., 2015). Three studies reported implantation of human bone-, amnion- or muscle-derived

Copyright © 2016 John Wiley & Sons, Ltd.

DOI: 10.1002/term

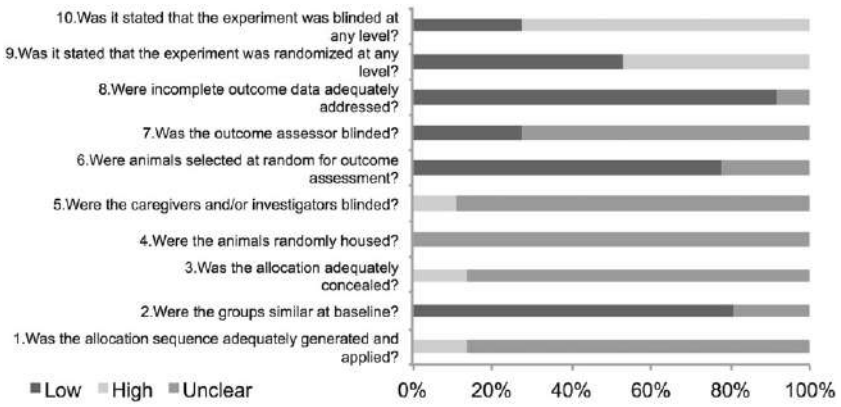

Figure 3. Frequency distribution (%) of the risk of bias assessment for each item of the modified SYRCLE RoB tool in all studies included. Items 1–8 were judged as 'yes', 'no', or 'unclear'; items 9 and 10 were judged as 'yes' or 'no' (risk of bias; yes = low, no = high, unclear = unclear). Item 6 was always judged as 'yes' if all animals in both test and control groups were analysed at the same time-point.

cells in rats (Schliephake *et al*., 2009; Jiawen *et al*., 2014; Raposo-Amaral *et al*., 2014). No immunological reactions were reported in studies using allogeneic or human-derived cells, in either immunosuppressed or immunocompetent animals.

Most studies (55.5%) reported the use of bone marrow MSC; three studies used osteoblasts. Other MSC sources included dental pulp, alveolar bone and adipose tissue. Mesenchymal stem cells were used in early (1–6) passages, with (15 studies) or without osteogenic preinduction. One study compared the efficacy of osteogenically differentiated and undifferentiated MSCs in rats alveolar clefts: a trend towards superior regeneration with undifferentiated cells was observed (Korn *et al*., 2014). Primary cell cultures were expanded *ex vivo*; seeding densities ranged from 1×10^4 to 4×10^8 cells per scaffold. Cells were cultured on scaffolds for a specified period (range 30 min to 2 weeks), in basal or osteogenic media, before implantation.

Six studies reported the use of 'gene-modified' cells in rabbits or rats; cells were altered via viral vector-mediated gene transfer of osteogenic growth factors [bone morphogenetic proteins (BMPs)] (Jiang *et al*., 2006, 2009; Li *et al*., 2010; Zhao *et al*., 2010; Sun *et al*., 2013) or osteoclast inhibitors [osteoprotegerin (OPG)] (Su *et al*., 2015). Control groups in these studies included 'reporter' gene-modified cells [cells infected with adenovirus expressing enhanced green fluorescent protein (EGFP) (Jiang *et al*., 2006; Zhao *et al*., 2010) or β-galactosidase (LacZ) (Jiang *et al*., 2009)], unmodified cells and/or scaffold-only groups.

3.4.2. Scaffolds

A majority of studies (58.3%) reported the use of mineral-phase alloplastic [hydroxyapatite (HA), alpha−/beta-tricalcium-phosphate (α−/β-TCP), bioglass or coral] or xenogeneic (bovine, porcine or antler bone) scaffolds, used in the block, disc or particulate form. Five studies reported the use of non-mineral-phase scaffolds [platelet-rich plasma (PRP), polypeptides or collagen]. Seven studies reported the use of composite scaffolds, composed of a mineral- and non-mineral [(co)polymer] phase. Five studies reported the addition of growth factors [BMP-2, BMP-3 or transforming growth factor-β2 (TGF-β2)] known to stimulate osteogenesis, to the scaffolds in at least one experimental group. However, for the sake of homogeneity with regard to the property of 'defect-space maintenance', and to minimize any confounding influence of growth factors, only studies reporting mineral-phase, polymeric or composite scaffolds, without additional growth factors, were considered for the meta-analysis.

3.5. Meta-analysis

Twenty-two studies reporting histomorphometric data of cell-loaded vs. cell-free scaffolds in dogs (CSD or segmental defects), minipigs, rabbits (at 4 or 12 weeks) and rats (mandibular or maxillary CSD) were included in the meta-analysis (Figure 4). Separate analyses were performed for three studies in rabbits and two in rats, comparing BMP-gene-modified and 'unmodified' cell-groups (Figure 5), and in two studies in dogs comparing cell-loaded scaffolds and autogenous bone (Figure 6). As there were fewer than 10 studies in each meta-analysis, publication bias via funnel plots or statistical testing was not assessed because of the lack of power to distinguish chance from real asymmetry (Sterne *et al*., 2008).

Overall, the meta-analyses revealed three main findings: (1) a statistically significant effect in favour of cell-loaded vs. cell-free scaffolds [pooled estimate (WMD) range: 15.59–49.15% and 8.60–13.85% NBF in large- and small-animal models, respectively]; (2) a statistically significant effect in favour of BMP gene-modified cells vs. unmodified or EGFP/LacZ-modified cells (WMD range: 10.06–20.83% NBF in small-animal models); and (3) a marginally significant effect in favour of autogenous bone vs. cell-loaded scaffolds (WMD: 4.05% NBF in dogs). Heterogeneity in most cases was very high ($I^2 > 90\%$, $p < 0.05$). Robustness of findings of the meta-analysis, were confirmed by observation of similar 95% CI values in the sensitivity analyses, which excluded 0 for all comparisons except cell-loaded scaffolds vs. autogenous bone. Pooled WMD with 95% CI

Copyright © 2016 John Wiley & Sons, Ltd.

DOI: 10.1002/term

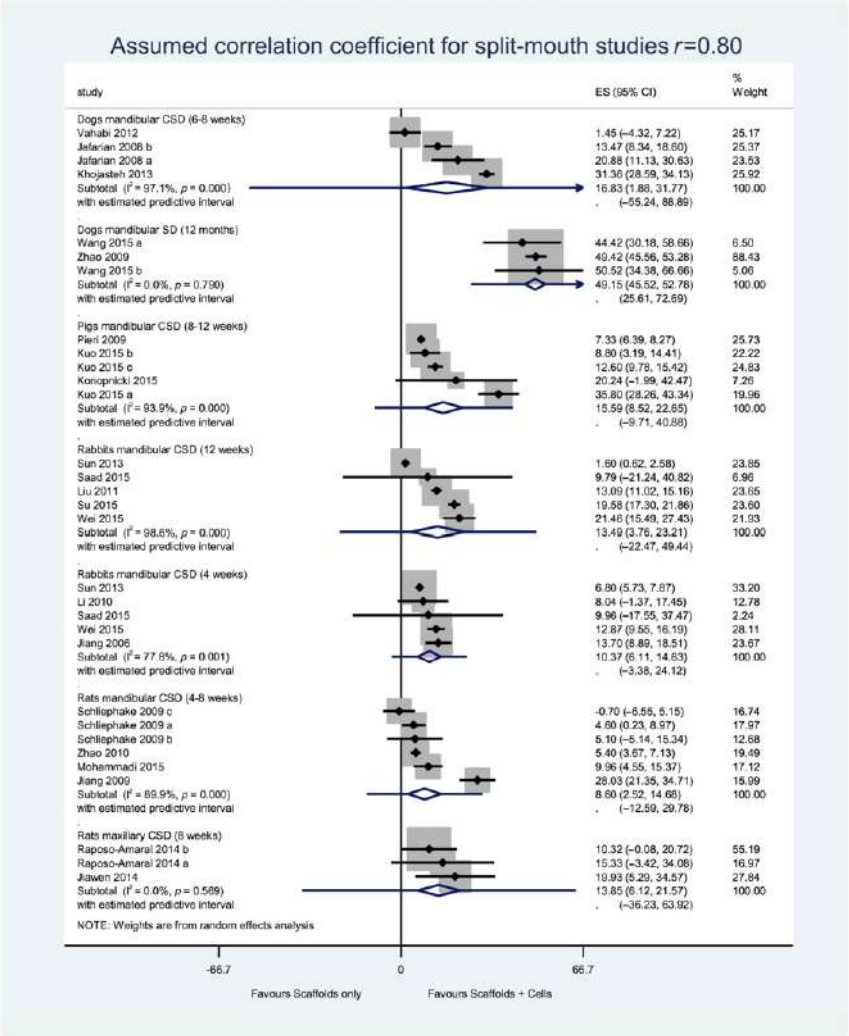

Figure 4. Forest plot for the comparison cell-loaded vs. cell-free scaffolds. The forest plot displays relative weight of the individual studies, the estimates of treatment effect (ES) expressed as weighted mean differences (WMD), 95% confidence intervals (CI) and a predictive interval, for the outcome percentage of new bone formation (%NBF). A diamond indicates the pooled estimate and its 95% CI. SD, segmental defect; CSD, critical-size defect. References on the left give first author and year. The letters a, b, and c represent different comparison groups within the same study.

and measures of heterogeneity for each of the subgroups are presented in the Supplementary material online, along with an example for interpretation.

4. Discussion

The aim of the present study was to systematically review the preclinical *in vivo* evidence for cell-based bone tissue engineering (BTE) strategies for alveolar bone regeneration. Systematic reviews and meta-analyses of animal studies can be useful for guiding the design of future clinical trials, detecting heterogeneity between studies and treatment effects, and improving the methodological quality of future studies (Hooijmans *et al*., 2014a). Recent systematic reviews of animal studies have reported favourable effects of BTE approaches for skeletal (Liao *et al*., 2014) and periodontal regeneration (Bright *et al*., 2015; Yan *et al*., 2015). Similar findings have been reported in systematic reviews of human clinical trials evaluating the effectiveness of BTE approaches for alveolar bone regeneration (Padial-Molina *et al*., 2015; Shanbhag and Shanbhag, 2015). However, because of the large variation in the methodology of studies, especially with regard to the nature of cells and biomaterial scaffolds used, no conclusive statements regarding the effectiveness of BTE exist in the literature. In addition, concerns regarding ethical aspects and cost-effectiveness have limited large-scale clinical application of BTE, and a need for further, more standardized, preclinical research on this topic has been highlighted (Cancedda *et al*., 2007).

Guidelines for designing preclinical animal models in BTE have been proposed; the model should: (1) simulate the target clinical and biological environment; (2) allow the use of quantifiable parameters to evaluate success and functional performance of regenerated tissues; and (3) allow detection of clinically relevant differences in biological performance between the regenerative therapies assessed (Muschler *et al*., 2010). The wide variation in bone anatomy, composition, biomechanics, size and biology between and within

Copyright © 2016 John Wiley & Sons, Ltd.

DOI: 10.1002/term

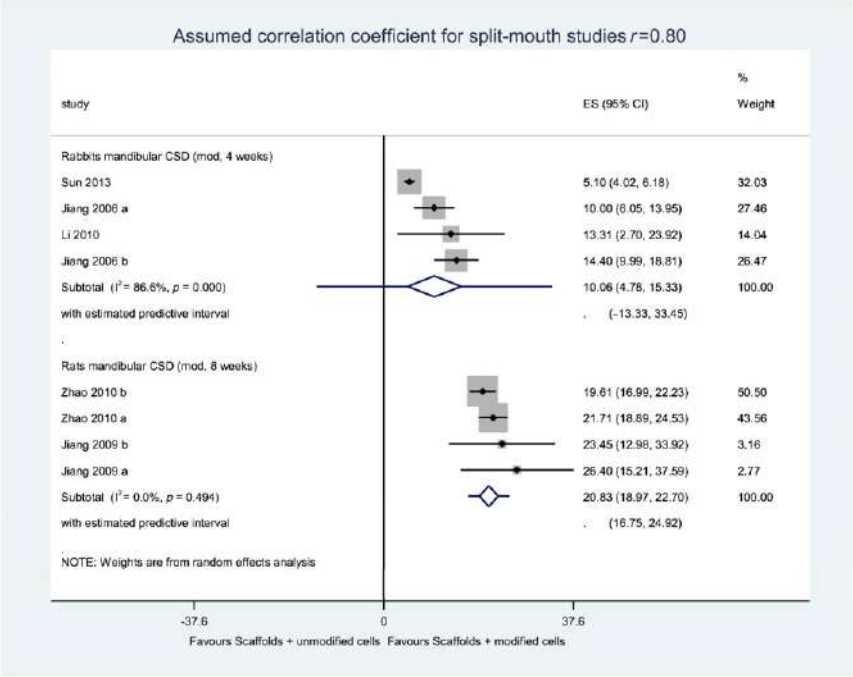

Figure 5. Forest plot for the comparison bone morphogenetic protein (BMP)-modified vs. unmodified cells. The forest plot displays relative weight of the individual studies, the estimates of treatment effect (ES) expressed as weighted mean differences (WMD), 95% confidence intervals (CI) and a predictive interval, for the outcome percentage of new bone formation (%NBF). A diamond indicates the pooled estimate and its 95% CI. CSD, critical-size defect. References on the left give first author and year. The letters a, b, and c represent different comparison groups within the same study.

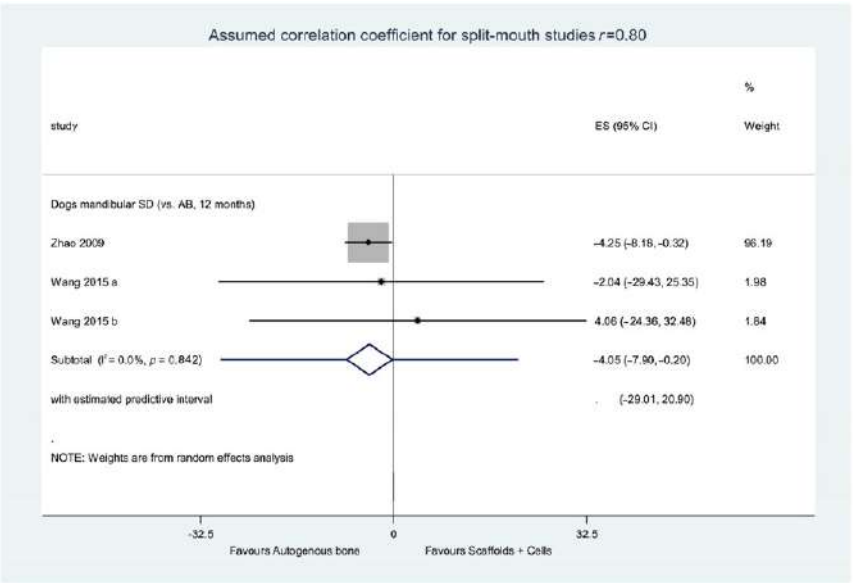

Figure 6. Forest plot for the comparison cell-loaded scaffolds vs. autogenous bone. The forest plot displays relative weight of the individual studies, the estimates of treatment effect (ES) expressed as weighted mean differences (WMD), 95% confidence intervals (CI) and a predictive interval, for the outcome percentage of new bone formation (%NBF). The diamond indicates the pooled estimate and its 95% CI. SD, segmental defect. References on the left give first author and year. The letters a, b, and c represent different comparison groups within the same study.

species, and in comparison with humans, often complicates translationability of the results in animal models. Generally, small-animal models constitute a starting point for proof-of-principle or feasibility studies before 'clinical modelling' and efficacy testing in larger animals (Pellegrini *et al.*, 2009; Li *et al.*, 2015). Therefore, the results herein are discussed in the context of small- and large-animal models.

4.1. Small-animal models

Small-animal models used in musculoskeletal research include primarily two species, rodents (rats or mice) and rabbits (O'Loughlin, 2008). Rodent models are often preferred over larger animals because of the significantly lower costs, easier housing and handling, and minimal social concern (Gomes and Fernandes, 2011). Rodents

Copyright © 2016 John Wiley & Sons, Ltd.

DOI: 10.1002/term

also have a well-defined and controlled genetic background, with less variation among individual animals in terms of biological response, which implies that fewer experimental units may be required to achieve statistically valid data, compared with larger animals (Stavropoulos *et al*., 2015). Rabbits, like rodents, provide advantages of small size and easy handling. Additional advantages include the achievement of skeletal maturity by 6 months of age and larger volumes of mandibular bone tissue, which allow the creation of more reliable CSD than in rodents (Stübinger and Dard, 2013).

In the present meta-analysis, a statistically significant effect in favour of cell-based approaches was observed in rats' maxillary and mandibular CSD after 4–8 weeks, and in rabbits' mandibular CSD after 4 weeks and 12 weeks. However, the significant differences in structure, composition and physiology of rodent, rabbit and human bone (e.g. trabecular content, metabolic rate, remodelling, etc.) must be considered when extrapolating results from these studies (Pearce *et al*., 2007).

4.2. Large-animal models

Advantages of large-animal models include the ability to easily create multiple CSD with clinically relevant dimensions (i.e. both Ex- and Co-groups within the same jaw of the animal), thus limiting inter-animal variation and the number of animals needed. Further, large-animal models allow longer observation times; for example, the longest observation time in the present review (12 months) was in studies involving canine segmental CSD. Biopsies of the regenerated sites can be obtained at the end of observation periods without the need for euthanasia (Pourebrahim *et al*., 2013; Behnia *et al*., 2014), which is consistent with the '3R's' principle (Russel and Burch, 1959). Importantly, for BTE research, large-animal models allow preparation of defects with clinically relevant diffusion distances, so that the influence of mass transport, hypoxia and vascularization on the survival of transplanted cells can be evaluated in a simulated clinical setting (Muschler *et al*., 2010).

A majority of studies (55.5%) included in the present review reported data from large-animal models (i.e., monkeys, dogs, sheep and minipigs); data from dogs and minipigs were included in the meta-analysis. Dogs and pigs are widely used animal platforms in musculoskeletal research, given the similarities in structure, composition and physiology between canine/porcine and human bone (Aerssens *et al*., 1998). Although some differences in the bone remodelling process do exist between the three species, both canine and porcine models are considered to be highly relevant: the rate of remodelling in pigs (1.2–1.5 μm/day) is comparable to that in humans (1.0–1.5 μm/day) but slower than that in dogs (1.5–2.0 μm/day) (Pearce *et al*., 2007). However, limitations of large animals include high costs, ethical issues in the case of dogs, and handling difficulty in the case of pigs. In context, minipigs represent a more suitable model because of more morphological similarities to human bone than other large-animal models (Mardas *et al*., 2014).

In the present meta-analysis, significantly greater bone regeneration was observed in favour of cell-based vs. cell-free approaches in mandibular CSD of dogs and minipigs. A similar result was reported in one study of sheep mandibular defects (Schliephake *et al*., 2001). Another recent study in sheep, which was excluded from the present analysis because of the use of uncultured autologous bone marrow (BM; see the Supplementary material online), also reported greater regeneration in mandibular defects augmented with BM-TCP vs. TCP-blood constructs; this was attributed to the possible 'osteopromotive' effects of MSC within the BM (Russmueller *et al*., 2015). These results are in agreement with a recent meta-analysis of the effectiveness of stem cell therapy for histological bone regeneration in all anatomical skeletal defects of large-animal models (Liao *et al*., 2014).

Non-human primates are considered the closest experimental model to humans, given their anatomical and biological similarities (Muschler *et al*., 2010). Only one study included herein used a mandibular segmental defect model in monkeys and found no significant benefit of autologous MSC-loaded polycaprolactone (PCL) scaffolds, over BMP-2-loaded PCL or PCL scaffolds alone, after 6 months of healing (Chanchareonsook *et al*., 2014b). However, previous studies, which were not included in the present review because they reported only qualitative outcomes (see the Supplementary material online), have observed superior regeneration, and even complete 'bridging', of mandibular segmental defects in monkeys following implantation of autologous bone marrow/BMSC-loaded PLGA or collagen scaffolds impregnated with BMP-2, compared with implantation of only BMSC- or BMP-2-loaded scaffolds (Seto *et al*., 2001, 2006). The combined delivery of osteogenic (BMSC) and osteoinductive (BMP-2) agents may have contributed to superior outcomes in the latter studies. Moreover, the choice of scaffold and its biological (osteoconductivity) and mechanical (load-bearing) properties, and cell–scaffold interactions are critical for the regenerative outcome.

4.3. Use of gene-modified cells

Five studies reported *ex vivo* gene transfer of BMP-2, −4 or −7 into cells via adenoviral vectors before implantation. The BMPs are osteoinductive growth factors that have been well established to regenerate CSD *in vivo* (Khojasteh *et al*., 2013). Gene transfer is a method by which growth factors can be introduced, either directly or via cells, into defect sites to enhance *in vivo* bone regeneration (Kofron and Laurencin, 2006). Gene transfer into cells is usually performed using viral or non-viral (e.g. liposomes) vectors. In the present meta-analysis, a significant effect in favour of BMP (viral-mediated)

Copyright © 2016 John Wiley & Sons, Ltd.

DOI: 10.1002/term

gene-modified cell groups over unmodified and control (EGFP/LacZ) gene-modified cell groups was observed in rabbit and rat mandibular CSD. Similarly, in one study, OPG-modified PDLSC enhanced regeneration compared with unmodified PDLSC in rabbits; OPG, also known as osteoclastogenesis inhibitory factor (OCIF), is an inhibitor of osteoclast differentiation and function (Su *et al*., 2015).

Implantation of gene-modified MSC has also been evaluated in studies of alveolar CSD, which were not included in the present analysis because they reported only qualitative outcomes (see the Supplementary material online). Use of BMP-2 gene-modified MSC has been reported in minipigs (Chang *et al*., 2003), mice (human BMSC; see the Supplementary material online, Steinhardt *et al*., 2008), and in normal (Park *et al*., 2003) and osteoporotic rats (Tang *et al*., 2008). In one of these studies, superior regeneration with BMSC modified by viral-mediated vs. liposome-mediated BMP-2 gene transfer, was observed (Park *et al*., 2003). Other studies that were excluded reported gene transfer of osteoinductive factors such as LIM mineralization protein-3 (LMP-3) to dermal fibroblasts in rats (see the Supplementary material online: Lattanzi *et al*., 2008; Parrilla *et al*., 2010), and basic fibroblast growth factor (bFGF) to BMSC in rabbits (see the Supplementary material online: Yang *et al*., 2013). Gene-mediated suppression of osteo-inhibitory factors, e.g., *noggin*-suppression in adipose MSC (*noggin* is an inhibitor of BMP-signalling), was also reported (see the Supplementary material online, Fan *et al*., 2014). All the above studies consistently reported superior bone regeneration in gene-modified vs. unmodified and/or control (EGFP/LacZ) gene-modified cell-groups, in small- and large-animal models (see the Supporting information online).

4.4. Tissue-engineered vs. autogenous bone

Among the studies involving large-animal models, only one study (Pourebrahim *et al*., 2013) reported significantly greater regeneration with autogenous bone compared with MSC/HA–β-TCP constructs, in a canine alveolar cleft defect; all other studies reported no significant differences between cell/scaffold constructs or autogenous bone in CSD or cleft defects. For canine segmental defects, a marginally significant effect in favour of autogenous bone was observed in the meta-analysis, but disappeared in the sensitivity analyses, suggesting insufficient evidence to detect true differences between the groups (Hooijmans *et al*., 2014a). In smaller animals, one study in rabbits reported significantly greater regeneration with autogenous bone compared with DPSC/nano-HA–PLA constructs (Liu *et al*., 2011), while another study in rats reported no significant differences between AB and MSC/α-TCP or HA constructs (Raposo-Amaral *et al*., 2014). In summary, the current evidence seems to indicate that tissue-engineered constructs may result in comparable alveolar bone regeneration with what is achieved with the 'gold standard' autogenous bone; however, the evidence is limited and thus it should be considered inconclusive regarding the effectiveness of this approach.

4.5. Implantation of human-derived cells in experimental animals

Three studies reported implantation of human muscle- (Raposo-Amaral *et al*., 2014), amnion- (Jiawen *et al*., 2014) or femoral bone-derived cells (Schliephake *et al*., 2009) in either immunocompetent or immunosuppressed rats, with no remarkable inflammatory or immunological reactions. In one study, an 'immunomodulatory' effect of amnion-derived cells was observed when implanted with β-TCP scaffolds in immunocompetent rats, via suppression of the physiological host response and milder macrophage infiltration, compared with cell-free scaffolds (Jiawen *et al*., 2014). Interestingly, two studies reported implantation of SHED or DPSC in large animals – dogs (Behnia *et al*., 2014) and minipigs (Kuo *et al*., 2015) – without adverse reactions. Similar results were reported in other studies of alveolar CSD (not included in the present review because they reported only qualitative outcomes; see the Supplementary material online), following implantation of human-derived cells in minipigs (placenta-MSCs; Lee *et al*., 2010), rabbits (adipose-MSCs; see the Supplementary material online, Linero and Chaparro, 2014), rats (adipose-MSCs; see the Supplementary material online, Streckbein *et al*., 2013; and gingiva-MSC; see the Supplementary material online, Wang *et al*., 2011), and mice (maxillofacial-BMSCs; see the Supplementary material online, Steinhardt *et al*., 2008). These data are consistent with previous reports of uneventful implantation of human MSC in CSD of non-immunosuppressed animals (de Mendonça Costa *et al*., 2008; Bueno *et al*., 2009; Daei-Farshbaf *et al*., 2014).

The biocompatibility of MSC within and across species can be attributed to their hypoimmunogenic, immunomodulatory and anti-inflammatory properties. Mesenchymal stem cells are reported to exert these effects via three broad mechanisms: (1) their lack or limited expression of major histocompatibility complex (MHC)-I and MHC-II molecules; (2) via direct and indirect modulation of T-cell responses; and (3) secretion of various anti-inflammatory cytokines, making them a promising resource for allogeneic transplantation in regenerative therapies (De Kok *et al*., 2003; Ryan *et al*., 2005). A recent randomized controlled trial reported favourable 2-year outcomes and no adverse reactions in patients after transplantation of allogeneic BMSCs for knee meniscus regeneration (Vangsness *et al*., 2014).

4.6. Meta-analysis and heterogeneity

A random effects model was chosen for the present meta-analysis to account for the expected between-study variance (Hooijmans *et al*., 2014a). The distribution of effect sizes was provided by WMD and measures of I^2. The

Copyright © 2016 John Wiley & Sons, Ltd.

DOI: 10.1002/term

I^2-value is a measure of 'true' inconsistency between the study results, owing to between-study differences and not simply chance (Hooijmans *et al*., 2014a), and was found to be very high within most categories in the meta-analyses. A large heterogeneity may have questioned the validity of the results, if the direction of the effects varied greatly, as was not the case in the present meta-analyses. This heterogeneity could be due to biological factors related to the animals and/or methodological differences between the studies. Biological factors may include the animals' species, gender, age, immunological status, etc., while methodological differences in the study design (e.g. sample sizes, randomization), nature of interventions (e.g. use of autologous vs. allogeneic or human cells, osteogenic induction of cells before implantation), and outcome evaluation (e.g. methods of bone histomorphometry) could possibly explain the large heterogeneity observed in the meta-analyses.

All attempts were made to minimize heterogeneity when performing the meta-analyses. Care was taken to pool only those studies with similar characteristics in terms of PICO, observation times, nature of experimental models and interventions (e.g. type of scaffold used). Subgroup analyses were performed for each animal model. Although sample sizes were generally small and sample size calculation was never reported, the majority of studies involved split-mouth designs, which is a more efficient design in terms of sample size. Split-mouth and 'parallel group' studies were combined using recommended statistical methods (Higgins *et al*., 2008; Smaïl-Faugeron *et al*., 2014), thus increasing the overall power to detect treatment effects. It should be noted that sample size has an impact only on the precision of the estimates and heterogeneity during the synthesis. Baseline differences are not applicable and are irrelevant in terms of bias in split-mouth designs. Finally, comparisons of gene-modified cell groups were evaluated separately from those of 'unmodified' cell-groups, to avoid the influence of confounders (BMP gene-transfer) on the outcomes.

4.7. Outcome measures

Histomorphometry is considered the 'gold standard' method for evaluation of bone structure (Vidal *et al*., 2012; Rentsch *et al*., 2014). All studies included in the meta-analysis reported relatively consistent methods for calculating the main parameter of interest (i.e. %NBF), which is calculated as the percentage of newly formed bone tissue relative to the total defect space (i.e. area or volume). A majority of studies (66.7%) reported decalcified paraffin-embedded preparation of samples for histology. Microscopic images of central sections (three, on average) were analysed by computerized software for quantitative estimation of new bone and residual graft material. No remarkable variation in terms of bone regeneration should be expected among studies because of the method of histological analysis (decalcified or non-decalcified); in a recent report, similar relative amounts of calcified tissue components within augmented periodontal intrabony defects were calculated from decalcified and non-decalcified histological sections (Park *et al*., 2015). However, variation in the studies regarding processing methods (e.g. section thickness, number of sections analysed per implant, software used for analysis, etc.; Chappard *et al*., 1999; Kopp *et al*., 2012; Stewart *et al*., 2013), difficulty in differentiating between mineralized scaffolds and regenerated mineralized bone (Schliephake *et al*., 2009) and investigator-related factors (e.g. inter-observer/intra-method variation, lack of blinding, etc.; Wright *et al*., 1992), may have introduced heterogeneity in the meta-analysis.

Conventional histomorphometry is considered to be destructive, time-consuming and limited to two-dimensional assessment of tissue sections; a third dimension can be added on the basis of stereology (Müller *et al*., 1998). Recently, micro-computed tomography (micro-CT) has been proposed as an alternative method for assessing three-dimensional bone microarchitecture with high resolution and accuracy, in a fast and non-destructive manner. Several studies have reported high correlation between micro-CT and histomorphometry (Müller *et al*., 1998; Thomsen *et al*., 2005; Vandeweghe *et al*., 2013). For this reason, 11 studies reporting quantitative micro-CT-based or CT-based outcomes were also considered in the present review (see the Supplementary material online). Although a wide variation was observed in the parameters evaluated, a majority of studies (63.6%) reported significantly greater regeneration in defects implanted with cell–scaffold constructs compared with scaffolds alone. Moreover, in three studies, no significant differences in regeneration were observed between cell–scaffold constructs and autogenous bone. However, care should be taken when interpreting outcomes of CT or micro-CT because of the difficulties in differentiating between mineralized scaffolds and newly formed bone.

4.8. Experimental models

Unlike calvarial CSD, alveolar CSD models have not been well characterized in the literature in terms of defect location, size and morphology. Defect dimensions varied between studies for the same animal model/species, and, in many cases, selection of a particular model appeared to be based on one previously established by the same, or related, research group(s). Only 16 studies reported inclusion of an 'empty' or untreated control group to determine whether the defects were truly of critical size, as demonstrated by minimal or no bone formation at the end of the observation period, although many studies based their CSD models on previous reports. To place this in context, even a very small size of defect would be of critical size, provided that the experiment is of short enough duration; meaningful results regarding the ability of an intervention to enhance bone formation

Copyright © 2016 John Wiley & Sons, Ltd.

DOI: 10.1002/term

can be produced only if the defects have relevant dimensions. A relatively large variation in the location, size and morphology of alveolar CSD was observed within and between animal models, which could likely have also contributed to heterogeneity in the present meta-analysis. Indeed previous studies have highlighted the influence of alveolar CSD characteristics, such as defect site(s) (e.g. 'marrow-rich' vs. 'marrow-poor' sites; Guo *et al*., 2012), preservation or removal of bony cortices (e.g. 'partial-thickness' vs. 'full-thickness' defects; Young *et al*., 2008) and preservation vs. removal of the periosteum (Huh *et al.*, 2005; Ma *et al*., 2009) on regenerative outcomes.

The results of the present review can also be discussed in light of CSD models in other skeletal sites, more frequently reported in the orthopaedic literature. These commonly include CSD in the tibiae or femur of small animals, or more extensive CSD in the long bones of larger animals (Li *et al*., 2015). A recent study reviewed various large-animal defect models, mostly in the extremities (tibial, radial, ulnar and femoral) for cell-based BTE (Liao *et al*., 2014). The meta-analysis identified: (1) a significant effect in favour of cell-based vs. other therapies for histological new bone formation (WMD 17.79%, 95% CI 10.54, 25.03, I^2 99%); (2) a superior effect of cells in combination with matrix scaffolds vs. direct cell injection; and (3) no variation in effects based on the type of animal or cells, such as BMSC vs. other cell types (Liao *et al*., 2014).

4.9. Quality of reporting

The reliability of results of meta-analyses directly depends on the quality of the primary studies (Hooijmans *et al*., 2014a). The overall methodological quality of the studies included, as assessed by compliance with the ARRIVE guidelines (Kilkenny *et al*., 2010), was found to be moderate. The ARRIVE guidelines have been developed to improve the reporting quality of animal studies and have been widely used for assessment of preclinical research in implant dentistry (Berglundh and Stavropoulos, 2012). Moreover, the SYRCLE tool, which addresses particular aspects of bias that play a role in animal experimental studies, was also utilized (Hooijmans *et al*., 2014b). Nevertheless, a clear need for more standardized reporting of animal studies was identified herein, to allow reliable future reproduction and synthesis.

4.10. Clinical relevance

Clinical meta-analyses aim to obtain a combined estimate or size of treatment effect, while preclinical meta-analyses aim to summarize the effect of an intervention, where the direction rather than size is meaningful, because of the large inherent variations in animal studies (Hooijmans *et al*., 2014a; Vesterinen *et al*., 2014). Thus, although numerical values from the present meta-analysis should not be directly translated to the human situation, it can be inferred that a similar response, or direction of treatment effect, could also be expected in humans (Stavropoulos *et al*., 2015). For example, the ~17% additional bone regeneration observed in dogs' mandibular CSD augmented with cell-loaded biomaterial scaffolds compared with scaffolds alone, would not translate to 17% (or '*x*-times' 17%) more bone, if the same procedure was performed in humans. Other inherent limitations of animal models that must be considered, are: (1) underestimation of clinical variation, with regard to both local (defect size, morphology, mass transfer, etc.) and systemic (age, co-morbidities, etc.) biological environments; and (2) overestimation of clinical performance, especially in the context of CSD, where uniform defects are surgically created most often in healthy animals with sound surrounding tissues and generally uncompromised blood supply, which is often not the case in clinical scenarios (Faggion *et al*., 2010; Muschler *et al*., 2010). In perspective, meta-analyses of animal studies tend to be exploratory rather than confirmatory. Standardization of alveolar CSD models to better represent the clinical scenario and standardization of study reporting should be important considerations in future studies of alveolar BTE.

Several reviews of clinical BTE strategies in humans have recently been published (Chanchareonsook *et al*., 2014a; Gamie *et al*., 2014; Gothard *et al*., 2014; Shanbhag and Shanbhag, 2015; Roux *et al*., 2015). Overall, the findings suggest that BTE, especially cell-based, approaches have shown promising clinical results with minimal adverse reactions in orthopaedic and maxillofacial applications. However, the evidence is based on few controlled studies, usually with small sample-sizes and short observation times. Large heterogeneity between studies regarding the nature of BTE approaches in terms of the cells, scaffolds and/or growth factors used, and *in vitro* processing methods, limit the drawing of reliable conclusions. Long-term evaluations of the safety of cell therapy appear to be lacking (Lalu *et al*., 2012). Notably, adverse effects have been reported following clinical use of recombinant human BMP (Carreira *et al*., 2014). Finally, further research is needed to evaluate: (1) the safety and efficacy of allogeneic 'off-the-shelf' cell-based products; (2) strategies to enhance vascularization of constructs, especially in large defects; (3) optimization of the *ex vivo* expansion process and it's duration; and (4) the cost-effectiveness of cell-based therapy, to facilitate clinical translation.

5. Conclusions

The pre-clinical *in vivo* evidence reviewed can be summarized as follows:

1. Based on results of both small- and large-animal models, the addition of osteogenic cells (MSCs or OB) to biomaterial scaffolds can enhance histomorphometric alveolar bone regeneration.

Copyright © 2016 John Wiley & Sons, Ltd.

DOI: 10.1002/term

2. Based on results of small-animal models, *ex vivo* BMP gene-transfer to MSCs and OB can enhance their *in vivo* osteogenic potential.
3. Limited evidence suggests that tissue-engineered constructs may result in comparable alveolar bone regeneration with what is achieved with the 'gold standard' (i.e. autogenous bone).
4. The results should be interpreted with caution because of the large heterogeneity between studies resulting from biological and methodological variability.

Acknowledgements

The authors thank all the corresponding authors of the primary studies who provided additional information for the review.

Conflict of interest

The authors declare no conflict of interest and no external funding was obtained for performing the current review.

References

Aerssens J, Boonen S, Lowet G, *et al*. 1998; Interspecies differences in bone composition, density, and quality: potential implications for *in vivo* bone research. *Endocrinology* **139**: 663–670.

Al-Nawas B, Schiegnitz E. 2014; Augmentation procedures using bone substitute materials or autogenous bone – a systematic review and meta-analysis. *Eur J Oral Implantol* **7**: 219–234.

Arosarena OA, Falk A, Malmgren L, *et al*. 2003. Defect repair in the rat mandible with bone morphogenic proteins and marrow cells. *Arch. Facial Plast. Surg.* **5**: 103–108.

Bagi CM, Berryman E, Moalli MR. 2011; Comparative bone anatomy of commonly used laboratory animals: implications for drug discovery. *Comp Med* **61**: 76–85.

Behnia A, Haghighat A, Talebi A, Nourbakhsh N, Heidari F. 2014; Transplantation of stem cells from human exfoliated deciduous teeth for bone regeneration in the dog mandibular defect. *World J Stem Cells* **6**: 505–510.

Berglundh T, Stavropoulos A. 2012; Preclinical *in vivo* research in implant dentistry. Consensus of the eighth European workshop on periodontology. *J Clin Periodontol* **39**(Suppl 1): 1–5.

Bright R, Hynes K, Gronthos S, *et al*. 2015; Periodontal ligament-derived cells for periodontal regeneration in animal models: a systematic review. *J Periodontal Res* **50**: 160–172.

Bueno DF, Kerkis I, Costa AM, *et al*., 2009; New source of muscle-derived stem cells with potential for alveolar bone reconstruction in cleft lip and/or palate patients. *Tissue Eng Part A* **15**: 427–435.

Cancedda R, Giannoni P, Mastrogiacomo M. 2007; A tissue engineering approach to bone repair in large animal models and in clinical practice. *Biomaterials* **28**: 4240–4250.

Carreira AC, Lojudice FH, Halcsik E, *et al*. 2014; Bone morphogenetic proteins: facts, challenges, and future perspectives. *J Dent Res* **93**: 335–345.

Chanchareonsook N, Junker R, Jongpaiboonkit L, *et al*. 2014a; Tissue-engineered mandibular bone reconstruction for continuity defects: a systematic approach to the literature. *Tissue Eng Part B Rev* **20**: 147–162.

Chanchareonsook N, Tideman H, Feinberg SE, *et al*. 2014b; Segmental mandibular bone reconstruction with a carbonate-substituted hydroxyapatite-coated modular endoprosthetic poly(ε-caprolactone) scaffold in *Macaca fascicularis*. *J Biomed Mater Res B Appl Biomater* **102**: 962–976.

Chang SC-N, Chuang HL, Chen YR, *et al*. 2003; *Ex vivo* gene therapy in autologous bone marrow stromal stem cells for tissue-engineered maxillofacial bone regeneration. *Gene Ther* **10**: 2013–2019.

Chappard D, Legrand E, Pascaretti C, *et al*. 1999; Comparison of eight histomorphometric methods for measuring trabecular bone architecture by image analysis on histological sections. *Microsc Res Tech* **45**: 303–312.

Corbella S, Taschieri S, Weinstein R, *et al*. 2015; Histomorphometric outcomes after lateral sinus floor elevation procedure: a systematic review of the literature and meta-analysis. *Clin Oral Implants Res* doi: 10.1111/clr.12702.

Daei-Farshbaf N, Ardeshirylajimi A, Seyedjafari E, *et al*. 2014; Bioceramic-collagen scaffolds loaded with human adipose-tissue derived stem cells for bone tissue engineering. *Mol Biol Rep* **41**: 741–749.

Deeks JJ, Higgins JPT, Altman DG. 2008; Analysing data and undertaking meta-analyses. In: *Cochrane Handbook for Systematic Reviews of Interventions* John Wiley and Sons, Ltd, Chichester: 243–296.

Faggion CM Jr, Chambrone L, Gondim V, *et al*. 2010; Comparison of the effects of treatment of peri-implant infection in animal and human studies: systematic review and meta-analysis. *Clin Oral Implants Res* **21**: 137–147.

Fretwurst T, Gad LM, Nelson K, *et al*. 2015; Dentoalveolar reconstruction. *Curr Opin Otolaryngol Head Neck Surg* **23**: 316–322.

Gamie Z, MacFarlane RJ, Tomkinson A, *et al*. 2014; Skeletal tissue engineering using mesenchymal or embryonic stem cells: clinical and experimental data. *Expert Opin Biol Ther* **14**: 1611–1639.

Gomes PS, Fernandes MH. 2011; Rodent models in bone-related research: the relevance of calvarial defects in the assessment of bone regeneration strategies. *Lab Anim* **45**: 14–24.

Gothard D, Smith EL, Kanczler JM, *et al*. 2014; Tissue engineered bone using select growth factors: a comprehensive review of animal studies and clinical translation studies in man. *Eur Cell Mater* **28**: 166–208.

Götz C, Warnke PH, Kolk A. 2015; Current and future options of regeneration methods and reconstructive surgery of the facial skeleton. *Oral Surg Oral Med Oral Pathol Oral Radiol* **120**: 315–323.

Guo J, Meng Z, Chen G, *et al*. 2012; Restoration of critical-size defects in the rabbit mandible using porous nanohydroxyapatite–polyamide scaffolds. *Tissue Eng Part A* **18**: 1239–1252.

Haghighat A, Akhavan A, Hashemi-Beni B, *et al*. 2011; Adipose derived stem cells for treatment of mandibular bone defects: An autologous study in dogs. *Dent Res J (Isfahan)* **8**: S51–S57.

Higgins JPT, Deeks JJ. 2008; Selecting studies and collecting data. In: *Cochrane Handbook for Systematic Reviews of Interventions.*. John Wiley and Sons, Ltd, Chichester; 151–185.

Higgins JPT, Deeks JJ, Altman DG. 2008; Special topics in statistics. In: *Cochrane Handbook for Systematic Reviews of Interventions*. John Wiley and Sons, Ltd, Chichester; 481–529.

Hooijmans CR, IntHout J, Ritskes-Hoitinga M, *et al*. 2014a; Meta-analyses of animal studies: an introduction of a valuable instrument to further improve healthcare. *ILAR J* **55**: 418–426.

Hooijmans CR, Rovers MM, de Vries RB, *et al*. 2014b; SYRCLE's risk of bias tool for animal studies. *BMC Med Res Methodol* **14**: 43.

Huang J, Tian B, Chu F, *et al*. 2015; Rapid maxillary expansion in alveolar cleft repaired with a tissue-engineered bone in a canine model. *J Mech Behav Biomed Mater* **48**: 86–99.

Huh J-Y, Choi B-H, Kim B-Y, *et al*. 2005; Critical size defect in the canine mandible. *Oral Surg Oral Med Oral Pathol Oral Radiol Endod* **100**: 296–301.

Ichikawa Y, Watahiki J, Nampo T, *et al*. 2015; Differences in the developmental origins of the periosteum may influence bone healing. *J Periodontal Res* **50**: 468–478.

Jafarian M, Eslaminejad MB, Khojasteh A, *et al*. 2008; Marrow-derived mesenchymal stem cells-directed bone regeneration in the dog mandible: a comparison between biphasic calcium phosphate and natural bone mineral. *Oral Surg., Oral Med., Oral Pathol., Oral Radiol. Endod*. **105**: e14–e24.

Jiang X, Gittens SA, Chang Q, *et al*. 2006; The use of tissue-engineered bone with human bone morphogenetic protein-4-modified bone-marrow stromal cells in repairing mandibular defects in rabbits. *Int J Oral Maxillofac Surg* **35**: 1133–1139.

Jiang X, Zhao J, Wang S, *et al*. 2009; Mandibular repair in rats with premineralized silk scaffolds and BMP-2-modified bMSCs. *Biomaterials* **30**: 4522–4532.

Jiawen S, Jianjun Z, Jiewen D, *et al*. 2014; Osteogenic differentiation of human amniotic epithelial cells and its application in alveolar defect restoration. *Stem Cells Transl Med* **3**: 1504–1513.

Khojasteh A, Behnia H, Naghdi N, *et al*. 2013; Effects of different growth factors and carriers on bone regeneration: a systematic review. *Oral Surg Oral Med Oral Pathol Oral Radiol* **116**: e405–e423.

Kilkenny C, Browne WJ, Cuthill IC, *et al*. 2010; Improving bioscience research reporting: the ARRIVE guidelines for reporting animal research. *PLoS Biol* **8**: e1000412.

Kofron MD, Laurencin CT. 2006; Bone tissue engineering by gene delivery. *Adv Drug Deliv Rev* **58**: 555–576.

De Kok IJ, Peter SJ, Archambault M, *et al*. 2003; Investigation of allogeneic mesenchymal stem cell-based alveolar bone formation: preliminary findings. *Clin Oral Implants Res* **14**: 481–489.

Konopnicki S, Sharaf B, Resnick C, *et al*. 2015; Tissue-engineered bone with 3-dimensionally printed β-tricalcium phosphate and polycaprolactone scaffolds and early implantation: an in vivo pilot study in a porcine mandible model. *J. Oral Maxillofac. Surg* **73**: 1016.e1–1016.e11.

Kopp S, Warkentin M, Öri F, *et al*. 2012; Section plane selection influences the results of histomorphometric studies: the example of dental implants. *Biomed Tech (Berl)* **57**: 365–370.

Korn P, Schulz MC, Range U, *et al*. 2014; Efficacy of tissue engineered bone grafts containing mesenchymal stromal cells for cleft alveolar osteoplasty in a rat model. *J Craniomaxillofac Surg* **42**: 1277–1285.

Kuo T, Lee S-Y, Wu H-D, *et al*. 2015; An *in vivo* swine study for xeno-grafts of calcium sulfate-based bone grafts with human dental pulp stem cells (hDPSCs). *Mater Sci Eng C Mater Biol Appl* **50**: 19–23.

Lalu MM, McIntyre L, Pugliese C, *et al*. 2012; Safety of cell therapy with mesenchymal stromal cells (SafeCell): a systematic review and meta-analysis of clinical trials. *PLoS One* **7**: e47559.

Lee ES, Seo BM, Rim JS, *et al*. 2010; Placenta derived mesenchymal stem cells in combination with polycaprolactone–20% tricalcium phosphate scaffolds for the treatment of critical-sized defects of the mandible. *Tissue Eng Regen Med* **7**: 276–282.

Li J, Li Y, Ma S, *et al*. 2010; Enhancement of bone formation by BMP-7 transduced MSCs on biomimetic nano-hydroxyapatite/polyamide composite scaffolds in repair of mandibular defects. *J Biomed Mater Res Part A* **95A**: 973–981.

Li Y, Chen S-K, Li L, *et al*. 2015; Bone defect animal models for testing efficacy of bone substitute biomaterials. *J Orthop Transl* **3**: 95–104.

Liao Y, Zhang X-L, Li L, *et al*. 2014; Stem cell therapy for bone repair: a systematic review and meta-analysis of preclinical studies with large animal model. *Br J Clin Pharmacol* **78**: 718–726.

Liebschner MAK. 2004; Biomechanical considerations of animal models used in tissue engineering of bone. *Biomaterials* **25**: 1697–1714.

Copyright © 2016 John Wiley & Sons, Ltd.

Liu H-C, E L-L, Wang D-S, *et al*. 2011; Reconstruction of alveolar bone defects using bone morphogenetic protein 2 mediated rabbit dental pulp stem cells seeded on nano-hydroxyapatite/collagen/poly(L-lactide). *Tissue Eng Part A* **17**: 2417–2433.

Ma J-L, Pan J-L, Tan B-S, *et al*. 2009; Determination of critical size defect of minipig mandible. *J Tissue Eng Regen Med* **3**: 615–622.

Mardas N, Dereka X, Donos N, *et al*. 2014; Experimental model for bone regeneration in oral and cranio-maxillofacial surgery. *J Investig Surg* **27**: 32–49.

de Mendonça Costa A, Bueno DF, Martins MT, *et al*. 2008; Reconstruction of large cranial defects in nonimmunosuppressed experimental design with human dental pulp stem cells. *J Craniofac Surg* **19**: 204–210.

Milinkovic I, Cordaro L. 2014; Are there specific indications for the different alveolar bone augmentation procedures for implant placement? A systematic review. *Int J Oral Maxillofac Surg* **43**: 606–625.

Mohammadi R, Amini K. 2015; Guided bone regeneration of mandibles using chitosan scaffold seeded with characterized uncultured omental adipose-derived stromal vascular fraction: an animal study. *Int. J. Oral Maxillofac. Implants* **30**: 216–222.

Moher D, Liberati A, Tetzlaff J, *et al*. 2009; Preferred reporting items for systematic reviews and meta-analyses: the PRISMA statement. *PLoS Med* **6**: e1000097.

Müller R, Van Campenhout H, Van Damme B, *et al*. 1998; Morphometric analysis of human bone biopsies: a quantitative structural comparison of histological sections and micro-computed tomography. *Bone* **23**: 59–66.

Muschler GF, Raut VP, Patterson TE, *et al*. 2010; The design and use of animal models for translational research in bone tissue engineering and regenerative medicine. *Tissue Eng Part B Rev* **16**: 123–145.

Nkenke E, Neukam FW. 2014; Autogenous bone harvesting and grafting in advanced jaw resorption: morbidity, resorption and implant survival. *Eur J Oral Implantol* **7** (Suppl 2): S203–S217.

O'Loughlin PF. 2008; Selection and development of preclinical models in fracture-healing research. *J Bone Joint Surg* **90**: 79–84.

Oppenheimer AJ, Mesa J, Buchman SR. 2012; Current and emerging basic science concepts in bone biology: implications in craniofacial surgery. *J Craniofac Surg* **23**: 30–36.

Padial-Molina M, Valle F, Lanis A, *et al*. 2015; Clinical application of mesenchymal stem cells and novel supportive therapies for oral bone regeneration. *Biomed Res Int* **2015**: 16.

Park J, Ries J, Gelse K, *et al*. 2003; Bone regeneration in critical size defects by cell-mediated BMP-2 gene transfer: a comparison of adenoviral vectors and liposomes. *Gene Ther* **10**: 1089–1098.

Park J-B, Lee K, Lee W, *et al*. 2013; Establishment of the chronic bone defect model in experimental model mandible and evaluation of the efficacy of the mesenchymal stem cells in enhancing bone regeneration. *Tissue Eng. Regen. Med.* **10**: 18–24.

Park S-H, Choi H, Han J-S, *et al*. 2015. Comparative study of decalcification versus nondecalcification for histological evaluation of one-wall periodontal intrabony defects in dogs. *Microsc Res Tech* **78**: 94–104.

Pearce AI, Richards RG, Milz S, *et al*. 2007; Animal models for implant biomaterial research in bone: a review. *Eur Cell Mater* **13**: 1–10.

Pellegrini G, Seol YJ, Gruber R, *et al*. 2009; Pre-clinical models for oral and periodontal reconstructive therapies. *J Dent Res* **88**: 1065–1076.

Peric M, Dumic-Cule I, Grcevic D, *et al*. 2015. The rational use of animal models in the evaluation of novel bone regenerative therapies. *Bone* **70**: 73–86.

Pieri F, Lucarelli E, Corinaldesi G, *et al*. 2009; Effect of Mesenchymal Stem Cells and Platelet-Rich Plasma on the Healing of Standardized Bone Defects in the Alveolar Ridge: A Comparative Histomorphometric Study in Minipigs. *J. Oral Maxillofac. Surg.* **67**: 265–272.

Pourebrahim N, Hashemibeni B, Shahnaseri S, *et al*. 2013; A comparison of tissue-engineered bone from adipose-derived stem cell with autogenous bone repair in maxillary alveolar cleft model in dogs. *Int J Oral Maxillofac Surg* **42**: 562–568.

Quarto N, Wan DC, Kwan MD, *et al*. 2010; Origin matters: differences in embryonic tissue origin and Wnt signaling determine the osteogenic potential and healing capacity of frontal and parietal calvarial bones. *J Bone Miner Res* **25**: 1680–1694.

Raposo-Amaral CE, Bueno DF, Almeida AB, *et al*. 2014; Is bone transplantation the gold standard for repair of alveolar bone defects? *J Tissue Eng* **5**: 2041731413519352.

Rentsch C, Schneiders W, Manthey S, *et al*. 2014. Comprehensive histological evaluation of bone implants. *Biomatter* **4**: e27993.

Roux BM, Cheng M-H, Brey EM. 2015; Engineering clinically relevant volumes of vascularized bone. *J Cell Mol Med* **19**: 903–914.

Russel WMS, Burch RL. 1959; *The Principles of Humane Experimental Technique*. Methuen & Co., London (special edition published by Universities Federation for Animal Welfare, 1992).

Russmueller G, Moser D, Spassova E, *et al*. 2015. Tricalcium phosphate-based biocomposites for mandibular bone regeneration d A histological study in sheep. *J. Cranio-Maxillofacial Surg.* **43**: 696–704.

Ryan JM, Barry FP, Murphy JM, *et al*. 2005; Mesenchymal stem cells avoid allogeneic rejection. *J Inflamm (Lond)* **2**: 8.

Saad KA-E, Abu-Shahba AGT, El-Drieny EA-E, *et al*. 2015; Evaluation of the role of autogenous bone-marrow-derived mesenchymal stem cell transplantation for the repair of mandibular bone defects in rabbits. *J. Craniomaxillofac. Surg.* **43**: 1151–1160.

Schliephake H, Knebel JW, Aufderheide M, *et al*. 2001; Use of cultivated osteoprogenitor cells to increase bone formation in segmental mandibular defects: an experimental pilot study in sheep. *Int J Oral Maxillofac Surg* **30**: 531–537.

Schliephake H, Zghoul N, Jäger V, *et al*. 2009; Bone formation in trabecular bone cell seeded scaffolds used for reconstruction of the rat mandible. *Int J Oral Maxillofac Surg* **38**: 166–172.

Schmitz JP, Hollinger JO. 1986; The critical size defect as an experimental model for craniomandibulofacial nonunions. *Clin Orthop Relat Res* **205**: 299–308.

Schwarz F, Iglhaut G, Becker J. 2012; Quality assessment of reporting of animal studies on pathogenesis and treatment of peri-implant mucositis and peri-implantitis. A systematic review using the ARRIVE guidelines. *J Clin Periodontol* **39**(Suppl 1): 63–72.

Seto I, Asahina I, Oda M, *et al*. 2001; Reconstruction of the primate mandible with a combination graft of recombinant human bone morphogenetic protein-2 and bone marrow. *J Oral Maxillofac Surg* **59**: 53–61.

Seto I, Marukawa E, Asahina I. 2006; Mandibular reconstruction using a combination graft of rhBMP-2 with bone marrow cells expanded in vitro. *Plast Reconstr Surg* **117**: 902–908.

Shanbhag S, Shanbhag V. 2015; Clinical Applications of cell-based approaches in alveolar bone augmentation: a systematic review. *Clin Implant Dent Relat Res* **17**: e17–e34.

Smaïl-Faugeron V, Fron-Chabouis H, Courson F, *et al*. 2014; Comparison of intervention effects in split-mouth and parallel-arm randomized controlled trials: a meta-epidemiological study. *BMC Med Res Methodo* **14**: 64.

Stavropoulos A, Sculean A, Bosshardt DD, *et al*. 2015; Pre-clinical *in vivo* models for the screening of bone biomaterials for oral/craniofacial indications: focus on small-animal models. *Periodontol* **68**: 55–65.

Sterne JAC, Egger M, Moher D. 2008; Addressing reporting biases. In: *Cochrane Handbook for Systematic Reviews of Interventions*. John Wiley and Sons, Ltd, Chichester; 297–333.

Stübinger S, Dard M. 2013; The rabbit as experimental model for research in implant dentistry and related tissue regeneration. *J Investig Surg* **26**: 266–282.

Stewart MC, McCormick LE, Goliath JR, *et al*. 2013; A comparison of histomorphometric data collection methods. *J Forensic Sci* **58**: 109–113.

Su F, Liu S-S, Ma J-L, *et al*. 2015. Enhancement of periodontal tissue regeneration by transplantation of osteoprotegerin-engineered periodontal ligament stem cells. *Stem Cell Res Ther* **6**: 22.

Sun M, Tan W, Wang K, *et al*. 2013; Effects of allogenous periosteal-derived cells transfected with adenovirus-mediated BMP-2 on repairing defects of the mandible in rabbits. *J Oral Maxillofac Surg* **71**: 1789–1799.

Tang Y, Tang W, Lin Y, *et al*. 2008; Combination of bone tissue engineering and BMP-2 gene transfection promotes bone healing in osteoporotic rats. *Cell Biol, Int.* **32**: 1150–1157.

Thomsen JS, Laib A, Koller B, *et al*. 2005; Stereological measures of trabecular bone structure: comparison of 3D micro computed tomography with 2D histological sections in human proximal tibial bone biopsies. *J Microsc* **218**: 171–179.

Vahabi S, Amirizadeh N, Shokrgozar MA, *et al*. 2012; A comparison between the efficacy of Bio-Oss, hydroxyapatite tricalcium phosphate and combination of mesenchymal stem cells in inducing bone regeneration. *Chang Gung Med. J.* **35**: 28–37.

Vajgel A, Mardas N, Farias BC, *et al*. 2014; A systematic review on the critical size defect model. *Clin Oral Implants Res* **25**: 879–893.

Vandeweghe S, Coelho PG, Vanhove C, *et al*. 2013; Utilizing micro-computed tomography to evaluate bone structure surrounding dental implants: a comparison with histomorphometry. *J Biomed Mater Res Part B Appl Biomater* **101**: 1259–1266.

Vangsness CT, Farr J, Boyd J, *et al*. 2014; Adult human mesenchymal stem cells delivered via intra-articular injection to the knee following partial medial meniscectomy: a randomized, double-blind, controlled study. *J Bone Joint Surg* **96**: 90–98.

Vesterinen HM, Sena ES, Egan KJ, *et al*. 2014; Meta-analysis of data from animal studies: a practical guide. *J Neurosci Methods* **221**: 92–102.

Vidal B, Pinto A, Galvão MJ, *et al*. 2012; Bone histomorphometry revisited. *Acta Reum Port* **37**: 294–300.

Wang S, Zhao J, Zhang W, *et al*. 2015; Comprehensive evaluation of cryopreserved bone-derived osteoblasts for the repair of segmental mandibular defects in canines. *Clin Implant Dent Relat Res* **17**: 798–810.

Wei J, Xu M, Zhang X, *et al*. 2015; Enhanced Osteogenic Behavior of ADSCs Produced by Deproteinized Antler Cancellous Bone and Evidence for Involvement of ERK Signaling Pathway. *Tissue Eng. Part A* **21**: 1810–1821.

Wright CD, Vedi S, Garrahan NJ, *et al*. 1992; Combined inter-observer and inter-method variation in bone histomorphometry. *Bone* **13**: 205–208.

Yamada Y, Ito K, Nakamura S, *et al*. 2011; Promising cell-based therapy for bone regeneration using stem cells from deciduous teeth, dental pulp, and bone marrow. *Cell Transplant* **20**: 1003–1013.

Yamada Y, Ueda M, Naiki T, *et al*. 2004; Autogenous injectable bone for regeneration with mesenchymal stem cells and platelet-rich plasma: tissue-engineered bone regeneration. *Tissue Eng.* **10**: 955–964.

Yan X-Z, Yang F, Jansen JA, *et al*. 2015; Cell-based approaches in periodontal regeneration: a systematic review and meta-analysis of periodontal defect models in animal experimental work. *Tissue Eng Part B Rev* **21**: 411–426.

Yoshimi R, Yamada Y, Ito K, *et al*. 2009; Self-assembling peptide nanofiber scaffolds, platelet-rich plasma, and mesenchymal stem cells for injectable bone regeneration with tissue engineering. *J. Craniofac. Surg.* **20**: 1523–1530.

Young S, Bashoura AG, Borden T, *et al*. 2008; Development and characterization of a rabbit alveolar bone nonhealing defect model. *J Biomed Mater Res A* **86**: 182–194.

Zhang D, Chu F, Yang Y, *et al*. 2011; Orthodontic tooth movement in alveolar cleft repaired with a tissue engineering bone: an experimental study in dogs. *Tissue Eng Part A* **17**: 1313–1325.

Zhao J, Zhang Z, Wang S, *et al*. 2009; Apatite-coated silk fibroin scaffolds to healing mandibular border defects in canines. *Bone* **45**: 517–527.

Zhao J, Hu J, Wang S, *et al*. 2010; Combination of beta-TCP and BMP-2 gene-modified bMSCs to heal critical size mandibular defects in rats. *Oral Dis* **16**: 46–54.

Zheng Y, Liu Y, Zhang CM, *et al*. 2009; Stem cells from deciduous tooth repair mandibular defect in swine. *J. Dent. Res.* **88**: 249–254.

Supporting information on the internet

The following supporting information may be found in the online version of this article:

Copyright © 2016 John Wiley & Sons, Ltd.

DOI: 10.1002/term

Table S1. Search strategy for MEDLINE.
Table S2. Checklist for quality assessment of studies according to modified ARRIVE guidelines and a predefined grading system.
Table S3. Assessment of risk of bias (RoB) in studies included using a modified SYRCLE's RoB tool.
Table S4. Summary of results of the meta-analysis and sensitivity analyses.
Table S5. Summary of studies excluded after full-text analysis.
Table S6. Summary of studies with quantitative radiographic outcomes.
Text S1. References: studies excluded

Copyright © 2016 John Wiley & Sons, Ltd.

DOI: 10.1002/term

Press release

Siddharth Shanbhag graduated as a dentist from India and received his postgraduate training in UK (London), Sweden (Malmö), and Norway (Bergen). Since 2016, Shanbhag has been a prominent researcher at the Department of Clinical Dentistry (IKO), Faculty of Medicine, UiB, focusing on the development of novel strategies for regeneration of bone defects.

Replacement of lost/missing teeth is important to restore individuals' speech, appearance, function, and quality of life. Very often, it is necessary to first regenerate the lost bone in order to safely and predictably reconstruct the dental tissues. Shanbhag has been developing novel strategies to regenerate bone defects using human stem cells based on the principles of 'tissue engineering'. This work has been presented in high-impact publications in scientific journals and at reputed international scientific meetings.

For his doctoral thesis (PhD), Shanbhag focused on 'cell-based' strategies for bone regeneration mainly using adult mesenchymal stem cells from the bone marrow and dental tissues. Notably, Shanbhag optimized a safe and efficient method to grow these cells free of animal products for clinical applications, resulting in a new product called 'BergenLys'. This strategy will now be used in the new Ex Vivo Facility at Haukeland University Hospital to manufacture stem cells for clinical trials in Bergen. Shanbhag also contributed to a European workshop to develop clinical guidelines for oral bone regeneration.

Despite its tremendous promise, cell therapy is currently limited by high costs and stringent regulations from health authorities. Moreover, recent studies show that stem cells mainly act by secreting potent molecules, such as growth factors. Therefore, in addition to his work on cell-based therapies, Shanbhag is investigating 'cell-free' strategies using biologically active molecules derived from stem cells. This strategy offers a potentially simpler, safer, and more cost-effective alternative to cell therapy for tissue regeneration. Shanbhag is currently leading an international consortium on this project with partners in Norway, Spain, and Austria with support from major funding agencies.

Shanbhag has received several awards and research grants from prestigious organizations such as the International Association for Dental Research (USA), ITI Foundation (Switzerland) and Osteology Foundation (Switzerland). He is currently a Postdoctoral Fellow at the Laboratory Clinic, Haukeland University Hospital, a Researcher at the Centre for Translational Oral Research, UiB, and a visiting Researcher at the Faculty of Odontology, University Complutense of Madrid, Spain.

Cristin-person-ID: 779503
Email: Siddharth.Shanbhag@uib.no